HAL
open science

Cartographie golgienne des enzymes de synthèse des polysaccharides complexes pariétaux et recherche de complexes enzymatiques.

Sophie Bernard

To cite this version:

Sophie Bernard. Cartographie golgienne des enzymes de synthèse des polysaccharides complexes pariétaux et recherche de complexes enzymatiques.. Biologie moléculaire. Université de Rouen, 2013. Français. NNT : . tel-02053665

HAL Id: tel-02053665

https://normandie-univ.hal.science/tel-02053665

Submitted on 13 Jun 2019

HAL is a multi-disciplinary open access archive for the deposit and dissemination of scientific research documents, whether they are published or not. The documents may come from teaching and research institutions in France or abroad, or from public or private research centers.

L'archive ouverte pluridisciplinaire **HAL**, est destinée au dépôt et à la diffusion de documents scientifiques de niveau recherche, publiés ou non, émanant des établissements d'enseignement et de recherche français ou étrangers, des laboratoires publics ou privés.

UNIVERSITE DE ROUEN
UFR DES SCIENCES ET TECHNIQUES

THESE DE DOCTORAT
Ecole Doctorale Normande de Biologie Intégrative, Santé et Environnement
Spécialité : Biologie Cellulaire

Soutenue le 03 décembre 2013 par :
SOPHIE BERNARD

Cartographie golgienne des enzymes de synthèse des polysaccharides complexes pariétaux et recherche de complexes enzymatiques.

Directeur de thèse : Pr. Azeddine Driouich
Co-encadrant de thèse : Dr. Marie-Laure Follet-Gueye

Membres du jury

Mme Anne-Sophie Blervacq	Maître de Conférences, Université de Lille 1	Rapporteur
Mr Benoît St Pierre	Professeur, Université François Rabelais – Tours	Rapporteur
Mr Patrice Lerouge	Professeur, Université de Rouen	Président
Mme Maïté Montero-Hadjadje	Professeur, Université de Rouen	Examinateur
Mme Catherine Rayon	Maître de Conférences, Université Jules Verne- Amiens	Examinateur

Remerciements

En premier lieu, je tiens à remercier les rapporteurs Mme Anne-Sophie Blervacq, maître de conférences à l'université de Lille 1, et Mr Benoît St Pierre, professeur à l'université de Tours, d'avoir accepté d'évaluer mon mémoire de thèse. Je remercie également tous les membres du jury pour leur présence à cette soutenance de thèse et l'évaluation de mes travaux de recherche.

Ces travaux de recherche ont été réalisés à l'université de Rouen au sein du laboratoire de recherche universitaire « Glycobiologie et Matrice Extracellulaire Végétale » (Glyco-MEV, UPRES-EA4358 ; http://www.univ-rouen.fr/Glyco-MEV/), co-fondé et co-dirigé par les Prs. Patrice Lerouge et Azeddine Driouich. Ma thèse a été effectuée sous la direction du Pr. Azeddine Driouich et le co-encadrement du Dr. Marie-Laure Follet-Gueye.

Je remercie la région Haute-Normandie et l'université de Rouen pour leur soutien financier durant ma thèse, ainsi que l'école doctorale Normande de Biologie Intégrative, Santé et Environnment (EdNBISE) pour ses formations de qualité et qui me sont toujours utiles pour mon métier d'ingénieur.

Mon aventure au sein du laboratoire Glyco-MEV a commencé en octobre 2004 lorsque le Pr. Azeddine Driouich m'a acceptée en stage de Master, puis a accepté de réitérer l'expérience pour trois années de plus en étant mon directeur de thèse. Après une année en tant qu'ATER, les Prs. Patrice Lerouge et Azeddine Driouich m'ont proposé un poste au laboratoire en tant qu'ingénieur d'étude en microscopie électronique à transmission. Je vous remercie sincèrement tout les deux d'avoir cru en mon potentiel et de m'avoir donné l'opportunité de faire un métier que j'aime profondément.

Je souhaite remercier maintenant mes deux chefs de thèse, Azeddine et Marie-Laure. Honneur aux femmes, je commencerai donc par Marie-Laure. Marie, je te remercie sincèrement pour ton encadrement et tes conseils qui ont commencé à mon arrivée en stage de master (il y a 9 ans déjà !). Tu m'as fait découvrir le monde de la microscopie électronique à transmission, et surtout tu me l'as fait aimer grâce à ton envie de transmettre et à ta patience pour me former à ces techniques qui demandent beaucoup de minutie. Azeddine, grâce à vous, je suis passée du stade « étudiante stagiaire » pas vraiment autonome à celui d'une véritable scientifique « chercheuse ». Par vos remarques et vos commentaires (qui m'ont fait grogner plus d'une fois, mais qui je l'espère continueront ☺), vous m'avez appris à communiquer à l'oral, à l'écrit, à aller au fond des choses, à être exigente sur la qualité d'un travail et à avoir l'esprit critique. Sachez que c'est grâce à vous deux si aujourd'hui je suis devenue ingénieur en microscopie électronique à transmission.

Durant ma thèse, j'ai eu l'opportunité de faire deux séjours scientifiques dans des laboratoires de recherche universitaires étrangers. Je remercie le Dr. Ahmed Faîk de m'avoir accueillie au sein du laboratoire « *Plant cell wall biotechnology: cell wall elaboration* », à l'université d'Athens (Ohio, USA). Je remercie également le Pr. Henrik Vibe Scheller de m'avoir accueillie chaleureusement au sein du laboratoire de recherche « *Molecular plant biology: Cell wall* », à l'université de Copenhague. Je remercie tout particulièrement le Dr. Yumiko Sakuragi qui m'a parfaitement encadrée durant ce séjour. Je remercie également tous mes collègues croisés au cours de ces séjours : Matthew, Wei, Ying-Ying, Jesper, Jacob, etc… pour leur aide au laboratoire et nos soirées multi-culturelles.

Je tiens à remercier Laurence Chevalier, également ingénieur en microscopie électronique, qui m'a beaucoup appris durant mes premières années de thèse et qui m'a fait découvrir le métier d'ingénieur.

C'est maintenant le tour de mes anciens collègues thésards. Ayant commencé ma thèse en octobre 2005, il y en a eu un certain nombre ☺ Un gros merci à ma « première génération » de complices de thèse : So, Bubu, Max, Fred, Olive et tous les autres, vous m'avez donné envie de commencer une thèse et vous m'avez fait partager votre expérience de thésard. Passons maintenant à ma « deuxième génération » de thésards : Caro, Bébé, Barbie, Marco, Pépé, Romain, Flavien, grâce à vous j'ai tenu bon malgré une période de doutes… et malgré le fait que vous m'ayez créé mon étiquette « doyenne des thésards » ☺. Et bien sûr, le point commun de ces deux générations que je n'oublierai pas, ce sont nos soirées mémorables !!

Je tiens à remercier l'ensemble de mes collègues du laboratoire Glyco-MEV, vous m'avez tous apporté à un moment ou à un autre votre aide, des conseils ou des réponses à mes questions lorsque j'étais thésarde. Aujourd'hui, je tiens également à vous remercier car à partir de septembre 2009, j'ai pu évoluer sans difficulté au sein du laboratoire de mon statut de thésarde à mon statut d'ingénieur et trouver ma place en tant qu'ingénieur.

Je remercie également mes collègues de la plateforme d'imagerie Primacen, avec qui j'ai un grand plaisir à travailler, et qui me font découvrir d'autres facettes du métier d'ingénieur que j'apprécie énormément.

Quant à la dernière génération de thésards, cà y est, je rends mon titre de « doyenne des thésards », à qui dois-je le donner ?? Dorénavant, il faudra m'appelé Madame la Docteur ☺. Et ne vous inquiétez pas, en toute simplicité Madame la Docteur continuera à vous dire qu'il faut : mettre sa blouse, mettre des gants, ranger sa paillasse, faire et ranger sa vaisselle, ranger les produits, prendre soin du matériel, participer au ménage du lundi matin… Bref, tout ce qui fait que vous m'adorez !!

Enfin, je remercie ma famille qui m'a toujours soutenue dans mes choix d'études, et qui a toujours été là pour m'épauler et me remonter le moral dans les périodes de doutes. Je vous aime de tout mon cœur. Papa, Maman, Vivi et les papis/mamies, çà y est, vous pourrez enfin dire que votre fille, sœur, petite-fille a enfin fini ses études ! Et vous ne pourrez plus me poser LA fameuse question « Au fait, quand est-ce que tu finis ta thèse ? ». Il va falloir en trouver une autre (je me doute déjà de ce que sera cette fameuse question…☺).

Et dire que je vous avais affirmé que je n'irai jamais étudier à l'université et que je ne ferai jamais d'études longues … comme quoi la vie est pleine de surprises ! En tout cas, je ne regrette aucun de mes choix, car j'ai trouvé mon métier.

Préambule

La paroi primaire des plantes des dicotylédones vraies est constituée de microfibrilles de cellulose, de protéines et de polysaccharides complexes, représentés par les hémicelluloses et les pectines. Chez la plante modèle *Arabidopsis thaliana*, le xyloglucane (XyG) et le rhamnogalacturonane-I (RG-I) constituent les catégories majeures des hémicelluloses et des pectines respectivement. Avant d'être transportés vers la paroi, le XyG et le RG-I sont synthétisés au sein de l'appareil de Golgi, notamment *via* l'action d'enzymes d'interconversion des sucres et de glycosyltransférases, qui vont générer et assembler les différents sucres pour former les polysaccharides.

L'objectif de ce projet de recherche a été d'effectuer la cartographie golgienne d'épitopes polysaccharidiques et de différentes enzymes impliquées dans la synthèse du XyG et du RG-I, ainsi que de rechercher l'existence de complexes enzymatiques, en utilisant les techniques de microscopie confocale à balayage laser, de microscopie électronique à transmission et d'immunocytochimie quantitative.

Ce manuscrit s'organise en quatre chapitres :

- Une introduction où les polysaccharides constitutifs de la paroi primaire des plantes eudicotylédones sont présentés, ainsi que les enzymes participant à la synthèse de deux polysaccharides majoritaires : le XyG et le RG-I. Dans une dernière partie, l'organisation structurale et fonctionnelle de l'appareil de Golgi (lieu de synthèse des polysaccharides complexes) sont décrites.
- Un chapitre Matériel et Méthodes où le matériel végétal, les conditions expérimentales, ainsi que les techniques auxquelles j'ai été formée sont décrites en détail.
- Les résultats obtenus au cours de mes travaux de thèse selon quatre parties : le développement méthodologique, la synthèse golgienne du XyG, la synthèse golgienne du RG-I et les travaux effectués dans le cadre d'une collaboration avec l'équipe du Dr Y. Sakuragi (Université de Copenhague, Danemark). Pour chaque partie, un résumé présente les résultats clefs, puis les résultats sont décrits en détail sous forme d'articles scientifiques (publiés ou soumis à publication).
- Enfin, un dernier chapitre relatif aux discussions et conclusion reprend les données clefs de ces travaux et propose des hypothèses sur la synthèse golgienne du XyG et du RG-I.

Sommaire

LISTE DES ABREVIATIONS 7
CHAPITRE I : INTRODUCTION 11
PARTIE A : COMPOSITION DE LA PAROI PRIMAIRE VEGETALE CHEZ LES PLANTES EUDICOTYLEDONES 13
I- Généralités 13
II- Organisation de la paroi primaire 14
III-La cellulose 17
IV-Les hémicelluloses 19
IV-1- Le xyloglucane (XyG) 19
IV-2- Les glucuronoarabinoxylanes (GAX) 21
IV-3-Les polysaccharides mannanes 22
V- Les pectines 23
V-1-Les homogalacturonanes 23
V-2- Les xylogalacturonanes 24
V-3-Le rhamnogalacturonane-II 25
V-4- Le rhamnogalacturonane-I 26
PARTIE B : LES ENZYMES IMPLIQUEES DANS LA SYNTHESE DU XYLOGLUCANE ET DU RHAMNOGALACTURONANE-I 29
I- Généralités 29
II- Les enzymes d'interconversion des nucléotides-sucres 30
II-1- La production de l'UDP- D-xylose 30
II-2- La production de l'UDP- D-galactose 31
II-3- Production du GDP-L- fucose 31
II-4- Production de l'UDP-D-acide galacturonique 32
II-5- Production de l'UDP-L- rhamnose 33
II-6- Production de l'UDP-L-arabinose 34
II-6-1- Les UDP-D-xylose 4-épimerases 34
II-6-2- Les UDP-arabinose mutases 34
III- Les transporteurs des nucléotides-sucre 35
IV-Les glycosyltransférases impliquées dans la synthèse du XyG 36
IV-1- La Glucane synthase 37
IV-2- Les α(1,6)Xylosyltransférases 37
IV-3- Les β(1,2)Galactosyltransférases 38
IV-4- La α(1,2)Fucosyltransferase 39
V- Les glycosyltransférases impliquées dans la synthèse du RG-I 40
V-1- Les β(1,4)galactosyltransférases 41
V-2- Les β(1,3)galactosyltransférases 42
V-3- Les α(1,5)arabinosyltransférases 42
V-4- Les α(1,2) et α(1,3)arabinosyltransférases 43
V-5- Les β(1,3)arabinosyltransférases 43
PARTIE C : LA SYNTHESE GOLGIENNE DES POLYSACCHARIDES NON CELLULOSIQUES CHEZ LES PLANTES EUDICOTYLEDONES 44
I- L'appareil de Golgi 44
I-1- Généralités 44

I-2- L'appareil de Golgi est une structure évolutive et mobile 45
I-3-Techniques développées pour étudier l'appareil de Golgi..... 46
II- Biogenèse et structure de l'appareil de Golgi..... 47
II-1- Différents modèles de synthèse 47
II-1-1- Synthèse *de novo* à partir du réticulum endoplasmique 47
II-1-2- Duplication par maturation 48
II-1-3- Coexistence des 2 modèles 49
II-2- Le réseau *trans*-golgien..... 50
II-3- Comment est conservée l'intégrité d'un empilement golgien ?..... 51
II-3-1- Les éléments inter-citernes 51
II-3-2- La matrice golgienne..... 51
II-4- Le système endomembranaire golgien 52
II-4-2- Transports antérograde et rétrograde entre le RE et les empilements golgiens..... 53
II-4-3- Transport post-Golgi..... 54
III- La synthèse golgienne des PS complexes 57
III-1- Généralités..... 57
III-2- La rétention des glycosyltransférases au sein du Golgi..... 58
III-2-1- Longueur et nature du domaine transmembranaire des protéines 58
III-2-2-Un signal de rétention dans la séquence protéique 59
III-2-3-La composition lipidique des membranes golgiennes 59
III-2-4-Ancrage des enzymes par les éléments inter-citernes..... 60
III-2-5- L'oligomérisation des protéines 60
III-3- Les enzymes de synthèse fonctionnent en complexes..... 60
III-3-1- Généralités..... 60
III-3-2-Complexes enzymatiques impliqués dans la synthèse du XyG 62
III-3-2-Complexes enzymatiques impliqués dans la synthèse du RG-I..... 63
III-4- Les enzymes de synthèse sont spécifiques d'un compartiment golgien..... 64
PARTIE D : OBJECTIFS DE MES TRAVAUX DE THESE..... 84
CHAPITRE II : MATERIEL ET METHODES..... 85
PARTIE A : CULTURE DU MATERIEL VEGETAL..... 87
I- Culture des plants de tabac *Nicotiana tabacum*..... 87
II- Culture des cellules de tabac *Nicotiana tabacum cv Bright Yellow* -2 (BY-2)..... 87
PARTIE B : CREATION DES PROTEINES DE FUSION 88
I- Construction des protéines de fusion avec la *Green Fluorescent Protein* 88
I-1- Clonage *via* l'utilisation des endonucléases de restriction..... 88
I-1-1- Amplification PCR 88
I-1-2- Insertion dans le plasmide pBLTI221sGFP..... 89
I-1-3- Contrôle de l'ADN plasmidique amplifié et extrait 91
I-1-4- Sous-clonage dans le vecteur d'expression pBLTI-121..... 91
I-2- Clonage par recombinaison : le système GATEWAY 92
I-2-1- Principe du Gateway..... 92
I-2-2- Amplification PCR 93
I-2-3- Insertion du gène d'intérêt dans le vecteur d'entrée pENTR-D-TOPO ® 94
I-2-4- Digestion contrôle Asc1/Not1 94
I-2-5- Séquençage..... 95
I-2-6- Insertion dans le vecteur d'expression pMDC : la réaction de LR clonase..... 95

II- Construction des protéines de fusion pour la *Bimolecular Fluorescence Complementation* 96
II-1- Clonage *via* l'utilisation de la méthode USER™ 96
II-1-1- Principe du USER™ (uracil-specific excision reagent) 96
II-1-2- Amplification PCR du gène d'intérêt 97
II-1-3- Digestion de l'ADN matrice par Dpn I 98
II-1-4- Digestion du vecteur de clonage BJH MP27 98
II-1-5- Ligation via l'enzyme USER 98
PARTIE C : EXPRESSION DES PROTEINES DE FUSION 99
I- Utilisation d'Agrobacterium tumefaciens 99
I- 1- Mise en compétence d'*Agrobacterium tumefaciens* 99
I-1-1- Préparation d'agrobactéries chiomiocompétentes 99
I-1-2- Préparation d'agrobactéries électrocompétentes 99
I - 2 - Transformation des agrobactéries 100
I-2-1- Transformation des agrobactéries chiomiocompétentes 100
I-2-2- Transformation des agrobactéries électrocompétentes 100
II- Transformation de cellules végétales 101
II-1- Transformation transitoire des cellules épidermiques de feuilles de tabac *Nicotiana tabacum* 101
II-2- Transformation stable des cellules de tabac Bright Yellow-2 (BY-2) 101
PARTIE D : LOCALISATION DES PROTEINES DE FUSION 102
I- Analyse par Microscopie Confocale à Balayage Laser (MCBL) 102
I-1- Principe de la microscopie confocale à balayage laser (MCBL). 102
I-2- Préparation des échantillons 103
I-3- Paramètres d'observations 103
II- Microscopie Electronique à Transmission 103
II-1-Principe du microscope électronique à transmission 103
II-2- Cryoimmobilisation haute pression 104
II-2-1- Préparations des échantillons à la congélation 104
II-2-2 Cryofixation des échantillons sous haute pression 105
II-2-3- Cryosubstitution et enrésinement 106
II-3- Réalisation des coupes ultrafines 107
II- 4- Immunocytochimie 107
II-4 -1- Immunomarquage des polysaccharides complexes 107
II-4-2- Immunomarquage des protéines fusionnées à la GFP 108
II-5- Coloration et observation des coupes ultrafines 108
II-6- Tests statistiques 109
II-6-1-Spécificité de marquage : Test du khi-deux 109
II-6-2- Distribution golgienne des particules d'or : Test du RLI 110
PARTIE E : TECHNIQUE D ETUDE POUR LA RECHERCHE DE COMPLEXES ENZYMATIQUES : LA COMPLEMENTATION DE FLUORESCENCE BIMOLECULAIRE(BIFC) 111
I- Principe de la Bimolecular Fluorescence Complementation (BiFC) 111
II- Préparation des échantillons 111
III- Les paramètres d'observation 112
CHAPITRE III: RESULTATS 113
PARTIE A : DÉVELOPPEMENTS METHODOLOGIQUES 115
PARTIE B : SYNTHESE GOLGIENNE DU XYLOGLUCANE 153

PARTIE C : SYNTHESE GOLGIENNE DU RHAMNOGALACTURONANE-I 173
PARTIE D: TRAVAUX EFFECTUES DANS LE CADRE D'UNE COLLABORATION 225
CHAPITRE IV: DISCUSSION 257
PARTIE A : LA SYNTHESE GOLGIENNE DU XYLOGLUCANE 258
I- Quels compartiments golgiens sont impliqués dans la synthèse du XyG ? 258
II- Les glycosyltransférases participant à la synthèse golgienne du XyG sont-elles organisées en complexes ? 259
PARTIE B : LA SYNTHESE GOLGIENNE DU RG-I 261
I- Quels compartiments golgiens sont impliqués dans la synthèse du RG-I ? 261
II- Les glycosyltransférases participant à la synthèse golgienne des chaînes arabinanes du RG-I sont-elles organisées en complexes ? 263
PARTIE C : CONCLUSION 265
BIBLIOGRAPHIE 267
CURICULUM VITAE 289

Figure 1 : Classification phylogénique des angiospermes (APG III). 14
Figure 2 : Premiers modèles proposés pour l'organisation de la paroi primaire végétale. 15
Figure 3 : Derniers modèles proposés pour la structure de la paroi primaire végétale. 16
Figure 4 : Structure et synthèse de la cellulose (Lerouxel et al., 2006). 17
Figure 5 : Les différentes sources de glucose pour la synthèse de cellulose (Endler et Persson, 2011)..... 18
Figure 6 : Spécificité structurale et de liaison des hémicelluloses (Scheller et Ulvskov, 2010). 19
Figure 7 : Nomenclature des chaînes du xyloglucane (Fry et al., 1993)..... 20
Figure 8 : Structures typiques des fragments de xyloglucane retrouvées chez les Brassicales. 20
Figure 9 : Structures typiques des fragments de xyloglucane retrouvés chez les Solanales . . 21
Figure 10 : Structure des glucuronoarabinoxylanes. 22
Figure 11 : Galactoglucomannanes présents chez *Nicotiana tabacum* (Eda et al., 1985). 22
Figure 12 : Arabinoglucuronomannanes présents chez *Nicotiana tabacum* (Mori et Kato, 1981) 23
Figure 13 : Structure des homogalacturonanes (Scheller et al., 2007) 23
Figure 14: Association des chaînes HG *via* des ponts calciques : modèle en « boîtes à œufs ». 24
Figure 15 : Structure des xylogalacturonanes (Scheller et al., 2007) 24
Figure 16: Structure du Rhamnogalacturonane-II. 25
Figure 17 : Structures des chaînes arabinanes et galactanes rencontrées dans le RG-I (Adapté de Mohnen, 2008) 26
Figure 18 : Structures des chaînes arabinogalactanes rencontrées dans le RG-I (Adapté de Mohnen, 2008) 27
Figure 19 : Schéma représentant la prise en charge des UDP-sucres au cours de la synthèse golgienne des polysaccharides complexes 29
Figure 20 : Interconversion des UDP-sucres *via* l'action des différentes enzymes d'interconversion (Yin et al., 2011). 30
Figure 21 : Vue générale des transporteurs d'UDP-sucres pouvant exister (adapté de Reboul et al., 2011)..... 36
Figure 22 : Morphologie générale d'un empilement golgien..... 45
Figure 23 : L'association entre le RE et l'appareil de Golgi mise en évidence dans des cellules de tabac (Hawes et Satiat-Jeunemaitre, 2005) 47
Figure 24 : Synthèse *de novo* des saccules golgiennes (Donohoe et al., 2013) 48
Figure 25 : Duplication par maturation d'un empilement golgien (Staehelin et Kang, 2008) 49
Figure 26 : Morphologie des différents types de TGN (Staehelin et Kang, 2008). 50
Figure 27 : Les éléments inter-citernes (Kristen, 1978)..... 51
Figure 28 : Morphologie de la matrice golgienne (Donohoe et al., 2013) 52
Figure 29 : Le modèle "Dock, pluck, and go" du transport RE/Golgi (Staehelin et Kang, 2008) 53
Figure 30 : Transport antérograde et rétrograde entre le RE et les empilements golgiens (Staehelin et Kang, 2008) 54
Figure 31 : Formations des vésicules de transport au niveau du TGN (Surma et al., 2012). .. 55
Figure 32 : Modèle de maturation des corps multivésiculaires (MVBs) à partir du TGN (Scheuring et al., 2011). 57
Figure 33 : Différents mécanismes de rétention des protéines membranaires (adapté de Banfield, 2011). 58

Figure 34 : Les différents types de protéines (adapté de Banfield et al., 2011). 61
Figure 35 : Association des protéines AtGAUT1 et AtGAUT7 (adapté de Oikawa et al., 2012). 61
Figure 36 : Association des protéines AtFX/GER1 et AtMUR1/GMD2 (Nakayama et al., 2003). 62
Figure 37 : Oligomérisation des protéines RGPs (De Pino et al., 2013). 64
Figure 38 : Plant de tabac *Nicotiana tabacum* âgé de 7/8 semaines..... 87
Figure 39 : Cal (a) et suspension cellulaire (b) de *Nicotiana tabacum* cv Bright Yellow 2(BY-2) 88
Figure 40 : Paramètres des cycles PCR (dénaturation, hybridation et élongation). 89
Figure 41 : Représentation schématique du vecteur de clonage pBLTI221sGFP. 89
Figure 42 : Représentation schématique du vecteur de clonage pBLTI221sGFP 91
Figure 43 : Principe de la recombinaison par site spécifiques entre le phage λ et *E.coli*. 92
Figure 44 : Principe du clonage Gateway par réactions BP ou LR (Invitrogen)..... 93
Figure 45 : Paramètres des cycles PCR (dénaturation, hybridation et élongation). 93
Figure 46 : Représentation schématique du vecteur d'entrée pENTR/D-TOPO..... 94
Figure 47 : Représentation schématique du vecteur d'expression pMDC83 95
Figure 48 : Principe du clonage USER..... 97
Figure 49 : Paramètres des cycles PCR (dénaturation, hybridation et élongation). 97
Figure 50 : Représentation schématique du plasmide BJH MP27 98
Figure 51 : Principe d'un microscope confocal à balayage laser 102
Figure 52 : Principe du microscope électronique à transmission 104
Figure 53 : Les différentes formes de l'eau dans une cellule. 105
Figure 54 : Apppareil de cryofixation sous haute pression EMPACT1, Leica (Studer et al., 2001)..... 106
Figure 55 : Automate de cryosubstitution AFS1, Leica 107
Figure 56 : Ultramicrotomie 107
Figure 57 : Principe de la complémentation de fluorescence bimoléculaire 111
Figure 58 : Synthèse du xyloglucane (adapté de http://www.bmb.msu.edu/faculty/keegstra/cellwall.html et Davis, 2010)..... 259
Figure 59 : Modèle représentant les grandes étapes de la synthèse du RG-I dans les différents compartiments golgiens. 262
Figure 60 : Représentation schématique des enzymes potentiellement impliquées dans la synthèse golgienne des chaînes arabinanes du RG-I. 263

Tableau 1 : Primers utilisés pour l'amplification PCR 89
Tableau 2 : Primers utilisés pour l'amplification PCR 93
Tableau 3 : Primers utilisés pour l'amplification PCR 97
Tableau 4 : Tableau de calcul pour le test du khi-deux..... 109

LISTE DES ABREVIATIONS

χ_2 : Khi-deux

2-AB : 2-aminobenzamide

ABC : ATP-binding cassette

ADN_c : Acide désoxyribonucléique codant

AFS : Automate Freeze Substitution

AG : appareil de Golgi

AGPs : arabinogalactanes protéines

Amp : Ampicilline

APG III : Angiosperm Phylogeny Group classification III

arad1 : arabinan deficient 1

Ara*f* : arabinofuranose

Ara*p* : arabinopyranose

A.thaliana : Arabidopsis thaliana

BFA : Brefeldin A

BiFC : Bimolecular Fluorescence Complementation

BSA : Bovin serum albumin

BY-2 : Bright Yellow-2

C1RGP : RGP de classe 1

C2RGP : RGP de classe 2

CAZy : Carbohydrate-Active enZYmes

CCV : vésicule à manteaux de clathrine

CesA : cellulose synthase

COPI : coat protein I

COPII : coat protein II

CPCs : coat protein complexes

CSL : cellulose synthase like

D-Gal : D-galactose

Dha : acide 2-céto-3-déoxy-D-lyxo-heptulosarique

dNTP : désoxynucléotide tri-phosphate

DPI : Day Post Infection

DRPs : dynamin-related GTPases

E.Coli : Escherichia coli

EE : early endosome

ERES : Endoplasmic Reticulum Exit Site

ESCRT : Endosomal Sorting Complex Required for Transport

EST : Expressed Sequence Tag

FF : forming face

Fru : fructose

GAE : Glucuronic Acid Epimerase

GalA : acide galacturonique

Gal*p* : galactopyranose

gals : galactan synthase

GAX : glucuronoarabinoxylane

GDP : guanosine diphosphate

GDP-D-Man : GDP-D-mannose

GDP-L-Fuc : GDP-L-fucose

GER : GDP-4-céto-6-désoxy-D-mannose-3,5-épimérase-4-réductase

GFP : Green Fluorescent Protein

Glc : glucose

GMD : GDP-D-mannose-4,6-déshydratase

GME : GDP-D-mannose-3,5-épimérase

GPL : glycérophospholipides

GT : glycosyltransférase

GV : golgi vesicles

HG : homogalacturonane

HPF : High Pressure Freezing

IHF : Integration Host Factor

Kan : kanamycine

Kdo : acide 2-céto-3-désoxy-D-manno-octulosonique

KH_2PO_4 : dihydrogénophosphate de potassium

KOH : hydroxyde de potassium

LB : Luria-Bertani

LE : late endosome

LRW : London Resin White

lrx1 : LRR-extensin1

MCLB : microscopie confocale à balayage laser

med : médian

MES : 2-(N-morpholino)ethanesulfonic acid

MET : microscopie électronique à transmission

MF : maturing face

$MgCl_2$: chlorure de magnesium

MS : Murashige et Skoog

mum4 : mucilage modified 4

mur : murus

MVBs : multivesicular bodies

NaCl : chlorure de sodium

NGS : normal goat serum

NIE : nucleotide interconversion enzyme

NST : nucleotide sugar transporter

NSR/ER : nucléotide-rhamnose synthase/épimérase-réductase

N. tabacum : Nicotiana tabacum

PCR : polymerase chain reaction

P. pastoris : Pichia pastoris

PM : membrane plasmique

PMT : photo-multiplicateur

PRIMACEN : Plate-forme régionale de recherche en imagerie cellulaire de Haute-Normandie

PS : polysaccharide

RE : réticulum endoplasmique

RFP : Red Fluorescent Protein

RG-I : rhamnogalacturonane - I

RG-II : rhamnogalacturonane - II

RGPs : Riversibly Glycosylated Polypeptides

RHM : UDP-L-rhamnose synthase

RLI : relative labeling index

rol1 : repressor of Irx1

rpm : rotations par minute

RT : room temperature

SL : sphingolipides

SNAREs : soluble N-ethylmaleimide-sensitive factor attachment protein receptors

Suc : sucrose

SuSy : sucrose synthase

SV : secreted vesicles

TBS : tris buffer saline

TGN : *trans*-Golgi network

Ti : tumor inducing

TMD : domaine transmembranaire

UAM : UDP-arabinose mutase

UAXS : UDP-D-apiose/UDP-D-xylose synthase

UDP : uridine diphosphate

UDP-Araf : UDP-arabinofuranose

UDP-D-Gal : UDP-D-galactose

UDP-D-GalA : UDP-D-acide galacturonique

UDP-D-Glc : UDP-D-glucose

UDP-GlcA : UDP-D-acide glucuronique

UDP-GlcAE : UDP-D-acide glucuronique-4-épimérase

UDP-L-Ara : UDP-L-arabinose

UDP-L-Rha : UDP-L-rhamnose

UDP-D-Xyl : UDP-D-xylose

UGD : UDP-D-glucose déshydrogénase

UGE : UDP-glucose-4-épimérase

UGlcAE : GDP-4-céto-6-désoxy-D-mannose-3,5-épimérase-4-réductase

UGPase : UDP-glucose pyrophosphorylase

UXE : UDP-xylose-4-épimérase

UV : ultra-violet

UXS : UDP-xylose synthase

USER ^{TM} : uracil-specific excision reagent

XGA : xylogalacturonane

xlt2 : xyloglucan L-side chain galactosyltransferase position 2

xxt5 : xyloglucan xylosyltransferase 5

XyG : xyloglucane

YC : fragment $C_{terminal}$ de la YFP

YFP : Yellow Fluorescent Protein

YN : fragment $N_{terminal}$ de la YFP

CHAPITRE I : INTRODUCTION

PARTIE A : COMPOSITION DE LA PAROI PRIMAIRE VEGETALE CHEZ LES PLANTES EUDICOTYLEDONES

I- Généralités

Les cellules végétales sont caractérisées par la présence d'une matrice extracellulaire de structure moléculaire diverse et hétérogène, appelée paroi (Popper et al., 2011). Il existe une paroi primaire et secondaire constituées d'une grande variété de polysaccharides complexes, dont la composition et les propriétés structurales sont contrôlées dans l'espace et le temps, ainsi qu'aux niveaux tissulaire et cellulaire. Cette paroi est essentielle pour les plantes, puisqu'elle joue un rôle dans la croissance, la différenciation cellulaire, la communication intercellulaire, les mouvements d'eau et la défense (Cosgrove, 2005 ;Vicré et al., 2005 ; Moore et al., 2006).

La paroi végétale a également un intérêt industriel important puisqu'elle représente la matière première nécessaire pour le textile, le papier, le bois de construction, les agents texturants, etc…. Plus récemment, l'industrie s'est aussi intéressée aux propriétés de la paroi végétale en tant que source de biocarburant (Jordan et al., 2012).

Mon projet de recherche s'est principalement intéressé à la localisation subcellulaire d'enzymes participant à la synthèse de la paroi primaire de la plante modèle *Arabidopsis thaliana*. De plus, *Nicotiana tabacum*, autre modèle végétal très répandu, a été utilisé comme système d'expression de ces enzymes impliquées dans la synthèse des composés pariétaux. D'après la troisième version de la classification phylogénétique des angiospermes **(figure 1)**, la plante *Arabidopsis thaliana* est issue de l'ordre des Brassicales qui fait partie de l'embranchement des Rosidées, tandis que *Nicotiana tabacum* est issu de l'ordre des Solanales qui fait partie de l'embranchement des Asteridées. Les Rosidées et les Astéridées font partie de l'embranchement du noyau des dicotylédones vraies ou « Core Eudicots », c'est pourquoi nous nous focaliserons dans cette introduction bibliographique, sur la présentation des caractéristiques pariétales de cet embranchement.

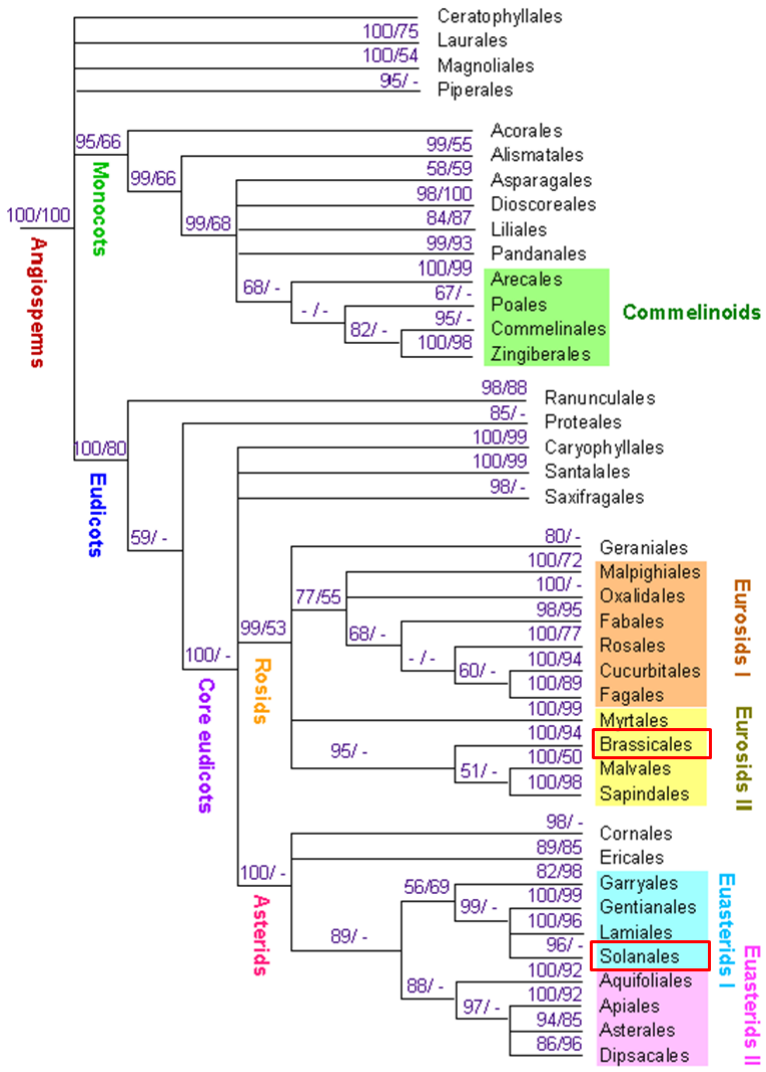

Figure 1 : Classification phylogénique des angiospermes (APG III).

II- Organisation de la paroi primaire

Au sein des parois primaires des plantes du noyau des dicotylédones vraies sont présents des microfibrilles de cellulose, des protéines et des polysaccharides non cellulosiques (également nommés polysaccharides complexes). Ces derniers sont définis par deux catégories : les hémicelluloses et les pectines. Les hémicelluloses regroupent le xyloglucane (hémicellulose majeure chez les dicotylédones vraies), les xylanes, les mannanes et les glucomannanes. Les pectines regroupent 4 classes majeures : les homogalacturonanes, les homogacturonanes substitués représentés par les xylogalacturonanes et le rhamnogalacturonane-II, et le rhamnogalacturonane-I.

L'organisation de ces différents composés pour former la paroi primaire végétale a donné lieu à plusieurs modèles. L'un des premiers modèles a initialement représenté cette paroi comme une grosse structure avec de nombreux liens covalents entre les microfibrilles de cellulose, les hémicelluloses et les pectines **(figure 2A)** (Keegstra et al., 1973). Vingt ans plus tard, Talbott et Ray (1992) ont proposé un modèle « multi-couches » **(figure 2B)**, dans lequel la cellulose est intégrée dans des couches d'hémicelluloses et où les pectines remplissent les interstices.

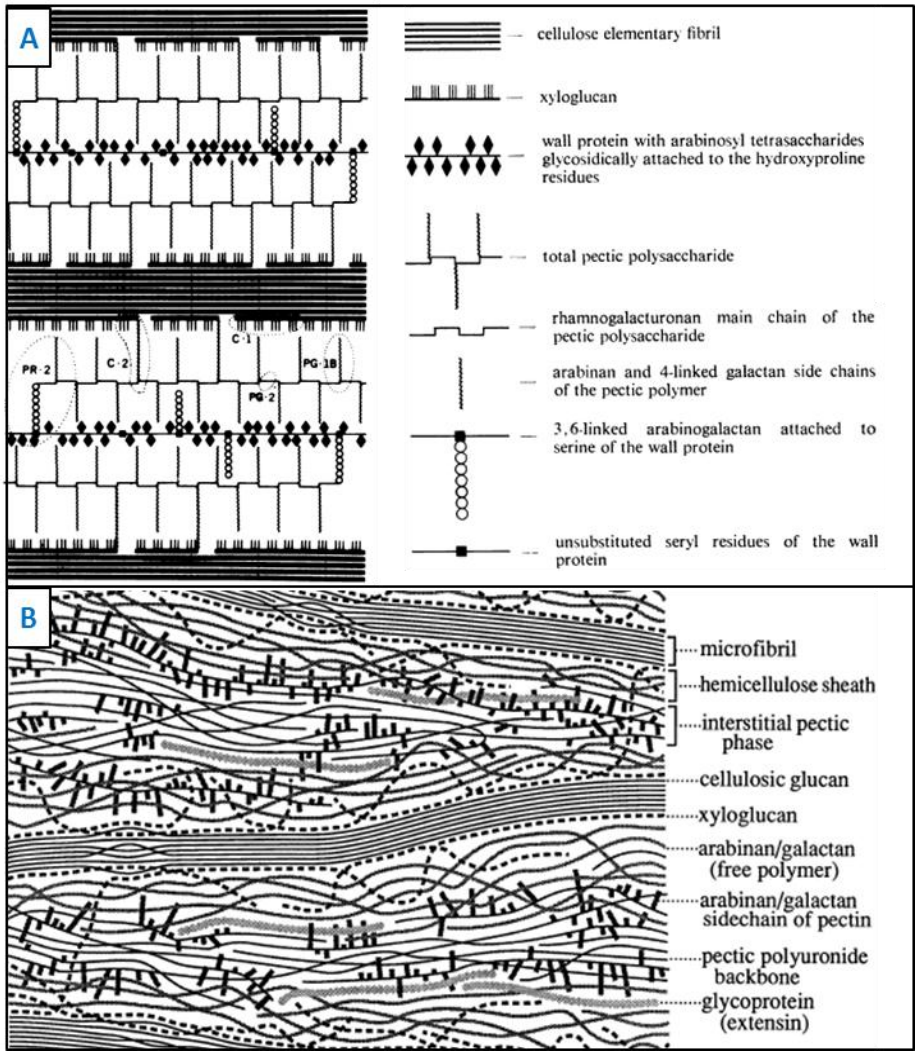

Figure 2 : Premiers modèles proposés pour l'organisation de la paroi primaire végétale.
A- Modèle « grosse structure » proposé par Keegstra et al., 1973
B- Modèle « multi-couches » proposé par Talbott et Ray, 1992

A cette même période, McCann & Roberts (1991) proposèrent un modèle nommé « réseau collant » **(figure 3A)**, en insistant sur le rôle central de l'hémicellulose xyloglucane qui, *via* des liaisons non covalentes, permet d'attacher les microfibrilles de cellulose entre elles, tout en les séparant d'un espace de 20 à 40 nm. C'est ce modèle qui a été

communément admis ces dernières années. Toutefois, celui-ci a récemment été remis en cause. En effet, Park et Cosgrove (2012), ont proposé un nouveau modèle où le xyloglucane n'aurait plus un rôle central, mais serait un adhésif sur des zones limitées là où 2 microfibrilles sont suffisamment proches pour le prendre en sandwich et former une sorte d'amalgame cellulose/xyloglucane **(figure 3B)**.

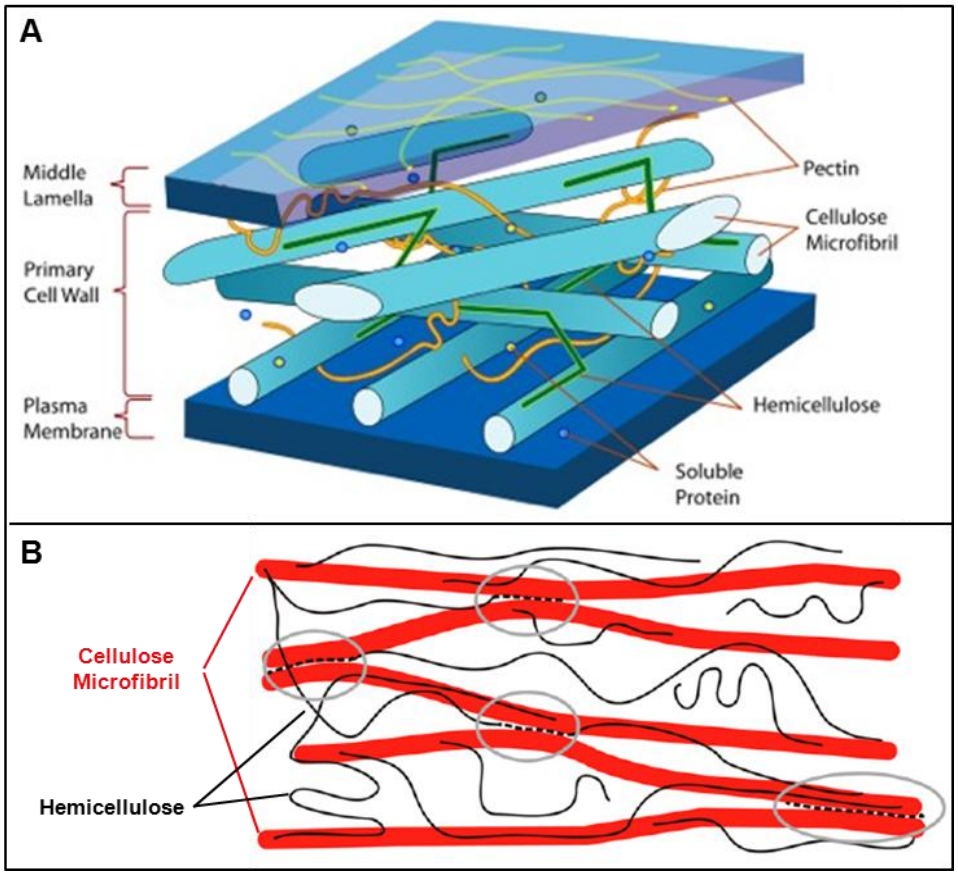

Figure 3 : Derniers modèles proposés pour la structure de la paroi primaire végétale.
A- Modèle de McCann & Roberts (1991) où le XyG joue un rôle central dans l'attachement des microfibrilles de cellulose entre elles.
B- Modèle proposé par Park et Cosgrove (2012), où le XyG relie les microfibrilles de cellulose uniquement sur des zones où les deux molécules sont suffisamment proches.

III-La cellulose

Les fibres de cellulose sont constituées de macrofibrilles, constituées à leur tour d'un assemblage de microfibrilles **(figure 4A)**. Celles-ci sont formées de chaînes parallèles de β(1,4)-D-glucose, liées par des liaisons hydrogènes inter- et intramoléculaires, et par des forces de Van der Waals.

La biosynthèse de la cellulose a lieu au niveau de la membrane plasmique (Brown, 1996), grâce à des complexes protéiques formant des hexamères appelés « rosettes » **(figure 4B)**. Une rosette, dont le diamètre est d'environ 20 à 30 nm, est constituée de 6 complexes globulaires dans lesquels se trouvent des cellulose synthases, nommées CesA (Kimura et al., 1999). Un complexe globulaire possèderait jusqu'à 6 protéines CesA, qui représentent les sous-unités catalytiques, permettant la synthèse simultanée de 36 chaînes de β(1,4)glucanes.

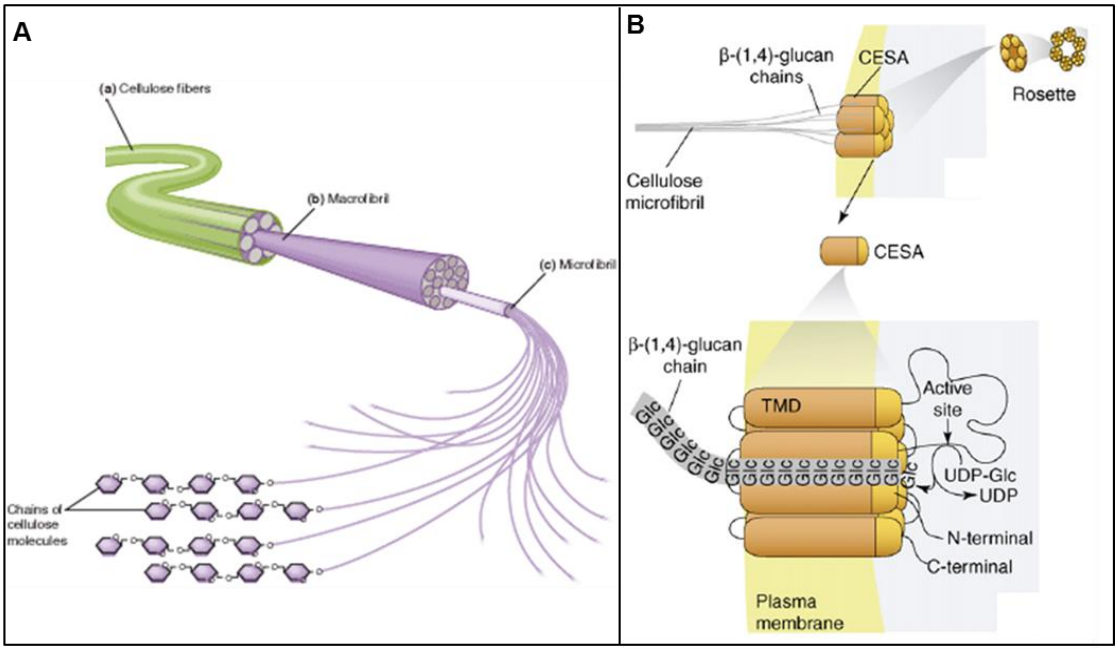

Figure 4 : Structure et synthèse de la cellulose (Lerouxel et al., 2006).
A - Représentation schématique d'une fibre de cellulose, composée de macrofibrilles, elles-mêmes constituées de microfibrilles formées à partir de chaînes glucanes. **B**- Structure d'une « rosette », constituée d'un hexamère de complexes globulaires CesA. Chaque complexe est lui-même formé par 6 sous-unités catalytiques (les protéines CesA) au sein de la membrane plasmique. (TMD, domaine transmembranaire ; UDP-Glc, uridine di-phosphate glucose).

Chez Arabidopsis, 10 gènes codant pour les protéines CesA ont été identifiés. Les protéines CesA1, -2, -3, -5, -6 et -9 sont impliquées dans la synthèse de la cellulose de la

paroi primaire, tandis que les protéines CesA4, -7 et -8 interviennent pendant la synthèse de la paroi secondaire (Endler et Persson, 2011).

Plusieurs modèles concernant le déroulement de l'initiation, de l'élongation, et de la terminaison des chaînes β(1,4)-glucane au sein des complexes CesA ont été proposés, revus par Endler et Persson (2011), et sont résumés **figure 5**. Les complexes CesA, formant une structure en rosette avec un large domaine cytosolique, utilisent l'UDP-glucose (UDP-Glc) pour la polymérisation des chaînes. Celui-ci peut être synthétisé dans le cytosol par une sucrose synthase (SuSy) ou une UDP-glucose pyrophosphorylase (UGPase). Lorsque SuSy est attachée sous forme phosphorylée à la membrane plasmique, elle fournit l'UDP-Glc pour la production de chaîne β(1,4)-glucane. Cette protéine a également été décrite comme appartenant à un large complexe soluble associé au complexe CesA (Fujii et al., 2010). Ainsi, les invertases cytosoliques fourniraient le glucose dans les cellules non photosynthétiques (Barratt et al., 2009), alors que les steryl glycosides, tels que le sisterol-β-glucoside, pourraient agir comme primers pour initier la polymérisation de la cellulose (Peng et al., 2002) et/ou pourraient créer un environnement membranaire favorable à la synthèse de la cellulose (Schrick et al., 2004).

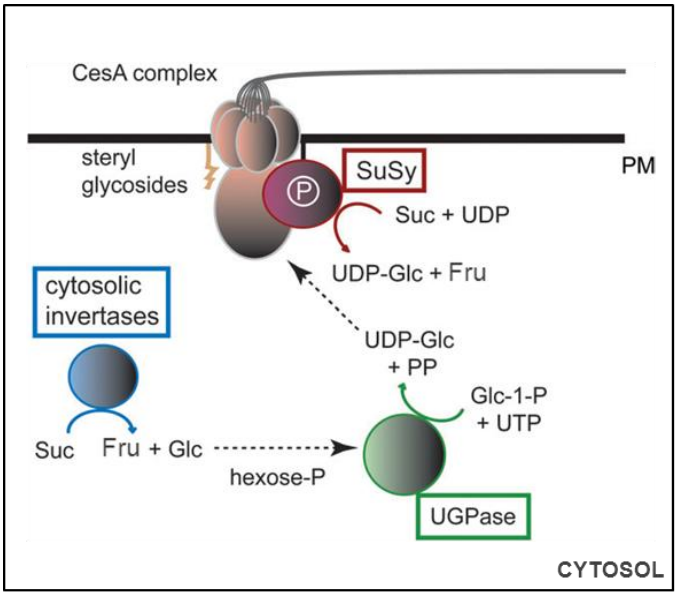

Figure 5 : Les différentes sources de glucose pour la synthèse de cellulose (Endler et Persson, 2011).
Les enzymes SuSy et UGPase, mais également des invertases, apportent l'UDP-Glc nécessaire à la synthèse de chaîne glucane *via* l'action des complexes CesA au sein de la membrane plasmique. La présence de steryl glycosides semble essentielle pour l'initiation de la synthèse des chaînes glucanes (CesA : cellulose synthase ; Fru, fructose ; Glc, glucose ; Suc, sucrose ; PM, membrane plasmique ; SuSy, sucrose synthase ; UGPase, UDP-glucose pyrophosphorylase).

IV-Les hémicelluloses

Les hémicelluloses sont définies comme des polysaccharides insolubles dans l'eau, mais que l'on peut extraire par une solution alcaline de 1M ou 4M de KOH. Elles sont également définies comme les polysaccharides pariétaux ayant une chaîne principale de résidus β-D-pyranosyl (glucose, xylose ou mannose) liés en 1,4 ; où l'oxygène *O*-4 est en orientation équatoriale **(figure 6)** (Scheller et Ulvskov, 2010).

.

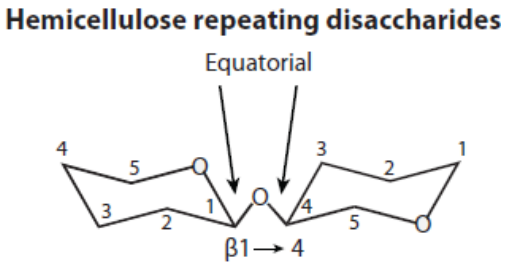

Figure 6 : Spécificité structurale et de liaison des hémicelluloses (Scheller et Ulvskov, 2010).

Chez les plantes dicotylédones vraies, les hémicelluloses sont très majoritairement représentées par le xyloglucane (XyG) qui représente 20 à 25% de la quantité de polysaccharides pariétaux, ainsi que la présence d'environ 5% de glucuronoarabinoxylanes (GAX) (Darvill et al., 1980 ; Zablackis et al., 1995 ; Scheller et Ulvskov, 2010). Chez certains ordres, on détecte également de 3 à 5% de (gluco)mannanes (Eda et al., 1985 ; Sims et al., 1997 ; Schröder et al., 2001).

Les hémicelluloses jouent un rôle structural au niveau de la paroi primaire, et par conséquent régulent l'expansion cellulaire (Scheller et Ulvskov, 2010). Ce sont également des sources de molécules signal (McDougall et Fry, 1989) et des molécules de réserves au sein de la graine (Meier et Reid, 1982 ; Reid, 1985).

IV-1- Le xyloglucane (XyG)

Le xyloglucane est constitué d'une chaîne principale de β-D-(1,4)-glucose pouvant être substituée par des chaînes latérales contenant des sucres variés, dont l'identification repose sur l'utilisation d'une endoglucanase générant des fragments oligosaccharidiques analysés ensuite par spectrométrie de masse. Une nomenclature a été mise en place par Fry et al. en 1993, afin de nommer et d'identifier facilement ces fragments oligosaccharidiques

définissant les chaînes latérales. Ainsi, une lettre a été attribuée à chaque résidu β(1,4)-D-glucose de la chaîne principale qui est lié à une chaîne latérale. Cette lettre désigne les substituants constituant la chaîne latérale, à partir du sucre terminal de cette dernière. La lettre G est utilisée dans le cas où le glucose n'est pas substitué. Cette nomenclature est présentée **figure 7**.

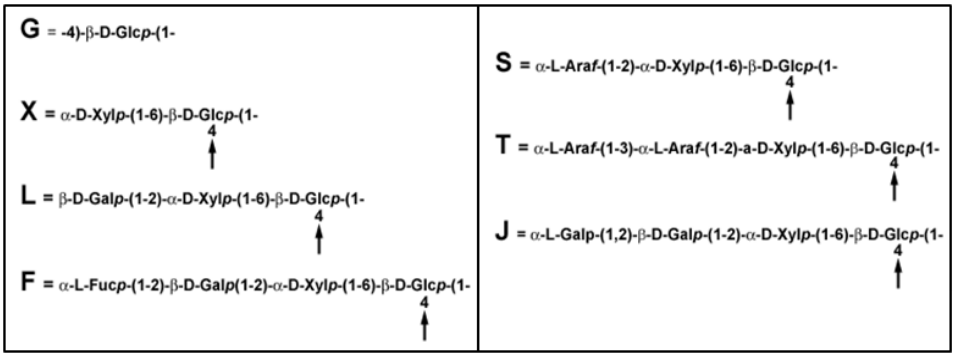

Figure 7 : Nomenclature des chaînes du xyloglucane (Fry et al., 1993).

Après plusieurs études, il a été montré qu'il existe deux grands types de xyloglucane nommés XXXG ou XXGG (Vincken et al., 1997). Le type XXXG possède 3 résidus glucose consécutifs substitués par un xylose et un dernier non substitué, tandis que le type XXGG possède 2 résidus glucose consécutifs substitués par un xylose et deux non substitués.

Le traitement à l'endoglucanase des XyG de type XXXG génère des oligosaccharides qui ont été très bien définis. Par exemple, les études effectuées sur les Rosidées telles que les suspensions cellulaires d'*Arabidopsis thaliana* (Ordre des Brassicales) (Pauly et al., 2001) ou les suspensions cellulaires de sycamore *Acer pseudoplatanus* (Ordre des Sapindales) (Hisamatsu et al., 1992) ont montré que les chaînes latérales sont principalement constituées de résidus xylose, xylose-galactose et xylose-galactose-fucose, pour donner des structures de type XXFG, XXXG et XLFG **(figure 8)**. Ces structures peuvent être partiellement acétylées sur le carbone 6 du galactose.

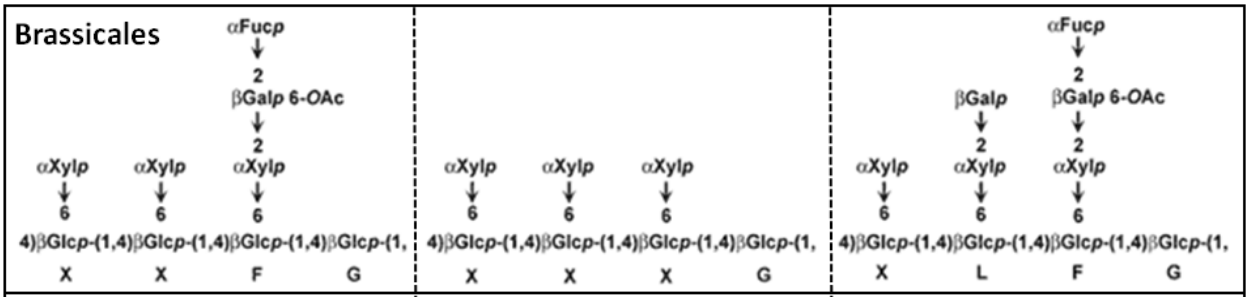

Figure 8 : Structures typiques des fragments de xyloglucane retrouvées chez les Brassicales.

(Complex Carbohydrate Research Center, http://www.ccrc.uga.edu/~mao/xyloglc/Xtext.htm#xyloglucan)

L'étude des XyG de type XXGG, s'est avérée un peu plus complexe de par la présence de groupement *O*-acétyl sur les glucoses de la chaîne principale, empêchant ainsi l'action de l'endoglucanase. Cependant, les études effectuées sur les Astéridées Solanales, telles que les suspensions cellulaires de tabac *Nicotiana tabacum* (Eda et al., 1983 ; York et al., 1996) et *Nicotiana plumbaginifolia* (Sims et al., 1996) ou bien les suspensions cellulaires de tomate *Lycopersicon esculentum* (Jia et al., 2003), puis sur d'autres représentants des Astéridées (Hoffman et al., 2005) ont montré que les chaînes latérales sont principalement constituées de résidus xylose, xylose-arabinose, xylose-galactose ou xylose-arabinose-arabinose, pour donner des structures de type XSGG, LSGG et XTGG **(figure 9)**. Ces structures peuvent être acétylées sur le carbone 5 de l'arabinose et sur le carbone 6 d'un glucose non substitué.

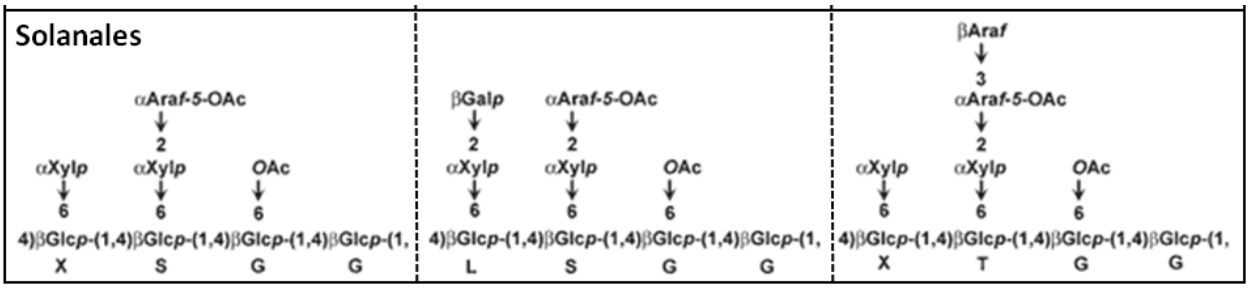

Figure 9 : Structures typiques des fragments de xyloglucane retrouvés chez les Solanales .
(Complex Carbohydrate Research Center, http://www.ccrc.uga.edu/~mao/xyloglc/Xtext.htm#xyloglucan)

Le XyG est étroitement associé aux microfibrilles de cellulose grâce à leur homologie conformationnelle, ce qui lui permet de contrôler leur relachement ou leur resserrement. Cette interaction assure le maintien de l'intégrité cellulaire durant les processus de croissance et de différenciation (Scheller et Ulvskov, 2010 ; Hayashi et Kaida, 2011).

IV-2- Les glucuronoarabinoxylanes (GAX)

Des études menées sur des suspensions cellulaires de sycamore *Acer pseudoplatanus* (Darvill et al., 1980) et des feuilles d'Arabidopsis (Zablackis et al., 1995), ont révélé que les glucuronoarabinoxylanes (GAX) sont composés d'une chaîne principale de β-D-(1,4)-xylose , substitués par des chaînes latérales neutres ou acides **(Figure 10)**.

Les chaînes neutres sont constituées de résidus arabinose et/ou xylose, tandis que les chaînes acides sont terminées par des résidus d'acide glucuronique ou de 4-*O*-méthyl acide

glucuronique. Les résidus xylose de la chaîne principale peuvent être *O*-acétylés et les résidus arabinose des chaînes latérales peuvent être estérifiés par de l'acide férulique.

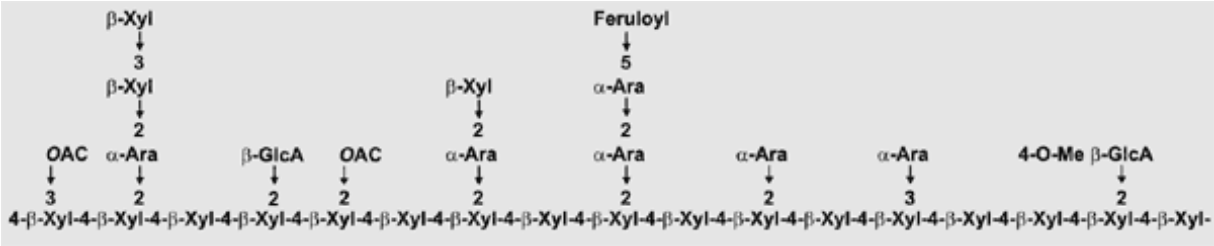

Figure 10 : Structure des glucuronoarabinoxylanes.
(Complex Carbohydrate Research Center, http://www.ccrc.uga.edu/~mao/wallmab/Hemicel/hemi.htm)

IV-3-Les polysaccharides mannanes

Les mannanes regroupent différents types de polysaccharides : les mannanes, polymères de résidus mannose liés en β(1,4), et les glucomannannes qui contiennent une chaîne principale de résidus glucose et mannose liés en β(1,4). Les résidus mannose ou glucomannane peuvent être substitués avec un résidu galactose lié en α(1,6), on les nomme alors galactomannanes ou galactoglucomannanes. Les mannanes et glucomananes sont parfois acétylés (Scheller et Ulskov, 2010).

Chez *Arabidopsis thaliana*, il n'a pas été détecté de mannanes dans la paroi primaire (Zablackis et al ; 1995), et il ne semble pas qu'il y ait d'étude montrant la présence de ce type de polysaccharide dans la paroi primaire des Rosidées. Cependant, chez les Astéridées telles que le tabac *Nicotiana tabacum* (Eda et al., 1985), *Nicotiana plumbaginifolia* (Sims et al., 1997) ou le kiwi *Actinidia deliciosa* (Schröder et al., 2001), on trouve des galactoglucomannanes constitués d'une chaîne principale de résidus D-glucopyranose et D-mannopyranose liés en β(1,4), avec une majorité de mannoses substitués en *O*-6 par un ou deux résidus β-D-galactopyrannosyl **(figure 11)**.

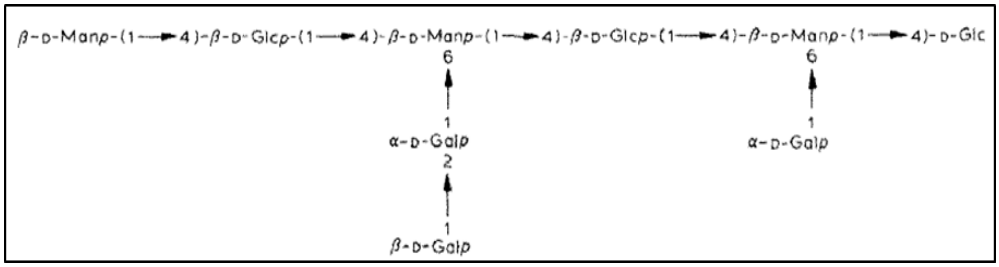

Figure 11 : Galactoglucomannanes présents chez *Nicotiana tabacum* (Eda et al., 1985).

Chez *Nicotiana tabacum*, la présence d'arabinoglucuromannanes (Mori et Kato, 1981) constitués d'une chaîne principale d'acide D-glucopyranosyluronique et de D-mannopyranose, substitué en *O*-3 par un résidu α-L-arabinofuranose a également été mis en évidence **(figure 12).**

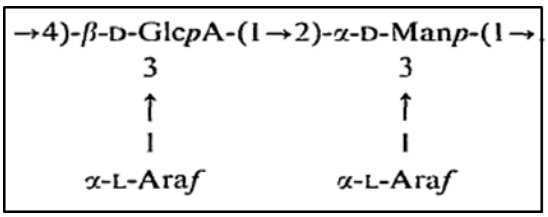

Figure 12 : Arabinoglucuronomannanes présents chez *Nicotiana tabacum* (Mori et Kato, 1981) .

V- Les pectines

Les pectines sont définies comme des polysaccharides facilement extractibles avec un acide à chaud ou des chélateurs, et contenant une grande proportion de résidus d'acide galacturonique. Chez les plantes « Core Eudicots », les pectines constituant la paroi primaire sont représentées par les homogalacturonanes, les homogalacturonanes substitués : le xylogalacturonne et le rhamnogalacturonane-II, et le rhamnogalacturonane-I.

Les pectines sont structurellement complexes et très hétérogènes, elles jouent un rôle clef dans le contrôle de l'architecture pariétale (porosité, adhésion,…). Elles jouent également un rôle dans la défense des plantes, car elles servent de cibles primaires lors d'attaques microbiennes et peuvent servir d'éliciteurs (Cosgrove, 2005 ; Caffall et Mohnen, 2009).

V-1-Les homogalacturonanes

Les homogalacturonanes (HG) consistent en une chaîne linéaire de résidus d'acide galacturonique liés en α(1,4), avec un degré de polymérisation typique de 100/150, pouvant être méthylée et/ou acétylée **(figure 13)** (Caffall et Mohnen, 2009 ; Wolf et al., 2009).

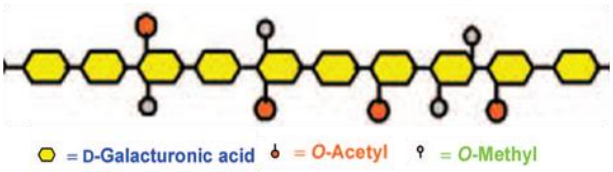

Figure 13 : Structure des homogalacturonanes (Scheller et al., 2007)

Les HG semblent représenter la chaîne principale des pectines (Coenen et al., 2007), même s'il a également été suggéré que les HG seraient une chaîne latérale du rhamnogalacturonane-I (Vincken et al., 2003). Les blocs d'HG non estérifiés peuvent être liés par des ponts calciques **(figure 14)**, pour former des chaînes d'HG fortement compactées, appelé modèle en « boîte à œufs », participant ainsi à la rigidité de la paroi. Le degré de méthyl estérification des HG influe directement sur leur affinité pour les ions calcium, et donc également sur la formation d'un gel pectique essentiel pour l'adhésion (Jarvis, 1984 ; Orfila et al., 2001 ; Caffall et Mohnen, 2009).

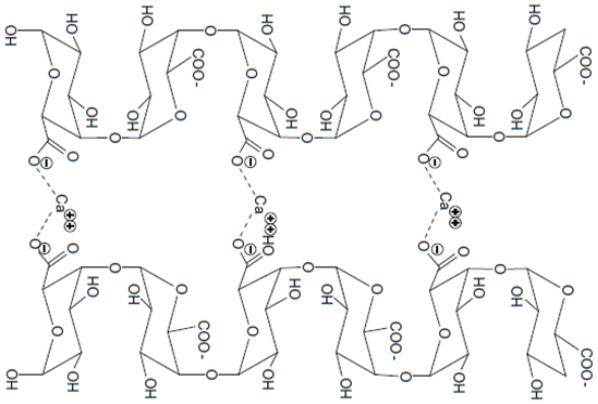

Figure 14: Association des chaînes HG *via* des ponts calciques : modèle en « boîtes à œufs ».
(Caffall et Mohnen, 2009)

V-2- Les xylogalacturonanes

Les xylogalacturonanes (XGA) sont constitués d'une chaîne de résidus d'acide galacturonique liés en α(1,4), pouvant être acétylés et méthylés, et substitués en *O*-3 avec un β-D-xylose terminal **(figure 15)** ou de courtes chaînes de xylanes.

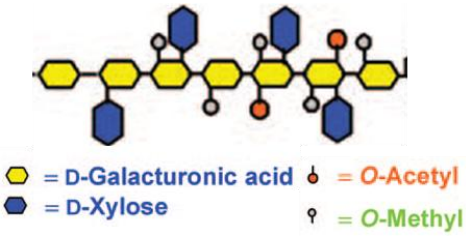

Figure 15 : Structure des xylogalacturonanes (Scheller et al., 2007)

Les courtes chaînes de xylanes peuvent varier dans leur type de liaison. Chez les Rosidées, les chaînes de xylanes ont des liaisons β(1,4) pour la pomme (Oechslin et al., 2003), β(1,4) et β(1,2) pour le soja (Nakamura et al., 2002), β(1,2) et β(1,3) pour le pois (LeGoff et al., 2001). Chez les Astéridées, les liaisons sont de type β(1,4) comme pour la pomme de terre (Zandleven et al., 2006).

V-3-Le rhamnogalacturonane-II

Le rhamnogalacturonane-II (RG-II) **(figure 16)** est le polysaccharide pectique le plus complexe d'un point de vue structural, puisqu'il est constitué d'au moins une douzaine de monosaccharides différents et de plus d'une vingtaine de liaisons (Ridley et al., 2001).

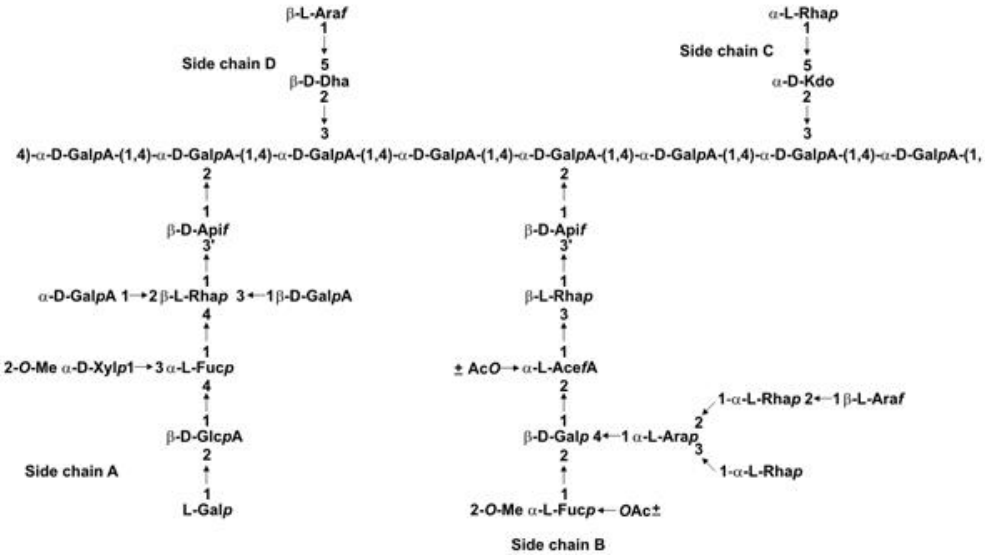

Figure 16: Structure du Rhamnogalacturonane-II.
(Complex Carbohydrate Research Center, http://www.ccrc.uga.edu/~mao/rg2/intro.htm#rhamnogalacturonan II)

Sa chaîne principale est constituée d'au moins 8 résidus α-D-(1,4)-GalA sur lesquels sont substituées 4 chaînes latérales, notées A, B, C et D. Les chaînes A et B sont liées en C-2 du résidu acide galacturonique (GalA) de la chaîne principale, tandis que les chaînes C et D sont substituées en C-3 (O'Neill et al., 2004). Les chaînes A et B sont constituées de 8 à 10 monosaccharides et attachées *via* un résidu β-D-apiose en *O*-2. La chaîne B possède également un résidu D-galactosyl (D-Gal). Les chaînes C et D sont des chaînes courtes constituées par un disaccharide. La chaîne C est formée par un résidu rhamnose et un résidu acide 2-céto-3-déoxy-D-manno-octulosonique (Kdo), tandis que la chaîne D est constituée d'un résidu acide 2-céto-3-déoxy-D-lyxo-heptulosarique (Dha) et d'un résidu arabinose (O'Neill et al., 2004).

Le RG-II joue un rôle essentiel dans la régulation de la porosité et des propriétés mécaniques de la paroi primaire (Ishii et al., 2001), car il existe sous forme d'un dimère lié par des di-esters de borate (Matoh et al., 1993; Kobayashi et al., 1996; Ishii et Matsunaga, 1996; O'Neill et al., 1996). Chez Arabidopsis, des mutations portant sur la synthèse ou la

dimérisation du RG-II entrainent des altérations majeures de la croissance et du développement des plantes (O'Neill et al., 2001; Reuhs et al., 2004, Voxeur et al., 2011).

V-4- Le rhamnogalacturonane-I

Le rhamnogalacturonane-I (RG-I) représente 20 à 35% des pectines, et il est le plus variable d'un point de vue structural, dû à la variabilité des chaînes latérales. Sa chaîne principale est constituée du disaccharide [-4-α-D-GalA-(1,2)-α-L-Rha-(1-)]$_n$. De 20 à 80% des résidus rhamnose sont substitués par des chaînes latérales dont la composition et la longueur varient en fonction de l'espèce et du stade de développement (Albersheim, 1996). Ces chaînes latérales sont majoritairement constituées de galactanes, d'arabinanes et d'arabinogalactanes (McNeil et al., 1982, Vincken et al., 2003; Mohnen, 2008).

Les galactanes sont principalement des chaînes linéaires de β(1,4)-D-galactopyranose (Gal*p*) **(Figure 17B et 17C)**. Les arabinanes sont des chaînes de α(1,5)-L-arabinofuranose (Ara*f*) linéaires ou substituées en *O*-3 et parfois en *O*-2 **(Figure 17A, 17D et 17E)**. Les chaînes arabinanes ou galactanes sont souvent substituées par des esters phénoliques terminaux permettant la liaison avec d'autres polymères (Ralet et al., 2005).

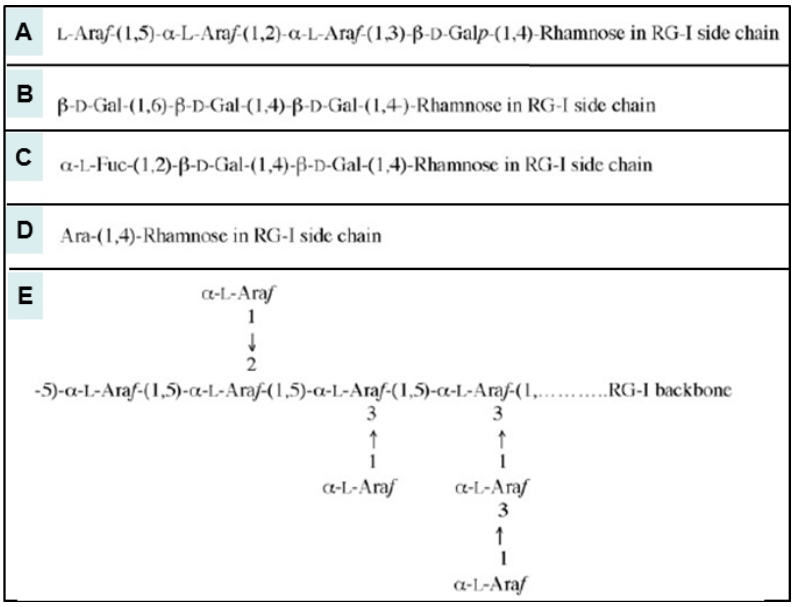

Figure 17 : Structures des chaînes arabinanes et galactanes rencontrées dans le RG-I (Adapté de Mohnen, 2008)
B,C : exemples de chaînes galactanes, A,D,E : exemples de chaînes arabinanes.

Plusieurs types de chaînes arabinogalactanes ont été identifiés. Les arabinogalactanes de type I **(Figure 18F et 18G)** consistent en une chaîne de β(1,4) galactanes avec des résidus arabinose branchés en *O*-3 ou d'autres sucres tels que le fucose et l'acide glucuronique (Ridley et al., 2001; Nakamura et al., 2002; Øbro et al., 2004).

Les arabinogalactanes de type II **(Figure 18H)** consistent en une chaîne de β(1,3) galactanes substituée par de courtes chaînes β(1,6) galactanes, elles-mêmes branchées par des résidus arabinose, rhamnose, et acide glucuronique. Ce type de chaîne est typique de la composition glycannique des arabinogalactanes protéines (AGPs), et le débat reste encore ouvert pour savoir si les chaînes identifiées dans les fractions enrichies en RG-I sont effectivement liées à ce polysaccharide ou bien si elles proviennent d'une co-extraction des AGPs (Mohnen, 2008; Verhoef et al., 2009).

Un autre type de chaîne arabinogalactane a été identifié chez les Rosidées telles que la pomme (Schols et al., 1990) ou le soja (Huisman et al., 2001). Elle consiste en un résidu galactose ou une courte chaîne de galactane liée en β(1,3), branchée à une chaîne d'arabinanes liés en α(1,5) et substitués en -2 ou en -3 **(figure 18I)**.

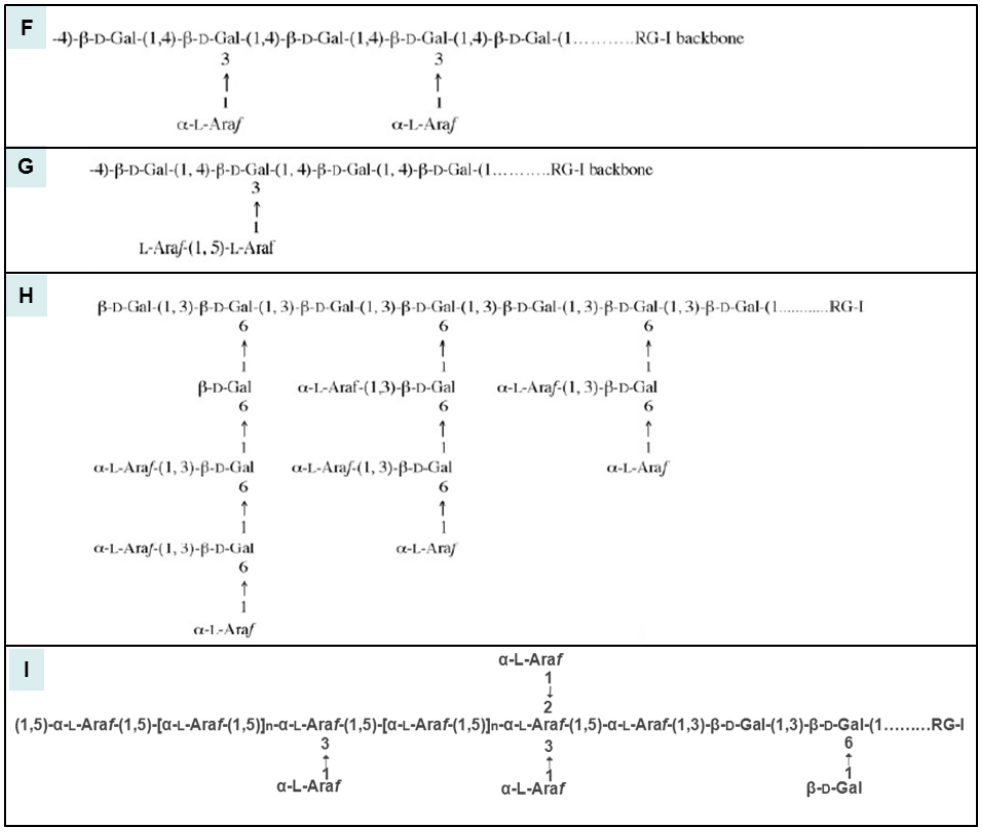

Figure 18 : Structures des chaînes arabinogalactanes rencontrées dans le RG-I (Adapté de Mohnen, 2008)
F,G : exemples de chaînes arabinogalactane de type I ; H : exemple de chaîne arabinogalactane de type II ; I : autre type de chaîne arabinogalactane.

Les chaînes latérales du RG-I influencent les propriétés mécaniques de la paroi car elles diminuent la capacité des molécules pectiques à créer un réseau pour former un gel stable (Hwang et Kokini, 1991). Les chaînes latérales jouent également un rôle important dans l'adhésion cellulaire (Orfila et al., 2001) et dans l'ouverture et la fermeture des stomates, grâce à l'action des chaînes arabinanes qui maintiendraient la flexibilité en prévenant l'association des homogalacturonanes (Jones et al., 2003).

De plus, il a été montré que la structure et la distribution tissulaire des chaînes riches en arabinanes ou galactanes sont régulées durant la croissance cellulaire et le développement chez de nombreuses espèces (voir les revues Willats et al., 2001 ; Scheller et al., 2007 ; Harholt et al., 2010).

PARTIE B : LES ENZYMES IMPLIQUEES DANS LA SYNTHESE DU XYLOGLUCANE ET DU RHAMNOGALACTURONANE-I

I- Généralités

Chez les plantes, environ 10% de leurs gènes sont dédiés à la biosynthèse et au remodelage de la paroi végétale (Arabidopsis genome initiative, 2000; Tuskan et al., 2006). Comme décrit précédemment, les polysaccharides pariétaux non cellulosiques sont des structures complexes constituées d'au moins 14 monosaccharides différents et d'une grande variété de liaisons glycosidiques (Scheible et Pauly, 2004). Afin d'assembler ces différents polysaccharides non cellulosiques, dont la synthèse a lieu au sein de l'appareil de Golgi, l'action de différents types d'enzymes et de transporteurs est nécessaire.

Dans un premier temps, les monosaccharides sont générés majoritairement dans le cytosol sous forme de nucléotide-sucres, puis ils sont amenés dans la lumière des saccules golgiennes grâce à l'action de transporteurs de nucléotides-sucres, avant d'être pris en charge par des glycosyltransférases golgiennes (dont le site catalytique est luminal) spécifiques d'un nucléotide-sucre et d'un type de liaison, afin de les assembler pour générer les différents types de polysaccharides.

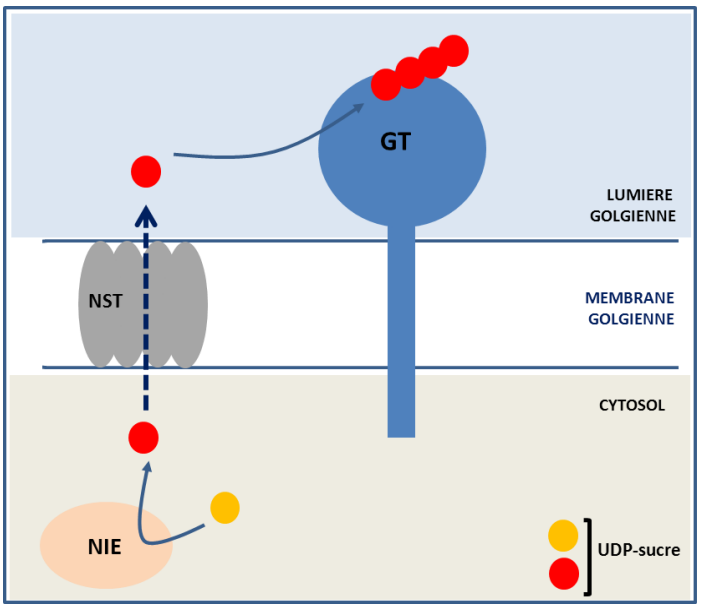

Figure 19 : Schéma représentant la prise en charge des UDP-sucres au cours de la synthèse golgienne des polysaccharides complexes .
Les monosaccharides sont générés majoritairement dans le cytosol sous forme de nucléotide-sucres par des enzymes d'interconversion d'UDP-sucre (NIE), puis ils sont amenés dans la lumière des saccules golgiennes *via* l'action de transporteurs de nucléotides-sucres (NST), avant d'être pris en charge par des glycosyltransférases golgiennes (GT) dont le site catalytique est luminal, afin de les assembler pour générer des polysaccharides.

II- Les enzymes d'interconversion des nucléotides-sucres

Les différents monosaccharides sont générés sous forme de nucléotides-sucre par une conversion séquentielle de l'UDP-glucose, grâce à l'action d'enzymes d'interconversion comprenant des épimérases, des décarboxylases, des déshydratases, des réductases et des mutases **(Figure 20)**.

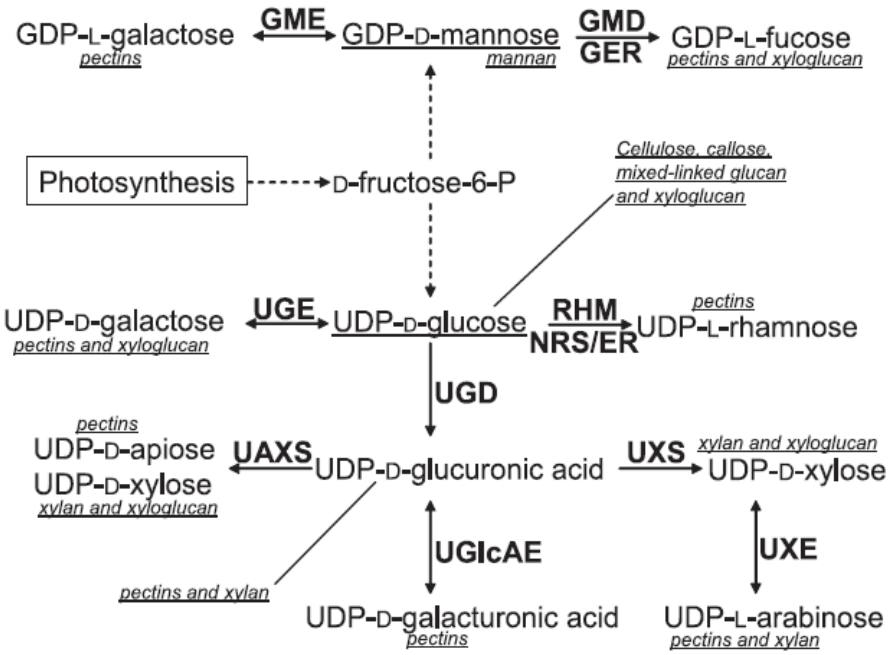

Figure 20 : Interconversion des UDP-sucres *via* l'action des différentes enzymes d'interconversion (Yin et al., 2011).
(GER : GDP-4-keto-6-désoxy-D-mannose-3,5-épimérase-4-réductase, GMD : GDP-D-mannose-4,6-déhydratase, GME : GDP-D-mannose-3,5-épimérase, RHM : UDP-L-rhamnose synthase, NRS/ER : nucléotide-rhamnose synthase/épimérase-réductase, UGE : UDP-glucose-4-épimérase, UGlcAE : GDP-4-céto-6-désoxy-D-mannose-3,5-épimérase-4-réductase, UAXS : UDP-D-apiose/UDP-D-xylose synthase, UXE : UDP-xylose-4-épimérase, UXS : UDP-D-xylose synthase)

II-1- La production de l'UDP- D-xylose

Harper et Bar-Peled (2002) ont identifié cinq UDP-xylose synthases (UXS) chez *Arabidopsis thaliana*, par comparaison avec celle identifiée chez *Cryptococcus neoformans*, qu'ils ont nommées AtUXS. D'après les analyses *in silico*, AtUXS3 et -5 seraient solubles, tandis que AtUXS1, -2 et -4 seraient transmembranaires de type II.

Leur activité UDP-acide glucuronique décarboxylase, pour convertir l'UDP-GlcA en UDP-Xyl, a été démontrée chez *Escherichia coli* par expression hétérologue. En 2005, Pattathil et al., ont démontré qu'AtUXS2 était effectivement une protéine transmembranaire de type II de localisation golgienne et qu'AtUXS3 était cytosolique.

II-2- La production de l'UDP- D-galactose

La première UDP-glucose-4-épimérase (UGE), qui convertit l'UDP-Glc en UDP-Gal, a été identifiée chez *Arabidopsis thaliana*, par comparaison de séquences avec les UDP-glucose épimérases identifiées chez les bactéries, le rat et les champignons (Dörmann et Benning, 1996). Son activité épimérase a été démontrée par expression hétérologue chez *Saccharomyces cerevisiae* et *Escherichia coli*.

Par la suite, un groupe de 5 isoformes a été défini par homologie de la séquence d'AtUGE1 (Seifert, 2004) et les caractéristiques de chacune ont été étudiées (Barber et al., 2006). Il est ressorti des différences au niveau de leurs propriétés enzymatiques, de la régulation de leur transcrit et de leur localisation subcellulaire. AtUGE2, -4, et -5 auraient plutôt tendance à convertir l'UDP-Glc en UDP-Gal, tandis qu'AtUGE1 et -3 feraient la réaction inverse. La localisation subcellulaire d'AtUGE1, -2 et -4 a montré une localisation uniquement cytosolique, excepté pour AtUGE4 qui semble pouvoir être aussi associée aux membranes golgiennes.

Rösti et al. (2007) ont montré qu'AtUGE4 influence la croissance racinaire et la quantité de galactose au sein de la paroi, en agissant de façon synergique avec AtUGE2, et de façon moindre avec AtUGE1 et -5. Cependant, AtUGE4 influence à elle seule la galactosylation du XyG au niveau racinaire. AtUGE3, avec l'aide d'AtUGE2, est spécialisée dans le développement du pollen. Enfin, AtUGE5 pourrait agir en situation de stress, car son niveau de transcription varie en fonction de la température et du niveau d'acide abscissique et des teneurs en sel. De plus, les auteurs ont émis l'hypothèse qu'AtUGE5 pourrait apporter de l'UDP-Gal pour la synthèse de galactinol, qui serait un osmoprotectant pour la tolérance à la sécheresse.

II-3- Production du GDP-L- fucose

La synthèse du GDP-L-fucose (ou 6-désoxy-L-galactose) à partir du GDP-D-mannose nécessite 3 types de réactions séquentielles : une 4,6-déshydratation, une 3,5-épimérisation et une 4-réduction.

Bonin et al. (1997) ont isolé chez Arabidopsis deux séquences d'ADN_C d'intérêt, en utilisant un EST (*Expressed Sequence Tag*) ayant une forte similarité de séquence avec des séquences codant des GDP-D-mannose-4,6-déshydratases bactériennes. Ces gènes ont été nommés *GMD1* and *GMD2* (guanosine-diphospho-D-mannose-4,6-déshydratase). Il s'est

avéré que *GMD2* était en fait un ADNc dérivé du gène *MUR1*. Le mutant chimique Arabidopsis *mur1* est un mutant nain, qui est justement déficient en GDP-L-fucose (Reiter et al., 1993). L'activité GDP-D-mannose-4,6-déshydratase de la protéine soluble et cytosolique AtGMD2/MUR1 par expression hétérologue dans *E.coli* et par complémentation du mutant *mur1* a ensuite été démontrée.

La protéine AtGMD2/MUR1 est exprimée partout dans la plante, alors que la protéine AtGMD1 est exprimée principalement dans la pointe de la racine. L'expression différentielle des deux isoformes AtGMD1 et -2 montre que la synthèse du GDP-L-fucose est contrôlée de façon cellule spécifique (Bonin et al., 2003).

Ce même laboratoire a également identifié chez Arabidopsis l'enzyme responsable des 2 autres réactions, une 3,5-épimérase-4-réductase, nommée AtGER1/FX, ainsi que la présence d'un homologue potentiel d'AtGER1/FX, nommé AtGER2. Ainsi, ils ont pu convertir du GDP-mannose en GDP-fucose *in vitro* en coexprimant AtGER1/FX et AtGMD2/MUR1 dans *E.coli*, démontrant ainsi leur activité (Bonin et Reiter, 2000).

II-4- Production de l'UDP-D-acide galacturonique

Une UDP-D-acide glucuronique-4-épimérase (UGlcAE, ou GAE pour *Glucuronic Acid Epimerase*) catalyse l'épimérisation de l'UDP-α-D-acide glucuronique (UDP-GlcA) en l'UDP-α-D-acide galacturonique (UDP-GalA). Par comparaison de séquence avec une UDP-D-acide glucuronique-4-épimérase bactérienne, le gène codant pour AtUGlcAE1/GAE4 a été identifié chez Arabidopsis et l'activité de l'enzyme a été démontrée par expression hétérologue de la protéine (délétée de son domaine transmembranaire) chez *E.coli* (Gu et Bar-Peled, 2004). Les auteurs ont montré que l'activité d'AtUGlcAE1 n'était pas inhibée par l'UDP-Glc, l'UDP-Gal, mais qu'elle était inhibée par l'UDP-Xyl et l'UDP-Ara, suggérant un rôle de ces nucléotides-sucres dans la régulation de la synthèse des pectines.

Le gène *AtUGlcAE1* fait partie d'une famille de gènes déshydrogénases/réductases composée de 6 isoformes, dont tous les membres codent pour des protéines putatives transmembranaires de type II. En 2004, Usadel et al. (a) ont identifié, cloné et caractérisé la protéine AtUGlcAE2/GAE6 chez Arabidopsis, et la même année la protéine AtUGlcAE3/GAE1 a été caractérisée par Mølhøj et Reiter. L'activité de ces deux protéines a été démontrée *in vitro* chez *Pichia pastoris*.

L'analyse de l'expression des différentes isoformes montre qu'AtUGlcAE3/GAE1 est fortement exprimée dans tous les tissus (Mølhøj et Reiter, 2004). Toutes les isoformes sont exprimées au cours du développement du pollen et leur expression au niveau racinaire est différentielle. En effet, AtUGlcAE3/GAE1 et AtGAE2 sont exprimées dans toute la racine, alors que AtGAE3 et AtUGlcAE2/GAE6 sont exprimées uniquement dans la zone pilifère et AtUGlcAE1/GAE4 à la pointe racinaire (Usadel et al., 2004a).

II-5- Production de l'UDP-L- rhamnose

La première UDP-L-rhamnose synthase (RHM) a été identifiée chez Arabidopsis grâce au mutant *mum4* (*mucilage modified 4*) qui a une quantité réduite de rhamnose et d'acide galacturonique dans le mucilage des graines (Western et al., 2004 ; Usadel et al., 2004b). La protéine AtMUM4 est exprimée de façon ubiquitaire et code certainement pour une UDP-L-rhamnose synthase requise pour la synthèse du RG-I, puisque c'est le composant majoritaire du mucilage des graines d'Arabidopsis. *MUM4* est un membre d'une famille de gènes décrite *in silico* par Reiter et Vanzin en 2001, et constituée de 3 membres *AtRHM1*, *AtRHM2/MUM4* et *AtRHM3*.

La deuxième UDP-L-rhamnose synthase a été identifiée *via* l'étude d'un mutant suppresseur, le mutant *rol1* (*repressor of lrx1*) (Diet et al., 2006). A partir d'un mutant chimique *lrx1* (*LRR-extensin1*) présentant des poils racinaires morphologiquement aberrants, un *screening* a été effectué pour identifier les gènes liés à l'expression de *lrx1* au cours du développement, et le mutant *rol1* a été identifié. *ROL1* est allélique à *AtRHM1*, et les mutations sur le gène *AtRHM1/ROL1* modifient la structure du RG-I et RG-II. Il a été montré que AtRHM1 est une protéine cytosolique fortement exprimée dans les racines et les cotylédons de plantules (Wang et al., 2009), et que sa surexpression chez Arabidopsis entraîne une augmentation de 40% de rhamnose dans les feuilles, et que ce surplus est utilisé pour la synthèse de RG-I et/ou RG-II.

Oka et al. (2007) ont démontré que les 3 isoformes avaient une activité cytoplasmique UDP-D-glucose 4,6-déshydratase, UDP-4-céto-6-désoxy-D-glucose-3,5-épimérase et UDP-4-céto-L-rhamnose 4-céto-réductase lorsqu'elles étaient exprimées chez *Saccharomyces cerevisiae*, pour former de l'UDP-L-rhamnose à partir de l'UDP-glucose. Lors de cette étude, il a été montré que la partie N-terminale de AtRHM2/MUM4 ayant l'activité

UDP-D-glucose-4,6-déshydratase était fortement inhibée par l'UDP-L-rhamnose, UDP-D-xylose et l'UDP, mais pas par les autres nucléotides-sucres.

II-6- Production de l'UDP-L-arabinose

II-6-1- Les UDP-D-xylose 4-épimerases

En 1999, Burget et Reiter ont étudié chez Arabidopsis le mutant chimique *mur4*, qui présente une réduction de 50% du monosaccharide L-arabinose dans la plupart des organes. De façon plus fine, une réduction de moitié des teneurs en L-arabinose dans les fractions pectines, xylanes et xyloglucane est observée chez le mutant *mur4*, ainsi qu'une plus grande mobilité électrophorétique des arabinogalactanes protéines traduisant une modification de charge et/ou de masse. Le mutant *mur4* présente une déficience dans la conversion de l'UDP-D-xylose en UDP-L-arabinose. La protéine AtMUR4 (Burget et al., 2003) a ensuite été caractérisée et son activité UDP-D-xylose 4-épimerase démontrée après expression chez *Pichia pastoris*. AtMUR4 est une protéine transmembranaire de type II, localisée au niveau de l'appareil de Golgi, ayant ainsi son activité épimérase dans la lumière des saccules golgiennes. Trois autres isoformes d'AtMUR4 existent chez Arabidopsis.

En 2004, Seifert a normalisé leur dénomination en les appelant UXE (pour UDP-D-xylose 4-épimerase), pour donner AtUXE1/MUR4, AtUXE2, -3 et -4. Le gène *AtUXE1/MUR4* est allélique au gène *AtHSR8*, isolé chez le mutant *high sugar response 8* (Li et al., 2007) et le gène *AtUXE3* est allélique au gène *AtMEE25*, identifié lors de l'identification de gènes requis pour le développement gamétophyte femelle (Pagnussat et al., 2004).

II-6-2- Les UDP-arabinose mutases

Les épimérases précitées génèrent de l'UDP-L-arabinopyranose, or *in planta* les pectines contiennent du L-arabinofuranose transféré par des arabinosyltransférases. L'action intermédiaire d'UDP-arabinose mutases (UAM) convertissant l'UDP-arabinopyranose en UDP-arabinofuranose est donc nécessaire.

La première UDP-arabinose mutase a été caractérisée chez le riz (Konishi et al., 2007b), et il a été montré qu'elle partageait plus de 80% d'identité avec une famille de 5 protéines chez Arabidopsis nommées RGPs, pour *Reversibly Glycosylated Polypeptides*, capables de s'autoglycosyler.

Une première étude de la localisation de ces protéines exprimées de façon transitoire chez *N.tabacum* a montré que AtRGP1 à 4 étaient des protéines solubles délivrées au plasmodesme *via* l'appareil de Golgi (Sagi et al., 2005). Cependant, lorsque ces protéines ont été exprimées chez Arabidopsis soit dans le tube pollinique (Drakakaki et al., 2006) ou dans la plante entière (Rautengarten et al., 2011), il a été montré que AtRGP1, -2 et -5 étaient des protéines cytosoliques, avec AtRGP1 et -2 également associées aux vésicules golgiennes.

Les différentes études d'activité tendent à montrer que AtRGP1, -2 et -3, qui forment les RGPs de classe 1, ont une activité UDP-arabinose mutase ; contrairement à AtRGP4 et -5 qui forment les RGPs de classe 2 (Delgado et al., 1998 ; Konishi et al., 2007a ; Rautengarten et al., 2011). Rautengarten et al., (2011) ont montré que les transcrits d'AtRGP1, -2 et -5 étaient détectés dans tous les tissus, avec une plus forte présence au niveau des fleurs, des graines et des siliques en développement. Les transcrits d'AtRGP3 et -4 sont quasiment uniquement retrouvés dans les siliques.

III- Les transporteurs des nucléotides-sucre

Une fois les différents nucléotides-sucre synthétisés dans le cytosol, ils vont être transportés jusque dans la lumière des saccules golgiennes *via* des transporteurs de nucléotides-sucre (NST), qui sont des protéines golgiennes ayant 6 à 10 domaines transmembranaires (Reyes et Orellana, 2008). Peu de NST pouvant participer à la synthèse des polysaccharides complexes, et plus particulièrement du XyG ou du RG-I, ont été identifiés chez Arabidopsis. Actuellement, seuls des NSTs pouvant transporter l'UDP-glucose et /ou l'UDP-galactose ont été identifiés et leur activité démontrée : AtUTr1 (Norambuena et al., 2002) et AtUTr7 (Handford et al., 2012) transportent l'UDP-glucose et l'UDP-galactose ; tandis qu'AtUTr2 (Norambuena et al., 2005), UDP-GalT1 et -2 (Bakker et al., 2005) et AtNST-KT1 (Rollwitz et al., 2006) transportent uniquement l'UDP-galactose.

L'identité de NSTs transportant l'UDP-xylose ou le GDP-fucose nécessaires à la synthèse du xyloglucane, ou bien l'UDP-acide galacturonique, l'UDP-rhamnose et l'UDP-arabinose nécessaires à la synthèse du RG-I n'est pas encore connue. Cependant, tous ces transporteurs ne sont peut-être pas nécessaires, car plusieurs enzymes d'interconversion de nucléotides-sucre sont des protéines transmembranaires de type II également présentes dans les saccules golgiennes, avec une activité luminale.

Par exemple, le transport d'UDP-acide glucuronique au sein des saccules golgiennes pourrait fournir un substrat pour la synthèse d'UDP-acide galacturonique, d'UDP-xylose et d'UDP-arabinose au sein des saccules. En effet, toutes les UDP-acide glucuronique 4-épimérases (AtGAE) identifiées sont de type II, donc semblent générer de l'UDP-acide galacturonique uniquement au sein des saccules golgiennes. Certaines UDP-xylose synthases sont également de type II (AtUXS1, -2 et -4) et peuvent générer de l'UDP-xylose à partir de l'UDP-acide glucuronique. Enfin, l'UDP-arabinose peut être généré à partir de l'UDP-xylose, grâce à une UDP-xylose 4-épimérase dont une, nommée AtUXE1/MUR4 est de type II **(Figure 21)**.

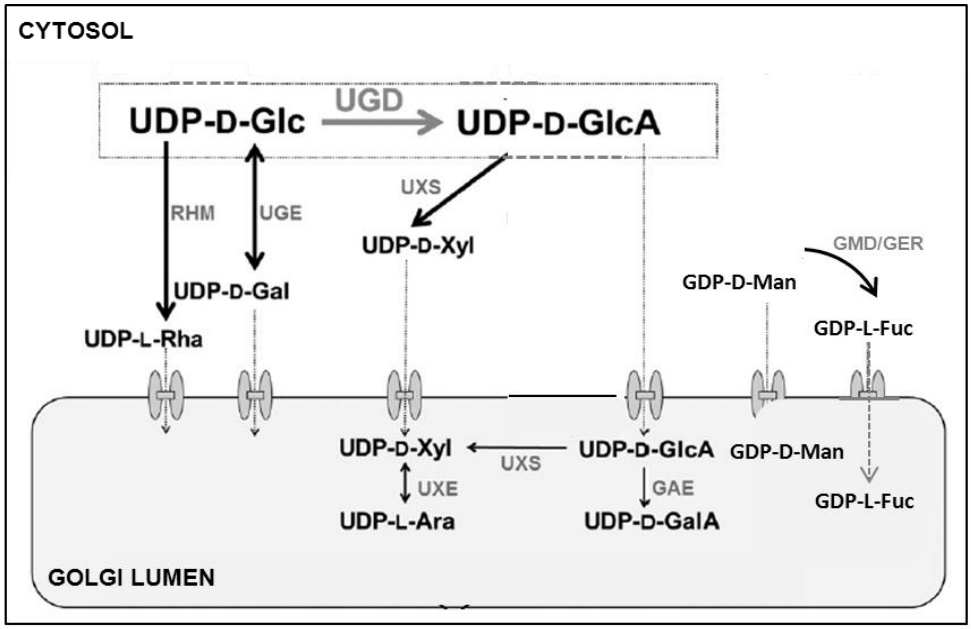

Figure 21 : Vue générale des transporteurs d'UDP-sucres pouvant exister (adapté de Reboul et al., 2011)
GAE : UDP-D-acide glucuronique-4-épimérase ; GMD/GER GDP-D-mannose 4,6-déshydratase/ 3,5-épimérase-4-réductase; RHM : UDP-L-rhamnose synthase; UGD : UDP-D-glucose déshydrogénase ; UGE:UDP-D-glucose 4-épimérase ; UXE : UDP-D-xylose-4-épimérase ; UXS : UDP-D-xylose synthase
GDP-D-Man : Guanidine-diphosphate-D-mannose; GDP-L-Fuc : Guanidine-diphosphate-L-fucose; UDP-D-Gal :uridine diphosphate-D-galactose; UDP-D-Glc : uridine diphosphate-D-glucose; UDP-D-GlcA : uridine diphosphate-D-acide glucuronique; UDP-D-GalA : uridine diphosphate-D-acide galacturonique; UDP-L-Ara : uridine diphosphate-D-arabinose; UDP-L-Rha : uridine diphosphate-L-rhamnose.

IV-Les glycosyltransférases impliquées dans la synthèse du XyG

L'étude des mutants chimiques d'Arabidopsis, puis l'utilisation de la génomique fonctionnelle ont permis d'identifier et de caractériser les principales glycosyltransférases qui participent à la synthèse du XyG de type XXXG. Cette dernière requiert une glucane synthase pour l'assemblage de la chaîne principale, et différentes glycosyltransférases pour

la synthèse des chaînes latérales, qui sont principalement de type xylosyltransférase, gactosyltransférase et fucosyltransférase.

IV-1- La Glucane synthase

Identifier un ou plusieurs gènes responsables de la synthèse de la chaîne principale de β(1,4)-D-glucose du XyG n'a pas été aisé, car sa structure est similaire à celle de la cellulose. Cependant, la famille de gènes *CSL* (*cellulose synthase like*) a été identifiée chez Arabidopsis comme étant un bon candidat (Richmonds et Somerville, 2001) pour la synthèse des polysaccharides non cellulosiques. En 2007, Cocuron et al., ont identifié un gène chez la capucine (*Tropaeolum majus*), puis ont ensuite trouvé un gène très proche chez *Arabidopsis thaliana*, nommé *AtCSLC4*. Ils ont exprimé ce gène dans *Pichia pastoris*, en le coexprimant avec le gène d'une xylosyltransférase (*AtXXT1*), puisque de précédentes études ont montré qu'ils devaient certainement agir ensemble pour la biosynthèse du XyG (Hayashi et al., 1981 ; Faik et al., 2002). Bien que Cocuron et al. n'aient pas réussi à détecter d'activité glucane synthase, ils ont montré une accumulation de β(1,4)-D-glucose chez les cotransformants de Pichia, qui est naturellement riche en β(1,3)-D-glucose et pauvre en β(1,4)-D-glucose. De plus, des analyses *in silico* révèlent que ce gène est coexprimé avec d'autres gènes participant à la synthèse du XyG, tel que le gène *XTH22* codant pour une xyloglucane endotransglucosylase/hydrolase.

Ces résultats tendent à montrer que AtCSLC4 est une glucane synthase impliquée dans la synthèse du XyG, et que la famille de gènes AtCSLC est impliquée dans la synthèse du XyG (Liepman et Cavalier, 2012). AtCSLC4 est une protéine golgienne constituée de plusieurs domaines transmembranaires (probablement six), avec son site actif situé sur la face cytosolique (Cocuron et al., 2007 ; Davis et al., 2010). AtCSLC4 fonctionnerait probablement de façon analogue aux protéines CESA, puisque sa topologie est très proche, permettant ainsi l'ajout d'UDP-glucose sur un polymère en cours de synthèse et la traversée de la membrane des vésicules golgiennes (Davis et al., 2010 ; Davis, 2012).

IV-2- Les α(1,6)Xylosylstransférases

La première α(1,6)xylosylstransférase, a été identifiée chez Arabidopsis par homologie de séquence d'une α(1,6)galactosyltransférase du fenugrec (Edwards et al., 1999) qui a conduit à 7 candidats possibles (Faik et al., 2002). L'activité d'AtXXT1 (*xyloglucan*

xylosyltransferase 1) a été montrée par expression hétérologue dans *Pichia pastoris*. Un cellopentaose de type GGGGG a été utilisé comme accepteur, et AtXXT1 y a transféré principalement un résidu xylose sur le deuxième résidu glucose à partir de l'extrémité non réductrice, pour donner GXGGG.

Cavalier et Keegstra (2006) ont identifié AtXXT2, dont le gène est très proche d'AtXXT1. Cette fois-ci, l'activité de la protéine a été démontrée par expression hétérologue dans des cellules d'insectes, car cela ne fonctionnait pas avec *Pichia pastoris*. L'activité d'AtXXT1 et AtXXT2 a été testée sur un cellopentaose et un cellohexaose comme accepteur. Les deux enzymes ont permis l'ajout d'un résidu xylose pour donner GXGGG ou GGXGGG. De plus, les auteurs ont montré qu'en augmentant le ratio UDP-xylose/cellohexaose et le temps de réaction, AtXXT1 et AtXXT2 pouvaient ajouter un deuxième résidu xylose pour donner GGXXGG.

Zabotina et al. (2008) ont étudié une autre enzyme, nommée AtXXT5, ayant potentiellement une activité α(1,6)xylosyltransférase. L'étude du XyG des graines du mutant T-DNA *xxt5* d'Arabidopsis, après traitement à l'endoglucanase, a montré une diminution des fragments xylosylés (XXXG, XXFG et XXLG) et une augmentation de fragments avec un seul xylose (GXXG et XXG), comparé au type sauvage. De plus, ils ont montré que le mutant *xxt5* était complémenté par la protéine AtXXT5 et retrouvait un XyG comparable au type sauvage. Enfin, des analyses immunohistochimiques effectuées sur le mutant *xxt5*, ont montré une diminution spécifique des épitopes du XyG des parois (reconnus par les anticorps CCRCM1, CCRCM39 et CCRCM58), alors que les épitopes d'autres polysaccharides étaient inchangés. Bien que l'activité *in vitro* de la protéine n'ait pas été démontrée, ces résultats semblent montrer que AtXXT5 peut être une α(1,6)xylosyltransférase impliquée dans la synthèse du XyG.

IV-3- Les β(1,2)Galactosyltransférases

La première β(1,2)galactosyltransférase a été identifiée chez Arabidopsis grâce à l'étude du mutant chimique *mur3* qui possède un XyG très différent du type sauvage (Madson et al., 2003). En effet, chez le type sauvage, après traitement à l'endoglucanase, des fragments typiques d'Arabidopsis XXXG, XLXG, XXLG, XXFG, XLLG et XLFG étaient détectés, tandis que chez le mutant *mur3*, seuls les fragments XXXG et XLXG étaient présents. Ceci tendait à montrer que le gène *mur3* codait certainement pour une

β(1,2)galactosyltransférase spécifique du troisième résidu glucose portant un xylose. Une fois le gène identifié, l'activité de la protéine AtMUR3 a été montrée par expression hétérologue dans *Pichia pastoris*, montrant l'incorporation spécifique du galactose sur le troisième résidu glucose portant un xylose, pour donner le fragment XXLG et son équivalent fucosylé XXFG. Grâce à AtMUR3, 10 régions codantes proches de sa séquence ont été identifiées, et l'étude des mutants d'insertion T-DNA a fait ressortir 2 candidats (AtGT13/At2G32740 et AtGT18/At5G62220) montrant une diminution en galactose, qui pourraient coder pour une galactosyltransférase (Li et al., 2004).

En 2012, Jensen et al., ont effectué une étude transcriptomique sur des graines de capucine, qui sont riches en XyG non fucosylé, afin d'identifier de nouvelles enzymes impliquées dans la synthèse de ce polysaccharide. Parmi les gènes très exprimés, ils ont recherché les gènes orthologues chez *Arabidopsis thaliana*, et le candidat AtGT18/At5G62220, précédemment cité comme une potentielle galactosyltransférase est ressorti. Ainsi, ils ont étudié le phénotype du XyG chez le mutant qu'ils ont nommé *xlt2* (*Xyloglucan L-side chain galactosylTransferase position 2*), et ont montré par les techniques de HPAEC–PAD et OLIMP que les fragments XLXG and XLFG n'étaient pas détectés, alors que les fragments XXLG et XXFG étaient bien présents. Ces résultats démontrent que AtXLT2 incorpore spécifiquement du galactose sur le deuxième résidu glucose portant un xylose, pour donner le fragment XLXG et son équivalent fucosylé XFXG. Pour confirmer que ce phénotype était bien dû à l'absence de la protéine AtXLT2, ils ont complémenté le mutant avec AtXLT2 sauvage et réussi à restaurer un phénotype structural typique de XyG d'Arabidopsis.

IV-4- La α(1,2)Fucosyltransferase

En 1999, Perrin et al., ont identifié et caractérisé une xyloglucane α(1,2)fucosyltransférase chez *Arabidopsis thaliana*. A partir de fractions microsomales d'épicotyles de pois, ils ont purifié la protéine et testé son activité sur du XyG de tamarin ou de graine de capucine (qui possèdent un XyG non fucosylé). Une fois l'activité confirmée, ils ont recherché un candidat orthologue chez *A.thaliana*, nommé AtFUT1, et démontré son activité α(1,2)fucosyltransférase sur le XyG.

AtFUT1 a permis de mettre en évidence une famille de gènes contenant 9 autres glycosyltransférases potentielles, notées AtFUT2 à -10, qui ont été étudiées pour voir si

certaines étaient redondantes avec AtFUT1, ou bien étaient des fucosyltransférases impliquées dans la synthèse d'autres polysaccharides non cellulosiques (Sarria et al., 2001). L'activité de AtFUT3, -4 et -5 a été testée *in vitro* sur du xyloglucane (de tamarin), des arabinogactanes (de mélèze) et des arabinogalactanes protéines (de radis), mais aucun transfert de fucose n'a eu lieu. AtFUT3, -4 et -5 ont ensuite été surexprimées chez Arabidopsis pour voir si la composition monosaccharidique pariétale était modifiée. AtFUT4 et -5 induisaient une augmentation de fucose (ainsi qu'une augmentation de xylose, et une diminution d'arabinose et de galactose) dans la composition pariétale des feuilles et de la tige, comparé au type sauvage. AtFUT3 avait un profil pariétal différent d'AtFUT4 et -5, ainsi que du type sauvage. Ces résultats suggèrent qu'AtFUT4 et -5 possèdent des fonctions similaires, mais distinctes d'AtFUT3.

En 2002, Vanzin et al., ont étudié le mutant chimique d'Arabidopsis *mur2*, qui possède un phénotype normal, bien qu'il contienne moins de 2% de XyG fucosylé comparé au type sauvage, et ce à cause d'une mutation dans le gène *AtFUT1*. Cette mutation engendre la perte de fucosylation du XyG dans presque toute la plante, indiquant qu'AtFUT1 est la seule enzyme responsable de la fucosylation du XyG chez *Arabidopsis thaliana*.

V- Les glycosyltransférases impliquées dans la synthèse du RG-I

Il existe peu de données sur l'identification et la caractérisation des glycosyltransférases impliquées dans la synthèse du RG-I, comparé aux connaissances sur le xyloglucane. En 2009, Caffall et Mohnen ont postulé que 34 glycosyltransférases ayant une activité spécifique pourraient être requises.

A ce jour, aucune donnée n'existe quant à l'identification de l'activité de glycosyltransférases impliquées dans la synthèse de la chaîne principale, qui est constituée du disaccharide $[\text{-4-}\alpha\text{-D-GalA-(1,2)-}\alpha\text{-L-Rha-(1-)}]_n$, ainsi seules les glycosyltransferases potentiellement impliquées dans la synthèse des chaînes ramifiées seront présentées.

Cependant, ces dernières années, plusieurs équipes ont réussi à synthétiser artificiellement un tétrasaccharide ou un hexasaccharide de la chaîne principale (Nemati al., 2008 ; Reiffarth et al., 2008 ; Zakharova et al., 2013). Ainsi, ils pourront servir de substrats pour tester et montrer l'activité de glycosyltransférases candidates pour la synthèse de la chaîne principale, mais aussi pour des glycosyltransférases qui pourraient initier la synthèse des chaînes ramifiées à partir de la chaîne principale.

V-1- Les β(1,4)galactosyltransférases

Plusieurs études ont permis d'identifier des activités β(1,4)galactosyltransférases, notamment chez le soja (Rosidée, *Glycine max Merr*) (Konishi et al., 2004, 2007a) et la pomme de terre (Astéridée, *Solanum tuberosum L.*) (Geshi et al., 2002, 2004).

Konishi et al. (2004) ont réussi à transférer quelques résidus galactose sur des galactanes pectiques commerciaux de lupin partiellement hydrolysés, par une préparation membranaire issue d'hypocotyles étiolés de soja. Ils ont montré que le transfert nécessite au moins 5 résidus galactose. En 2007, les mêmes auteurs ont augmenté le transfert jusque 25 résidus galactose, avec une fraction plus purifiée, et ont montré qu'au-delà de 7 résidus galactose, l'efficacité de transfert diminuait fortement.

Geshi et al. (2002) ont démontré une activité β(1,4)galactan galactosyltransférase à partir de fractions microsomales issues de suspensions cellulaires de pomme de terre, puis ont prouvé que cette activité était intra-golgienne (Geshi et al., 2004).

Récemment, Liwanag et al. (2012) ont réussi à identifier une β(1,4)galactan β(1,4)galactosyltransférase dans la famille CAZy GT92, qui possède chez Arabidopsis 3 candidats potentiels nommés AtGALS1, -2 et -3. Ces 3 mutants d'insertion montrent une diminution significative de galactose dans la paroi. De façon plus fine, l'analyse de sucre a montré une réduction significative du contenu en galactose dans les tiges chez les mutants *gals1-1* et *gals3-1*, mais pas chez le mutant *gals2-1* ; et une faible réduction dans les graines pour les mutants *gals1* et *gals2*. Les 3 protéines sont des protéines transmembranaires de type II, et la protéine AtGALS1 est golgienne. Les protéines AtGALS2 et -3 ont été identifiées comme des protéines potentiellement golgiennes, d'après une étude protéomique effectuée sur des fractions golgiennes purifiées de cellules d'Arabidopsis (Parsons et al., 2013).

Les auteurs ont exprimé la protéine AtGALS1, fusionnée à un *tag* (FLAG ou YFP), chez *Nicotiana benthamiana* et ont démontré que les fractions microsomales contenant la protéine AtGALS1 pouvaient transférer un galactose sur un β(1,4)galactopentaose. Les auteurs suggèrent que cette protéine n'est certainement pas une enzyme qui ajoute le premier galactose sur la chaîne principale du RG-I, puisque son substrat est un β(1,4)galactopentaose, mais n'ont pas de preuve qu'elle pourrait être processive.

V-2- Les β(1,3)galactosyltransférases

Une étude bioinformatique a permis d'identifier chez *Arabidopsis thaliana* des β(1,3)galactosyltransférases potentielles (Qu et al., 2008), par comparaison avec des séquences de β(1,3)galactosyltransférases issues de l'*Homo sapiens*. Une vingtaine de candidats a été identifiée, tous issus de la famille GT31, dont une β(1,3)galactosyltransférase impliquée dans la synthèse des N-glycannes, et caractérisée chez *A. thaliana* (Strasser et al., 2007). Sur ces 20 candidats, 13 protéines sont prédites comme des protéines transmembranaires de type II, avec une localisation golgienne, après une analyse *in silico* des séquences.

V-3- Les α(1,5)arabinosyltransférases

Chez Arabidopsis, une première α(1,5)arabinosyltransférase potentiellement impliquée dans la synthèse des chaînes arabinanes du RG-I a été identifiée grâce à la génération d'un mutant d'insertion T-DNA *arad 1* (*arabinan deficient 1*). Il présente une réduction d'arabinose d'environ 75% dans les feuilles et 46% dans les tiges (Harholt et al., 2006). Une étude immunohistochimique a montré que cette diminution était spécifique des arabinanes, de plus le RG-I du mutant présentait seulement 30% d'arabinose comparé au sauvage. Enfin, lorsque la protéine AtARAD1 a été exprimée sous promoteur fort chez le mutant *arad 1-1*, elle a permis de restaurer un niveau d'arabinose équivalent au type sauvage. Bien que l'activité de la protéine n'ait pu être testée *in vitro*, ces résultats tendent à montrer que la protéine AtARAD1 est très certainement une α(1,5)arabinan arabinosyltransférase impliquée dans la synthèse du RG-I. De plus, les auteurs ont constaté que même si la quantité d'arabinose diminuait, le pourcentage de substitution de rhamnose de la chaîne principale restait identique, indiquant une diminution de la longueur des chaînes arabinanes. Ces résultats tendent à montrer que cette arabinosyltransférase a certainement une activité processive.

Chez une autre Rosidée, le haricot mungo, Konishi et al. (2007a) ont démontré une activité α(1,5)arabinofuranosyltransférase dans des fractions membranaires golgiennes issues d'hypocotyles étiolés. Ils ont démontré qu'il y avait transfert d'un résidu UDP-arabinofuranose (UDP-Ara*f*) à la fois sur un oligomère d'arabinofuranoses liés en α(1,5) et marqués au 2-AB (2-aminobenzamide), montrant une activité non processive. Lorsque cet

oligomère possédait un arabinopyranose (Ara*p*) en position terminale, il n'y avait aucun ajout. Les auteurs ont donc émis l'hypothèse que l'ajout d'Ara*p* sur une chaîne α(1,5)arabinane était certainement le moyen de stopper l'élongation d'une chaîne et donc de contrôler la longueur des chaînes.

V-4- Les α(1,2) et α(1,3)arabinosyltransférases

Actuellement, aucune étude n'a mis en évidence de candidats potentiels pour une activité α(1,2) ou α(1,3) arabinofuranosyltransférase pouvant participer à la synthèse du RG-I. Cependant, une étude récente portant sur la famille CAZy GT61, a démontré l'activité d'une α(1,3)arabinofuranosyltransférase spécifique de la synthèse des xylanes (Anders et al., 2012). Cette famille possède d'autres candidats qui potentiellement peuvent participer à la synthèse du RG-I.

V-5- Les β(1,3)arabinosyltransférases

Une activité β(1,3)arabinopyranosyltransférase permettant le transfert d'un résidu arabinopyranose sur un accepteur L-arabinofuranose-oligosaccharide lié en α(1,5) marqué au 2-AB a été identifiée sur une préparation d'hypocotyle de haricot mungo (*Vigna radiate L. Wilezek*) (Ishii et al., 2005). Les résultats ont démontré que l'arabinopyranose transféré était lié en β(1,3) sur le *O*-3 d'un résidu arabinofuranose terminal de l'oligosaccharide, et que le degré de polymérisation le plus efficace s'effectuait avec un oligomère de 8 arabinofuranoses.

PARTIE C : LA SYNTHESE GOLGIENNE DES POLYSACCHARIDES NON CELLULOSIQUES CHEZ LES PLANTES EUDICOTYLEDONES

I- L'appareil de Golgi

I-1- Généralités

L'appareil de Golgi fut découvert par Camillo Golgi, professeur de pathologie générale à l'Université de Pavie (Italie) en 1883. Il étudiait la structure du cervelet à l'aide d'une coloration au nitrate d'argent, où il décrivit un « appareil réticulaire interne » dans le cytoplasme des cellules de Purkinje, qui fut ensuite nommé « appareil de Golgi ». Plus tard, ce dernier fut décrit à l'échelle de la microscopie électronique comme « un empilement de lamelles courbes à surface lisse entourées par des vacuoles de taille variable » (Sjostrand et Hanzon, 1954). Ces lamelles courbes sont appelées citernes ou saccules.

Contrairement à l'appareil de Golgi (AG) des cellules animales qui est formé par une structure fixe unique périnucléaire, celui des végétaux est constitué de nombreux empilements golgiens mobiles dans le cytoplasme. Cependant, il existe des exceptions, telles que la Drosophile et chez certaines cellules de mammifères où l'appareil de Golgi peut aussi exister en plusieurs petites unités (Kondylis et Rabouille, 2009). Grâce aux différentes études de microscopie électronique réalisées chez les plantes (Staehelin et al., 1990; Staehelin and Kang, 2008), l'appareil de Golgi a pu être défini comme des empilements de citernes constitués de 3 compartiments nommées *cis*, médian et *trans*, qui se distinguent par leur position dans l'empilement golgien et leur morphologie unique (**Figure 22A**).

Les citernes *cis* sont les plus larges et sont les moins contrastées. Les citernes médian sont plus étroites et plus denses aux électrons. Les citernes *trans* ont la plupart du temps leur domaine central avec leur lumière complètement collapsée et sont visualisées par un trait épais denses aux électrons. Chacune de ces saccules ont des extrémités bourgeonnantes. Un réseau *trans*-golgien (TGN, *trans-Golgi network*) peut être associé, situé très proche des saccules *trans*. Il est constitué de nombreuses vésicules bourgeonnantes ayant différents types de contraste. Des éléments interciternes situés entre les citernes *trans* et le TGN peuvent également être présents. Les saccules et le TGN sont englobés dans une zone sans ribosomes, appelée matrice golgienne. De nos jours, la technique de tomographie électronique, qui permet d'obtenir une image de microscopie électronique en 3 dimensions,

ouvre de nouvelles perspectives sur la vision que nous avons de l'appareil de Golgi (**Figure 22B**).

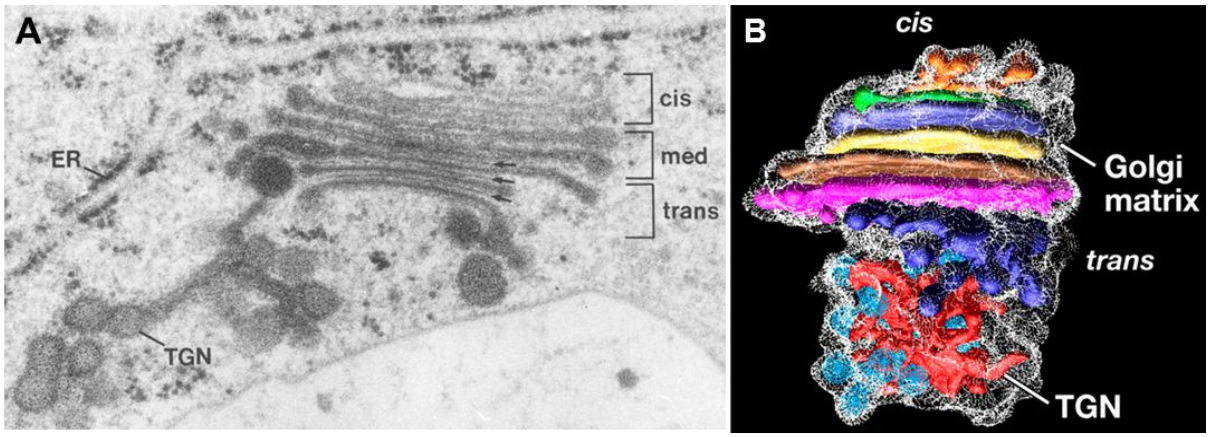

Figure 22 : Morphologie générale d'un empilement golgien.
A- Micrographie électronique montrant la structure 2-D des 3 catégories de saccules *cis*, médian, *trans* et le TGN, chacun différenciés par la largeur de leur saccule et leur contraste spécifiques (Staehelin et al., 1990).
B- Tomogramme électronique représentant la structure 3-D d'un empilement golgien avec les différentes saccules et le TGN englobés dans la matrice golgienne (Staehelin et Kang, 2008).
(ER : réticulum endoplasmique, med : médian ; TGN : réseau *trans*-golgien)

I-2- L'appareil de Golgi est une structure évolutive et mobile

La première difficulté pour définir un modèle général de la structure de l'appareil de Golgi réside dans le fait que ce n'est pas une structure fixe. Le nombre d'empilements golgiens par cellule, le nombre de citernes par empilement, la présence ou l'absence de TGN et d'éléments interciternes varient en fonction du type cellulaire, du stade de développement de la cellule et des espèces (Staehelin et al., 1990; Zhang and Staehelin, 1992).

Cette variabilité est due au fait que l'appareil de Golgi joue un rôle central dans le trafic membranaire intracellulaire. En premier lieu, au sein de l'appareil de Golgi, les protéines sont glycosylées et les polysaccharides non cellulosiques sont synthétisés, puis chacun est trié pour être envoyé à sa destination finale selon les différentes voies (sécrétion, lysosome, vacuole, endocytose,..). Son activité peut donc être variable selon les besoins de la cellule.

De plus, à l'échelle d'un empilement golgien, deux points de vue ont longtemps été débattus quant à son évolution dans le temps, à savoir si un empilement golgien est constitué de saccules dont la nature reste fixe, formant une sorte de sous-organites

distincts ; ou bien si les saccules évoluent du *cis* vers le *trans*. Ce deuxième modèle, appelé « modèle de maturation des citernes », propose que de nouvelles citernes se forment du côté *cis* de l'empilement golgien, et maturent à travers l'empilement dans une direction *cis-trans*, puis se dissipent en formant des vésicules dans le réseau *trans*-golgien.

De nos jours, c'est plutôt ce modèle qui est finalement accepté, car il a été mis en évidence chez la levure *Saccharomyces cerevisiae* (Losev et al., 2006; Matsuura-Tokita et al., 2006), les algues (Becker et al., 1995), les mammifères (Bonfanti et al., 1998), et chez les plantes (voir les revues Moreau et al., 2007 ; Staehelin et Kang, 2008 ; Hawes et al., 2010).

L'autre difficulté pour étudier l'appareil de Golgi est que, chez les plantes, les empilements golgiens sont mobiles dans la cellule, des études l'ont notamment démontré chez le tabac (Boevink et al., 1998 ; Nebenführ et al. 1999 ; Yang et al. 2005 ; Ito et al., 2012). De plus, ce déplacement est dépendant des éléments du cytosquelette (système actine/myosine) (Boevink et al., 1998 ; Nebenführ et al. 1999).

I-3-Techniques développées pour étudier l'appareil de Golgi

Pour répondre à ces 2 difficultés, les techniques d'imagerie par microscopie confocale à balayage laser et par microscopie électronique à transmission ont été développées et admises comme étant les 2 méthodes complémentaires permettant l'étude structurale et fonctionnelle de l'appareil de Golgi chez les plantes. La première permet une observation *in vivo* de la dynamique des empilements golgiens dans leur environnement, quand la deuxième permet une observation avec une plus grande résolution, pour observer l'ultrastructure des empilements golgiens à un instant donné.

A ces techniques ont été ajouté différents outils, dont la Brefeldin A (BFA). La BFA est un métabolite fongique qui bloque le système endomembranaire de sécrétion, et plus particulièrement le transport entre le RE et le compartiment *cis*-Golgi. L'intérêt de cette molécule est qu'elle induit une disparition des empilements golgiens, et que son action est réversible après un simple lavage de l'échantillon traité. Ainsi, on peut induire la reformation d'un empilement golgien après un traitement à la BFA (Hawes et al., 2010).

L'utilisation de marqueurs de l'appareil de Golgi et de son environnement proche a également été développée afin de suivre la néosynthèse des empilements. Ces marqueurs peuvent être des protéines transmembranaires ou cytosoliques fusionnées à la *Green Fluorescent protein* (GFP) ou l'un de ses variants (RFP, YFP) exprimées dans le système

étudié, ou bien des anticorps couplés à des fluorochromes et dirigés contre des marqueurs constitutifs. Ces marqueurs sont souvent des enzymes résidentes des empilements golgiens ou des protéines associées aux vésicules impliquées dans le système endomembranaire de sécrétion situées dans l'environnement très proche des saccules.

Ainsi, les paragraphes suivants sont une synthèse des résultats obtenus en utilisant une approche combinée de ces différents outils.

II- Biogenèse et structure de l'appareil de Golgi

II-1- Différents modèles de synthèse

II-1-1- Synthèse *de novo* à partir du réticulum endoplasmique

Chez les plantes, lorsqu'on colocalise le réticulum endoplasmique (RE) et l'appareil de Golgi, on observe une distribution des empilements golgiens parfaitement liée au réseau du RE (**Figure 23**), en particulier sur des zones spécifiques du RE, appelées « site d'export du RE » (ERES, *endoplasmic reticulum exit site*) (Hawes et Satiat-Jeunemaitre, 2005 ; Sparkes et al., 2009, Hawes et al., 2010).

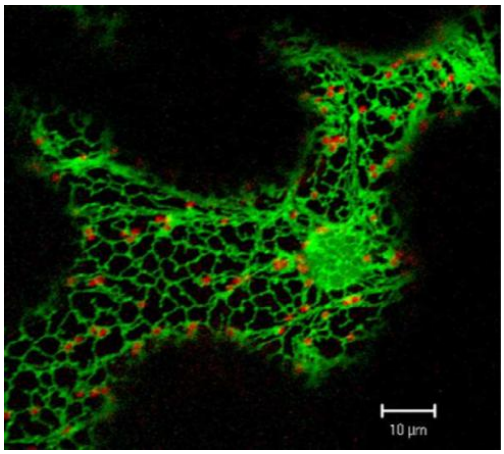

Figure 23 : L'association entre le RE et l'appareil de Golgi mise en évidence dans des cellules de tabac (Hawes et Satiat-Jeunemaitre, 2005)
Coexpression d'un marqueur du RE couplé à la GFP (vert) formant un réseau en toile d'araignée, et d'un marqueur golgien couplé à la RFP (rouge) formant des spots, dans des cellules épidermiques de feuille de tabac. Notez la colocalisation de signal des empilements golgiens (rouge) avec le réseau du RE (vert).

Les empilements golgiens étant constitués de saccules évolutives qui maturent du *cis* vers le *trans*, l'hypothèse a été posée que c'était peut-être au niveau des ERES que les empilements golgiens étaient synthétisés *de novo*.

Récemment, une étude effectuée sur différents types d'algues (*Scherffelia dubia*, *Chlamydomonas reinhardtii*) et sur des cellules de pointe de racine d'Arabidopsis a montré à l'échelle ultrastructurale la mise en place des premières saccules *cis* au niveau des sites ERES (Donohoe et al., 2013). Au départ, plusieurs vésicules intervenant dans le système de sécrétion, appelées COPII, vont fusionner pour donner une structure tubulaire, puis une structure plate qui sera définie comme étant la première saccule *cis*. Une fois générée, cette première petite saccule va évoluer en une saccule *cis* plus tardive, qui va grossir en taille grâce à la fusion d'autres vésicules COPII par les extrémités de la saccule (**Figure 24A**). Une fois les saccules *cis* formées, elles maturent en saccules median, puis en saccules *trans*, puis vont former le réseau *trans*-golgien (**Figure 24B**).

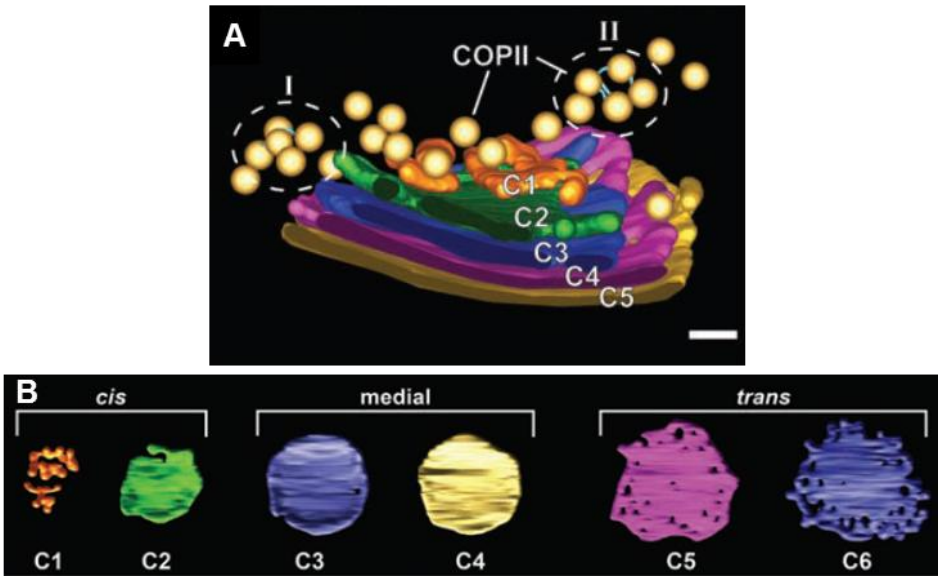

Figure 24 : Synthèse *de novo* des saccules golgiennes (Donohoe et al., 2013)
A- Tomogramme électronique montrant les vésicules COPII (représentées en jaune) qui s'associent en petits groupes (cercle en pointillés notés I et II), puis fusionnent pour donner une structure tubulaire, la première saccule *cis* (notée C1 en orange). Puis la saccule C1 va former une « vraie » saccule *cis*, nommée C2, et ainsi de suite. De C2 à C5, les saccules *cis* grossissent grâce à la fusion par les extrémités de vésicules COPII. Barre d'échelle : 100 nm. B- Tomogramme électronique montrant les vues de face des différents types de saccules, *cis*, median et *trans*.

II-1-2- Duplication par maturation

Une autre hypothèse sur la synthèse de l'appareil de Golgi a été formulée. En effet, durant le cycle cellulaire de cellules méristématiques d'Arabidopsis, il a été montré que le nombre d'empilements golgiens, doublait durant la phase G2, précédant la mitose (Segui-Simarro et al., 2006). Plus tard, la même équipe a montré *via* la tomographie qu'à partir d'un empilement golgien constitué de deux demi-citernes *cis*, on pouvait obtenir deux nouveaux empilements golgiens (Staehelin et Kang, 2008). Ces derniers ayant des saccules qui

maturent du *cis* vers le *trans*, les deux saccules *cis* servent de matrice de départ, et vont ensuite évoluer en median, puis en *trans* pour donner un nouvel empilement golgien (**Figure 25**).

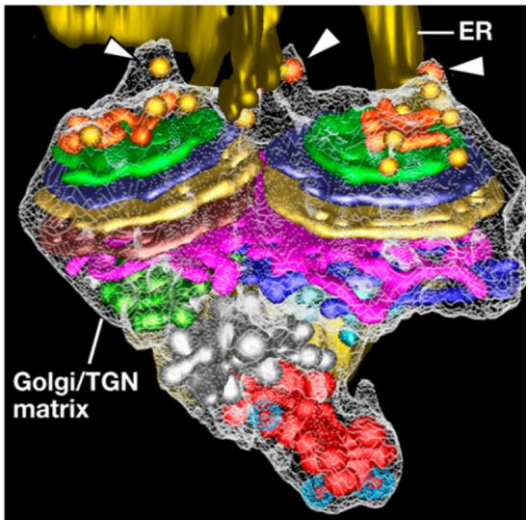

Figure 25 : Duplication par maturation d'un empilement golgien (Staehelin et Kang, 2008)
Tomogramme électronique montrant un empilement golgien en cours de division au niveau d'un ERES dans une cellule méristématique de racine d'Arabidopsis. Les saccules *cis* (orange et vert) et médian (bleu et beige) sont doublées et maintenues ensemble *via* une grande saccule *trans* (rose). Au-dessous, on peut observer différents TGN (vert, blanc rouge). L'ensemble est entouré dans une matrice Golgienne (maillage blanc). On observe également la fusion de vésicules COPII (sphères jaunes) pour former les premières saccules *cis*.

II-1-3- Coexistence des 2 modèles

Récemment, Abiodun et Matsuoka (2013) ont démontré que la synthèse des empilements golgiens chez les cellules de tabac BY-2 se faisait selon les 2 systèmes. Pour ce faire, ils ont utilisé des protéines fluorescentes photoconvertibles (Hawes et al., 2010) couplées à des marqueurs golgiens. L'intérêt de ces protéines est de pouvoir différencier *in vivo* des empilements golgiens préexistants et des empilements nouvellement synthétisés. Ainsi, on s'affranchit de l'utilisation de la BFA pour destructurer puis reconstruire des empilements golgiens, et la création de possibles artéfacts est minimisée.

Le principe est le suivant : les cellules de tabac exprimant les marqueurs golgiens couplés à la protéine photoconvertible sont exposées à une lumière violette, transformant le marquage initial en vert des empilements golgiens en marquage rouge. Les cellules sont ensuite cultivées normalement, puis de nouveau observées au microscope. Le marqueur golgien nouvellement formé émettra en vert, et lorsqu'il sera transporté dans les empilements golgiens, ces derniers auront donc un marquage rouge, vert et jaune.

Ils ont observé une diminution rapide d'empilements golgiens « rouges » et « jaunes », et une augmentation d'empilements golgiens « verts » dès le début de leur

analyse, indiquant que la synthèse *de novo* à partir du RE et la division d'empilements préexistants après avoir accepté la protéine marqueur provenant du RE nouvellement synthétisée se fait en parallèle dans des cellules de tabac en croissance.

II-2- Le réseau *trans*-golgien

Staehelin et Kang (2008), ont mis en évidence l'existence de deux types de TGN, nommés TGN précoce et TGN tardif, ayant une morphologie bien distincte. Le TGN précoce possède un domaine central plat, provenant certainement d'une saccule *trans* et quelques vésicules en bourgeonnement, et situé très près du compartiment *trans* de l'empilement golgien. Le TGN tardif présente plutôt une structure en grappe, constitué de vésicules et de quelques restes de saccules, il peut être proche ou éloigné du TGN précoce **(Figure 26)**.

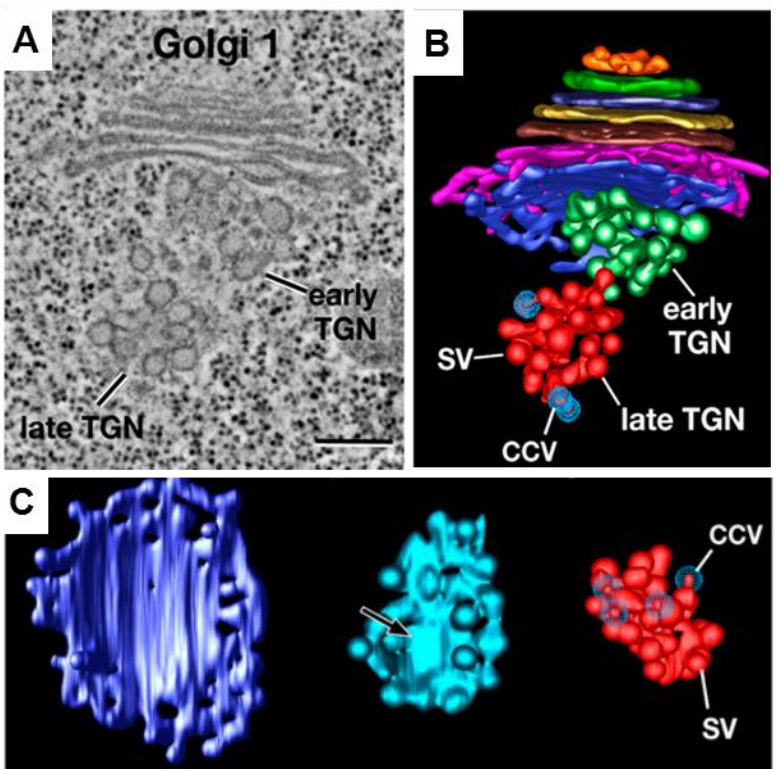

Figure 26 : Morphologie des différents types de TGN (Staehelin et Kang, 2008).
Micrographe (A) et tomogramme électronique (B) présentant la morphologie d'un empilement golgien, avec les TGN précoce et tardif. En (C), tomogramme électronique montrant une vue de face d'une saccule *trans* (bleu), du TGN précoce (turquoise) et du TGN tardif (rouge). (CCV : vésicules à manteau de clathrine ; SV : vésicules de sécrétion)

Il a également été montré que le TGN tardif en tant que structure disparaissait complètement, puisque la totalité de ses membranes servait à la formation des vésicules de sécrétion et des vésicules à manteau de clathrine. Ainsi, le TGN tardif peut être considéré

comme une structure à « usage unique », dont la durée de vie varierait en fonction des besoins cellulaires (Kang et al., 2011 ; Kang, 2011).

II-3- Comment est conservée l'intégrité d'un empilement golgien ?

II-3-1- Les éléments inter-citernes

Les éléments inter-citernes sont des éléments fibreux, opaques aux électrons, avec une structure régulière, et majoritairement détectés entre les saccules *trans* (Kristen, 1978 ; Staehelin et al., 1990) **(Figure 27A)**. Ces éléments sont supposés effectuer une compression de la région centrale des citernes, afin de restreindre le gonflement des saccules et le bourgeonnement de vésicules aux extrémités des saccules. En effet, une citerne avec un contenu hypertonique aura tendance à devenir sphérique **(Figure 27B)**. Kristen (1978) a émis l'hypothèse que la compression des citernes par les éléments inter-citernes pouvait engendrer un changement de distribution de charges électriques dans les membranes, permettant ainsi une attraction des surfaces internes de ces dernières et conduisant à des saccules très collapsées.

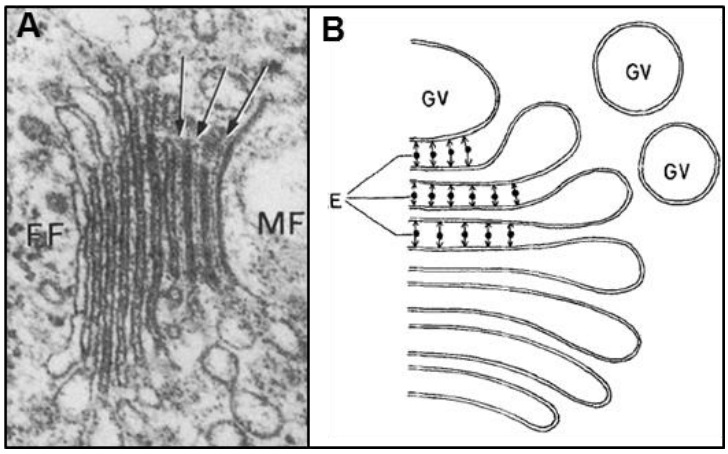

Figure 27 : Les éléments inter-citernes (Kristen, 1978)
(A) Micrographe montrant la morphologie des éléments inter-citernes, indiqués par les flèches noires.
(B) Schéma présentant le rôle possible des éléments inter-citernes. Ces derniers sont représentés en points noirs entre les saccules trans, les flèches représentent la direction de la force de compression. (E : éléments inter-citernes; FF : *forming face* (face *cis*); GV : *golgi vesicles*; MF : *maturing face* (face *trans*))

II-3-2- La matrice golgienne

La matrice golgienne est définie par une zone entourant les empilements golgiens d'où sont exclus les ribosomes, suggérant une densité plus forte que le cytoplasme dans lequel se trouvent les empilements golgiens (**Figure 28**).

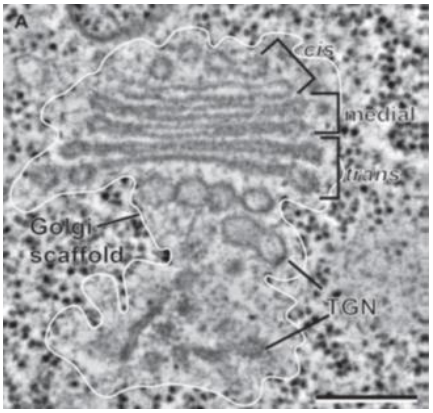

Figure 28 : Morphologie de la matrice golgienne (Donohoe et al., 2013)
Micrographie montrant un empilement golgien inclut dans une zone exclue de ribosomes, la matrice golgienne, délimitée par un trait blanc. Barre d'échelle : 300 nm.

La nature et le rôle de cette matrice sont encore peu définis. Les golgines, une classe de protéines avec une structure en superhélice, ont été identifiées dans la matrice golgienne de plusieurs systèmes eucaryotes, et leur rôle commence à être mieux compris. Les golgines semblent avoir un rôle dans le trafic membranaire et la structure des empilements golgiens. De nombreuses golgines possèdent un site de fixation pour les GTPases de la famille Rab, ce qui amène à penser que les golgines pourraient agir de façon collective pour former une matrice golgienne qui capture les membranes coatées avec la protéine Rab à proximité des saccules (Munro, 2011 ; Renna et al., 2013).

Aujourd'hui, encore peu de golgines ont été identifiées chez les plantes, mais les premiers résultats montrent une grande conservation de ces protéines dans les différents systèmes (Latijnhouwers et al., 2007), et suggèrent donc un rôle similaire, ou du moins en partie.

II-4- Le système endomembranaire golgien

II-4-1- L'appareil de Golgi et les sites ERES

La nature du contact entre les sites ERES et les empilements golgiens fait débat, puisque deux hypothèses sont proposées : les ERES et les empilements golgiens sont associés de façon stable pour former une unité sécrétoire mobile (Brandizzi et al., 2002a ; daSilva et al., 2004) ou les empilements golgiens s'associent de façon transitoire aux ERES (Nebenführ et al., 1999 ; Yang et al., 2005).

Staehelin et Kang (2008) ont proposé un modèle appelé « *Dock, Plug and Go* » **(Figure 29)**. A l'échelle de la tomographie électronique, ils ont observé qu'au niveau d'un site

ERES, les vésicules COPII bourgeonnent et s'entourent d'une couche d'où sont exclus les ribosomes. Un empilement golgien qui passe sur son filament d'actine va être « arrimé » par cette couche qui va l'orienter du côté de sa face *cis*, et l'entourer comme dans une sorte de cocon, le décrochant du filament d'actine. Les vésicules COPII délivrent alors leurs molécules par fusion avec l'empilement golgien, puis une fois ce processus terminé, l'empilement golgien est de nouveau libre de continuer son mouvement sur le filament d'actine. La nature des molécules constituant la couche est très certainement constitué de golgines structurées en super-hélice (Latijnhouwers et al., 2007).

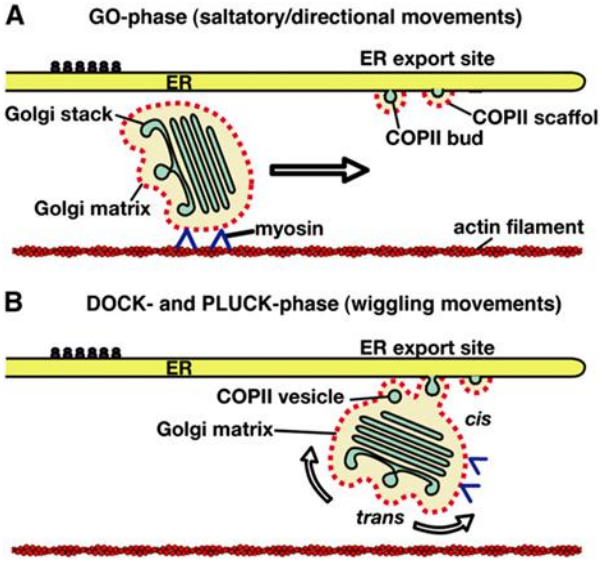

Figure 29 : Le modèle "Dock, pluck, and go" du transport RE/Golgi (Staehelin et Kang, 2008)
(A) « Phase *Go* » : Les empilements golgiens circulent sur les filaments d'actine propulsés par les moteurs de myosine. (B) « Phase *Dock- and Pluck* : la couche située sur les vésicules COPII en bourgeonnement va arrimer l'empilement golgien et l'orienter sur sa face *cis*, et le décrocher du filament d'actine. Les vésicules COPII vont délivrer leur molécules, puis l'empilement Golgien sera libre et de nouveau sur le filament d'actine.

II-4-2- Transports antérograde et rétrograde entre le RE et les empilements golgiens

Un transport antérograde est effectué par les vésicules COPII, originaires du RE, qui se chargent de transporter les molécules du RE vers le compartiment *cis*, et participent activement à la génération des saccules comme vu au paragraphe II-1-1. Un transport rétrograde est effectué par les vésicules COPI, originaires des saccules golgiennes, qui se chargent de ramener des protéines « échappées » du RE et du transport intra-golgien. En effet, puisqu'un empilement golgien est une structure dont les saccules maturent en permanence, les vésicules COPI maintiennent la composition membranaire de chaque type de saccule.

Il a été montré par tomographie électronique (Staehelin et Kang, 2008) qu'il existait deux groupes de vésicules COPI, nommés COPIa et COPIb. Les vésicules COPIa bourgeonnant uniquement des saccules *cis*, sont confinées dans l'environnement RE/*cis*-Golgi, et colocalisent avec les vésicules COPII. Au contraire, les vésicules COPIb bourgeonnant exclusivement des saccules median, *trans* et du TGN précoce, sont confinées dans l'environnement proche de ces saccules (**Figure 30**).

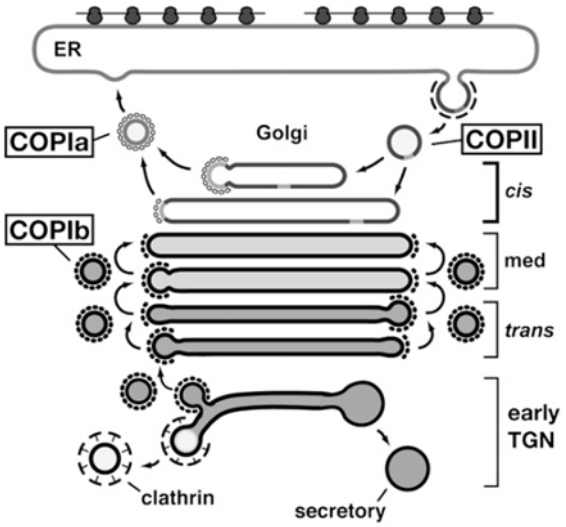

Figure 30 : Transport antérograde et rétrograde entre le RE et les empilements golgiens (Staehelin et Kang, 2008)
Les vésicules COPII effectuent le transport antérograde du RE vers les saccules *cis*, tandis que les vésicules COPIa se chargent du transport *cis* vers le RE, et les vésicules COPIb se chargent du transport rétrograde au niveau des saccules médian, *trans* et du TGN précoce.

II-4-3- Transport post-Golgi

Le réseau *trans*-golgien est le point de départ du transport post-Golgi, qui joue un rôle essentiel dans la voie de sécrétion, mais également dans les voies d'endocytose et de recyclage des membranes. Ces transports font appel à des vésicules bourgeonnant à partir du TGN, *via* la nature lipidique particulière des membranes ou grâce à l'action de protéines manteaux, comme détaillé ci-après.

Les vésicules à manteaux (**Figure 31**, «*Coat-mediated budding*») se forment grâce à l'action des *coat protein complexes* (CPCs) qui vont faciliter la reconnaisance de la molécule à transporter et la déformation de la membrane, et à l'action des *dynamin-related GTPases* (DRPs) qui participent à la tubulation et à la scission de la vésicule ainsi formée. Puis, l'intervention des Rab GTPases (membre des Ras), des protéines d'attachement et des SNAREs (*soluble N-ethylmaleimide-sensitive factor attachment protein receptors*) vont permettre le guidage, l'ancrage et la fusion de la vésicule au niveau de la membrane

réceptrice (Fujimoto et al., 2012). Pour les vésicules formées à partir de domaines lipidiques (**Figure 31**, «*Domain-mediated budding*»), de petits radeaux lipidiques vont fusionner pour former une plateforme lipidique plus large et plus stable qui va également emprisonner les molécules cargo. Les différents lipides créent des forces de tension qui vont recourber la membrane, et ce avec l'aide d'autres facteurs (Melser et al., 2011 ; Surma et al., 2012).

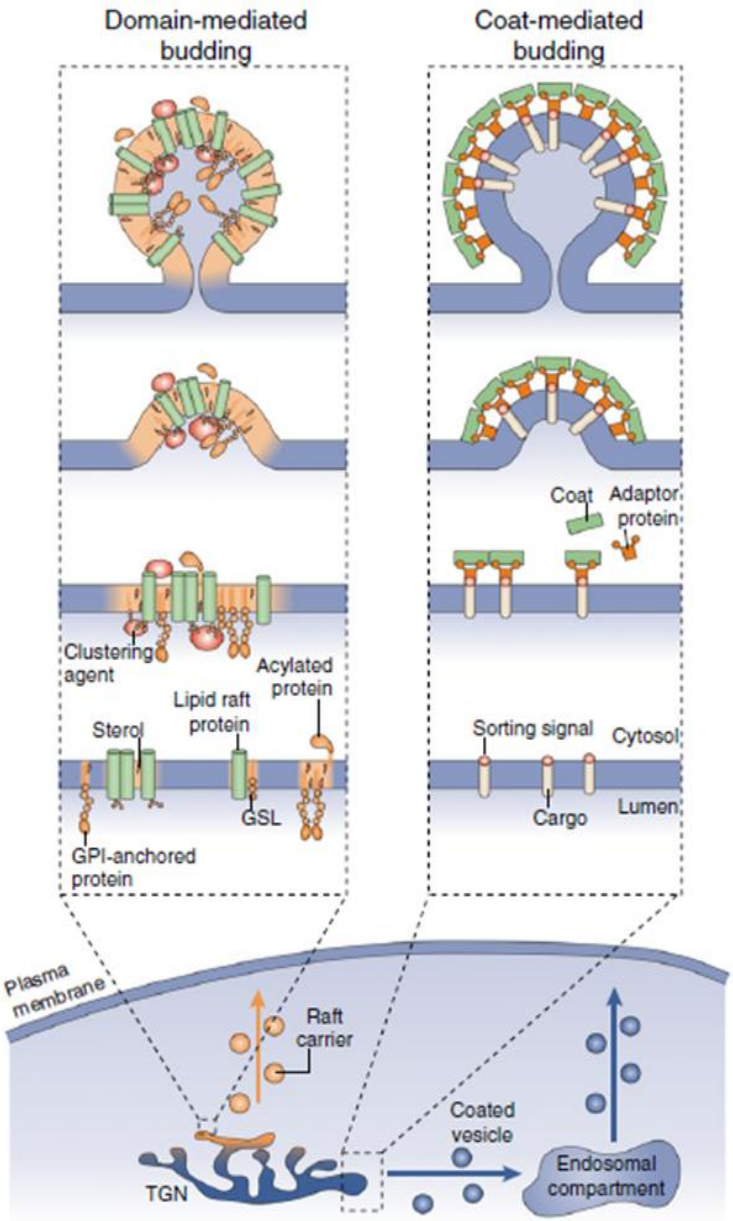

Figure 31 : Formations des vésicules de transport au niveau du TGN (Surma et al., 2012).
Droite : formation des vésicules à manteau. La molécule cargo est intégrée dans une vésicule de transport par l'action de protéines « adaptateur » et de protéines manteaux qui vont induire une déformation de la membrane. Gauche : la formation du radeau lipidique est induite avec l'aide d'agents aidant à l'agglomération des lipides et des molécules cargo. Les différents lipides créent des forces de tension qui vont recourber la membrane, et ce avec l'aide d'autres facteurs.

L'idée que le bourgeonnement de certaines vésicules au niveau du TGN a lieu spécifiquement au niveau de microdomaines lipidiques distincts est de plus en plus présente (Melser et al., 2011 ; Surma et al., 2012). Effectivement, le TGN a été observé comme le lieu privilégié pour la formation de microdomaines lipidiques, également nommés « radeaux lipidiques » (Klemm et al., 2009). Récemment, une étude a montré le rôle déterminant des sphingolipides et des stérols dans le trafic endomembranaire (Yang et al., 2013). Ils ont étudié un transporteur ABC (ATP-binding cassette) chez Arabidopsis et ont montré qu'une fois traversé l'empilement golgien, son départ au niveau du TGN dépendait du contenu membranaire en stérols.

Cela présente plusieurs avantages. Premièrement, cette organisation en microdomaines ne nécessite pas l'intervention d'autres molécules qu'il faudrait ensuite stocker au niveau de l'appareil de Golgi. De plus, ce système représente un bon moyen pour exclure les protéines transmembranaires résidentes de l'appareil de Golgi des vésicules en bourgeonnement, parce qu'elles seront riches en cholestérol/sphingolipides, et ainsi les retenir indirectement dans l'empilement golgien (Bretscher et Munro, 1993).

En 2006, Dettmer et al., ont émis l'hypothèse que le TGN ne jouait pas uniquement un rôle dans le système de sécrétion, mais également dans le système d'endocytose, en représentant un endosome précoce. Ainsi, le TGN a été nommé TGN/EE pour *Early Endosome*. La même équipe a également observé que les TGN/EE se dissociaient de l'appareil de Golgi et pouvaient s'associer à d'autres TGN par le biais d'une interaction homotypique réversible (Viotti et al., 2010). Enfin, ils ont démontré que les corps multivésiculaires (MVBs, *Multivesicular Bodies*), représentant les endosomes tardifs (LE, *Late Endosome*), étaient dérivés du TGN/EE par maturation, et que la formation des vésicules intraluminales commençait dès le TGN/EE, *via* l'action d'ESCRT (*Endosomal Sorting Complex Required for Transport*) et l'action d'annexines pour l'étape finale de libération des MVBs comme transporteur jusqu'à la vacuole. Ainsi, ils ont également démontré que le transport post-TGN vers les vacuoles lytiques n'était pas dépendant des vésicules à clathrines (Scheuring et al., 2011) **(Figure 32)**.

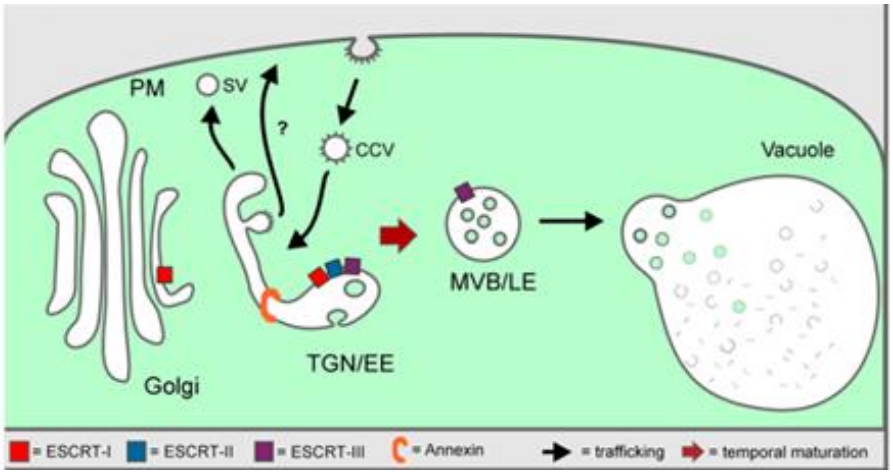

Figure 32 : Modèle de maturation des corps multivésiculaires (MVBs) à partir du TGN (Scheuring et al., 2011). Le TGN/EE se subdivise probablement en différents domaines, certains vont donner les vésicules de sécrétion vers la membrane plasmique, d'autres domaines vont maturer pour former un MVB/LE, *via* l'action des complexes ESCRT et d'annexine, qui fusionnera avec une vacuole lytique.
(CCV : vésicules à manteau de clathrine ; MVB/LE : corps multivésiculaire/endosome tardif ; TGN/EE : réseau *trans*-golgien/endosome précoce ; SV : vésicule de sécrétion)

III- La synthèse golgienne des PS complexes

III-1- Généralités

Les premières études ayant démontré l'implication de l'appareil de Golgi dans la synthèse des PS pariétaux datent des années 60 et 70 (Pickett-Heaps, 1966, 1968; Harris et Northcote, 1971; Dauwalder et Whaley, 1974). Elles ont montré que l'appareil de Golgi était riche en glucides de même nature que ceux contenus dans la paroi. Puis, d'autres études ont montré le rôle de l'appareil de Golgi dans la synthèse des PS non cellulosiques par la présence d'activités glycosyltransférases spécifiques dans les membranes golgiennes (Gardiner and Chrispeels, 1975; Green et Northcote, 1978; Ray, 1980 ; Camirand et al., 1987; Brummell et al., 1990; Gibeaut et Carpita, 1994).

Les glycosyltransférases impliquées dans la synthèse du xyloglucane et du rhamnogalacturonane-I qui ont été caractérisées (voir partie B ; Scheller et al., 2010 ; Atmodjo et al., 2013) sont des protéines transmembranaires de type II résidentes de l'appareil de Golgi.

III-2- La rétention des glycosyltransférases au sein du Golgi

Plusieurs mécanismes de rétention des protéines membranaires semblent coexister (**Figure 33**), impliquant la nature de leur séquence primaire, ainsi que leur relation avec la composition lipidique des membranes golgiennes.

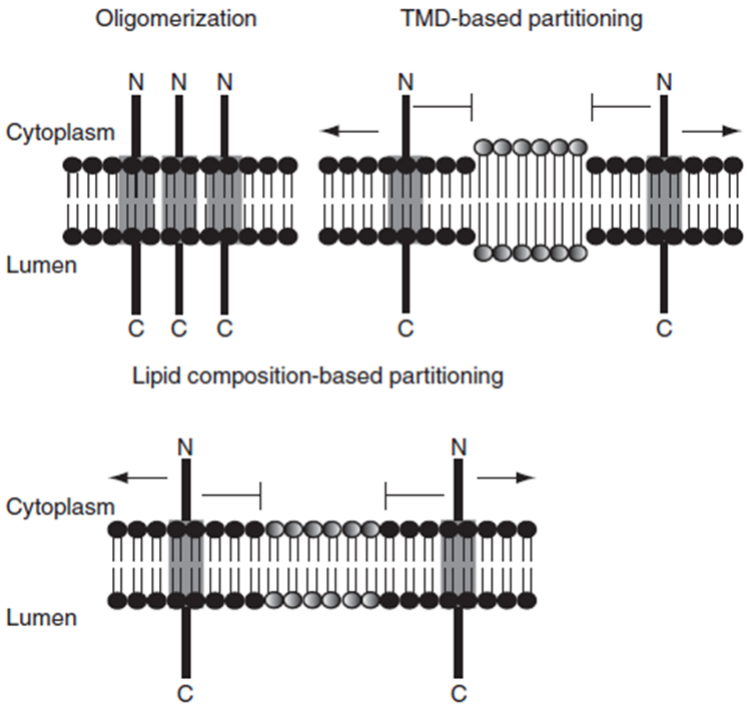

Figure 33 : Différents mécanismes de rétention des protéines membranaires (adapté de Banfield, 2011). « *Oligomerization* »: rétention par oligomérisation des protéines ; « *TMD-based partitioning* »: rétention selon la longueur et la nature du domaine transmembranaire de la protéine ; « *Lipid composition-based partitioning* »: rétention de la protéine selon la composition lipidique membranaire du compartiment.

III-2-1- Longueur et nature du domaine transmembranaire des protéines

En 1993, Bretscher et Munro ont observé que les protéines transmembranaires de type II localisées dans la membrane plasmique avaient un domaine transmembranaire en moyenne plus long que des protéines golgiennes transmembranaires de type II. Ce modèle propose que le domaine transmembranaire plus court des protéines golgiennes de type II empêche leur entrée dans les vésicules de sécrétion à destination de la membrane plasmique, ces dernières ayant une bicouche plus épaisse enrichie en stérols. Ainsi, la longueur et la composition riche en acides aminés aromatiques du domaine transmembranaire des protéines golgiennes seraient déterminantes pour leur rétention dans le Golgi.

Une étude menée chez le tabac a clairement démontré que la longueur du domaine transmembranaire jouait un rôle déterminant sur la localisation d'une protéine transmembranaire de type I (Brandizzi et al., 2002b). Enfin, une récente étude de protéomique effectuée sur des cals d'Arabidopsis a comparé la structure des domaines transmembranaires de 304 protéines localisées dans le RE, 197 localisées dans l'appareil de Golgi et 208 dans la membrane plasmique. Comparées aux protéines de la membrane plasmique, les protéines golgiennes ont des domaines transmembranaires plus courts, avec des séquences qui possèdent plus d'acides aminés hydrophobes volumineux comme la leucine, la phénylalanine, la tyrosine. Leur queue cytosolique est quant à elle inférieure à 45 acides aminés (Nikolovski et al., 2012).

III-2-2-Un signal de rétention dans la séquence protéique

Pour les protéines transmembranaires de type II, il n'y a pas de motif directement lié à une rétention dans l'appareil de Golgi, comme il peut exister pour le RE (motif H/KDEL). Cependant, plusieurs études tendent à montrer que la queue cytosolique joue un rôle essentiel, mais pas suffisant dans la rétention au sein de l'appareil de Golgi (Dirnberger et al., 2002 ; Saint-Jore-Dupas et al., 2006). Ainsi, il semblerait que la présence d'acides aminés basiques (Arginine/Lysine) situés dans la queue cytosolique de glycosyltransférases soit importante pour faciliter l'export de ces protéines au niveau du RE (Schoberer et al., 2009 ; Strasser et al., 2006).

Dès lors, une glycosyltransférase de type II pourrait résider dans l'appareil de Golgi par un signal de rétention « indirect », à savoir un export immédiat du RE, puis une localisation dans l'appareil de Golgi par son domaine transmembranaire ou *via* une interaction avec d'autres protéines partenaires (Banfield, 2011).

III-2-3-La composition lipidique des membranes golgiennes

En 2008, Patterson et al., ont proposé que les protéines transmembranaires golgiennes se séparaient dans des domaines membranaires spécifiques selon un ratio lipidique, en particulier celui des glycérophospholipides/sphingolipides (GPL/SL). En effet, ce dernier est plus faible du côté *cis* et plus important du côté *trans*. Ainsi, chaque protéine transmembranaire irait vers le compartiment dont le ratio lipidique lui convient (Patterson et al. 2008; Lippincott-Schwartz et Phair 2010; Sharpe et al., 2010).

III-2-4-Ancrage des enzymes par les éléments inter-citernes

Staehelin et al. (1990) ont proposé que les éléments inter-citernes, situés principalement au niveau du *trans*-Golgi, aient pour fonction principale de servir de point d'ancrage pour les enzymes transmembranaires ou les complexes enzymatiques au sein des saccules golgiennes afin de prévenir leur sorties dans les vésicules de sécrétion. Cependant, aucune étude n'a démontré cette hypothèse.

III-2-5- L'oligomérisation des protéines

Il a été observé dans le monde animal et le monde végétal que les protéines membranaires résidentes de l'appareil de Golgi, peuvent exister sous forme de monomères, mais également sous forme d'homo- ou hétéro-oligomères (Banfield, 2011 ; Oikawa et al., 2013). Un des rôles proposés pour cette oligomérisation est que ces protéines seraient exclues des vésicules de transport car le complexe formé serait trop large, les préservant ainsi de leur sortie d'un empilement golgien (Nilsson et al., 1993). La capacité à former des oligomères dépendrait des caractéristiques du domaine transmembranaire (longueur et composition en acides aminés) et/ou de leur région luminale (Banfield, 2011).

III-3- Les enzymes de synthèse fonctionnent en complexes

III-3-1- Généralités

La synthèse golgienne des polysaccharides pariétaux, tels que le xyloglucane et le rhamnogalacturonane-I, nécessite l'action concertée d'enzymes d'interconversion des nucléotides-sucres, des transporteurs de nucléotides-sucres et de glycosyltransférases, dont un certain nombre a été identifié, comme décrit dans la partie B de ce chapitre.

Les glycosyltransférases sont des protéines membranaires de type II, ayant un seul domaine transmembranaire, avec un site catalytique dans la lumière d'une saccule golgienne. Les enzymes d'interconversion des nucléotides-sucres peuvent également être des protéines transmembranaires de type II ou bien des protéines solubles, souvent périphériques et associées à un empilement golgien, et d'autres peut-être situées dans la lumière d'une saccule golgienne. Enfin, les transporteurs de nucléotides-sucre sont des protéines membranaires présentent dans la memebrane golgienne et possédant plusieurs domaines transmembranaires (**Figure 34**).

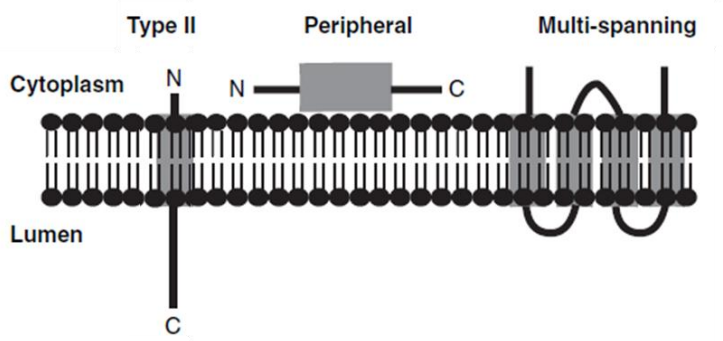

Figure 34 : Les différents types de protéines (adapté de Banfield et al., 2011).
« *Type II* » : Les protéines ont un domaine transmembranaire avec un domaine catalytique luminal, « *Peripheral* » : ce sont des protéines solubles souvent associées à des partenaires transmembranaires, « *Multispanning* » : protéines avec plusieurs domaines transmembranaires.

Les approches de biochimie, de bio-informatique et d'imagerie ont permis d'apporter des preuves plus ou moins directes sur le fonctionnement de ces différents acteurs en complexes enzymatiques golgiens pour la synthèse des polysaccharides pariétaux. Par exemple, il a été montré que pour la synthèse de l'homogalacturonane (Atmodjo et al., 2011), la galacturonosyltransférase AtGAUT1 fonctionne en complexe avec une autre protéine nommée AtGAUT7, qui bien que présentant des similarités avec AtGAUT1, n'a pas d'activité transférase. Ces deux protéines sont membranaires de type II, mais la région N-terminale et le domaine transmembranaire de AtGAUT1 seraient clivés et son site catalytique serait lié par des liaisons covalentes et non-covalentes au site catalytique de AtGAUT7 (**Figure 35**). Une analyse protéomique a également démontrée qu'une douzaine d'autres protéines étaient potentiellement associées à ce complexe.

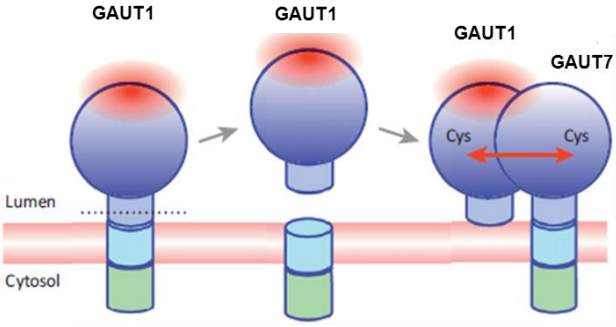

Figure 35 : Association des protéines AtGAUT1 et AtGAUT7 (adapté de Oikawa et al., 2012).
La partie N-terminale et le domaine transmembranaire d'AtGAUT1 sont clivés, puis la partie C-terminale possédant le site catalytique est associé *via* des cystéines à la partie C-terminale d'AtGAUT7.

III-3-2-Complexes enzymatiques impliqués dans la synthèse du XyG

Il a été montré que la glucane synthase AtCSLC4 et la xylosyltransférase AtXXT1 fonctionnaient certainement en complexe d'après des études biochimiques effectuées *in vitro* (Hayashi et al., 1981, 1988). Plus récemment, Chou et al. (2012) ont démontré par différentes méthodologies *in vitro* et *in vivo* l'existence d'homodimères de la glucane synthase AtCSLC4-AtCSLC4 et de la xylosyltransférase AtXXT2-AtXXT2 (également montré par Pattathil et al., 2005) , et d'hétérodimères AtXXT1-AtXXT2, AtXXT2-AtXXT5 et AtXXT5-AtCSLC4.

L'UDP-glucose épimérase AtUGE4, qui transforme l'UDP-glucose en UDP-galactose, participe à la galactosylation du XyG. Elle est cytosolique, mais également localisée en périphérie de l'appareil de Golgi, et pourrait ainsi être associée à la galactosyltransférase AtMUR3 (Barber et al., 2006 ; NGuema-Ona et al., 2006). AtUGE2, une autre épimérase, agit synergiquement avec AtUGE4, et ces deux protéines solubles peuvent former des homodimères et également des hétérodimères entre elles, mais avec une faible interaction (Rosti et al., 2007).

La synthèse du GDP-L-fucose (ou 6-désoxy-L-galactose) à partir du GDP-D-mannose nécessite l'action d'une GDP-D-mannose-4,6-déshydratase AtGMD2/MUR1 et d'une 3,5-épimérase-4-réductase AtGER1/FX. Nakayma et al. (2003) ont montré que ces deux protéines cytosoliques formaient un complexe, et que la protéine AtGER1/FX était même importante pour garder l'intégrité de la protéine AtGMD2/MUR1 (**Figure 36**).

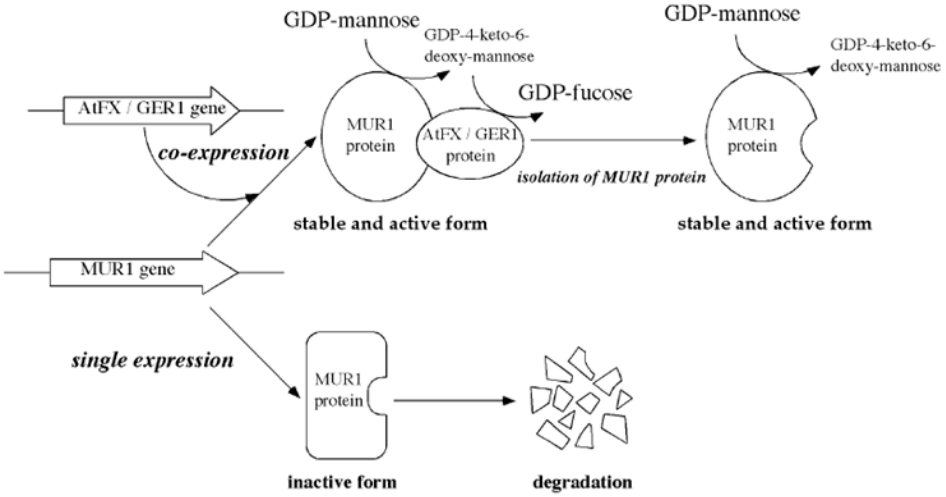

Figure 36 : Association des protéines AtFX/GER1 et AtMUR1/GMD2 (Nakayama et al., 2003).
L'association de la protéine AtGER1/FX à la protéine AtGMD2/MUR1 permet de maintenir cette dernière dans une forme stable et active.

III-3-2-Complexes enzymatiques impliqués dans la synthèse du RG-I

Comme il a été vu dans la partie B, peu de glycosyltransférases impliquées dans la synthèse du RG-I ont été identifiées. Récemment, Liwanag et al. (2012) ont réussi à identifier une β(1,4)galactan β(1,4)galactosyltransférase AtGALS1, mais il n'ont pas testé si cette dernière était associée en oligomères.

L'UDP-L-arabinopyrannose est synthétisé par les UDP-D-xylose 4-épimérases, or *in planta* les pectines contiennent du L-arabinofuranose transféré par des arabinosyltransférases. L'action intermédiaire d'UDP-arabinose mutases, nommées RGP (voir partie B), convertissant l'UDP-arabinopyranose en UDP-arabinofuranose est donc nécessaire. En 2011, Rautengarten et al. ont montré *in vitro* l'existence de différents hétéro-oligomères AtRGP1-AtRGP2-AtRGP5 ; AtRGP3-AtRGP1 et AtRGP4-AtRGP2-AtRGP1. De plus, les auteurs ont montré qu'AtRGP1, -2 et -5 s'associent *in vivo* en complexes cytosoliques, dans l'environnement très proche des vésicules golgiennes.

De Pino et al. (2007), ont montré que la glycosylation des RGPs facilitait leur association en complexe, et ont proposé que l'intérêt de ces protéines de fonctionner en complexe serait de faciliter leur association aux vésicules golgiennes. Plus récemment, ces mêmes auteurs ont confirmé et affiné leur hypothèse en étudiant les RGPs du riz (De Pino et al., 2013). Ils ont montré que la formation de complexes s'effectuait à des moments spécifiques du développement, puisqu'ils sont présents sur de jeunes plantules et absents sur des graines non germées. La formation d'un complexe est donc très probablement associée à la synthèse d'un polysaccharide durant l'élongation de la plante. De plus, une expression différentielle des transcrits des RGPs de classe 1 et 2 a été observée. Ainsi, ils proposent que les RGPs de classe 1 soient glycosylées dans le cytosol, ce qui enclenche le recrutement de RGPs de classe 2, voire de classe 1. Une fois les RGPs complexées, une RGP de classe 2 pourrait se lier aux vésicules golgiennes (**Figure 37**). Les RGPs de classe 2 n'ont pas d'activité mutase.

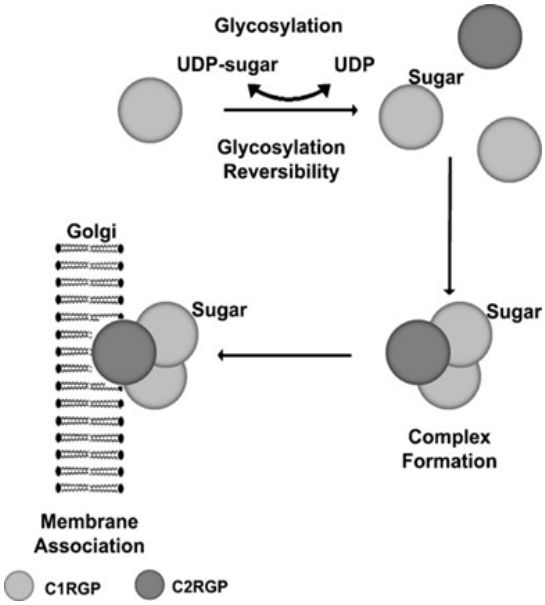

Figure 37 : Oligomérisation des protéines RGPs (De Pino et al., 2013).
Une fois la glycosylation d'une RGP de classe 1, le recrutement de RGPs de classe 2, voire de classe 1, peut s'effectuer, puis le complexe formé peut être lié aux vésicules golgiennes via une RGP de classe 2 (C1RGP : RGP classe 1, C2RGP : RGP classe 2)

III-4- Les enzymes de synthèse sont spécifiques d'un compartiment golgien

Schoberer et Strasser (2011) ont résumé plusieurs études ayant utilisé les techniques d'imagerie *in vivo* pour compartimenter les glycosyltransférases impliquées dans la synthèse golgienne des N-glycanes chez les plantes (ce sont aussi des protéines membranaires de type II). Ces études ont testé la présence ou non d'une colocalisation des différentes glycosyltransférases testées avec l'α2,6-sialyltransférase de rat, qui est un marqueur reconnu de la face *trans*-Golgi à l'échelle de la microscopie électronique à transmission (Boevink et al., 1998 ; Wee et al., 1998).

D'autres études effectuées à l'échelle de la microscopie électronique à transmission ont montré que ces enzymes étaient spécifiquement localisées dans un seul type de compartiment golgien *cis* ou médian (Nebenführ et al., 1999; Pagny et al., 2003 ; Saint-Jore-Dupas et al. 2006 ; Reichardt et al., 2007; Staehelin and Kang, 2008).

Actuellement, la cartographie à l'échelle de la microscopie électronique au sein de l'appareil de Golgi des enzymes impliquées dans la synthèse du XyG ou du RG-I est très peu connue (Chevalier et al., 2010). Cependant, plusieurs études d'immunomarquage ont permis d'effectuer la cartographie golgienne d'épitopes polysaccharidiques spécifiques de la chaîne principale ou de chaînes ramifiées fucosylées du XyG (Zhang and Staehelin, 1992; Driouich et

al., 1993; Staehelin et Driouich, 1997). Celles-ci ont montré que ces épitopes étaient associés aux citernes *trans* et au réseau *trans*-golgien. Zhang et Staehelin (1992) ont également étudié la cartographie golgienne d'un épitope polysaccharidique associé à la chaîne principale du RG-I, qui a été détecté dans les citernes *cis* et median.

En tant que préambule à l'ensemble de ces travaux, nous avons écrit et publié une revue synthétisant l'ensemble des connaissances sur la synthèse golgienne et la sécrétion des polysaccharides de la paroi primaire des plante supérieures, présentée ci-après.

Papier N°1: Revue scientifique

Introduction :

Golgi-mediated synthesis and secretion of matrix polysaccharides of the primary cell wall of higher plants.

Azeddine Driouich, Marie-Laure Follet-Gueye, Sophie Bernard, Sumaira Kousar, Laurence Chevalier, Maite Vicré-Gibouin, Olivier Lerouxel

Frontiers in Plant Science (2012) 3: 79.

frontiers in
PLANT SCIENCE

REVIEW ARTICLE
published: 30 April 2012
doi: 10.3389/fpls.2012.00079

Golgi-mediated synthesis and secretion of matrix polysaccharides of the primary cell wall of higher plants

Azeddine Driouich[1]*, Marie-Laure Follet-Gueye[1], Sophie Bernard[1], Sumaira Kousar[3], Laurence Chevalier[2], Maïté Vicré-Gibouin[1] and Olivier Lerouxel[3]

[1] *Laboratoire «Glycobiologie et Matrice Extracellulaire Végétale», UPRES EA 4358, Institut Federatif de Recherche Multidisciplinaire sur les Peptides, Plate-forme de Recherche en Imagerie Cellulaire de Haute Normandie, Université de Rouen, Mont Saint Aignan, France*
[2] *Institut des Matériaux/UMR6634/CNRS, Faculté des Sciences et Techniques, Université de Rouen, St. Etienne du Rouvray Cedex, France*
[3] *Centre de Recherches sur les Macromolécules végétales–CNRS, Université Joseph Fourier, Grenoble, France*

Edited by:
Marisa Otegui, University of Wisconsin at Madison, USA

Reviewed by:
Markus Pauly, University of California Berkeley, USA
Paul Knox, University of Leeds, UK

****Correspondence:***
Azeddine Driouich, Laboratoire "Glycobiologie et Matrice Extracellulaire Végétale" UPRES EA 4358, Institut Federatif de Recherche Multidisciplinaire sur les Peptides, Plate-forme de Recherche en Imagerie Cellulaire de Haute Normandie, Université de Rouen, Rue Tesnière, Bâtiment Henri Gadeau de Kerville, 76821. Mont Saint Aignan, Cedex, France.
e-mail: azeddine.driouich@univ-rouen.fr

The Golgi apparatus of eukaryotic cells is known for its central role in the processing, sorting, and transport of proteins to intra- and extra-cellular compartments. In plants, it has the additional task of assembling and exporting the non-cellulosic polysaccharides of the cell wall matrix including pectin and hemicelluloses, which are important for plant development and protection. In this review, we focus on the biosynthesis of complex polysaccharides of the primary cell wall of eudicotyledonous plants. We present and discuss the compartmental organization of the Golgi stacks with regards to complex polysaccharide assembly and secretion using immuno-electron microscopy and specific antibodies recognizing various sugar epitopes. We also discuss the significance of the recently identified Golgi-localized glycosyltransferases responsible for the biosynthesis of xyloglucan (XyG) and pectin.

Keywords: cell wall, immunocytochemistry, glycosyltransferases, Golgi, polysaccharides, plants

INTRODUCTION

One of the most important functional properties of the plant Golgi apparatus is its ability to synthesize complex matrix polysaccharides of the cell wall. Unlike cellulose which is synthesized at the plasma membrane and glycoproteins whose protein backbones are generated in the endoplasmic reticulum, the cell wall matrix polysaccharides (pectin and hemicelluloses) are assembled exclusively in the Golgi cisternae and transported to the cell surface within Golgi-derived vesicles (Driouich et al., 1993; Lerouxel et al., 2006).

The synthesis of cell wall matrix polysaccharides occurs through the concerted action of hundreds of glycosyltransferases. These enzymes catalyze the transfer of a sugar residue from an activated nucleotide–sugar onto a specific acceptor. The activity of these enzymes depends, in turn upon nucleotide–sugar synthesizing/interconverting enzymes in the cytosol, and also on the nucleotide–sugar transporters necessary for sugar transport into the lumen of Golgi stacks and subsequent polymerization.

Because cell wall matrix polysaccharides exhibit a high structural complexity, their biosynthesis must be adequately organized and a certain degree of spatial organization/coordination must prevail within Golgi compartments, not only between glycosyltransferases themselves, but also between glycosyltransferases nucleotide–sugar transporters and nucleotide–sugar interconverting enzymes (Seifert, 2004; Reiter, 2008).

Cell wall matrix polysaccharides are known to confer important functions to the cell wall in relation with many aspects of plant life including cell growth, morphogenesis and responses to abiotic, and biotic stresses. Plant cell walls are also an important source of raw materials for textiles, pulping and, potentially, for renewable biofuels or food production for humans and animals (Cosgrove, 2005; Pauly and Keegstra, 2010).

THE PRIMARY CELL WALL IS COMPOSED OF DIVERSE COMPLEX CARBOHYDRATES

Plants invest a large proportion of their genes (~10%) in the biosynthesis and remodeling of the cell wall (Arabidopsis Genome Initiative, 2000; International Rice Genome Sequencing Project, 2005; Tuskan et al., 2006).

Cell walls of flowering plants are highly diverse and heterogeneous (Popper et al., 2011). They are composed of a variety of complex carbohydrates whose compositional and structural properties are controlled spatially and temporally as well as at the tissue and cell levels (Roberts, 1990; see also Burton et al., 2010).

The primary wall of eudicotyledonous plants comprises cellulose microfibrils and a xyloglucan network embedded within a matrix of non-cellulosic polysaccharides and proteins (i.e., glycoproteins and proteoglycans). Four major types of non-cellulosic polysaccharides are found in the primary walls of plant cells (in taxa outside the gramineae), namely the neutral hemicellulosic polysaccharide xyloglucan (XyG) and three main pectic polysaccharides, homogalacturonan (HG), rhamnogalacturonan I and

rhamnogalacturonan II (RG-I and RG-II; Carpita and Gibeaut, 1993; Mohnen, 2008; Scheller and Ulvskov, 2010).

XyG consists of a β-D-(1-4)-glucan backbone to which are attached side chains containing xylosyl, galactosyl–xylosyl, or fucosyl–galactosyl–xylosyl residues. In eudicotyledonous plants, XyG is the principal polysaccharide that cross-links the cellulose microfibrils. It is able to bind cellulose tightly because its β-D-(1-4)-glucan cellulose-like backbone can form numerous hydrogen bonds with the microfibrils. A single XyG molecule can therefore interconnect separate cellulose microfibrils. This XyG-cellulose network forms a major load-bearing structure that contributes to the structural integrity of the wall and the control of cell expansion (Cosgrove, 1999, 2005; Scheller and Ulvskov, 2010).

The pectic matrix is structurally complex and heterogeneous. HG domains consist of α-D-(1-4)-galacturonic acid (GalA) residues, which can be methyl-esterified, acetylated, and/or substituted with xylose to form xylogalacturonan (Willats et al., 2001; Vincken et al., 2003). De-esterified blocks of HG can be cross-linked by calcium producing a gel matrix which is believed to be essential for cell adhesion (Jarvis, 1984). RG-I domains contain repeats of the disaccharide [-4-α-D-GalA-(1-2)-α-L-Rha-(1-)] and the rhamnosyl residues can possess oligosaccharide side chains consisting predominantly of β-D-(1—4)-galactosyl- and/or α-L-(1-5)-arabinosyl-linked residues (McNeil et al., 1982). Side chains of RG-I can also contain α-L-fucosyl, β-D-glucuronosyl, and 4-*O*-methyl β-D-glucuronosyl residues and vary in length depending on the plant source (O'Neill et al., 1990). These chains are believed to decrease the ability of pectic molecules to cross-link and form a stable gel network, and are thereby able to influence the mechanical properties of the cell wall (Hwang and Kokini, 1991). In addition, the structure and tissue distribution of arabinan- or galactan-rich side chains of RG-I have been shown to be regulated during cell growth and development of many species (for review see Willats et al., 2001; Scheller et al., 2007; Harholt et al., 2010).

RG-II is the most structurally complex pectic polysaccharide discovered so far in plants and is of a relatively low molecular mass (5–10 Kda; Ridley et al., 2001). It occurs in the cell walls of all higher plants as a dimer (dRG-II-B) that is cross-linked by borate di-esters (Matoh et al., 1993; Ishii and Matsunaga, 1996; Kobayashi et al., 1996; O'Neill et al., 1996). The backbone of RG-II is composed of a HG-like structure containing at least eight α-D-(1-4)-GalA-linked residues to which four structurally different oligosaccharide chains, denoted A, B, C, and D, are attached. The C and D side chains are attached to C-3 of the GalA residues of the backbone whereas A and B are attached to C-2 of GalA residues (O'Neill et al., 2004). The C chain corresponds to a disaccharide that contains rhamnose and 2-keto-3-deoxy-D-*manno*-octulosonic acid (Kdo), whereas the D chain is a disaccharide of 2-keto-3-deoxy-D-lyxo-heptulosaric acid (Dha) and arabinose (O'Neill et al., 2004). The A and B oligosaccharide chains are both composed of eight to ten monosaccharides and are attached by a β-D-apiose residue to O-2 of the backbone. A D-galactosyl residue (D-Gal) occurs on the B chain. RG-II plays an important role in the regulation of porosity and mechanical properties of primary cell walls (Ishii et al., 2001). This in turn has an important impact on growth and development as has been shown from studies using various *Arabidopsis* mutants (O'Neill et al., 2001; Reuhs et al., 2004; Voxeur et al., 2011).

As for hemicellulosic polysaccharides, it is worth to note that glucurono(arabino)xylan (GAX) does exist in the primary cell walls of eudicotyledonous although at very limited amounts. It is however mostly present in the secondary walls of eudicotyledonous as well as in both the primary and secondary walls of grasses (see also Vogel, 2008 for a difference in polysaccharide composition of the cell walls between grasses and eudicots). GAX of eudicotyledonous primary cell wall is composed of a linear β-D-(1 —4)-xylose backbone substituted with both neutral and acidic side chains. The acidic side chains are terminated with glucuronosyl or 4-*O*-methyl glucuronosyl residues, whereas the neutral side chains are composed of arabinosyl and/or xylosyl residues (Darvill et al., 1980; Zablackis et al., 1995; Vogel, 2008). GAX is also known to be synthesized within Golgi stacks and significant advances have recently been made in understanding its biosynthesis (Faik, 2010). However, this is beyond the focus of this review and only major polysaccharides of the primary cell walls of eudicotyledonous are considered here below.

THE ROLE OF THE GOLGI APPARATUS IN COMPLEX POLYSACCHARIDE BIOSYNTHESIS

THE GOLGI IMPLICATION IN THE CONSTRUCTION OF THE CELL WALL

In higher plants, the Golgi apparatus plays a fundamental role in "the birth" of the cell wall. During cytokinesis, a new cell wall is formed and starts to assemble with the transport of Golgi-derived secretory vesicles to the center of a dividing cell. Fusion of these vesicles gives rise to a thin membrane-bound structure, the cell plate, which undergoes an elaborate process of maturation leading to a fully functional cell wall (Staehelin and Hepler, 1996; Cutler and Ehrhardt, 2002; Segui-Simarro et al., 2004). Also to perform the plant cell growth, new polysaccharides are delivered to growing cell wall by fusion of Golgi vesicles with the plasma membrane (Cosgrove, 2005).

The Golgi apparatus of plant cells is a dynamic and organized organelle consisting of a large number of small independent Golgi stacks that are randomly dispersed throughout the cytoplasm. At the confocal microscopy level, individual green fluorescent protein (GFP)-tagged Golgi stacks (around 1 μm in diameter) appear as round disks, small rings, or short lines depending on their orientation (Nebenführ et al., 1999; Ritzenthaler et al., 2002). At the level of transmission electron microscopy in high pressure frozen/freeze substituted cells, each stack appears to consist of three types of cisternae, designated *cis*, medial, and *trans* that are defined based on their position within a stack and their unique morphological features (Staehelin et al., 1990; Staehelin and Kang, 2008). This morphological polarity reflects different functional properties of Golgi compartments (**Figure 1**; Staehelin et al., 1990; Driouich and Staehelin, 1997). The number of stacks per cell, as well as the number of cisternae within an individual stack, varies with the cell type, the developmental stage of the cell and the plant species (Staehelin et al., 1990; Zhang and Staehelin, 1992).

The *trans* Golgi network (TGN) is a branched tubulo-vesicular structure that is frequently located close to *trans* cisternae. However, the TGN can be found remote from the Golgi stack located

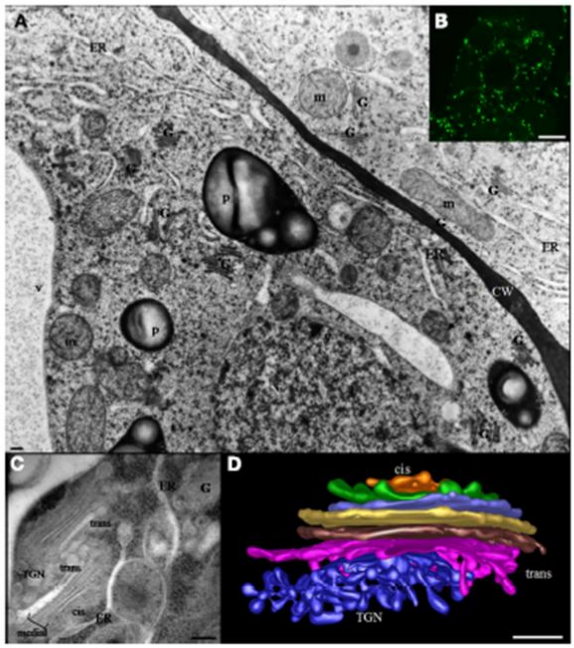

FIGURE 1 | (A) Electron micrograph of suspension-cultured tobacco cells preserved by high pressure freezing showing the random distribution of Golgi stacks throughout the cytoplasm. The bar represents 0.5 μm. **(B)** Confocal microscopy image showing distribution of Golgi stacks in suspension-cultured tobacco (BY-2) cells. Golgi stacks-expressing the Golgi XyG-synthesizing enzyme (XyG –GalT/MUR3) fused to GFP are visible as bright green spots. The bar represents 8 μm. **(C)** Two Golgi stacks and associated *trans* Golgi network (TGN) in a tobacco BY-2 suspension-cultured cell. *Cis*-, medial, and *trans* type of cisternae as well as the TGN are indicated. The bar represents 0.1 μm. **(D)** Electron tomographic model of a Golgi stack in a columella root cell of *Arabidopsis*. CW, cell wall; ER, endoplasmic reticulum; G, Golgi stack; m, mitochondria; N, nucleus; P, plastid; TGN, trans Golgi network; V, vacuole.

throughout the cytosol as an independent compartment. Two types of TGN compartments have been described and referred to as an early and a late TGN (see Staehelin and Kang, 2008). The plant TGN plays a major role in sorting of proteins and it represents a meeting point of secretory, endocytosis, and membrane recycling pathways. Recent studies have shown that certain TGN types, can serve also as early endosomes and thus have been termed TGN-Early endosomes (Dettmer et al., 2006; Richter et al., 2009; Viotti et al., 2010).

In contrast to the Golgi complex in mammalian cells that has a fixed location near the centrosomes, Golgi units in plants appear to move actively throughout the cytoplasm (Boevink et al., 1998; Nebenführ et al., 1999). GFP-fusions have allowed the study of Golgi dynamics *in vivo* and have shown that each Golgi unit can move at a slow or high speed (up to 5 μm/s) without loosing structural integrity (Boevink et al., 1998; Nebenführ et al., 1999; Brandizzi et al., 2002). In addition, cytoskeletal depolymerization studies have indicated that the movement of Golgi stacks depends on actin filaments rather than on microtubules (Nebenführ et al., 1999). Indeed, it is now established that the movement of Golgi stacks in plant cells occurs along actin filaments driven by myosin motors (Staehelin and Kang, 2008). In the context of this review, it is worth noting that actin filaments interact with Golgi stacks *via* an actin-binding protein, KATAMARI 1/MURUS3 – that is also known as a glycosyltransferase required for cell wall biosynthesis (see below; Tamura et al., 2005). KATAMARI 1 has been shown to be involved in maintaining the organization and dynamics of Golgi membranes.

As in animal cells (Rabouille et al., 1995), the plant Golgi apparatus functions in the processing and modification of N-linked glycoproteins (Pagny et al., 2003; Saint Jore Dupas et al., 2006; Schoberer and Strasser, 2011); but the bulk of the biosynthetic activity of this organelle is devoted to the assembly of different subtypes of complex, non-cellulosic polysaccharides of the cell wall such as pectin and hemicelluloses.

The first studies implicating plant Golgi stacks in cell wall biogenesis date back to the 60 and 70 and involved cytochemical staining as well as autoradiographic experiments with radiolabeled sugars (Pickett-Heaps, 1966, 1968; Harris and Northcote, 1971; Dauwalder and Whaley, 1974). These investigations have shown that Golgi cisternae and Golgi-derived vesicles are rich in carbohydrates and that a similar carbohydrate content is found in the cell plate, the cell wall and in Golgi-enriched fractions. Additionally, biochemical evidence for the role of the Golgi apparatus in the assembly of cell wall polysaccharides was obtained from fractionation experiments in which several glycosyltransferase activities (e.g., xylosyltransferase, arabinosyltransferase, fucosyltransferase) were detected in Golgi membranes (Gardiner and Chrispeels, 1975; Green and Northcote, 1978; Ray, 1980). Further biochemical investigations, reported in the eighties and nineties, allowed the identification and partial characterization of Golgi-associated enzymes specifically involved in the synthesis of XyG and pectic polysaccharides (Camirand et al., 1987; Brummell et al., 1990; Gibeaut and Carpita, 1994).

More recently, a proteomic method called LOPIT, for Localization of Organelle Proteins by Isotope Tagging, has been developed in order to determine the subcellular localization of membrane proteins in organelles of the secretory pathway such as Golgi stacks (Dunkley et al., 2004, 2006). This approach has allowed the identification of the α1,6-xylosyltransferase (AtXT1) involved in XyG biosynthesis, in the Golgi apparatus (Dunkley et al., 2004).

In connection with XyG biosynthesis, it is remarkable to note that the structure of XyG present in isolated Golgi membranes has been investigated using oligosaccharide mass profiling (OLIMP) method (Obel et al., 2009). This study has revealed subtle differences in the structure of the polymer with XXG and GXXG fragments being more abundant in Golgi-enriched fraction as compared to the cell wall. However, due to the inability of subfractionating plant Golgi stacks into *cis*, medial, and *trans* cisternae, it is not possible to associate a XyG oligosaccharide to a specific sub-compartment of the Golgi apparatus. For similar reasons, it is still not possible neither to determine how the enzymes are spatially organized and how complex polysaccharides are assembled within Golgi sub-compartments using biochemical methods.

SPATIAL ORGANIZATION OF THE COMPLEX POLYSACCHARIDE ASSEMBLY PATHWAY IN GOLGI STACKS: INSIGHTS FROM IMMUNO-ELECTRON MICROSCOPY

Progress toward understanding the compartmentalization of matrix cell wall polysaccharide biosynthesis has come from immuno-electron microscopical analyses with antibodies directed against specific sugar epitopes. In most cases, these immunolabeling studies have been performed on a variety of cells prepared by high pressure freezing, a cryofixation technique that is recognized as providing excellent preservation of Golgi stacks thereby allowing different cisternal subtypes to be easily distinguished (Staehelin et al., 1990; Zhang and Staehelin, 1992; Driouich et al., 1993; Follet-Gueye et al., 2012). More recently, a combination of cryofixation/freeze substitution with Tokuyasu cryosectioning have been used to immunolocalize polysaccharide epitopes in Golgi stacks of *Arabidopsis* (Stierhof and El Kasmi, 2010). This technology is quite promising and should be able to provide interesting information on the localization of epitopes within plant Golgi cisternae.

Quantitative immunolabeling experiments using antibodies recognizing either the XyG backbone (anti-XG antibodies: Moore et al., 1986; Lynch and Staehelin, 1992) or an α-L-Fuc*p*-(1-2)-β-D-Gal*p* epitope of XyG side chains in sycamore cultured cells have shown that the epitopes localize to *trans* cisternae and the TGN (Zhang and Staehelin, 1992). These data suggested that the synthesis of XyG occurs exclusively in late compartments of the Golgi and that no precursor forms of XyG are made in *cis* and medial cisternae. The use of these antibodies on clover and *Arabidopsis* root tip cells have also suggested that the synthesis of XyG takes place in *trans* Golgi cisternae and the TGN (Moore et al., 1991; Driouich et al., 1994). Nevertheless, it could be argued that the sugar epitopes recognized by both antibodies are not accessible until they reach the *trans* and TGN compartments, or that the antibodies do not bind XyG precursor forms in *cis* and medial cisternae. More recently, Viotti et al. (2010) have also shown that fucosylated epitopes of XyG occur preferentially in *trans* cisternae and the TGN using thawed ultrathin cryosections of high pressure frozen/freeze substituted and rehydrated *Arabidopsis* root tip cells. Therefore, it is necessary to localize XyG-synthesizing enzymes within Golgi cisternae to determine whether XyG synthesis is exclusively limited to *trans* and TGN cisternae. Although no antibody against any XyG-synthesizing enzyme is currently available, one possible approach of addressing this issue is to produce transgenic plants expressing GFP-tagged glycosyltransferases, followed by localization with anti-GFP antibodies. Such a strategy has been successfully used to study the compartmentation of enzymes involved in the processing of N-linked glycoproteins, including a β-1,2-xylosyltransferase responsible for the addition of β-1,2 xylose residues and an α-1,2-mannosidase responsible for the removal of α-1,2 mannose residues in tobacco suspension-cultured cells (Follet-Gueye et al., 2003; Pagny et al., 2003; Saint Jore Dupas et al., 2006). The same strategy has been recently applied to enzymes involved in the biosynthesis of XyG side chains including α-1,6-xylosyltransferase (AtXT1), β-1,2-galactosyltransferase (AtMUR3), and α-1,2-fucosyltransferase (AtFUT1; Chevalier et al., 2010). Immunogold localization of these GFP-tagged glycosyltransferases has demonstrated that AtXT1–GFP is mainly located in the *cis* and medial cisternae, AtMUR3–GFP is predominantly associated with medial cisternae and AtFUT1–GFP mostly detected over *trans* cisternae suggesting that initiation of XyG side chains occurs in early Golgi compartments in tobacco suspension-cultured (BY-2) cells.

Another interesting approach to study sub-Golgi localization of glycosyltransferases is through development of *in silico* predictors based on the transmembrane domain of these enzymes. Such an approach employing a support vector machine (SVM) algorithm has been recently used to predict the localization of several human and mouse glycosyltransferases and glycohydrolases within Golgi sub-compartments (van Dijk et al., 2008). This is an interesting methodology to apply for the prediction of sub-Golgi localization of the known plant glycosyltransferases involved in cell wall biosynthesis. Using this approach AtRGXT1 and AtRGXT2 -two α-1,3-xylosyltransferases involved in the synthesis of the pectic polysaccharide RG-II- have been predicted to be confined to the TGN (P. Ulskov, personal communication).

As for XyG synthesis, similar immunocytochemical studies using antibodies raised against pectin epitopes (including JIM7, anti-PGA/RG-I, and CCRCM2) has allowed a partial characterization of the assembly pathway of homogalacturonan (HG) and RG-I within Golgi cisternae (Zhang and Staehelin, 1992). The polyclonal anti-PGA/RG-I antibodies (recognizing un-esterified HG) were shown to label mostly *cis* and medial cisternae in suspension-cultured sycamore cells as well as in clover root cortical cells (Moore et al., 1991; Zhang and Staehelin, 1992). In contrast, JIM7 (specific for methyl-esterified HG) labeling was mostly confined to medial and *trans* cisternae (**Figure 2**). Consistent with this data is the localization of the putative pectin methyltransferase, QUASIMODO2 (Mouille et al., 2007) fused to GFP which was found mainly in medial and *trans* cisternae of Golgi stacks in *Arabidopsis* root tip cells (Chevalier et al., unpublished; **Figure 2**). In addition, the mAb CCRCM-2 which is believed, but not proven, to bind RG-I side chains was found to label *trans* cisternae in sycamore cultured cells (Zhang and Staehelin, 1992). These data suggest that HG is synthesized in its un-esterified form in *cis* and medial Golgi cisternae and, that (i) the methylesterification occurs in both medial and *trans* compartments, and (ii) that side chains of RG-I are added in *trans* cisternae. However, as discussed above for XyG labeling, the absence of labeling in *trans* cisternae and the TGN by anti-PGA/RG-I antibodies, might be due to the inaccessibility of the recognized epitopes in these compartments (because of the methylesterification for instance). This idea is supported by the fact that the same epitopes are localized predominantly in *trans* Golgi cisternae and the TGN in the epidermal cells of clover. Thus, it is not surprising that the compartmentation of cell wall matrix polysaccharides within Golgi cisternae varies in a cell type specific manner. The distribution of XyG and HG in Golgi membranes has also been investigated immunocytochemically in root hair cells of *Vicia villosa* preserved by high pressure freezing (Sherrier and VandenBosch, 1994). Although no quantitative analyses were performed, methyl-esterified HG epitopes recognized by JIM7 were detected within medial and *trans* cisternae, whereas the fucose-containing epitope of XyG (recognized by CCRCM1) was found over *trans* Golgi cisternae. These observations are consistent with those made in sycamore suspension-cultured cells and clover root cortical cells using the same antibodies (Moore et al., 1991; Zhang

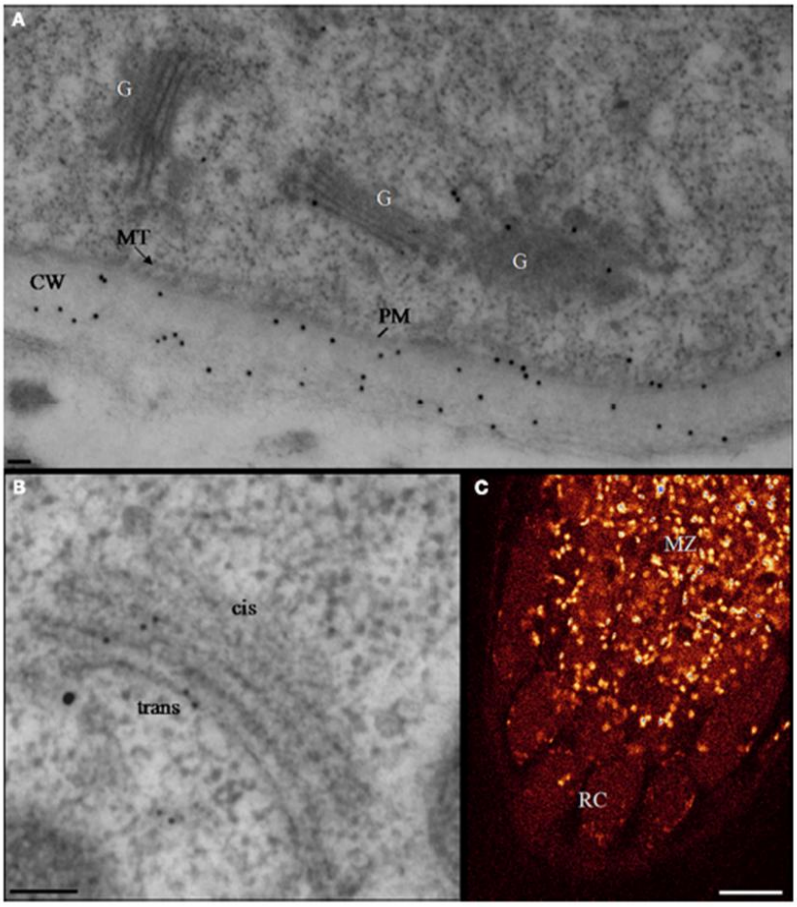

FIGURE 2 | Homogalacturonan localization in transgenic *Arabidopsis* root tips expressing the QUA2–GFP fusion protein. **(A,B)** Electron micrographs illustrating typical double-immunogold labeling of Golgi stacks (G) in *Arabidopsis* root cells with the mAbs JIM7 (20 nm gold particles) or with anti-GFP (10 nm gold particles). HG epitopes and the QUA2–GFP are predominantly associated with the *trans* cisternae and the TGN. The cell wall (CW) is labeled with JIM 7. Bar represents 100 nm. **(C)** A confocal laser fluorescence image of *Arabidopsis* root tip expressing the fusion protein QUA2–GFP. Bright spots represent GFP-stained Golgi units. Scale Bar: 16 μm (Chevalier et al., unpublished). CW, cell wall; G, Golgi stack; MT, microtubule; PM, plasma membrane; MZ, meristematic zone; RC, root cap.

and Staehelin, 1992). However, the *V. villosa* study did not address the issue of RG-I side chain distribution within Golgi stacks using the mAb CCRCM2. Therefore, the use of the more recently produced monoclonal antibodies LM5 and LM6, recognizing β-1,4-D-galactan and α-1,5-D-arabinan epitopes, respectively (Jones et al., 1997; Willats et al., 1998) should prove very useful for extending the "current map" of the pectin assembly pathway within the Golgi cisternae of sycamore cultured cells and *V. villosa* root hairs. Both antibodies have been widely used to study the distribution of galactan and arabinan epitopes within the cell walls, but relatively very little is known concerning their localization within the endomembrane system. In flax root cells, LM5-containing epitopes have been shown to be present mostly in *trans* cisternae and the TGN (Vicré et al., 1998). Similarly, epitopes recognized by LM5 and LM6 have been quantitatively localized to TGN in tobacco (BY-2) cultures (Bernard et al., unpublished). Therefore, it appears that galactan- and arabinan-containing side chains of RG-I are assembled in the TGN. Whether the enzymes responsible for the addition of these residues are confined to the same Golgi subcompartments remains to be determined by future studies. One of the genes involved in the synthesis of RG-I side chains, namely *ARAD1* (encoding a putative α-1,5-D-arabinosyltransferase) has been recently identified and cloned (see below). The generation of specific antibodies against this glycosyltransferase, or the generation of a GFP-tagged protein should help us to understand more about its specific localization within Golgi compartments. To extend our understanding of RG-I synthesis within Golgi stacks, the use of the new monoclonal antibodies specifically raised against the RG-I backbone (Ralet et al., 2010) or the LM13 recognizing longer oligoarabinosides than LM6, should be very helpful.

In contrast to RG-I, information on the localization and assembly of RG-II within the endomembrane system is missing. RG-II has a complex structure consisting of a HG-like backbone and four side chains that contain specific and unusual sugars including Kdo and apiose (see above). It would certainly be interesting to find out whether the backbone is assembled in the same compartments as the side chains and whether different side chains are assembled in the same or distinct compartments. The elucidation of RG-II assembly within sub-compartments of Golgi stacks requires the generation of antibodies specific for the sugar epitopes of the backbone and for the epitopes associated with different side chains, as well as the associated immuno-electron microscopy studies.

It is generally accepted that the transport of Golgi products, including glycoproteins and complex polysaccharides, to the cell surface occurs by bulk flow (Hadlington and Denecke, 2000). To date, no specific signals responsible for targeting and transport of such products to the cell wall have been found associated with any protein or polysaccharide. It has been shown that Golgi-derived secretory vesicles mediating such a transport vary in size and are capable of carrying mixed classes of complex polysaccharides (Sherrier and VandenBosch, 1994) or both polysaccharides and glycoproteins (see Driouich et al., 1994). Nevertheless, using secretory carrier membrane protein 2 (SCAMP2) from *Nicotiana tabacum*, a mobile secretory vesicle cluster (SVC) generated from the TGN has been recently identified in *Arabidopsis* tissues and tobacco suspension-cultured BY-2 cells (Toyooka et al., 2009). These clusters formed by budding of clathrin coated vesicles from the late TGN, are highly labeled with antibodies specific for either complex glycan or homogalacturonan epitopes (JIM7), suggesting that SVC are involved in mass transport from Golgi stacks to the cell surface. It is also possible that the processing of Golgi products such as cell wall polymers may continue to occur within the vesicles during their transport to the cell surface (Zhang et al., 1996).

GLYCOSYLTRANSFERASES AND SUGAR-CONVERTING ENZYMES INVOLVED IN THE ASSEMBLY OF COMPLEX POLYSACCHARIDES

The Golgi-mediated assembly of complex polysaccharides requires the action of a set of Golgi glycosyltransferases, in addition to nucleotide–sugar transporters and nucleotide–sugar interconversion enzymes (Keegstra and Raikhel, 2001; Seifert, 2004; Reiter, 2008; Reyes and Orellana, 2008). It has been postulated that these partners could interact physically to form complexes within Golgi membranes that would coordinate sugar supply and polymer synthesis (Seifert, 2004; Nguema-Ona et al., 2006).

XYLOGLUCAN BIOSYNTHESIS: GLYCOSYLTRANSFERASES AND OTHER PROTEINS

XyG biosynthesis has long been an interesting, but a challenging, area of investigation. Biosynthesis of the XyG core is expected to require two different catalytic activities, a glucan synthase activity for the backbone and a xylosyltransferase activity adding xylosyl substitutions. Interestingly, Ray (1980) suggested a "cooperative action of β-glucan synthase and UDP-xylose xylosyltransferase in Golgi membranes for the synthesis of a XyG-like polysaccharide." In that study, a UDP-xylose xylosyltransferase activity was measured in Golgi membranes isolated from pea, and the incorporation of xylose was shown to be stimulated by the addition of UDP-glucose. Furthermore, the stimulating effect of UDP-glucose on xylosyltransferase activity was shown to occur only in a pH range where β-glucan synthase is active, suggesting that UDP-glucose stimulates UDP-xylose incorporation by promoting β-glucan synthase activity. Here, the β-glucan synthase produces the required β-1,4-glucan substrate molecule necessary for XyG xylosyltransferase activity. At about the same time, Hayashi and Matsuda (1981a,b) performed a detailed characterization of XyG synthase activity in soybean suspension-cultured cells and demonstrated that XyG synthesis requires the cooperation of XyG β-1,4-glucan synthase and the XyG xylosyltransferase. The authors not only demonstrated that the incorporation of one sugar (xylose or glucose) depended on the presence of the other, but also that xylose was not transferred to a preformed β-1,4-glucan. This observation strongly supports the existence of a multienzyme complex responsible for XyG biosynthesis where glucan synthase and xylosyltransferase activities cooperate tightly (Hayashi, 1989). Since then, considerable efforts have been devoted to the characterization of XyG biosynthesis at the molecular level using functional genomics and the model plant *Arabidopsis thaliana* (Lerouxel et al., 2006; Scheller and Ulvskov, 2010).

We have currently gained a better picture of XyG biosynthesis by identifying and characterizing some of the genes involved (**Table 1**), although without much (if any) understanding of how these enzymes could potentially cooperate to achieve the biosynthesis. For example, the XyG fucosyltransferase AtFUT1 (CAZy GT37, Cantarel et al., 2009) was the first type II glycosyltransferase characterized at the biochemical level (Perrin et al., 1999), and for a long time the only member of this gene family containing nine putative glycosyltransferases to be characterized, as analyses of three other members failed to demonstrate any XyG fucosylation activity (Sarria et al., 2001). Wu et al. (2010) have recently demonstrated the involvement of AtFUT4 and AtFUT6 genes in arabinogalactan proteins fucosylation.

Later, the identification and characterization of the *mur2* mutant of *Arabidopsis* provided the unequivocal proof that the *AtFUT1* gene encodes the unique α-1,2-fucosyltransferase activity responsible for XyG fucosylation in *Arabidopsis* plants (Vanzin et al., 2002). Likewise, one XyG β-1,2-galactosyltransferase (AtMUR3; CAZy GT47) activity was successfully characterized using both mutant analysis (*mur3*) and heterologous expression of the enzyme (Madson et al., 2003). Nevertheless, as the galactose residue of the XyG molecule can be found in two different positions, it seems that at least one XyG galactosyltransferase remains to be identified and characterized. The galactosyl-residues of XyG are known to be *O*-acetylated and only one XyG-*O*-acetyltransferase (AXY4) has been identified so far (Gille et al., 2011) and found to be localized within Golgi stacks.

An important contribution to understanding XyG biosynthesis was also made by the characterization of two α-1,6-xylosyltransferase activities required for XyG xylosylation (CAZy GT34). First, one xylosyltransferase activity (named AtXT1) was identified based on sequence homology with a previously identified α-1,6-galactosyltransferase from fenugreek (Edwards et al., 1999), and characterized as an α-1,6-xylosyltransferase using heterologous expression in *Pichia pastoris* (Faik et al., 2002). Cavalier

Table 1 | List and characteristics of the glycosyltransferase and nucleotide–sugar interconversion enzymes.

Gene		Enzyme characteristics			Arabidopsis mutant		Notes	
Designation	Code	CAZy	Activity	Localization	Designation	Phenotypes	Category	Reference
AtCSLC4	At3g28180	GT2	β-l,4-Glucan synthase	Golgi	None	None		Cocuron et al. (2007)
AtXT1	At3g62720	GT34	α-1,6-Xylosyltransferase	Golgi	*xxt1*	10% Reduction in XyG; *xxt1 xxt2* Double mutant lacks		Faik et al. (2002), Cavalier and Keegstra (2006), Cavalier et al. (2008)
AtXT2	At4g02500	GT34	α-1,6-Xylosyltransferase	Golgi	*xxt1*	20% Reduction in XyG; Detectable amountof XyG	Xyloglucan	Cavalier and Keegstra (2006), Cavalier et al. (2008)
AtMUR3	At2g20370	GT47	β-1,2-Galactosyltransferase	Golgi	*mur3*	Hypocotyls wall strength is 50% reduced, xyloglucan lacks fucogalactosyl sidechain		Madson et al. (2003), Pena et al. (2004)
AtFUT1	At2g03220	GT37	α-1,2-Fucosyltransferase	Golgi	*Mur2*	Hypocotyls wall strength is slightly reduced, xyloglucan lacks fucose substitution		Perrin et al. (1999), Vanzin et al. (2002)
AXY4	Atlg70230	GT	*O*-Acetyltransferase	Golgi	*axy4*	Cell wall XyG extract is non-acetylated		Pena et al. (2004), Gille et al. (2011)
AtFUT4	At2gl5390	GT37	α-1,2-Fucosyltransferase	Golgi	None	None	Arabinogalactan proteins	
AtFUT6	Atlgl4080	GT37	α-1,2-Fucosyltransferase putative	Golgi	None	None		
AtQUA1	At3g25140	GT8	α-1,4-Galacturonosyltransferase	Predicted Golgi	*qua1*	Dwarf, reduced cell adhesion, 25% reduction in cell wall GalA content		Bouton et al. (2002)
AtGAUT1	At3g61130	GT8	α-1,4-Galacturonosyltransferase	Golgi	None	None		Sterling et al. (2006), Dunkley et al. (2004)
AtRGXT1	At4g01770	GT77	α-1,3-Xylosyltransferase	Golgi	*rgxt1*	RG-II from mutant (but not from WT) is an acceptor for a-l,3-xylosyltransferase acitvity		Egelund et al. (2006)
AtRGXT2	At4g01750	GT77	α-1,3-Xylosyltransferase	Golgi	*rgxt2*	RG-II from mutant (but not from WT) is an acceptor for a-l,3-xylosyltransferase acitvity		Egelund et al. (2006)
AtRGXT4	At4g01220	GT77	Xylosyltransferase	Golgi	*mgp4*	Defective for root and pollen tube growth		Fangel et al. (2011), Liu et al. (2011)
AtARAD1	At2g35100	GT47	α-1,5-Arabinosyltransferase	Predicted Golgi	*arad1*	Cell wall composition altered, decrease in RG-I arabinose content	Pectins	Harholt et al. (2006)
AtXGD1	At5g33290	GT47	β-1,3-Xylosyltransferase	Golgi	*xgd1*	*xgd1* mutant lacks detectable XGA in pectin enriched fraction		Jensen et al. (2008)

(Continued)

Table 1 | Continued

Gene		Enzyme characteristics			Arabidopsis mutant		Notes	
Designation	**Code**	**CAZy**	**Activity**	**Localization**	**Designation**	**Phenotypes**	**category**	**Reference**
NpGUT1	–	GT47	Putative β-glucuronytransferase	Predicted Golgi	*nolac-H18*	Callus harbored a cell-cell adhesion defect, and a reduced RG-II dimerisation ability		Iwai et al. (2002)
AtEPC1	At3g55830	GT64	Unknown	Predicted Golgi	*epc1*	Reduced growth habit, defects in vascular formation and reduced cell-cell adhesion in hypocotyls		Singh et al. (2005)
AtQUA2	At1g78240	–	Putative methyltransferase	Golgi	*qua2/tsd2*	Dwarf, reduced cell adhesion, 50% reduction in HG content		Mouille et al. (2007), Krupková et al. (2007)
AtQUA3	At4g00740		Putative methyltransferase	Golgi	*qua3*	No detectable phenotype		Miao et al. (2011)
AtCGR3	At5g65810	–	Putative methyltransferase	Golgi	*cgr3*	Decrease HG methylesterification		Held et al. (2011)
AtUGE4	At1g64440		UDP-glucose epimerase	Cytosolic and Golgi associated	*rhd1* (*uge4*); *reb1*	Reduced root elongation rate, bulging of trichoblast cells, xyloglucan, and arabinogalactan galactosylation defects in roots		Andème-Onzighi et al. (2002), Seifert et al. (2002), Barber et al. (2006), Nguema-Ona et al. (2006)
AtRGP1	At3g02230	GT75	Putative UDP-arabinopyranose mutase	Cytosolic and Golgi associated	*rgp1*	Decrease in L-Ara, l development altered; *rgp1 rgp2* double mutant is lethal (pollen development altered)	Interconversion enzymes	Rautengarten et al. (2011)
AtRGP2	At5g15650	GT75	Putative UDP-arabinopyranose mutase	Cytosolic and Golgi associated	*rgp2*	Decrease in L-Ara; *hpRGP1/2 cell wall is deficient in L-Ara*		

arad1, arabinose deficient 1; At, Arabidopsis thaliana; CSLC4, cellulose synthase-like C4; cgr3, cotton golgi-related 3; epc1, ectopically parting cells1; FUT, fucosyltransferase; hpRGP1/2, hairpin construct targeting RGP1 and RGP2 genes; mgp4, male gametophyte defective 4; nolac-H18, non-organogenic callus with loosely attached cells-H18; Np, Nicotiana plumbaginifolia; qua1, quasimodo1; qua2, quasimodo2; reb1, root epidermal bulging1;rgp1, reversibly glycosylated protein1; rgp2, reversibly glycosylated protein2; rhd1, root hair deficent1; rgxt1, rhamnogalacturonane II xylosyltransferase1; rgxt2, rhamnogalacturonan II xylosyltransferase2; xgd1, xylogalacturonan deficient1; xxt1, xyloglucan xylosyltransferase1; xxt2, xyloglucan xylosyltransferase2.

and Keegstra (2006) extended this work to the characterization of a second xylosyltransferase activity (named AtXT2), encoded by a gene closely related to AtXT1, that promotes an identical reaction to the one catalyzed by AtXT1. Interestingly, the authors also demonstrated that both AtXT1 and AtXT2 are able to catalyze multiple addition of xylosyl residues onto contiguous glucosyl residues of a cellohexaose acceptor *in vitro* (even though the β-linkage introduce a 180° rotation from one glucosyl residue to the other), but non-xylosylated cellohexaose was the preferred acceptor. The observation that both AtXT1 and AtXT2 xylosyltransferase activities were able to perform multiple xylosylation might indicate a reduced substrate specificity of these enzymes as compared to the high specificity of the XyG fucosyl- or galactosyl-transferases. Nevertheless, these results raise the intriguing possibility that AtXT1 and AtXT2 would be fully redundant *in planta* and that both would be able to perform multiple xylosylation. Such a hypothesis is consistent with the characterization of an *Arabidopsis* double mutant for AtXT1 and AtXT2 genes (named *xxt1 xxt2*; xyloglucan xylosyltransferase 1 and 2), which is lacking detectable amounts of XyG *in planta* (Cavalier et al., 2008).

Another enzyme involved in XyG biosynthesis is glucan synthase. While XyG glucan synthase activity has long been studied biochemically (discussed above), efforts to purify and ultimately characterize this enzyme have not been successful. A gene from the Cellulose Synthase-Like C family (*AtCSLC4*; CAZy GT2) was shown to encode a Golgi-localized β-1,4-glucan synthase activity providing a strong candidate for the, as yet, unidentified XyG β-glucan synthase (Cocuron et al., 2007). The candidate gene was identified using a transcriptional profiling strategy taking advantage of nasturtium's capacity to perform rapidly XyG biosynthesis during seed development (Desveaux et al., 1998). This observation supports the hypothesis that the β-1,4-glucan synthase activity identified was involved in XyG biosynthesis. Interestingly, this study also indicates that *AtCSLC4* is co-regulated with *AtXT1* at the transcriptional level and that some degree of interaction occurs at the protein level could possibly alter the length of the β-1,4-glucan synthesized by the AtCSLC4 protein (Cocuron et al., 2007). The results of this study are consistent with earlier reports showing that *in vitro* synthesis of XyG was shown to involve a cooperative action between the glucan synthase and the xylosyltransferase activities (Hayashi, 1989). Recently, the topology of AtCSLC4 was examined using protease protection experiments (Davis et al., 2010). AtCSLC4 was predicted to have six transmembrane domains and the active site facing the cytosol. These data suggest that AtCSLC4 protein would delimitate a pore, the glucan chain being synthesized at the cytosolic side of Golgi cisternae, translocated into the lumen and further substituted by an α-1,6-xylosyltransferase to prevent β-1,4-glucan chain aggregation. A physical cooperation between AtCSLC4 and AtXT1 or AtXT2 could then be envisioned to rationalize this process. Recently, Chevalier et al. (2010) have shown that AtXT1–GFP is mainly associated with *cis* and medial Golgi cisternae in transformed tobacco suspension-cultured (BY-2) cells. A similar approach to localize the AtCSL4 would be highly instructive. Another approach would be the design of a tagged version of either AtXT1 or AtXT2, taking advantage of the characterization of *xxt1/xxt2* double mutant (Cavalier et al., 2008) and further use the tagged version of the xylosyltransferases to pull down interacting candidate proteins. Then the interaction could be examined using bimolecular fluorescence complementation (BiFC) approach as previously performed for cellulose biosynthesis (Desprez et al., 2007).

XyG biosynthesis does not only depend upon the cooperation between glycosyltransferase activities, but might also require close interaction between glycosyltransferases and nucleotide–sugar interconversion enzymes. The study on the *reb1/rhd1* mutant of *Arabidopsis*, deficient in one of the five UDP-glucose 4-epimerase isoforms (UGE4) involved in the synthesis of UDP-D-galactose, provided indirect evidence for a possible interaction between UGE4 and a XyG-β-1,2-galactosyltransferase (Nguema-Ona et al., 2006). The authors showed that the galactosylation of XyG, unlike that of pectins (RG-I and RG-II), was absent in specific cells of the mutant and that UGE4 and XyG- β-1,2-galactosyltransferase are co-expressed at the transcriptional level in the root. Thus, it was postulated that the two enzymes might be associated in specific protein complexes involved in the galactosylation of XyG within Golgi membranes. Such an association could be required for an efficient galactosylation of XyG, where UGE4 would channel UDP-Gal to XyG-galactosyl-transferases. The existence of such a hypothetical association was supported by the demonstration that UGE4 was not only present in the cytoplasm but also found associated with Golgi membranes (Barber et al., 2006).

Although it is not the focus of this review, it is of interest to note that some glycosylhydrolases involved in XyG modification have been identified and characterized (Sampedro et al., 2001, 2012; Günl and Pauly, 2011; Günl et al., 2011). These are known to be transported via Golgi-derived vesicles to the apoplastic compartment where they act on the polymers. However, whether these enzymes are transported in the same Golgi vesicles and whether they are able to act on polymers within the vesicles during transport remain to be elucidated.

PECTIN BIOSYNTHESIS: TOWARD IDENTIFICATION OF THE GLYCOSYLTRANSFERASES INVOLVED

Because there is a considerable diversity of monosaccharide units and glycosidic linkages making up pectic polysaccharides, it has been proposed that a minimum of 67 glycosyltransferases would be needed for pectin biosynthesis (Mohnen, 2008). In addition, the complexity of pectic polysaccharides has made the identification and characterization of such glycosyltransferases difficult and, consequently, only a handful have been assigned precise biochemical functions (Egelund et al., 2006; Sterling et al., 2006; Jensen et al., 2008) or suggested to have certain functions (Iwai et al., 2001, 2002; Bouton et al., 2002; Harholt et al., 2006, 2010; Egelund et al., 2007; Fangel et al., 2011; Held et al., 2011; Liu et al., 2011). An additional degree of complexity in pectin synthesis is related to the control of the homogalacturonan methylesterification that requires specific methyltransferase activities, but also specific esterases to adjust methyl-esterification level during plant development (Wolf et al., 2009).

As for XyG biosynthesis, many biochemical studies have been devoted to the characterization of the enzymes involved in HG biosynthesis (Doong and Mohnen, 1998; Scheller et al., 1999). These studies showed that α-1,4-galacturonosyltransferase (GalAT) and HG methyltransferase activities are located in the

lumen of isolated Golgi membranes (Goubet and Mohnen, 1999; Sterling et al., 2001). A HG-GalAT activity was partially purified from solubilized membrane proteins isolated from *Arabidopsis* suspension-cultured cells and trypsin-digested peptides sequencing led to the identification of a candidate gene, named *AtGAUT1* for GAlactUronosylTransferase1 (Sterling et al., 2006). Genome analysis revealed that AtGAUT1 belongs to a large gene family comprising 25 members in *Arabidopsis* that is present in CAZy GT8 along with galactinol synthases and bacterial α-galactosyltransferase (Yin et al., 2010). Among the 25 homolog genes to AtGAUT1 in the *Arabidopsis* genome, two distinct group have been described for the GAUT genes and the GAUT-related genes (GATL), which comprise 15 and 10 genes, respectively (Sterling et al., 2006). Heterologous expression of AtGAUT1 in human embryonic kidney cells, showed that *AtGAUT1* cDNA encodes a galacturonosyltransferase activity able to transfer radiolabeled GalA onto α-1,4-oligogalacturonide acceptors, whereas the heterologous expression of *AtGAUT7* cDNA (36% amino-acid sequence identity with AtGAUT1) carried out in parallel did not yield any transferase activity. More recently, Atmodjo et al. (2011) have demonstrated that the association of AtGAUT1 with AtGAUT7 is necessary to retain GAUT1 galacturonosyltransferase activity in Golgi membranes. In that study the authors have proposed that two GAUT1 proteins would remain associated to each other (and thus retain) *via* one GAUT7 protein anchored in the Golgi membrane. However, whether the AtGAUT1 activity is directly responsible for the biosynthesis of the backbone of HG or that of RG-II polysaccharide in *Arabidopsis* has not been determined. Characterization of cell wall composition of *Arabidopsis* mutants altered for 13 out of the 15 GAUT genes and 3 of the 10 GATL genes has failed to clearly establish which polysaccharide is affected (Caffal et al., 2009; Kong et al., 2011).

The *Arabidopsis* mutant *quasimodo1* (*qua1*) is characterized by a reduced cell adhesion phenotype combined with a 25% decrease in cell wall galacturonic acid content, supporting the hypothesis that the *AtQUA1* gene encodes a putative glycosyltransferase activity involved in pectin biosynthesis (Bouton et al., 2002; Durand et al., 2009). AtQUA1 (also named AtGAUT8) belongs to CAZy GT 8 family and shows 77% similarity to AtGAUT1 which has a characterized HG-galacturonosyltransferase activity (Sterling et al., 2006). In addition, α-1,4-galacturonosyltransferase activity was shown to be significantly reduced in *qua1* providing further support for AtQUA1 involvement in pectin biosynthesis (Orfila et al., 2005). Another *Arabidopsis* mutant *quasimodo2* (*qua2*), having a 50% decrease in HG content, has been described (Mouille et al., 2007). Interestingly, AtQUA2 does not show any similarity with other glycosyltransferases, but it is a Golgi-localized protein (**Figure 2**) that contains a putative *S*-adenosyl methionine dependent methyltransferase domain, and appears strongly co-regulated with AtQUA1. This study supports the hypothesis that AtQUA2 is a pectin methyltransferase required for HG biosynthesis and that both enzymes work interdependently. The observation that an alteration in a putative methyltransferase can impair HG synthesis led the authors to suggest the existence of a protein complex containing galacturonosyltransferase and methyltransferase where the latter enzyme would be essential for the functioning of the protein complex (Mouille et al., 2007). Whereas *Arabidopsis* genome contains 29 putative genes encoding for pectin methyltransferases (Krupková et al., 2007), in addition to the AtQUA2, a novel putative *S*-adenosyl methionine dependent HG methyltransferase, showing a high amino-acid similarity with AtQUA2, the AtQUA3 has been recently characterized (Miao et al., 2011). AtQUA3 is a Golgi-localized type II membrane protein which is highly expressed and abundant in *Arabidopsis* suspension-cultured cells. More recently, it has been shown that AtQUA3 is co-expressed with AtGAUT1 and AtGAUT7; supporting the idea that HG methylation is closely associated with HG synthesis (Atmodjo et al., 2011). In addition, Held et al. (2011) have identified an *Arabidopsis* ortholog of a cotton protein containing a domain similar to SAM methyltransferase domain named cotton Golgi-related 3 (CGR3) involved in the methylesterification of HG. Finally, a third *Arabidopsis* mutant – *ectopically parting cells 1* (*epc1*) – was characterized on the basis of cell adhesion defects, however cell wall analyses did not support the hypothesis that pectin biosynthesis was specifically altered in *epc1* (Singh et al., 2005).

The HG backbone in *Arabidopsis* can also be decorated with β-1,3-xylose residues thus forming a xylogalacturonan domain (Zandleven et al., 2007). The characterization of the *xylogalacturonan deficient1* (*xgd1*) *Arabidopsis* mutant along with the heterologous expression of XGD1 protein in *Nicotiana benthamiana* led to the demonstration that the *XGD1* gene is involved in XGA biosynthesis (Jensen et al., 2008).

Four other genes involved in pectin biosynthesis, encoding a small glycosyltransferase family with four members named RG-II xylosyltransferase (RGXT1–4; CAZy GT77), have been described (Egelund et al., 2006, 2008; Fangel et al., 2011; Liu et al., 2011). The authors convincingly demonstrated that *AtRGXT1*, *AtRGXT2*, *AtRGXT3*, and *AtRGXT4* encode α-1,3-xylosyltransferase activities that are involved in the synthesis of the pectic polysaccharide RG-II. Whereas no mutant has been found for *RGXT3* (Egelund et al., 2008), *Arabidopsis* mutants have been described for *RGXT1*, *RGXT2* (Egelund et al., 2006) and *RGXT4* (Liu et al., 2011). Among these, only *rgxt4* mutant, also named male gametophyte defective 4 (*mgd4*), presents visible phenotypes in both RG-II structure and pollen tube growth (Liu et al., 2011). The peculiar role of *RGXT4* could be explained by its ubiquitous expression in vegetative and reproductive organs whereas *RGXT1* and *RGXT2* expression is restricted to the vegetative organs. Other genes have also been proposed to function in pectin biosynthesis although their involvement has not been firmly established. Mutant lines altered in pectin biosynthesis have been screened based on cell adhesion defects – a process that involves pectin (Iwai et al., 2001, 2002; Bouton et al., 2002; Mouille et al., 2007). A gene named *NpGUT1*, for *Nicotiana plmbaginifolia* glucuronyltransferase 1, has been identified using *nolac-H18*, a tobacco callus mutant line that exhibits a "loosely attached cells" phenotype (Iwai et al., 2002). It was proposed that *NpGUT1* encodes a putative glucuronyltransferase involved in RG-II biosynthesis based on the analysis of *nolac-H18* mutant cell walls. However, recent studies have shown that homologs of *Arabidopsis NpGUT1* are related to the biosynthesis of the hemicellulosic polysaccharide glucuronoxylan rather than to that of RG-II (Wu et al., 2009).

As compared to HG and RG-II biosynthesis, relatively little is known about the glycosyltransferases involved in RG-I

biosynthesis and only one glycosyltransferase has been characterized so far. A reverse genetics approach with putative glycosyltransferases from the CAZy GT47 family led to the identification of the *arabinan deficient 1 (arad1)* mutant of *Arabidopsis* showing a reduced arabinose content in the cell wall (Harholt et al., 2006) Characterization of the *arad1* cell wall demonstrated that the *ARAD1* gene probably encodes an arabinan α-1,5-arabinosyltransferase activity important for RG-I biosynthesis. Another Golgi glycosyltransferase of GT47 family sharing a high homology with ARAD1, named ARAD2, has been recently characterized (Harholt et al., 2012). Using biochemical and microscopical approaches, the study has revealed that ARAD1 and ARAD2 form homo and heterodimers when they are co-expressed in *N. benthamiana* plants (Harholt et al., 2012). It is interesting to note that although arabinofuranose is normally incorporated in RG-I during its biosynthesis *in planta*, it is the arabinopyranose that is actually incorporated during *in vitro* assays, using detergent-solubilized membranes. To explain this discrepancy between *in planta* and *in vitro* observations, it has been hypothesized that a mutase activity responsible for the conversion is lost upon solubilization (Nunan and Scheller, 2003). A UDP-arabinose mutase (UAM) that converts UDP-arabinopyranose into UDP-arabinofuranose was characterized in rice (Konishi et al., 2007) and found to share more than 80% identity with the reversibly glycosylated proteins (RGPs) of *Arabidopsis* that have long been known to be cytosolic proteins capable of associating with Golgi membranes (Dhugga et al., 1991, 1997; Delgado et al., 1998). Based on the fact that RGPs can be reversibly glycosylated by glucose, xylose, and galactose residues, it has been postulated that they could be involved in XyG or xylan biosynthesis. Among the five isoforms of RGPs (RGP1–5) identified in the *Arabidopsis* genome, the mutase activity has been recently shown for AtRGP1, AtRGP2, and AtRGP3 (Rautengarten et al., 2011). This UAM activity of RGPs suggests their potential role in the biosynthesis of arabinofuranosyl-containing polymers such pectin or arabinogalactan proteins. A double mutant *rgp1/rgp2* was shown to harbor pollen development defects, thereby leading the authors to hypothesize that RGPs might be involved in cell wall polysaccharide biosynthesis (Drakakaki et al., 2006). Moreover, Rautengarten et al. (2011) analyzed the phenotype of homozygous T-DNA insertion mutants (*rgp1–1* and *rgp1–2*), and described severe developmental phenotypes associated with subsequent reduction (≥69%) in cell wall arabinose content.

CONCLUDING REMARKS

The knowledge of XyG and pectin biosynthesis has progressed significantly over the past 10 years with respect to the identification of the enzymes involved in their biosynthesis, using functional genomics. The challenge now is, to determine how these players (and partners) cooperate, in a timely and probably spatially resolved manner, in order to achieve the coordinated and efficient synthesis of these polymers.

In plants, the only approach that has so far provided evidence for the compartmental organization of the Golgi with regards to complex polysaccharide biosynthesis is immunogold microscopy using antibodies raised against specific sugars of different polysaccharides (Follet-Gueye et al., 2012). Now we need to move forward with studies addressing how the glycosyltransferases are distributed within plant Golgi stacks and to determine whether distinct enzymes are preferentially compartmentalized within distinct Golgi cisternae, or if they are always localized in all Golgi sub-compartments and in all cell types. Another interesting issue relates to whether glycohydrolases are able to act on polysaccharides within Golgi-derived vesicles before secretion. Finally, in light of the recent identification of glycosyltransferase complexes involved in HG and arabinan synthesis (Atmodjo et al., 2011; Harholt et al., 2012), as well determination of their membrane topologies (Søgaard et al., 2012), it is of special interest to understand location and interactions of glycosyltransferases with partners including nucleotide–sugar interconversion enzymes and sugar transporters within Golgi membranes. Clearly, a better understanding of such interactions, their dynamics along with membrane topologies of the enzymes and their distribution within Golgi cisternae will provide new mechanistic insights into the biosynthesis and secretion of cell wall polysaccharides in flowering plants.

ACKNOWLEDGMENTS

Very special thanks are due to Pr. A. Staehelin (who retired recently) for having passionately launched AD onto the path of plant Golgi research. The authors wish to thank Pr. S. Hawkins and Dr. J. Moore for their critical reading of the manuscript as well as Pr. B. H. Kang for providing **Figure 1D**. We also thank Dr. G. Mouille (INRA, Versailles) for providing the GFP-QUA2 line. Work in AD laboratory is supported by the University of Rouen, le Conseil Régional de Haute Normandie via le Grand Réseau de Recherche VASI (Végétal, Agronomie, Sol, Innovation), le CNRS and l'ANR.

REFERENCES

Andème-Onzighi, C., Sivaguru, M., Judy-March, J., Baskin, T. I., and Driouich, A. (2002). The reb1-1 mutation of *Arabidopsis* alters the morphology of trichoblasts, the expression of arabinogalactan-proteins and the organization of cortical microtubules. *Planta* 215, 949–958.

Arabidopsis Genome Initiative. (2000). Analysis of the genome sequence of the flowering plant *Arabidopsis thaliana*. *Nature* 408, 796–815.

Atmodjo, M. A., Sakuragi, Y., Zhu, X., Burell, A. J., Mohanty, S. S., Atwood III, J. A., Orlando, R., Scheller, H. V., and Mohnen, D. (2011). Galacturonosyltransferase (GAUT)1 and GAUT7 are the core of a plant cell wall pectin biosynthetic homogalacturonan:galacturonosyltransferase complex. *Proc. Natl. Acad. Sci. U.S.A.* 108, 20225–20230.

Barber, C., Rösti, J., Rawat, A., Findlay, K., Roberts, K., and Seifert, G. J. (2006). Distinct properties of the five UDP-D-glucose/UDP-D-galactose 4-epimerase isoforms of *Arabidopsis thaliana*. 281, 17276–17285.

Boevink, P., Oparka, K., Sant Cruz, S., Martin, B., Betteridge, A., and Hawes, C. (1998). Stacks on tracks: the plant Golgi apparatus traffics on an actin/ER network. *Plant J.* 15, 441–447.

Bouton, S., Leboeuf, E., Mouille, G., Leydecker, M. T., Talbotec, J., Granier, F., Lahaye, M., Höfte, H., and Truong, H. N. (2002). QUASIMODO1 encodes a putative membrane-bound glycosyltransferase required for normal pectin synthesis and cell adhesion in *Arabidopsis*. *Plant Cell* 14, 2577–2590.

Brandizzi, F, Snapp, E. L., Roberts, A. G., Lippincott-Schwartz, J., and Hawes, C. (2002). Membrane protein transport between the endoplasmic reticulum and the Golgi in tobacco leaves is energy dependent but cytoskeleton independent: evidence from selective photobleaching. *Plant Cell* 14, 1293–1309.

Brummell, D. A., Camirand, A., and Maclachlan, G. A. (1990). Differential distribution of xyloglucan glycosyl transferases in pea Golgi dictyosomes and secretory vesicles. *J. Cell Sci.* 96, 705–710.

Burton, R. A., Gidley, M. J., and Fincher, G. B. (2010). Heterogeneity in the chemistry, structure and function of plant cell walls. *Nat. Chem. Biol.* 724–732.

Caffal, K. H., Pattathil, S., Phillips, S. E., Hahn, M. G., and Mohnen, D. (2009). *Arabidopsis thaliana* T-DNA mutants implicate GAUT genesin the biosynthesis of pectin and xylan in cell walls and seed testa. *Mol. Plant* 2, 1000–1014.

Camirand, A., Brummell, D. A., and Maclachlan, G. A. (1987). Fucosylation of xyloglucan: localization of the transferase in dictyosomes of pea stem cells. *Plant Physiol.* 113, 487–492.

Cantarel, B. L., Coutinho, P. M., Rancurel, C., Bernard, T., Lombard, V., and Henrissat, B. (2009). The carbohydrate-active enzymes database (CAZy): an expert resource for glycogenomics. *Nucleic Acids Res.* 37, D233–D238.

Carpita, N. C., and Gibeaut, D. M. (1993). Structural models of primary cells in flowering plants: consistency of molecular structure with the physical properties of the walls during growth. *Plant J.* 3, 1–30.

Cavalier, D. M., and Keegstra, K. (2006). Two xyloglucan xylosyltransferases catalyze the addition of multiple xylosyl residues to cellohexaose. *J. Biol. Chem.* 281, 34197–34207.

Cavalier, D. M., Lerouxel, O., Neumetzler, L., Yamauchi, K., Reinecke, A., Freshour, G., Zabotina, O. A., Hahn, M. G., Burgert, I., Pauly, M., Raikhel, N. V., and Keegstra, K. (2008). Disrupting Two *Arabidopsis thaliana* xylosyltransferase genes results in plants deficient in xyloglucan, a major primary cell wall component. *Plant Cell* 20, 1519–1537.

Chevalier, L., Bernard, S., Ramdani, Y., Lamour, R., Bardor, M., Lerouge, P., Follet-Gueye, M. L., and Driouich, A. (2010). Subcompartment localization of the side chain xyloglucan-synthesizing enzymes within Golgi stacks of tobacco suspension-cultured cells. *Plant J.* 64, 977–989.

Cocuron, J. C., Lerouxel, O., Drakakaki, G., Alonso, A. P., Liepman, A. H., Keegstra, K., Raikhel, N., and Wilkerson, C. G. (2007). A gene from the cellulose synthase-like C family encodes a beta-1,4 glucan synthase. *Proc. Natl. Acad. Sci. U.S.A.* 104, 8550–8555.

Cosgrove, D. J. (2005). Growth of the plant cell wall. *Nat. Rev. Mol. Cell Biol.* 6, 850–861.

Cosgrove, D. J. (1999). Enzymes and others agents that enhance cell wall extensibility. *Annu. Rev. Plant Physiol. Plant Mol. Biol.* 50, 391–417.

Cutler, S. R., and Ehrhardt, D. W. (2002). Polarized cytokinesis in vacuolate cells of *Arabidopsis*. *Proc. Natl. Acad. Sci. U.S.A.* 99, 2812–2817.

Darvill, J. E., McNeil, M., Darvill, A. G., and Albersheim, P. (1980). Structure of Plant Cell Walls: XI. Glucuronoarabinoxylan, a second hemicellulose in the primary cell walls of suspension-cultured sycamore cells. *Plant Physiol.* 66, 1135–1139.

Dauwalder, M., and Whaley, W. G. (1974). Patterns of incorporation of (3H)galactose by cells of *Zea mays* root tips. *J. Cell Sci.* 14, 11–27.

Davis, J., Brandizzi, F., Liepman, A. H., and Keegstra, K. (2010). *Arabidopsis* mannan synthase CSLA9 and glucan synthase CSLC4 have opposite orientations in the Golgi membrane. *Plant J.* 64, 1028–1037.

Delgado, I. J., Wang, Z., de Rocher, A., Keegstra, K., and Raikhel, N. V. (1998). Cloning and characterization of AtRGP1. A reversibly autoglycosylated Arabidopsis protein implicated in cell wall biosynthesis. *Plant Physiol.* 116, 1339–1350.

Desprez, T., Juraniec, M., Crowell, E. F., Jouy, H., Pochylova, Z., Höfte, H., Gonneau, M., and Vernhettes, S. (2007). Organization of cellulose synthase complexes involved in primary cell wall synthesis in *Arabidopsis thaliana*. *Proc. Natl. Acad. Sci. U.S.A.* 104, 15572–15577.

Desveaux, D., Faik, A., and Maclachlan, G. (1998). Fucosyltransferase and the biosynthesis of storage and structural xyloglucan in developing nasturtium fruits. *Plant Physiol.* 118, 885–894.

Dettmer, J., Hong-Hermesdorf, A., Stierhof, Y. D., and Schumacher, K. (2006). Vacuolar H^+-ATPase activity is required for endocytic and secretory trafficking in *Arabidopsis*. *Plant Cell* 18, 715–730.

Dhugga, K. S., Tiwari, S. C., and Ray, P. M. (1997). A reversibly glycosylated polypeptide (RGP1) possibly involved in plant cell wall synthesis: purification, gene cloning, and trans-Golgi localization. *Proc. Natl. Acad. Sci. U.S.A.* 94, 7679–7684.

Dhugga, K. S., Ulskov, P., Gallagher, S. R., and Ray, P. M. (1991). Plant Polypeptide reversibly glycosylated by UDP-glucose. Possible components of Golgi beta-glucan synthase. *J. Biol. Chem.* 94, 7679–7684.

Doong, R. L., and Mohnen, D. (1998). Solubilization and characterization of a galacturonosyltransferase that synthesizes the pectic polysaccharide homogalacturonan. *Plant J.* 13, 363–374.

Drakakaki, G., Zabotina, O., Delgado, I., Robert, S., Keegstra, K., and Raikhel, N. (2006). *Arabidopsis* reversibly glycosylated polypeptides 1 and 2 are essential for pollen development. *Plant Physiol.* 142, 1480–1492.

Driouich, A., Faye, L., and Staehelin, L. A. (1993). The plant Golgi apparatus: a factory for complex polysaccharides and glycoproteins. *Trends Biochem. Sci.* 18, 210–214.

Driouich, A., Levy, S., Staehelin, L. A., and Faye, L. (1994). Structural and functional organization of the Golgi apparatus in plant cells. *Plant Physiol.* 32, 731–749.

Driouich, A., and Staehelin, L. A. (1997). "The plant Golgi apparatus: Structural organization and functional properties," in *The Golgi Apparatus*, ed. E. G. Berger (Basel: J. Roth Birkhauser), 275–301.

Dunkley, T. P., Hester, S., Shadforth, I. P., Runions, J., Weimar, T., Hanton, S. L., Griffin, J. L., Bessant, C., Brandizzi, F., Hawes, C., Watson, R. B., Dupree, P., and Lilley, K. S. (2006). Mapping the *Arabidopsis* organelle proteome. *Proc. Natl. Acad. Sci. U.S.A.* 103, 6518–6523.

Dunkley, T. P. J., Watson, R., Griffin, J. L., Dupree, P., and Lilley, K. S. (2004). Localization of organelle proteins by isotope tagging (LOPIT). *Mol. Cell. Proteomics* 3, 1128–1134.

Durand, C., Vicré-Gibouin, M., Moreau, M., Duponchel, L., Follet-Gueye, M. L., Lerouge, P., and Driouich, A. (2009). The organization pattern of root border-like cells in *Arabidopsis* is dependent on homogalacturonan. *Plant Physiol.* 150, 1411–1421.

Edwards, M. E., Dickson, C. A., Chengappa, S., Sidebottom, C., Gidley, M. J., and Reid, J. S. (1999). Molecular characterization of a membrane-bound galactosyltransferase of plant cell wall matrix polysaccharide biosynthesis. *Plant J.* 19, 691–697.

Egelund, J., Damager, I., Faber, K., Olsen, C. E., Ulvskov, P., and Petersen, B. L. (2008). Functional characterisation of a putative rhamnogalacturonan II specific xylosyltransferase. *FEBS Lett.* 582, 3217–3222.

Egelund, J., Obel, N., Ulvskov, P., Geshi, N., Pauly, M., Bacic, A., and Petersen, B. L. (2007). Molecular characterization of two *Arabidopsis thaliana* glycosyltransferase mutants, rra1 and rra2, which have a reduced residual arabinose content in a polymer tightly associated with the cellulosic wall residue. *Plant Mol. Biol.* 64, 439–451.

Egelund, J., Petersen, B. L., Motawia, M. S., Damager, I., Faik, A., Olsen, C. E., Ishii, T., Clausen, H., Ulvskov, P., and Geshi, N. (2006). *Arabidopsis thaliana* RGXT1 and RGXT2 encode Golgi-localized (1,3)-alpha-D-xylosyltransferases involved in the synthesis of pectic rhamnogalacturonan-II. *Plant Cell* 18, 2593–2607.

Faik, A. (2010). Xylan biosynthesis: news from the grass. *Plant Physiol.* 153, 396–402.

Faik, A., Price, N. J., Raikhel, N. V., and Keegstra, K. (2002). An *Arabidopsis* gene encoding an alpha-xylosyltransferase involved in xyloglucan biosynthesis. *Proc. Natl. Acad. Sci. U.S.A.* 99, 7797–7802.

Fangel, J. U., Petersen, B. L., Jensen, N. B., Willats, W. G. T, Bacic, A., and Egelund, J. (2011). A putative *Arabidopsis thaliana* glycosyltransferase, At4g01220, which is closely related to three plant cell wall-specific xylosyltransferases, is differentially expressed spatially and temporally. *Plant Sci.* 180, 470–479.

Follet-Gueye, M. L., Mollet, J. C., Vicré-Gibouin, M., Bernard, S., Chevalier, L., Plancot, B., Dardelle, F., Ramdani, Y., Coimbra, S., and Driouich, A. (2012). "Immuno-glyco-imaging in plant cells: localization of cell wall carbohydrate epitopes and their biosynthesizing enzymes," in *Applications of Immunocytochemistry*, ed. H. Dehghani (Rijeka: In Tech), 297–320.

Follet-Gueye, M. L., Pagny, S., Faye, L., Gomord, V., and Driouich, A. (2003). An improved chemical fixation method suitable for immunogold localization of green fluorescent protein in the Golgi apparatus of tobacco Bright Yellow (BY-2) cells. *J. Histochem. Cytochem.* 51, 931–940.

Gardiner, M., and Chrispeels, M. J. (1975). Involvement of the Golgi apparatus in the synthesis and secretion of hydroxyproline-rich cell wall glycoproteins. *Plant Physiol.* 55, 536–541.

Gibeaut, D. M., and Carpita, N. C. (1994). Biosynthesis of plant cell wall polysaccharides. *FASEB J.* 8, 904–915.

Gille, S., de Souza, A., Xiong, G., Benz, M., Cheng, K., Schultink, A., Reca, I. B., and Pauly, M.

(2011). O-acetylation of *Arabidopsis* hemicellulose xyloglucan requires AXY4 or AXY4L, proteins with a TBL and DUF231 domain. *Plant Cell* 23, 4041–4053.

Goubet, F., and Mohnen, D. (1999). Solubilization and partial characterization of homogalacturonan-methyltransferase from microsomal membranes of suspension-cultured tobacco cells. *Plant Physiol.* 121, 281–290.

Green, J. R., and Northcote, D. H. (1978). The structure and function of glycoproteins synthesized during slime-polysaccharide production by membranes of the root-cap cells of maize (*Zea mays*). *Biochem. J.* 170, 599–608.

Günl, M., Neumetzler, L., Kraemer, F., de Souza, A., Schultink, A., Pena, M., York, W. S., and Pauly, M. (2011). AXY8 encodes an (α-fucosidase, underscoring the importance of apoplastic metabolism on the fine structure of *Arabidopsis* cell wall polysaccharides. *Plant Cell* 23, 4025–4040.

Günl, M., and Pauly, M. (2011). AXY3 encodes a (α-xylosidase that impacts the structure and accessibility of the hemicellulose xyloglucan in *Arabidopsis* plant cell walls. *Planta* 233, 707–719.

Hadlington, J. L., and Denecke, J. (2000). Sorting of soluble proteins in the secretory pathway of plants. *Curr. Opin. Plant Biol.* 3, 461–468.

Harholt, J., Jensen, J. K., Sørensen, S. O., Orfila, C., Pauly, M., and Scheller, H. V. (2006). ARABINAN DEFICIENT 1 is a putative arabinosyltransferase involved in biosynthesis of pectic arabinan in *Arabidopsis*. *Plant Physiol.* 140, 49–58.

Harholt, J., Jensen, J. K., Verhertbruggen, Y., Casper Søgaard, C., Bernard, S., Nafisi, M., Poulsen, C. P., Geshi, N., Sakuragi, Y., Driouich, A., Knox, J. P., and Vibe Scheller, H. (2012). ARAD proteins associated with pectic Arabinan biosynthesis form complexes when transiently overexpressed in planta. *Planta*. doi:10.1007/s00425-012-1592-3. [Epub ahead of print].

Harholt, J., Suttangkakul, A., and Vibe Scheller, H. (2010). Biosynthesis of pectin. *Plant Physiol.* 153, 384–395.

Harris, P. J., and Northcote, D. H. (1971). Polysaccharide formation in plant Golgi bodies. *Biochem. Biophys. Acta* 237, 56–64.

Hayashi, T. (1989). Xyloglucans in the primary cell wall. *Annu. Rev. Plant Physiol. Plant Mol. Biol.* 40, 139–168.

Hayashi, T., and Matsuda, K. (1981a). Biosynthesis of xyloglucan in suspension-cultured soybean cells. Occurrence and some properties of xyloglucan 4-beta-D-glucosyltransferase and 6-alpha-D-xylosyltransferase. *J. Biol. Chem.* 256, 11117–11122.

Hayashi, T., and Matsuda, K. (1981b). Biosynthesis of Xyloglucan in Suspension-cultured soybean cells. Evidence that the enzyme system of xyloglucan synthesis does not contain ß-1,4-glucan 4-ß-D-glucosyltransferase activity (EC 2.4.1.12). *Plant Cell Physiol.* 22, 1571–1584.

Held, M. A., Be, E., Zemelis, S., Withers, S., Wilkerson, C., and Brandizzi, F. (2011). CGR3: a Golgi-localized protein influencing homogalacturonan methylesterification. *Mol. Plant.* 4, 832–844.

Hwang, J. W., and Kokini, J. L. (1991). Structure and rheological function of side branches of carbohydrate polymers. *J. Texture Stud.* 22, 123–167.

International Rice Genome Sequencing Project. (2005). The map-based sequence of the rice genome. *Nature* 436, 793–800.

Ishii, T., and Matsunaga, T. (1996). Isolation and characterization of a boron-rhamnogalacturonan II complex from cell walls of sugar beet pulp. *Carbohydr. Res.* 284, 1–9.

Ishii, T., Matsunaga, T., and Hayashi, N. (2001). Formation of Rhamnogalacturonan II-borate dimer in pectin determines cell wall thickness of pumpkin tissue. *Plant Physiol.* 126, 1698–1705.

Iwai, H., Ishii, T., and Satoh, S. (2001). Absence of arabinan in the side chains of the pectic polysaccharides strongly associated with cell walls of *Nicotiana plumbaginifolia* non-organogenic callus with loosely attached constituent cells. *Planta* 213, 907–915.

Iwai, H., Masaoka, N., Ishii, T., and Satoh, S. (2002). A pectin glucuronyltransferase gene is essential for intercellular attachment in the plant meristem. *Proc. Natl. Acad. Sci. U.S.A.* 99, 16319–11624.

Jarvis, M. C. (1984). Structure and properties of pectin gels in plant cell wall. *Plant Cell Environ.* 7, 153–164.

Jensen, J. K., Sørensen, S. O., Harholt, J., Geshi, N., Sakuragi, Y., Møller, I., Zandleven, J., Bernal, A. J., Jensen, N. B., Sørensen, C., Pauly, M., Beldman, G., Willats, W. G., and Scheller, H. V. (2008). Identification of a xylogalacturonan xylosyltransferase involved in pectin biosynthesis in *Arabidopsis*. *Plant Cell* 20, 1289–1302.

Jones, L., Seymour, G. B., and Knox, J. P. (1997). Localization of pectic galactan in tomato cell walls using a monoclonal antibody specific to (1-4)-β-D-galactan. *Plant Physiol.* 113, 1405–1412.

Keegstra, K., and Raikhel, N. V. (2001). Plant glycosyltransferases. *Curr. Opin. Plant Biol.* 4, 219–224.

Kobayashi, M., Matoh, T., and Azuma, J. (1996). Two chains of rhamnogalacturonan-II are cross-linked by borate-diol ester bonds in higher plant cell walls. *Plant Physiol.* 110, 1017–1020.

Kong, Y., Zhou, G., Yin, Y., Xu, Y, Pattathil, S., and Hahn, M. G. (2011). Molecular analysis of a family of *Arabidopsis* genes related to galacturonosyltransferases. *Plant Physiol.* 155, 1791–1805.

Konishi, T., Takeda, T., Miyazaki, Y., Ohnishi-Kameyama, M., Hayashi, T., O'Neill, MA., and Ishii, T. (2007). A plant mutase that interconverts UDP-arabinofuranose and UDP-arabinopyranose. *Glycobiology* 17, 345–354.

Krupková, E., Immerzeel, P., Pauly, M., and Schmülling, T. (2007). The TUMOROUS SHOOT DEVELOPMENT2 gene of *Arabidopsis* encoding a putative methyltransferase is required for cell adhesion and coordinated plant development. *Plant J.* 50, 735–750.

Lerouxel, O., Cavalier, D. M., Liepman, A. H., and Keegstra, K. (2006). Biosynthesis of plant cell wall polysaccharides – a complex process. *Curr. Opin. Plant Biol.* 9, 621–630.

Liu, X. L., Liu, L., Niu, Q. K., Xia, C., Yang, K. Z., Li, R., Chen, L. Q., Zhang, X. Q., Zhou, Y., and Ye, D. (2011). Male gametophyte defective 4 encodes a rhamnogalacturonan II xylosyltransferase and is important for growth of pollen tubes and roots in *Arabidopsis*. *Plant J.* 65, 647–660.

Lynch, M. A., and Staehelin, L. A. (1992). Domain-specific and cell type-specific localization of two types of cell wall matrix polysaccharides in the clover root tip. *J. Cell Biol.* 118, 467–479.

Madson, M., Dunand, C., Li, X., Verma, R., Vanzin, G. F., Caplan, J., Shoue, D. A., Carpita, N. C., and Reiter, W. D. (2003). The MUR3 gene of *Arabidopsis* encodes a xyloglucan galactosyltransferase that is evolutionarily related to animal exostosins. *Plant Cell* 15, 1662–1670.

Matoh, T., Ishigaki, K., Ohno, K., and Azuma, J. (1993). Isolation and characterization of a boron-polysaccharide complex from radish roots. *Plant Cell Physiol.* 34, 639–642.

McNeil, M., Darvill, A. G., and Albersheim, P. (1982). Structure of plant cell walls. Identification of seven glycosyl residues attached to O-4 of the 2-4 linked L-rhamnosyl residues of rhamnogalacturonan I. *Plant Physiol.* 70, 1586–1591.

Miao, Y., Li, H. Y., Shen, J., Wang, J., and Jiang, L. (2011). QUASIMODO 3 (QUA3) is a putative homogalacturonan methyltransferase regulating cell wall biosynthesis in *Arabidopsis* suspension-cultured cells. *J. Exp. Bot.* 62, 5063–5078.

Mohnen, D. (2008). Pectin structure and biosynthesis. *Curr. Opin. Plant Biol.* 11, 266–277.

Moore, P. J., Darvill, A. G., Albersheim, P., and Staehelin, L. A. (1986). Immunogold localization of xyloglucan and rhamnogalacturonan I in the cell walls of suspension-cultured sycamore cells. *Plant Physiol.* 82, 787–794.

Moore, P. J., Swords, K. M., Lynch, M. A., and Staehelin, L. A. (1991). Spatial organization of the assembly pathways of glycoproteins and complex polysaccharides in the Golgi apparatus of plants. *J. Cell Biol.* 112, 589–602.

Mouille, G., Ralet, M. C., Cavelier, C., Eland, C., Effroy, D., Hématy, K., McCartney, L., Truong, H. N., Gaudon, V., Thibault, J. F., Marchant, A., and Höfte, H. (2007). Homogalacturonan synthesis in *Arabidopsis thaliana* requires a Golgi-localized protein with a putative methyltransferase domain. *Plant J.* 50, 605–614.

Nebenfuhr, A., Gallagher, L., Dunahay, T. G., Frohlick, J. A., Mazurkiewicz, A. M., Meehl, J. B., and Staehelin, L. A. (1999). Stop-and-go movements of plant Golgi stacks are mediated by the acto-myosin system. *Plant Physiol.* 121, 1127–1141.

Nguema-Ona, E., Andème-Onzighi, C., Aboughe-Angone, S., Bardor, M., Ishii, T., Lerouge, P., and Driouich, A. (2006). The reb1-1 mutation of *Arabidopsis*. Effect on the structure and localization of galactose-containing cell wall polysaccharides. *Plant Physiol.* 140, 1406–1417.

Nunan, K. J., and Scheller, H. V. (2003). Solubilization of an arabinan arabinosyltransferase activity from mung bean hypocotyls. *Plant Physiol.* 132, 331–342.

Obel, N., Erben, V., Schwarz, T., Kühnel, S., Fodor, A., and Pauly, M. (2009). Microanalysis of plant cell wall polysaccharides. *Mol. Plant.* 2, 922–932.

O'Neill, M. A., Albersheim, P., and Darvill, A. G. (1990). "The pectic polysaccharides of primary cell walls," in *Methods in Plant Biochemistry*, Vol. 2, ed. D. M. Dey (London: Academic Press), 415–441.

O'Neill, M. A., Ishii, T., Albersheim, P., and Darvill, A. G. (2004). Rhamnogalacturonan II: structure and function of a borate cross-linked cell wall pectic polysaccharide. *Annu. Rev. Plant Biol.* 55, 109–139.

O'Neill, M. A., Warrenfeltz, D., Kates, K., Pellerin, P., Doco, T., Darvill, A. G., and Albersheim, P. (1996). Rhamnogalacturonan-II, a pectic polysaccharide in the walls of growing plant cell, forms a dimer that is covalently crosslinked by a borate ester. *J. Biol. Chem.* 271, 22923–22930.

O'Neill, M. A, Eberhard, S., Albersheim, P., and Darvill, A. G. (2001). Requirement of borate cross-linking of cell wall rhamnogalacturonan II for Arabidopsis growth. *Science* 294, 846–849.

Orfila, C., Sørensen, S. O., Harholt, J., Geshi, N., Crombie, H., Truong, H. N., Reid, J. S., Knox, J. P., and Scheller, H. V. (2005). QUASIMODO1 is expressed in vascular tissue of *Arabidopsis thaliana* inflorescence stems, and affects homogalacturonan and xylan biosynthesis. *Planta* 222, 613–622.

Pagny, S., Bouissonié, F., Sarkar, M., Follet-Gueye, M. L., Driouich, A., Schachter, H., Faye, L., and Gomord, V. (2003). tructural requirements for *Arabidopsis* β-1,2-xylosyltransferase activity and targeting to the Golgi. *Plant J.* 33, 189–203.

Pauly, M., and Keegstra, K. (2010). Plant cell walls as precursors for biofuels. *Curr. Opin. Plant Biol.* 13, 305–312.

Pena, M. J., Ryden, P., Madson, M., Smith, A. C., and Carpita, N. C. (2004). The galactose residues of xyloglucan are essential to maintain mechanical strength of the primary cell walls in *Arabidopsis* during growth. *Plant Physiol.* 134, 443–451

Perrin, R. M., DeRocher, A. E., Bar-Peled, M., Zeng, W., Norambuena, L., Orellana, A., Raikhel, N. V., and Keegstra, K. (1999). Xyloglucan fucosyltransferase, an enzyme involved in plant cell wall biosynthesis. *Science* 284, 1976–1979.

Pickett-Heaps, J. D. (1966). Incorporation of radiactivity into wheat xylem walls. *Planta* 71, 1–14.

Pickett-Heaps, J. D. (1968). Further ultrastructural observations on polysaccharide localization in plant cells. *J. Cell Sci.* 3, 55–64.

Popper, Z. A., Michel, G., Hervé, C., Domozych, D. S., Willats, W. G., Tuohy, M. G., Kloareg, B., and Stengel, D. B. (2011). Evolution and diversity of plant cell walls: from algae to flowering plants. *Annu. Rev. Plant Biol.* 62, 567–590.

Rabouille, C., Hui, N., Hunte, F., Kieckbusch, R., Berger, E. G., Warren, G., and Nilsson, T. (1995). Mapping the distribution of Golgi enzymes involved in the construction of complex oligosaccharides. *J. Cell Sci.* 108, 1617–1627.

Ralet, M. C., Tranquet, O., Poulain, D., Moïse, A., and Guillon, F. (2010). Monoclonal antibodies to rhamnogalacturonan I backbone. *Planta* 231, 1373–1383.

Rautengarten, C., Ebert, B., Herter, T., Petzold, C. J., Ishii, T., Mukhopadhyay, A., Usadel, B., and Scheller, H. V. (2011). The interconversion of UDP-arabinopyranose and UDP-arabinofuranose is indispensable for plant development in *Arabidopsis*. *Plant Cell* 23, 1373–1390.

Ray, P. M. (1980). Cooperative action of beta-glucan synthetase and UDP-xylose xylosyl transferase of Golgi membranes in the synthesis of xyloglucan-like polysaccharide. *Biochim. Biophys. Acta* 629, 431–444.

Reiter, W. D. (2008). Biochemical genetics of nucleotide sugar interconversion reactions. *Curr. Opin. Plant Biol.* 11, 236–243.

Reuhs, B. L., Glenn, J., Stephens, S. B., Kim, J. S., Christie, D. B., Glushka, J. G., Zablackis, E., Albersheim, P., Darvill, A. G., and O'Neill, M. A. (2004). L-galactose replaces L-fucose in the pectic polysaccharide rhamnogalacturonan II synthesized by the L-fucose-deficient mur1 *Arabidopsis* mutant. *Planta* 219, 147–157.

Reyes, F., and Orellana, A. (2008). Golgi transporters: opening the gate to cell wall polysaccharide biosynthesis. *Curr. Opin. Plant Biol.* 11, 244–251.

Richter, S., Voss, U., and Jürgens, G. (2009). Post-Golgi traffic in plants. *Traffic* 10, 819–828.

Ridley, B. L., O'Neill, M. A., and Mohnen, D. (2001). Pectins: structure, biosynthesis, and oligogalacturonide-related signaling. *Phytochemistry* 57, 929–967.

Ritzenthaler, C., Nebenführ, A., Movafeghi, A., Stussi-Garaud, C., Behnia, L., Pimpl, P., Staehelin, L. A., and Robinson, D. G. (2002). Reevaluation of the effects of brefeldin A on plant cells using tobacco bright yellow 2 cells expressing Golgi-targeted green fluorescent protein and COPI antisera. *Plant Cell* 14, 237–261.

Roberts, K. (1990). Structure at the plant cell surface. *Curr. Opin. Cell Biol.* 2, 920–928.

Saint Jore Dupas, C., Nebenführ, A., Boulaflous, A., Follet-Gueye, M. L., Plasson, C., Hawes, C., Driouich, A., Faye, L., and Gomord, V. (2006). Plant N-glycan processing enzymes employ different targeting mechanisms for their spatial arrangement along the secretory pathway. *Plant Cell* 18, 3182–3200.

Sampedro, J., Gianzo, C., Iglesias, N., Guitián, E., Revilla, G., and Zarra, I. (2012). AtBGAL10 is the main xyloglucan β-galactosidase in *Arabidopsis*, and its absence results in unusual xyloglucan subunits and growth defects. *Plant Physiol.* 158, 1146–1157.

Sampedro, J., Sieiro, C., Revilla, G., González-Villa, T., and Zarra, I. (2001). Cloning and expression pattern of a gene encoding an alpha-xylosidase active against xyloglucan oligosaccharides from *Arabidopsis*. *Plant Physiol.* 126, 910–920.

Sarria, R., Wagner, T. A., O'Neill, M. A., Faik, A., Wilkerson, C. G., Keegstra, K., and Raikhel, N. V. (2001). Characterization of a family of *Arabidopsis* genes related to xyloglucan fucosyltransferase1. *Plant Physiol.* 127, 1595–1606.

Scheller, H. V., Doong, R. L., Ridley, B. L., and Mohnen, D. (1999). Pectin biosynthesis: a solubilized α1,4-galacturonosyltransferase from tobacco catalyzes the transfer of galacturonic acid from UDP-galacturonic acid onto the non-reducing end of homogalacturonan. *Planta* 207, 512–517.

Scheller, H. V., Jensen, J. K., Sørensena, S. O., Harholt, J., and Geshi, N. (2007). Biosynthesis of pectin. *Physiol Plant* 129, 283–295.

Scheller, H. V., and Ulvskov, P. (2010). Hemicelluloses. *Annu. Rev. Plant Biol.* 61, 263–289.

Schoberer, J., and Strasser, R. (2011). Sub-compartmental organization of Golgi-resident N-glycan processing enzymes in plants. *Mol. Plant* 4, 220–228.

Segui-Simarro, J. M., Austin, J. R., White, E. A., and Staehelin, A. (2004). Electron tomographic analysis of somatic cell plate formation in meristematic cells of *Arabidopsis* preserved by high-pressure freezing. *Plant Cell* 16, 836–856.

Seifert, G. J. (2004). Nucleotide sugar interconversions and cell wall biosynthesis: how to bring the inside to the outside. *Curr. Opin. Plant Biol.* 7, 277–284.

Seifert, G. J., Barber, C., Wells, B., Dolan, L., and Roberts, K. (2002). Galactose biosynthesis in *Arabidopsis*: genetic evidence for substrate channeling from UDP-D-galactose into cell wall polymers. *Curr. Biol.* 12, 1840–1845.

Sherrier, D. J., and VandenBosch, K. A. (1994). Secretion of cell wall polysaccharides in Vicia root hairs. *Plant J.* 5, 185–195.

Singh, S. K., Eland, C., Harholt, J., Scheller, H. V., and Marchant, A. (2005). Cell adhesion in *Arabidopsis thaliana* is mediated by ECTOPICALLY PARTING CELLS 1– a glycosyltransferase (GT64) related to the animal exostosins. *Plant J.* 43, 384–397.

Søgaard, C., Stenbæk, A., Bernard, S., Hadi, M., Driouich, A., Scheller, H. V., and Sakuragi, Y. (2012). GO-PROMTO illuminates protein membrane topologies of glycan biosynthetic enzymes in the Golgi apparatus of living tissues. *PLoS ONE* 7, e31324. doi:10.1371/journal.pone.0031324

Staehelin, L. A., Giddings, T. H. Jr., Kiss, J. Z., and Sack, F. D. (1990). Macromolecular differentiation of Golgi stacks in root tips of *Arabidopsis* and Nicotiana seedlings as visualized in high pressure frozen and freeze-substituted samples. *Protoplasma* 157, 75–91.

Staehelin, L. A., and Hepler, P. K. (1996). Cytokinesis in higher plants. *Cell* 84, 821–824.

Staehelin, L. A., and Kang, B. H. (2008). Nanoscale architecture of endoplasmic reticulum export sites and of Golgi membranes as determined by electron tomography. *Plant Physiol.* 147, 1454–1468.

Sterling, J. D., Atmodjo, M. A., Inwood, S. E., Kumar Kolli, V. S., Quigley, H. F., Hahn, M. G., and Mohnen, D. (2006). Functional identification of an *Arabidopsis* pectin biosynthetic homogalacturonan galacturonosyltransferase. *Proc. Natl. Acad. Sci. U.S.A.* 103, 5236–5241.

Sterling, J. D., Quigley, H. F., Orellana, A., and Mohnen, D. (2001). The catalytic site of the pectin biosynthetic enzyme alpha-1,4-galacturonosyltransferase is located in the lumen of the Golgi. *Plant Physiol.* 127, 360–371.

Stierhof, Y. D., and El Kasmi, F. (2010). Strategies to improve the antigenicity, ultrastructure preservation and visibility of trafficking compartments in *Arabidopsis* tissue. *Eur. J. Cell Biol.* 89, 285–297.

Tamura, K., Shimada, T., Kondo, M., Nishimura, M., and Nishimura, I. H. (2005). KATAMARI1/MURUS3 is a novel Golgi membrane protein that is required for endomembrane organization in *Arabidopsis*. *Plant Cell* 17, 1764–1776.

Toyooka, K., Goto, Y., Asatsuma, S., Koizumi, M., Mitsui, T., and Matsuoka, K. (2009). A mobile secretory vesicle cluster involved in mass transport from the Golgi to the plant cell exterior. *Plant Cell* 21, 1212–1229.

Tuskan, G. A., Difazio, S., Jansson, S., Bohlmann, J., Grigoriev, I., and Hellsten, U. (2006). The genome of black cottonwood, Populus trichocarpa (Torr and Gray). *Science* 313, 1596–1604.

van Dijk, A. D., ter Braak, C. J., Immink, R. G., Angenent, G. C., and van Ham, R. C. (2008). Predicting and understanding transcription factor interactions based on sequence level determinants of combinatorial control. *Bioinformatics* 24, 26–33.

Vanzin, G. F., Madson, M., Carpita, N. C., Raikhel, N. V., Keegstra, K., and Reiter, W. D. (2002). The mur2 mutant of *Arabidopsis thaliana* lacks fucosylated xyloglucan because of a lesion in fucosyltransferase AtFUT1. *Proc. Natl. Acad. Sci. U.S.A.* 99, 3340–3345.

Vicré, M., Jauneau, A., Knox, J. P., and Driouich, A. (1998). Immunolocalization of β(1-4) and β (1-6)-D-galactan epitope in the cell wall and Golgi stacks of developing flax root tissues. *Protoplasma* 203, 26–34.

Vincken, J. P., Schols, H. A., Oomen, R. J. F. J., Beldman, G., Visser, R. G. F., and Voragen, A. G. J. (2003). "Pectin – the hairy thing," in *Advances in Pectin and Pectinase Research*, eds A. G. J. Voragen, H. Schols and R. Visser (Dordrecht: Kluwer Academic Publishers), 47–59.

Viotti, C., Bubeck, J., Stierhof, Y. D., Krebs, M., Langhans, M., van den Berg, W., van Dongen, W., Richter, S., Geldner, N., Takano, J., Jürgens, G., de Vries, S. C., Robinson, D. G., and Schumacher, K. (2010). Endocytic and secretory traffic in *Arabidopsis* merge in the trans-Golgi network/early endosome, an independent and highly dynamic organelle. *Plant Cell* 22, 1344–1357.

Vogel, J. (2008). Unique aspects of the grass cell wall. *Curr. Opin. Plant Biol.* 11, 301–307.

Voxeur, A., Gilbert, L., Rihouey, C., Driouich, A., Rothan, C., Baldet, P., and Lerouge, P. (2011). Silencing of the GDP-D-mannose 3,5-epimerase affects the structure and cross-linking of the pectic polysaccharide rhamnogalacturonan II and plant growth in tomato. *J. Biol. Chem* 286, 8014–8020.

Willats, W. G. T., Marcus, S. E., and Knox, J. P. (1998). Generation of a monoclonal antibody specific to (1-5)-α-L-arabinan. *Carbohydr. Res.* 308, 149–162.

Willats, W. G. T., McCartney, L., Mackie, W., and Knox, J. P. (2001). Pectin: cell biology and prospects for functional analysis. *Plant Mol. Biol.* 47, 9–27.

Wolf, S., Mouille, G., and Pelloux, J. (2009). Homogalacturonan methylesterification and plant development. *Mol Plant* 2, 851–860.

Wu, A. M., Rihouey, C., Seveno, M., Hörnblad, E., Singh, S. K., Matsunaga, T., Ishii, T., Lerouge, P., and Marchant, A. (2009). The *Arabidopsis* IRX10 and IRX10-LIKE glycosyltransferases are critical for glucuronoxylan biosynthesis during secondary cell wall formation. *Plant J.* 57, 718–731.

Wu, Y., Williams, M., Bernard, S., Driouich, A., Showalter, A. M., and Faik, A. (2010). Functional identification of two non-redundant *Arabidopsis* α(1,2)fucosyltransferases specific to arabinogalactan-proteins. *J. Biol. Chem.* 285, 13638–13645.

Yin, Y., Chen, H., Hahn, M. G., Mohnen, D., and Xu, Y. (2010). Evolution and function of the plant cell wall synthesis-related glycosyltransferase family 8. *Plant Physiol.* 153, 1729–1746.

Zablackis, E., Huang, J., Müller, B., Darvill, A. G., and Albersheim, P. (1995). Characterization of the cell-wall polysaccharides of *Arabidopsis thaliana* leaves. *Plant Physiol.* 107, 1129–1138.

Zandleven, J., Sørensen, S. O., Harholt, J., Beldman, G., Schols, H. A., Scheller, H. V., and Voragen, A. J. (2007). Xylogalacturonan exists in cell walls from various tissues of *Arabidopsis thaliana*. *Phytochemistry* 68, 1219–1226.

Zhang, G. F., Driouich, A., and Staehelin, L. A. (1996). Monensin-induced redistribution of enzymes and products from Golgi stacks to swollen vesicles in plant cells. *Eur. J. Cell Biol.* 71, 332–340.

Zhang, G. F., and Staehelin, L. A. (1992). Functional compartmentalization of the Golgi apparatus of plant cells: an immunochemical analysis of high pressure frozen/freeze substituted sycamore suspension-cultured cells. *Plant Physiol.* 99, 1070–1083.

Conflict of Interest Statement: The authors declare that the research was conducted in the absence of any commercial or financial relationships that could be construed as a potential conflict of interest.

Received: 10 February 2012; paper pending published: 23 February 2012; accepted: 09 April 2012; published online: 30 April 2012.

Citation: Driouich A, Follet-Gueye M-L, Bernard S, Kousar S, Chevalier L, Vicré-Gibouin M and Lerouxel O (2012) Golgi-mediated synthesis and secretion of matrix polysaccharides of the primary cell wall of higher plants. Front. Plant Sci. ***3****:79. doi: 10.3389/fpls.2012.00079*

This article was submitted to Frontiers in Plant Cell Biology, a specialty of Frontiers in Plant Science.

Copyright © 2012 Driouich, Follet-Gueye, Bernard, Kousar, Chevalier, Vicré-Gibouin and Lerouxel. This is an open-access article distributed under the terms of the Creative Commons Attribution Non Commercial License, which permits non-commercial use, distribution, and reproduction in other forums, provided the original authors and source are credited.

PARTIE D : OBJECTIFS DE MES TRAVAUX DE THESE

Cette étude bibliographique montre que les voies de biosynthèse golgienne du xyloglucane et du rhamnogalacturonane-I à l'échelle des différents compartiments golgiens sont encore peu documentées. Afin de compléter les connaissances dans ce domaine, nous avons mené des études ayant pour objectifs :

1) développer une méthode de préparation d'échantillons qui préserve la qualité d'ultrastructure et les épitopes, pour l'observation à l'échelle de la microscopie électronique à transmission, en utilisant la cryofixation et la cryosubstitution,

2) effectuer la cartographie golgienne d'épitopes glucidiques spécifiques du XyG et du RG-I à l'échelle de la microscopie électronique à transmission, sur des suspensions cellulaires de tabac BY-2,

3) réaliser la cartographie golgienne de différentes enzymes impliquées dans la synthèse du XyG et du RG-I à l'échelle de la microscopie électronique à transmission, sur des suspensions cellulaires de tabac BY-2 exprimant ces protéines couplées à la *Green Fluorescent Protein*,

4) rechercher *in vivo* l'existence de complexes d'enzymes impliquées dans la synthèse du RG-I à l'échelle de la microscopie confocale à balayage laser, sur des cellules épidermiques de feuilles de tabac *N.tabacum*.

CHAPITRE II : MATERIEL ET METHODES

PARTIE A : CULTURE DU MATERIEL VEGETAL

I- Culture des plants de tabac *Nicotiana tabacum*

Les graines de *Nicotiana tabacum* sont mises à germer en terreau préalablement stérilisé, dans un phytotron avec une photopériode de 16h de jour à 25°C, et 8h de nuit à 22°C, et un taux d'humidité de 60%. Après 4 semaines, les jeunes plants sont rempotés individuellement, puis utilisés pour l'expression transitoire des protéines de fusion entre 2 et 3 semaines après le rempotage **(Figure 38)**.

Figure 38 : Plant de tabac *Nicotiana tabacum* âgé de 7/8 semaines

II- Culture des cellules de tabac *Nicotiana tabacum cv Bright Yellow* -2 (BY-2)

Les cals de tabac **(Figure 39a)** sont cultivés sur milieu BY-2 composé comme suit : Murashige et Skoog (MS) 4,3g/L (Sigma M5524), saccharose 30g/L, di-hydrogénophosphate de potassium (KH_2PO_4) 100 mg/L, myo-inositol 51mg/L, thiamine 1mg/L, acide 2,4 dichlorophénoxyacétique 0,22mg/L et bacto agar 8g/L. Le pH du milieu est ajusté avec une solution molaire d'hydroxyde de potassium (KOH) à 5,6-5,8, puis stérilisé. Pour les cals transgéniques, un ou deux antibiotiques de sélection est ajouté aux concentrations adéquates. Les cals sont repiqués toutes les 4 semaines sur milieu neuf, et maintenus à 24°C à l'obscurité.

Les suspensions cellulaires de tabac **(Figure 39b)** sont initiées à partir des cals. Elles sont cultivées en milieu BY-2 liquide (composition identique à celui des cals de tabac, exempté de bacto-agar). Après 3 repiquages du cal transgénique sur milieu avec antibiotique de sélection, un morceau de cal âgé de 3 semaines est déposé dans un erlenmeyer de 80 mL contenant 30 mL de milieu BY-2 liquide frais. On maintient sous agitation permanente (140 rpm) à 24°C et à l'obscurité durant 8/ 10 jours afin de resuspendre le cal, puis on repique 10

mL dans 150 mL de milieu frais. Chaque semaine, 10 mL de suspension sont repiqués dans 150 mL de milieu BY-2 frais. Toutes les manipulations de culture de cellules sont réalisées en conditions aseptiques sous hotte à flux laminaire horizontal.

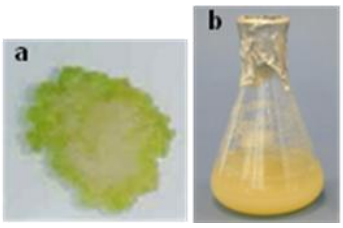

Figure 39 : Cal (a) et suspension cellulaire (b) de *Nicotiana tabacum* cv Bright Yellow 2(BY-2)

PARTIE B : CREATION DES PROTEINES DE FUSION

I- Construction des protéines de fusion avec la *Green Fluorescent Protein*

I-1- Clonage *via* l'utilisation des endonucléases de restriction

Les protéines AtXT1, AtMUR3, AtFUT1, AtARAD1 et AtMUR4 ont été fusionnées à l'extrémité N terminale de la sGFP (Pédelacq et al., 2006) selon la méthode suivante.

Le clonage par l'utilisation des endonucléases de restriction est la méthode la plus ancienne. Cette méthode est assez longue et fastidieuse, puisque pour sous-cloner une séquence d'intérêt en utilisant les enzymes de restriction, il faut s'assurer que la séquence d'intérêt ne porte pas les sites reconnus par les enzymes choisies pour le sous-clonage. Par conséquent, cette méthode de clonage est complètement dépendante de la séquence nucléotidique considérée et la stratégie doit être ajustée au cas par cas.

I-1-1- Amplification PCR

Le gène de chaque protéine est amplifié grâce à la réaction de polymérisation en chaîne (PCR). Les couples de primers utilisés sont décrits **tableau 1**.

AtXT1 (At3g62720)	For BamH1 5'-CGCGGATCCCGATGATAGAGAAGTGTATAGGA-3' Rev Nhe1 5'-CTAGCTAGCCGTCGTCGTCGTACTAAGCTT-3'
AtMUR3 (At2g20370)	For Kpn1 5'-GGGGTACCCCATGTTTCCAAGGGTTTCT-3' Rev Nhe1 5'-CTAGCTAGCCTGTGTCTTATCTCTCTG-3'
AtFUT1 (At2g03220)	For BamH1 5'-CGCGGATCCCGATGGATCAGAATTCGTACAGG-3' Rev Spe1 5'-GGACTAGTTACTAGCTTAAGTCCCCAGCT-3'

ARAD1 (At2g35100)	For Kpn I 5'-GGGGTACCCCATGGCGCGTAAATCTTCC-3' Rev Spe I 5'-GGACTAGTAATGGAAGTGATAAGACC-3'
MUR4 (At1g30620)	For BamH I 5'-CGCGGATCCCGATGTTTAGTTTTGGCCGAGCA-3' Rev SpeI 5'-GGACTAGTGTAAACCGAGACCGATGAGGT-3'

Tableau 1 : Primers utilisés pour l'amplification PCR

Le milieu réactionnel était constitué comme suit : 100 à 200ng d'ADN, 5 µL de tampon *Thermo pol. buffer* 10X (Biolabs), 1 µL de chaque primer à 10 µM, 2 µL de mix de dNTP à 10mM et 1 µL de *VENT DNA polymerase*, Biolabs, complété à 50 µL avec de l'eau stérile. Pour *xt1*, ce milieu réactionnel ne fonctionnant pas, nous avons utilisé : 100 à 200ng d'ADN, 5 µL de tampon *Mg free buffer* , 5 µL de MgCl2 25 mM (Biolabs), 1 µL de chaque primer à 10 µM, 2 µL de mix de dNTP à 10mM et 1 µL de *Taq polymerase*, Biolabs, complété à 50 µL avec de l'eau stérile. Les paramètres de températures de la réaction PCR sont décrits **Figure 40**.

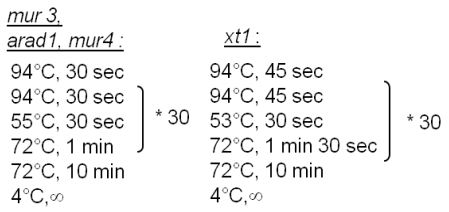

Figure 40 : Paramètres des cycles PCR (dénaturation, hybridation et élongation).

Une fois la réaction de PCR effectuée, chaque échantillon est mis à migrer par électrophorèse sur un gel d'agarose à 0,8% + bromure d'éthidium à 0,3µg/mL**,** dans un tampon de migration TBE 1X (TBE 5X : Tris Base 54g ; Acide borique 27,5g ; EDTA 2,92g ; pH 8,2). Le marqueur de taille utilisé est le « 1kb DNA ladder », Invitrogen. Chaque bande ADN d'intérêt est ensuite découpée et purifiée grâce au « Gel Purification Kit », Proméga.

I-1-2- Insertion dans le plasmide pBLTI221sGFP

Le plasmide pBLTI221sGFP a été utilisé comme vecteur de clonage, présenté **Figure 41**.

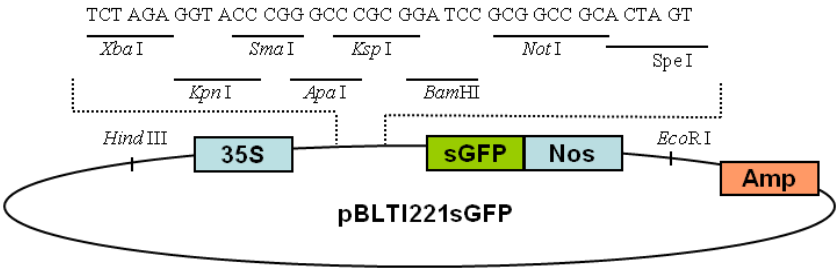

Figure 41 : Représentation schématique du vecteur de clonage pBLTI221sGFP.
35S : promoteur CaMV35S du virus de la mosaïque du chou-fleur, sGFP: séquence codante pour la sGFP,
Nos : terminateur nos 3 du gène de la nopaline synthase, Amp : gène de résistance à l'ampicilline.

Afin de créer des extrémités complémentaires pour insérer les séquences d'ADN amplifiées dans le vecteur de clonage, on les digère par le couple d'enzymes de restriction choisi en tableau 1. De façon générale, 1µg d'ADN est digéré avec 2µL de tampon enzymatique (10X), 5 à 10 unités d'enzyme de restriction, et complété avec de l'eau stérile à 20µL. La digestion a lieu à température optimale de l'enzyme durant 2 à 4h.

La ligation entre le vecteur de clonage et le fragment d'ADN digérés est effectuée avec un ratio molaire Vecteur/Insert 1/3, 1/1 et 3/1, avec 1µL de tampon ligase 10X, 1 unité de T4 DNA ligase, et complété avec de l'eau stérile à 10µL. Ce milieu réactionnel est ensuite laissé sur la nuit à température ambiante.

L'ADN plasmidique obtenu est ensuite amplifié en mélangeant 5 µL du mix de ligation à 50 µL d'*E.coli* DH5α chimiocompétentes (Invitrogen). Ce mélange est laissé 30 min sur la glace, puis 30s à 42°C exactement, et remis dans la glace 2 min. Ensuite, ajouter 950 µL de milieu LB (Sigma) et incuber 1h à 37°C à 150 rpm. Enfin, étaler 10µL sur boite LB supplémentées en ampicilline 100µg/mL, et incuber sur la nuit à 37°C.

L'ADN amplifié est ensuite extrait *via* l'utilisation du « Gene Elut Plasmid Miniprep Kit », Sigma. Le protocole a été modifié afin d'optimiser le rendement final. Lancer une préculture sur 2 colonies dans 2 mL de milieu LB additionné d'antibiotique de sélection, incuber 24h à 37°C (150 rpm). Puis, 200 µL sont repris dans 10 mL de milieu LB + antibiotique de sélection et incubés 24h à 37°C (150 rpm). La préculture est centrifugée 8 min à 7000 rpm, et le culot est repris dans 200 µL de tampon de suspension, auxquels ont été ajoutés 2 µL de lyzozyme à 50 mg/mL (afin d'augmenter l'efficacité de la lyse), et laissé 5 min à température ambiante (RT). Puis, 200 µL de tampon de lyse sont ajoutés, et le mélange est laissé 5 min à RT. Trois cent cinquante microlitres de tampon de neutralisation sont ajoutés, puis le tube est centrifugé 1 min à 13000 rpm. Parallèlement, la colonne d'extraction est préparée avec 500 µL de tampon de préparation et centrifugée 1min à 13000 rpm. Le surnagent est transféré sur la colonne, et centrifugé 1min à 13000 rpm. Puis, 750 µL de tampon de lavage sont ajoutés, et la colonne est centrifugée 1min à 13000 rpm. Après 1 min de séchage à RT, l'ADN est élué de la colonne par 120 µL de la solution d'élution, préalablement chauffée à 50°C, puis centrifuger 1min à 13000 rpm.

I-1-3- Contrôle de l'ADN plasmidique amplifié et extrait

Afin de contrôler la bonne insertion du gène dans le pBLTI221sGFP, plusieurs clones de chaque construction plasmidique obtenue sont digérés par les endonucléases de restriction choisies pour insérer les séquences d'intérêt, selon le protocole décrit en I-1-2, et ainsi vérifier la bonne taille de l'insert.

Une fois les digestions contrôles effectuées, chaque clone est séquencé au laboratoire, avec le système d'analyses génétiques CEQ™, afin de vérifier l'exactitude de la séquence et le respect du cadre de lecture de la sGFP. Les primers ev1 (situé dans le promoteur 35S) et sGFPRev (situé au début de la GFP) ont été utilisés, ainsi que le kit de séquençage « Dye Terminator Cycle Sequencing Quick Start Kit », Beckman Coulter.

I-1-4- Sous-clonage dans le vecteur d'expression pBLTI-121

Le vecteur pBLTI121 (Pagny et al., 2000), représenté **Figure 42**, est un vecteur binaire utilisé pour la transformation des cellules végétales par *Agrobactérium tumefaciens*.

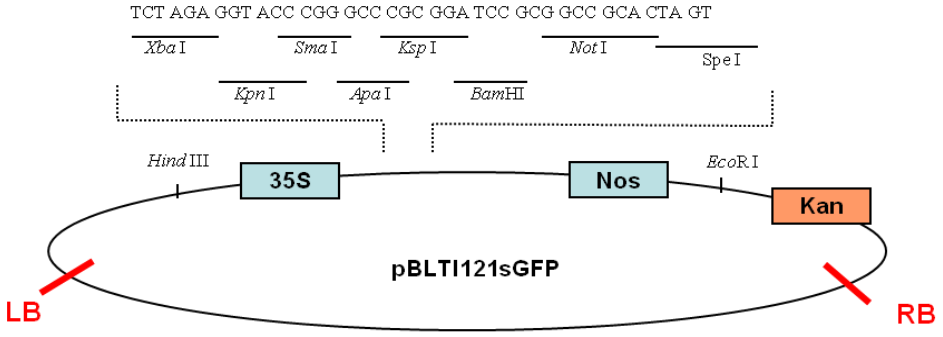

Figure 42 : Représentation schématique du vecteur de clonage pBLTI221sGFP
35S : promoteur CaMV35S du virus de la mosaïque du chou-fleur, Nos : terminateur nos 3 du gène de la nopaline synthase, Kan : gène de résistance à la kanamycine.

Les constructions obtenues dans le vecteur de clonage pBLTI221sGFP sont digérées par le couple d'enzymes BamH1/Sac1, afin de sortir la cassette d'expression contenant la protéine fusionnée à la sGFP, et de l'insérer dans le vecteur pBLTI121, préalablement digéré par BamH1/Sac1. Les méthodes de digestion, ligation, d'amplification, et d'extraction du plasmide sont identiques au protocole décrit en I-1-2.

I-2- Clonage par recombinaison : le système GATEWAY

Cette partie du travail a été effectuée en 2008 durant mon stage doctoral (6 mois) au sein du laboratoire de recherche « *Plant cell wall biotechnology: cell wall elaboration* », dirigé par le Dr Ahmed Faik, à l'université d'Athens, Ohio, USA.

I-2-1- Principe du Gateway

Les protéines homologues d'AtMUR4/UXE1, à savoir At2g20460/UXE2 et At2g34850/UXE3, ont été fusionnées à l'extrémité N terminale de la GFP selon la méthode suivante.

La technologie Gateway a été développée par la société Invitrogen. Elle utilise les propriétés de recombinaison sites spécifiques utilisées par le phage λ pour intégrer son ADN dans le chromosome d'*E.coli.* Les 2 organismes ont des sites de recombinaison spécifiques : *att*P dans le phage λ et *att*B dans *E.coli*. L'intégration de l'ADN est catalysé par 2 enzymes : la protéine Int (integrase) pour le phage λ et la protéine IHF (Integration Host Factor) pour *E.coli*. Après intégration, la recombinaison des sites *att*B (25nt) et *att*P (243nt) va générer des sites *att*L (100nt) et *att*R (168nt) flanquants l'ADN intégré du phage λ, comme montré **Figure 43.**

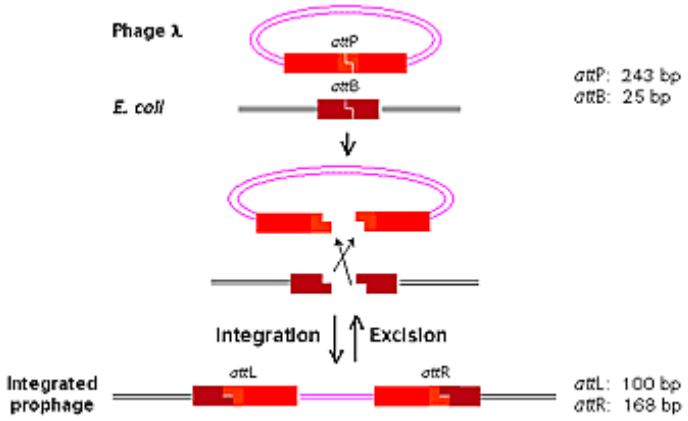

Figure 43 : Principe de la recombinaison par site spécifiques entre le phage λ et *E.coli*.

Cette réaction étant réversible, on peut donc faire des intégrations ou des excisions. La société Invitrogen a donc développé des vecteurs possédant des régions *att*, pour obtenir des vecteurs d'entrée ou de destination. Ici, nous avons utilisé le vecteur d'entrée pENTR-D-TOPO (Invitrogen) pour intégrer notre séquence d'intérêt, qui permet un clonage directionnel du gène, grâce à des extrémités spécifiquement sensibles à l'action de la

Topoisomérase I. Le clone d'entrée ainsi obtenu constitue le point de départ de la deuxième étape, la réaction LR, qui permet de transférer la séquence d'intérêt dans un vecteur de destination, pour donner le « clone d'expression », comme montré **Figure 44**.

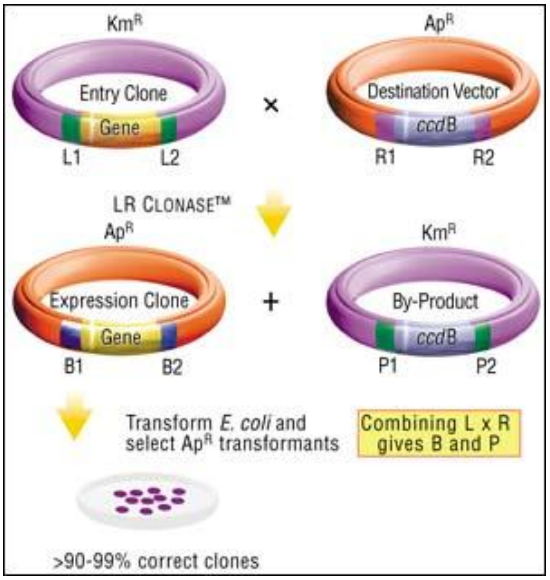

Figure 44 : Principe du clonage Gateway par réactions BP ou LR (Invitrogen)

I-2-2- Amplification PCR

Le gène de chaque protéine est amplifié grâce à la réaction de polymérisation en chaîne (PCR). Les couples de primers utilisés sont décrits **Tableau 2**.

At4g20460	For 5'-CACCATGGCTGCTCATGGTGTGAAG-3' Rev 5'-CATGTATGCAGAAACCAAGGA-3'
At2g34850	For 5'-CACCATGGGCAAGATTATCTTGGTT-3' Rev 5'-CATAAACTTTTTTTCTTTCT-3'

Tableau 2 : Primers utilisés pour l'amplification PCR

Le milieu réactionnel était constitué comme suit : 100 à 200ng d'ADN, 2,5 µL de *Accu prime Pfxreaction mix* (avec dNTP) Invitrogen, 1 µL de chaque primer à 10 µM, 0,5 µL de *Pfx DNA polymerase* Invitrogen, complété à 25 µL avec de l'eau stérile. Les paramètres de températures de la réaction PCR sont décrits **Figure 45**.

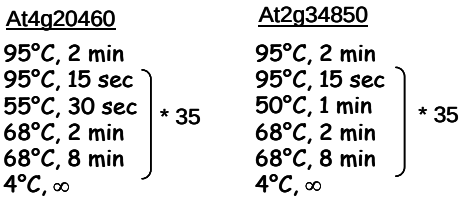

Figure 45 : Paramètres des cycles PCR (dénaturation, hybridation et élongation).

I-2-3- Insertion du gène d'intérêt dans le vecteur d'entrée pENTR-D-TOPO ®

Le gène d'intérêt est dans un premier temps intégré au vecteur d'entrée pENTR-D-TOPO **(Figure 46)**, *via* l'utilisation du « pENTR-D-TOPO cloning kit », Invitrogen.

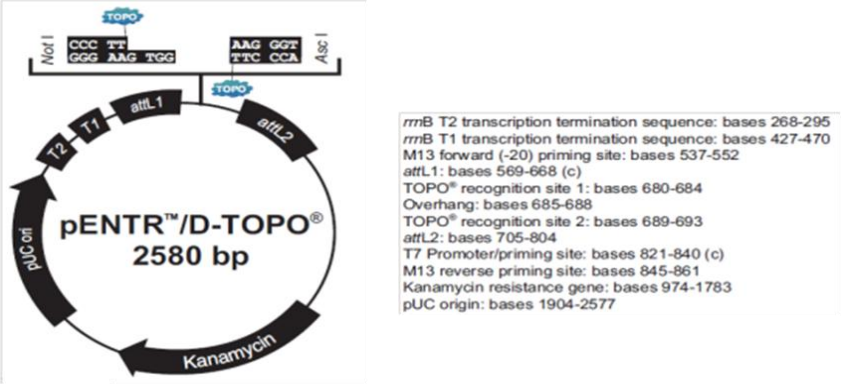

Figure 46 : Représentation schématique du vecteur d'entrée pENTR/D-TOPO

Mélanger 4µL du mix de produit PCR + 1µL de « Salt solution » + 1µL du vecteur pENTR-D-TOPO. Mélanger doucement et laisser 30 min à température ambiante.

Afin d'amplifier le plasmide, ce dernier est inséré dans *E.coli*, selon le protocole suivant. Mélanger 2µL du mix de ligation à 50 µL de *E.coli* TOP10 (Invitrogen), laisser 30 min sur la glace, puis 45 sec à 42°C exactement. Laisser 1 min dans la glace, puis ajouter 250 µL de milieu SOC (Invitrogen). Agiter à 150 rpm durant 1h à 37°C, puis étaler 10µL et 50µL sur boîte LB + antibiotique de sélection. Laisser sur la nuit à 37°C. Quatre colonies sont piquées et mises en culture séparément dans 2 mL de milieu LB additionné d'antibiotique de sélection, sur la nuit à 37°C (200 rpm), avant d'être traités par le kit « Qiaprep Spin Miniprep », Qiagen

I-2-4- Digestion contrôle Asc1/Not1

Afin de vérifier le sens d'insertion du gène, chaque clone est digéré par des enzymes de restriction selon le protocole suivant. Mélanger 5 µL de miniprep à 1 µL de l'enzyme Asc I (New England Biolabs) + 2 µL de tampon NEB 4 (10X). Ajuster à 20 µL avec de l'eau stérile, puis digérer sur la nuit à 37°C. Purifier le mélange de digestion avec le « QIAquick purification kit», Qiagen. Le plasmide purifié est ensuite digéré par 1 µL de l'enzyme Not1 (New England Biolabs) + 3,5 µL de tampon NEB 3 (10X) + 1 µL de BSA (100X), 4h à 37°C.

I-2-5- Séquençage

Une fois les digestions contrôles effectuées, chaque clone a été envoyé à séquencer au laboratoire « Ohio University Genomics Facility », pour vérifier l'exactitude de la séquence. Les primers M13For et M13Rev ont été utilisés.

I-2-6- Insertion dans le vecteur d'expression pMDC : la réaction de LR clonase

Nous avons choisi le vecteur d'expression pMDC83, représenté **Figure 47**, qui provient d'une banque de vecteur créée par Curtis et Grossniklaus en 2003 (« Marks vector gateway page » : http://botserv1.uzh.ch/home/grossnik/curtisvector/index_2.html), et commercialisée par l'ABRC stock center.

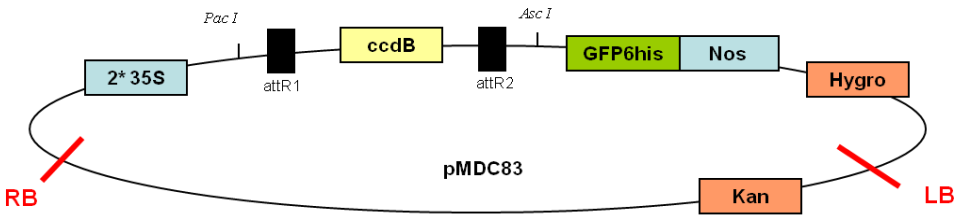

Figure 47 : Représentation schématique du vecteur d'expression pMDC83

Avant d'effectuer la réaction de LR clonase, il est important de digérer le PENTR-D-TOPO contenant le gène d'intérêt avec une enzyme de restriction, afin de linéariser le vecteur. En effet, le vecteur pENTR-D-TOPO et le vecteur pMDC possèdent le même antibiotique de résistance. Il faut tout d'abord digérer 5 µL de pENTR-D-TOPO contenant le gène d'intérêt + 5 µL d'enzymes Mlu I (New England Biolabs) + 2 µL NEB 3 (10 X) + 8 µL d'eau stérile, sur la nuit à 37°C ; puis laisser 10 min à 80°C pour inactiver l'enzyme.

La réaction de LR clonase se déroule comme suit :

- mélanger 2 µL de vecteur pENTR-D-TOPO contenant le gène d'intérêt (et digéré par Mlu I) + 3 µL de vecteur pMDC + 4 µL de tampon TE 1X + 2 µL d'enzyme LR clonase (Invitrogen) ;
- vortexer, et laisser 2h à température ambiante ;
- ajouter 1 µL de protéinase K pour stopper la réaction, puis laisser 10 min à 37°C.

Le plasmide est ensuite amplifié selon la méthode décrite en I-2-3. Puis, plusieurs clones sont piqués et testés par une réaction PCR, comme décrit en I-2-2.

II- Construction des protéines de fusion pour la *Bimolecular Fluorescence Complementation*

Cette partie du travail a été effectuée en 2007 sous responsabilité du Dr. Yumiko Sakuragi durant mon stage doctoral (2 mois) au sein du laboratoire de recherche « *Molecular plant biology: Cell wall* », dirigé par le Pr. Henrik Vibe Scheller, à l'université de Copenhague.

II-1- Clonage *via* l'utilisation de la méthode USER™

II-1-1- Principe du USER™ (uracil-specific excision reagent)

Les protéines AtARAD1 et AtARAD2 ont été fusionnées en Cter ou Nter des moitiés de la YFP, nommées Yn ou Yc pour l'étude des complexes par la technique de complémentation de fluorescence bimoléculaire (BiFC).

Cette nouvelle méthode de clonage ne dépend pas de site de restriction enzymatique ou d'une ligase pour insérer un produit PCR dans un vecteur (Nour-Eldin et al., 2006 et 2010). Dans un premier temps, on créé des primers contenant un uracyl et on amplifie le produit PCR avec une Taq polymérase. Puis, le produit PCR est digéré par l'enzyme USER™, constituée d'un mélange d'uracile DNA glycosylase et de DNA glycosylase-lyase endo VIII, créant au final une extrémité 3' dépassante de 8 nucléotides. En parallèle, un vecteur possédant une cassette de clonage user, appellée cassette PacI, est digéré par les enzymes PacI et N.BbvC pour créer des extrémités 3' dépassantes de 8 nucléotides et complémentaire de celles du produit PCR. Le principe de cette méthode est représenté **Figure 48**. Chacune des extrémités dépassantes n'étant pas complémentaires au sein du produit PCR ou du vecteur, cela permet une insertion orientée du produit PCR et évite un repliement du vecteur sur lui-même.

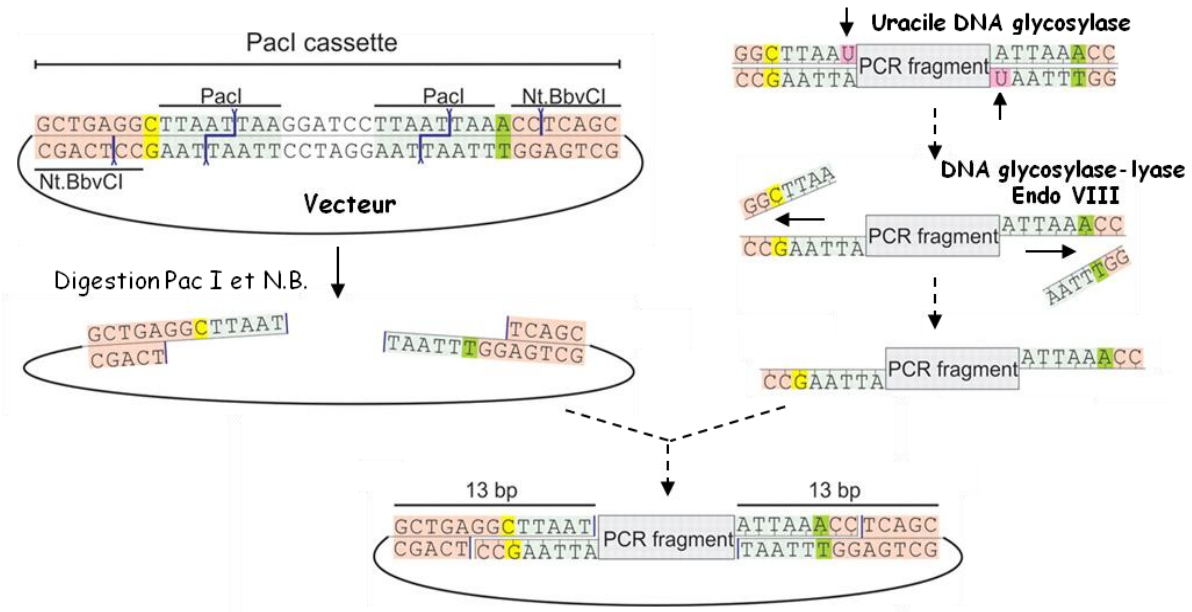

Figure 48 : Principe du clonage USER

II-1-2- Amplification PCR du gène d'intérêt

Le gène de chaque protéine est amplifié grâce à la réaction de polymérisation en chaîne (PCR). Les couples de primers utilisés sont décrits **Tableau 3**.

AtARAD1	For GGCTTAAUATGGCGCGTAAATCTTCCCT Rev GGTTTAAUCCAATGGAAGTGATAAGACCGGT
AtARAD2	For GGCTTAAUATGAACCCCAAAATCAGA Rev GGTTTAAUCCGACACCATGGATGATCCC

Tableau 3 : Primers utilisés pour l'amplification PCR

Le milieu réactionnel était constitué comme suit : 100 à 150ng d'ADN, 5µL de *Turbo Cx Buffer* 10X, 5µL de chaque primer à 5µM, 5µL de dNTP à 2mM, 0,5µL de *Pfx Cx Hot Start Polymerase* NEB, complété à 50 µL avec de l'eau stérile. Les paramètres de températures de la réaction PCR sont décrits **Figure 49**.

94°C, 2min
94°C, 30 sec
50°C, 30 sec
72°C, 1 min 30 sec
} * 30
72°C, 10 min
12°C,∞

Figure 49 : Paramètres des cycles PCR (dénaturation, hybridation et élongation).

II-1-3- Digestion de l'ADN matrice par Dpn I

Cette étape permet de s'affranchir d'un gel de purification, si et seulement si le gène amplifié n'est pas coupé par DpnI. Ajouter 1 µL d'enzyme de restriction DpnI aux 50 µL du mix PCR, incuber 2 heures à 37°C. Puis, inactiver l'enzyme par une incubation de 20 min à 80°C. Ainsi, le mélange est directement utilisable pour la ligation.

II-1-4- Digestion du vecteur de clonage BJH MP27

Nous avons utilisé comme vecteur de clonage le plasmide BJH MP27, représenté **Figure 50**.

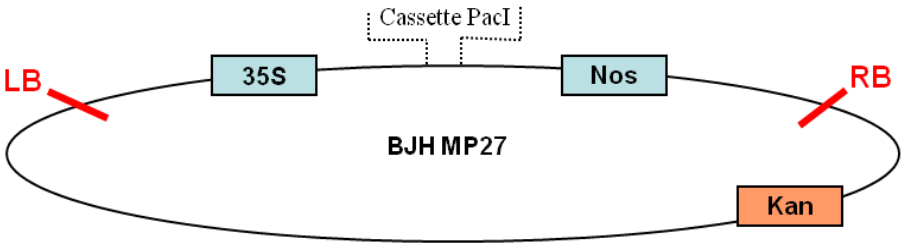

Figure 50 : Représentation schématique du plasmide BJH MP27

Le milieu réactionnel est constitué comme suit : 1µg d'ADN, 2µL de NEB buffer 1 (10X), 2 µL de BSA (10X), 2µL d'enzyme PacI et de l'eau stérile pour compléter à 20µL. Incuber le mélange réactionnel sur la nuit à 37°C, puis ajouter 1 µL d'enzyme N.BbvC et incuber 5h à 37°C. Puis, ajouter 40 µL d'eau stérile, et inactiver l'enzyme *via* un traitement de 20 min à 80°C. Vérifier la digestion sur gel agarose 0,8% + BET 0,3µg/mL, en utilisant le vecteur non digéré comme contrôle. Le mélange est directement utilisable pour la ligation.

II-1-5- Ligation via l'enzyme USER

Le milieu réactionnel est constitué comme suit : 2µL de vecteur digéré par PacI/N.BbvC, 5 µL de produit PCR et 0,5 µL d'enzyme USER. Incuber 30 min à 37°C, puis 30 min à 25°C. Utiliser 4 µL de ce mélange pour l'amplification du plasmide par *E.coli*. L'ADN plasmidique est amplifié et extrait comme décrit en I-1-2.

PARTIE C : EXPRESSION DES PROTEINES DE FUSION

I- Utilisation d'Agrobacterium tumefaciens

Les agrobactéries sont des bactéries pathogènes des plantes. Les souches utilisées en laboratoire renferment un plasmide Ti (Tumor inducing) désarmé, c'est-à-dire qu'il ne contient plus les gènes induisant la tumeur, mais conserve les facteurs de virulence responsables de l'insertion d'un ADN exogène dans le génome des cellules eucaryotes.

Deux souches d'*Agrobacterium tumefaciens* ont été utilisées durant ce travail de thèse : GV3101pMP90RK (Koncz et Schell, 1986) et EHA105 (Hood et al., 1993).

I- 1- Mise en compétence d'*Agrobacterium tumefaciens*

I-1-1- Préparation d'agrobactéries chiomiocompétentes

Une colonie d'agrobactérie est repiquée dans 4 mL de milieu LB stérile, puis laissé 24 h à 28°C sous agitation. Cette préculture est transférée dans 100 mL de milieu LB stérile et incubée à 28°C jusqu'à obtention d'une absorbance lue à 600 nm, égale à 1. Une fois transféré dans 2 cornings de 50 mL, laisser 5min sur la glace, puis centrifuger 5 min à 3000 rpm. Chaque culot est rincé avec 10 mL de $CaCl_2$ 20 mM froid et stérile, puis centrifuger. Le culot est remis en suspension avec 1mL de $CaCl_2$, puis aliquoté par 100 µL dans des eppendorfs, ces derniers sont plongés dans l'azote liquide, puis conservés a -80°C dans du glycérol 20% (Xu et Li, 2008).

I-1-2- Préparation d'agrobactéries électrocompétentes

Une colonie d'agrobactérie est repiquée dans 4 mL de milieu LB stérile, puis laissé 24 h à 28°C sous agitation. Cette préculture est transférée dans 100 mL de milieu frais, et incubée à 28°C jusqu'à obtention d'une absorbance lue à 600 nm, égale à 1. Deux tubes à centrifuger froids sont ensuite transférer dans la glace et laisser 20 min, avant une centrifugation à + 4°C à 4000g durant 15 min. Puis, le surnagent est éliminé et le culot resuspendu dans 50 mL d'eau stérile froide. Les cellules sont lavées 4 fois pour éliminer toutes traces de sels, puis doucement resuspendues dans du glycérol froid et stérile à 10%.

Enfin, aliquoter 50 µL de cellules, et les plonger dans de l'azote liquide, avant de les stocker à - 80°C.

I - 2 - Transformation des agrobactéries

I-2-1- Transformation des agrobactéries chiomiocompétentes

Un microgramme d'ADN plasmidique est ajouté stérilement à 50 µL d'agrobactéries compétentes (souches GV3101 ou EHA105), préalablement décongelées sur glace. Le tube est mélangé et plongé dans l'azote liquide durant 1 min, puis 5 min dans un bain à 37°C. Une fois le choc thermique effectué, 150 µL de milieu LB sont ajoutés et le tube est incubé 4h à 28°C sous agitation. Dix microlitres de cette préculture sont ensuite étalés sur une boite de milieu LB supplémenté en antibiotique de sélection et incubé 2 jours à 28°C.

Afin de préparer un stock d'agrobactéries transformées, une colonie est repiquée et mise dans 3 mL de milieu LB supplémenté en antibiotique de sélection et laissé 24h à 28°C. La préculture est centrifugée 10 min à 3000 rpm, le culot est repris dans 500 µL de LB stérile, additionné de 200 µL de glycérol 80%, dans des tubes cryogéniques. Ces derniers sont plongés 3 min dans l'azote liquide et mis à -80°C.

I-2-2- Transformation des agrobactéries électrocompétentes

Mélanger doucement 200 ng d'ADN à 50 µL d'agrobactéries électrocompétentes, et transférer dans une cuvette d'électroporation pré refroidie en déposant la goutte au milieu de la cuvette. Insérer la cuvette dans l'appareil d'électroporation (Bio-Rad, « Cap Exterior pulse»), puis créer le choc électrique, selon les paramètres suivants : Capacitance 25 µF ; Voltage 2,4 kV ; Sample resistance 200 Ω ; Pulse length 5 ms. Puis, ajouter 1 mL de milieu LB, transférer dans un eppendorff, et incuber 4h à 28°C (200 rpm). Etaler 1 à 10 µL sur boîte LB supplémentée en antibiotique de sélection.

II- Transformation de cellules végétales

II-1- Transformation transitoire des cellules épidermiques de feuilles de tabac *Nicotiana tabacum*

Une préculture fraîche d'agrobactérie transformée est réalisée en prenant 50 µL d'une préculture mère dans 3 mL de milieu LB stérile additionné de l'antibiotique de sélection, et laissé 24h à 28°C. La préculture est transférée dans un tube corning et centrifugée 10 min à 4000 rpm. Le culot est remis en suspension dans du milieu LB pour un volume final d'environ 200 µL. L'absorbance est ensuite mesurée à 600 nm par spectrophotométrie pour connaître la concentration en agrobactéries.

Puis, ces dernières sont diluées dans un milieu d'infiltration (MgCl2 1mM, MES 1mM, Acétosyringone 10 µM) selon la concentration en agrobactérie désirée pour l'étude, et laissées 1h à température ambiante. (L'acétosyringone contenue dans le milieu d'infiltration permet l'activation des gènes de virulence des agrobactéries). A l'aide d'une seringue de 2 mL, les agrobactéries sont infiltrées au sein de la couche de cellules épidermiques, situées sur la partie inférieure des feuilles de tabac. Il est important de ne pas infecter plus de 75% de la surface de chaque feuille, sinon elles meurent. Les plantes sont ensuite maintenues 1 à 3 jours dans les conditions optimales de cultures.

II-2- Transformation stable des cellules de tabac Bright Yellow-2 (BY-2)

Afin d'insérer la protéine au sein du génôme de la plante, une transformation stable des cellules BY-2 de tabac par *Agrobacterium tumefaciens* est effectuée.

Cinq millilitres de suspension cellulaire BY-2 sauvage, âgée de 3 à 4 jours, sont mis en contact avec 100 µL d'une préculture d'agrobactérie transformée (agée de 24h), durant 48h à 22°C et à l'obscurité. Cette coculture est ensuite lavée 3 fois avec du milieu BY-2 frais (v/v) supplémenté en céfotaxime à 250 mg/mL (détruit les agrobactéries) avec 5 min d'attente, et centrifugée 3 min à 3000 rpm. Le culot est resuspendu dans 1mL de milieu BY-2 et étalé sur milieu BY-2 solide contenant de la céfotaxime à 250 mg/mL et les antibiotiques de sélection. Quatre à six semaines sont nécessaires pour obtenir des microcals transformés.

PARTIE D : LOCALISATION DES PROTEINES DE FUSION

I- Analyse par Microscopie Confocale à Balayage Laser (MCBL)

I-1- Principe de la microscopie confocale à balayage laser (MCBL).

La microscopie confocale à balayage laser (ou MCBL) est une technique de microscopie optique permettant de réaliser des images de faible profondeur de champ, appelées « section optiques ». Ainsi, on limite la perte de résolution due à la superposition d'informations issues des plans adjacents. La MCBL permet d'isoler la fluorescence d'un unique plan focal, grâce à l'utilisation d'un diaphragme variable (ou pinhole) en amont du détecteur. Le principe de cette technique est illustré **Figure 51**.

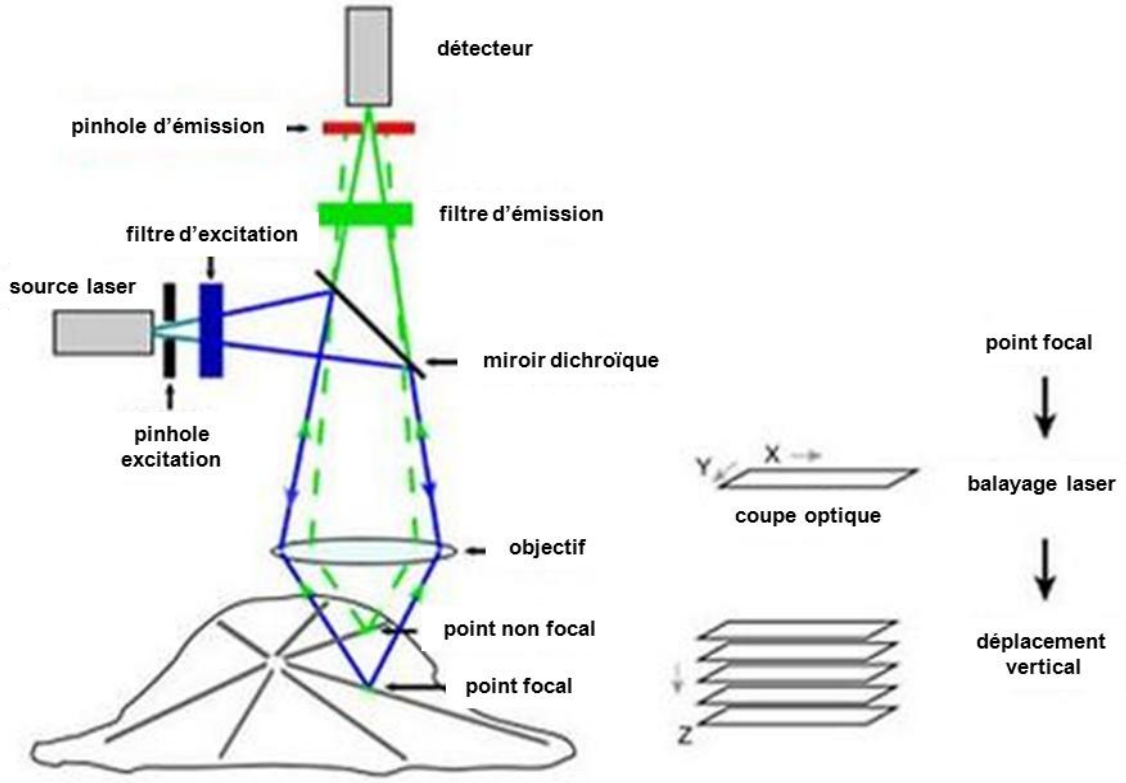

Figure 51 : Principe d'un microscope confocal à balayage laser

Le rayon laser excitateur pénètre l'échantillon préalablement marqué par un ou plusieurs types de fluorochromes. Si la longueur d'onde du rayon laser correspond à la longueur d'onde d'excitation d'un type de fluorochromes, ces derniers émettront des rayons lumineux de différents plans optiques. Ces rayons seront ensuite filtrés par le diaphragme, afin d'isoler ceux ne provenant que d'un plan focal et d'éliminer le signal des plans voisins. Les rayons

filtrés sont ensuite réceptionnés par des photo-multiplicateurs (PMT) qui vont sélectionner les fenêtres spectrales d'intérêt, et convertir le signal lumineux en un signal numérique. Ce signal numérique sera transmis à l'ordinateur qui permettra la modélisation et la reconstitution de l'image.

I-2- Préparation des échantillons

Pour l'observation de l'expression transitoire des protéines de fusion, 3 sections de 1 cm^2 de feuilles de tabac sont découpées et observées en milieu hydrophile, entre une lame de verre et une lamelle couvre-objet. Pour l'étude de l'expression stable des protéines de fusion, une goutte de suspensions cellulaires de tabac âgées de 3/4 jours est observée entre une lame de verre et une lamelle couvre-objet.

I-3- Paramètres d'observations

Les observations ont été réalisées sur le microscope confocal droit TCS SP2 Leica de la Plate-forme régional de recherche en imagerie cellulaire de Haute-Normandie (PRIMACEN), localisée sur le campus de Mont Saint Aignan. Deux marqueurs fluorescents ont été utilisés pour les différentes observations : la *Green Fluorescent Protein* (sGFP) et la *Red Fluorescent Protein* (mRFP). Pour chaque marqueur, un λscan est effectué afin de définir la fenêtre spectrale optimale, pour capter les longueurs d'ondes d'émission spécifiques sur notre échantillon. Les paramètres retenus sont les suivants : pour la sGFP $\lambda_{excitation}$ = 488nm et $\lambda_{émission}$ = 500-520nm et pour la mRFP $\lambda_{excitation}$ = 543nm et $\lambda_{émission}$ = 580-620nm. Les réglages du gain (limite haute du PMT) et de l'offset (limite basse du PMT) sont réglés pour chaque observation, afin de diminuer au maximum les signaux de fluorescence non spécifiques.

II- Microscopie Electronique à Transmission

II-1-Principe du microscope électronique à transmission

Dans un microscope électronique (**Figure 52**), des électrons accélérés sont générés par un canon à électrons comprenant une source et un champ électrique produit par une différence de potentiel entre la source et une anode, puis focalisés sur l'échantillon par des lentilles magnétiques ou électrostatiques. Le faisceau d'électrons interagit avec un échantillon suffisamment mince, avec un contraste spatial résultant de différences de densité ou de composition chimique, et mesuré par un détecteur permettant ainsi de former

une image de l'échantillon. Le système de lentilles magnétiques permet de projeter l'image de l'échantillon sur un écran phosphorescent qui transforme l'image électronique en image optique. Les observations ont été effectuées sur un microscope électronique à transmission FEI Tecnai 12 Biotwin sous une tension de 80 kV, avec une caméra CCD Gatan ES500W Erlangshen.

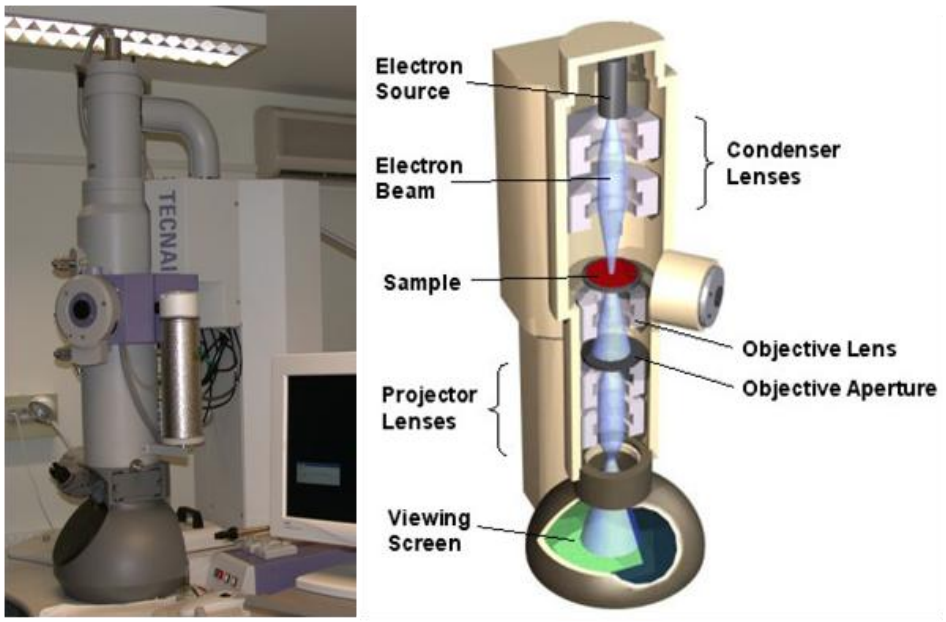

Figure 52 : Principe du microscope électronique à transmission

II-2- Cryoimmobilisation haute pression

II-2-1- Préparations des échantillons à la congélation

Avant leur congélation, les suspensions cellulaires de tabac âgées de 3 à 4 jours (transformées ou non), sont concentrées par filtration sur une membrane de nylon de 50µm. Les cellules sont d'abord cryoprotégées par des bains de glycérol. Elles sont incubées successivement dans du milieu BY-2 contenant 5% glycérol, puis 10% glycérol 1h à + 4°C chaque bain. Les cellules sont ensuite transférées dans du milieu BY-2 additionné de 20% glycérol. Sous stéréomicroscope, les cellules sont rapidement transférées dans les anneaux de cryofracture (diamètre extérieur de 1,2 mm ; cavité ouverte de 100 µm d'épaisseur) ou dans des cupules d'or (diamètre 1,2mm et 200 µm de profondeur), et l'excédent de liquide est délicatement absorbé avec une pointe de papier filtre tout en veillant à ne pas déshydrater sévèrement l'échantillon avant sa congélation.

II-2-2 Cryofixation des échantillons sous haute pression

La cryofixation sous haute pression apporte plusieurs avantages comparée aux méthodes dites « classiques » de fixation. Elle permet une fixation physique de l'échantillon, évitant ainsi les artéfacts de préparation dus à l'utilisation des fixateurs chimiques classiques. De plus, l'échantillon étant congelé très rapidement et à très basse température, il est congelé non pas sous forme de « glace cristalline » mais sous forme de « glace vitreuse » qui n'altère pas son ultrastructure et préserve au mieux son état natif, comme il est montré **Figure 53.**

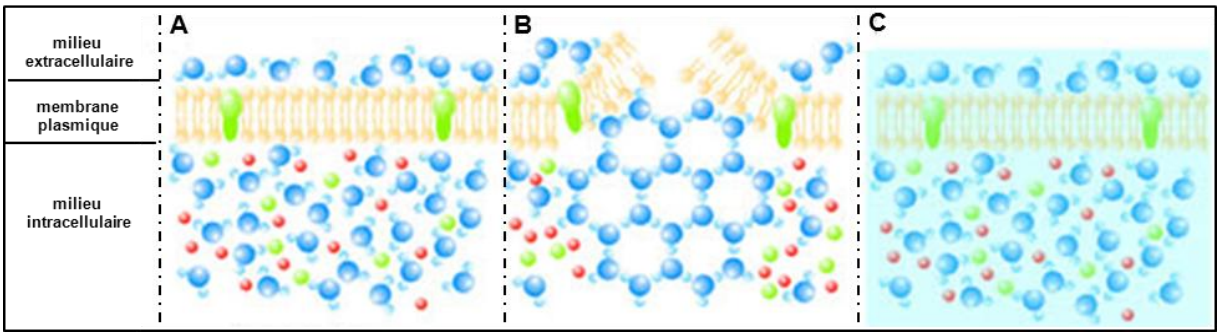

Figure 53 : Les différentes formes de l'eau dans une cellule.
A- Echantillon à température ambiante avec un milieu intracellulaire sous forme liquide, B- Echantillon congelé et endommagé par la glace cristalline formée, C- Echantillon congelé sous forme de glace vitreuse et non endommagé.

La congélation sous haute pression a été réalisée avec l'appareil HPF-EMPACT I (Leica-Vienne) **(Figure 54)** dont le mode d'action est parfaitement détaillé par Studer et al., 2001. Brièvement, la pression est générée par un système hydraulique faisant intervenir le méthylcyclohexane comme liquide de compression. Le cryogène utilisé est l'azote liquide. La pression (2000 bars), appliquée à l'intérieur de l'échantillon est synchronisée avec le refroidissement (jet d'azote liquide) appliqué à l'extérieur de l'échantillon entraînant une congélation ultrarapide de l'échantillon. Pour une pression d'entrée de 9,5 bars, des taux de refroidissements variant de 12 000°C/sec à 15000°C/sec sont obtenus. Lorsque l'échantillon est congelé, il tombe automatiquement dans un réservoir d'azote où il est conservé en attendant son transfert dans l'automate de substitution.

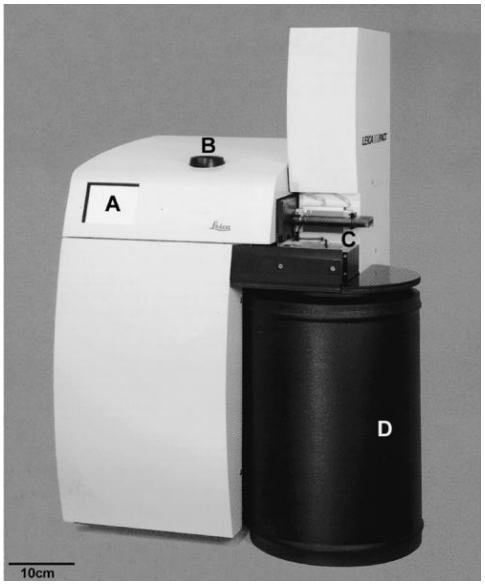

Figure 54 : Apppareil de cryofixation sous haute pression EMPACT1, Leica (Studer et al., 2001)
A- Ecran de contrôle, B- Réservoir pour le liquide de haute pression (Méthylcyclohexane), C- Zone de chargement du porte-échantillon et de transfert dans l'azote liquide après la cryofixation, D- Deware contenant la réserve d'azote liquide.

II-2-3- Cryosubstitution et enrésinement

Après congélation sous haute pression, les échantillons sont transférés dans l'automate de substitution AFS (Freeze-substitution- Leica Vienne) **(Figure 55)** pré-refroidi à -140°C. Les échantillons sont substitués dans l'acétone anhydre contenant 0,5% d'acétate d'uranyle à -90°C pendant 72h. La température est graduellement augmentée de 2°C/h jusqu'à -60°C et maintenue pendant 12h. La température est de nouveau remontée à -30°C (2°C/h). Après un pallier de 12h à -30°C, les échantillons sont maintenus à -15°C.

Les échantillons sont rincés deux fois 15 min dans l'éthanol sec. L'infiltration est réalisée à -15°C dans un mélange London Resin White (LRW) : éthanol (ratio 1:2; 1:1; 2:1, 8h chaque étape) puis en résine pure 2x24h. La polymérisation a lieu sous ultra-violet à -15°C pendant 48h. La résine LRW est une résine acrylique polyhydroxyaromatique. Pour polymériser cette résine sous UV, il est nécessaire de lui ajouter un catalyseur d'éther de benzoïne dans une proportion de 0,5% w/v.

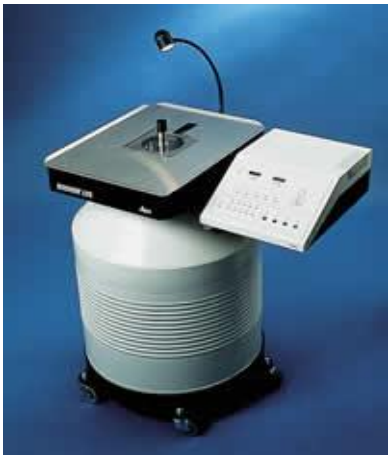

Figure 55 : Automate de cryosubstitution AFS1, Leica

II-3- Réalisation des coupes ultrafines

Comme montré **Figure 56**, les sections ultra-fines de 90 nm ont été obtenues sur un ultramicrotome UCT (Leica-Vienne) avec un couteau de diamant Diatome 45°. Les sections ont été recueillies sur des grilles nickel 100 mesh à trames hexagonales recouvertes d'une membrane formvar-carbone.

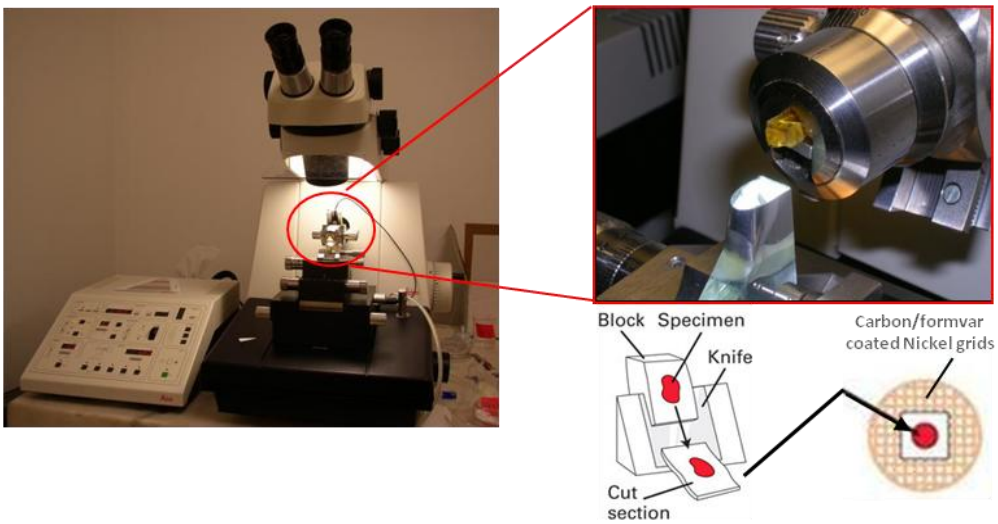

Figure 56 : Ultramicrotomie

II- 4- Immunocytochimie

II-4 -1- Immunomarquage des polysaccharides complexes

Les anticorps primaires testés LM5, LM6, LM13, LM15, LM16 (Plant probes) sont des anticorps monoclonaux produits chez le rat, et les anticorps INRARU1 et INRARU2 sont des anticorps produits chez la souris. L'anticorps secondaire utilisé est un anticorps anti rat ou anti souris conjugué à une particule d'or de 10 nm (Tebu, British BioCell).

Afin de saturer les sites non spécifiques, les sections sont incubées durant 30 min dans un tampon TBS (Tris 20 mM ; NaCl 150 mM) + BSA 0,2% + Lait écrémé 3%, avant d'être rincée 2 min dans un tampon (TBS + BSA 0,2%). Puis, les coupes sont incubées dans l'anticorps primaire pur durant 3h, à 25°C, avant d'être rincées 6x5 min dans le tampon (TBS + BSA 0,2%). L'incubation dans l'anticorps secondaire dilué au 1/20 dans une solution de (TBS + BSA 0,2% + NGS 1/30) s'effectue 1h à 25°C. Les rinçages sont effectués 6x5 min avec du tampon (TBS + BSA 0,2%), puis 5 min dans du TBS seul. Afin de fixer les complexes immuns, on incube 10 min dans une solution de (TBS + glutaraldéhyde 2 %). Les coupes sont ensuites rincées 1x5 min dans du TBS, puis 2x5 min dans l'eau milliQ, avant d'être séchées à l'air.

II-4-2- Immunomarquage des protéines fusionnées à la GFP

L'anticorps primaire Av peptide living color testé (Clontech) est un anticorps polyclonal produit chez le lapin, qui reconnaît la GFP, même fusionnée à une autre protéine. L'anticorps secondaire utilisé est un anticorps anti lapin conjugué à une particule d'or de 10 nm (Tebu, British BioCell).

Afin de saturer les sites non spécifiques, les sections sont incubées durant 15 min dans un tampon TBS (Tris 20 mM ; NaCl 150 mM) + BSA 0,2% + Tween 20 0,05%, avant d'être rincée 2 min dans un tampon (TBS + BSA 0,2%). Puis, les coupes sont incubées dans l'anticorps primaire Av peptide dilué au 1/5 dans une solution de (TBS + BSA 0,2% + NGS 1/30) durant 2h, à 25°C, avant d'être rincées 6x5 min dans le tampon (TBS + BSA 0,2%). L'incubation dans l'anticorps secondaire dilué au 1/20 dans une solution de (TBS + BSA 0,2% + NGS 1/30) s'effectue 1h à 25°C. Les rinçages sont effectués 6x5 min avec du tampon (TBS + BSA 0,2%), puis 5 min dans du TBS seul. Afin de fixer les complexes immuns, on incube 10 min dans une solution de (TBS + glutaraldéhyde 2 %). Les coupes sont ensuites rincées 1x5 min dans du TBS, puis 2x5 min dans l'eau milliQ, avant d'être séchées à l'air.

II-5- Coloration et observation des coupes ultrafines

Les échantillons ainsi préparés transparents aux électrons, il faut donc les contraster. Dans un premier temps, les grilles sont mises en présence de vapeur d'une solution à tétroxyde d'osmium à 2%. Puis, nous faisons agir une solution d'acétate d'uranyle à 0,5% dans le méthanol pendant 10 min. Après rinçage dans de l'eau milliQ, les grilles sont

incubées 10min dans une solution de citrate de plomb, puis rincées dans l'eau milliQ. Les observations ont été réalisées avec le microscope électronique à transmission TECNAI 12 Biotwin (FEI company, Eindhoven, NL) sous une tension d'accélération de 80 kV. Les images ont été acquises avec une caméra CCD Erlangshen ES500W (GATAN) pilotée par le logiciel Digital Micrograph (GATAN).

II-6- Tests statistiques

II-6-1-Spécificité de marquage : Test du khi-deux

Afin d'évaluer la spécificité de la distribution des particules d'or pour le marquage des épitopes polysaccharidiques ou des protéines fusionnées à la GFP, comparé à un témoin négatif, nous avons effectué un test du khi-deux (Mayhew et al., 2002). Pour le marquage des épitopes polysaccharidiques, nous avons considéré l'hypothèse nulle « Pas de différence de distribution des particules d'or entre le témoin contrôle sans anticorps primaire et le test avec l'anticorps primaire et secondaire ». Pour le marquage des protéines fusionnées à la GFP, nous avons considéré l'hypothèse nulle « Pas de différence de distribution des particules d'or entre les cellules sauvages et les cellules transformées ». Pour chaque test khi-deux, le nombre de particules d'or dans les compartiments golgiens (*cis*, median, *trans* et TGN) a été analysé.

Une table de contingence (2 colonnes X 4 lignes) a été créée comme décrit T**ableau 4** (Mayhew et al., 2002).

	Test avec l'anticorps primaire et secondaire Ou Cellules transformées			Témoin sans anticorps primaire Ou Cellules sauvages			
Compartiment golgien	Nombre de particules observées	Nombre de particules attendues	χ^2 partiel	Nombre de particules observées	Nombre de particules attendues	χ^2 partiel	TOTAL
cis							
median							
trans							
TGN							
TOTAL							

Tableau 4 : Tableau de calcul pour le test du khi-deux.

Dans cette analyse, le « nombre attendu de particules d'or » est calculé comme suit : *(nombre total particules de la colonne X nombre total particules de la ligne) / grand total*.

Chacun étant définit comme suit : *Nombre total particules de la colonne* = nombre de particules issu des 4 compartiments golgiens, *Nombre total particules de la ligne* = nombre de particules d'un seul compartiment golgien issu du témoin négatif et du test, *Grand total* = nombre total de particules des 4 compartiments issu du témoin négatif et du test.

Une fois ces valeurs obtenues, les valeurs de khi-deux partiel ont été calculées comme suit : (nombre de particules observées – nombre de particules attendues)^2 / nombre de particules attendues. La valeur du khi-deux total est ensuite comparée à la valeur du khi-deux référence dans une table de contingence, avec un degré de liberté égal à 3 [ddl = (Nombre de colonne-1)*(Nombre de ligne-1)], voir Mayhew et al., 2002.

II-6-2- Distribution golgienne des particules d'or : Test du RLI

Afin d'évaluer si le marquage des épitopes polysaccharidiques et des protéines de fusion au sein de saccules golgiennes est aléatoire, ou au contraire spécifique d'un ou plusieurs compartiments golgiens, nous avons effectué un test du RLI, qui signifie *Relative Labeling Index*.

La quantification a été effectuée, comme décrit dans Mayhew et al. (2002) et Mayhew (2011), sur un total de 35 à 50 saccules golgiennes ayant les 4 sous-compartiments (*cis*, médian, *trans*, TGN) parfaitement définis et photographiés au grossissement X60000. Puis, pour chaque photo, une région d'intérêt a été définie pour définir la saccule golgienne, et donc la zone de comptage. Dans un premier temps, les particules de chaque compartiment ont été comptées et définies comme le « *Nombre de particules observées,(n_0)* ». Puis, on superpose sur chaque photo un maillage fait de croix disposées de façon aléatoire (voir Mayhew et al., 2002 pour la création du maillage), et on compte le nombre de croix dans chaque compartiment, qui représente le « *Nombre de points observés,(P)* ». Une fois ces données obtenues, on calcule le « *Nombre de particules attendues, (n_e)* » (qui représente la distribution aléatoire), comme suit : $n_e = (P * n_{0\ total}) / P_{total}$, où « $n_{0\ total}$ » et « P_{total} » représentent les valeurs tous compartiments confondus.

Les valeurs des « *nombres particules observées et attendues* » permettent de calculer le RLI = (n_0 / n_e), pour chaque compartiment golgien. Pour une distribution aléatoire, la valeur du RLI est inférieure ou égale à 1. Pour un compartiment golgien préférentiellement marqué, la valeur du RLI doit être strictement supérieure à 1 et la valeur du χ2 du compartiment doit être supérieure à 10% du χ2 total (Mayhew, 2011).

PARTIE E : TECHNIQUE D ETUDE POUR LA RECHERCHE DE COMPLEXES ENZYMATIQUES : LA COMPLEMENTATION DE FLUORESCENCE BIMOLECULAIRE(BIFC)

I- Principe de la Bimolecular Fluorescence Complementation (BiFC)

Cette technique repose sur l'observation de la fluorescence résultant de la reconstitution de la *Yellow Fluorescent Protein* ou d'autres variants de la *Green Fluorescent Protein* (Hu et Kerppola, 2002 ; Kerppola, 2008). Son principe est résumé F**igure 57**.

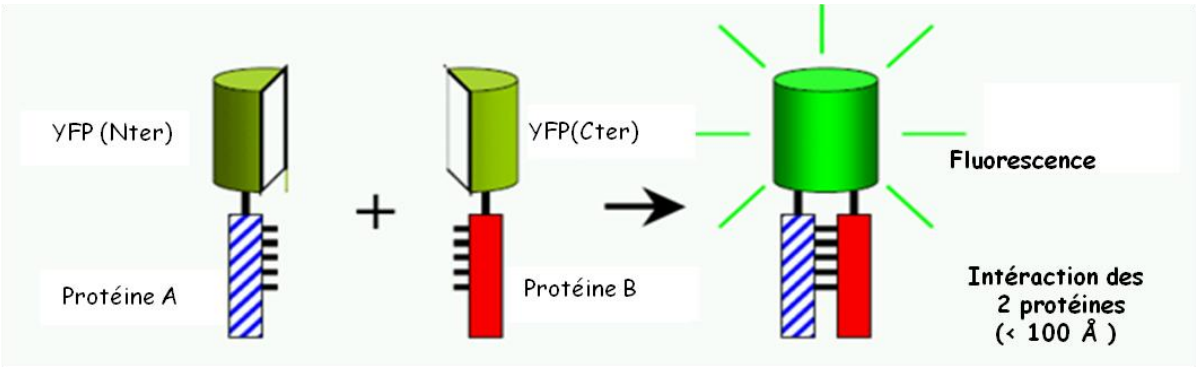

Figure 57 : Principe de la complémentation de fluorescence bimoléculaire

La YFP est séparée en deux fragments, l'un étant porté par une protéine A et l'autre par une protéine B. En cas de forte proximité des protéines A et B, les deux portions YFP (YN: fragment $N_{terminal}$ de la YFP; YC: fragment $C_{terminal}$ de la YFP) s'assemblent et émettent un rayonnement après excitation; cet attachement ne pouvant se faire de manière spontanée entre les fragments de YFP. Au contraire, si les protéines A et B sont distantes de plus de 100Å, la YFP ne peut se reconstituer, et aucune émission de fluorescence n'est observable après excitation.

II- Préparation des échantillons

Pour cette étude, les protéines MUR4, ARAD1 et ARAD2 ont été fusionnées à la YFP, ou à ses portions YN et YC, et exprimées sous le contrôle du promoteur CaMV 35S. Dans un premier temps, les vecteurs d'expression de ces protéines de fusion ont été insérés dans des agrobactéries. Grâce à ces dernières, les 2 protéines de fusion seront coexprimées

transitoirement dans des cellules épidermiques de tabac, puis la fluorescence sera observée par microscopie confocale.

Les constructions disponibles vont être utilisées en de multiples combinaisons, afin de nous fournir des témoins négatifs et positifs, mais également pour étudier les homo- et hétéro-dimérisations.

III- Les paramètres d'observation

Après la transformation transitoire des feuilles de tabac, 3 sections de 1 cm^2 sont découpées et observées en milieu hydrophile entre une lame de verre et une lamelle couvre-objet à 3, 4 et 5 jours après l'infection (ou DPI: *day post infection*) par *Agrobacterium tumefaciens*.

Les observations ont été réalisées sur le microscope confocal à balayage laser TCS SP2 de Leica, appartenant à la plateforme régionale de recherche en imagerie cellulaire de Haute Normandie (PRIMACEN). Le marqueur fluorescent utilisé est un variant de la *Green Fluorescent Protein* (GFP), la *Yellow Fluorescent Protein*-Venus (YFP-Venus). Cette protéine possède des caractéristiques spectrales modifiées (longueur d'onde d'excitation: 514 nm ; longueur d'onde d'émission: 527 nm) et une fluorescence 13 fois supérieure à la YFP classique pour la technique du BiFC (Shyu et *al*., 2006). On utilise la raie 514 nm du laser argon comme longueur d'onde d'excitation de la YFP-venus. Un λscan préalablement effectué a permis de définir la fenêtre spectrale optimale, pour capter les longueurs d'ondes d'émission spécifiques de la protéine reporteur. Celle-ci est délimitée entre 520 nm et 550 nm grâce au système de fentes spectrales. Les réglages du gain (limite haute du PMT) et de l'offset (limite basse du PMT) sont effectués sur les feuilles de tabac transformées et adaptés pour chaque observation, afin de diminuer au maximum les signaux de fluorescence non spécifiques.

CHAPITRE III: RESULTATS

PARTIE A : DÉVELOPPEMENTS METHODOLOGIQUES

Un des volets de mes travaux de recherche était d'effectuer la cartographie golgienne d'épitopes glucidiques et d'enzymes impliquées dans la synthèse du XyG et du RG-I à l'échelle de la microscopie électronique à transmission, sur des suspensions cellulaires de tabac BY-2. Ainsi, en premier lieu, nous avons développé au sein du laboratoire une technique de préparation d'échantillons pour l'observation en microscopie électronique. Celle-ci devait être adaptée pour préserver l'ultrastructure des appareils de Golgi et pour préserver les épitopes glucidiques ou les protéines fusionnées à la GFP dans des suspensions cellulaires de tabac BY-2.

Brièvement, avant d'être observé au microscope électronique à transmission un échantillon doit être fixé, déshydraté puis enrésinné en résine acrylique (LRW). Le bloc de résine obtenu est ensuite coupé avec un ultramicrotome, puis les coupes sont traitées par immunomarquage, contrastées et enfin observées au microscope. Les étapes de fixation, déshydratation et enrésinnement par les systèmes classiques peuvent apporter des artéfacts, c'est pourquoi les techniques appelées « cryométhodes » ont été développées. Ici, nous avons utilisé la technique de congélation sous haute pression (HPF, *High Pressure Freezing*), pour l'étape de fixation, suivie de la substitution à froid (FS, *Freeze Substitution*) pour l'étape de déshydratation et d'enrésinnement.

Lors du traitement par HPF, les suspensions cellulaires de tabac sont fixées physiquement par congélation ultrarapide (taux de refroidissement 10 000°C/s) *via* un tir d'azote liquide. Le tir est effectué sous haute pression (2000 bars) pour obtenir un échantillon congelé sous forme vitreuse, et ainsi éviter son éclatement. La difficulté réside dans le fait que les cellules de tabac BY-2 sont des échantillons très hydratés, un prétraitement par un cryoprotectant pour minimiser les artéfacts durant la congélaton est donc nécessaire. Des cryoprotectants non pénétrants (sucrose, dextran) et pénétrants (glycérol) ont été testés. Pour l'étape de substitution à froid (FS), plusieurs milieux de substitution ont été testés, avec de l'acétate d'uranyle et/ou du tétroxyde d'osmium.

Il s'est avéré que pour une procédure HPF/FS sur des suspensions cellulaires de tabac BY-2, un prétraitement par le glycérol comme cryoprotectant, ainsi que l'utilisation d'un mélange acétate d'uranyle/acétone comme milieu de substitution, étaient le plus efficace pour préserver une très bonne ultrastructure des empilements golgiens et les épitopes associés aux protéines fusionnées à la GFP. Ces résultats sont présentés en détail dans l'article ci-après **page 117** :

Chevalier L., Bernard S., Vicré-Gibouin M., Driouich A., and Follet-Gueye ML. (2011) Cryopreparation of tobacco Bright Yellow-2 (BY-2) suspension-cultured cells and application to immunogold localization of Green Fluorescent Protein-tagged-membrane- proteins. *Journal of Biological Research-Thessaloniki*, 16:212-216

Ce protocole de préparation des cellules de tabac BY-2 a été utilisé pour effectuer la cartographie golgienne d'épitopes glucidiques spécifiques du XyG et du RG-I et de différentes enzymes impliquées dans la synthèse du XyG et du RG-I. Ainsi, nous avons également appliqué une méthode statistique à notre problématique, nommée *Relative Labelling Index* (RLI). Les différents protocoles développés sont détaillés dans le sous-chapitre 4 **«** Spatial organization of non-cellulosic cell wall polysaccharides at the ultrastructural level », ci-après **page 135** :

Follet-Gueye ML., Mollet JC., Vicré-Gibouin M., Bernard S., Chevalier L., Plancot B., Dardelle F., Ramdani Y, Coimbra S. and Driouich A. (2012) Applications of Immunocytochemistry. Chapter 14: Immuno-Glyco-Imaging in Plant Cells:Localization of Cell Wall Carbohydrate Epitopes and Their Biosynthesizing Enzymes. Ed. Hesam Dehghani ISBN 978-953-51-0229-8. pp 297-320

Papier N° 2: Article scientifique

Résultats : Développements techniques

Cryopreparation of tobacco Bright Yellow-2 (BY-2) suspension-cultured cells and application to immunogold localization of Green Fluorescent Protein-tagged-membrane- proteins.

Chevalier L., Bernard S., Vicré-Gibouin M., Driouich A., and Follet-Gueye ML

Journal of Biological Research-Thessaloniki (2011) 16:212-216

Journal of Biological Research-Thessaloniki **16**: 202–216, 2011
J. Biol. Res.-Thessalon. is available online at http://www.jbr.gr
Indexed in: WoS (Web of Science, ISI Thomson), SCOPUS, CAS (Chemical Abstracts Service) and DOAJ (Directory of Open Access Journals)

Cryopreparation of tobacco Bright Yellow-2 (BY-2) suspension-cultured cells and application to immunogold localization of Green Fluorescent Protein-tagged-membrane-proteins

Laurence CHEVALIER[1], Sophie BERNARD[2], Maïté VICRÉ-GIBOUIN[2], Azeddine DRIOUICH[2] and Marie-Laure FOLLET-GUEYE[2*]

[1] *Groupe de Physique des Matériaux, UMR6634 – CNRS, Institut des Matériaux Université de Rouen – Faculté des Sciences et Techniques BP 12 – Technopôle du Madrillet, Avenue de l'Université, 76801 St Etienne du Rouvray cedex*

[2] *Laboratoire "Glycobiologie et Matrice Extracellulaire Végétale", UPRES EA 4358, Institut Fédératif de Recherche Multidisciplinaire sur les Peptides 23, Plate-forme de Recherche en Imagerie Cellulaire de Haute Normandie (PRIMACEN), IBiSA, Université de Rouen, 76821 Mont-Saint Aignan Cedex, France*

Received: 16 November 2010 Accepted after revision: 9 March 2011

Electron microscopy investigations require excellent ultrastructure preservation, coupled with high antigenicity signal in specific applications of Golgi enzyme localization. The optimal detection of membrane-bound proteins needs appropriate specimen preparation techniques, such as cryo-methods known to provide higher cell structure and antigen preservation than conventional techniques. Two cryopreparation methods (high-pressure freezing and Tokuyasu techniques) applied to tobacco cultured cell lines are presented in this study. Two transgenic lines of tobacco cultured cells expressing GFP-fused proteins (Man-I-GFP and MUR3-GFP) were used to assess antigenicity under various conditions of cryomethods. According to cell morphology and immunolabeling detection, pre-freezing treatments are discussed in detail for high pressure freezing and freeze substituted samples embedded in both Spurr's and London Resin White. In a same approach, the effect of two fixative solutions was investigated for cryosectioned suspension-cultured tobacco cells using Tokuyasu technique. Integrity during the thawing step and subsequent immunolabeling were analysed under chemical fixation conditions.

Key words: Cryosectioning, GFP-tagged Golgi proteins, high-pressure freezing, immunogold labeling, tobacco BY-2 cells.

INTRODUCTION

The plant Golgi apparatus is involved in the processing of glycoproteins and also in the synthesis of cell wall matrix polysaccharides, such as hemicelluloses and pectins (Driouich *et al.* 1993; Saint-Jore-Dupas *et al.*, 2004). These biosynthetic functions rely on the activities of glycosidases or glycosyltransferases, the genes of which have been identified (Arabidopsis Genome Initiative, 2000). Information on the distribution and dynamics of these enzymes are currently obtained by using green fluorescent protein (GFP) technologies and confocal laser microscopy (Brandizzi *et al.*, 2004). Transgenic tobacco Bright Yellow-2 (BY-2) suspension-cultured cells (Saint-Jore *et al.*, 2002; Pagny *et al.*, 2003; Yang *et al.*, 2005; Dhanoa *et al.*, 2006; Saint-Jore-Dupas *et al.*, 2006) were often used as a model system for the expression of GFP-tagged proteins. Immuno-electron microscopy is the only approach to study the distribution of GFP-labeling at the organelle level, in contrast to light-based microscopy. Therefore, a central issue for immunogold at transmission electron microscopy (TEM) level is to

* Corresponding author: tel.: +33 235140039, fax: +33 235146615, e-mail: marie-laure.follet-gueye@univ-rouen.fr

preserve the epitopes of interest while minimizing the loss of ultrastructural details. As previously reported by Follet-Gueye *et al.* (2003) on the distribution of N-glycan-β (1-2) xylosyltransferase, conventional techniques using chemical fixatives have provided valuable information on the subcellular locations of GFP-fused proteins. In order to increase the specific labeling, additional treatments are often necessary after the chemical fixation step, and are known to induce a potential loss of structural details of membranes. To overcome these problems, it is now well established that the cryomethods (mainly cryofixation and cryosectioning) offer the best alternatives to conventional chemical techniques for ultrastructural and immunocytochemical investigations. Under high pressure and extremely low temperature, cryofixation allows immobilization of cellular structures by achieving amorphous state in few milliseconds, thus minimizing disturbance of natural processes (Studer *et al.*, 2001). When coupled to specific antibodies, high-pressure freezing (HPF) combined with freeze substitution (FS) have proven their efficiency in the localization of cell wall matrix polysaccharides and glycoproteins (Zhang & Staehelin 1992; Driouich *et al.*, 1993; Driouich & Starehelin, 1997), actin cytoskeleton (Lancelle & Hepler, 1992), storage proteins (Jolliffe *et al.*, 2004) and vacuolar receptors (Hinz *et al.*, 2007) in many plant species. Compared to HPF/FS, Tokuyasu cryosectioning (Tokuyasu, 1973) remains the most suitable approach for the detection of membrane-bound proteins. This technique optimizes immunolabeling as evidenced by the excellent preservation of the epitopes, while the embedding and dehydration steps are omitted. These promising techniques have, however, scarce applications in plant suspension-cultured cells. Only a few studies were devoted to protein or GFP-tagged protein localization in tobacco BY-2 suspension-cultured cells using the HPF/FS method (Samuels *et al.*, 1995; Nebenführ *et al.*, 1999; Tse *et al.*, 2004; Langhans *et al.*, 2007; Toyooka *et al.*, 2009; Chevalier *et al.*, 2010) as well as on other plant cells (Zhang & Staehelin, 1992; Driouich *et al.*, 1993; Zhang *et al.*, 1993; Driouich & Staehelin, 1997; Lam *et al.*, 2007; Ebine *et al.*, 2008). Moreover, the Tokuyasu immuno-cryosectioning method is widely used in animal systems to study the distribution of membrane proteins, such as receptor molecules (Liou *et al.*, 1997; Klumperman *et al.*, 1998) but few applications are available in plant systems so far. In *Arabidopsis* root cells, immuno-cryosectioning has allowed localization of coat components such as COPI, as well as of many other proteins involved in vacuolar trafficking, including syntaxin, a transmembrane receptor protein called BP-80, μ-adaptin and vacuolar H^+/ ATPase (Conceiçao *et al.*, 1997; Sanderfoot *et al.*, 1998; Hinz *et al.*, 1999; Pimpl *et al.*, 2000; Happel *et al.*, 2004; Dettmer *et al.*, 2006). More recently, Von der Fecht-Bartenbach *et al.* (2007) localized a chloride transporter (AtCLC-d-GFP) to the *trans* side of Golgi stacks in ultrathin cryosections of *Arabidopsis* root epidermal cells. Applied to tobacco BY-2 suspension-cultured cells, the Tokuyasu immuno-cryosectioning method has been published in a limited number of articles (Saint-Jore-Dupas *et al.*, 2006).

In this context, we report an overview of the technical conditions for tobacco BY-2 suspension-cultured cells preparation, using HPF/FS or cryosectioning methods. The impact of different pre-cooling and freeze substitution media prior to HPF and pre-fixative solutions for cryosectioning were assessed on both the quality of endomembrane preservation in tobacco BY-2 cells and immunogold localization of GFP-tagged Golgi proteins. Despite their high level of hydration, we demonstrate that BY-2 cells were successfully prepared by these cryomethods which could be routinely applied for the detection of Golgi-membrane-bound proteins in this plant model.

MATERIALS AND METHODS

Growth conditions

Tobacco BY-2 suspension-cultured cells were grown *in vitro* as described previously (Gomord *et al.*, 1998). Cells were harvested by filtration 3 d after subculturing and were immediately used for experiments.

Construction of GFP-tagged proteins and transformation of plant cells

The coding sequence of a xyloglucan-β (1-2) galactosyltransferase (At2g20370) from *Arabidopsis thaliana* (MUR3) (Madson *et al.*, 2003) was amplified by PCR without the stop codon, using respectively Forward Kpn1 (5′- GGGGTACCCCATGTTTCCAAGGGTT TCT-3′) and Reverse Nhe1 (5′- CTAGCTAGCCTG TGTCTTATCTCTCTG-3′) primers. The SALK cDNA clones were used as template (S81470). The amplified cDNA was then introduced into the pBLTI221 binary vector containing the sGFP, allowing a N-terminal fusion to the sGFP, and the resulting construct was verified by sequencing. Finally, the cassette containing the chimeric protein was introduced into pBLTI121

binary vector to allow plant transformation. Transformation of *Nicotiana tabacum* (cv. BY-2) cells with *Agrobacterium tumefaciens* was performed as described by Gomord *et al.* (1998). Transgenic lines expressing β (1-2) galactosyltransferase fused to GFP (MUR3-GFP) were obtained as described by Chevalier *et al.* (2010). Transgenic lines of tobacco BY2 suspension-cultured cells expressing the first 99 amino acids of soybean β (1-2) mannosidase I (Nebenführ *et al.*, 1999) membrane protein fused to GFP (ManI-GFP) were obtained as described by Saint-Jore-Dupas *et al.* (2006).

High-pressure freezing, freeze substitution and freeze drying

HPF was performed with the freezer HPF-EM PACT I Leica-microsystems (Studer *et al.*, 2001). Prior to freezing, 3 d-old tobacco (BY-2) suspension-cultured cells were treated with different cryoprotectants such as: 20% (v/v) glycerol (Sigma), 0.4 M (w/v) sucrose (Sigma), 20% (w/v) Bovine Serum Albumin (BSA) (Sigma), 20% (w/v) arabic gum (Sigma) or 25% (w/v) dextran 70 KD (Sigma) diluted in culture medium. For glycerol treatment, the cells were concentrated on 50 µm nylon membrane and incubated successively in 5% and 10% glycerol (v/v) for 1 h at +4°C and under light stirring. Cells were subsequently transferred to 20% (v/v) glycerol and immediately frozen. For the other pre-cooling treatment, cells were incubated for a few minutes in Murashige and Skoog (MS) medium (Sigma) supplemented by cryoprotectants.

Tobacco BY-2 cells pre-treated or not were concentrated on 50 µm nylon membrane and transferred into the cavity of a copper ring used for cryofracture, which is 100 µm in depth and 1.2 mm in diameter. Excess medium was lightly absorbed by filter paper. Using a horizontal loading station, the specimen carriers were tightened securely to the pod of specimen holder. After fixation on the loading device, specimens were frozen according to a maximum cooling rate of 10°C/s, incoming pressure of 7.5 bars and working pressure of 4.8 bars. Rings containing frozen samples were stored in liquid nitrogen until the freeze substitution procedure was initiated.

After HPF the samples were transferred to a FS automate (AFS, Leica Vienna Austria) pre-cooled to –140°C. FS conditions followed a modified procedure from D. Studer (personnal communication). For ultrastructure analyses, substitution media consisted of anhydrous acetone, supplemented with 2% (w/v) osmium tetroxide (Polysciences Inc.). The samples were substituted at –90°C for 72 hrs. The temperature was gradually raised (2°C/hr) to –60°C and stabilized during 12 hrs, then gradually raised (2°C/hr) to –30°C (12 hrs) and gradually raised again (2°C/hr) to 0°C for 2 hrs. The samples were washed at room temperature with fresh anhydrous acetone (Fischer). Infiltration was done at +4°C in acetone-Spurr's resin (Polysciences Inc.) (ratio 2v:1v; 1v:1v; 1v:2v, 8 hrs each step) and with pure resin for at least 2 d. Polymerization was performed at 60°C for 16 hrs. Samples destined for immunocytochemistry were substituted in anhydrous acetone +0.5% (w/v) uranyl acetate (Polysciences Inc.), using a similar program as that described above, except that the final substitution step was performed at –15°C. The samples were rinsed twice with anhydrous ethanol (VWR). Infiltration was processed at –15°C in a solution containing ethanol: London Resin White (LRW) (Polysciences Inc.) (ratio 2v:1v; 1v:1v; 1v:2v, 8 hrs each step) and with pure resin for 2 x 24 hrs. Polymerization was performed into the AFS apparatus at –15°C under UV light for 48 hrs.

Cryosectioning

For cryosectioning (Tokuyasu, 1973 modified), 3 d-old tobacco BY-2 cells were harvested by filtration on 50 µm nylon membrane and fixed at +4°C with a mixture of 1.5% (v/v) paraformaldehyde (PAF) (Prolabo) and 0.2% (v/v) glutaraldehyde (GA) (Agar) (fixative solution 1) or 2% (v/v) PAF and 2% (v/v) GA (fixative solution 2) in 0.1 M Na-phosphate, pH 7.2 buffer (PB) for 16 hrs. After successive washing with a mixture containing 0.1 M glycine (Fischer) in PB saline (PBS: 0.01 M Na-phosphate pH 7.2, Sigma), and 0.15 M NaCl (Fischer), the cells were progressively embedded in 12% gelatin (w/v) in 0.1 M PB. Small blocks (1 to 2 mm^3) of gelatin were cut at + 4°C and transferred into 1.2 M sucrose in 0.1 M PB for 1 hr, then into 2.3 M sucrose in 0.1 M PB for 2 hrs, followed by infiltration with fresh 2.3 M sucrose in 0.1 M PB overnight and then into successive solutions of 2.3 M sucrose in 0.1 M PB for 72 hr periods. The sucrose infiltration method mentioned just above was performed at + 4°C with stirring. Gelatin cubes were then mounted onto specimen stubs, frozen in liquid nitrogen by plunging, and cut into 70 nm ultrathin sections at –120°C with Ultracut UCT microtome (Leica Vienna Austria). Frozen sections were picked up as described by Liou *et al.* (1996) by using a mixture of 2.3 M sucrose in PB and 2% (w/v) methylcellulose and transferred on formvar-coated nickel grids stabilized with carbon.

Immunogold labeling of GFP-tagged membrane protein

Ultrathin sections (50-70 nm; ultracut UCT Leica Vienna Austria) of HPF-prepared tobacco BY-2 cells expressing MUR3-GFP fusion protein were collected on carbon-formvar-coated nickel grids and blocked in Tris-Buffered Saline (TBS: Tris HCl 20 mM pH 7.2, Fischer, 200 mM NaCl) supplemented with 0.2% (w/v) BSA and 0.05% (w/v) Tween 20 (Sigma) for 15 min. Sections were then incubated with the polyclonal anti-GFP antibody (BD living colors A.v peptide antibody – Clontech) at 1:5 dilution in TBS + 0,2% (w/v) BSA and Normal Goat Serum 1:30 (NGS; British Biocell International) for 2 hrs at room temperature. After washing in TBS + BSA, the grids were incubated for 1 hr at room temperature in the anti-rabbit secondary antibody conjugated to 10 nm gold particles (Tebu-British Biocell International). After washing and fixing in TBS + 2% (v/v) GA, the sections were first stained with 4% (w/v) vapour osmium followed by classical staining (uranyl acetate and lead citrate).

Cryosections of tobacco BY-2 cells expressing the soybean β (1-2) mannosidase I-GFP fusion protein were immunolabelled with anti-GFP antibodies derived from a rabbit's polyclonal serum (Pagny *et al.*, 2003). To this purpose, grids with frozen sections were first incubated in PBS containing 0.1% (w/v) glycine to inactivate any residual fixative. The grids were blocked in PBS with 1% (w/v) BSA for 2 min and then incubated with the anti-GFP antibodies diluted 1:100 in blocking buffer for 30 min. After washing in PBS, the grids were blocked in NGS 1:30 in PBS containing 0.1% (w/v) BSA. After incubation with the secondary antibody (British Biocell International, EM gold conjugates, goat-anti-rabbit IgG-10 nm) diluted 1:25 in blocking buffer for 30 min, the grids were incubated with glutaraldehyde 1% (v/v) in PBS for 5 min and finally washed in water. The specimens were stained for 5 min with cold 2% (w/v) methyl cellulose (Sigma) containing 0.4% (w/v) uranyl acetate, at pH 4. Two controls were systematically done by labeling sections of non-transformed tobacco cells and by omitting the first antibody.

Observations were made with a Tecnai 12 Biotwin TEM (FEI company Eindhoven NL) at 80 KV. Image acquisitions were made with a coupled charge device Megaview II camera controlled by AnalySis software (Eloise Paris France).

RESULTS

HPF/FS and Tokuyasu cryosectioning methods were used to process 3 d-old tobacco BY-2 suspension-cultured cells before TEM investigations. With the HPF/FS approach, five types of components for freezing conditions were tested on subcellular preservation, using a standard osmium tetroxide/acetone condition for FS followed by Spurr's resin embedding. The best conditions were then selected to determine their impact on the detection of xyloglucan-galactosyltransferase fused to GFP (MUR3-GFP), using acetone/uranyl acetate as FS medium followed by LRW embedding. According to the Tokuyasu method, the effect of two fixative solutions were assessed on ultrastructural patterns of the cells as well as immunogold labeling of another glycosyltransferase fused to GFP, the N-Glycan-mannosidase I (ManI – GFP).

Ultrastructural preservation of high pressure frozen and freeze substituted tobacco BY-2 suspension-cultured cells

Freezing medium composition was firstly studied on the subcellular structure of 3 d-old BY-2 cells. Freezing of cells directly in their culture medium MS without any additive induces important ice damage leading to very poor preservation of the cell structure (data not shown). Similar damage was observed in samples in which freeze drying and FS were applied as dehydration processes. Noticeable injuries came from an inefficiency of freezing, including tonoplast disruption, segregation phase and extremely low integrity of organelles within the cytoplasm (data not shown). As for Golgi membrane preservation, those conditions were not sufficient to obtain a well preserved ultrastructure. Thus, to get an optimal freezing of this organelle in BY-2 cells, cryoprotectants are required (Figs 1 and 2).

Pre-freezing treatment with glycerol or sucrose and embedding in Spurr's resin

Figure 1A-E shows the general appearance of a tobacco BY-2 suspension-cultured cells frozen in culture medium containing 20% (v/v) glycerol. The cytoplasm presented no visible ice damage and was deprived of any phase segregation. Its ground appeared densely stained with granular texture and was particularly rich in organelles, demonstrating that no extraction occurred during sample preparation. The nucleus was well preserved, showing a smooth nuclear

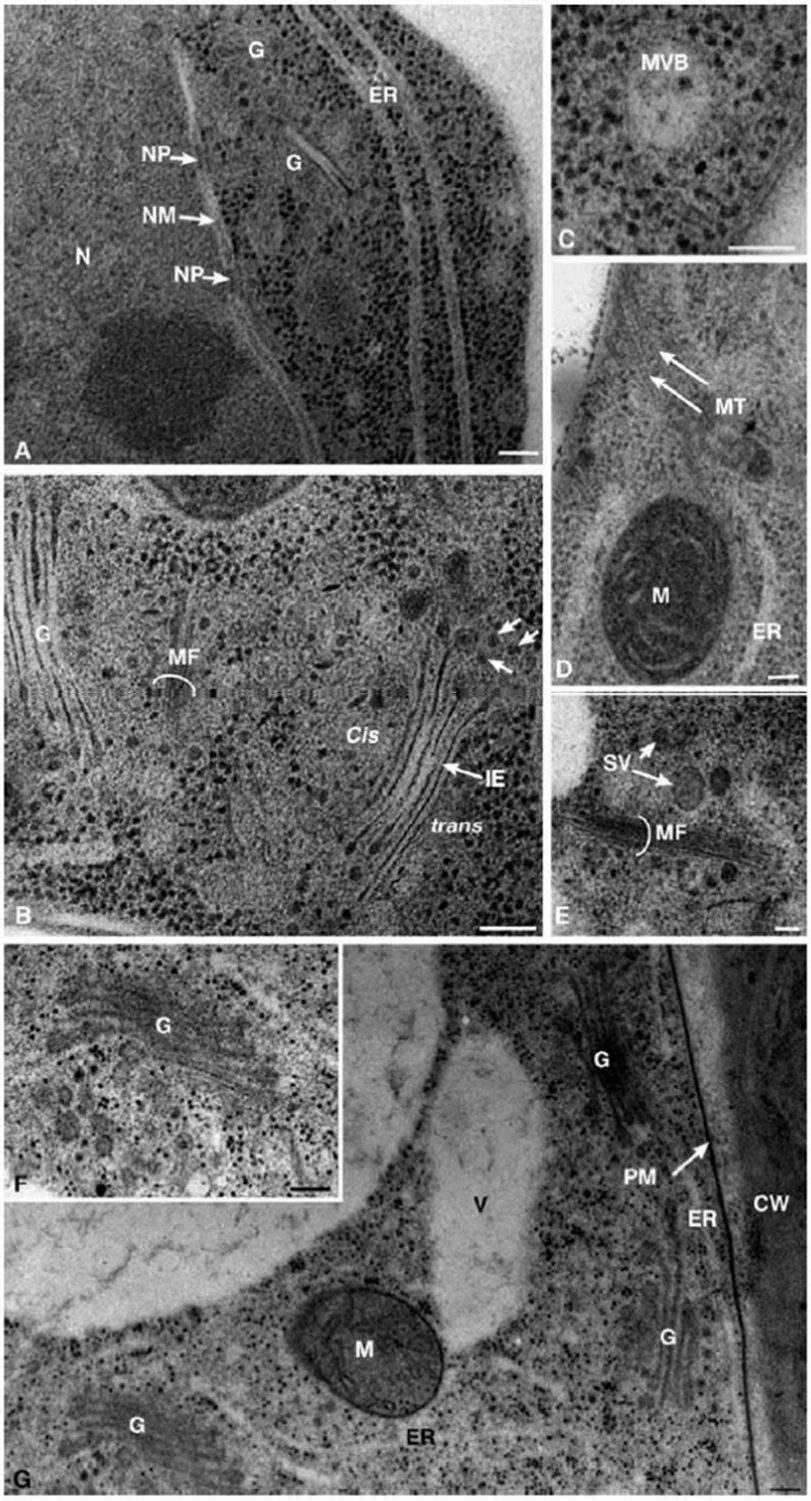

FIG. 1. Electron micrographs of tobacco BY2 suspension-cultured cells cryofixed by HPF. Cells were frozen in 20% (v/v) glycerol (A-E) or in 0.4 M sucrose (F, G). Cryofixed cells were substituted in acetone + 2% (w/v) osmium tetroxide and embedded in Spurr's resin. CW: cell wall; ER: endoplasmic reticulum; G: Golgi stacks; IE: intercisternal elements; M: mitochondria; MF: microfilaments; MT: microtubules; MVB: multi-vesicular body; N: nucleus; NM: nuclear membrane; NP: nuclear pore; PM: plasma membrane; SV: secretory vesicles; V: vacuole. Scale bars = 100 nm.

membrane which exhibited regular disconnections corresponding to nuclear pores. In our conditions, the condensed chromatin showed no evidence of ice crystal damage and appeared as flocculent substances in localized areas. Figure 1C-E depicts the fine ultrastructural details of organelles reported to be particularly susceptible to ice damage. As illustrated in Fig. 1B, Golgi stacks were well preserved. Figure 1B shows *trans* cisternae characterized by a lumen filled with densely stained material and the presence of intercisternal elements. It is worth noting that in plant cells, intercisternal elements are maintained only in cryofixed material showing optimal preservation (see Driouich & Staehelin, 1997). Endoplasmic reticulum membranes were frequently observed with ribosomes lining up their surface. Multi-vesicular bodies and mitochondria both exhibited a typical rounded shape (Fig. 1C-D). Aggregated microfilaments (Fig. 1E) supposed to be actin filaments could often be observed in the vicinity of Golgi vesicles as shown in Fig. 1B. Microtubules were also frequently observed (Fig. 1D) proving that the freezing protocol used is appropriate.

We also assessed the impact of 0.4 M sucrose on the freezing of tobacco BY-2 suspension-cultured cells. This pre-freezing condition provided similar results as glycerol regarding cytoplasm and endomembrane preservation (Fig. 1F, G). The abundance of ribosomes and other organelles throughout the cytoplasm indicated that little or no extraction had occur-

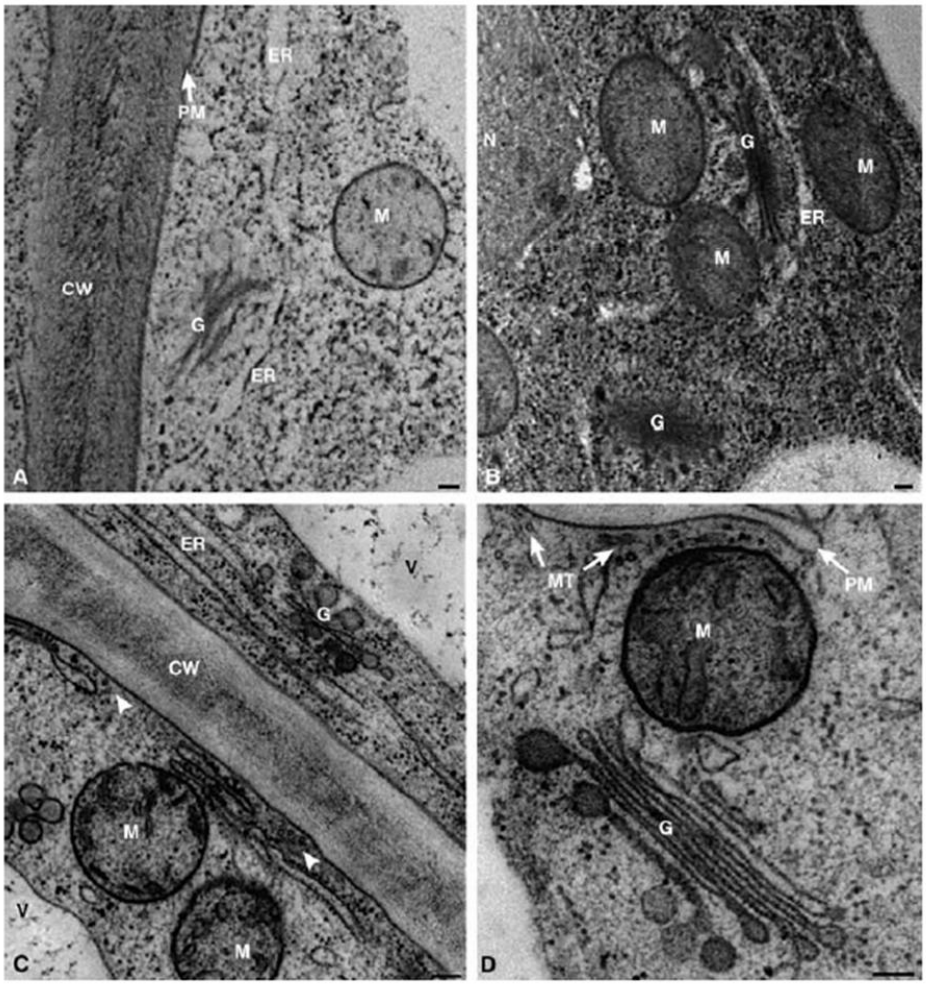

FIG. 2. Electron micrographs of tobacco BY-2 suspension-cultured cells cryofixed by HPF. Cells were frozen in 20% (w/v) BSA (A), 20% (w/v) arabic gum (B) and 25% (w/v) dextran (C, D). Cryofixed cells were substituted in acetone + 2% (w/v) osmium tetroxide and embedded in Spurr's resin. CW: cell wall; ER: endoplasmic reticulum; G: Golgi stacks; M: mitochondria; MT: microtubules; N: nucleus; PM: plasma membrane; V: vacuole. Scale bars = 100 nm.

red (Fig. 1G). Plasma membrane appeared regular as a straight line with no cracks (Fig. 1G). Golgi stacks and associated vesicles were also clearly discernable (Fig. 1F, G). The vacuolar sap, filled with dense material, was also well preserved (Fig. 1G). Comparing images obtained by glycerol (Fig. 1A-E) and sucrose (Fig. 1F, G), constrasting differences appeared on the membranes. It seems that membranes are "negatively" stained by glycerol pre-treatment and positively stained by sucrose.

Pre-freezing treatment with high molecular weight compounds and embedding in Spurr's resin

We have also assessed the ultrastructural preservation of BY-2 cells by supplementing the freezing medium with some high molecular weight cryoprotectants (Fig. 2). The addition of 20% (w/v) BSA was not sufficient enough to preserve well the cell structures (Fig. 2A). Similar damage was observed as in samples that were not cryoprotected before freezing. Although scattered ice defaults were present, treatment with arabic gum before freezing enhanced the quality of morphological preservation (Fig. 2B). The cytoplasm was dense with numerous ribosomes and some well preserved and clearly discernable Golgi stacks. Nevertheless, the last freezing medium tested, which consisted of MS medium with 25% (w/v) dextran, yielded the best ultrastructural preservation of BY-2 cells (Fig. 2C, D). In addition to the excellent preservation of different cellular organelles, including Golgi stacks, endoplasmic reticulum, mitochondria and tonoplast, cells appeared turgescent with the plasma membrane tightly appressed to the cell wall (Fig. 2C). Excellent preservation of Golgi stacks was obtained, making the *cis*-to-*trans* polarity very easily recognizable (Fig. 2D). The well preserved cytoplasm was however confined to small areas of the cell.

Pre-freezing treatment with glycerol, sucrose or dextran and embedding in LRW resin

FS for ultrastructural analyses was performed in acetone containing 2% (w/v) osmium tetroxide as a standard substitution medium, according to McCully & Canny (1985). Osmium-free substitution method was secondly investigated for subsequent LRW embedding (Fig. 3). Tobacco BY-2 suspension-cultured cells

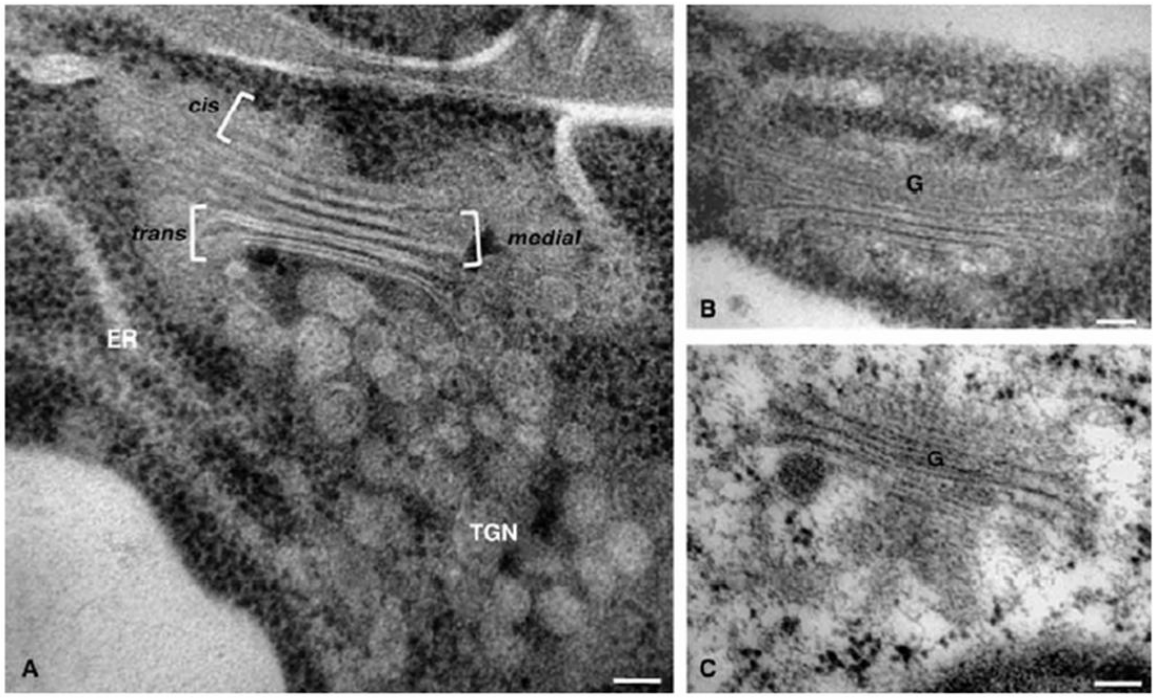

FIG. 3. Electron micrographs of tobacco BY-2 suspension-cultured cells frozen by high pressure in 20% (v/v) glycerol (A), in 0.4 M sucrose (B), and 25% (w/v) dextran (C). Cells were substituted in acetone + 0.5% (w/v) uranyl acetate and embedded in LRW resin. ER: endoplasmic reticulum; G: Golgi stacks; TGN: trans-Golgi network. Scale bars = 100 nm.

frozen in glycerol (Fig. 3A) or sucrose (Fig. 3B) and freeze-substituted in acetone containing 0.5% (w/v) uranyl acetate presented excellent ultrastructural preservation. The well preserved Golgi cisternae were easily distinguishable with *cis* to *trans* polarity and secretory vesicles of various sizes. It is worth noting that, under these conditions of FS, BY-2 cells frozen in glycerol yielded the highest quality of preservation. In contrast, cells frozen in dextran followed by FS in uranyl acetate/acetone presented ice crystal damage throughout the whole cytoplasm. In general, organelle preservation was poor and endomembranes, including Golgi cisternae, were hardly discernable (Fig. 3C).

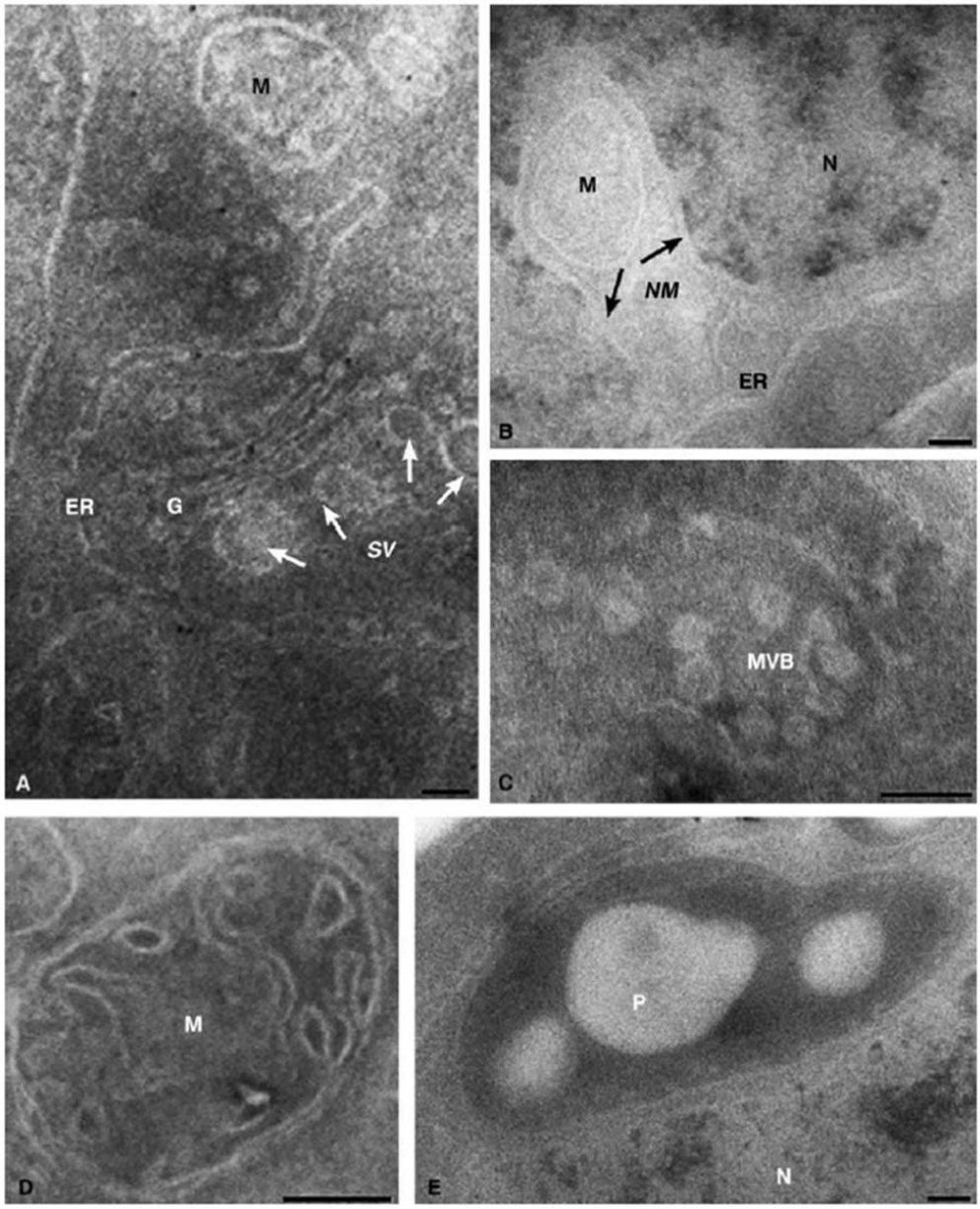

FIG. 4. Electron micrographs of transgenic tobacco suspension-cultured BY-2 cells preserved by cryosectioning method. Cells were chemically pre-fixed with 1.5% (w/v) PAF + 0,2% (v/v) GA (A) or 2% (w/v) PAF+ 2% (v/v) GA (B-E). ER: endoplasmic reticulum; G: Golgi stacks; M: mitochondria; MVB: multi-vesicular body; N: nucleus; NM: nuclear membrane; P: plastid; SV: secretory vesicles. Scale bars = 100 nm.

Ultrastructure of cryosectioned suspension-cultured BY-2 cells

Chemical fixation is a prerequisite for cryosections to maintain integrity during thawing and subsequent immunolabeling. Therefore, the effect of two fixative solutions was investigated on subcellular features of BY-2 cells that were fixed for 16 hrs with 1.5% (v/v) PAF – 0.2% (v/v) GA (fixative solution 1) or 2% (v/v) PAF – 2% (v/v) GA (fixative solution 2) prior to cryosectioning.

The use of fixative solution 1 affected drastically the preservation of cellular organelles (data not shown). Membranes were not clearly discernable and the cytoplasm did not appear uniformly preserved, suggesting that extraction occurred. As illustrated in Fig. 5C, similar results were observed for Golgi stacks whose *cis* to *trans* polarity was not preserved.

Increasing concentration of GA to 2% (v/v) (fixative solution 2) enhanced the quality of ultrastructure (Fig. 4A-E) and the visualization of membranes limiting different organelles, including the nuclear membrane (Fig. 4A), endoplasmic reticulum (Fig. 4B), multi-vesicular bodies (Fig. 4C), mitochondria (Fig. 4D) and plastids (Fig. 4E). Compared to the first fixative solution, Golgi stacks have preserved their structural integrity with distinct compartments as well as the a-

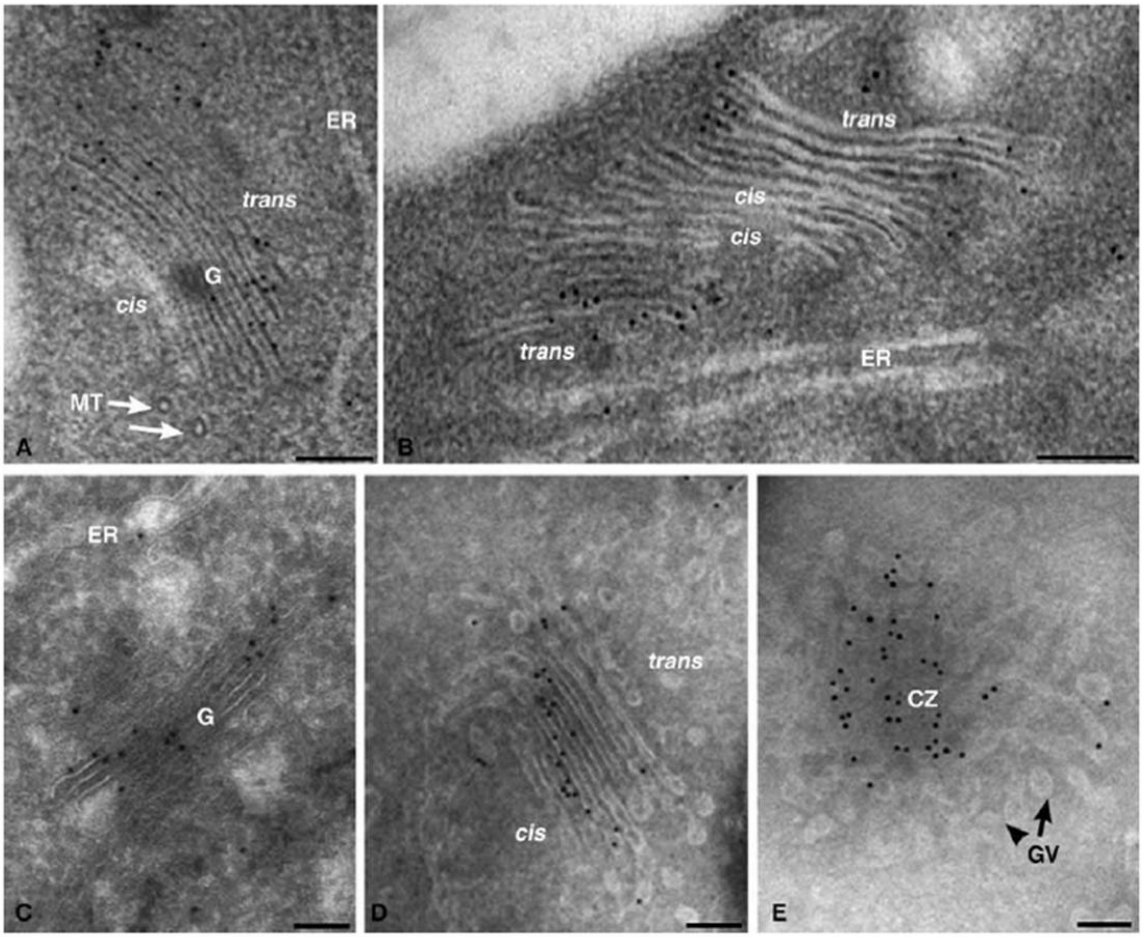

FIG. 5. Electron micrographs showing immunogold localization of GFP-tagged Golgi proteins under cryopreparation methods in transgenic tobacco BY-2 suspension-cultured cells. (A, B) Distribution of MUR3-GFP in cells prepared with HPF/FS, pretreated by 0.4 M sucrose (A) or 20% (v/v) glycerol (B), shows labeling in Golgi stacks (A) and in *medial/trans* Golgi margins (B). (C-E) Distribution of ManI-GFP in cryosectioned cells pre-fixed with 1.5% (w/v) PAF + 0.2% (v/v) GA (C) or 2% (w/v) PAF + 2% (v/v) GA (D, E). A cross-section view (D) of Golgi apparatus or a top view (E) of cisternae showing abundant labeling of the central zone as compared to the margins. CZ: central zone; ER: endoplasmic reticulum; G: Golgi stacks; GV: Golgi vesicles; MT: microtubules. Scale bars = 100 nm.

bundance of Golgi-derived vesicles (see Fig. 4A and Fig. 5D, E). It appeared that the original structure of Golgi stacks is better stabilized with high concentration of GA, allowing the identification of different subtypes of cisternae (Fig. 5C, D) according to the *cis*, *medial* and *trans* polarity previously described (Staehelin *et al.*, 1990; Zhang & Staehelin, 1992; Driouich *et al.*, 1993). Moreover, Figs 4B and 5D, E showed the presence of numerous secretory vesicles in the vicinity of Golgi, illustrating that the quality of endomembrane preservation was improved using those conditions.

Immunogold localization of GFP tagged-Golgi proteins under HPF/FS method

To assess antigenicity preservation of our samples prepared under various conditions, we used transgenic lines of BY-2 cells expressing GFP-fused proteins. A xyloglucan-galactosyltransferase from *Arabidopsis* (MUR3-GFP) and a soybean mannosidase I (ManI-GFP) were localized respectively using HPF/FS and cryosectioning procedures. Since the best conditions of HPF/FS amenable to immunocytochemistry were obtained by using sucrose and glycerol as freezing medium, only these two treatments were applied to the MUR3-GFP detection (Fig. 5A, B). As shown in Fig. 5B, labeling with the polyclonal GFP-antibodies was found specifically over Golgi stacks and mostly detected in the margins of *medial/trans* cisternae. Similar results in terms of localization were observed for samples frozen in sucrose (Fig. 5A).

Immunogold localization of GFP tagged-Golgi proteins with Tokuyasu method

The impact of the two fixative solutions on the immunogold localization of ManI-GFP within the Golgi stacks was also examined. Detection of GFP-labeling over Golgi stacks was possible in both conditions as shown in Fig. 5C-E. With an improved ultrastructure quality, Fig. 5D illustrates specifically the distribution of the ManI-GFP with most of the labeling over the *cis* moiety of the Golgi stacks, on cryosectioned transformed BY-2 cells prepared with 2% (v/v) PAF-2% (v/v) GA (fixative solution 2). In addition, the top view of the Golgi cisternae (Fig. 5E) showed that the majority of gold particles were associated with the central zone of the cisternae. The density of labeling was compared and found to be higher in conditions with great concentration of GA (Fig. 5D) than in low GA concentration (Fig. 5C): an average of 21 ± 4.2 gold particles per Golgi stack was numbered with 2% (v/v) GA, compared to 9 ± 1.4 with 0.5 % (v/v) GA.

DISCUSSION

HPF/FS and cryosectioning are recognized respectively as the best established fixation and immunodetection methods. Nevertheless, in spite of the availability of those tools, relatively few studies on plant suspension-cultured cells have been reported to date. In our work, technical conditions in HPF/FS and cryosectioning for tobacco BY-2 cell preparations were overviewed with a particular focus on the Golgi apparatus and their impact on GFP-tagged protein localization is discussed below.

In the HPF/FS procedure, the most critical phase of the whole fixation process is undoubtedly the preceding preparation prior to freezing of specimen, as very well described in the recent upgrade published by McDonald *et al.* (2007). In our study, the use of FS media free of strong fixatives amenable for immunoanalysis, provided optimal freezing quality. It is well known that the water content of vacuolated cells (such as tobacco suspension cells) is a crucial factor for vitrification of hydrated specimens. The complex interactions between water and intracellular compounds and the various forms of water present in the different compartments, including vacuoles, cytoplasm and apoplast, greatly influence phase transitions during cooling procedures in spite of high cooling rate generated by HPF. Studer *et al.* (1995) demonstrated the dependence of vitrification on proteoglycan concentration and water content in articular cartilage. Similarly, Lepeault *et al.* (1997) studied vitrification of water and showed that amorphous ice of pure water could be obtained by HPF only by adding at least 20% (w/v) sucrose.

In the case of tobacco suspension-cultured cells, it was already described that freezing without any cryoprotectant gives some sufficient ultrastructural result to immuno-analysis of specific vacuolar or vesicular compartment, and multi-vesicular bodies (Tse *et al.*, 2004; Oliviusson *et al.*, 2006; Langhans *et al.*, 2007). In our work, we showed that freezing tobacco cells without any additive induced important ice damage leading to poor preservation of cell structures, including the Golgi stacks. These ice injuries are not dependent on the dehydration process but result in the lack of efficiency of vitrification. In this context, cryoprotectants become essential to improve the quality of freezing by ensuring a rapid heat removal from the

sample without the formation of ice crystals. Usually, cryoprotectants are divided into two categories, including non-penetrating (e.g. dextran, BSA, arabic gum and sucrose) and penetrating compounds (e.g. glycerol). Extracellular compounds act as an "embedding agent", thereby increasing the viscosity of the outside medium. Thus, by preventing freezing outside the cell, the ice nucleation within the cell is delayed and ice damage is prevented (Echlin, 1992). They are often more suitable than intracellular cryoprotectants, which might change cell physiology. However, another classification of these agents, based on their osmotic activities, should be considered. Dextran, BSA and arabic gum are molecules with low osmotic activity, compared to sucrose or glycerol. Dextran and sucrose have previously been used in large HPF/ FS applications on sycamore or tobacco suspension-cultured cells (Driouich *et al.*, 1993; Zhang *et al.*, 1993; Samuels *et al.*, 1995; Driouich & Staehelin, 1997; Winicur *et al.*, 1998; Nebenführ *et al.*, 1999) in contrast to glycerol. As shown in our results, dextran could be an effective cryoprotectant when tobacco suspension-cultured cells were freeze-substituted in osmium tetroxide and embedded in Spurr's resin (Fig. 2C, D) but not when FS conditions deprived of strong fixatives followed by LRW resin were applied (Fig. 3C). In this case, segregation compartments caused by crystallization were present. These data are in line with the previous report of Matsko & Müller (2005), who demonstrated that Spurr's components were involved in the stabilization of fine structures after HPF, resulting in higher quality of ultrastructure compared to LRW resin. Nevertheless, the major drawback in the use of dextran is its incompatibility with substitution fluids such as acetone supplemented with uranyl acetate suitable for immunolabeling. The possible interaction of dextran with uranyl salts (Kiss *et al.*, 1990; Giddings, 2003) leads to an important reduction of freeze substitution efficiency inducing re-crystallization when temperature increases during the substitution process. In those conditions, ultrastructure is damaged. In addition, high concentration of dextran may exert a non colligative osmotic pressure involved in some membrane shrinkage.

Freezing in glycerol or sucrose provided good preservation with LRW resin (Fig. 3A, B), avoiding the necessity of using osmium tetroxide in the freeze substitution medium as generally proposed in the literature (Nebenführ *et al.*, 1999; Toyooka *et al.*, 2009). Glycerol is a natural compound found in the plant cell membranes and known to play a key role in tolerance to various abiotic stresses such as cold or dehydration (Eastmond, 2004). Although glycerol is identified as a penetrating cryoprotectant, its entry into the plant cell may be limited by the cell wall (McGann, 1978; Echlin, 1992; Hayat, 2000). In our experiments, glycerol incubation was performed gradually on non-fixed cells at +4°C, which decreased greatly the cell glycerol penetration (McGann, 1978; Echlin, 1992). Thus, in this context, the glycerol played the role of an osmotic agent, like sucrose. The good ultrastructural preservation of Golgi stacks obtained with sucrose and glycerol treatment is due to an osmotic effect that does not occur with dextran. This finding suggests that the optimal freezing of BY-2 cells requires their light dehydration. To preserve the integrity of endomembranes, osmotical action of sucrose or glycerol is more successful than dextran.

The lack of membrane staining when glycerol is used as cryoprotectant, compared to sucrose, could be explained by the behaviour of membranes during high pressure freezing. Because of the structure and composition (phospholipids closely arranged to each other in a double lamellar layer) of membranes, the ultrarapid freezing process could be modified and became different of free water. Wolfe & Bryant (1999) have shown that membrane vitrification is dependent on the ability of cryoprotectants to diffuse in the interlamellar spaces and each side of phospholipid layers. A good vitrification of membrane can be achieved if the cryoprotectant diffuses efficiently in the interlamellar spaces. Otherwise, the presence of different types of ice in intra- or extra- compartments could induce drastic injuries, such as membrane cracks or swells (Wolfe & Bryant, 1999). We can also speculate that the visibility of membranes could be modified according to vitrification status. Although no link between vitrification quality and their contrast was established, some authors notice the poor staining of membranes after HPF/FS, and added low rate of water in the FS medium to increase membrane contrast (Walther & Ziegler 2002, Giddings, 2003).

When sucrose or glycerol is added to the freezing medium, no difference in immunogold localization of specific Golgi enzymes (Fig. 5A, B) was observed. These findings are illustrated by the localization of the MUR3-GFP fused protein involved in the synthesis of the xyloglucan, a major hemicellulosic polysaccharide of dicotyledonous primary cell wall (Carpita & McCann, 2000). In line with the previous work of Zhang & Staehelin (1992) on the distribution of oligosaccharide linked to xyloglucan, we recently

showed that the enzyme responsible for the galactosylation of this polymer is mostly localized in the *medial/trans* margins of Golgi cisternae (Chevalier *et al.*, 2010). We demonstrate here that whatever the precooling treatment applied to BY-2 cells, sucrose or glycerol, the localization of these GFP-Golgi fused proteins is the same. Given the fact that ultrastructural preservation is better with glycerol pretreatment, we also used this procedure to describe two other XyG synthesizing enzymes localization in BY-2 cells prepared by HPF/FS (Chevalier *et al.*, 2010).

Tokuyasu thawed cryosectioning technique is based on fixation with aldehydes, infiltration with high concentration of cryoprotectant, followed by plunging in liquid nitrogen and finally cryosectioning on a microtome cryo-chamber at –90°C and –130°C. During this process, two major difficulties are generally encountered: the cryoprotection step and the retrieval section. The presence of sucrose, widely used in high concentration, ensures the vitrification of the biological material when freezed upon plunging into liquid nitrogen. Thus infiltration of sucrose into the cell seems to be essential to prevent ice damage and to achieve vitrification, in contrast to the HPF/FS approach. Therefore, aldehyde fixation plays an important role by permeabilizing the plasma membrane, in addition to stabilizing cell structure. Despite that fixed cells are permeable to sucrose, the infusion rate into cell is dependent on the fixation intensity (Hayat, 2000). When applied to plant cell material, sucrose infiltration is obviously impaired by the presence of cell wall, which constitutes a great biological barrier. This results generally in severe plasmolysis of the cell, which can be overcome by increasing fixative concentration and length of incubation to 72 hrs, in gradual sucrose solutions.

Section retrieval step in the cryo-chamber is known to be a critical step in the cryosectioning approach. This step can induce damage of the cell endomembranes (Skepper, 2000) and must be performed rapidly to avoid the freezing of the retrieval medium. When 2.3M sucrose solution is used, the time needed to retrieve sections in a cryo-chamber maintained at –100°C was estimated at 3 sec (Skepper, 2000). An alternative mixture of 2% (w/v) methyl cellulose and 2.3M sucrose helps to avoid tissue over-streching caused by the strong osmotic activity of sucrose (Griffiths, 1993). Consequently, this solution freezes faster than sucrose, shortening the section retrieval time. Thus, we believe that improving pre-fixation will prevent damage occurring at this critical stage. Indeed, fixation with 1.5% (v/v) PAF – 0.2% (v/v) GA for 16 hrs at +4°C resulted in insufficient ultrastructural preservation (see Fig. 5C) with a quality below that obtained after chemical co-fixation method (Follet-Gueye *et al.*, 2003).

Increasing the fixative concentration proved a marked improvement of cellular preservation. In particular, the morphology of the endomembrane system was very well preserved, matching that obtained with HPF technique in BY-2 cells (see Fig. 5). This method also allowed a clear distinction of the *cis* to *trans* Golgi polarity. Despite the good patterns of cell ultrastructural preservation, the use of a high fixative concentration is known to hamper epitope accessibility. In our work, use of 2% (v/v) GA fixative combined to PAF afforded a high density of gold particles (Fig. 5C, D) and the precise GFP localization within Golgi membranes (Fig. 5C, D). We observed that the GFP localization was predominantly associated with the *cis* and less frequently in the *medial* Golgi cisternae compartments, as previously described (Saint-Jore-Dupas *et al.*, 2006). Similar distribution of this Golgi membrane protein was obtained using either high-pressure frozen tobacco BY-2 cells (Nebenführ *et al.*, 1999) or chemically co-fixed cells (data not shown), but the density of labeling was much weaker than that obtained in cryosectioned samples. More recently, Staehelin & Kang (2008), in a paper dedicated to EM tomography, showed also that the native β mannosidase was predominantly located to the central zone of the medial cisternae in *Arabidopsis* root tip as presented here in Fig. 5D, E.

Impacts of Tokuyasu cryosectioning *versus* HPF/FS preparations on antigenicity are highly dependent either on the sample and the antigen (Lauber *et al.*, 1997; Hess, 2007; Stierhof & Kasmi, 2010). Provided that antigens were maintained in their original location and not extracted during chemical fixation and sucrose infiltration, the accessibility of epitopes at the thawed cryosection surface is better when compared to that of the resin section surface. Moreover, in the Tokuyasu cryosectioning approach, because tissues are only fixed with low concentrations of aldehydes and remain in an aqueous environment prior to immunolabeling, epitope detection would sometime turn out to be more favorable. Here, in the Tokuyasu technique, to perform the ultrastructural preservation of tobacco BY-2 cells, we fixed them with an aldehyde mixture containing 2% (v/v) PAF and 2% (v/v) GA and then infiltrated them slowly with 2.3M sucrose. We show here that this process is not deleteri-

ous to GFP-tag detection in transgenic BY-2 cells. On the other hand, we also reveal that the GFP-tag is insensitive to HPF/FS procedure following by LRW resin embedding.

Whereas Tokuyasu cryosectioning is often assumed to be the most suitable approach to label membrane-bound proteins (Liou *et al*., 1996; Griffiths & Posthuma, 2002), the ultrastructural features of BY-2 cells was often inferior to HPF/FS experiments. The major drawback is the great cell plasmolysis which is reduced by a progressive sucrose infiltration and stronger fixation. Alternatively, it would be interesting to combine the quality of the ultra-rapid cooling with the sensitiveness of thawed frozen section technique. In practice, a modified approach was proposed by Van Donselaar *et al*. (2007) and Ripper *et al.* (2008) named the "rehydration method". It combines HPF/FS procedure followed by a rehydration step, infiltration in sucrose and cryo-sectioning. The rehydration method is particularly sufficient to investigate some extractable epitopes like polysaccharides that are often lost during Tokuyasu process and was recently used to immunolocalize epitopes associated with a hemicellulosic compound, the xyloglucan (Viotti *et al.*, 2010). This new approach was also successfully applied to *Arabidopsis thaliana* plant model on pollen grains, cotyledons and root tip (Stierhof & Kasmi, 2010) but never described on tobacco BY-2 cells. Considering the high hydration level of BY-2 cells, successive dehydration and rehydration steps might be delicate. However, it could be of interest to adapt the rehydration method to plant suspension cells like tobacco BY-2 cells.

ACKNOWLEDGMENTS

The work described here was done at the Service de Microscopie Electronique de la Plate-forme de Recherche en Imagerie Cellulaire de Haute Normandie (PRIMACEN) supported by CNRS and Université de Rouen. Thanks are due to Marie-Françoise Carroll for her reading of the manuscript and to Drs Christian Bordat and Dany Studer for their helpful comments.

REFERENCES

Arabidopsis Genome Initiative, 2000. Analysis of the genome sequence of the flowering plant *Arabidopsis thaliana*. *Nature*, 408: 796-815.

Brandizzi F, Irons SL, Johansen J, Kotzer A, Neumann U, 2004. GFP is the way to glow: Bioimaging of the plant endomembrane system. *Journal of Microscopy*, 214: 138-158.

Carpita N, McCann M, 2000. The cell wall. In: Buchanan BB, Gruissem W, Jones RL, eds. *Biochemistry and molecular biology of plants*. American Society of Plant Physiologists, Rockville, Maryland: 52-108.

Chevalier L, Bernard S, Ramdani Y, Lamour R, Bardor M, Lerouge P, Follet-Gueye ML, Driouich A, 2010. Subcompartment localization of the side chain xyloglucan-synthesizing enzymes within Golgi stacks of tobacco suspension-cultured cells. *Plant Journal*, 64: 977-989.

Conceiçao AdS, Marty-Mazars D, Bassham DC, Sanderfoot AA, Marty F, Raikhel NV, 1997. The synaxin homolog AtPAP12p resides on a late post-Golgi compartment in plants. *Plant Cell*, 9: 571-582.

Dettmer J, Hong-Hermesdorf A, Stierhof YD, Schumacher K, 2006. Vacuolar H^+-ATPase activity is required for endocytic and secretory trafficking in *Arabidopsis*. *Plant Cell*, 18: 715-730.

Dhanoa PK, Sinclair AM, Mullen TR, Mathur J, 2006. Illuminating subcellular structures and dynamics in plants: a fluorescent protein tool box. *Canadian Journal of Botany*, 84: 515-522.

Driouich A, Faye L, Staehelin LA, 1993. The plant Golgi apparatus: a factory for complex polysaccharides and glycoproteins. *Trends in Biochemical Sciences*, 18: 210-214.

Driouich A, Staehelin LA, 1997. 7-dehydrobrefeldin A, a natural-occuring BFA derivative, inhibits secretion and causes a *cis*-to-*trans* breakdown of Golgi stacks in plants cells. *Plant Physiology*, 113: 487-492.

Eastmond P, 2004. Glycerol –insensitive *Arabidopsis* mutants: gli1 seedlings lack glycerol kinase accumulate glycerol and are more resistant to biotic stress. *Plant Journal*, 37: 617-625.

Ebine K, Okatani Y, Uemura T, Goh T, Shoda K, Niihama M, Morita MT, Spitzer C, Otegui MS, Nakano A, Ueda T, 2008. A SNARE complex unique to seed plants is required for protein storage vacuole biogenesis and seed development of *Arabidopsis thaliana*. *Plant Cell*, 20: 3006-3021.

Echlin P, 1992. *Low temperature microscopy and analysis*. Plenum Press, New York.

Follet-Gueye ML, Pagny S, Faye L, Gomord V, Driouich A, 2003. An improved chemical fixation method suitable for immunogold localization of green fluorescent protein in the Golgi apparatus of tobacco Bright Yellow (BY-2) cells. *Journal of Histochemistry and Cytochemistry*, 51: 931-940.

Giddings TH, 2003. Freeze substitution protocols for improved visualization of membranes in high pressure frozen samples. *Journal of Microscopy*, 212: 53-61.

Gomord V, Fitchette AC, Denmat LA, Michaud D, Faye L, 1998. Production of foreign proteins in tobacco cell suspension culture. In: Cunningham C, Porter AJ, eds.

Methods in biotechnology. Totowa Humana Press Inc., Vol. 3: 155-164.

Griffiths, G, 1993. *Fine structure immunocytochemistry*. Springer-Verlag, Heidelberg.

Griffiths JM, Posthuma G, 2002. A reliable and convenient method to store ultrathin thawed cryosections prior to immunolabeling. *Journal of Histochemistry and Cytochemistry*, 50: 57-62.

Happel N, Höning S, Neuhaus JM, Paris N, Robinson DG, Holstein SHE, 2004. *Arabidopsis* µA-adaptin interacts with the tyrosine motif of the vacuolar sorting receptor VSR-PS1. *Plant Journal*, 37: 678-693.

Hayat MA, 2000. *Principles and techniques of electron microsocpy: biological applications*. Fourth edition. Cambridge University Press, Cambridge.

Hess MW, 2007. Cryopreparation methodology for plant cell biology. *Methods in Cell Biology*, 79: 57-100.

Hinz G, Hilmer S, Bäumer M, Hohl I, 1999. Vacuolar storage proteins and the putative vacuolar sorting receptor BP-80 exit the Golgi apparatus of developing pea cotyledons in different transport vesicles. *Plant Cell*, 11: 1509-1524.

Hinz G, Colanesi S, Hillmer S, Rogers JC, Robinson DG, 2007. Localization of vacuolar transport receptors and cargo proteins in the Golgi apparatus of developing *Arabidopsis* embryos. *Traffic*, 8: 1452-1464.

Jolliffe NA, Brown JC, Neumann U, Vicré M, Bachi A, Hawes C, Ceriotti A, Roberts LM, Frigerio L, 2004. Transport of ricin and 2S albumin precursors to the storage vacuoles of *Ricinus communis* endosperm involves the Golgi and VSR-like receptors. *Plant Journal*, 39: 821-833.

Kiss JZ, Giddings TH, Staehelin LA, Sack FD, 1990. Comparison of the ultrastructure of conventionnally fixed and high pressure frozen/freeze substituted root tips of *Nicotiana* and *Arabidopsis*. *Protoplasma*, 157: 64-74.

Klumperman J, Kuliawat R, Griffiths JM, Geuze HJ, Arvan P, 1998. Mannose 6-phosphate receptors are stored from immature secretory granules via adaptor protein AP-1, clathrin and synaxin 6-positive vesicles. *Journal of Cell Biology*, 141: 359-371.

Lam SK, Siu CL, Hillmer S, Jang S, An G, Robinson DG, Jiang L, 2007. Rice SCAMP1 defines clathrin-coated, trans-Golgi-located tubular-vesicular structures as an early endosome in tobacco BY-2 cells. *Plant Cell*, 19: 296-319.

Lancelle SA, Hepler PK, 1992. Ultrastructure of freeze-substituted pollen tubes of *Lilium longiflorum*. *Protoplasma*, 167: 215-230.

Langhans M, Hawes C, Hillmer S, Hummel E, Robinson DG, 2007. Golgi regeneration after Brefeldin A treatment in BY2 cells entails stack enlargement and cisternal growth followed by division. *Plant Physiology*, 145: 527-538.

Lauber MH, Waizenegger I, Steinmann T, Schwarz H, Mayer U, Hwang I, Lukowitz W, Jürgens G, 1997. The *Arabidopsis* KNOLLE protein is a cytokinesis-specific syntaxin. *Journal of Cell Biology*, 139: 1485-1493.

Lepeault J, Bigot D, Studer D, Erk I, 1997. Freezing of aqueous specimen: an X ray diffraction study. *Journal of Microscopy*, 187: 158-166.

Liou W, Geuze HJ, Slot JW, 1996. Improving structural integrity of cryosections for immunogold labeling. *Histochemistry and Cell Biology*, 106: 41-58.

Liou W, Geuze HJ, Geelen MJH, Slot JW, 1997. The autophagic and endocytic pathways converge at the nascent autophagic vacuoles. *Journal of Cell Biology*, 136: 61-70.

Madson M, Dunand C, Li X, Verma R, Vanzin GF, Caplan J, Shoue DA, Carpita NC, Reiter WD, 2003. The *MUR3* gene of *Arabidopsis* encode a xyloglucan galactosyltransferase that is evolutionarily related to animal exostosins. *Plant Cell*, 15: 1662-1670.

Matsko N, Mueller M, 2005. Epoxy resin as fixative during freeze substitution. *Journal of Structural Biology*, 152: 92-103.

McCully ME, Canny MJ, 1985. The stabilization of labile configurations of plant cytoplasm by freeze substitution. *Journal of Microscopy*, 139: 27-33.

McDonald KL, Morphew M, Verkade P, Müller-Reichert T, 2007. Recent advances in high-pressure freezing: equipment and specimen loading methods. In: Kuo J, ed. *Electron microscopy: methods and protocols*, second edition. Humana press Inc, Totowa, NJ: 143-173.

McGann LE, 1978. Differing actions of penetrating and non-penetrating cryoprotective agents. *Cryobiology*, 15: 382-390.

Nebenführ A, Gallagher LA, Dunahay TG, Frohlick JA, Mazurkiewicz AM, Meehl JB, Staehelin LA, 1999. Stop-and-go movements of plant Golgi stacks are mediated by the acto-myosin system. *Plant Physiology*, 121: 1127-1141.

Oliviusson P, Heinzerling O, Hilmer S, Hinz G, Tse YC, Jiang L, Robinson D, 2006. Plant retromer localized to the prevacuolar compartment and microvesicles in *Arabidopsis* may interact with vacuolar sorting receptors. *Plant Cell*, 18: 1239-1252.

Pagny S, Bouissonié F, Sarkar M, Follet-Gueye ML, Driouich A, Schachter H, Faye L, Gomord V, 2003. Structural requirements for *Arabidopsis* alpha1,2xylosystransferase activity and targeting to the Golgi. *Plant Journal*, 33: 189-203.

Pimpl P, Movafeghi A, Coughlan S, Denecke J, Hillmer S, Robinson DG, 2000. *In situ* localization and *in vitro* induction of plant COPI-coated vesicles. *Plant Cell*, 12: 2219-2235.

Ripper D, Scwartz H, Stierhof YD, 2008. Cryo-section immunolabeling of difficult to preserve specimens: advantages of cryofixation, freeze-substitution and rehydration. *Biology of the Cell*, 100: 109-123.

Saint-Jore C, Evins J, Brandizzi F, Moore I, Hawes C,

2002. Redistribution of membrane proteins between the Golgi apparatus and endoplasmic reticulum in plants is reversible and not dependent on cytoskeletal networks. *Plant Journal*, 29: 661-678.

Saint-Jore-Dupas C, Gomord V, Paris N, 2004. Protein localization in the Golgi apparatus and the trans Golgi network. *Cellular and Molecular Life Sciences*, 61: 159-171.

Saint-Jore-Dupas C, Nebenführ A, Follet-Gueye ML, Boulaflous A, Plasson C, Hawes C, Driouich A, Faye L, Gomord V, 2006. The transmembrane domain length plays a key role in intra-Golgi targeting of soybean α-1,2-mannosidase I. *Plant Cell*, 18: 3182-3200.

Samuels AL, Giddings TH, Staehelin LA, 1995. Cytokinesis in tobacco BY2 and root tip cells: A new model of cell plate formation in higher plants. *Journal of Cell Biology*, 130: 1345-1357.

Sanderfoot AA, Ahmed SU, Marty-Mazars D, Rapoport I, Kirchhausen T, Marty F, Raikhel NV, 1998. A putative vacuolar cargo receptor partially colocalizes with AtPEP12p on a prevacuolar compartment in *Arabidopsis* roots. *Proceedings of the National Academy of Sciences USA*, 95: 9920-9925.

Skepper JN, 2000. Immunocytochemical strategies for electron microscopy choice or compromise. *Journal of Microscopy*, 199: 1-36.

Staehelin LA, Giddings Jr TH, Kiss JZ, Sack FD, 1990. Macromolecular differentiation of Golgi stacks in root tip of *Arabidopsis* and *Nicotiana* seedlings as visualized in high pressure frozen and freeze-substitued samples. *Protoplasma*, 157: 75-91.

Staehelin LA, Kang BH, 2008. Nanoscale architecture of endoplasmic reticulum export sites and of Golgi membranes as determined by electron tomography. *Plant Physiology*, 147: 1454-1468.

Stierhof YD, El Kasmi F, 2010. Strategies to improve the antigenicity, ultrastructure preservation and visibility of trafficking compartments in *Arabidopsis* tissue. *European Journal of Cell Biology*, 89: 285-297.

Studer D, Michel M, Wohlwend M, Hunziker EB, Buschman MD, 1995. Vitrification of articular cartilage by high-pressure freezing. *Journal of Microscopy*, 179: 321-333.

Studer D, Graber W, Al-amoudi A, Eggli P, 2001. A new approach for cryofixation by high pressure freezing. *Journal of Microscopy*, 203: 285-294.

Tokuyasu KT, 1973. A technique for ultracryomicrotomy of cells suspensions and tissues. *Journal of Cell Biology*, 57: 551-565.

Toyooka K, Goto Y, Asatsuma S, Koizumi M, Mitsui T, Matsuoka K, 2009. A mobile secretory vesicle cluster involved in mass transport from the Golgi to the plant cell exterior. *Plant Cell*, 21: 1212-1229.

Tse YC, Mo B, Hilmer S, Zhao M, Lo SW, Robinson DG, Jiang L, 2004. Identification of multivesicular bodies as pre-vacuolar compartments in *Nicotiana tabacum* BY-2 cells. *Plant Cell*, 16: 672-693.

Van Donselaar E, Posthuma G, Zeuschner D, Humbel BM, Slot JW, 2007. Immunogold labeling of cryosections from high-pressure frozen cells. *Traffic*, 8: 471-485.

Viotti C, Bubeck J, Stierhof YD, Krebs M, Langhans M, van den Berg W, van Dongen W, Richter S, Geldner N, Takano J, Jürgens G, de Vries SC, Robinson DG, Schumacher K, 2010. Endocytic and secretory traffic in *Arabidopsis* merge in the trans-Golgi network/early endosome, an independent and highly dynamic organelle. *Plant Cell*, 22: 1344-1357.

Von der Fecht-Bartenbach J, Bogner M, Krebs M, Stierhof YD, Schumacher K, Ludewig U, 2007. Function of the anion transporter At*CLC*-d in the *trans*-Golgi network. *Plant Journal*, 50: 466-474.

Walther P, Ziegler A, 2002. Freeze substitution of high pressure frozen samples: the visibility of biological membranes is improved when the substitution medium contains water. *Journal of Microscopy*, 208: 3-10.

Winicur ZM, Zhang GF, Steahelin LA, 1998. Auxin deprivation induces synchronous Golgi differentiation in suspension-cultured tobacco BY-2 cells. *Plant Physiology*, 117: 501-513.

Wolfe J, Bryant G, 1999. Freezing, drying, and/or vitrifcation of membrane-solute-water systems. *Cryobiology*, 39: 103-129.

Yang YD, Elamawi R, Bubeck J, Pepperkok R, Ritzenhaler C, Robinson DG, 2005. Dynamics of COPII vesicles and the Golgi apparatus in cultured *Nicotiana tabacum* BY 2 cells provides evidence for transient association of Golgi stacks with endoplasmic reticulum exit sites. *Plant Cell*, 17: 1513-1531.

Zhang GF, Staehelin LA, 1992. Functional compartmentalization of the Golgi apparatus of plant cells. An immunochemical analysis of high pressure frozen and freeze substituted sycomore maple suspension-cultured cells. *Plant Physiology*, 99: 1070-1083.

Zhang, GF, Driouich A, Staehelin LA, 1993. Effect of monensin on plant Golgi: re-examination of the monensin-induced changes in cisternal architecture and functional activities of the Golgi apparatus of sycomore suspension-cultured cells. *Journal of Cell Science*, 104: 819-831.

Papier N°3: Chapitre d'ouvrage

Résultats: Développements techniques

Applications of Immunocytochemistry. Chapter 14: Immuno-Glyco-Imaging in Plant Cells : Localization of Cell Wall Carbohydrate Epitopes and Their Biosynthesizing Enzymes.

Sous chapitre 4: Spatial organization of non-cellulosic cell wall polysacharides at the ultrastructural level.

Follet-Gueye ML., Mollet JC., Vicré-Gibouin M., Bernard S., Chevalier L., Plancot B., Dardelle F., Ramdani Y, Coimbra S. and Driouich A.

Ed. Hesam Dehghani ISBN 978-953-51-0229-8. (2012) pp 297-320

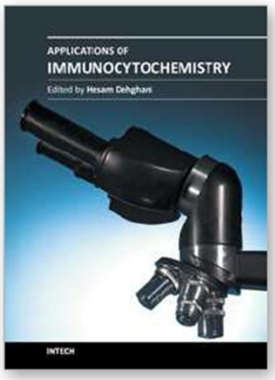

Applications of Immunocytochemistry

Edited by Dr. Hesam Dehghani

ISBN 978-953-51-0229-8
Hard cover, 320 pages
Publisher InTech
Published online 09, March, 2012
Published in print edition March, 2012

Immunocytochemistry is classically defined as a procedure to detect antigens in cellular contexts using antibodies. However, over the years many aspects of this procedure have evolved within a plethora of experimental setups. There are different ways to prepare a given specimen, different kinds of antibodies to apply, different techniques for imaging, and different methods of analyzing the data. In this book, various ways of performing each individual step of immunocytochemistry in different cellular contexts are exemplified and discussed. Applications of Immunocytochemistry offers technical and background information on different steps of immunocytochemistry and presents the application of this technique and its adaptations in cell lines, neural tissue, pancreatic tissue, sputum cells, sperm cells, preimplantation embryo, arabidopsis, fish gonads, and Leishmania.

How to reference

In order to correctly reference this scholarly work, feel free to copy and paste the following:

Marie-Laure Follet-Gueye, Mollet Jean-Claude, Vicré-Gibouin Maïté, Bernard Sophie, Chevalier Laurence, Plancot Barbara, Dardelle Flavien, Ramdani Yasmina, Coimbra Silvia and Driouich Azeddine (2012). Immuno-Glyco-Imaging in Plant Cells: Localization of Cell Wall Carbohydrate Epitopes and Their Biosynthesizing Enzymes, Applications of Immunocytochemistry, Dr. Hesam Dehghani (Ed.), ISBN: 978-953-51-0229-8, InTech, Available from: http://www.intechopen.com/books/applications-of-immunocytochemistry/immuno-glyco-imaging-in-plant-cells-localization-of-cell-wall-carbohydrate-epitopes

INTECH
open science | open minds

InTech Europe
University Campus STeP Ri
Slavka Krautzeka 83/A
51000 Rijeka, Croatia
Phone: +385 (51) 770 447
Fax: +385 (51) 686 166
www.intechopen.com

InTech China
Unit 405, Office Block, Hotel Equatorial Shanghai
No.65, Yan An Road (West), Shanghai, 200040, China
中国上海市延安西路65号上海国际贵都大饭店办公楼405单元
Phone: +86-21-62489820
Fax: +86-21-62489821

microscopy observations, labelling of Golgi units is hardly detectable. In contrast, the complete removal of the cell wall in protoplasts allows the access of the MAb CCRC-M86 to the Golgi-associated epitopes (Fig. 4B). Moreover, it is well recognized that cell wall polymer synthesis is stimulated in protoplasts thus contributing to the increase of labelling of the endomembranes. With this procedure, we have clearly shown that sugar motifs associated with XyG (Fig. 4) or pectins (data not shown) are present in the Golgi units. These are numerous and dispersed throughout the cytoplasm (see numerous fluorescent spots on Fig. 4B).

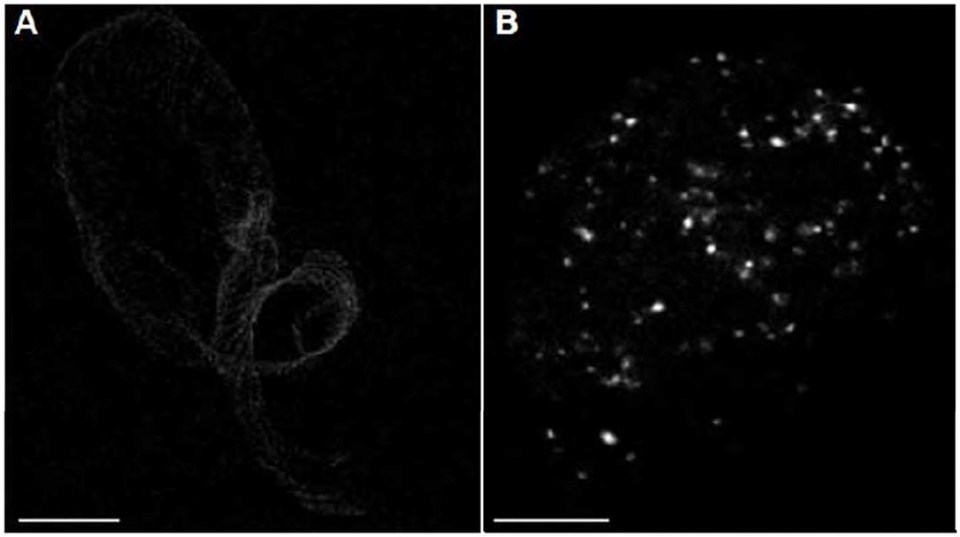

Fig. 4. Immunocytochemical localization of XyG epitopes in partially-digested tobacco BY-2 suspension-cultured cells and protoplasts with the MAb CCRC-M86. A- Confocal microscope images showing fluorescent staining of the cell surface and B- Golgi bodies. CCRC-M86 epitopes localize to both the cell wall and Golgi stacks of tobacco cell or protoplasts, respectively. Bars = 8 µm.

4. Spatial organization of non-cellulosic cell wall polysaccharides at the ultrastructural level

Due to the unability to subfractionate the plant Golgi stacks into *cis*, medial and *trans* cisternae, our knowledge, concerning the assembly of complex polysaccharides within the Golgi subcompartments, remains scarce. Progress towards the understanding of compartmentalization of matrix cell wall polysaccharide biosynthesis has come from immuno-electron microscopical analyses (Staehelin et al., 1990, Zhang & Staehelin, 1992; Driouich et al., 1993). These immunolabeling studies have been performed on samples prepared by HPF, a cryofixation technique that provides excellent preservation of Golgi stacks thereby allowing different cisternal subtypes to be easily distinguished. For ultrastructural and immunocytochemical investigations, we used the HPF coupled to freeze substitution (FS) technologies to prepare Arabidopsis root tips and pollen tubes, or tobacco

suspension-cultured cells. We present and discuss here protocols allowing epitopes detection associated with polysaccharides and membrane proteins (e.g., glycosyltransferases responsible for polysaccharide biosynthesis).

4.1 TEM sample preparation

4.1.1 High-Pressure Freezing/Freeze Substitution (HPF/FS)

4.1.1.1 Pre-cooling treatment

Prior to freezing, 3 day-old tobacco (BY-2) suspension-cultured cells were concentrated on 50 µm nylon membrane and incubated successively in MS + 5% glycerol, then in MS+10% glycerol for 1h each, at +4°C and under light stirring. Cells were then transferred to MS+20% glycerol and immediately frozen (see § 4.1.1.2). Root tips of seven day-old arabidopsis seedlings were first immersed in 2-(N-morpholino) ethanesulfonic acid (MES) buffer (20mM, $CaCl_2.2H_2O$ 2mM, KCl 2mM, Sucrose 0.2M; pH 5.5) containing a small drop of red ruthenium (to allow visualisation of the roots) for 5 min. Roots were then incubated with 0.2M sucrose in MES buffer for 5 min before freezing. Six hour-old pollen tubes were kept in the germination medium (GM) before freezing.

4.1.1.2 High pressure freezing

High-pressure freezing was performed with the freezer HPF-EM PACT I Leica-microsystems (Studer et al., 2001). Tobacco cells were concentrated on 50µm nylon membrane and transferred into the cavity of a copper ring used for cryofracture which is 100µm in depth and 1.2 mm in diameter. Excess medium was lightly absorbed with filter paper. Using a horizontal loading station, the specimen carriers were tightened securely into the pod of specimen holder. After fixation on the loading device, specimens were frozen according to a maximum cooling rate of 13000°C/s, incoming pressure of 7.5 bars and working pressure of 4.8 bars. Rings containing frozen samples were stored in liquid nitrogen until the freeze substitution procedure was initiated.

Root tips of *Arabidopsis thaliana* (1 to 2 mm) were excised with a fine razor blade in freezing media (0.2M sucrose in MES buffer). Three or four roots were placed in a gold platelet (200 mm in depth and 1.2 mm in diameter) carrier pre-filled with the freezing medium and coated with soybean lecithin (100 mg mL^{-1} in chloroform). Specimens were immediately frozen in the EM PACT freezer under similar conditions of pressure and cooling rate as for the tobacco cells (see above). Time between excision of the root tips and freezing was <1 min.

Like root tips, centrifuged 6-h-old pollen tubes were transferred into the cavity of gold cupules coated with soybean lecithin (100 mg mL^{-1} in chloroform). Excess medium was removed using a filter paper and were frozen as describe above.

4.1.1.3 Freeze substitution and resin embedding

After HPF, pollen tubes were transferred to a freeze substitution automate (EM-AFS; Leica) precooled to -140°C. Freeze substitution conditions followed a modified procedure from D. Studer (personal communication). Substitution media were composed of 2% osmium in anhydrous acetone. Samples were substituted at -90°C for 72 h. The temperature was gradually raised (2°C h^{-1}) to -60°C and stabilized during 12 h, then gradually raised (2°C $^{-1}$)

to -30°C (12 h) and gradually raised again (2°C h^{-1}) to 0°C for 2 h. Samples were washed at room temperature with fresh anhydrous acetone. Infiltration was done at +4°C in acetone-Spurr resin (2:1, 1:1, 1:2, 8 h each step) and with pure resin for at least 2 days. Polymerization was performed at 60°C for 16 h. Samples destined for protein immunocytochemistry (Arabidopsis root tips and BY-2 cells) were substituted in anhydrous acetone + 0.5% uranyl acetate (UA) using similar program as that described above except that the final substitution step was performed at -15°C. Samples were rinsed twice with anhydrous ethanol. Infiltration was processed at -15°C in a solution containing Ethanol : LR White (ratio 2:1; 1:1; 1:2, 8h each step) and with pure resin for 2x24 h. Polymerisation was performed into the AFS apparatus at -15°C under ultra violet light for 48h. Using an ultracut EM-UC6 (Leica), thin sections (90 nm) were mounted on formvar-coated nickel grids.

4.2 Immunogold staining

4.2.1 Single immunogold labelling

4.2.1.1 Cell wall immunogold labeling on epoxy sections

Grids, with pollen tube sections, were rehydrated in a Tris-buffered saline buffer (TBS) + 0.2% BSA and blocked in a TBS/BSA 0.2%/milk 3% solution for 30 min. After three brief rinses in TBS/BSA 0.2% solution, grids were incubated 3 h at 25°C in primary antibodies: non diluted for LM15 and CCRC-M1 or diluted (LM6, 1:2; anti-callose, 1:100) in TBS/BSA 0.2% buffer. Then, grids were washed (six times for 5 min each) in TBS/BSA 0.2% and incubated for 1 h at 25°C in a 1:20 secondary antibody (goat anti-rat for LM6 and LM15, goat anti-mouse for CCRC-M1 and anti-callose) conjugated to 10-nm gold particles (British Biocell International). Finally, grids were washed (six times for 5 min each) in a TBS + BSA 0.2% buffer, 1 min in TBS, 10 min in TBS + glutaraldehyde 2%, 5 min in TBS, and then two times for 5 min each in double deionized water. The sections were stained with 0.5% (w/v) UA in methanol for 10 min in the dark, rapidly rinsed 10 times with water and stained with lead citrate for 10 min, and briefly rinsed 10 times with water. In this experiment, epoxy resin was used as embedding medium. It is generally well admitted that Epoxy resin, which allow good cellular structure preservation, is not recommended for immunocytochemical studies. In the case of XyG and callose epitopes studied in Arabidopsis pollen grain and pollen tube, the detection was done with success (Fig. 5). Subcellular observation of Arabidopsis pollen grains showed that the intine cell wall contains the hemicellulose epitopes associated with fucogalactoXyG (Fig. 5A) and XyG (Fig. 5B). On the exine wall, pollen coat material is also visible. In the pollen tube, a double cell wall can be detected back from the tip region with the inner cell wall containing callose (Fig. 5C).

4.2.1.2 Immunogold labeling of polysaccharides and synthesizing-enzymes in Golgi stacks on acrylic sections

Ultrathin sections of tobacco cells or Arabidopsis root tips were blocked in TBS (Tris-buffered saline: Tris–HCl 20 mM pH 7.2, 200 mM NaCl) supplemented with 0.2% of BSA and milk 3% for 30 min. Sections were then incubated with monoclonal antibodies CCRC-M86 at a 1/5 dilution in TBS + BSA and normal goat serum (NGS; British Biocell International) for 3 h at room temperature. After washing in TBS + BSA 0.2% buffer, grids were incubated for 1 h at room temperature in the rat secondary antibody conjugated to 10-nm gold particles (Tebu-British Biocell International, http://www.tebu-bio.com). After

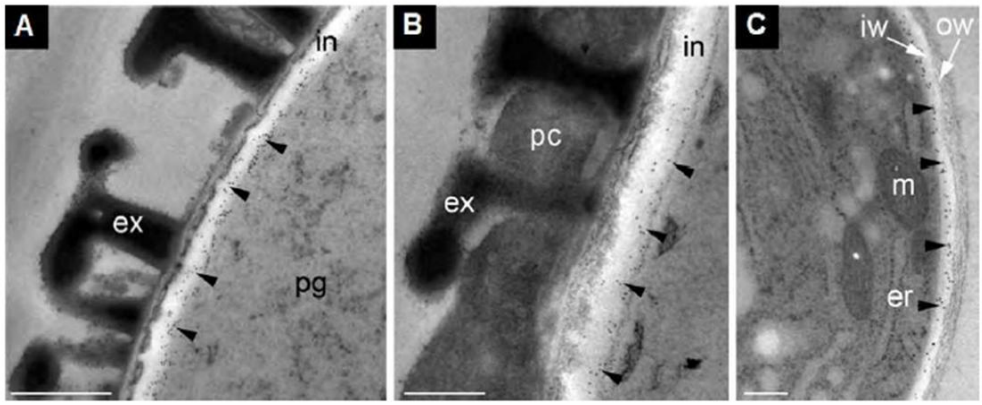

Fig. 5. A. Localization of fucosylated XyG in the intine wall of the pollen grain using the CCRC-M1 MAb. B. Localization of the motif XXXG found in XyG in the intine wall of the pollen grain using the LM15 MAb. C. Localization of callose in the inner cell wall of the pollen tube using the anti-callose antibody. Arrowhead, gold particles; er, endoplasmic reticulum; ex, exine; in, intine; iw, inner cell wall; m, mitochondria; ow, outer cell wall; pc, pollen coat; pg, pollen grain. Bars = 0.2 µm.

washing and fixation in TBS + 2% glutaraldehyde, sections were first stained with 4% vapour osmium for 3 h on a hotplate warmed to 40°C placed under a fume hood. For this step, the grids were put closed to 4% osmium droplets on a parafilm paper. This system was put in a small glass Petri dish who was kept hermetically closed until the total osmium evaporation. Then sections were classically stained 10 min with 0.5% UA diluted in methanol and 10 min in lead citrate.

Ultrathin sections of frozen cells expressing AtXT1-Green Fluorescent GFP (GFP) or AtMURUS 3 (MUR3)-GFP fusion proteins (Chevalier et al., 2010) were blocked in TBS (Tris-HCl 20 mM pH 7.2, 200 mM NaCl) supplemented with 0.2% of BSA and Tween 20 0.05% for 15 min. Sections were then incubated with the polyclonal anti-GFP antibody (BD living colors A.v peptide antibody - Clontech) at a 1/5 dilution in TBS + BSA and NGS for 2 h at room temperature. After washing in TBS + BSA 0.2% buffer, grids were incubated for 1 h at room temperature in the rabbit secondary antibody conjugated to 10 nm gold particles (Tebu-British Biocell International). After washing and fixation in TBS + 2% GA, sections were stained as described above with osmium vapours, uranyl acetate and lead citrate.

The combined use of HPF-FS and cryo-embedding in acrylic resin is particularly adapted to immunodetection of either membrane proteins or cell wall polysaccharides (Fig. 6 & Fig. 7). The cryo-immobilisation by HPF ensures the sample vitrification without modification of molecular structures. While chemical fixatives (such as aldehydes or osmium tetroxyde) are relatively inert with sugar molecules, proteins are often covalently cross linked with fixatives, which can disturb the epitope structure. During the cryo-dehydration step, we have lightly fixed the cells by adding 0.5% uranyl acetate to avoid the modification of the protein epitope. To enhance the electron micrograph contrast, the contact with osmium vapour prior to classical uranyl acetate and lead citrate staining is efficient (Fig. 6, Fig. 7, Fig.8 & 9) to enhance Golgi stack morphology. The non-fucosylated sugar motifs associated

with XyG, already detected in Golgi units in tobacco protoplasts (Fig. 4B), are mainly localized to the secretory vesicles of *trans* Golgi network (TGN) (Fig. 6A). With the same preparation procedure, it is also possible to immunolocalize XyG-synthesizing enzymes fused to GFP (e.g., AtXT1-GFP), within Golgi cisternae in transformed BY-2 cells (Fig. 6B). AtXT1-GFP was shown to localize mainly to the cis Golgi compartment (Chevalier et al., 2010).

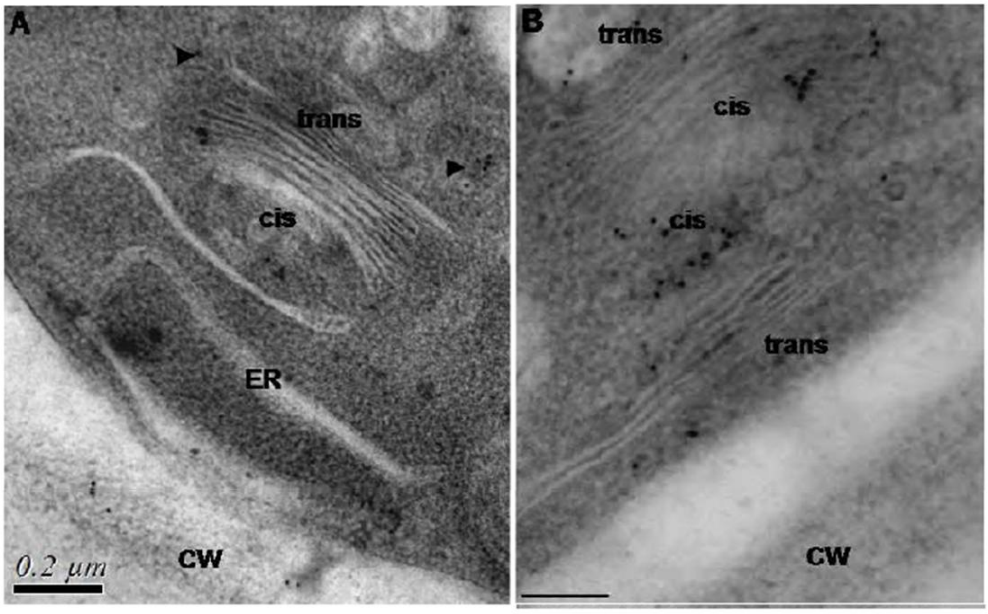

Fig. 6. Electron micrographs of HPF/FS and LR White embedded tobacco cells illustrating immunogold labelling of Golgi stacks and the cell wall. A- Non fucosylated motifs of XyG were immunodetected with the MAb CCRC-M86. B- AtXT1-GFP fusion protein was labelled with anti-GFP Ab, in Golgi stacks of transformed tobacco BY-2 suspension-cultured cells. The black head arrows indicate the secretory vesicles labelled. CW, cell wall; ER, endoplasmic reticulum; bars = 200 nm.

4.2.2 Double immunogold labeling

Information on the distribution of Golgi localized enzymes are currently obtained by using GFP technologies and confocal laser microscopy (Brandizzi et al., 2004). Immuno-electron microscopy is the only approach to study the distribution of GFP-labelling within a given organelle. Therefore, a central issue for immunogold at TEM level is to preserve epitopes of interest while minimizing the loss of ultrastructural details. Here, we study the localization of QUASIMODO2 protein (QUA2) in *qua2* mutant transgenic plants expressing the QUA2-GFP fusion protein (Mouille et al., 2007). QUA2 is a putative methyltransferase involved in the methylesterifcation of HG. It is well admitted that HG are synthesized in their methylesterified form and then possibly de-esterified by pectin methylesterases in the cell wall (Micheli, 2001).

With the sample substituted in 0.5% AU medium and embedded in LR White resin, we have been able to perform a double immunolabeling to localize Golgi enzymes fused to GFP and cell-wall polysaccharides. Ultrathin sections of Arabidopsis root tips of *qua2*-QUA2-GFP (Mouille et al., 2007) were blocked as describe above and incubated 2h at 25°C with the polyclonal anti-GFP antibody (BD living colors A.v peptide antibody – Clontech) at a 1/5 dilution in TBS + BSA and normal goat serum. After washing in TBS + BSA 0.2% buffer, sections were again saturated with 3% milk, 0.2% BSA in TBS buffer for 30 min. Incubation with the MAb JIM7 diluted to 1/5 in TBS + BSA and normal goat serum was done for 2h at 25°C. After six rinsing for 5 min with TBS buffer containing 0.2% BSA, grids were incubated for 1 h at room temperature in the rabbit secondary antibody conjugated to 10 nm gold particles diluted to 1/20 in TBS + BSA 0.2% + NGS 3%. Sections were then washed three times in TBS buffer + BSA 0.2%, and incubated 1 h at 25°C in the goat anti-rat secondary antibodies conjugated to 20-nm gold particles (Tebu-British Biocell International, http://www.tebu-bio.com). Sections were rinsed six times for 5 min with TBS buffer containing BSA 0.2%, and were followed by one washing in TBS buffer. After fixation in TBS + 2% GA, sections were stained as described above with osmium vapours, uranyl acetate and lead citrate.

The fusion protein is detected in the *trans* Golgi cisternae (Fig. 7C) while the methylesterified HG are immunolocalized not only in the *trans* cisternae but also in the TGN as previously described (Zhang & Steahelin, 1992; Toyooka et al., 2009). The lack of strong fixative in the substitution medium like osmium tetroxide or glutaraldehyde, allows the combined detection of pectic epitopes and its Golgi-associated biosynthetic enzyme. The cell wall labelling of the methylesterified HG epitopes (Fig. 7A & 7B) shows that the sample preparation did not alter the polymer localization. Given that the protein epitope is not impaired by strong fixatives, the double labelling of the product (HG) and the Golgi-localized methyltransferase is now possible. Our results suggest that HG methylation is likely to start in trans Golgi cisternae.

4.3 Quantitative mapping of polysaccharide-synthesizing enzymes within Golgi stacks

Statistical analysis of immunogold labelling was used to map XyG-glycosyltransferases within Golgi cisternae (Chevalier et al., 2010). As no antibodies directed against these enzymes are currently available, we have chosen to investigate their localization indirectly by using anti-GFP antibodies in transgenic tobacco cells expressing the glycosyltransferases fused to GFP. Immunogold labelling was quantified over each Golgi cisternae (fifty Golgi stacks with distinguishable cisternal subtypes) and subjected to chi-squared (χ^2) test to check for labelling specificity in transformed BY-2 cells versus wild type. The relative labelling index (RLI) was also determined to evaluate specific gold particles distribution within different subtypes of Golgi cisternae (Mayhew et al., 2002; Mayhew, 2011).

4.3.1 Labelling specificity of signal in transformed BY-2 cells

To evaluate the distribution of gold particles in Golgi stacks of transformed cells as compared with wild type cells, we used a chi-squared test (χ^2) as described by Mayhew et al., (2002). We considered the null hypothesis as 'no difference of gold distribution between wild type and transformed cells'. We analyzed gold labelling in different compartments of Golgi stacks: *cis*, medial, *trans* and the TGN (Fig. 8).

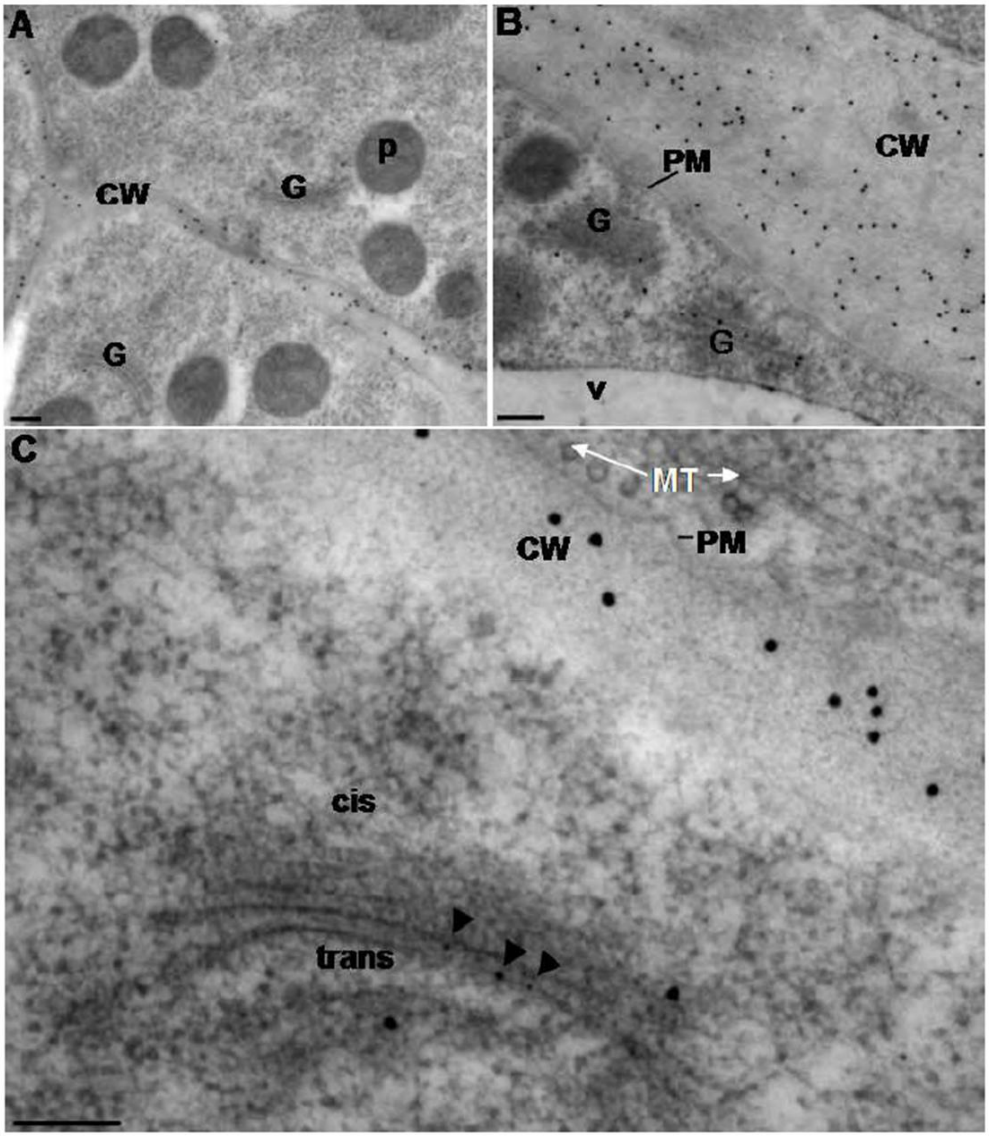

Fig. 7. Electron micrographs of HPF/FS and LR White-embedded ultrathin sections of Arabidopsis root tips of *qua2*-QUA2-GFP. Double localization of AtQUA2-GFP with anti-GFP antibody (10 nm gold particles) and of highly methylesterified HG with MAb JIM7 (20 nm gold particles) in Arabidopsis root meristematic cells. A-B: Note abundant labelling of HG epitopes in the cell wall and in the last Golgi compartments. C, the black arrow heads indicate the 10 nm gold particles corresponding to GFP labelling in the *trans* Golgi cisternae. CW, cell wall; G, Golgi ; MT, cortical microtubules ; P, plastid; PM, plasma membrane ; V, vacuole. Bars = 100 nm.

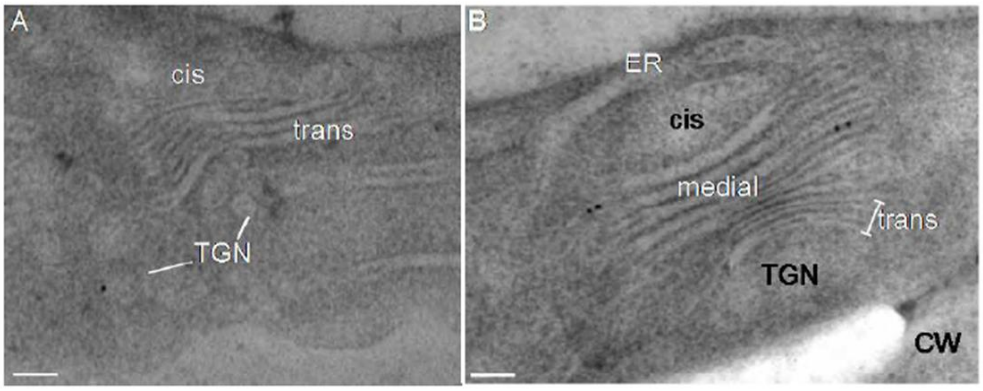

Fig. 8. Electron micrographs of GFP immunodetection on A- 3 day-old wild type BY-2 cells or B- transformed cells expressing the fusion protein AtMUR3-GFP. 50 similar images are used to determine the number of gold particles observed in each Golgi compartment: *cis*, medial, *trans* cisternae and the *trans* Golgi network (TGN). CW, cell wall; ER, Endoplasmic reticulum; At MUR3 is a XyG-galactosyltransferase, bars = 100 nm.

To compare the distribution of gold particles in these compartments between the two tobacco lines, we counted the gold particles observed over 50 Golgi units both in non-transformed cells (Wild type cells, termed WT cells) and transformed tobacco cells (expressing Golgi-enzyme fused to GFP, termed GFP-cells), immunolabelled with anti-GFP antibodies (Fig. 8). We prepared a table of gold particles counted for each tobacco lines and their repartition in different Golgi compartments (Table 2).

For each Golgi compartment, we calculated the expected gold particle number (Eij) according to the null hypothesis as 'no difference of gold distribution between wild type and transformed cells and that the gold particles are randomly distributed across the Golgi units'. The expected gold count (Eij) at two line cells for each selected Golgi compartment are calculated by using the table 2 values1, from the product of column (total gold particles observed in all Golgi stacks for wild type or transformed tobacco lines) and row totals (total gold particles observed in all BY-2 lines for the selected compartment) divided by the big total (total gold particles observed in four Golgi compartments, in wild type and transformed BY-2 cells).

	cis (j_1)	medial (j_2)	*trans* (j_3)	TGN (j_4)	Row Total (j_5)
WT cells (i_1)	O_{11}	O_{12}	O_{13}	O_{14}	O_{15}
GFP cells (i_2)	O_{21}	O_{22}	O_{23}	O_{24}	O_{25}
Column Total (i_3)	O_{31}	O_{32}	O_{33}	O_{34}	O_{35}

Table 2. Gold particles counted (Oij) over 50 Golgi stacks from Wild type tobacco cells (WT cells) or transformed BY-2 cells by Golgi localized enzymes fused to GFP (GFP cells). Oij designates the gold particle number indicated in the row (i) and the column (j). O_{15} and O_{25} designate the total gold particle number in WT cells and GFP cells, respectively. O_{31} to O_{34} correspond to the total gold count in the four Golgi compartments of the two tobacco lines. O_{35} is the big total (four Golgi compartments, in WT and GFP cells).

Example for the *cis* compartment of WT cells, expected gold number (E_{11}) is calculated as described below[1]:

$$E_{11}=[(O_{31} X\ O_{15})/O_{35}] \quad (1)$$

To compare the distribution of gold particles between the two tobacco lines in these compartments, we created a contingency table (two columns; four rows) as described in Mayhew et al. (2002) and also in table 3. In this contingency table we report the observed (Oij) and expected (Eij) numbers of gold particles. For each tobacco line, total column should be equal ($O_{15}=E_{15}$; $O_{25}=E_{25}$). If expected number is superior to 5, the χ^2 test can then be applied. The corresponding partial χ^2 value is calculated as the square of the difference between observed and expected gold particle numbers divided by the expected gold number.

Example for the *cis* compartment of WT cells, χ^2 value (χ_{11}^2) is calculated as described below[2]:

$$\chi_{11}^2=[(O_{11}-E_{11})^2/\ E_{11}] \quad (2)$$

The total χ^2 value ($\chi_{15}^2 + \chi_{25}^2$) is compared with χ^2 value in contingency table analysis with a degree of freedom equal to 3 in our experiment and corresponding to[3]:

$$\text{Degree of freedom}=[(\text{row number } -1)\times(\text{column number } -1)] \quad (3)$$

When the total χ^2 value ($\chi_{15}^2 + \chi_{25}^2$) is found to be superior to that of the contingency table, $\chi_{table}^2 = 12.38$ (with a degree of freedom of 3 and an uncertainty degree $\alpha = 0.005$) indicating that labelling is specific in Golgi stacks of transformed BY-2 cells.

	WT cells			GFP cells			Total observed gold
	(Oij)	(Eij)	χij^2	(Oij)	(Eij)	χij^2	
cis	O_{11}	E_{11}	χ_{11}^2	O_{21}	E_{21}	χ_{21}^2	O_{31}
medial	O_{12}	E_{12}	χ_{12}^2	O_{22}	E_{22}	χ_{22}^2	O_{32}
trans	O_{13}	E_{13}	χ_{13}^2	O_{23}	E_{23}	χ_{23}^2	O_{33}
TGN	O_{14}	E_{14}	χ_{14}^2	O_{24}	E_{24}	χ_{24}^2	O_{34}
Column Total	O_{15}	E_{15}	χ_{15}^2	O_{25}	E_{25}	χ_{25}^2	O_{35}

Table 3. Model of contingency table use for quantitative analysis of anti-GFP labelling over Golgi stacks in tobacco BY-2 cells expressing Golgi enzyme–GFP. This table contains two columns (Oij and Eij) and four rows (related to the four Golgi compartments studied).

4.3.2 Determination of fusion protein distribution in Golgi stacks

Quantification of the labelling was done according to Mayhew et al. (2002), on a total of 50 Golgi stacks with clearly distinguishable subtypes of cisternae (Fig. 9A) from transformed BY-2 cells expressing enzyme-GFP fused construct (noted GFP cells). First, gold particles were counted in each Golgi compartment (*cis*, medial, *trans* and the TGN) in 50 Golgi stacks from WT or GFP cells as described in § 4.3.1. The *'observed gold particles'* (n_0) in a given Golgi compartment in GFP cells is determined by subtracting the number of gold particles found in this compartment (Oij, GFP cells, 50 Golgi stacks) from the one counted in WT cells (Oij,

WT)[4]. Example for the *cis* compartment of WT cells, n_0 value is determined as described below[4]:

$$n_{011} = O_{21} - O_{11} \quad (4)$$

Second, each electron micrograph is calibrated and a lattice of test points was superimposed on each Golgi stack (so as to be random in position) by the plungins function of Image J computer software (Fig. 9B); hit points were counted (*'Observed points'*, P) in each compartment of the Golgi stack.

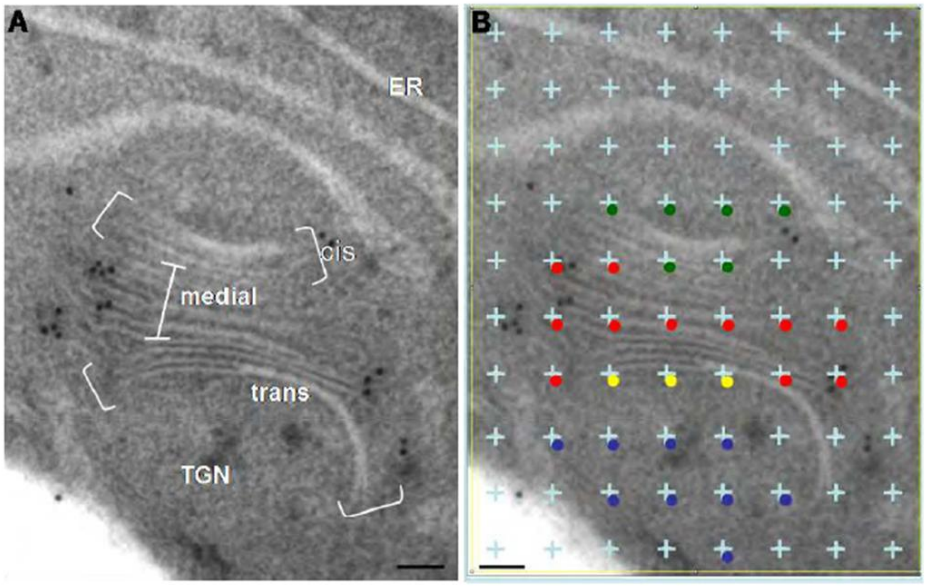

Fig. 9. Electron micrograph of a Golgi unit from At-MUR3-GFP transformed BY-2 cells. (A) *cis*, medial, *trans* and *trans* Golgi network (TGN) are clearly distinguishable. (B) Lattice (1015,43 area per point) was superimposed on the same electron micrograph calibrated (1nm/1.01 pixels) by using Image J computer software. In this example, 6 *'Observed points*, P' are present in the *cis* (green points), 11 in the medial (red points), 3 in the *trans* (yellow points) and 9 in the TGN (blue points) compartments. Scale bars = 100 nm.

"Observed gold particles, n_0" and "*observed points*, P" are put in the relative labelling index (RLI) table (Table 4). Then, the *'expected golds particles'* (n_e) (i.e. random distribution) is calculated for each Golgi compartment[5] from the product of the observed points in the Golgi compartments and column total of observed gold particles (total gold particles observed in four Golgi compartments, $n_{0\,51}$), divided by the column total of observed points (total points observed in four Golgi compartments, P_{52}). Example for the *cis* compartment of WT cells, n_e value is determined as described[5]:

$$n_{e\,13} = (P_{12} \times n_{0\,51}) / P_{52}. \quad (5)$$

Observed (n_0) and expected (n_e) gold particles distribution allowed calculation of the relative labelling index[6] (RLI):

$$RLI = (n_0/n_e) \quad (6)$$

For a random distribution, the relative labelling index (RLI) is inferior or equal to 1, and for a compartment preferentially labelled RLI is superior to 1.

	Observed gold particles (n_0)	Observed points (P)	Expected gold particles (n_e)	RLI (n_0/n_e)
cis	$n_{0\,11}$	P_{12}	$n_{e\,13}$	$n_{0\,11}/\ n_{e\,13}$
medial	$n_{0\,21}$	P_{22}	$n_{e\,23}$	$n_{0\,21}/\ n_{e\,23}$
trans	$n_{0\,31}$	P_{32}	$n_{e\,33}$	$n_{0\,31}/\ n_{e\,33}$
TGN	$n_{0\,41}$	P_{42}	$n_{e\,43}$	$n_{0\,41}/\ n_{e\,43}$
Column total	$n_{0\,51}$	P_{52}	$n_{e\,53}$	

Table 4. Model of relative labelling index (RLI) table comprising 3 columns (n_0, P and n_e) and four rows (related to four Golgi compartments studied). Total observed gold particles and total of expected gold particles must be equal ($n_{0\,51} = n_{e\,53}$).

In a recent published study, we have applied this quantitative analysis to determine the Golgi mapping of three XyG synthesis enzymes in transformed tobacco cell lines (Chevalier et al., 2010). We show that the labelling of AtXT1-GFP (Fig. 6B) was mostly associated with *cis* and medial cisternae, whereas the labelling of AtMUR3-GFP (Fig. 8B & Fig.9) was mainly detected in medial and *trans* cisternae of Golgi stacks. In addition to HPF-FS protocol described here for BY-2 cell preparation, Tokuyasu cryo-sectioning approach is also amenable to this plant cell model (Chevalier et al., 2011). A new approach named the "rehydration method" was proposed by Van Donselaar et al. (2007). It combines HPF/FS procedure followed by a rehydration step, infiltration in sucrose and cryo-sectioning, and is particularly efficient to investigate the localization of epitopes from polysaccharides that are often lost during Tokuyasu process and was recently used to immunolocalize epitopes associated with XyG (Viotti et al., 2010). It could be of interest to adapt the rehydration method to plant suspension cells like tobacco BY-2 cells for quantitative study of cell wall polymers such as hemicelluloses or pectins.

5. Conclusion

In conclusion, many immuno-microscopical methods are available to investigate plant cell walls. A number of antibodies against cell wall carbohydrate epitopes are also available and can be used to examine the distribution of polysaccharides. It is however important to perform experiments with varying parameters to determine the best conditions for a given sample. Optical imaging instrumentation, based on confocal laser scanning microscopy (CLSM), offers the ability to determine the spatial organisation of polymers at the cell surface, across the cell wall compartment as well as within the endomembrane system. The CLSM minimizes interference of innate plant autofluorescence from chlorophylls or vacuole content and provides a quite precise picture of polysaccharides distribution. Moreover, cryo-sample preparation for immunogold EM studies has significantly improved the immunodetection at the subcellular level of the cell wall components and their synthesizing enzymes. Finally, the preservation quality of both the cell ultrastructure and epitopes allows the quantification of the labelling within specific membrane-bound compartments (e.g; Golgi stacks). A careful

combination of microscopical and quantification methodologies is very promising for future studies devoted to imaging of cell wall glycomolecules and synthesizing enzymes.

6. Acknowledgments

Work in authors laboratories is/was supported by the Centre National de la Recherche Scientifique (CNRS), l'Université de Rouen, le Conseil Régional de Haute Normandie, the Plant Research Network VATA of Haute Normandie, the French ministry of Research and the FCT (Fundação para a Ciência e Tecnologia, Portugal) within the project PTDC/AGR-GPL/67971/2006.

7. References

Baskin T.I., Busby C.H., Fowke L.C., Saturant M. & Gubler F. (1992) Improvements in immunostaining samples embedded in methacrylate: localization of microtubules and other antigens throughout developing organs in plants of diverse taxa. *Planta*, Vol. 187, pp. 405-413

Boavida, L.C. & McCormick, S. (2007) Temperature as a determinant factor for increased and reproducible in vitro pollen germination in Arabidopsis thaliana. *The Plant Journal*, Vol.52, pp. 570–582

Brandizzi F., Irons S.L., Johansen J., Kotzer A. & Neumann U. (2004) GFP is the way to glow: Bioimaging of the plantendomembrane system. *Journal of Microscopy*, Vol. 214, pp.: 138-158.

Cheung, A.Y., Wang, H. & Wu, H.M. (1995) A floral transmitting tissue-specific glycoprotein attracts pollen tubes and stimulates their growth. *Cell*, Vol.82, pp. 383-393

Chevalier, L., Bernard, S., Ramdani, Y., Lamour, R., Bardor, M., Lerouge, P., Follet-Gueye, M.L. & Driouich, A. (2010) Subcompartment localization of the side chain xyloglucan-synthesizing enzymes within Golgi stacks of tobacco suspension-cultured cells. *The Plant Journal*, Vol.64, pp. 977-989

Chevalier L., Bernard S., Vicré-Gibouin M., Driouich A. & Follet-Gueye M.L. (2011) Cryopreparation of tobacco Bright Yellow-2 (BY-2) suspensioncultured cells and application to immunogold localization of Green Fluorescent Protein-tagged-membrane-proteins. *Journal of Biological Research*, Vol.16, pp. 202-216

Clausen, M.H., Willats, W.G.T. & Knox, J.P. (2003) Synthetic methyl hexagalacturonate hapten inhibitors of anti-homogalacturonan monoclonal antibodies LM7, JIM5 and JIM7. *Carbohydrate Research*, Vol.338, pp. 1797-1800

Coimbra, S. & Salema, R. (1997). Immunolocalization of arabinogalactan proteins in *Amaranthus hypochondriacus* L. ovules. *Protoplasma*, Vol.199, pp. 75-82.

Coimbra, S. & Duarte, C. (2003). Arabinogalactan proteins may facilitate the movement of pollen tubes from the stigma to the ovules in *Actinidia deliciosa* and *Amaranthus hypochondriacus*. *Euphytica*, Vol.133, pp. 171-178

Coimbra, S., Almeida, J., Junqueira, V., Costa, M.L. & Pereira, L.G. (2007) Arabinogalactan proteins as molecular markers in Arabidopsis thaliana sexual reproduction. *Journal of Experimental Botany*, Vol.58, pp. 4027-4035

Dardelle, F., Lehner, A., Ramdani, Y., Bardor, M., Lerouge, P., Driouich, A. & Mollet JC (2010) Biochemical and immunocytological characterizations of Arabidopsis thaliana pollen tube cell wall. *Plant Physiology*, Vol.153, pp. 1563-1576

Driouich A., Faye L. & Staehelin L.A. (1993) The plant Golgi apparatus: a factory for complex polysaccharides and glycoproteins. *Trends in Biochemistry. Science.*, Vol. 18, pp. 210-214

Driouich A., Durand C. & Vicré-Gibouin M. (2007) Formation and separation of root border cells. *Trends in Plant Science*, Vol. 12, pp.14–19

Driouich A. & Baskin T. (2008). Intercourse between cell wall and cytoplasm exemplified by arabinogalactan-proteins and cortical microtubules in the root of *Arabidopsis thaliana*. *Am. J. Botany*. 95: 1491-1497.

Durand C., Vicré-Gibouin M., Follet-Gueye M.L., Duponchel L., Moreau M., Lerouge P. & Driouich A. (2009) The organization pattern of root border-like cells of Arabidopsis is dependent on cell wall homogalacturonan. *Plant Physiology*, Vol.3, pp 1411-1421

Ellis, M., Egelund, J., Schultz, C.J. & Bacic, A. (2010) Arabinogalactan-proteins: key regulators at the cell surface? *Plant Physiology*, Vol.153, pp. 403-419

Fitchette A.C., Cabanes-Macheteau M., Marvin L., Martin B., Satiat-Jeunemaitre B., Gomord V., Crooks K., Lerouge P., Faye L. & Hawes C. (1999) Biosynthesis and immunolocalization of Lewis a-containing N-glycans in the plant cell. *Plant Physiology*, Vol. 121, pp. 333-44

Follet-Gueye, M.L., Pagny, S., Faye, L., Gomord, V. & Driouich, A. (2003) An improved chemical fixation method suitable for immunogold localization of green fluorescent protein in the Golgi apparatus of tobacco bright yellow (BY-2) cells. *Journal of Histochemistry and Cytochemistry*, Vol. 51, pp.931–940

Gibeaut D.M. & Carpita N.C. (1994) Biosynthesis of plant cell wall polysaccharides. *FASEB J.*, Vol. 8, pp. 904-915

Gilbert, H.J. (2010) The biochemistry and structural biology of plant cell wall deconstruction. *Plant Physiology*, Vol.153, pp. 444-455

Harholt J., Jensen J.K., Sørensen S.O., Orfila C., Pauly M. & Scheller H.V. (2006) ARABINAN DEFICIENT 1 is a putative arabinosyltransferase involved in biosynthesis of pectic arabinan in Arabidopsis. *Plant Physiology*, Vol. 140, pp. 49–58

Harris P.J. & Northcote D.H., (1971). Polysaccharide formation in plant Golgi bodies. *Biochemistry and Biophysical Acta.*, Vol. 237, pp. 56-64

Hawes M.C., Bengough G., Cassab G. & Ponce G. (2003) Root caps and rhizosphere. *Journal of Plant Growth Regulation*, Vol. 21, pp.352–367

Hématy, K., Cherk, C. & Somerville, S. (2009) Host-pathogen warfare at the plant cell wall. *Current Opinion in Plant Biology*, Vol.12, pp. 406-413

Jauh, G.Y. & Lord E.M. (1996) Localization of pectins and arabinogalactan-proteins in lily (*Lilium longiflorum* L.) pollen tube and style, and their possible roles in pollination *Planta*, Vol.199, pp. 251-261

Johnson-Brousseau, S.A. & McCormick, S. (2004) A compendium of methods useful for characterizing Arabidopsis pollen mutants and gametophytically expressed genes. *The Plant Journal*, Vol. 39, pp. 761–775

Jones, L., Seymour, G.B., & Knox, J.P. (1997) Localization of pectic galactan in tomato cell walls using a monoclonal antibody specific to (1->4)-beta-D-galactan. *Plant Physiology*, Vol.113, pp. 1405-1412.

Langhans M., Förster S., Helmchen G. & Robinson D.G. (2011) Differential effects of the brefeldin A analogue (6R)-hydroxy-BFA in tobacco and Arabidopsis. *Journal of Experimental Botany*,. Vol. 62, pp. 2949-2957

Lee, K.J.D., Marcus S.E. & Knox J.P. (2011) Cell wall biology: Perspectives from cell wall imaging. *Molecular Plant*, Vol.4, pp. 212-219

Lehner, A., Dardelle, F., Soret-Morvan, O., Lerouge, P., Driouich, A., & Mollet, J.C. (2010) Pectins in the cell wall of *Arabidopsis thaliana* pollen tube and pistil. *Plant Signaling and Behavior*, Vol.5, pp. 1282-1285

Li, Y.Q., Bruun, L., Pierson, E.S. & Cresti, M. (1992) Periodic deposition of arabinogalactan epitopes in the cell wall of pollen tubes of *Nicotiana tabacum L. Planta*, Vol.188, pp. 532-538

Liepman, A.H., Wightman, R., Geshi, N., Turner, S.R. & Scheller, H.V. (2010) Arabidopsis - a powerful model system for plant cell wall research. *The Plant Journal*, Vol.61, pp. 1107-1121

Marcus, S.E., Verhertbruggen, Y., Herve, C., Ordaz-Ortiz, J.J., Farkas, V., Pedersen, H.L., Willats, W.G.T. & Knox, J.P. (2008) Pectic homogalacturonan masks abundant sets of xyloglucan epitopes in plant cell walls. *BioMedCentral Plant Biology*, Vol.8, pp. 60-71

Mayhew, T.M., Lucocq, J.M. & Griffiths, G. (2002) Relative labelling index: a novel stereological approach to test for non-random immunogold labelling of organelles and membranes on transmission electron microscopy thin sections. *Journal of Microscopy*, Vol. 205, pp.153–164

Mayhew T.M. (2011) Quantifying immunogold localization on electron microscopic thin sections: a compendium of new approaches for plant cell biologists. *Journal of Experimental Botany*, Vol. 62, pp. 4101-4113

Micheli F. (2001) Pectin methylesterases: cell wall enzymes with important roles in plant physiology. Trends in Plant Sciences, Vol. 6, pp.414-419

Moller, I., Marcus, S.E., Haeger, A., Verhertbruggen, Y., Verhoef, R., Schols, H., Mikklesen, J.D., Knox, J.P. & Willats, W. (2008) High-throughput screening of monoclonal antibodies against plant cell wall glycans by hierarchial clustering of their carbohydrate microarray binding profiles. *Glycoconjugate Journal* Vol. 25, pp. 37-48.

Mollet, J.C., Park, S.Y., Nothnagel, E.A. & Lord, E.M. (2000) A lily stylar pectin is necessary for pollen tube adhesion to an in vitro stylar matrix. *The Plant Cell*, Vol.12, 1737-1749

Mollet, J.C., Kim, S., Jauh, G.Y. & Lord, E.M. (2002) AGPs, pollen tube growth and the reversible effects of Yariv phenylglycoside. *Protoplasma*, Vol.219, pp. 89-98

Mollet, J.C., Faugeron, C. & Morvan, H. (2007) Cell adhesion, separation and guidance in compatible plant reproduction, In: *Plant Cell separation and adhesion*, Roberts, J. & Gonzalez-Carranza, Z. (Ed.), *Annual Plant Reviews*, Vol.25, pp. 69-90

Mouille, G., Ralet, M.C., Cavelier, C., Eland, C., Effroy, D., Hématy, K., McCartney, L., Truong, H.N., Gaudon, V., Thibault, J.F., Marchant, A. & Höfte, H. (2007) Homogalacturonan synthesis in Arabidopsis thaliana requires a Golgi-localized protein with a putative methyltransferase domain. *The Plant Journal*, Vol.50, pp. 605–614

Pagny S., Bouissonnie F., Sarkar M., Follet-Gueye M.L., Driouich A., Schachter H., Faye L. & Gomord V. (2003) Structural requirements for Arabidopsis beta1,2-xylosyltransferase activity and targeting to the Golgi. *The Plant Journal*, Vol. 33, pp. 189-203

Pattathil, S., Avci, U., Baldwin, D., Swennes, A.G., McGill, J.A., Popper, Z., Bootten, T., Albert, A., Davis, R.H., Chennareddy, C., Dong, R., O'Shea, B., Rossi, R., Leoff, C., Freshour, G., Narra, R., O'Neil, M., York, W.S. & Hahn, M.G. (2010) A comprehensive toolkit of Plant cell wall glycan-directed monoclonal antibodies. *Plant Physiology*, Vol.153, pp. 514-525.

Pennell, R.I., Janniche, L., Kjellbom, P., Scofield, G.N., Peart, J.M. & Roberts, K. (1991) Developmental regulation of a plasma membrane arabinogalactan protein epitope in oilseed rape flowers. *The Plant Cell*, Vol.3, pp. 1317-1326.

Puhlmann, J., Bucheli, E., Swain, M.J., Dunning, N., Albersheim, P., Darvill, A.G. & Hahn, M.G. (1994) Generation of monoclonal antibodies against plant cell wall polysaccharides. I. Characterization of a monoclonal antibody to a terminal alpha-(1,2)-linked fucosyl-containing epitope. *Plant Physiology*, Vol.104, pp. 699-710

Qin, Y. & Zhao, J. (2006). Localization of arabinogalactan proteins in egg cells, zygotes, and two-celled proembryos and effects of β-D-glucosyl Yariv reagent on egg cell

fertilization and zygote division in *Nicotiana tabacum* L. *Journal of Experimental Botany*, Vol.57, pp. 2061-2074

Ray P.M. (1980) Cooperative action of beta-glucan synthetase and UDP-xylose xylosyl transferase of Golgi membranes in the synthesis of xyloglucan-like polysaccharide. *Biochimistry and Biophysical Acta*, Vol. 629, pp. 431-444

Sandhu, A.P.S., Randhawa, G.S. & Dhugga, K.S. (2009) Plant cell wall matrix polysaccharide biosynthesis. *Molecular Plant*, Vol. 2, pp. 840-850

Seifert, G.J. & Blaukopf, C. (2010) Irritable walls: the plant extracellular matrix and signaling. *Plant Physiology*, Vol.153, pp. 467-478

Smyth, D.R., Bowman, J.L. & Meyerowitz, E.M. (1990) *Early flower development in* Arabídopsis. The Plant Cell, *Vol.2, pp. 755-767*

Staehelin L.A., Giddings T.H. Jr, Kiss J.Z. & Sack F.D. (1990) Macromolecular differentiation of Golgi stacks in root tips of Arabidopsis and Nicotiana seedlings as visualized in high pressure frozen and freeze-substituted samples. *Protoplasma*, Vol. 157, pp. 75-91

Studer, D., Graber, W., Al-Amoudi, A. & Eggli, P. (2001) A new approach for cryofixation by high-pressure freezing. *Journal of Microscopy*, Vol. 203, pp.285–294

Toyooka K., Goto Y., Asatsuma S., Koizumi M., Mitsui T. & Matsuoka K. (2009) A mobile secretory vesicle cluster involved in mass transport from the Golgi to the plant cell exterior. *The Plant Cell*, Vol. 4, pp. 1212-1229

Van Donselaar E., Posthuma G., Zeuschner D., Humbel B.M. & Slot J.W. (2007). Immunogold labeling of cryosections from high-pressure frozen cells. *Traffic*, 8: 471-485

Vicré, M., Santaella, C., Blanchet, S., Gateau, A. & Driouich, A. (2005) Root border-like cells of Arabidopsis. Microscopical characterization and role in the interaction with rhizobacteria. *Plant Physiology*, Vol.138, pp. 998-1008

Viotti C., Bubeck J., Stierhof Y.D., Krebs M., Langhans M., van den Berg W., van Dongen W., Richter S., Geldner N., Takano J., Jürgens G., de Vries S.C., Robinson D.G. & Schumacher K. (2010) Endocytic and secretory traffic in Arabidopsis merge in the trans-Golgi network/early endosome, an independent and highly dynamic organelle. *The Plant Cell*, Vol. 22, pp. 1344-1357

Willats, W.G.T., Marcus, S.E. & Knox, J.P. (1998) Generation of a monoclonal antibody specific to (1->5)-alpha-L-arabinan. *Carbohydrate Research*, Vol.308, pp. 149-152.

Willats W.G., McCartney L. & Knox J.P. (2001) In-situ analysis of pectic polysaccharides in seed mucilage and at the root surface of Arabidopsis thaliana. *Planta*, Vol. 213, pp. 37-44

Willats W.G., McCartney L., Steele-King C.G., Marcus S.E., Mort A., Huisman M., van Alebeek G.J., Schols H.A., Voragen A.G., Le Goff A., Bonnin E., Thibault J.F. & Knox J.P. (2004) A xylogalacturonan epitope is specifically associated with plant cell detachment. *Planta*, Vol. 218, pp.673-81

Wu, H., de Graaf, B., Mariani, C. & Cheung, A. Y. (2001). Hydroxyproline rich glycoproteins in plant reproductive tissues: structure, functions and regulation. *Cell and Molecular Life Sciences*, Vol.58, pp. 1418-1429

Yates, E.A., Valdor, J.-F., Haslam, S.M., Morris, H.R., Dell, A., Mackie, W. & Knox, J.P. (1996) Characterization of carbohydrate structural features recognized by anti-arabinogalactan-protein monoclonal antibodies. *Glycobiology*, Vol.6, pp. 131-139.

Zhang G.F. & Staehelin L.A. (1992) Functional compartmentalization of the Golgi apparatus of plant cells: an immunochemical analysis of high pressure frozen/freeze substituted sycamore suspension-cultured cells. *Plant Physiology*, Vol. 99, pp. 1070-1083

PARTIE B : SYNTHESE GOLGIENNE DU XYLOGLUCANE

Le xyloglucane est le polysaccharide hémicellulosique majoritaire des plantes eudicotylédones vraies, et joue un rôle clef dans leur développement, comme énoncé dans le chapitre d'introduction. De précédentes études ont focalisé sur la cartographie golgienne d'épitopes glucidiques spécifiques de la chaîne principale du XyG et des chaînes latérales fucosylées, et ont montré que seules les saccules *trans* et le réseau *trans*-golgien (TGN) présentaient ces épitopes. Ainsi, les auteurs ont proposé que la synthèse du XyG auraient lieu uniquement dans les compartiments tardifs de l'appareil de Golgi (Zhang and Staehelin, 1992, Driouich et al., 1993, Staehelin and Driouich, 1997).

Pour compléter ces premiers résultats, nous avons effectué la cartographie golgienne de trois glycosyltransférases d'Arabidopsis participant à la synthèse des chaînes latérales du XyG, fusionnées à la GFP, puis exprimées dans des suspensions cellulaires de tabac : la α(1,6)xylosyltransférase (AtXXT1), la β(1,2)galactosyltransférase (AtMUR3) et la α(1,2)fucosyltransférase (AtFUT1). Nous avons traité les cellules de tabac exprimant ces protéines de fusion selon la méthode que nous avions développée au laboratoire : traitement des cellules par un cryoprotectant, puis par congélation haute pression/substitution à froid. Un immunomarquage a été effectué ensuite et la cartographie des protéines déterminée d'après méthode statistique quantitative nommée *Relative Labelling Index* (RLI).

Nos conclusions sont les suivantes : la protéine AtXXT1 est majoritairement associée aux saccules *cis* et median, la protéine AtMUR3 est associée aux saccules median et la protéine AtFUT1 associée aux saccules *trans*, suggérant que tous les compartiments golgiens seraient impliqués dans la synthèse du XyG et que les enzymes agiraient de façon séquentielle au sein des différents types de saccules. L'ensemble de ce travail est décrit dans l'article suivant, **page 155**:

Chevalier L*, Bernard S*, Ramdani Y, Lamour R, Bardor M, Lerouge P, Follet-Gueye ML, Driouich A. (2010) Subcompartment localization of the side chain xyloglucan-synthesizing enzymes within Golgi stacks of tobacco suspension-cultured cells. *Plant Journal* 64(6):977-89

Papier N°4: Article scientifique

Résultats: Synthèse golgienne du xyloglucane

Subcompartment localization of the side chain xyloglucan-synthesizing enzymes within Golgi stacks of tobacco suspension-cultured cells.

Chevalier L*, Bernard S*, Ramdani Y, Lamour R, Bardor M, Lerouge P, Follet-Gueye ML, Driouich A.
*equal contribution

Plant Journal (2010) ; 64(6):977-89

the plant journal

SEB Society for Experimental Biology

The Plant Journal (2010) **64**, 977–989 doi: 10.1111/j.1365-313X.2010.04388.x

Subcompartment localization of the side chain xyloglucan-synthesizing enzymes within Golgi stacks of tobacco suspension-cultured cells

Laurence Chevalier[†,‡], Sophie Bernard[‡], Yasmina Ramdani, Romain Lamour, Muriel Bardor, Patrice Lerouge, Marie-Laure Follet-Gueye and Azeddine Driouich[*]

Laboratoire 'Glycobiologie et Matrice Extracellulaire Végétale,' UPRES EA 4358, Institut Fédératif de Recherche Multidisciplinaire sur les Peptides 23, Plate-forme de Recherche en Imagerie Cellulaire de Haute Normandie (PRIMACEN), IBiSA, Université de Rouen, 76821 Mont-Saint Aignan Cedex, France

Received 24 July 2010; revised 10 September 2010; accepted 21 September 2010; published online 15 November 2010.
[*]For correspondence (fax +33 235146615; e-mail azeddine.driouich@univ-rouen.fr).
[†]Present address: Groupe de Physique des Matériaux, UMR6634-CNRS, Institut des Matériaux Université de Rouen – Faculté des Sciences et Techniques BP 12 – Technopôle du Madrillet, Avenue de l'Université, 76801 St Etienne du Rouvray cedex.
[‡]These authors contributed equally to this work. This paper is dedicated to the memory of our colleague Pr. S. Barray.

SUMMARY

Xyloglucan is the dominant hemicellulosic polysaccharide of the primary cell wall of dicotyledonous plants that plays a key role in plant development. It is well established that xyloglucan is assembled within Golgi stacks and transported in Golgi-derived vesicles to the cell wall. It is also known that the biosynthesis of xyloglucan requires the action of glycosyltransferases including α-1,6-xylosyltransferase, β-1,2-galactosyltransferase and α-1,2-fucosyltransferase activities responsible for the addition of xylose, galactose and fucose residues to the side chains. There is, however, a lack of knowledge on how these enzymes are distributed within subcompartments of Golgi stacks. We have undertaken a study aiming at mapping these glycosyltransferases within Golgi stacks using immunogold-electron microscopy. To this end, we generated transgenic lines of tobacco (*Nicotiana tabacum*) BY-2 suspension-cultured cells expressing either the α-1,6-xylosyltransferase, AtXT1, the β-1,2-galactosyltransferase, AtMUR3, or the α-1,2-fucosyltransferase AtFUT1 of *Arabidopsis thaliana* fused to green-fluorescent protein (GFP). Localization of the fusion proteins within the endomembrane system was assessed using confocal microscopy. Additionally, tobacco cells were high pressure-frozen/freeze-substituted and subjected to quantitative immunogold labelling using anti-GFP antibodies to determine the localization patterns of the enzymes within subtypes of Golgi cisternae. The data demonstrate that: (i) all fusion proteins, AtXT1–GFP, AtMUR3–GFP and AtFUT1–GFP are specifically targeted to the Golgi apparatus; and (ii) AtXT1–GFP is mainly located in the *cis* and medial cisternae, AtMUR3–GFP is predominantly associated with medial cisternae and AtFUT1–GFP mostly detected over *trans* cisternae suggesting that initiation of xyloglucan side chains occurs in early Golgi compartments in tobacco cells.

Keywords: cell wall, cryofixation, green-fluorescent protein, Golgi, immunocytochemistry, xyloglucan.

INTRODUCTION

Plant growth and morphology are largely dependent on the biosynthesis of the cell wall. In dicotyledonous plants, the primary cell wall comprises cellulose microfibrils and a xyloglucan network embedded within a matrix of non-cellulosic polysaccharides and proteins (i.e. glycoproteins and proteoglycans). Four major types of non-cellulosic polysaccharides are found in the primary walls of plant cells (*in taxa* outside the graminae), namely the neutral hemicellulosic polysaccharide xyloglucan (XyG), and three main pectic polysaccharides, homogalacturonan (HG), rhamnogalacturonan I and II (RG-I and RG-II) (Cosgrove, 2005).

XyG consists of a β-D-(1 → 4)-glucan backbone to which are attached side chains containing xylosyl, galactosyl-xylosyl or fucosyl-galactosyl-xylosyl residues. In dicotyledonous and non-grass monocotyledonous plants, XyG is

The Plant Journal © 2010 Blackwell Publishing Ltd
No claim to original US government works

the principal polysaccharide that cross-links the cellulose microfibrils. It is able to bind cellulose tightly because its β-D-(1 → 4)-glucan cellulose-like backbone can form numerous hydrogen bonds with the microfibrils, whereas the side chains give rise to regions where microfibril binding is interrupted. A single XyG molecule can therefore interconnect separated cellulose microfibrils. This XyG-cellulose network forms a major load-bearing structure that contributes to the structural integrity of the cell wall and the control of cell expansion during growth (Cosgrove, 2005).

XyG biosynthesis has long been an interesting area of investigation. It mainly requires, among others, a glucan synthase activity for backbone assembly and several glycosyltransferases involved in the addition of the side chains, including xylosyltransferase, galactosyltransferase and fucosyltransferase activities.

Early studies on pea stems have demonstrated that all the glycosyltransferases necessary for XyG biosynthesis are associated with Golgi membranes (Ali *et al.*, 1986; Camirand and MacLachlan, 1986; Camirand *et al.*, 1987). Hayashi and Matsuda (1981) and Hayashi *et al.* (1981) have shown that the β-glucan synthase produces the required β-1,4-glucan substrate molecule necessary for XyG xylosyltransferase activity. In addition, it has been demonstrated that XyG synthesis requires the cooperation of XyG β-1,4-glucan synthase and the XyG xylosyltransferase within Golgi membranes supporting the existence of a multienzyme complex responsible for XyG biosynthesis (Hayashi *et al.*, 1988).

Since then, considerable efforts have been devoted to the identification and characterization of the genes involved in XyG biosynthesis using functional genomics and the model plant *Arabidopsis thaliana* (see Lerouxel *et al.*, 2006). For example, the XyG fucosyltransferase AtFUT1 (CAZy GT37) was the first type-II glycosyltransferase characterized at the biochemical level (Perrin *et al.*, 1999). AtFUT1 has been identified as one member of a large family containing nine putative glycosyltransferases. However, further analyses of the enzymes have shown that three members of this family are not involved in the fucosylation of XyG (Sarria *et al.*, 2001). Later on, the identification and characterization of the *mur2* mutant of arabidopsis provided compelling evidence that the AtFUT1 gene encodes the unique α-1,2-fucosyltransferase activity responsible for XyG fucosylation (Vanzin *et al.*, 2002). Similarly, one XyG β-1,2-galactosyltransferase (AtMUR3; CAZy GT47) activity was successfully characterized using both mutant analysis (*mur3*) and heterologous expression of the enzyme (Madson *et al.*, 2003). Nevertheless, as the galactose residue of the XyG molecule can be found in two different positions, it seems that at least one XyG galactosyltransferase remains to be identified. AtMUR3 acts specifically on the third xylose of the XXXG core structure of XyG. An important contribution to understanding XyG biosynthesis was also made by the characterization of two α-1,6-xylosyltransferases activities required for XyG xylosylation (CAZy GT34). First, one xylosyltransferase activity (named AtXT1) was identified based on sequence homology with a previously identified α-1,6-galactosyltransferase from fenugreek (Edwards *et al.*, 1999), and characterized as a α-1,6-xylosyltransferase using heterologous expression in *Pichia pastoris* (Faik *et al.*, 2002). Cavalier and Keegstra (2006) extended this work by the characterization of a second xylosyltransferase activity (named AtXT2), encoded by a gene closely related to AtXT1. AtXT1 and AtXT2 preferentially add the first xylosyl residue to the fourth glucosyl residue at the reducing end of the acceptor XyG oligosaccharides. More recently, Zabotina *et al.* (2008) have identified another XyG-xylosyltransferase named XXT5 that has also been localized to Golgi bodies by using confocal microscopy.

Another enzyme involved in XyG biosynthesis is the glucan synthase. Recently, a gene from the Cellulose Synthase-Like C family (*AtCSLC4;* CAZy GT2) was shown to encode a Golgi localized β-1,4-glucan synthase activity providing a strong candidate for the, as yet, unidentified XyG β-glucan synthase (Cocuron *et al.*, 2007).

Another approach that has helped understanding XyG biosynthesis within Golgi stacks is immunocytochemistry using transmission electron microscopy and anti-XyG antibodies specific either for the backbone or for the fucosylated side chains. Based on this methodology, it was suggested that the assembly of XyG occurs exclusively in the late compartments of Golgi stacks namely *trans* cisternae, the *trans*-Golgi network (Zhang and Staehelin, 1992; Driouich *et al.*, 1993; Staehelin and Driouich, 1997). So far, such a Golgi compartmentalization of XyG-associated sugar epitopes has not been investigated for the glycosyltransferases involved in the biosynthesis of this hemicellulosic polysaccharide. Therefore and as a starting point towards understanding how all functional activities involved in XyG biosynthesis are organized within Golgi cisternae, we have investigated Golgi compartmentalization of three glycosyltransferases (namely AtXT1, AtMUR3 and AtFUT1) involved in the assembly of XyG side chains in transformed tobacco BY-2 cells expressing GFP-tagged AtXT1, AtMUR3 or AtFUT1. To this end, immunogold electron microscopy with anti-GFP antibodies along with quantitative analysis of antibody binding within Golgi cisternae based on relative labelling index calculations were used. Our findings show that fusion proteins, AtXT1–GFP, AtMUR3–GFP and AtFUT1–GFP were targeted to Golgi stacks of tobacco BY-2 suspension-cultured cells. In addition, labelling of AtXT1–GFP was mostly associated with *cis* and medial cisternae, and labelling of AtMUR3–GFP and ATFUT1–GFP was mainly detected in medial and *trans* cisternae of Golgi stacks respectively. These findings suggest that the assembly of XyG side chains involves all subtypes of Golgi cisternae.

RESULTS

Structural analysis of XyG isolated from tobacco BY-2 suspension-cultured cells

Prior to any expression or localization studies of XyG-synthesizing enzymes in BY-2 suspension-cultured cells, we performed a structural analysis of XyG isolated from the cell wall of these cells via the enzymatic oligosaccharide fingerprinting procedure as previously described (Lerouxel *et al.*, 2002; Ray *et al.*, 2004). The population of xyloglucan oligosaccharides generated by endoglucanase treatment of BY-2 cell walls was analyzed by MALDI-TOF mass spectrometry. As described in suspension-cultured cells of *Nicotiana plumbaginifolia* (Sims *et al.*, 1996), the main ions were assigned to $(M + Na)^+$ adducts of XXGG-type XyG fragments partially acetylated and substituted with arabinosyl residues (S) (Figure 1). In addition, minor non-fucosylated XXXG-type oligosaccharides were detected, including an acetylated monogalactosylated XXLG or XLXG fragment.

Subcellular localization of XyG-glycosyltransferases fused to green fluorescent protein

To establish the subcellular localization of XyG-glycosyltransferases, AtXT1, AtMUR3 and AtFUT1 in tobacco leaf epidermal cells using confocal microscopy, we created fluorescent protein fusions of these enzymes (see Materials and methods). All three glycosyltransferases are type II membrane-bound proteins containing a transmembrane domain and supposed to be localized in the Golgi apparatus.

As illustrated in Figure 2, transformed tobacco epidermal cells with AtXT1–GFP (Figure 2a), AtMUR3–GFP (Figure 2d) or AtFUT1–GFP (Figure 2g) displayed a punctate pattern of GFP fluorescence, as would be expected from the dispersed organization of Golgi stacks in plant cells (Nebenführ *et al.*, 1999; Pagny *et al.*, 2003). To confirm Golgi localization, we co-expressed each glycosyltransferase–GFP with the well known fluorescent Golgi marker, α2,6-sialyltransferase (ST) fused to YFP, in the same epidermal leaf cells. As shown in Figure 2(c, f, i), AtXT1–GFP, AtMUR3–GFP and AtFUT1–GFP fluorescence signals co-localized with ST–YFP fluorescence to punctate and mobile structures typical of Golgi bodies.

To investigate the localization of the glycosyltransferases in the Golgi bodies using transmission electron microscopy, we could not use transiently transformed epidermal cells, mostly because the transformation yield was very low. We therefore generated stably transformed tobacco-suspension-cultured BY-2 cells expressing AtXT1–GFP, AtMUR3–GFP or AtFUT1–GFP at a high level (up to 90% of the cells expressed GFP). Then, we also studied the subcellular localization of the three fusion proteins in the stably transformed suspension cultured BY-2 cells using confocal imaging. In all cases and as for transiently expressed cells, we observed fluorescent and mobile spots (of 1 μm in size) consistent with Golgi localization for AtXT1–GFP, AtMUR3–GFP and AtFUT1–GFP (Figure 2j, k, l). None of the transient or stably transformed cells showed any additional fluorescence in any other organelles of the endomembrane system. These data demonstrate that AtXT1–GFP, AtMUR3–GFP and AtFUT1–GFP of arabidopsis have Golgi localization in tobacco leaf epidermal and suspension-cultured cells.

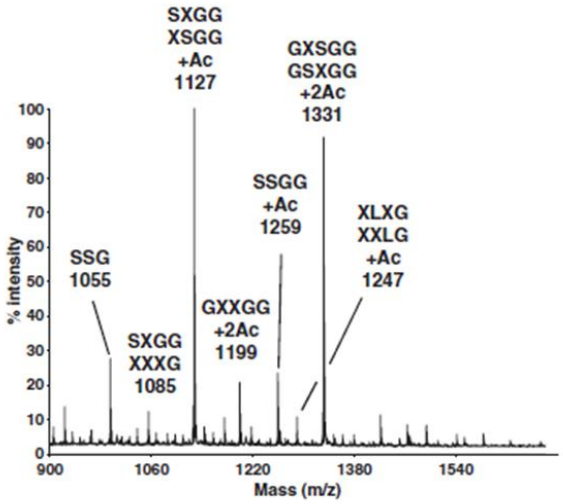

Figure 1. MALDI-TOF mass spectrum of xyloglucan fragments released by endoglucanase treatment of XyG extracted from tobacco BY-2 suspension-cultured cells. XXGG, XSG, SXG, SSGG, XXLG, XLXG refer to XXGG-type or XXXG-type fragments according to Fry *et al.* (1993).

Ultrastructural organization of Golgi stacks in high pressure frozen/freeze substituted tobacco BY-2 cells

We first examined the quality of ultrastructural preservation of BY-2 suspension-cultured cells prepared by high pressure freezing and freeze-substitution in acetone containing 0.5% uranyl acetate (but no osmium), and embedded in London Resin White (LRW) for immunocytochemistry. As shown in Figure 3(a), BY-2 cells exhibited very well preserved subcellular structures including the nucleus, nuclear membrane, mitochondria, vacuole, endoplasmic reticulum, secretory vesicles and Golgi stacks. In the context of this paper, Golgi stacks were clearly distinguishable and their organization was typical of plant suspension-cultured cells (Zhang and Staehelin, 1992; Andreeva *et al.*, 1998; Winicur *et al.*, 1998). Also and as illustrated in Figure 3(b,c), were consistently discernable based on their very well characterized ultrastructure as previously described (Staehelin *et al.*, 1990; Zhang and Staehelin, 1992; Driouich *et al.*, 1993). *Cis* cisternae exhibited the most irregular contour, were faintly stained and had the widest lumen. Medial cisternae had a narrower lumen, were more elongated and picked up more stain than *cis* cisternae. There is often a gradation of luminal staining of the medial cisternae in a *cis*-to-*trans* direction. *Trans* cisternae presented a very thin, collapsed lumen that

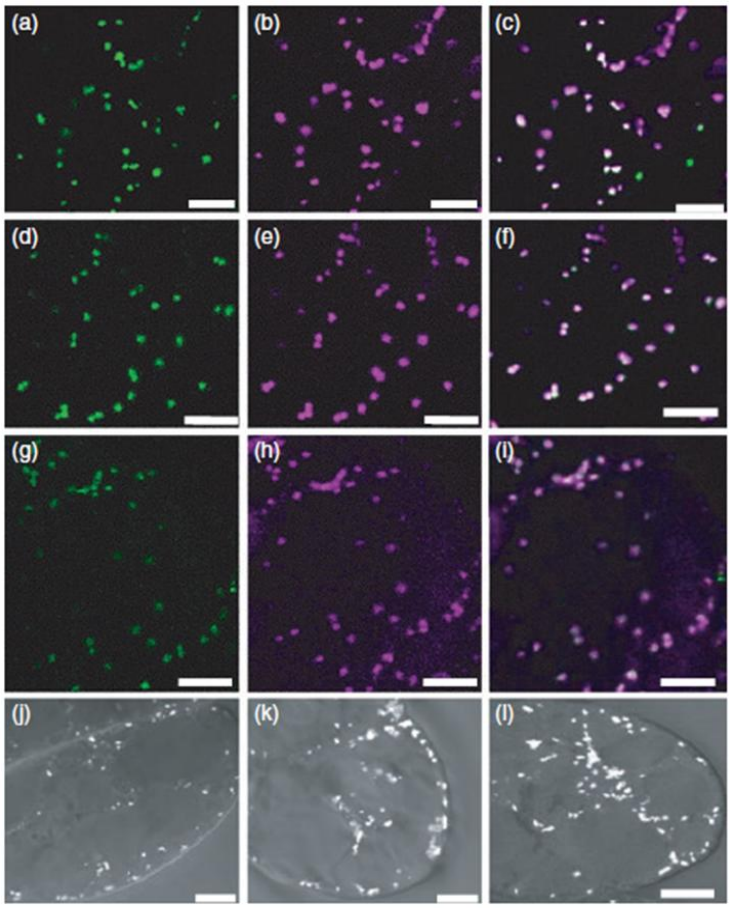

Figure 2. Distribution of AtXT1–GFP, AtMUR3–GFP and AtFUT1–GFP in living tobacco cells.
Images of epidermal leaf cells (a–i).
Images of suspension-cultured cells (j-l).
Brightly fluorescent spots typical of Golgi localization are seen following transient expression of AtXT1–GFP (a), AtMUR3-GFP (d) and AtFUT1–GFP (g) in leaf epidermal cells. Localization of the Golgi marker, α 2,6-sialyltransferase (ST), fused to YFP in epidermal leaf cells (b, e, h). Golgi stacks are visible as bright spots. Co-localization of AtXT1–GFP (c), AtMUR3–GFP (f) or AtFUT1–GFP (i) with ST–YFP in epidermal leaf cells confirming Golgi localization of the XyG-glycosyltransferases. Stable expression of AtXT1–GFP (j), AtMUR3–GFP (k) and AtFUT1–GFP (l) in tobacco BY-2 cultured cells also shows fluorescent spots typical of Golgi localization. Scale bars 8 μm.

is always densely stained even more than medial cisternae. The *trans*-Golgi network was observed as a branched tubulo-vesicular structure that is frequently, but not systematically, located close to *trans* cisternae consistent with previous findings (Zhang and Staehelin, 1992).

Immunolocalization of XyG epitopes in tobacco cells

Prior to any investigation of XyG-synthesizing enzymes at the electron microscopical level, we immunolocalized XyG epitopes in tobacco BY-2 suspension-cultured cells using confocal imaging and immunogold electron microscopy with the mAb CCRC-M86 (kindly provided by Prof. M. Hahn; University of Georgia, USA), which recognizes non-fucosylated xyloglucan (Pattathil *et al.*, 2010). On immunodot assay, the CCRC-M86 antibody reacted strongly with native tamarind XyG but not with a hydrolyzed sample of the polymer (Figure S1 in Supporting Information). It also reacted with XyG isolated from tobacco suspension-cultured cells.

Confocal imaging of immunostained cells with the mAb CCRC-M86 showed a punctate fluorescence in the cytosol and a quite uniform staining at the cell surface (Figure 4a,b). This is consistent with the CCRC-M86-recognized XyG-associated epitopes being located in Golgi stacks and cell wall, two compartments where XyG is known to occur.

Immunogold labelling of cryo-fixed BY-2 cultured cells showed XyG epitopes over Golgi stacks and in the cell wall (Figure 4c,d). Gold particles were mainly found over medial and *trans* cisternae, the *trans*-Golgi network and Golgi-derived transport vesicles. Also, labelling of the cell wall was mostly associated with the closest zone to the plasma membrane (Figure 4d). In contrast, no labelling was found in BY-2 cells using the mAb CCRC-M1 (data not shown) specific for an α-L-Fuc*p*-(1–2)-β-D-Gal*p* epitope of XyG, consistent with the previously published data showing that tobacco XyG does not contain fucosyl residues (Hoffman *et al.*, 2005).

Immunogold localization of the glycosyltransferases–GFP within Golgi cisternae

Once we confirmed Golgi localization of XyG epitopes and glycosyltransferases using confocal microscopy (see

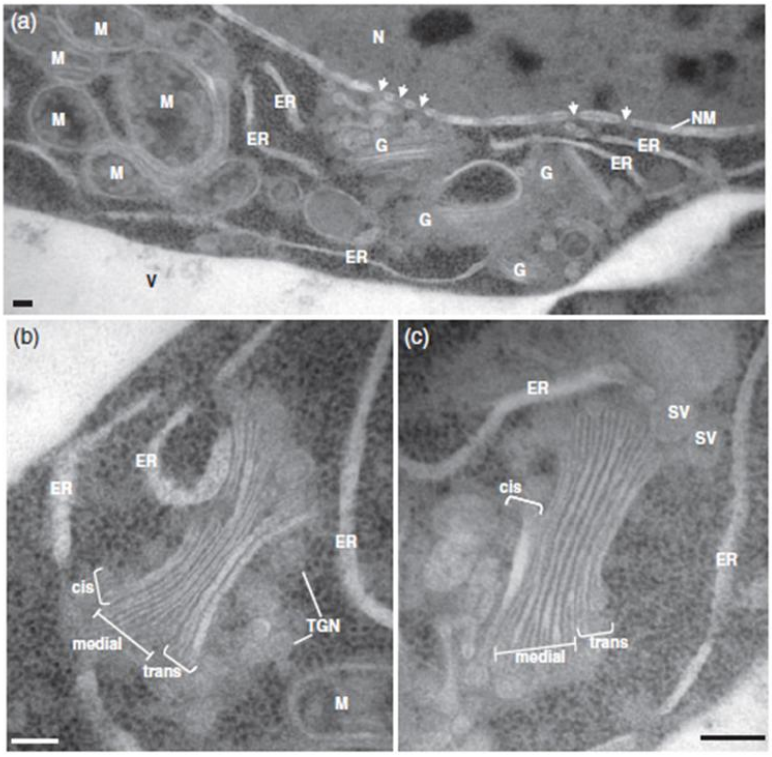

Figure 3. Ultrastructural organization of BY-2 Golgi stacks.
Electron micrographs of tobacco BY2-suspension-cultured cells preserved by high pressure freezing.
(a) A view of the cytoplasm showing different organelles including Golgi stacks, endoplasmic reticulum, vacuole, mitochondria and nucleus. White arrowheads indicate nuclear pores.
(b, c) Images of Golgi stacks exhibiting different subtypes of cisternae including *cis*, medial and *trans*. Note that the trans-Golgi network is not always associated with all Golgi stacks. ER, endoplasmic reticulum, G, Golgi stack; NM, nuclear membrane; N, nucleus; M, mitochondria; SV, secretory vesicles; TGN, *trans*-Golgi network; V, vacuole. Scale bars: 100 nm.

above), we investigated distribution of the enzymes within Golgi cisternae using immunogold-electron microscopy. Labelling of AtXT1–GFP, AtMUR3–GFP and AtFUT1–GFP was performed by employing anti-GFP antibodies in stably transformed BY-2 cells prepared by HPF/FS technique.

Immunogold labelling was quantified over each Golgi cisterna (fifty Golgi stacks with distinguishable cisternal subtypes) and subjected to chi-squared (χ^2) test to check for labelling specificity in transformed BY-2 cells versus wild type. The relative labelling index (RLI) was also determined to evaluate specific gold particles distribution within different subtypes of Golgi cisternae (Mayhew *et al.*, 2002) (see Materials and methods).

Golgi distribution of AtXT1–GFP

Immunogold labelling of Golgi stacks of AtXT1–GFP transgenic BY-2 cultured cells with anti-GFP antibodies is illustrated in Figure 5(a,b). Gold particles were mainly localized over *cis*- and medial-Golgi cisternae and also in transport vesicles associated with Golgi margins.

Quantification of labelling and chi-square test were performed (Table 1a) to confirm the specificity of the signal in cells expressing AtXT1–GFP BY-2 versus wild type cells. The total chi-squared value (31.28) was found to be superior to that of the contingency table, χ^2_{table} = 12.38 (with a degree of freedom of 3 and an uncertainty degree α = 0.005) indicating that labelling is specific in Golgi stacks. In addition, distribution of GFP-tagged AtXT1 within subtypes of Golgi cisternae in transformed cells was assigned based on RLI determination. The RLI values for *cis* and medial cisternae were found to be superior to 1 (1.66 for *cis* cisternae and 1.27 for medial cisternae; see Table 1b), indicating a specific and preferential labelling of these two Golgi compartments with anti-GFP antibodies.

Golgi distribution of AtMUR3–GFP

Localization of AtMUR3 was performed using the same procedure. Immunogold labelling of Golgi stacks of AtMUR3–GFP transgenic BY-2 cultured cells with anti-GFP antibodies is shown in Figure 6(a,b). Gold particles were also mainly localised in Golgi stacks and seemed to be preferentially in the medial-Golgi cisternae. Quantification of labelling and chi-square tests were performed as for cells expressing AtXT1–GFP (see above). The total chi-squared value (25.69), was found to be greater than that of the contingency table, χ^2_{table} = 12.38 (with a degree of freedom of 3 and an uncertainty degree α = 0.005) indicating that labelling in Golgi stacks is specific (Table 2a). In addition, analysis of AtMUR3–GFP distribution based on RLI determination indicates a preferential labelling of medial cisternae (RLI value 1.67 for medial cisternae; see Table 2b).

No claim to original US government works

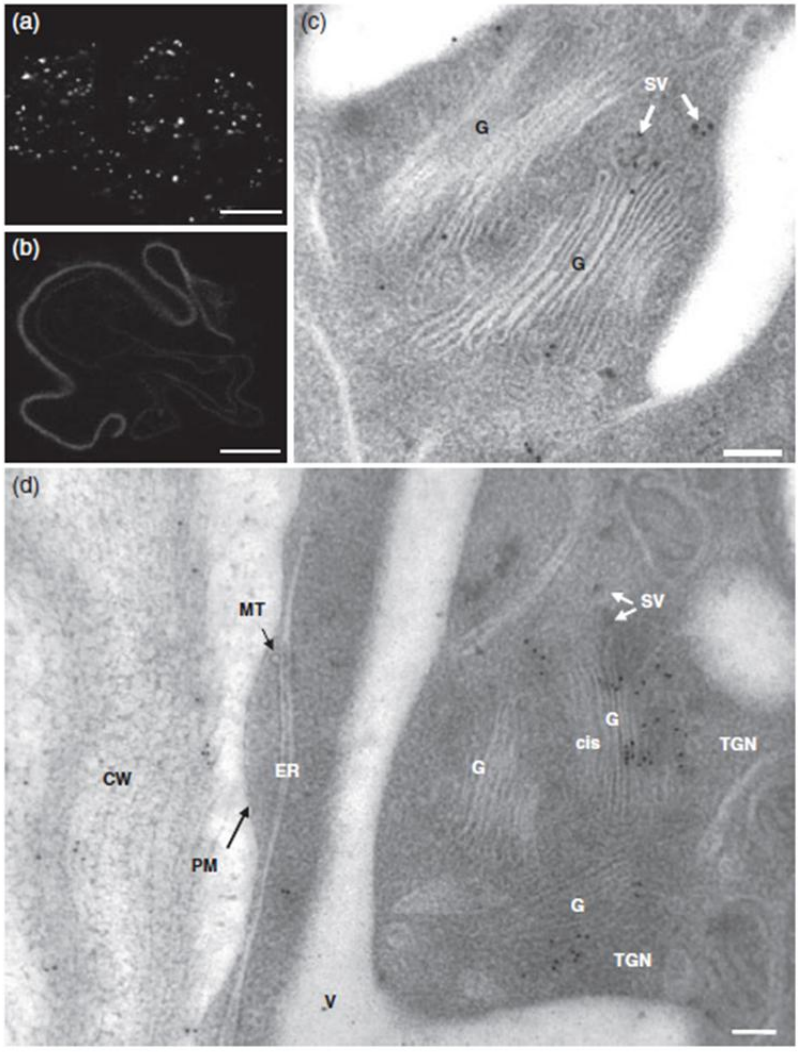

Figure 4. Immunocytochemical localization of XyG epitopes in tobacco BY-2 suspension-cultured cells with the mAb CCRC-M86.
(a, b) Confocal microscope images showing fluorescent staining of Golgi bodies (a) and the cell surface (b). CCRC-M86 epitopes localize to both Golgi stacks and the forming cell wall of tobacco protoplasts.
(c, d) Electron micrographs of HPF/FS cells illustrating immunogold labelling of Golgi stacks and the cell wall. Note that labelling is found over Golgi cisternae Golgi-derived secretory vesicles (c, d) and the TGN (d). CW, Cell wall; ER, endoplasmic reticulum; G, Golgi stack; MT, microtubule; PM, plasma membrane; SV, secretory vesicles; TGN, *trans*-Golgi network; V, vacuole. Scale bars 8 μm (a, b), 100 nm (c, d).

Golgi distribution of AtFUT1–GFP

Quantification of immunogold labelling, of Golgi stacks in transgenic BY-2 cultured cells expressing AtFUT1–GFP, and a chi-squared test were performed as for AtXT1–GFP and AtMUR3–GFP. The total chi-squared value (22.41), was found to be superior compared with that of the contingency table, $\chi^2_{table} = 12.38$ (with a degree of freedom of 3 and an uncertainty degree $\alpha = 0.005$) indicating that labelling in Golgi stacks is specific (Table S1 in Supporting Information). The RLI values were found to be 1.00 for *cis* cisternae, 0.84 for medial cisternae, 1.61 for *trans* cisternae and 0.97 for the TGN. The data indicate a preferential labelling of *trans*-Golgi cisternae as the RLI is superior to 1.

Together the immunogold labelling data coupled to quantitative and statistical analysis of the binding pattern of GFP indicate that in tobacco BY-2 suspension-cultured cells, the AtXT1 is mostly located in *cis* and medial cisternae, whereas AtMUR3 and ATFUT1 are predominantly associated with medial- and *trans*-Golgi cisternae, respectively.

DISCUSSION

The goal of the present study was to gain insights onto the spatial organization of the biosynthesis of the complex polysaccharide XyG within Golgi stacks of higher plants. Therefore, we mapped three glycosyltransferases, namely AtXT1, AtMUR3 and AtFUT1 that are involved in the biosynthesis of the side chains of XyG within different subtypes of Golgi cisternae of tobacco BY-2 cells. As no antibodies directed against these enzymes are currently available, we have chosen to investigate their localization indirectly by using anti-GFP antibodies in transgenic tobacco cells expressing the glycosyltransferases fused to GFP. We have previously used such a strategy to localize various glycosyltransferases involved in the assembly of *N*-linked glycoproteins (see Follet-Gueye *et al.*, 2003; Pagny *et al.*, 2003;

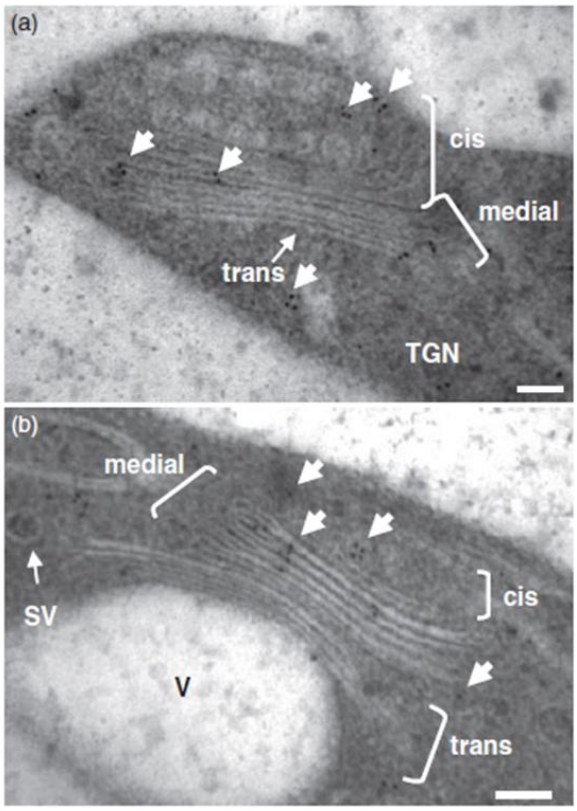

Figure 5. Immunogold localization of the AtXT1–GFP fusion protein in Golgi stacks of transformed tobacco BY-2 suspension-cultured cells with anti-GFP antibodies.
(a, b) Two electron micrographs illustrating immunolocalization of AtXT1–GFP fusion protein within Golgi stacks (see also Table 1 for quantification of labelling).
SV, secretory vesicles; TGN, *trans*-Golgi network; V, vacuole. Scale bars 100 nm.

Saint-Jore-Dupas *et al.*, 2006) within specific compartments of tobacco Golgi stacks. We show in the present study that the three enzymes are associated with all compartments of Golgi stacks with AtXT1, mainly found over *cis* and medial cisternae, AtMUR3 being mostly associated with medial cisternae and AtFUT1 in *trans* cisternae. These findings suggest that all Golgi cisternae are involved in XyG assembly by the Golgi apparatus of plant cells.

XyG is known to be synthesized in the Golgi lumen before its delivery via Golgi-derived vesicles to the cell wall (Ray, 1980; Camirand *et al.*, 1987; Moore and Staehelin, 1988; Driouich *et al.*, 1993). The biosynthesis of this polysaccharide, predictably, requires the activities of a β-glucan synthase; one or possibly more α-xylosyltransferases; at least two β-galactosyltransferases; and an α-fucosyltransferase (Lerouxel *et al.*, 2006); as well as additional enzymes, such as nucleotide sugar transporters and nucleotide sugar interconversion enzymes (Seifert *et al.*, 2004; Nguema-Ona *et al.*, 2006).

In the past, only the products of XyG-synthesizing enzymes, carrying specific sugar epitopes, have been mapped within Golgi cisternae using anti-sugar antibodies and immunogold electron microscopy (Zhang and Staehelin, 1992). Quantitative immunolabelling experiments using antibodies recognizing either the XyG backbone (anti-XG antibodies: Lynch and Staehelin, 1992; Moore *et al.*, 1986) or an α-L-Fuc*p*-(1 → 2)-β-D-Gal*p* epitope of XyG side chains in sycamore cultured cells have shown that the epitopes localize to *trans* cisternae and the TGN (Zhang and Staehelin, 1992). Based on these observations, the authors proposed that the biosynthesis of XyG is exclusively confined to *trans* cisternae and the TGN with the addition the β-1,4-linked glucosyl backbone being confined to *trans* cisternae and the fucosylation of the side chains associated partly with the *trans* cisternae and partly with the TGN. The authors also suggested that no XyG precursors are formed in *cis* or medial cisternae. Nevertheless, it could be argued that the sugar epitopes recognized by both antibodies used in that study are not accessible (and thus not detectable) until they reach the *trans* and the TGN compartments, or that the antibodies do not bind XyG precursor forms in *cis* and medial cisternae. In contrast to the study of Zhang and Staehelin (1992), the study of Brummell *et al.* (1990) on XyG-glycosyltransferase distribution in pea using biochemical assays of enzyme activities on separated Golgi membranes suggested that all Golgi cisternae are involved in XyG biosynthesis. These authors postulated that the glucose-xylose backbone of XyG is initiated in *cis* cisternae, continued in medial cisternae and completed in *trans,* where the fucosylation of the side chains is also initiated.

We first demonstrated that the GFP-tagged enzymes (AtXT1, AtMUR3 and AtFUT1) were targeted to Golgi stacks in tobacco cells as revealed by confocal imaging of transgenic plants. All the enzymes are predicted to be localized in the Golgi apparatus. We considered both C- and N-terminal fusions and we found that C-terminal fusions had no impact on subcellular localization of the enzymes. A similar observation (Golgi localization) was made when the *MUR3* gene was tagged with RFP at C-terminal position in Arabidopsis plants (Tamura *et al.*, 2005). In contrast, we found N-terminal fusion of GFP to MUR3 led to a dual localization, Golgi and cytosol (not shown). Tagging proteins with GFP at the C-terminal is generally known to preserve the localization of the native protein better than tagging at N-terminal position (Palmer and Freeman, 2004).

Zhang and Staehelin (1992) have suggested that only *trans* cisternae and TGN are involved in XyG biosynthesis in sycamore cells. In contrast our immunogold labelling data presented herein do favor the participation of all Golgi cisternae in XyG assembly. The fact that AtXT1 and AtMUR3 are detected in *cis* and medial cisternae of Golgi stacks implies the involvement of these early compartments in the biosynthesis of XyG. This is assuming that the enzymes are

Table 1 Quantitative analysis of anti-GFP labelling over Golgi stacks in tobacco BY-2 cells expressing AtXT1–GFP. (a) Comparison of gold particles distribution in Golgi cisternae of wild type and transformed cells (expressing AtXT1–GFP) of BY-2 cultured cells. (b) Observed and expected distribution of gold particles in subtypes of Golgi cisternae of tobacco BY-2 cells expressing AtXT1–GFP and relative labelling index values

	Wild type cells			Transformed cells			
Compartment	Observed gold particles	Expected gold particles	χ^2 values	Observed gold particles	Expected gold particles	χ^2 values	Total observed gold particles
(a)							
Cis	18	29.26	4.33	124	112.74	1.12	142
Medial	33	43.89	2.70	180	169.11	0.70	213
Trans	32	19.37	8.24	62	74.63	2.14	94
TGN	19	9.48	9.56	27	36.52	2.48	46
Column totals	102	102	24.83	393	393	6.44	495

Compartment	Observed gold particles, n_o	Observed points, P	Expected gold particles, n_e	Relative labelling index n_o/n_e
(b)				
Cis	106	898	64.04	1.66[a]
Medial	156	1719	122.58	1.27[a]
Trans	41	952	67.89	0.60
TGN	2	708	50.49	0.04
Column totals	305	4277	305	

Quantification of labelling was done on 68 Golgi stacks for each line. The total chi-squared value (24.83 + 6.44) compared with that of contingency table analysis, with a degree of freedom of 3, confirms specificity of gold particles distribution between wild-type and transformed cells.
[a]Identify Golgi compartments that are preferentially labelled.

Table 2 Quantitative analysis of anti-GFP labelling over Golgi stacks in tobacco BY-2 cells expressing AtMUR3–GFP. (a) Comparison of gold particles distribution in Golgi cisternae of wild type and transformed cells (expressing AtMUR3–GFP) of tobacco BY-2 cultured cells. (b) Observed and expected distribution of gold particles in subtypes of Golgi cisternae of tobacco BY-2 cells expressing AtMUR3–GFP and relative labelling index values

	Wild type cells			Transformed cells			
Compartment	Observed gold particles	Expected gold particles	χ^2 values	Observed gold particles	Expected gold particles	χ^2 values	Total observed gold particles
(a)							
Cis	15	13.49	0.17	48	49.51	0.05	63
Medial	26	34.89	2.27	137	128.11	0.62	163
Trans	5	10.49	2.87	44	38.51	0.78	49
TGN	24	11.13	14.9	28	40.87	4.05	52
Column totals	70	70	20.19	257	257	5.50	327

Compartment	Observed gold particles, n_o	Observed points, P	Expected gold particles, n_e	Relative labelling index n_o/n_e
(b)				
Cis	33	595	35.62	0.93
Medial	116	1159	69.38	1.67[a]
Trans	27	613	36.69	0.74
TGN	4	640	38.31	0.10
Column totals	180	3007	180	

Quantification of labelling was done on 57 Golgi stacks for each line. The total chi-squared value (20.19 + 5.50) compared with that of contingency table analysis, with a degree of freedom of 3, confirms specificity of gold particles distribution between wild-type and transformed cells.
[a]Identify Golgi compartments that are preferentially labeled.

functional within these compartments. Thus, our results are in favor of the model described by Brummell *et al.* (1990), which involves all Golgi cisternae in XyG biosynthesis. Our data, however, do not necessarily contradict the model proposed by Zhang and Staehelin (1992) because the absence of XyG backbone labelling in *cis* and medial

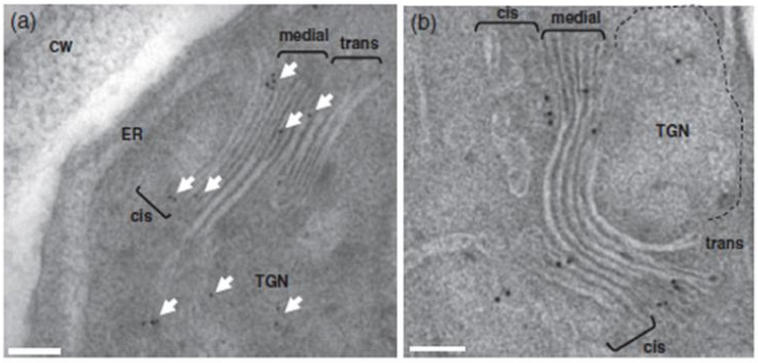

Figure 6. Immunogold localization of the AtMUR3–GFP fusion protein in Golgi stacks of transformed tobacco BY-2 suspension-cultured cells with anti-GFP antibodies.
(a, b) Two electron micrographs illustrating immunogold localization of AtMUR3–GFP fusion protein within Golgi stacks (see also Table 2 for quantification of labelling).CW, Cell wall; ER, endoplasmic reticulum; TGN, *trans*-Golgi network. Scale bars 100 nm.

cisternae observed in that study could only be due to inaccessibility (or masking) of sugar epitopes recognized by anti-XG antibodies. The possible explanation is that, in sycamore cells, the backbone of XyG could be initiated in *cis* and medial cisternae by the action of the corresponding enzymes but that the sugar epitopes (products of the enzymes) would not be detectable until they reach the *trans* cisternae and the TGN.

Early studies on the biosynthesis of XyG *in vitro* have clearly shown that the incorporation of glucose and xylose into this polymer occurs by cooperative addition (Ray, 1980; Hayashi and Matsuda, 1981). Thus, it is possible that the AtXT1 and the glucan synthase, responsible for the biosynthesis of the backbone, enzymes co-exist as a multi-protein complex to efficiently initiate the synthesis of XyG within Golgi stacks of tobacco cells. Although localization of the glucan synthase responsible for the generation of the backbone remains to be established, it is likely that this enzyme co-localizes with the xylosyltransferase (XT1) in the same Golgi cisternae (i.e. *cis* and medial compartments). Such a hypothesis will await further studies on Golgi localization of the XyG-glucan synthase.

Also, unlike the addition of glucose and xylose, it has been shown that the incorporation of galactose is independent of that of fucose and that the galactosylation precedes fucosylation of XyG (Camirand and MacLachlan, 1986; Farkas and MacLachlan, 1988). Therefore, fucosylation may begin at least in the compartment where galactosylation occurs (AtMUR3 is mostly found over medial cisternae in this study) but might also start only in later compartments, *trans* cisternae and the TGN, as suggested previously in both studies of Zhang and Staehelin (1992) and Brummell *et al.* (1990). The preferential localization of AtFUT1 to *trans* cisternae (Table S1) in our tobacco system is consistent with this hypothesis. Nevertheless, fucosylated XyG does not occur in wild-type tobacco BY-2 cells.

To summarize, the present study is an examination of immunogold electron microscopy-based distribution of XyG-synthesizing enzymes within Golgi stacks of higher plants. Our findings do show that the enzymes involved in the biosynthesis of XyG side chains are distributed all over Golgi stacks with some maxima occurring in given Golgi compartments. Thus, the majority of xylosylation, galactosylation and fucosylation of XyG is likely to occur sequentially in *cis*, medial and *trans* compartments of Golgi stacks in plants.

MATERIALS AND METHODS

Plant material and growth conditions

Suspension cells of *Nicotiana tabacum cv. Bright Yellow 2* (BY-2) were cultured in the Murashige and Skoog liquid medium (Sigma M5524, http://www.sigmaaldrich.com): 4.3 g L^{-1} in sucrose 30 g L^{-1}, KH_2PO_4 100 mg L^{-1}, myo-inositol 51 mg L^{-1}, thiamine 1 mg L^{-1}, 2.4 dichlorophenoxyacetic acid 0.22 mg L^{-1}, pH 5.6, in dark, at 22°C, 140 rpm. Cells were subcultured every week by transferring 10 ml of suspension cells in 150 ml of fresh medium.

Nicotiana tabacum plants were grown in soil in a growth chamber under a 16 h photoperiod condition, 22–24°C and 60% relative humidity. Seven- to 8-week-old plants were used for the subcellular localization studies.

Cell wall extraction and purification

BY-2 suspension cells (15 g fresh weight) were filtered and crushed in liquid nitrogen, then heated at 70°C for 30 min in 25 ml of 96% ethanol, before being centrifuged at 5500 ***g*** for 15 min. The pellet was solubilized in 25 ml 96% ethanol and homogenized in a potter (Tenbroeck), before heating again at 70°C for 15 min and centrifugation at 5000 rpm for 10 min. The pellet, called cell wall residue (CWR), was freeze-dried. To remove lipids, the CWR was mixed with chloroform/methanol (1:1 v/v) for 24 h, filtered, washed with acetone and dried at 45°C (see Nguema-Ona *et al.*, 2006).

Xyloglucan extraction

The alkali-soluble hemicellulosic fraction was extracted from the CWR as previously described by Nguema-Ona *et al.*, 2006. Briefly, CWR was treated sequentially with 0.1% CDTA (*trans*-1.2-diaminocyclohexane-N,N,N′,N′-tetraacetic acid) and 4 M KOH containing 1% (w/v) $NaBH_4$. The 4 M KOH hemicellulosic extract was neutralized with 10% (v/v) of acetic acid, dialyzed and finally freeze-dried.

MALDI-TOF mass spectrometry (MS) analysis

XyG fragments were generated by treating 2 mg of cell wall extract with 5 units of endo (1 → 4)-β-D-glucanase (EC 3.2.1.4, Megazyme International, http://www.megazyme.com) in 500 µl of 10 mM

No claim to original US government works

ammonium acetate buffer, pH 5, overnight at 37°C. Glucanase-resistant material was removed by centrifugation after addition of EtOH to reach a final concentration of 80%. The EtOH soluble XyG oligosaccharides were evaporated and concentrated under a stream of air. MALDI-TOF MS of the XyG oligosaccharides generated by endoglucanase was recorded on a Voyager DE-Pro MALDI-TOF mass spectrometer (Applied Biosystems, http://www.appliedbiosystems.com) equipped with a nitrogen laser operating at 337 nm. Mass spectra were performed in the reflector delayed extraction mode using 2,5-dihydroxybenzoic acid (Sigma-Aldrich, http://www.sigmaaldrich.com) as matrix. The matrix, freshly dissolved at 5 mg ml^{-1} in a 70:30 acetonitrile/0.1% TFA, was mixed with the water solubilized oligosaccharides in a ratio 1:1 (v/v). These spectra were recorded in a positive mode, using an acceleration voltage of 20 000 V with a delay time of 100 ns and above 50% of the laser energy. One thousand shots were accumulated for one spectrum and the data presented here are the sum of 5 acquired spectrum. The spectra were externally calibrated using commercially available peptides mixture from Applied Biosystems (Sequazyme™ Peptide Mass Standard kit).

Cloning procedure

The coding sequence of AtXT1, AtMUR3 and AtFUT1, were amplified by PCR without the stop codon using respectively. Forward *Bam*H1 (5′-CGCGGATCCCGATGATAGAGAAGTGTATAGGA-3′) and Reverse *Nhe*1 (5′-CTAGCTAGCCGTCGTCGTCGTACTAAGCTT-3′) primers for AtXT1; Forward *Kpn*1 (5′- GGGGTACCCCATGTTTC-CAAGGGTTTCT-3′) and Reverse *Nhe*1 (5′- CTAGCTAGCCTGT GTCTTATCTCTCTG-3′) primers for MUR3; Forward *Bam*H1 (5′-CGCGGATCCCGATGGATCAGAATTCGTACAGG-3′) and Reverse *Spe*1 (5′-GGACTAGTTACTAGCTTAAGTCCCCAGCT-3′) primers for AtFUT1. The SALK cDNA clones were used as template (respectively U14458, S81470 and U24263).

Then, the amplified cDNA were introduced into the pBLTI221 (Pagny *et al.*, 2000) binary vector containing the sGFP, allowing a fusion of the protein to the Nter part of the sGFP, and each resulting construct was verified by sequencing. Finally, each cassette containing the chimeric protein was introduced into pBLTI121 binary vector to allow plant transformation.

Stable and transient expression in *Nicotiana tabacum*

The generated plasmids were transferred into *Agrobacterium tumefaciens* (strain GV3101 pMP90) by heat shock, and transformed agrobacterium were selected on YEB medium (beef extract 5 g L^{-1}, yeast extract 1 g L^{-1}, sucrose 5 g L^{-1}, $MgSO_4.7H_2O$ 0.5 g L^{-1}) containing kanamycin (100 mg L^{-1}).Transformation of *N. tabacum* (cv BY-2) cells was performed as described by Gomord *et al.* (1998). Transformed cells were selected on the Murashige and Skoog medium (see above) containing kanamycin (100 mg L^{-1}) and cefotaxime (250 mg L^{-1}) and only micro-calli expressing GFP, screened for their fluorescence by confocal microscopy, were used to initiate suspension cultures.

Transformation of leaves of *N. tabacum* was obtained as follows: the agrobacteria were cultured for 20 h at 28°C in YEB media and then centrifuged at 3700 ***g*** to concentrate them. The excess medium was eliminated and the initial density of OD_{600} was measured. Then, each construct was resuspended in an infiltration medium (MES 10 mM, $MgCl_2$ 10 mM, Acetosyringone 100 μM) to obtain a final density of OD_{600} = 0.1 for Sialyltransferase::YFP (ST-YFP represents the first 52 amino acid of a rat α-2,6-sialyltransferase). AtXT1–GFP, AtMUR3–GFP and AtFUT1–GFP fusion proteins were tested with a final density of OD_{600} = 0.1–0.8. Finally, ST-YFP and the AtXT1–GFP, AtMUR3–GFP and AtFUT1–GFP were incubated together for 1 h at room temperature before the co-infiltration in leaves. Microscopic observation of leaf epidermal cells was made 2 days after infiltration.

Localization of fusion proteins in *N. tabacum*

Subcellular localization of fusion proteins were examined using a Leica TCS SP2 AOBS confocal laser scanning microscope. GFP fluorescence of epidermal cells and suspension cultured cells were imaged using an excitation wavelength of 488 nm with the emission wavelength at 500–520 nm. For colocalization of sGFP and YFP-venus in epidermal cells, a 488 and 514 nm argon ion laser were used simultaneously. Fluorescence signals were separated using an acoustic-optical beam splitter; emission signal was 495–510 nm for sGFP and 540–580 nm for YFP-venus. The power of each laser, gain and offset were identical for each experiment to compare images. Appropriate controls were performed to exclude the possibility of crosstalk between the two fluorochromes before image acquisition.

Dot blot

Five microliters containing 10 μg of purified xyloglucan from tamarind seeds, or 5–50 μg of tobacco BY-2 cell wall are deposited on PVDF membrane. The membrane saturation was done overnight in PBS buffer (137 mM NaCl, 2.7 mM KCl, 100 mM Na_2HPO_4, 2 mM KH_2PO_4 pH 7.5) + half milk 5%. The mAbs CCRC-M86 (kindly provided by Dr M. Hahn, Complex Carbohydrate Research Center, University of Georgia, USA) and CCRC-M1 were diluted 1/10 in PBS + 5% dry milk, and the membrane was incubated at room temperature for 2 h. The mAb CCRC-M1 was used as a negative control, as it recognizes fucosylated xyloglucan. After washing in PBS + milk (3 × 10 min), the membrane was incubated 2 h in a secondary antibody 1/500 (Anti mouse polyvalent Ig Alkaline phosphatase conjugate – Sigma). The membrane was washed again 2 × 10 min in PBS + milk and 2 × 10 min in PBS, before signal detection using the 'BCIP/NBT color development substrate' from Promega (http://www.promega.com).

Localization of xyloglucan epitopes in tobacco BY-2 cells

Immunolocalization of XyG epitopes using the mAb CCRC-M86 at the confocal microscopy level was done on protoplasts.

Protoplast preparation. Four-day-old BY-2 cells (400 μl) were plasmolyzed in 800 μl plasmolysis medium (20 mM MES buffer pH 5.6; 0.6 M mannitol; 0.5 mM $CaCl_2$; 0.25 mM $MgCl_2$) for 15–20 min. Then the cell wall was digested overnight at 25°C by incubation in 1 ml enzymatic mixture of 1% cellulase (Sigma) and 1% pectinase (Sigma) diluted in plasmolysis medium containing 0.1% bovine serum albumin (BSA). After three washes with plasmolysis medium, protoplasts were fixed 1 h on the glass slide with 4% paraformaldehyde in PBS (phosphate-buffered saline: 8 g L^{-1} NaCl, 0.29 g L^{-1} KCl, 1.45 g L^{-1} Na_2HPO_4, 0.24 g L^{-1} KH_2PO_4) and washed four times with PBS. Then, protoplasts were sequentially incubated 10 min with 0.5% Triton X100 in PBS, with 1% BSA and 3% half-milk in PBS, and washed three times with 3% BSA in PBS.

Immunostaining and confocal microscopy. Protoplasts were incubated overnight at 4°C, with the primary antibody CCRC-M86 diluted at 1/10 in PBS containing 1% BSA, 3% normal goat serum (NGS). After six washes in PBS containing 1% BSA, protoplasts were incubated 1 h at 25°C with a secondary antibody (goat IgG anti-rat TRITC conjugate from Sigma) diluted at 1/50 in PBS containing 1% BSA, 3% NGS. Finally protoplasts were washed three times in PBS containing 1% BSA. Observation of XyG-epitope staining was done using a Leica TCS SP2 AOBS confocal laser

scanning microscope. TRITC fluorescence was imaged using an excitation wavelength of 543 nm with the emission wavelength at 565–585 nm.

High pressure freezing (HPF) and freeze substitution (FS)

Pre-cooling treatment prior to HPF. Before use, 3-day-old tobacco (BY-2) suspension cultured cells were checked for their GFP expression based on fluorescence observation by confocal microscopy. GFP expressing cells were then concentrated on 50 μm nylon membrane and incubated successively in 5% and 10% glycerol for 1 h at +4°C. Cells were subsequently transferred to 20% glycerol and immediately frozen.

High-pressure freezing. High-pressure freezing was performed with the freezer HPF–EM PACT I Leica-microsystems (Studer *et al.*, 2001). Tobacco BY-2 cells pre-treated were concentrated on 50 μm nylon membrane and transferred into the cavity of a copper ring used for cryofracture which is 100 μm in depth and 1.2 mm in diameter. Excess medium was lightly absorbed by filter paper. Using a horizontal loading station, the specimen carriers were tightened securely to the pod of specimen holder. After fixation on the loading device, specimens were frozen according to a maximum cooling rate of 10 000°C sec^{-1}, incoming pressure of 7.5 bars and working pressure of 4.8 bars. Rings containing frozen samples were stored in liquid nitrogen until the freeze substitution procedure was initiated.

Freeze substitution. After high-pressure freezing, samples were transferred to a freeze substitution automate (AFS, Leica, http://www.leica-microsystems.com) pre-cooled to −140°C. Freeze substitution conditions followed a modified procedure of Studer *et al.* (2001). Samples were substituted in anhydrous acetone +0.5% uranyl acetate at −90°C for 72 h. The temperature was gradually raised (2°C h^{-1}) to −60°C and stabilized during 12 h, then gradually raised (2°C h^{-1}) to −30°C (12 h) and gradually raised again (2°C h^{-1}) to −15°C for 2 h and finally rinsed twice with anhydrous ethanol. Infiltration was processed at −15°C in a solution containing ethanol:London Resin White (LRW) (ratio 2:1; 1:1; 1:2, 8 h each step) and with pure resin for 2 × 24 h. Polymerisation was performed into the AFS apparatus at −15°C under ultra violet light for 48 h.

Immunogold labelling of xyloglucan epitopes

Ultrathin sections (50–70 nm; ultracut UCT, Leica) of tobacco cells were collected on to carbon-formvar-coated nickel grids and blocked in TBS (Tris-buffered saline: Tris–HCl 20 mM pH 7.2, 200 mM NaCl) supplemented with 0.2% of BSA and milk 3% for 30 min. Sections were then incubated with the monoclonal antibody CCRC-M86 at a 1/5 dilution in TBS + BSA and normal goat serum (NGS) for 3 h at room temperature. After washing in TBS + BSA 0.2% buffer, grids were incubated for 1 h at room temperature in the rat secondary antibody conjugated to 10-nm gold particles (Tebu-British Biocell International, http://www.tebu-bio.com). After washing and fixation in TBS + 2% glutaraldehyde, sections were first stained with 4% vapour osmium for 3 h followed by classical staining using uranyl acetate and lead citrate. Sections were observed in a Philips, FEI Tecnai 12 Biotwin transmission electron microscope operating at 80 kV, with ES500W Erlangshen CCD camera (Gatan).

Immunogold labelling of GFP-tagged proteins

Ultrathin sections (50–70 nm; ultracut UCT, Leica, Vienna, Austria) of frozen cells expressing AtXT1–GFP, AtMUR3–GFP or AtFUT1–GFP fusion proteins were collected on to carbon-formvar-coated nickel grids and blocked in TBS (Tris–HCl 20 mM pH 7.2, 200 mM NaCl) supplemented with 0.2% of BSA and Tween 20 0.05% for 15 min. Sections were then incubated with the polyclonal anti-GFP antibody (BD living colors A.v peptide antibody – Clontech) at a 1/5 dilution in TBS + BSA and normal goat serum (NGS; British Biocell International) for 2 h at room temperature. After washing in TBS + BSA 0.2% buffer, grids were incubated for 1 h at room temperature in the rabbit secondary antibody conjugated to 10 nm gold particles (Tebu-British Biocell International). After washing and fixation in TBS + 2% GA, sections were stained as described above.

Quantifying immunogold labelling and statistic analysis

Quantification, specificity and statistical analysis of Golgi labelling were assessed using the method of Mayhew *et al.* (2002).

Labelling specificity of signal in transformed BY-2 cells. To evaluate the distribution of gold particles in Golgi stacks of transformed cells as compared with wild type cells, we used a chi-squared test (Mayhew *et al.*, 2002). We considered the null hypothesis as 'no difference of gold distribution between wild type and transformed cells'.

We analyzed gold labelling in different compartments of Golgi stacks: *cis*, medial, *trans* and the TGN. To compare distribution of gold particles between the two tobacco lines in these compartments, we created a contingency table (two columns × four rows) as described in Mayhew *et al.* (2002). In this analysis, the expected gold count at two line cells for each selected Golgi compartment are calculated from the product of column (total gold particles observed in all Golgi stacks for wild type or transformed tobacco line) and row totals (total gold particles observed in all BY-2 lines for the selected compartment) divided by the grand total (total gold particles observed in four Golgi compartments, in wild type and transformed BY-2 cells). The corresponding partial chi-squared value is calculated as the square of the difference between observed and expected gold particle numbers divided by the expected gold number. The total chi-squared value was compared with chi-squared value in contingency table analysis, with a degree of freedom equal to 3 (see Mayhew *et al.*, 2002).

Determination of fusion protein distribution in Golgi stacks

Quantification of labelling was done according to Mayhew *et al.* (2002), on a total of 50 Golgi stacks with distinguishable subtypes of cisternae. First, gold particles were counted in each Golgi compartment (*cis*, medial, *trans* and the TGN) and represented the 'observed golds particles' (n_0). Second, a lattice of test points was superimposed on each Golgi stacks (so as to be random in position); hit points were counted ('Observed points', P) in each compartment of Golgi stacks. Then, the 'expected golds particles' (n_e) (i.e. random distribution) is calculated as followed: $n_e = (P \times n_{0\ total})/P_{total}$. Observed and expected gold particles distributions allowed calculation of the relative labelling index: RLI (n_0/n_e) for each compartment. For a random distribution, the relative labelling index (RLI) is inferior or equal to 1, and for a compartment preferentially labelled RLI is superior to 1.

ACKNOWLEDGEMENTS

We would like to thank Yumiko Sakuragi (Department of Plant Biology and Biotechnology/Laboratory for Molecular Plant Biology, Copenhagen, Denmark) for providing us with the Golgi marker sialyltransferase fused to YFP (ST–YFP) and Pr. M. Hahn for providing CCRC-M86 antibody. Dr V. Gomord and S. Pagny (University

of Rouen) are acknowledged for helpful advices during early days of this work. Dr L. Galas and Dr J. Moore are also acknowledged for their help with confocal imaging and for critical reading of the manuscript. This work was supported by the University of Rouen, the CNRS and le GRR VATA 'Vegétal, Agronomie et transformation des Agroressources' de la Région de Haute Normandie.

SUPPORTING INFORMATION

Additional Supporting Information may be found in the online version of this article:

Figure S1. Immunodot blot analysis of the binding of the mAb CCRC-M86 to xyloglucan.

Table S1. Quantitative analysis of anti-GFP labelling over Golgi stacks in tobacco BY-2 cells expressing AtFUT1–GFP.

Please note: As a service to our authors and readers, this journal provides supporting information supplied by the authors. Such materials are peer-reviewed and may be re-organized for online delivery, but are not copy-edited or typeset. Technical support issues arising from supporting information (other than missing files) should be addressed to the authors.

REFERENCES

Ali, M.S., Mitsui, T. and Akazawa, T. (1986) Golgi-specific localization of transglycosylases engaged in glycoprotein biosynthesis in suspension-cultured cells of sycamore (*Acer pseudoplatanus* L.). *Arch. Biochem. Biophys.* **251**, 421–431.

Andreeva, A.V., Kutuzov, M.A., Evans, D.E. and Hawes, C.R. (1998) The structure and function of the Golgi apparatus: a hundred years of questions. *J. Exp. Bot.* **49**, 1281–1291.

Brummell, D.A., Camirand, A. and Maclachlan, G.A. (1990) Differential distribution of xyloglucan glycosyltransferase in pea Golgi dictyosomes and secretory vesicles. *J. Cell Sci.* **96**, 705–710.

Camirand, A. and MacLachlan, G. (1986) Biosynthesis of the fucose-containing xyloglucan nonasaccharide by pea microsomal membranes. *Plant Physiol.* **82**, 379–383.

Camirand, A., Brummell, D. and Maclachlan, G. (1987) Fucosylation of xyloglucan: localization of the transferase in dictyosomes of pea stem cells. *Plant Physiol.* **84**, 753–756.

Cavalier, D.M. and Keegstra, K. (2006) Two xyloglucan xylosyltransferase catalyze the addition of multiple xylosyl residues to a cellohexaose. *J. Biol. Chem.* **281**, 34197–34207.

Cocuron, J.C., Lerouxel, O., Drakakaki, G., Alonso, A.P., Liepman, A.H., Keegstra, K., Raikhel, N. and Wilkerson, C.G. (2007) A gene from the cellulose synthase-like C family encodes a beta-1,4 glucan synthase. *Proc. Natl Acad. Sci. USA*, **104**, 8550–8555.

Cosgrove, D.J. (2005) Growth of the plant cell wall. *Nat. Rev. Mol. Cell Biol.* **6**, 850–861.

Driouich, A., Zhang, G.F. and Staehelin, L.A. (1993) Effect of brefeldin A on the structure of the Golgi apparatus and on the synthesis and secretion of proteins and polysaccharides in sycamore maple suspension-cultured cells. *Plant Physiol.* **101**, 1363–1373.

Edwards, M.E., Dickson, C.A., Chengappa, S., Sidebottom, C., Gidley, M.J. and Reid, G.J.S. (1999) Molecular characterization of a membrane-bound galactosyltransferase of plant cell wall matrix polysaccharide biosynthesis. *Plant J.* **19**, 691–697.

Faik, A., Price, N.J., Raikhel, N.V. and Keegstra, K. (2002) An Arabidopsis gene encoding an α-xylosyltransferase involved in xyloglucan biosynthesis. *Proc. Natl Acad. Sci. USA*, **99**, 7797–7802.

Farkas, V. and MacLachlan, G. (1988) Fucosylation of exogenous xyloglucans by pea microsomal membranes. *Arch. Biochem. Biophys.* **264**, 48–53.

Follet-Gueye, M.L., Pagny, S., Faye, L., Gomord, V. and Driouich, A. (2003) An improved chemical fixation method suitable for immunogold localization of green fluorescent protein in the Golgi apparatus of tobacco bright yellow (BY-2) cells. *J. Histochem. Cytochem.* **51**, 931–940.

Fry, S.C., York, W.S., Albersheim, P. *et al.* (1993) An unambiguous nomenclature for xyloglucan-derived oligosaccharides. *Physiol. Plant.* **89**, 1–3.

Gomord, V., Fitchette-Laine, A.C., Denmat, L.A., Michaud, D. and Faye, L. (1998) Production of foreign proteins in tobacco cell suspension culture. In *Methods in Biotechnology*, **vol. 3** (Cunningham, C. and Porter, A.J.R., eds). Totowa NJ: Humana Press, pp. 155–164.

Hayashi, T. and Matsuda, K. (1981) Biosynthesis of xyloglucan in suspensions-cultured soybean cells: occurrence and some properties of xyloglucan 4-β-D glucosyltransferase and 6-alpha-D-xylosyltransferase. *J. Biol. Chem.* **256**, 1117–1122.

Hayashi, T., Kato, Y. and Matsuda, K. (1981) Biosynthesis of xyloglucan in suspensions-cultured soybean cells. An assay method for xyloglucan xylosyltransferase and attempted synthesis of xyloglucan from UDP-d-xylose. *J. Biochem.* **89**, 325–328.

Hayashi, T., Koyama, T. and Matsuda, K. (1988) Formation of UDP-Xylose and xyloglucan in soybean Golgi membranes. *Plant Physiol.* **87**, 341–345.

Hoffman, M., Jia, Z., Pena, M.J., Cash, M., Harper, A., Blackburn, A.R. II, Darvill, A. and York, W.S. (2005) Structural analysis of xyloglucans in primary cell walls of plants in the subclass Asteridae. *Carbohydr. Res.* **340**, 1826–1840.

Lerouxel, O., Choo, T.S., Séveno, M., Usabel, B., Faye, L., Lerouge, P. and Pauly, M. (2002) Rapid structural phenotyping of plant cell wall mutants by enzymatic oligosaccharide fingerprinting. *Plant Physiol.* **130**, 1754–1763.

Lerouxel, O., Cavalier, D.M., Liepman, A.H. and Keegstra, K. (2006) Biosynthesis of plant cell wall polysaccharides: a complex process. *Curr. Opin. Plant Biol.* **9**, 621–630.

Lynch, M.A. and Staehelin, L.A. (1992) Domain-specific and cell type specific localization of two types of cell wall matrix polysaccharides in the clover root tip. *J. Cell Biol.* **118**, 467–479.

Madson, M., Dunand, C., Li, X., Verma, R., Vanzin, G.F., Caplan, J., Shoue, D.A., Carpita, N.C. and Reiter, W.D. (2003) The *MUR3* gene of Arabidopsis encode a xyloglucan galactosyltransferase that is evolutionarily related to animal exostosins. *Plant Cell*, **15**, 1662–1670.

Mayhew, T.M., Lucocq, J.M. and Griffiths, G. (2002) Relative labelling index: a novel stereological approach to test for non-random immunogold labelling of organelles and membranes on transmission electron microscopy thin sections. *J. Microsc.* **205**, 153–164.

Moore, P.J. and Staehelin, L.A. (1988) Immunogold localization of the cell wall matrix polysaccharides rhamnogalacturonan I and xyloglucan during cell wall expansion and cytokinesis in *Trifolium pratense* L.: implications for secretory pathways. *Planta*, **174**, 433–445.

Moore, P.J., Darvill, A.G., Albersheim, P. and Staehelin, L.A. (1986) Immunogold localization of xyloglucan and rhamnogalacturonan I in the cell walls of suspension-cultured sycamore cells. *Plant Physiol.* **82**, 787–794.

Nebenführ, A., Gallagher, L., Dunahay, T.G., Frohlick, J.A., Mazurkiewicz, A.M., Meehl, J.B. and Staehelin, L.A. (1999) Stop-and-go movements of plant Golgi stacks are mediated by the acto-myosin system. *Plant Physiol.* **121**, 1127–1141.

Nguema-Ona, E., Andeme-Onzighi, C., Aboughe-Angone, S., Bardor, M., Ishii, T., Lerouge, P. and Driouich, A. (2006) The *reb1-1* mutation of Arabidopsis: effect on the structure and the localization of galactose containing cell wall polysaccharides. *Plant Physiol.* **140**, 1406–1417.

Pagny, S., Cabanes-Macheteau, M., Gillikin, J.W., Leborgne-Castel, N., Lerouge, P., Boston, R.S., Faye, L. and Gomord, V. (2000) Protein recycling from the Golgi apparatus to the endoplasmic reticulum in plants and its minor contribution to calreticulin retention. *Plant Cell*, **12**, 739–756.

Pagny, S., Bouissonieé, F., Sarkar, M., Follet-Gueye, M.L., Driouich, A., Schachter, H., Faye, L. and Gomord, V. (2003) Structural requirements for Arabidopsis β1-2 xylosyltransferase activity and targeting to the Golgi. *Plant J.* **33**, 189–203.

Palmer, E. and Freeman, T. (2004) Investigation into the use of C- and N-terminal GFP fusion proteins for subcellular localization studies using reverse transfection microarrays. *Comp. Funct. Genomics*, **5**, 342–353.

Pattathil, S., Avci, U., Baldwin, D. *et al.* (2010) A comprehensive toolkit of plant cell wall glycan-directed monoclonal antibodies. *Plant Physiol.* **153**, 514–525.

Perrin, R.M., DeRocher, A.E., Bar-Peled, M., Zeng, W., Norambuena, L., Orellana, A., Raikhel, N.V. and Keegstra, K. (1999) Xyloglucan fucosyltransferase, an enzyme involved in plant cell wall biosynthesis. *Science*, **284**, 1976–1979.

Ray, P.M. (1980) Cooperative action of beta-glucan synthetase and UDP-xylose xylosyl transferase of Golgi membranes in the synthesis of xyloglucan-like polysaccharide. *Biochim. Biophys. Acta* **629**, 431–444.

Ray, B., Loutelier-Bourhis, C., Lange, C., Condamine, E., Driouich, A. and Lerouge, P. (2004) Structural investigation of hemicellulosic

polysaccharides from *Argania spinosa*: characterisation of a novel xyloglucan motif. *Carbohydr. Res.* **339**, 201–208.

Saint-Jore-Dupas, C., Nebenführ, A., Boulaflous, A., Follet-Gueye, M.L., Plasson, C., Hawes, C., Driouich, A., Faye, L. and Gomord, V. (2006) Plant N-glycan processing enzymes employ different targeting mechanisms for their spatial arrangement along the secretory pathway. *Plant Cell*, **18**, 3182–3200.

Sarria, R., Wagner, T.A., O'Neill, M.A., Faik, A., Wilkerson, C.G., Keegstra, K. and Raikhel, N.V. (2001) Characterization of a family of Arabidopsis genes related to xyloglucan fucosyltransferase. *Plant Physiol.* **127**, 1595–1606.

Seifert, G.J., Barber, C., Wells, B. and Roberts, K. (2004) Growth regulators and the control of nucleotide sugar flux. *Plant Cell*, **16**, 723–730.

Sims, I.M., Munro, S.L.A., Currie, G., Craik, D. and Bacic, A. (1996) Structural characterization of xyloglucan secreted by suspension-cultured cells of *Nicotiana plumbaginifolia*. *Carbohydr. Res.* **293**, 147–172.

Staehelin, L.A. and Driouich, A. (1997) Brefeldin A effects in plants (are different Golgi responses caused by different sites of action?). *Plant Physiol.* **114**, 401–403.

Staehelin, L.A., Giddings, T.H. Jr, Kiss, J.Z. and Sack, F.D. (1990) Macromolecular differentiation of Golgi stacks in root tip of *Arabidopsis* and *Nicotiana* seedlings as visualized in high pressure frozen and freeze-substituted samples. *Protoplasma*, **157**, 75–91.

Studer, D., Graber, W., Al-Amoudi, A. and Eggli, P. (2001) A new approach for cryofixation by high-pressure freezing. *J. Microsc.* **203**, 285–294.

Tamura, K., Shimada, T., Kondo, M., Nishimura, M. and Hara-Nishimura, I. (2005) KATAMARI1/MURUS3 is a novel Golgi membrane protein that is required for endomembrane organization in Arabidopsis. *Plant Cell.* **17**, 1764–1776.

Vanzin, G.F., Madson, M., Carpita, N.C., Keegstra, K. and Reiter, W.D. (2002) The *mur*2 mutant of *Arabidopsis thaliana* lacks fucosylated xyloglucan because of a lesion in fucosyltransferase AtFUT1. *Proc. Natl Acad. Sci. USA*, **99**, 3340–3345.

Winicur, Z.M., Zhang, G.F. and Staehelin, A. (1998) Auxin deprivation induces Golgi differentiation in suspension-cultured tobacco BY-2 cells. *Plant Physiol.* **117**, 501–513.

Zabotina, O.A., van de Ven, W.T., Freshour, G., Drakakaki, G., Cavalier, D., Mouille, G., Hahn, M.G., Keegstra, K. and Raikhel, N.V. (2008) Arabidopsis XXT5 gene encodes a putative alpha-1,6-xylosyltransferase that is involved in xyloglucan biosynthesis. *Plant J.* **56**, 101–115. Erratum in *Plant J.* (2009) **57**, 386.

Zhang, G.F. and Staehelin, L.A. (1992) Functional compartmentation of the Golgi apparatus of plant cells: immunocytochemical analysis of high-pressure frozen- and freeze-substituted sycamore maple suspension culture cells. *Plant Physiol.* **99**, 1070–1083.

The Plant Journal © 2010 Blackwell Publishing Ltd, *The Plant Journal*, (2010), **64**, 977–989
No claim to original US government works

SUPPORTING INFORMATION

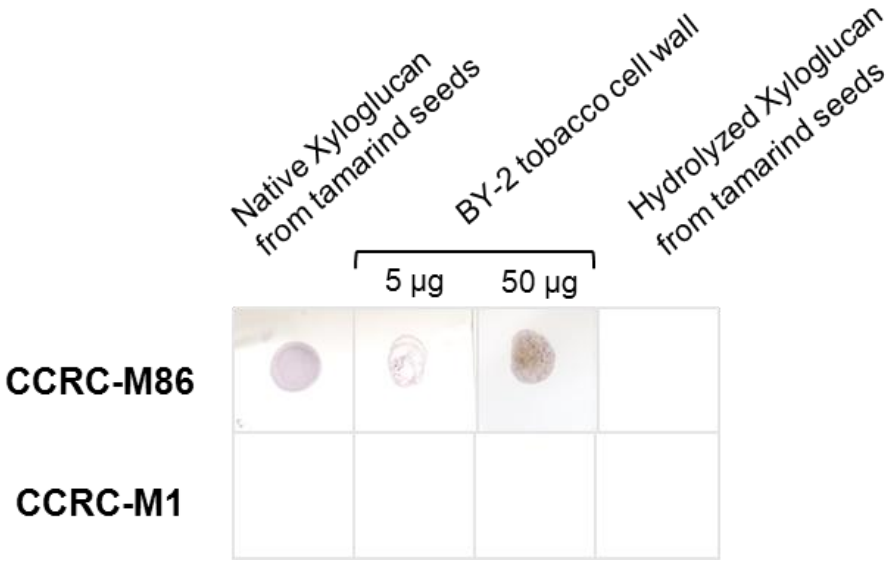

Figure S1. Immunodot blot analysis of the binding of the mAb CCRC-M86 to xyloglucan. CCRC-M86 were tested on purified native XyG from tamarind seeds, on hydrolyzed XyG (after endoglucanase treatment) and on XyG from BY-2 tobacco cell walls. CCRC-M1 was used as negative control as XyG from tamarind and from tobacco are not fucosylated.

SUPPORTING INFORMATION

(a)

Compartment	Wild type cells: Observed gold particles	Wild type cells: Expected gold particles	Wild type cells: $\chi 2$ values	Transformed cells: Observed gold particles	Transformed cells: Expected gold particles	Transformed cells: $\chi 2$ values	Total observed gold particles
Cis	17	18.58	0.13	95	93.42	0.03	112
Medial	31	23.23	2.60	109	116.77	0.52	140
Trans	21	13.27	4.50	59	66.73	0.90	80
TGN	3	16.92	11.45	99	85.08	2.28	102
Column totals	72	72	**18.68**	362	362	**3.73**	434

(b)

Compartment	Observed gold particles, n_o	Observed points, P	Expected gold particles, n_e	Relative Labelling Index n_o/n_e
Cis	77	1102	77.14	1.00
Medial	98	1666	116.63	0.84
Trans	56	498	34.86	**1.61***
TGN	92	1348	94.37	0.97
Column totals	323	4614	323	4.42

Table S1. Quantitative analysis of anti-GFP labelling over Golgi stacks in tobacco BY-2 cells expressing AtFUT1-GFP

(a) Comparison of gold particles distribution in Golgi cisternae of wild type and transformed cells (expressing AtFUT1-GFP) of BY-2 cultured cells. (b) Distribution of gold particles in subtypes of Golgi cisternae of tobacco BY-2 cells expressing AtFUT1-GFP and relative labelling index values.

PARTIE C : SYNTHESE GOLGIENNE DU RHAMNOGALACTURONANE-I

Le rhamnogalacturonane-I (RG-I) représente 20 à 35% des pectines constituant la paroi primaire des plantes eudicotylédones vraies. La composition et la longueur des chaînes latérales du RG-I varient en fonction de l'espèce et du stade de développement, c'est pourquoi nous avons en premier lieu étudié la composition monosaccharidique et les types de liaison présents dans le RG-I de la paroi des cellules de tabac BY-2, grâce à la spectrométrie de masse. Ainsi, nous avons observé que la chaîne principale de ce RG-I était substituée à 50% par des chaînes arabinanes branchées, des chaînes galactanes et des chaînes arabinogalactanes, confirmant une étude également effectuée sur des cellules de tabac (Eda *et al.*, 1983).

A ce jour, aucune étude n'a abordé la cartographie golgienne d'épitopes glucidiques spécifiques du RG-I. Ainsi, nous avons étudié la distribution au sein des différentes saccules golgiennes des épitopes spécifiques de la chaîne principale et des chaînes latérales, en utilisant des anticorps spécifiques. Après avoir quantifié cette distribution, les résultats statistiques (RLI) montrent que les épitopes de la chaîne principale sont principalement retrouvés dans les saccules médian, les épitopes des chaînes arabinanes sont situés dans les saccules *trans* et le TGN. Enfin, les épitopes des chaînes galactanes et arabinogalactanes sont retrouvés exclusivement dans le TGN.

Puis, nous avons complété cette étude par la cartographie golgienne d'enzymes d'Arabidopsis potentiellement impliquées dans la synthèse des chaînes arabinanes du RG-I : l'arabinan α(1,5)arabinosyltransférase (AtARAD1), l'UDP-xylose 4-épimérase (AtUXE1/MUR4) et son homologue (AtUXE3). Nous avons avons fusionné ces protéines à la GFP et exprimé dans des suspensions cellulaires de tabac. Nous avons utilisé la même méthodologie que pour la cartographie des enzymes de synthèse du XyG. Il est ressorti que les protéines AtARAD1 et AtUXE3 étaient majoritairement associées aux saccules median, tandis que la protéine AtUXE1/MUR4 est retrouvée dans le TGN.

L'arabinosyltransférase (AtARAD1), et la protéine AtUXE3, homologue de l'épimérase AtUXE1, étant situées toute les deux dans les saccules médian, nous avons postulé qu'elles

étaient peut-être associées dans un complexe multiprotéique impliquant également deux UDP-arabinose mutases nommées AtRGP1 et AtRGP2.

En effet, au niveau du cytosol dans l'environnement très proche du Golgi, l'épimérase potentielle AtUXE3 (qui n'a pas de domaine transmembranaire d'après les prédictions *in silico*) pourrait transformer l'UDP-xylose en UDP-arabinopyranose, ce dernier serait pris en charge par les mutases AtRGP1/2 pour devenir de l'UDP-arabinofuranose, traverserait la membrane golgienne *via* un transporteur, puis serait pris en charge par l'arabinosyltransférase AtARAD1 dans la lumière des saccules médian.

Ainsi, en collaboration avec l'équipe du Dr Y. Sakuragi, l'intéraction de chaque partenaire potentiel a été testée en utilisant le système de split ubiquitin : les mutases AtRGP1 et AtRGP2 forment des homo- et hétérodimères entre elles, mais l'arabinosyltransférase AtARAD1 ou l'épimérase potentielle AtUXE3 n'intéragissent avec aucun des partenaires testés.

Ces résultats sont détaillés dans l'article suivant **page 175**:

Bernard S, Have Lund C, Dardelle F, Ramdani Y, Loutelier-Bourhis C, Lerouge P, Sakuragi Y, Driouich A and Follet-Gueye ML. The Golgi compartmentalization of rhamnogalacturonan-I associated epitopes and enzymes potentially involved in arabinan biosynthesis in tobacco BY-2 suspension-cultured cells. *Soumis à Plant Journal*

Papier N°5: Article scientifique

Résultats: Synthèse golgienne du rhamnogalacturonane - I

THE GOLGI COMPARTMENTALIZATION OF RG-I ASSOCIATED EPITOPES AND ENZYMES POTENTIALLY INVOLVED IN ARABINAN BIOSYNTHESIS IN TOBACCO BY-2 SUSPENSION-CULTURED CELLS

Sophie Bernard, Christian Have Lund, Flavien Dardelle, Yasmina Ramdani, Corinne Loutelier-Bourhis, Patrice Lerouge, Yumiko Sakuragi, Azeddine Driouich* and Marie-Laure Follet-Gueye*.
*co-supervision of the work

Soumis à Plant Journal

THE GOLGI COMPARTMENTALIZATION OF RHAMNOGALACTURONAN I ASSOCIATED EPITOPES AND ENZYMES POTENTIALLY INVOLVED IN ARABINAN BIOSYNTHESIS IN TOBACCO BY-2 SUSPENSION-CULTURED CELLS

Sophie Bernard[1], Christian Have Lund[2], Flavien Dardelle[3], Yasmina Ramdani[4], Corinne Loutelier-Bourhis[5], Patrice Lerouge[1], Yumiko Sakuragi[2], Azeddine Driouich*[1] and Marie-Laure Follet-Gueye*[1].

*cosupervision of the study

[1]Glycobiology and Plant Extracellular Matrix laboratory-EA4358, Institute for Cell Imaging Research Platform of Normandy (PRIMACEN), Institut of Research and Innovation in Biomedecine (IRIB), Rouen University, France

[2]University of Copenhagen, Faculty of Science, Department of Plant and Evironmental sciences, Thorvaldsensvej 40, Frederiksberg DK-1871, Denmark

[3]Fitoplancton Marino, S.L., Dársena Comercial S/N, 11500 El Puerto de Santa María (Cádiz), Spain

[4]Laboratoire Inserm-ERI28, NeoVasc, Faculté de Médecine et de Pharmacie, Université de Rouen, 22, Boulevard Gambetta, 76183 Rouen Cedex

[5]Laboratoire CNRS-UMR6614, COBRA, Institut de Recherche en Chimie Organique Fine (IRCOF), Faculté des Sciences, Université de Rouen, Rue Tesnière, 76130 Mont Saint Aignan

RUNNING TITLE

Compartmentalization of RG-I synthesis within the Golgi stack of tobacco BY-2 suspension-cultured cells.

KEY WORDS

Rhamnogalacturonan I, Arabinan, Cell wall, Golgi, Quantitative immunogold, Electron microscopy, High Pressure Freezing

SUMMARY

Pectins are cell wall complex polysaccharides that play a central role in plant development. Rhamnogalacturonan I (RG-I), is a structurally heterogeneous pectic polysaccharide that consists of a rhamnogalacturonan backbone substituted with galactan, arabinan and arabinogalactan side chains. RG–I has been implicated in numerous cell wall properties. Like other complex polysaccharides, RG-I is synthesized within Golgi stacks before its transport to the cell wall. To gain more understanding on the spatial organization of RG-I assembly pathway within Golgi cisternae, we apply here a quantitative immunogold analysis using transmission electron microscopy on high pressure frozen and freeze substituted wild-type tobacco (*Nicotiana tabacum*) BY-2 suspension cultured-cells. We present a detailed Golgi mapping of major sugar epitopes associated with RG-I by using specific monoclonal antibodies. We also establish the Golgi compartmentalization of three enzymes potentially involved in the biosynthesis of RG-I, namely the arabinan α-1,5-arabinosyltransferase, AtARAD1 (arabinan deficient 1), two UDP-xylose 4-epimerases, AtUXE1/MURUS4 and AtUXE3. These enzymes have been fused to green-fluorescent protein (GFP) and stably expressed in tobacco cells. The data demonstrate that sugar motifs associated with RG-I backbone are preferentially present in the medial Golgi cisternae whereas linear unbranched arabinan chains are located to the trans cisternae and the ramified arabinan, galactan or arabinogalactan are mapped to *trans*-Golgi network. Finally, the fused proteins AtARAD1-GFP and AtUXE3-GFP are detected in the medial Golgi cisternae suggesting their possible cooperative action during the biosynthesis of the arabinose-containing cell wall polymers such as RG-I.

INTRODUCTION

Pectins are major polysaccharides of the primary cell wall. They consist of structurally complex and heterogeneous polysaccharides with galacturonic acid (GalUA) residues. The most abundant pectin is homogalacturonan (HG), a linear homopolymer of (1→4)-α-linked GalUA which can be methyl-esterified and/or acetylated (Willats *et al*., 2001; Vincken *et al.*, 2003; Knox, 2008). More complex in structure are the three other major pectic polysaccharides: xylogalacturonan (XGA), rhamnogalacturonan-II (RG-II) and rhamnogalacturonan-I (RG-I).

The RG-I represents 20-35% of pectin and is the most structurally variable pectic compound. It consists of a disaccharide repeat of [-4-α-D-GalUA-(1→2)-α-L-Rha-(1-)]$_n$ backbone. Between 20 and 80% of the backbone rhamnosyl residues are substituted and the side chain composition varies depending on plant species, tissues and developmental stage (Albersheim, 1996; Freshour *et al*., 1996; Willats *et al*., 2001; Guillemin *et al*., 2005; Lee *et al.,* 2013). Oligosaccharide side chains of RG-I consist predominantly of galactan, arabinan and arabinogalactan (AG) (Vincken *et al.*, 2003; Mohnen, 2008; Atmodjo *et al*., 2013). Galactans are mostly linear chains of (1→4)-β-D-galactopyrannose (Gal*p*) residues, whereas arabinans are chains of (1→5)-α-L-arabinofuranose (Ara*f*) that are frequently branched. In certain plant species, galactan and arabinan side chains could be substituted with terminal phenolic esters which can dimerize oxidatively to form links between polymers (Ralet *et al*., 2005). Several AG side chains of RG-I have been identified. Type I AG is composed of a linear (1→4)-β-D-galactan chains branched with single α-L-Ara*f* units at position *O*-3 of the galactosyl units or other sugars such as fucose and glucuronic acid (Ridley *et al.*, 2001; Nakamura *et al*., 2002; Øbro *et al*., 2004). The presence of type II AG in RG-I, that consists of an (1→3)-α-D-galactan backbone substituted by short (1→6)-β-D-galactan chains branched with Ara*f*, rhamnose and glucuronic acid and terminated by α-L-Ara*f*, has also been reported (Mohnen, 2008; Verhoef *et al*., 2009). Other types of arabinogalactan side chains of RG-I have been described consisting of galactosyl residues or short sequence of galactosyl residues between branched arabinan chains and the backbone (Schols *et al.*, 1990; Sakamoto and Sakai, 1995; Huisman *et al*., 2001).

Pectic polysaccharides of the cell wall are assumed to be synthesized in the Golgi apparatus (Zhang and Staehelin, 1992; Mohnen, 2008; Driouich *et al*., 2012) *via* the combined action of Golgi glycosyltransferases (GTs), nucleotide-sugar transporters (NSTs) and nucleotide-sugar interconversion enzymes (NIEs) (Keegstra and Raikhel, 2001; Seifert, 2004; Reiter, 2008; Reyes and Orellana, 2008). As compared to XyG, HG and RG-II biosynthesis, relatively little is known about the GTs involved in RG-I biosynthesis. Caffall and Mohnen (2009) postulated that 34 specific GTs activities may be required. None of the enzymes involved in the RG-I backbone assembly have been identified. The characterization of galactosyltransferase activity necessary for RG-I (1→4)-β-D-galactan chains biosynthesis was carried out in Golgi-membrane fractions from several eudicotyledonous plants (Goubet *et al.*, 1993; Brickell and Reid, 1996; Geshi *et al*., 2000; Kato *et al*., 2003; Konishi *et al*., 2004). Recently, Liwanag *et al.* (2012) demonstrated that the Arabidopsis galactan synthase 1 (AtGALS1) of GT92 family, is a β(1-4) galactan β(1-4) galactosyltransferase. Two putative arabinan arabinosyltransferases, AtARAD1 and AtARAD2, belonging to the GT47 family, have been identified (Harholt *et al.*, 2006; 2012). While pyranose ring is the utmost arabinose configuration found in plants, pectic arabinan incorporates UDP-L-arabinofuranose. An UDP-arabinose mutase (UAM) that converts UDP-arabinopyranose into UDP-arabinofuranose was characterized in rice (Konishi *et al*., 2007) and found to share more than 80% identity with the reversibly glycosylated proteins (RGPs) of Arabidopsis (Dhugga *et al.*, 1991, 1997; Delgado *et al*., 1998; De Pino *et al.*, 2007). The arabinose mutase activity has been recently shown for three (AtRGP1, 2 and 3) of the five isoforms of RGPs identified in the Arabidopsis genome (Rautengarten *et al*., 2011). Moreover, severe developmental phenotypes associated with subsequent reduction in cell wall arabinose content in homozygous T-DNA insertion *rgp1-1* and *rgp1-2* mutants have been observed, suggesting that RGPs could be involved in the biosynthesis of the arabinose-enriched cell wall polymers such as RG-I or AGPs.

RG-I biosynthesis in the Golgi apparatus requires cooperation between glycosyltransferases, nucleotide-sugar interconversion enzymes (NIEs) and potentially nucleotide-sugar transporters (NSTs). Actually, few NST have been functionally characterized (Baldwin *et al*., 2001; Norambuena *et al*., 2005; Handford *et al*., 2012). Five UDP-D-glucose-4-epimerases (UGEs) have been identified in

Arabidopsis thaliana. Whereas AtUGE4 was shown to be involved in AGPs and XyG galactosylation (Seifert *et al*., 2002; Nguema-Ona *et al*., 2006), other UGE isoforms are less selective and could contribute to RG-I galactosylation (Rösti *et al.*, 2007). A Golgi-localized UDP-D-xylose-4-epimerase, AtUXE1/MUR4, has been characterized in Arabidopsis (Burget *et al*., 1999; 2003). The authors have shown that the *mur4* mutant contains 50% of wild-type levels of cell wall arabinose affecting both pectic polysaccharides and AGPs.

To date, the spatial organization of RG-I assembly pathway within the plant Golgi stacks is not fully understood. Immuno-electron microscopical analyses using antibodies directed against specific sugar, Golgi enzyme or Golgi tagged-enzyme epitopes is a reliable method for investigating the compartmentalization of cell wall complex polysaccharide biosynthesis within Golgi cisternae (Zhang and Staehelin, 1992; Vicré *et al*., 1998; Chevalier *et al*., 2010; Follet-Gueye *et al*., 2012; Driouich *et al*., 2012).

To complete the knowledge with respect to RG-I assembly in the Golgi apparatus, we established the first immunogold quantitative analysis of epitopes associated to RG-I backbone, arabinan, galactan and arabinogalactan side chains, in tobacco BY-2 suspension cultured-cells. In addition, we investigated the Golgi compartmentalization of the xylose epimerase AtUXE1/MUR4 and its homolog AtUXE3, and a putative arabinan arabinosyltransferase (AtARAD1) in cells expressing AtARAD1-GFP, AtUXE1-GFP or AtUXE3-GFP. Finally, we tested if AtARAD1 and AtUXE3 were involved in a proteins complex with the mutases AtRGP1 and AtRGP2.

RESULTS

Structural analysis of Rhamnogalacturonan- I isolated from tobacco BY-2 suspension-cultured cells

The monosaccharide composition and sugar linkages of RG-I from tobacco cells were determined on a pectin-enriched fraction isolated from the whole cell wall of BY-2 suspension-cultured cells using hot 0.5% oxalate ammonium. The four main monosaccharides (Table 1a), representing 88% of the total sugar composition, were arabinose (Ara), galacturonic acid (GalUA), rhamnose (Rha) and galactose (Gal) consistent with previous data (Eda *et al.*, 1983).

Rha (18.0%) and GalUA (20.8%) are in a ratio close to 1 and can be attributed to the (4-α-D-GalUA*p*1→2-α-L-Rha*p*1) repeating unit of the backbone of the RG-I. Therefore, this pectic fraction is highly enriched in RG-I. Ara (38.8%) and Gal (11.8%), the main monosaccharides constitutive of the RG-I side chains (Scheller *et al*., 2007; Mohnen, 2008), represent about the half of the total sugars. The pectin-enriched fraction also contains low amount of xylose, suggesting the presence of XyG or XGA probably co-extracted with RG-I or linked to the pectins (Popper and Fry, 2005, Marcus *et al*., 2008). Mannose, glucuronic acid, glucose and galactose could possibly originate from residual arabinoglucuronomannan (Mori and Kato 1981), or galactoglucomannan as it has been described in *Nicotiana tabacum* (Eda *et al.,* 1985) and *Nicotiana plumbaginifolia* (Sims *et al.,* 1997).

The sugar linkage analysis (Table 1b) shows the presence of 2-linked (3.2%) and 2,4-linked (3.6%) rhamnosyl residues in similar ratio indicating that ~50% of the RG-I backbone is substituted on C4 of the rhamnosyl residue. Linkage analysis of arabinosyl residues shows a high percentage of 5-Ara*f* (22.9%) and a lower percentage of 3-Ara*f* (1.9%), indicating most of the Ara*f* residues are found in α(1-5) arabinan chains, and only a small proportion is found in α(1-3) arabinan chains. The presence of 3,5-Ara*f* (15.7 %) suggests that α(1-5) arabinan chains are highly substituted (around 40%). The presence of T-Ara*f* (T, terminal) (14.3%) reinforces this observation and suggests that substitutions are with single Ara*f* residues and with short secondary chains of α(1-5) arabinan and a minor part of α(1-3) arabinan. As for the galactose residues, these are mainly 4-Gal*p* (7.5%) and 3-Gal*p* (3.9%),

reflecting the presence of β(1-4) and β(1-3) galactan chains, and a small proportion found in β(1-6) galactan chain. Given the percentage of 4,6-Gal*p* (1.2%) and 3,6-Gal*p* (0.8%) substitutions, around 14% of β(1-4) galactan chains and 17% of β(1-3) galactan chains are substituted at position *O*-6 of galactosyl unit. Other substitution types were not detected. The presence of contaminating xyloglucan in the BY-2 pectin-enriched fraction was confirmed by the identification of T-Xyl*p*, 2-Xyl*p* and 4,6-Glc*p* in the sugar linkage analysis. The xyloglucan contamination in the pectin fraction most likely co-purified because of covalent linkages between xyloglucan and RG-I which have been reported to occur in Arabidopsis, sycamore, rose, tomato, spinach, maize and barley in addition to tobacco (Popper and Fry 2005).

Taken together, these analyses indicate that the pectic fraction isolated from the cell wall of tobacco BY-2 suspension-cultured cells using hot 0.5% oxalate ammonium is highly enriched in RG-I. Its backbone consists of (4-α-D-GalUA*p*1 → 2-α-L-Rha*p*1) repeating unit which is 50% substituted with branched arabinan, galactan, and arabinogalactan chains as possible side chains. These findings are in agreement and confirm previous studies on RG-I structure of BY-2 suspension-cultured cells by (Eda *et al.*, 1983).

Subcellular localization of RG-I epitopes in tobacco cells

The RG-I epitopes recognized by the set of antibodies we used are summarized in Table 2. To investigate the subcellular localization of these different epitopes within tobacco BY-2 suspension-cultured cells, we prepared protoplasts that were immunolabelled using a secondary antibody coupled to FITC. Figure 1 shows a punctate pattern of fluorescence with INRA-RU1 (Fig.1A), INRA-RU2 (Fig.1B), LM5 (Fig.1C), LM6 (Fig.1D), LM13 (Fig.1E) and LM16 (Fig.1F) antibodies typical of that Golgi stack labelling in plant cells (Nebenführ *et al*., 1999, Pagny *et al*., 2003; Chevalier et al., 2010).

Immunogold localization of RG-I epitopes in Golgi cisternae

We investigated the distribution of different pectic epitopes within Golgi cisternae using immunogold-electron microscopy on wild-type BY-2 suspension-cultured cells prepared by high pressure freezing (HPF), followed by freeze substitution (FS) technique. Figures 2A and 2B show immunogold-labelled Golgi stacks of wild-type tobacco BY-2 suspension-cultured cells. It is to note that the ultrastructural

organization of the Golgi stacks is well-preserved allowing distinction of different Golgi subcompartments as described previously in Chevalier *et al.,* 2010 (Figure 2B). Different labelling densities in Golgi stacks depending on the tested antibody were observed. LM6 and LM16 antibodies showed the strongest labelling density (Figures 2A and 2B), whereas INRA-RU1, LM5 and LM13 antibodies had a lower labelling density (Figures S1A, S1B and S1C respectively). Also, for LM13 epitopes, labelling of the cell wall was weaker than those observed with other sugar epitopes analyzed (data not shown). For INRA-RU2 antibody, we could not detect gold particles in Golgi stacks or in the cell wall, although fluorescence signals could be observed in Golgi stacks in protoplast (Figure 1B) and in cell walls of intact cells (Figure S2).

To start the statistical evaluation of the immunogold localization, we first checked the labelling specificity of different antibodies by using the immunolabelling condition without the primary antibody as control to do a chi-square test (χ^2). Our null hypothesis was: “there is a random distribution of gold particles with immunolabelling with primary antibody and immunolabelling without primary antibody”. For each antibody, we counted gold particles in the 3 compartments (*cis*, medial, *trans*) and the *trans*-Golgi Network (TGN) of 35 to 55 Golgi stacks. For LM6, LM16 and LM5 antibodies, the total chi-squared values were 30.91, 17.36, and 11.32, respectively (Table 3a for LM6, Table S2a and S3a, for LM5 and LM16). Those values were compared to reference values in a contingency table, with a degree of freedom = 3 (see M&M), and showed that we rejected the null hypothesis with a risk $\alpha < 0.005$ for LM6 and LM16, and $\alpha < 0.015$ for LM5. For LM13 antibody, the total chi-squared was 4.35 (see Table S4a). In this case, we rejected the null hypothesis with a risk $\alpha \leq 0.1$. A chi-square test was not necessary for INRA-RU1 as we have no gold particle on more than 55 Golgi stacks on the control without the primary antibody.

Secondly, we investigated Golgi distribution of the pectic epitopes recognized by these antibodies in the 3 compartments (*cis*, medial, *trans*) and the TGN using the relative labelling index (RLI) as described in Chevalier *et al*., (2010) and updated by Mayhew, (2011). According to Mayhew and Lucocq, (2008), RLI indicates the degree to which a compartment is preferentially labelled in comparison to the theoretical situation of random labelling considering the surface of each compartment. If RLI of the compartment is ≤ 1, it means that it is randomly labelled. But if the compartment

has RLI > 1 and its partial χ2 > 10%, then it is preferentially labelled. Immunogold labelling of Golgi stacks of epitopes recognized by LM6 is illustrated in Figure 2A and Table 3b. Gold particles were found to be localized mainly over the TGN, as the RLI = 1.75 and χ^2 = 50.34%. Immunogold localization of epitopes recognized by the other antibodies are shown in supplemental data: for INRA-RU1 antibody, gold particles were mainly localized over medial Golgi cisternae (Figure S1A and Table S1), labelling of epitopes recognized by LM13 (Figure S1C and Table S4b) showed a localization in *trans* cisternae, whereas LM5 and LM16 epitopes (respectively Figures S1B and 2B; and Tables S2b and S3b) showed preferential localization in the TGN.

Subcellular localization of AtARAD1, AtUXE1 and AtUXE3 proteins fused to GFP

In addition to RG-I epitopes distribution within Golgi subcompartments, we first checked subcellular localization of the proteins potentially involved in RG-I synthesis by confocal microscopy. We focused on proteins that are good candidates for RG-I arabinan side chain synthesis: the putative arabinan arabinosyltransferase AtARAD1 (Harholt *et al*., 2006), the proven xylose epimerase AtUXE1/MUR4 (Burget *et al.,* 2003) and one of its homologs AtUXE3. AtARAD1 and AtUXE1 are Golgi type II membrane-bound proteins. AtUXE3 is a homolog of AtUXE1 that seems to have no transmembrane domain or signal peptide according to *in silico* analysis of the coding sequence with Aramemnon (http://aramemnon.uni-koeln.de/) (data not shown).

As illustrated in Figure 3, transformed BY-2 suspension-cultured cells expressing AtARAD1-GFP (Figure 3A) and AtUXE3-GFP (Figure 3B) displayed fluorescent and mobile spots (of 1 µm in size) confirming Golgi localization. Interestingly, AtUXE3-GFP (Figure 3C) showed a similar fluorescence signal again consistent with Golgi localization, and no any additional fluorescence associated with cytosolic localization.

Immunogold localization of AtARAD1, AtUXE1 and AtUXE3 proteins fused to GFP within Golgi cisternae

The labelling specificity of the proteins in transformed BY-2 suspension-cultured cells compared to wild-type was confirmed with a chi-square test (χ^2). Our null hypothesis was that there is no difference of gold distribution between wild-type and transformed

cells. We used the same procedure for immunogold localization of pectic epitopes (see above). For AtARAD1-GFP and AtUXE3-GFP, the total chi-squared values were 86.98 and 31.68 respectively (Table 4a and Table S5a), showing that with 3 degree of freedom the null hypothesis can be rejected with a risk $\alpha < 0.005$. For AtUXE1-GFP, the total chi-squared was 9.24 (Table S6a). In this case, we rejected the null hypothesis with a risk $\alpha < 0.03$.

Then, we investigated the Golgi distribution of these fusion proteins in the 3 sub-compartments (*cis*, medial, *trans*) and the TGN using the relative labelling index (RLI) as described earlier (Chevalier *et al*., 2010). Based on RLI value and partial χ^2 value, we found that AtARAD1-GFP and AtUXE3-GFP are both preferentially localized within medial Golgi cisternae (Table 4b and S5b respectively). Finally, AtUXE1-GFP was found mostly in the TGN (Table S6b).

Arabinan RG-I biosynthesis: a search for Golgi protein complex

As the putative arabinosyltransferase AtARAD1 and AtUXE3, the homolog of the xylose epimerase AtUXE1, seemed to localize to the same Golgi subcompartment, we investigated whether these proteins interact and form a Golgi protein complex. Also, we tested if the arabinose mutases AtRGP1 and AtRGP2 (Rautengarten *et al.*, 2011) could be part of such a putative complex in the Golgi apparatus.

The proteins AtARAD1, AtUXE3, AtRGP1 and AtRGP2 were tested in a binary protein-protein interaction screen using the split ubiquitin yeast system, to clarify if any direct interaction occurs between them. A modified split ubiquitin system commercially available from Dualsystems Biotech AG was used because it allows fusion of the reporters at the N-termini of tested proteins. The proteins are fused to the C-terminal ubiquitin moiety (Cub) fused to a transcription factor and the N-terminal ubiquitin moiety (NubG). The fusion proteins are designated as bait and prey, respectively.

The data are presented Figure 5. Functionality of bait (Cub) tested against the positive control interaction partner Ost1-NubI (Figure 5, lines 1 to 4) showed that all constructs were functional except for AtARAD1-Cub which did not produce any viable cell on the selection media and no blue color formation was observed in Xgal assay

(Figure 5, line 1). Interaction specificity of baits and preys were tested against an empty vector control (pPR3-N) and AtXXT2, an Arabidopsis type-II transmembrane xylosyltranferase involved in xyloglucan biosynthesis, respectively (Figure 5, lines 5 to 12). No random interaction was detected with the empty vector nor with AtXXT2-Cub.

Binary interaction assay was carried out among the four proteins. The binary interaction test with AtRGP1 and AtRGP2 showed positive signals, when reciprocal tagging with Cub or NubG, for the two homodimers, AtRGP1-AtRGP1 (Figure 5, line 18) and AtRGP2-AtRGP2 (Figure 5, line 23), and the heterodimer AtRGP1-AtRGP2 (Figure 5, lines 19 and 22), confirming results of Rautengarten *et al.* (2011). The interaction test with AtUXE3 showed no homodimerization (Figure 5, line 28), nor heterodimerization with AtRGP1 or AtRGP2 (Figure 5, lines 20, 24, 26 and 27). AtARAD1-NubG did not show positive signals with AtRGP1-Cub, AtRGP2-Cub or AtUXE3-Cub (Figure 5, lines 17, 21 and 25), suggesting no direct interaction with these proteins, however we cannot conclude if AtARAD1-NubG is functional.

DISCUSSION

Structural heterogeneity of RG-I in *Nicotiana tabacum* BY-2 suspension-cultured cells

Monosaccharide and linkage analyses combined with immunocytochemical labelling showed that RG-I in tobacco BY-2 suspension-cultured cells is composed of a backbone consisting of (4-α-D-GalUA*p*1→ 2-α-L-Rha*p*1) repeating unit where 50% of the rhamnosyl residues are substituted with arabinan, arabinogalactan and/or galactan side chains. Arabinan side chains are composed of (1→5)-α-L-arabinan chain branched at 40% with arabinose residues and/or short (1→5)-α-L-arabinan and/or short (1→3)-α-L-arabinan at *O*-3, as we detected 5-Ara*f*, 3-Ara*f*, 3,5-Ara*f* and T-Ara*f* in the RG-I-enriched fraction. Branched arabinans are common RG-I side chains already described in plants including apple (Schols *et al.*, 1990), soybean (Huismann *et al*., 2001; Nakamura *et al.*, 2002), sugar beet (Sakamoto and Sakai, 1995) and potato (Øbro *et al.*, 2004). AG side chains are often defined in the literature as (1→4)-β-D-galactan, which may be branched at *O*-3 with α-L-Ara*f* or arabinan, named type I AG; and (1→3)-β-D-galactan branched at *O*-6 with galactan or arabinogalactan, terminated by α-L-Ara*f*, named type II AG. Sometimes, (1→3)-α-L-Ara*f*-moieties, and other sugars such as Glc, Rha, and GlcUA can also be found in AG side chains. Here, we found 14% of (1→4)-β-D-galactan side chain substituted at *O*-6, but we could not detect any substitution at *O*-3. Therefore, it seems that, in tobacco BY-2 suspension-cultured cells, RG-I does not contain type I AG in its side chains. However, an *O*-6 substitution in (1→4)-β-D-galactan side chain by β-D-GlcUA and 4-*O*-methyl-β-D-GlcUA in RG-I of sycamore suspension cells has been described (An *et al.*, 1994). We detected a small amount of GlcUA (0.3%) in the monosaccharide composition, but the linkage analysis did not allow study of uronic acid sugars; therefore it is not possible to ascertain if this chain type exists in RG-I tobacco BY-2 suspension-cultured cells. Linkage analysis reveals also the presence of (1→3)-β-D-galactan, with 17% of *O*-6 substitution, and the presence of (1→6)-β-D-galactan showing type II AG side chains. This structure is typical of AGPs, and there is still no evidence that type II AG are side chains of RG-I or associated with a polymer, and co-extracted in the RG-I enriched fraction (Verhoef *et al*., 2009). The LM16 antibody suggested the presence of another type of AG side chains in RG-I

tobacco BY-2 suspension-cultured cells. This antibody has been obtained using RG-I isolated from apple fruit, which contains arabinogalactan side chains having (1→3)-β-D-galactose residues (that can be branched with galactose residues), between branched (1→5)-α-L-arabinan chain and RG-I backbone (Schols *et al.*, 1990). LM16 activity on sugar beet arabinan, whose AG side chain is composed of (1→4)-β-D-galactose residues, between branched (1→5)-α-L-arabinan chain and RG-I backbone (Sakamoto and Sakai, 1995), has been clearly shown by Verhertbruggen *et al.* (2009). Interestingly, the sugar linkage analysis, showing the presence of 4-Gal*p*, 3-Gal*p*, 3,6-Gal*p* and branched arabinan, coupled to LM16 immunolabelling, reveals that this type of AG side chain exists in the RG-I from BY-2 cells. Other arabinogalactan side chains with galactose residue between branched (1→5)-α-L-arabinan chain and RG-I backbone have been described in soybean (Huisman *et al.*, 2001) and could be present in RG-I from tobacco BY-2 suspension-cultured cells.

The assembly pathway of RG-I within Golgi cisternae

Quantitative immunocytochemical studies of specific RG-I sugar epitopes were applied to enhance understanding of RG-I synthesis and assembly in the Golgi apparatus (Table 5). In 1992, Zhang and Staehelin, by using the antibody anti-PGA/RG-I, which is supposed to recognize the transition region between unesterified homogalacturonan and the first (1→2)-α-rhamnosyl linked residue of RG-I (Moore *et al.*, 1991), detected PGA/RGI epitope in the *cis* and medial Golgi compartments of sycamore maple suspension-cultured cells. These data indicate that HG and RG-I backbone units are already assembled in this early Golgi compartment (see also Driouich *et al.*, 1993). In addition, it has been shown that HG and RG-I are covalently attached (Coenen *et al.*, 2007). As the INRA-RU1 sugar epitope, comprising at least six disaccharides repeats (4-α-D-GalUA*p*1 → 2-α-L-Rha*p*1) with no methylation and no acetylation (Ralet *et al.*, 2010; Macquet *et al.*, 2007), was localized to the medial cisternae, it could be postulated that RG-I backbone synthesis is initiated in the *cis* Golgi cisternae and extended in the medial cisternae. Then, (1→5)-α-L-arabinan chains could be added in *trans* cisternae, as labelling with the LM13 antibody which binds preferentially 5 to 11 (1→5)-α-L-arabinose residues forming unbranched and linearized arabinan chain (Moller *et al.*, 2008; Verhertbruggen *et al.*, 2009) was mainly found over that late subcompartment. In the TGN, where LM5 epitopes

consisting of at least 4 contiguous units of (1→4)-β-D-galactosyl residues were detected (Jones *et al.*, 1997), (1→4)-β-D- galactan chains could be initiated and/or elongated. We also detected a short (1→5)-α-L-arabinan chain recognized by LM6 antibody in the TGN. In accordance with the literature (Willats *et al.*, 1998; Lee *et al.*, 2005; Verhertbruggen *et al.*, 2009), our results support that the LM6 monoclonal antibody binds 2 to 6 arabinose residues from 1,5-linked arabinan sequences involved in branched backbone or short secondary side chains. Our immunogold data using LM16 indicate the presence of arabinogalactan chain composed of galactose/galactan stub with branched arabinan in the TGN.

To progress towards understanding the compartmentalization of RG-I assembly within Golgi cisternae, we performed a Golgi mapping of enzymes potentially involved in the arabinan chain synthesis: the putative arabinosyltransferase AtARAD1, the UDP-D-xylose-4-epimerase AtUXE1/MUR4, and its homolog AtUXE3. So far, few studies have been done on Golgi mapping of both sugar epitopes and enzymes (Zhang and Steahelin 1992; Chevalier *et al.*, 2010; Follet-Gueye *et al.*, 2012). Here, we show that AtARAD1-GFP and AtUXE3-GFP fused proteins are localized in the medial Golgi cisternae, and AtUXE1-GFP in the TGN.

Harholt *et al*. (2006) hypothesized that AtARAD1 is a processive arabinosyltransferase, probably involved in the arabinan backbone elongation. Different arabinosyltransferase activities are needed for the initiation, elongation and branching of the arabinan chains. Phylogenetic analysis of AtARAD1 homologs in Arabidopsis GT 47 family identified seven other proteins, among them AtARAD2, sharing 65% identity with AtARAD1. These two putative arabinan arabinosyltransferases are nonredundant (Harholt *et al*., 2012), and form homo and heterodimers when they were co-overexpressed transitory in epidermal cells of *N.benthamiana* (Harholt *et al*., 2012). *ARAD2* gene is less expressed in arabidopsis tissues compared to *ARAD1*, and the cell wall arabinose content of *arad2* mutant is not affected. A significant detection of LM13 epitope was observed at the root surface of *arad2* mutant compared to wild-type, *arad1* and *arad1/arad2* double mutant, suggesting an involvement of AtARAD2 in the arabinan branching. As both AtARAD1 and AtARAD2 are associated in a complex (Harholt *et al*., 2012) and AtARAD1 has been found in medial Golgi cisternae, we postulate that AtARAD2 also localized in

this same compartment, and therefore that arabinan backbone is possibly elongated and branched in the medial compartment. We have localized unbranched and linearized arabinan chain epitopes with a length of 5 to 11 α-(1→5)-L-arabinose residues in the *trans* cisternae with the LM13 antibody, and we have detected 1,5-linked arabinan sequences (2 to 6 arabinose residues) involved in branched backbone and short secondary side chains in the TGN with the LM6 antibody. It is therefore not surprising to detect the enzyme AtARAD1 in the medial cisternae and to detect linear arabinan chains (the "final" product) in a later compartment, since in the medial cisternae, arabinan chains assembly is in progress and the LM13 antibody needs at least 5 arabinose residues for recognition.

In which compartment is initiated the synthesis of arabinan, galactan or arabinogalactan side chains? As no specific antibody for initiation region is available, it remains difficult to draw a conclusion. But, as we have detected linear arabinan with LM13 and the putative arabinosyltransferase (AtARAD1-GFP) respectively in the *trans* and the medial cisternae, we propose that initiation of (1→5)-α-L-arabinan starts at least in the medial compartment. It remains to be determined if the synthesis of the RG-I side chains could be initiated directly on the backbone, or if the side chains could be added on the backbone after their initiation.

Arabinan RG-I biosynthesis: Golgi protein complex research

Arabinan side chains of RG-I is known to influence the mechanical properties of the cell wall (Ulvskov *et al.*, 2005; Moore *et al.*, 2006; Harholt *et al*., 2010). Arabinan synthesis involves the action of different partners within Golgi membranes. First, biosynthesis of UDP-Ara*p* residues occurs *via* 4-epimerization of UDP-Xyl, then UDP-Ara*p* is converted in UDP-Ara*f* by arabinose mutase, and carried by UDP-Ara*f* transporter and arabinosyltransferase. Using the split-ubiquitin system, we tested if the homolog of the xylose epimerase AtUXE1/MUR4, called AtUXE3, with the arabinose mutase AtRGP1 and AtRGP2, and the arabinosyltransferase AtARAD1 could be involved in a complex, as we localized AtUXE3 and AtARAD1 both in the same Golgi sub-compartment; namely the medial.

We confirm that AtRGP1 and AtRGP2 form homo and heterodimers (Rautengarten *et al.*, 2011). In contrast, we could not confirm that AtARAD1 forms homodimers (Harholt *et al.*, 2006), as AtARAD1-Cub was nonfunctional. We did not observe that AtUXE3 forms homo or heterodimers. Finally, we could not show any direct interactions between AtUXE3 and AtARAD1, AtRGP1 or AtRGP2 when using this system.

It could be helpful to explore the cell wall sugar content of *uxe3* mutant to determine whether AtUXE3 is really involved in RG-I arabinan synthesis, as well as more detailed studies of RG-I fractions in the *rgp* mutants to ensure that AtRGP-1 and -2 contribute to RG-I arabinan assembly. It should be noted that the lack of interaction in the split ubiquitin system does not indicate the lack of interaction *in vivo*. Furthermore, the proteins could be found within the same complexes without direct interaction. Recently, DePino *et al.* (2013) have examined RGP oligomerisation in *Solanum tuberosum*, and proposed that class 2 RGPs (*e.g.* AtRGP4 or AtRGP5), with no mutase activity, could be directly involved in Golgi membrane binding of RGP oligomers. According to this model, it is possible that AtRGP1 and AtRGP2 interact indirectly with Golgi membranes *via* AtRGP4/5, although this possibility remains to be tested. Further studies are required to verify potential interaction between AtUXE3 and AtARAD1, and perhaps AtARAD2. So far, none of the UDP-Ara*f* transporters has been characterized. Such transporters represent a good candidate partner linking mutases and arabinosyltransferases, from the cytosol to the Golgi lumen (Søgaard *et al*., 2012).

EXPERIMENTAL PROCEDURES

Plant material and growth conditions

Suspension cells of *Nicotiana tabacum* cv. Bright Yellow 2 (BY-2) were cultured in the Murashige and Skoog liquid medium (Sigma M5524, http://www.sigmaaldrich.com): 4.3 g/L in sucrose 30 g/L, KH2PO4 100 mg/L, myo-inositol 51 mg/L, thiamine 1 mg/L, 2.4 dichlorophenoxyacetic acid 0.22 mg/L, pH 5.6, in dark, at 22°C, 140 rpm. Cells were subcultured every week by transferring 10 mL of suspension cells in 150 mL of fresh medium.

Isolation of RG-I from tobacco BY-2 suspension-cultured cells

One hundred mL of 4 d-old tobacco BY-2 suspension-cultured cells were filtered, ground and heated twice in 70% ethanol at 70°C for 15 min. The homogenate was treated with a solution of chloroform/methanol (1/1, v/v) for 15 min following by acetone for 15 min before drying. The resulting alcohol insoluble residue was incubated in imidazole-HCl 500 mM pH 7 overnight. The pectin-enriched fraction was then extracted from the insoluble residue by boiling in 0.5% oxalate ammonium for 1 h. After centrifugation at 2,000 g, the supernatant was dialyzed against water and then freeze-dried.

Quantification of monosaccharides

Sugar composition of the pectin-enriched fraction was determined by gas liquid chromatography (GLC) analysis of the trimethylsilyl methylglycoside derivatives using inositol as internal standard. Briefly, samples were heated overnight in 1 M methanolic-HCl (Sigma) at 80°C for methanolysis. After evaporation of the reagent, the methylglycosides were converted into their trimethylsilyl derivatives by heating the samples for 20 min at 110°C in hexamethyldisilizane / trimethylchlorosilane / pyridine (3/1/9; Sigma). After evaporation, the samples were suspended in cyclohexane before being injected on a DB-1 column (DB-1 Supelco). Chromatographic data were integrated with GLC Star Workstation software (Varian), each surface being corrected according to its response factor.

Sugar linkage analysis

The permethylation analysis of the pectin-enriched fraction was carried out as reported in Ciucanu and Kerek (1984). The permethylated sample was then hydrolyzed, reduced and acetylated as described in Dardelle *et al.* (2010). No prior reduction of uronic acids was used in the protocol and as a consequence, linkage analysis of only neutral monosaccharides was performed. The partially methylated alditol acetates were separated by GLC (Hewlett-Packard 6890) on an Optima 5-MS capillary column (30 m i.d., 0.25 mm; Macherey Nagel) and analyzed by electron impact mass spectrometry (EIMS) using an Autospec mass spectrometer (Micromass) equipped with an Opus 3.1 data system.

Cloning procedure

The coding sequence of AtARAD1(At2g35100), AtUXE1/MUR4/HSR8 (At1g30620) and AtUXE3/MEE25 (At2g34850), were amplified by PCR without the stop codon using respectively Forward Kpn1 (5'-GGGGTACCCCATGGCGCGTAAATCTTCC -3') and Reverse Spe1(5'- GGACTAGTAATGGAAGTGATAAGACC-3') primers for AtARAD1; Forward BamH1 (5'- CGCGGATCCCGATGTTTAGTTTTGGCCGAGCA-3') and Reverse Spe1 (5'- GGACTAGTGTAAACCGAGACCGATGAGGT-3') primers for MUR4; and Forward (5'-CACCATGGCTGCTCATGGTGTGAAG-3') and Reverse (5'- CATGTATGCAGAAACCAAGGA-3') primers for AtUXE3. The SALK cDNA clones were used as template (respectively U67266, U21248 and U21365).

For AtARAD1 and AtUXE1, the amplified cDNA were introduced in vectors and fused to the sGFP as described in Chevalier *et al*. (2010). The amplified cDNA of AtUXE3 was introduced in pENTR-D-TOPO, and fused to the GFP by introducing in pMDC83 vector (Curtis and Grossniklaus, 2003) using Gateway technology by LR clonase reaction.

Stable expression in *Nicotiana tabacum*

The generated plasmids were transferred into *Agrobacterium tumefaciens* (strain GV3101 pMP90 for AtARAD1 and AtUXE1, and EHA105 for AtUXE3 as described in Chevalier *et al*. (2010).

Immunolocalization of Rhamnogalacturonan-I epitopes inside tobacco BY-2 protoplasts

Protoplasts preparation, immunostaining and confocal microscopy were done exactly as described in Chevalier et al., 2010. INRA-RU1 and INRA-RU2 antibodies (Dr Fabienne Guillon, INRA, UR1268 Biopolymères Interactions Assemblages, guillon@nantes.inra.fr) were diluted at 1/3 in incubation buffer and LM5, LM6, LM13 and LM16 (Plantprobes; http://www.plantprobes.net/) antibodies were not diluted.

Immunolocalization Rhamnogalacturonan-I epitopes in tobacco BY-2 cells wall

Immunostaining and observation were done as describe in Chevalier et al. (2010), but on entire BY-2 suspension-cultured cells using INRA-RU2 as primary antibody.

Localization of fusion proteins in *N. tabacum*

Subcellular localization of fusion proteins were examined using a Leica TCS SP2 AOBS confocal laser scanning microscope. GFP fluorescence of suspension cultured cells was imaged using an excitation wavelength of 488 nm with the emission wavelength at 500 nm to 520 nm.

High pressure freezing (HPF) and freeze substitution (FS)

BY-2 suspension-cultured cells were fixed by high pressure freezing and freeze substituted exactly as described in Chevalier *et al*., 2010.

Immunogold labelling of Rhamnogalacturonan - I epitopes

Ultrathin sections (90 nm; ultracut UCT Leica Vienna Austria) of tobacco cells were collected on to carbon-formvar-coated nickel grids and blocked in TBS (Tris-Buffered Saline: Tris-HCl 20mM pH 7.2, 200 mM NaCl) supplemented with 0.2% of BSA and milk 3% for 30 min. Sections were then incubated with the neat solution of monoclonal antibody (INRA-RU1, INRA-RU2, LM5, LM6, LM13, LM16) for 3h at room temperature. After washing in TBS + BSA 0.2% buffer, grids were incubated for 1h at room temperature in the mouse secondary antibody (INRA-RU1, INRA-RU2) or rat secondary antibody (LM5, LM6, LM13, LM16) conjugated to 10 nm gold particles (dilution 1/20, Tebu-British Biocell International). After washing and fixation in TBS+

2% glutaraldehyde, sections were first stained with 2% vapour osmium for 3 hours followed by classical staining using uranyl acetate and lead citrate. Sections were observed in a Philips, FEI Tecnai 12 Biotwin transmission electron microscope operating at 80 kV, with ES500W Erlangshen CCD camera (Gatan).

Immunogold labelling of GFP-tagged proteins

Immunolabelling was done exactly as described in Chevalier *et al.* (2010).

Quantifying immunogold labelling and statistical analysis

The procedure was done exactly as described in Chevalier *et al.* (2010).

Split ubiquitin assay

The split-ubiquitin assay was performed using the yeast strain NMY51 and the bait vectors pBT3-N or pDHB1 and the prey vector pPR3-N (Dualsystems Biotech AG).
Coding sequences of AtARAD1, AtRGP1, AtRGP2 and AtUXE3 were PCR amplified and subsequently ligated into the vectors using the SfiI restriction site (see Table S7, Dualsystems Biotech AG). AtARAD1 was cloned into the bait vector pBT3-N and the prey vector pPR3-N (Dualsystems Biotech AG). AtRGP1, AtRGP2 and AtUXE3 were cloned into the bait vector pDHB1, linking the soluble proteins to the ER membrane via Ost4 anchor domain, and the prey vector pPR3-N (Dualsystems Biotech AG). The plasmids were pairwise inserted into the yeast NMY51 using the LiAc transformation method (Gietz and Woods 2002), plated on SD-Leu-Trp plates and grown at 30°C for 3 days. Yeast carrying both vectors were picked and grown O/N in liquid SD-Leu-Trp media and subsequently spotted in a SD-His-Leu-Trp-Ade plate in equal concentrations and grown for at 30°C for 3 days.
XGal assay, which tests β-Galactosidase activity, was performed in growing yeast on SD-His-Leu plates as in (Obrdlik, El-Bakkoury et al. 2004).Growth on the SD-His-Leu-Trp-Ade media and blue color formation, β-galactosidase activity, combined is an indication of interaction.

ACKNOWLEDGEMENTS

We would like to thank C.Rautengarten, Ph.D. (Joint BioEnergy Institute/Feedstocks Division, Lawrence Berkeley National Laboratory) for providing us the cDNA of ArRGP1 and 2; Pr A. Faik (Department of Plant Biology, Ohio University) for providing pENTR-D-TOPO and pMDC83 vectors for cloning and Dr F. Guillon (UR1268, INRA, Nantes, France) for providing INRA-RU1/2 antibodies. We would like to thank the Grand Réseau de Recherche named “Végétal, Agronomie, Sol, Innovation” (GRR VASI) and the Structure Fédérative de Recherche named Institut de Recherche et d’Innovation Biomédicale (SFR IRIB) for providing funding on “Protein trafficking in animal and plant systems”.

[a] *Monosaccharide composition (%)*	
Ara	38.8 ± 4.0
GalUA	20.8 ± 0.4
Rha	18.0 ± 0.6
Gal	11.8 ± 0.8
Xyl	6.9 ± 1.4
Fuc	1.7± 0.3
Man	1.7 ± 0.2
GlcUA	0.3 ± 0.1
[b] *Linkage analysis (%)*	
T-Ara*f*	14.3
3-Ara*f*	1.9
5-Ara*f*	22.9
3,5-Ara*f*	15.7
T-Gal*p*	3.6
3-Gal*p*	3.9
4-Gal*p*	7.5
6-Gal*p*	0.4
3,6-Gal*p*	0.8
4,3-Gal*p*	nd
4,6-Gal*p*	1.2
T-Rha*p*	0.2
2-Rha*p*	3.2
3-Rha*p*	0.2
2,4-Rha*p*	3.6
2,3,4-Rha*p*	0.6
T-Xyl*p*	3.8
2-Xyl*p*	3.8
2,3,4-Xyl*p*	0.9
T-Glc*p*	2.0
3-Glc*p*	2.3
4,6-Glc*p*	5.9

Table 1: Monosaccharide composition and linkage analysis of the pectin-enriched fraction. (a) The monosaccharide composition was determined by GLC analysis of trimethylsilyl methylglycosides and expressed as mol %. Values are means ± SEM from three independent experiments. (b) The sugar linkage analysis was determined by GLC-EIMS of partially methylated alditol acetate and expressed as mol %. nd: not detected. Ara: Arabinose; Fuc: Fucose; Gal: Galactose; GalUA: Galacturonic acid; Glc: Glucose; GlcUA: Glucuronic acid; Rha: Rhamnose; Xyl: Xylose.

Antibody	Reference	Epitope
INRA-RU1	Ralet *et al.*, 2010	[→2)-α-L-rhamnose *p*-(1→4)-α-D-galacturonic acid *p-(1→]*$_{6/7}$
INRA-RU2	Ralet *et al.*, 2010	[→2)-α-L-rhamnose *p*-(1→4)-α-D-galacturonic acid *p-(1→]*$_{2/7}$
LM13	Moller *et al.*, 2008; Verhertbruggen *et al.*, 2009	[unbranched α(1-5) arabinan]$_{5/11}$
LM6	Willats *et al.*, 1998	[α(1-5) arabinan]$_{5/6}$
LM16	Verhertbruggen *et al.*, 2009	Galactosyl residue/galactan stub between arabinan chain and RGI backbone
LM5	Jones *et al.*, 1997	[unbranched β(1-4) galactan]$_{>3}$

Table 2: Antibodies used in this study. Mouse monoclonal antibodies, INRA-RU1 and INRA-RU2 are specific for the backbone of RG-I. Rat monoclonal LM13 and LM6 antibodies bind arabinan side chains, whereas LM5 and LM16 recognize galactan and arabinogalactan branching respectively.

(a)

Compartment	Wild-type cells without primary antibody: Observed gold particles	Expected gold particles	$\chi 2$ values	Wild-type cells with primary antibody: Observed gold particles	Expected gold particles	$\chi 2$ values	Total observed gold particles
Cis	10	3.82	9.99	9	15.17	2.51	19
Medial	15	7.64	7.08	23	30.35	1.78	38
Trans	3	3.82	0.17	16	15.17	0.04	19
TGN	9	21.71	7.44	99	86.28	1.87	108
Column totals	37		**24.70**	147		**6.21**	184

(b)

Compartment	Observed gold particles, n_o	Observed points, P	Expected gold particles, n_e	RLI n_o/n_e	$\chi 2$	$\chi 2$ %
Cis	9	1314	35.8	0.25	18,57	32.02
Medial	23	1579	43.0	0.54	9,29	14.85
Trans	16	423	11.5	1.39	1,75	2.79
TGN	99	2084	56.7	**1.75***	30,02	**50.34***
Column totals	147	5400	147			

Table 3: Quantitative analysis of LM6 labelling over Golgi stacks in wild-type tobacco BY-2 suspension-cultured cells. (a) Comparison of gold particle distribution within Golgi subcompartments of wild-type cells immunolabelled with or without the primary antibody LM6. Quantification of labelling was done on 55 Golgi stacks for each line. The total $\chi 2$ value (24.70+6.21=30.91) compared to that of contingency table analysis, with a degree of freedom of 3, confirms that gold particles distribution is due to LM6 with $\alpha < 0.005$. (b) Observed and expected distribution of gold particles in subtypes of Golgi cisternae of wild-type tobacco BY-2 suspension-cultured cells and relative labelling index values. Asterisks (*) identify Golgi compartments that are preferentially labelled.

(a)

Compartment	Wild type cells: Observed gold particles	Wild type cells: Expected gold particles	Wild type cells: $\chi 2$ values	Transformed cells: Observed gold particles	Transformed cells: Expected gold particles	Transformed cells: $\chi 2$ values	Total observed gold particles
Cis	61	51.60	1.71	88	97.39	0.90	149
Medial	42	95.93	30.32	235	181.06	16.06	277
Trans	37	27.01	3.69	41	50.98	1.95	78
TGN	91	56.45	21.14	72	106.54	11.20	163
Column totals	231		**56.86**	436		**30.12**	667

(b)

Compartment	Observed gold particles, n_o	Observed points, P	Expected gold particles, n_e	RLI n_o/n_e	$\chi 2$	$\chi 2$ %
Cis	88	728	39.2	2.24	0,27	0.27
Medial	235	1286	69.2	**3.39***	52,54	**53.05***
Trans	41	444	23.9	1.71	1,88	1.90
TGN	72	1354	72.8	0.98	44,34	44.76
Column totals	436	3812	205			

Table 4: Quantitative analysis of anti-GFP labelling over Golgi stacks in tobacco BY-2 suspension-cultured cells expressing AtARAD1-GFP. (a) Comparison of gold particle distribution within Golgi subcompartments of wild-type and transformed cells (expressing AtARAD1-GFP) of BY-2 suspension-cultured cells. Quantification of labelling was done on 50 Golgi stacks for each line. The total $\chi 2$ value (56.86 + 30.12 = 86.98) compared to that of contingency table analysis, with a degree of freedom of 3, confirms specificity of gold particle distribution between wild-type and transformed cells with $\alpha < 0.005$. (b) Observed and expected distribution of gold particles in subtypes of Golgi cisternae of tobacco BY-2 suspension-cultured cells expressing AtARAD1-GFP and relative labelling index values. Asterisks (*) identify Golgi compartments that are preferentially labelled.

Golgi compartment labeled	Antibody used	Corresponding epitope detected	Possible reaction occuring in this compartment
cis	PGA/RG-I	Transition region between deesterified HG and the first Rha linked residue of RG-I	• Association of HG and RG-I backbone • Initiation of RG-I backbone synthesis
medial	PGA/RG-I	Transition region between deesterified HG and the first Rha linked residue of RG-I	• Elongation of RG-I backbone
	INRA-RU1	6 to 7 [GalUA /Rha] units which are unbranched, non-methylated and non-acetylated	
trans	PGA/RG-I after deesterification treatment	Transition region between deesterified HG and the first Rha linked residue of RG-I	• Methylesterification of GalA
	LM13	Long (5 to 11 Ara), unbranched and linear arabinan chain	• Elongation of (1→5)-α-L-arabinan chain
TGN	PGA/RG-I after deesterification treatment	Transition region between deesterified HG and the first Rha linked residue of RG-I	• (Methylesterification of GalA ?)
	LM5	Short (4 Gal) galactan chain	• Elongation of galactan chain
	LM6	Short (2 to 6 Ara), possibly branched and non linear arabinan chain	• Branching of linear arabinan chain with 2- or 3-linked arabinose
	LM16	Galactosyl residue/galactan stub between arabinan chain and RG-I backbone	• Branching of branched arabinan on galactose residue or galactan stub to form arabinogalactan chain

Table 5: A proposed pathway RG-I synthesis and assembly in the Golgi apparatus. PGA/RG-I epitopes were detected in sycamore maple suspension-cultured cells (Zhang and Staehelin, 1992; Driouich et al., 1993). Here, quantitative immunogold analysis (see also table 3) of INRA-RU1, LM5, LM6, LM13 and LM16 was performed in tobacco BY-2 suspension-cultured cells (deep squares). First, data suggest that RG-I backbone synthesis is initiated in the *cis* Golgi subcompartment, extends in the *medial* subcompartment, and that arabinan and galactan or arabinogalactan side chains elongation occurs at least in the *trans* Golgi subcompartment and the TGN respectively. And, secondly, data confirm that the methylesterification of galacturonic acid residues takes place in the late Golgi compartment.

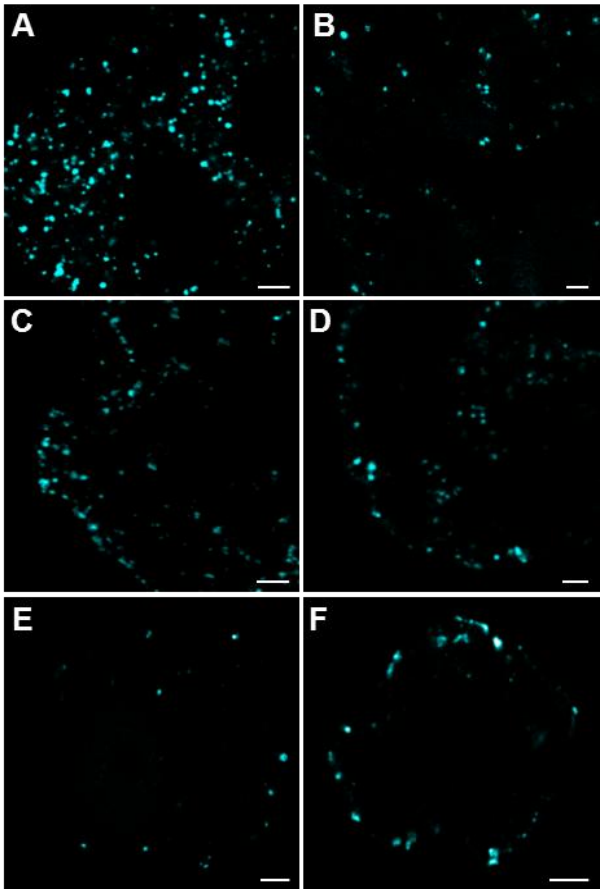

Figure 1: Confocal microscope images showing subcellular localization of rhamnogalacturonan-I epitopes within tobacco BY-2 protoplasts. Fluorescent spots (~1µm in diameter), that are typical of Golgi localization, are observed following labelling with INRA-RU1 (A), INRA-RU2 (B), LM5 (C), LM6 (D),LM13 (E) and LM16 (F). Scale bar = 5 µm.

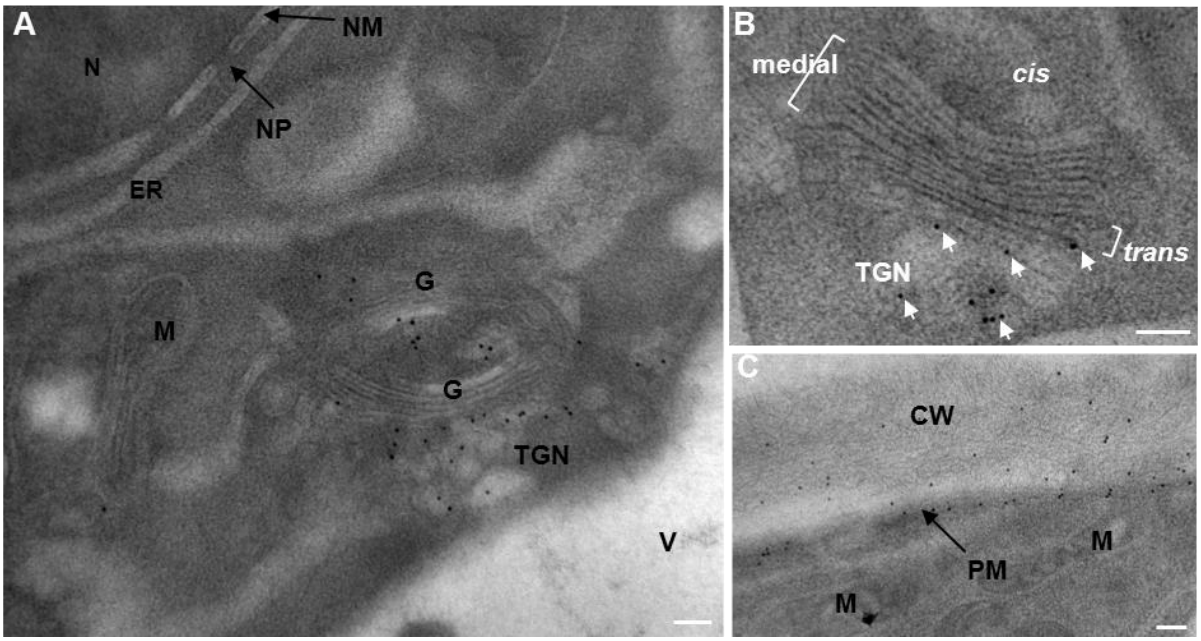

Figure 2: Immunogold localization of rhamnogalacturonan-I epitopes in HPF/FS tobacco BY-2 suspension-cultured cells. Electron micrographs illustrate labelling of Golgi units and secretory vesicles with the monoclonal antibody LM6 (A), and of Golgi stacks and the cell wall with the monoclonal antibody LM 16 (B, C). White arrows indicate gold particles in B. CW : cell wall, ER : endoplasmic reticulum, G : Golgi stacks, M : mitochondria, N, nucleus; NM : nuclear membrane, NP : nuclear pore, PM : plasma membrane; TGN : trans-Golgi network; V, vacuole. Scale bars = 100 nm.

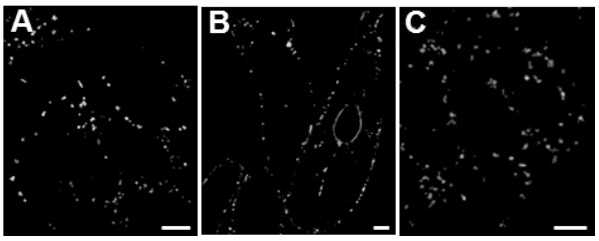

Figure 3

Figure 3: Distribution of AtARAD1-GFP, AtUXE1/MUR4-GFP, and AtUXE3-GFP in living tobacco BY-2 suspension-cultured cells. Stable expression of AtARAD1-GFP (A), AtUXE1/MUR4-GFP (B), and AtUXE3-GFP (C) in tobacco BY-2 suspension-cultured cultured cells also shows fluorescent spots typical of Golgi localization. Scale bars : 8 µm.

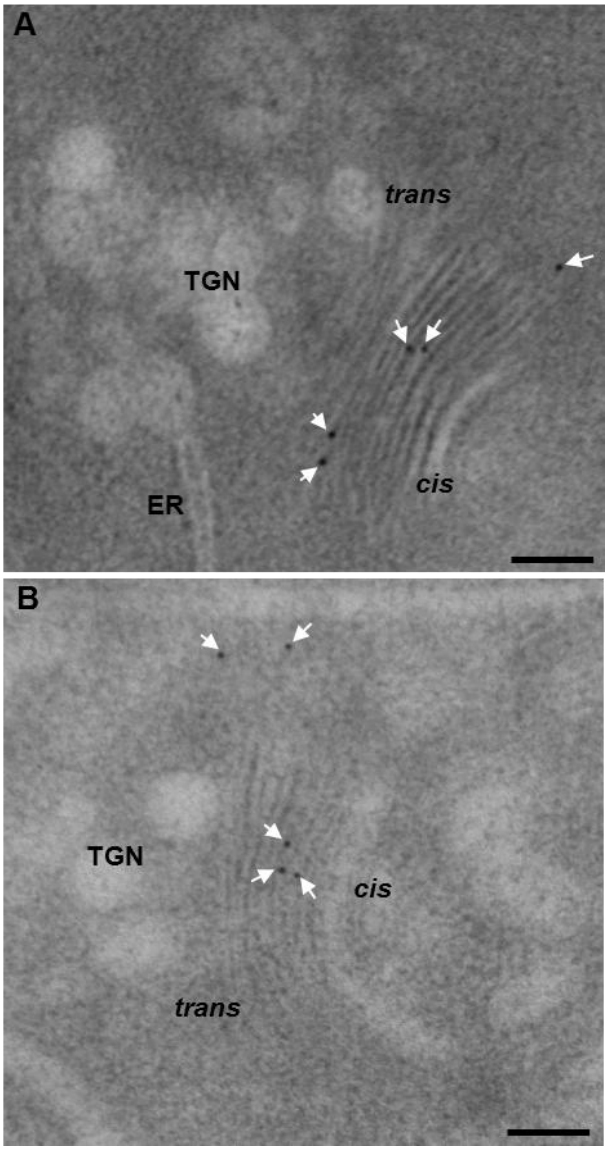

Figure 4: Immunogold localization of AtARAD1-GFP, AtUXE1/MUR4-GFP, and AtUXE3-GFP fusion protein in Golgi stacks of transformed tobacco BY-2 suspension-cultured cells with anti-GFP antibodies. ER, endoplasmic reticulum; TGN, *trans*-Golgi network. Arrows indicate gold particles. Scale bars: 100 nm.

Type of test	Line	Bait (Cub)	Prey (Nub)	Droptest	X
Bait functionality test	1	AtARAD1-BT3-N	pOst1-NubI		
	2	AtRGP1-DHB1	pOst1-NubI		
	3	AtRGP2-DHB1	pOst1-NubI		
	4	AtUXE3-DHB1	pOst1-NubI		
Bait randomly interaction test	5	AtARAD1-BT3-N	pPR3-N		
	6	AtRGP1-DHB1	pPR3-N		
	7	AtRGP2-DHB1	pPR3-N		
	8	AtUXE3-DHB1	pPR3-N		
Prey randomly interaction test	9	AtXXT2-BT3-N	AtARAD1-PR3-N		
	10	AtXXT2-BT3-N	AtRGP1-PR3-N		
	11	AtXXT2-BT3-N	AtRGP2-PR3-N		
	12	AtXXT2-BT3-N	AtUXE3-PR3-N		
Interaction test	13	AtARAD1-BT3-N	AtARAD1-PR3-N		
	14	AtARAD1-BT3-N	AtRGP1-PR3-N		
	15	AtARAD1-BT3-N	AtRGP2-PR3-N		
	16	AtARAD1-BT3-N	AtUXE3-PR3-N		
Interaction test	17	AtRGP1-DHB1	AtARAD1-PR3-N		
	18	AtRGP1-DHB1	AtRGP1-PR3-N		
	19	AtRGP1-DHB1	AtRGP2-PR3-N		
	20	AtRGP1-DHB1	AtUXE3-PR3-N		
Interaction test	21	AtRGP2-DHB1	AtARAD1-PR3-N		
	22	AtRGP2-DHB1	AtRGP1-PR3-N		
	23	AtRGP2-DHB1	AtRGP2-PR3-N		
	24	AtRGP2-DHB1	AtUXE3-PR3-N		
Interaction test	25	AtUXE3-DHB1	AtARAD1-PR3-N		
	26	AtUXE3-DHB1	AtRGP1-PR3-N		
	27	AtUXE3-DHB1	AtRGP2-PR3-N		
	28	AtUXE3-DHB1	AtUXE3-PR3-N		

Figure 5: Droptest and X-gal assay used to detect protein-protein interaction using the split-ubiquitin system between AtARAD1, AtRGP1, AtRGP2 and AtUXE3. Transformed yeast containing the indicated combinations of bait and prey proteins were spotted in equal concentrations on SD-His-Leu-Trp-Ade plates in a dilution series from 1x, 10x, 100x, to 1000x and incubated at 30°C for 3 days. Growth on SD-His-Leu-Trp-Ade plates indicates that two proteins of a given combination are interacting. X-Gal assay test for β-galactosidase activity, which is a reporter for interaction upon blue color formation. The baits when co-expressed with pOst1-NubI tests for functionality and when co-expressed with PR3-N tests for random interaction. The preys when co-expressed with the type II membrane protein AtXXT2 tests for random interaction.

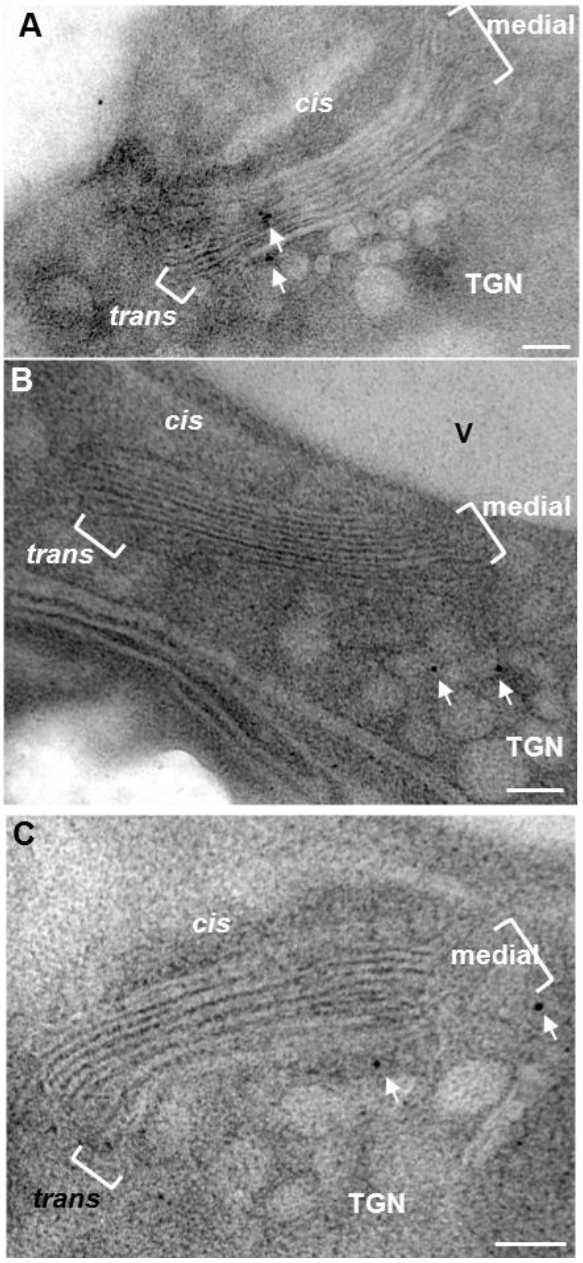

Figure S1: Immunogold localization of rhamnogalacturonan-I epitopes in tobacco BY-2 cells. INRA-RU1 (A), LM5 (B), LM13 (C). TGN, *trans*-Golgi network. Arrows indicate gold particle. Scale bars = 100 nm

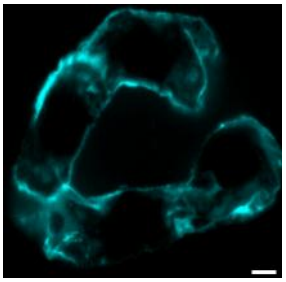

Figure S2: Immunocytochemical localization of rhamnogalacturonan-I epitopes recognized by the antibody INRA-RU2 in tobacco BY-2 suspension-cultured cells. Fluorescent signal is seen over the cell wall. Scale bar = 20 µm

Compartment	Observed gold particles, n_o	Observed points, P	Expected gold particles, n_e	RLI n_o/n_e	$\chi 2$	$\chi 2$ %
Cis	3	824	7.5	0.40	2,67	76.26
Medial	10	867	7.9	**1 .27***	0,59	**15.63***
Trans	3	243	2.2	1.36	0,29	7.73
TGN	13	1267	11.5	1.13	0,20	5.38
Column totals	29	3201	29			

Table S1: Quantitative analysis of INRA-RU1 labelling over Golgi stacks in wild-type tobacco BY-2 suspension-cultured cells. Observed and expected distribution of gold particles in subtypes of Golgi cisternae of wild-type tobacco BY-2 cells and relative labelling index values. Asterisks (*) identify Golgi compartments that are preferentially labelled.

(a)

Compartment	Wild-type cells without primary antibody: Observed gold particles	Expected gold particles	$\chi 2$ values	Wild-type cells with primary antibody: Observed gold particles	Expected gold particles	$\chi 2$ values	Total observed gold particles
Cis	9	7.37	0.35	8	9.62	0.27	17
Medial	14	9.10	2.62	7	11.89	2.01	21
Trans	3	2.16	0.31	2	2.83	0.24	5
TGN	10	17.34	3.11	30	22.65	2.38	40
Column totals	36		**6.41**	47		**4.91**	83

(b)

Compartment	Observed gold particles, n_o	Observed points, P	Expected gold particles, n_e	RLI n_o/n_e	$\chi 2$	$\chi 2$ %
Cis	8	862	11.3	0.71	0,94	10.23
Medial	7	971	12.7	0.55	2,54	27.65
Trans	2	249	3.3	0.62	0,48	5.23
TGN	30	1518	19.8	**1.51***	5,23	**56.89***
Column totals	47	3600	47			

Table S2: Quantitative analysis of LM5 labelling over Golgi stacks in wild-type tobacco BY-2 suspension cultured-cells. (a) Comparison of gold particles distribution in Golgi cisternae of wild-type cells immunolabelled without the primary antibody LM5 and wild-type cells immunolabelled with this antibody. Quantification of labelling was done on 45 Golgi stacks for each line. The total $\chi 2$ value (6.41+4.91=11.32) compared to that of contingency table analysis, with a degree of freedom of 3, confirms that gold particles distribution is due to LM5 with $\alpha < 0.015$. (b) Observed and expected distribution of gold particles in subtypes of Golgi cisternae of wild-type tobacco BY-2 cells and relative labelling index values. Asterisks (*) identify Golgi compartments that are preferentially labelled.

(a)

Compartment	Wild-type cells without primary antibody: Observed gold particles	Expected gold particles	$\chi 2$ values	Wild-type cells with primary antibody: Observed gold particles	Expected gold particles	$\chi 2$ values	Total observed gold particles
Cis	11	8.91	0.48	24	26.08	0.16	35
Medial	16	8.15	7.55	16	23.84	2.58	32
Trans	3	3.05	0.00	9	8.94	0.00	12
TGN	10	19.87	4.90	68	58.12	1.67	78
Column totals	40		**12.94**	117		**4.42**	157

(b)

Compartment	Observed gold particles, n_o	Observed points, P	Expected gold particles, n_e	RLI n_o/n_e	$\chi 2$	$\chi 2$ %
Cis	24	1306	30.0	0.80	1,19	6.73
Medial	16	1383	31.7	0.50	7,80	44.25
Trans	9	310	7.1	1.27	0,50	2.85
TGN	68	2101	48.2	**1.41***	8,13	**46.17***
Column totals	117	5100	117			

Table S3: Quantitative analysis of LM16 labelling over Golgi stacks in wild-type tobacco BY-2 susepnsion-cultured cells. (a) Comparison of gold particles distribution in Golgi cisternae of wild-type cells immunolabeled without the primary antibody LM6 and wild-type cells immunolabelled with this antibody. Quantification of labelling was done on 51 Golgi stacks for each line. The total $\chi 2$ value (12.94+4.42=17.36) compared to that of contingency table analysis, with a degree of freedom of 3, confirms that gold particles distribution is due to LM16 with $\alpha < 0.005$. (b) Observed and expected distribution of gold particles in subtypes of Golgi cisternae of wild-type tobacco BY-2 cells and relative labelling index values. Asterisks (*) identify Golgi compartments that are preferentially labelled.

(a)

Compartment	Wild-type cells without primary antibody: Observed gold particles	Expected gold particles	$\chi 2$ values	Wild-type cells with primary antibody: Observed gold particles	Expected gold particles	$\chi 2$ values	Total observed gold particles
Cis	7	5.65	0.32	13	14.34	0.12	20
Medial	11	9.04	0.42	21	22.95	0.16	32
Trans	0	2.26	2.26	8	5.73	0.89	8
TGN	8	9.04	0.12	24	22.95	0.04	32
Column totals	26		**3.12**	66		**1.23**	92

(b)

Compartment	Observed gold particles, n_o	Observed points, P	Expected gold particles, n_e	RLI n_o/n_e	$\chi 2$	$\chi 2$ %
Cis	13	976	17.0	0.77	0,92	30.43
Medial	21	1265	22.0	0.96	0,04	1.42
Trans	8	284	4.9	**1.62***	1,91	**63.02***
TGN	24	1275	22.1	1.08	0,16	5.13
Column totals	66	3800	66			

Table S4: Quantitative analysis of LM13 labelling over Golgi stacks in wild-type tobacco BY-2 suspension cultured-cells. (a) Comparison of gold particles distribution in Golgi cisternae of wild-type cells immunolabelled without the primary antibody LM13 and wild-type cells immunolabelled with this antibody. Quantification of labelling was done on 38 Golgi stacks for each line. The total $\chi 2$ value (3.12+1.23=4.35) compared to that of contingency table analysis, with a degree of freedom of 3, confirms that gold particles distribution is due to LM13 with $\alpha \leq 0.1$. (b) Observed and expected distribution of gold particles in subtypes of Golgi cisternae of wild-type tobacco BY-2 cells and relative labelling index values. Asterisks (*) identify Golgi compartments that are preferentially labelled.

(a)

Compartment	Wild type cells: Observed gold particles	Wild type cells: Expected gold particles	Wild type cells: $\chi 2$ values	Transformed cells: Observed gold particles	Transformed cells: Expected gold particles	Transformed cells: $\chi 2$ values	Total observed gold particles
Cis	0	4.21	4.21	15	10.79	1.64	15
Medial	4	10.65	4.16	34	27.35	1.62	38
Trans	0	1.96	1.96	7	5.04	0.76	7
TGN	26	13.18	12.48	21	32.82	4.86	47
Column totals	30		**22.80**	77		**8.88**	107

(b)

Compartment	Observed gold particles, n_o	Observed points, P	Expected gold particles, n_e	RLI n_o/n_e	$\chi 2$	$\chi 2$ %
Cis	15	48	18.8	0.79	0,75	31.93
Medial	34	73	28.5	**1.19** *	1,05	**44.36** *
Trans	7	15	5.9	1.19	0,22	9.33
TGN	21	61	23.8	0.88	0,34	14.35
Column totals	77	197	77			

Table S5: Quantitative analysis of anti-GFP labelling over Golgi stacks in tobacco BY-2 cells expressing AtUXE3-GFP. (a) Comparison of gold particle distribution over Golgi cisternae of wild-type and transformed cells (expressing AtUXE3-GFP) of BY-2 suspension-cultured cells. Quantification of labelling was done on 36 Golgi stacks for each line. The total $\chi 2$ value (22.80 + 8.88=31.68) compared to that of contingency table analysis, with a degree of freedom of 3, confirms specificity of gold particles distribution between wild-type and transformed cells with $\alpha < 0.005$. (b) Observed and expected distribution of gold particles in subtypes of Golgi cisternae of tobacco BY-2 cells expressing AtUXE3-GFP and relative labelling index values. Asterisks (*) identify Golgi compartments that are preferentially labelled.

(a)

Compartment	Wild type cells: Observed gold particles	Wild type cells: Expected gold particles	Wild type cells: $\chi 2$ values	Transformed cells: Observed gold particles	Transformed cells: Expected gold particles	Transformed cells: $\chi 2$ values	Total observed gold particles
Cis	61	65.10	0.26	143	138.91	0.12	204
Medial	42	49.77	1.22	114	106.22	0.57	156
Trans	37	25.84	4.82	44	55.16	2.26	81
TGN	91	90.29	0.01	192	192.71	0.00	283
Column totals	231		**6.29**	493		**2.95**	724

(b)

Compartment	Observed gold particles, n_o	Observed points, P	Expected gold particles, n_e	RLI n_o/n_e	$\chi 2$	$\chi 2$ %
Cis	143	1529	153.8	0.92	0,76	1.96
Medial	114	1640	165.0	0.69	15,75	40.71
Trans	44	343	34.5	1.27	2,61	6.75
TGN	192	1389	139.7	**1.37***	19,56	**50.56***
Column totals	493	4901	493			

Table S6: Quantitative analysis of anti-GFP labelling over Golgi stacks in tobacco BY-2 cells expressing AtUXE1/MUR4-GFP. (a) Comparison of gold particle distribution in Golgi cisternae of wild-type and transformed cells (expressing AtUXE1/MUR4-GFP) of BY-2 suspension-cultured cells. Quantification of labelling was done on 50 Golgi stacks for each line. The total $\chi 2$ value (6.29 + 2.95=9.24) compared to that of contingency table analysis, with a degree of freedom of 3, confirms specificity of gold particles distribution between wild-type and transformed cells with α <0.005. (b) Observed and expected distribution of gold particles in subtypes of Golgi cisternae of tobacco BY-2 suspension-cultured cells expressing AtUXE1/MUR4-GFP and relative labelling index values. Asterisks (*) identify Golgi compartments that are preferentially labelled.

Gene	Vector	Size	Primer (SfiI restriction site)	
AtARAD1	pBT3-N/ pPR3-N	1344bp	For	GGCCATTACGGCCATGGCGCGTAAATCTTCCC
			Rev	GGCCGAGGCGGCCTTAAATGGAAGTGATAAGACC
AtRGP1	pDHB1	1073bp	For	GGCCATTACGGCCATGGTTGAGCCGGCGAACAC
			Rev	GGCCGAGGCGGCCGCTTTAGTGGGTGGG
	pPR3-N	1074bp	For	GGCCATTACGGCCATGGTTGAGCCGGCGAACAC
			Rev	GGCCGAGGCGGCCTCAAGCTTTAGTGGGTGGG
AtRGP2	pDHB1	1083bp	For	GGCCATTACGGCCATGGTTGAGCCGGCGAATAC
			Rev	GGCCGAGGCGGCCCAAGCTTTGCCACTGGC
	pPR3-N	1084bp	For	GGCCATTACGGCCATGGTTGAGCCGGCGAATAC
			Rev	GGCCGAGGCGGCCTCAAGCTTTGCCACTGGC
AtUXE3	pDHB1	710bp	For	GGCCATTACGGCCATGGCTGCTCATGGTGTG
			Rev	GGCCGAGGCGGCCCAGTATGCAGAAACCAAGG
	pPR3-N	711bp	For	GGCCATTACGGCCATGGCTGCTCATGGTGTG
			Rev	GGCCGAGGCGGCCTCAGTATGCAGAAACCAAGG

Table S7: Primer sequences used to for cloning of AtARAD1, AtRGP1, AtRGP2 and AtUXE3 genes into the bait vector (pBT3-N or pDHB1) and prey vector (pPR3-N). Underline primer sequence correspond to the SfiI restriction digestion site used to insert the genes into the split-ubiquitin vector.

REFERENCES

Albersheim P, Darvill AG, O'Neill MA, Schols HA, Voragen AGJ (1996) An hypothesis: the same six polysaccharides are components of the primary cell walls of all higher plants. In Pectins and Pectinases. Edited by Visser J, Voragen AGJ. Amsterdam: Elsevier Sciences B.V.; p 47-53.

An J, O'Neill MA, Albersheim P, Darvill AG (1994) Isolation and structural characterization of beta-D-glucosyluronic acid and 4-O-methyl beta-D-glucosyluronic acid-containing oligosaccharides from the cell-wall pectic polysaccharide, rhamnogalacturonan I. *Carbohydr Res.* **252**:235-43.

Atmodjo MA, Hao Z, Mohnen D (2013) Evolving views of pectin biosynthesis. *Annu Rev Plant Biol.* **64**:747-79.

Atmodjo MA, Sakuragi Y, Zhu X, Burrell AJ, Mohanty SS, Atwood JA 3rd, Orlando R, Scheller HV, Mohnen D. (2011) Galacturonosyltransferase (GAUT)1 and GAUT7 are the core of a plant cell wall pectin biosynthetic homogalacturonan: galacturonosyltransferase complex. *Proc Natl Acad Sci U S A.* **108**(50):20225-30.

Baldwin TC, Handford MG, Yuseff MI, Orellana A, Dupree P. (2001) Identification and characterization of GONST1, a golgi-localized GDP-mannose transporter in Arabidopsis. *Plant Cell* **13**(10):2283-95.

Brickell LS, Reid JSG (1996) Biosynthesis in vitro of pectic (1–4)-beta-D-galactan. In: Visser J (ed) Pectins and pectinases.Elsevier, Amsterdam, pp 127–134

Burget EG, Verma R, Mølhøj M, Reiter WD. (2003) The biosynthesis of L-arabinose in plants: molecular cloning and characterization of a Golgi-localized UDP-D-xylose 4-epimerase encoded by the MUR4 gene of Arabidopsis. *Plant Cell*. **15**(2):523-31.

Burget EG, Reiter WD. (1999) The mur4 mutant of arabidopsis is partially defective in the de novo synthesis of uridine diphospho L-arabinose.*Plant Physiol*. **121**(2):383-9.

Caffall K.H., Mohnen D. (2009) The structure, function, and biosynthesis of plant cell wall pectic polysaccharides *Carbohydrate Research* **344**: 1879–1900.

Chevalier L, Bernard S, Ramdani Y, Lamour R, Bardor M, et al. (2010) Subcompartment localization of the side chain xyloglucan-synthesizing enzymes within Golgi stacks of tobacco suspension-cultured cells. *Plant J* **64**: 977–989.

Chou YH, Pogorelko G, Zabotina OA (2012) Xyloglucan xylosyltransferases XXT1, XXT2, and XXT5 and the glucan synthase CSLC4 form Golgi-localized multiprotein complexes. *Plant Physiol.* **159(**4):1355-66.

Ciucanu I. and Kerek F. (1984) A simple and rapid method for the permethylation of carbohydrates. *Carbohydr. Res.* **131:** 209-217.

Coenen GJ, Bakx EJ, Verhoef RP, Schols HA, Voragen AGJ (2007) Identification of the connecting linkage between homo- or xylogalacturonan and rhamnogalacturonan type I. *Carbohydrate Polymers* **70** :224–235.

Cocuron JC, Lerouxel O, Drakakaki G, Alonso AP, Liepman AH, Keegstra K, Raikhel N, Wilkerson CG. (2007) A gene from the cellulose synthase-like C family encodes a beta-1,4 glucan synthase. *Proc Natl Acad Sci USA.* **104**: 8550-8555.

Curtis MD, Grossniklaus U. (2003) A gateway cloning vector set for high-throughput functional analysis of genes in planta. *Plant Physiol*. **133**(2):462-9.

Dardelle F., Lehner A., Ramdani Y., Bardor M., Lerouge P., Driouich A. and Mollet J-C. (2010) Biochemical and immunocytological characterizations of Arabidopsis pollen tube cell wall. *Plant physiol.* **153**: 1563-1576.

Davis JK (2012) Combining polysaccharide biosynthesis and transport in a single enzyme: dual-function cell wall glycan synthases. *Frontiers in plant science* **3**:138.

Delgado IJ, Wang Z, de Rocher A, Keegstra K and Raikhel NV (1998) Cloning and Characterization of AtRGP11 - A Reversibly Autoglycosylated Arabidopsis Protein Implicated in Cell Wall Biosynthesis *Plant Physiol*. **116**: 1339–1349.

De Pino V, Marino Busjle C, Moreno S. (2013) Oligomerization of the reversibly glycosylated polypeptide: its role during rice plant development and in the regulation of self-glycosylation. *Protoplasma.* **250**(1):111-9.

De Pino V, Borán M, Norambuena L, González M, Reyes F, Orellana A, Moreno S. (2007) Complex formation regulates the glycosylation of the reversibly glycosylated polypeptide. *Planta.* **226**(2):335-45.

Dhugga KS, Tiwari SC, Ray PM. (1997) A reversibly glycosylated polypeptide (RGP1) possibly involved in plant cell wall synthesis: purification, gene cloning, and trans-Golgi localization. *Proc Natl Acad Sci U S A.* **94**(14):7679-84.

Dhugga KS, Ulvskov P, Gallagher SR, Ray PM. (1991) Plant polypeptides reversibly glycosylated by UDP-glucose. Possible components of Golgi beta-glucan synthase in pea cells. *J Biol Chem.* **266**(32):21977-84.

Driouich A, Follet-Gueye ML, Bernard S, Kousar S, Chevalier L, Vicré-Gibouin M, Lerouxel O. (2012) Golgi-mediated synthesis and secretion of matrix polysaccharides of the primary cell wall of higher plants. *Frontiers in Plant Science* **3**:79.

Driouich A, Zhang GF, Staehelin LA. (1993) Effect of Brefeldin A on the structure of the golgi apparatus and on the synthesis and secretion of proteins and polysaccharides in sycamore maple suspension-cultured cells. *Plant Physiol*. **101**: 1363-1373.

Eda S., Akiyama Y., Kato K. (1985) A galactoglucomannan from cell walls of suspension cultured tobacco (nicotiana tabacum) cells *Carbohydrate Research,* **137**: 173-181.

Eda S, Akiyama Y, Kato K (1983) Methylation Analysis of Cell Wall Polysaccharides from Suspension-cultured Cells of Nicotiana tabacum *Agric. Biol Chem.,* **47**(8): 1783-1789.

Follet-Gueye ML., Mollet JC., Vicré-Gibouin M., Bernard S., Chevalier L., Plancot B.,Dardelle F., Ramdani Y, Coimbra S. and Driouich A. (2012) Immuno-Glyco-Imaging in Plant Cells:Localization of Cell Wall Carbohydrate Epitopes and Their Biosynthesizing Enzymes. In Applications of Immunocytochemistry. Ed. Hesam Dehghani ISBN 978-953-51-0229-8. pp 297-320.

Freshour G, Clay RP, Fuller MS, Albersheim P, Darvill AG, Hahn MG (1996) Developmental and Tissue-Specific Structural Alterations of the Cell-Wall Polysaccharides of Arabidopsis thaliana Roots. *Plant Physiol.* **110**(4):1413-1429.

Geshi N, Pauly M and Ulvskov P (2002) Solubilization of galactosyltransferase that synthesizes 1,4-b-galactan side chains in pectic rhamnogalacturonan. *Physiologia Plantarum* **114**: 540–548.

Gietz, R. D. and R. A. Woods (2002). "Transformation of yeast by the liac/ss carrier dna/peg method." *Methods in Enzymology* **350**: 87-96.

Goubet F and Morvan C (1993) Evidence for Several Galactan Synthases in Flax (Linum usitassimum L.) Suspension-Cultured Cells. *Plant Cell Physiol***. 34**(8): 1297-1303.

Guillemin F, Guillon F, Bonnin E, Devaux MF, Chevalier T, Knox JP, Liners F, Thibault JF (2005) Distribution of pectic epitopes in cell walls of the sugar beet root. *Planta* **222**(2):355-71.

Handford M, Rodríguez-Furlán C, Marchant L, Segura M, Gómez D, Alvarez-Buylla E, Xiong GY, Pauly M, Orellana A. (2012) Arabidopsis thaliana AtUTr7 encodes a golgi-localized UDP-glucose/UDP-galactose transporter that affects lateral root emergence. *Mol Plant*. **5**(6):1263-80.

Harholt J, Jensen JK, Verhertbruggen Y, Søgaard C, Bernard S, Nafisi M, Poulsen CP, Geshi N, Sakuragi Y, Driouich A, Knox JP, Scheller HV.(2012) ARAD proteins associated with pectic Arabinan biosynthesis form complexes when transiently overexpressed in planta. *Planta.* **236**(1):115-28.

Harholt,J., Suttangkakul,A., and Vibe Scheller,H.(2010) Biosynthesis of pectin. *Plant Physiol.* **153**: 384–395.

Harholt J, Jensen JK, Sorensen SO, Orfila C, Pauly M, et al. (2006) ARABINAN DEFICIENT 1 is a putative arabinosyltransferase involved in biosynthesis of pectic arabinan in Arabidopsis. *Plant Physiol* **140**: 49–58.

Huisman MMH, Brüll LP, Thomas-Oates JE, Haverkamp J, Schols HA, Voragen AGJ (2001) The occurrence of internal (1-5)-linked arabinofuranose and arabinopyranose

residues in arabinogalactan side chains from soybean pectic substances. *Carbohydrate Research* **330**: 103–114.
Jones L., Seymour C. B., and Knox J.P (1997) Localization of Pectic Galactan in Tomato Cell Walls Using a Monoclonal Antibody Specific to (1 →4)-β-D-Galactan *Plant Physiol*. **113**: 1405-1412.

Kato H, Takeuchi Y, Tsumuraya Y, Hashimoto Y, Nakano H, Kovác P. (2003) In vitro biosynthesis of galactans by membrane-bound galactosyltransferase from radish (Raphanus sativus L.) seedlings. *Planta* **217**(2):271-82.

Keegstra K, Raikhel N. (2001) Plant glycosyltransferases. *Curr Opin Plant Biol.* **4**(3):219-24.

Knox JP (2008) Revealing the structural and functional diversity of plant cell walls. *Curr Opin Plant Biol.* **11**(3):308-13.

Konishi T, Kotake T, Tsumuraya Y (2007) Chain elongation of pectic β(1,4)-galactan by a partially purified galactosyltransferase from soybean (*Glycine max* Merr.) hypocotyls *Planta* **226**:571–579.

Konishi T, Mitome T, Hatsushika H, Md. Haque A, Kotake T, Tsumuraya Y (2004) Biosynthesis of pectic galactan by membrane-bound galactosyltransferase from soybean (Glycine max Merr.) seedlings *Planta* **218**: 833–842.

Lee KJ, Cornuault V, Manfield IW, Ralet MC, Paul Knox J. (2013) Multi-scale spatial heterogeneity of pectic rhamnogalacturonan I (RG-I) structural features in tobacco seed endosperm cell walls. *Plant J.* **75**(6):1018-27.

Lee, K.J.D., Sakata, Y., Mau, S.-L., Pettolino, F., Bacic, A., Quatrano,R.S., Knight, C.D. and Knox, J.P. (2005) Arabinogalactan-proteins are required for apical cell extension in the moss Physcomitrella patens. *Plant Cell* **17**: 3051–3065.

Liwanag AJ, Ebert B, Verhertbruggen Y, Rennie EA, Rautengarten C, Oikawa A, Andersen MC, Clausen MH, Scheller HV. (2012) Pectin biosynthesis: GALS1 in Arabidopsis thaliana is a β-1,4-galactan β-1,4-galactosyltransferase. *Plant Cell* **24**(12):5024-36.

Macquet A, Ralet M-C, Kronenberger J, Marion-Poll A, North HM (2007) In situ, chemical and macromolecular study of the composition of *Arabidopsis thaliana* seed coat mucilage. *Plant Cell Physiol* **48**:984–999.

Marcus Susan E , Verhertbruggen Yves , Hervé Cécile , Ordaz-Ortiz José J , Farkas Vladimir , Pedersen Henriette L Willats William GT and Knox Paul J (2008) Pectic homogalacturonan masks abundant sets of xyloglucane epitopes in plant cell walls *BMC Plant Biology* **8**:60-72.

Mayhew T. M. (2011) Quantifying immunogold localization on electron microscopic thin sections: a compendium of new approaches for plant cell biologists *J. Exp. Bot*. **62**(12): 4101-4113.

Mayhew T.M., Lucocq J.M. (2008) Developments in cell biology for quantitative immunoelectron microscopy based on thin sections: a review *Histochem Cell Biol* **130**:299–313.

Mohnen,D.(2008).Pectin structure and biosynthesis. *Curr.Opin.Plant Biol.* **11**: 266–277.

Moller, I., Marcus, S.E., Haeger, A., Verhertbruggen, Y., Verhoef, R.,Schols, H., Ulvskov, P., Mikkelsen, J.D., Knox, J.P. and Willats, W.(2008) High-throughput screening of monoclonal antibodies against plant cell wall glycans by hierarchical clustering of their carbohydrate microarray binding profiles. *Glycoconj. J*. **25**: 37–48.

Moore JP, Nguema-Ona E, Chevalier L, Lindsey GG, Brandt WF, Lerouge P, Farrant JM, Driouich A. (2006) Response of the leaf cell wall to desiccation in the resurrection plant Myrothamnus flabellifolius. *Plant Physiol.* **141**(2):651-62.

Moore, P. J., K. M. M. Swords, M. A. Lynch,and L. A. Staehelin. (1991) Spatial organization of the assembly pathways of glycoproteins and complex polysaccharides in the Golgi apparatus of plants. J. Cell Biol. 112(4):589-602.

Mori M. and Kato K. (1981) An arabinoglucuronomannan from suspension-cultured cells of *Nicotiana tabacum*. *Carbohydrate Research*. **91**: 49-58.

Nakamura, A., Furuta, H., Maeda, H., Takao, T., Nagamatsu, Y., (2002). Analysis of the molecular construction of xylogalacturonan isolated from soluble soybean polysaccharides. *Biosci. Biotechnol. Biochem.* **66**: 1155–1158.

Nebenführ, A., Gallagher, L., Dunahay, T.G., Frohlick, J.A., Mazurkiewicz, A.M., Meehl, J.B. and Staehelin, L.A. (1999) Stop-and-go movements of plant Golgi stacks are mediated by the acto-myosin system. *Plant Physiol*.**121**: 1127–1141.

Nguema-Ona E, Andeme-Onzighi C, Aboughe-Angone S, Bardor M, Ishii T, Lerouge P, Driouich A. (2006) The *reb1-1* mutation of Arabidopsis: Effect on the structure and the localization of galactose containing cell wall polysaccharides. *Plant Physiol*. **140**: 1406-1417.

Norambuena L, Nilo R, Handford M, Reyes F, Marchant L, Meisel L, Orellana A (2005) AtUTr2 is an Arabidopsis thaliana nucleotide sugar transporter located in the Golgi apparatus capable of transporting UDP galactose. Planta, **222**:521-529.

Øbro J, Harholt J, Scheller HV, Orfila C (2004) Rhamnogalacturonan I in Solanum tuberosum tubers contains complex arabinogalactan structures. *Phytochemistry* **65**:1429–1438.

Obrdlik, P., M. El-Bakkoury, et al. (2004). "K+ channel interactions detected by a genetic system optimized for systematic studies of membrane protein interactions." *PNAS - USA* **101**(33): 12242-12247.

Pagny, S., Bouissoniee´ , F., Sarkar, M., Follet-Gueye, M.L., Driouich, A., Schachter, H., Faye, L. and Gomord, V. (2003) Structural requirements for Arabidopsis b1-2 xylosyltransferase activity and targeting to the Golgi.*Plant J.* **33** : 189–203.

Popper ZA., Fry SC. (2005) Widespread occurrence of a covalent linkage between xyloglucan and acidic polysaccharides in suspension-cultured angiosperm cells. Annals of Botany. **96**: 91–99.

Ralet MC, André-Leroux G, Quéméner B, Thibault JF. (2005). Sugar beet (Beta vulgaris) pectins are covalently cross-linked through diferulic bridges in the cell wall. *Phytochemistry* **66**:2800–14.

Ralet MC, Tranquet O, Poulain D, Moïse A, Guillon F.(2010) Monoclonal antibodies to rhamnogalacturonan I backbone. *Planta*. **231**(6):1373-83 .

Rautengarten, C., B. Ebert, et al. (2011). "The Interconversion of UDP-Arabinopyranose and UDP-Arabinofuranose Is Indispensable for Plant Development in Arabidopsis." *The Plant Cell Online* **23**(4): 1373-1390.

Reiter WD (2008) Biochemical genetics of nucleotide sugar interconversion reactions. *Curr Opin Plant Biol.* **11**(3):236-43.

Reyes F, Orellana A. (2008) Golgi transporters: opening the gate to cell wall polysaccharide biosynthesis. *Curr Opin Plant Biol.* **11**(3):244-51.

Ridley, B.L., O'Neill, M.A., Mohnen, D. (2001). Pectins: structure, biosynthesis, and oligogalacturonide-related signaling. *Phytochemistry* **57**(6): 929-967.

Rösti J, Barton CJ, Albrecht S, Dupree P, Pauly M, Findlay K, Roberts K, Seifert GJ. (2007) UDP-glucose 4-epimerase isoforms UGE2 and UGE4 cooperate in providing UDP-galactose for cell wall biosynthesis and growth of Arabidopsis thaliana. *Plant Cell.* **19(**5):1565-79.

Sakamoto T, Sakai T (1995) Analysis of structure of sugar-beet pectin by enzymatic methods. *Phytochemistry* **39**(4):821-3.

Scheller, H.V, Jensen J.K, Sørensen S.O, Harholt J, Geshi N (2007) Biosynthesis of pectins. *Physiol. Plant.* **129**: 283–295.

Schols HA, Posthumus MA and Voragent AGJ (1990) Structural features of hairy regions of pectins isolated from apple juice produced by the liquefaction process. *Carbohydrate Research,* **206**: 17- 129.

Seifert GJ, Barber C, Wells B, Roberts K. (2004) Growth regulators and the control of nucleotide sugar flux. *Plant Cell*. **16**:723-730.

Seifert GJ, Barber C, Wells B, Dolan L, Roberts K (2002) Galactose biosynthesis in Arabidopsis: genetic evidence for substrate channeling from UDP-D-galactose into cell wall polymers. *Curr Biol.* **12**(21):1840-5.

Sims IM, Craik DJ, Bacic A (1997) Structural characterisation of galactoglucomannan secreted by suspension-cultured cells of *Nicotiana plumbaginifolia. Carbohydrate Research* **303**:79-92.

Søgaard C, Stenbaek A, Bernard S, Hadi M, Driouich A, Scheller HV, Sakuragi Y (2012) GO-PROMTO Illuminates Protein Membrane Topologies of Glycan Biosynthetic Enzymes in the Golgi Apparatus of Living Tissues. *PloS One*, **7**(2): e31324.

Ulvskov P, Wium H, Bruce D, Jørgensen B, Qvist KB, Skjøt M, Hepworth D, Borkhardt B, Sørensen SO. (2005) Biophysical consequences of remodeling the neutral side chains of rhamnogalacturonan I in tubers of transgenic potatoes. *Planta.* **220**(4):609-20.

Verhertbruggen Y., Marcus S. E., Haeger A., Verhoef R., Schols H.A., McCleary B.V., McKee L., Gilbert H. J. and Knox J. P. (2009) Developmental complexity of arabinan polysaccharides and their processing in plant cell walls *Plant J.* **59**(3):413-25.

Verhoef, R., Lu, Y., Knox, J.P., Voragen, A.G.J. and Schols, H.A. (2009) Fingerprinting complex pectins by chromatographic separation combined with ELISA detection. *Carbohydr. Res*. **344** : 1808-1817.

Vicré M, Jauneau A, Knox JP, Driouich A (1998) Immunolocalization of beta-(1 -> 4) and beta-(1 -> 6)-D-galactan epitopes in the cell wall and Golgi stacks of developing flax root tissues. *Protoplasma* **203**: 26-34.

Vincken,J.P.,Schols,H.A.,Oomen,R.J.,F.J.,Beldman,G.,Visser,R.G.F.,andVoragen,A. G.J.(2003).“Pectin–the hairy thing,” in *Advances in Pectin and Pectinase Research*, edsA.G. J. Voragen,H.ScholsandR.Visser (Dordrecht: Kluwer Academic Publishers), p 47–59.

Willats,W.G.,McCartney,L.,Mackie, W.,and Knox,J.P.(2001) Pectin: cell biology and prospects for functional analysis. *Plant Mol.Biol.* **47**: 9–27.

Willats, W.G., Marcus, S.E. and Knox, J.P. (1998) Generation of monoclonal antibody specific to (1 fi 5)-a- L-arabinan. *Carbohydr. Res*. **308**: 149–152.

Zhang GF, Staehelin LA. (1992); Functional compartmentation of the golgi apparatus of plant cells: immunocytochemical analysis of high-pressure frozen- and freeze-substituted sycamore maple suspension culture cells. *Plant Physiol.* **99**:1070-1083.

PARTIE D: TRAVAUX EFFECTUES DANS LE CADRE D'UNE COLLABORATION

Durant mon séjour au sein du laboratoire de recherche « *Molecular plant biology: Cell wall* », dirigé par le Pr. Henrik Vibe Scheller (Copenhague), le Dr. Yumiko Sakuragi m'a enseigné la pratique de la technique de complémentation de fluorescence bimoléculaire (BiFC). Cette technique a été développée pour tester *in vivo* si deux protéines forment un complexe.

Pour rappeler le principe, la *Yellow Fluorescent Protein* (YFP) est séparée en deux fragments, l'un étant porté par une protéine A et l'autre par une protéine B. En cas de forte proximité des protéines A et B, les deux portions YFP (YN: fragment N-terminal de la YFP; YC: fragment C-terminal de la YFP) s'assemblent et émettent un rayonnement après excitation; cet attachement ne pouvant se faire de manière spontanée entre les fragments de YFP. Au contraire, si les protéines A et B sont distantes de plus de 100Å, la YFP ne peut se reconstituer, et aucune émission de fluorescence n'est observable après excitation.

L'arabinosyltransférase AtARAD1 possède un homologue très proche nommé AtARAD2, qui a été étudié par le laboratoire du Pr HV Scheller. Comme pour AtARAD1, l'activité α(1,5)arabinosyltransférase d'AtARAD2 n'a pu être clairement démontrée. Cependant, l'étude du mutant *arad2* et du double mutant *arad1arad2*, montre que cette protéine est clairement impliquée dans la synthèse des chaînes arabinanes du RG-I, et que son activité n'est pas redondante avec la protéine AtARAD1. Dans le cadre de cette collaboration, j'ai participé à montrer que ces deux protéines formaient des homo- et des hétérodimères *in vivo* par la technique de BiFC.

Ces résultats sont détaillés dans l'article suivant **page 227**:

Harholt J, Jensen JK, Verhertbruggen Y, Søgaard C, Bernard S, Nafisi M, Poulsen CP, Geshi N, Sakuragi Y, Driouich A, Knox JP, Scheller HV.(2012) ARAD proteins associated with pectic Arabinan biosynthesis form complexes when transiently overexpressed in planta. *Planta* 236(1):115-28

L'équipe du Dr Y. Sakuragi a également utilisé la technique de BiFC pour développer un protocole simple permettant de connaître la topologie d'une protéine golgienne *in vivo*, grâce à l'utilisation de marqueurs golgiens de la face luminale et de la face cytosolique. Pour valider cette méthode, plusieurs enzymes participant à la synthèse du xyloglucane ou du rhamnogalacturonane-I ont été testées, afin de confirmer ou de montrer leur topologie.

Ainsi, pour les enzymes de synthèse du XyG, il a été confirmé que le site catalytique de la xylosyltransférase AtXXT1 était luminal, et il a été montré que le site catalytique de la xylosyltransférase AtXXT5, et de la galactosyltransférase AtMUR3 étaient également luminal. Pour les enzymes potentiellement impliquées dans la synthèse du RG-I, il a été montré que l'épimérase AtMUR4 et l'arabinosyltransférase AtARAD1 possédaient un site catalytique orienté dans la lumière du Golgi. Les résultats sont présentés dans l'article suivant **page 243**:

Søgaard C, Stenbæk A, Bernard S, Hadi M, Driouich A, Scheller HV, Sakuragi Y. (2012) GO-PROMTO illuminates protein membrane topologies of glycan biosynthetic enzymes in the Golgi apparatus of living tissues.*PLoS One* 7(2):e31324

Papier N°6: Article scientifique en collaboration avec Dr. Yumiko Sakuragi au sein du laboratoire de recherche « *Molecular plant biology: Cell wall* », dirigé par le Pr. Henrik Vibe Scheller, à l'université de Copenhague.

Résultats: Travaux effectués dans le cadre d'une collaboration

ARAD proteins associated with pectic Arabinan biosynthesis form complexes when transiently overexpressed in planta.

Harholt J, Jensen JK, Verhertbruggen Y, Søgaard C, Bernard S, Nafisi M, Poulsen CP, Geshi N, Sakuragi Y, Driouich A, Knox JP, Scheller HV.

Planta (2012) ; 236(1):115-28

Planta
DOI 10.1007/s00425-012-1592-3

ORIGINAL ARTICLE

ARAD proteins associated with pectic Arabinan biosynthesis form complexes when transiently overexpressed in planta

Jesper Harholt · Jacob Krüger Jensen · Yves Verhertbruggen · Casper Søgaard · Sophie Bernard · Majse Nafisi · Christian Peter Poulsen · Naomi Geshi · Yumiko Sakuragi · Azeddine Driouich · J. Paul Knox · Henrik Vibe Scheller

Received: 22 November 2011 / Accepted: 9 January 2012
© Springer-Verlag 2012

Abstract Glycosyltransferase complexes are known to be involved in plant cell wall biosynthesis, as for example in cellulose. It is not known to what extent such complexes are involved in biosynthesis of pectin as well. To address this question, work was initiated on ARAD1 (ARABINAN DEFICIENT 1) and its close homolog ARAD2 of glycosyltransferase family GT47. Using bimolecular fluorescence complementation, Förster resonance energy transfer and non-reducing gel electrophoresis, we show that ARAD1 and ARAD2 are localized in the same Golgi compartment and form homo-and heterodimeric intermolecular dimers when expressed transiently in *Nicotiana benthamiana*. Biochemical analysis of *arad2* cell wall or fractions hereof showed no difference in the monosaccharide composition, when compared with wild type. The double mutant *arad1 arad2* had an *arad1* cell wall phenotype and overexpression of *ARAD2* did not complement the *arad1* phenotype, indicating that ARAD1 and ARAD2 are not redundant enzymes. To investigate the cell wall structure of the mutants in detail, immunohistochemical analyses were carried out on *arad1*, *arad2* and *arad1 arad2* using the arabinan-specific monoclonal antibody LM13. In roots, the labeling pattern of *arad2* was distinct from both that of wild type, *arad1* and *arad1 arad2*. Likewise, in epidermal cell walls of inflorescence stems, LM13 binding differed between *arad2* and WILD TYPE, *arad1* or *arad1 arad2*. Altogether, these data show that ARAD2 is associated with arabinan biosynthesis, not redundant with ARAD1, and that the two glycosyltransferases may function in complexes held together by disulfide bridges.

Keywords Pectin · Arabinan · Glycosyltransferase · Disulfide bridges

J. Harholt · J. K. Jensen · C. Søgaard · M. Nafisi · C. P. Poulsen · N. Geshi · Y. Sakuragi · H. V. Scheller
Laboratory for Molecular Plant Biology, VKR Research Centre Pro-Active Plants, Department of Plant Biology and Biotechnology, University of Copenhagen, 1871 Frederiksberg C, Denmark

J. K. Jensen
Department of Plant Biology, DOE Great Lakes Bioenergy Research Center, Michigan State University, East Lansing, MI 48824, USA

Y. Verhertbruggen · J. P. Knox
Centre for Plant Sciences, Faculty of Biological Sciences, University of Leeds, Leeds LS2 9JT, UK

Y. Verhertbruggen · H. V. Scheller (✉)
Lawrence Berkeley National Laboratory, Physical Biosciences Division, Joint Bioenergy Institute, Berkeley, CA 94720, USA
e-mail: hscheller@lbl.gov

S. Bernard · A. Driouich
Laboratoire "Glycobiologie et Matrice Extracellulaire Végétale", UPRES EA 4358, Institut Fédératif de Recherche Multidisciplinaire sur les Peptides 23, Plate-forme de Recherche en Imagerie Cellulaire de Haute Normandie (PRIMACEN), IBiSA, Université de Rouen, 76821 Mont-Saint Aignan Cedex, France

H. V. Scheller
Department of Plant and Microbial Biology, University of California, Berkeley, CA 94720, USA

Introduction

Plant cells are surrounded by cell walls composed of cellulose microfibrils interwoven with hemicellulosic polysaccharides, pectins and proteins. Pectin consists mainly of homogalacturonan and rhamnogalacturonan I (RG-I), while minor components include rhamnogalacturonan II (RG-II) and xylogalacturonan (Mohnen 2008; Zandleven

Published online: 21 January 2012

et al. 2007). RG-I is a structurally complex molecule, consisting of a backbone of [-4-α-D-GalUA*p*-1,2-α-L-Rha*p*-1-] repeating units. The rhamnose residues often carry side chains of neutral sugars attached at the *O*-4 position. These side chains typically contain galactans, arabinans or branched type I arabinogalactans (Verhertbruggen and Knox 2009). Arabinans consist of a α-1,5-L-arabinofuranose backbone with possible further ramification by sidechains at C-2 and/or C-3 consisting of single α-linked L-arabinofuranosyl residues or small α-1,5-L-arabinofuranose oligomers. The exact arrangements of homogalacturonan, RG-I and xylogalacturonan within pectic networks are not known (Vincken et al. 2003; Verhertbruggen and Knox 2007), but RG-I and xylogalacturonan co-elute as a high molecular mass fraction after extraction from cell walls using endo-polygalacturonase, indicating that RG-I and xylogalacturonan are closely associated (Jensen et al. 2008).

The complex structure of pectin necessitates intricate biochemical machinery for its biosynthesis and assembly. So far, the progress in identifying glycosyltransferases involved in the biosynthesis of pectin has been modest. Of the many pectic glycosyltransferase activities predicted to be needed (Mohnen 2008), only three have been identified and verified biochemically by heterologous expression and in vitro assays, namely a homogalacturonan synthase (GAUT1, Sterling et al. 2006), an RG-II xylosyl transferase (RGXT1, RGXT2, and RGXT3, Egelund et al. 2006, 2008) and a xylogalacturonan xylosyltransferase (XGD1, Jensen et al. 2008). In addition, a putative arabinan arabinosyltransferase (ARAD1, Harholt et al. 2006) and a group of putative homogalacturonan synthases (QUA1, GAUT, Bouton et al. 2002; Caffall et al. 2009) have been identified based on mutant characterisation. Several of the *gaut* mutants show pleiotropic effects in other aspects of cell wall biosynthesis, but it is likely that some besides GAUT1 function as homogalacturonan synthases (Orfila et al. 2005; Caffall et al. 2009). ARAD1 has a close homolog in Arabidopsis designated ARAD2, and because *arad1* mutants have residual arabinan and ARAD1 and ARAD2 appear to be paralogs with a single common ortholog in rice, we hypothesized that ARAD1 and ARAD2 could be redundant proteins (Harholt et al. 2006). Pectin biosynthesis has recently been thoroughly reviewed (Scheller et al. 2007; Mohnen 2008; Caffall and Mohnen 2009; Harholt et al. 2010; Liepman et al. 2010).

The formation of complexes involved in pectin biosynthesis has been proposed by several authors (Scheller et al. 2007; Mohnen 2008; Ralet et al. 2008). It has furthermore been found that arabinose is incorporated into arabinose-containing polymers from the unstable and energetically unfavorable furanose configuration of UDP-arabinose (Konishi et al. 2006, 2007; Rautengarten et al. 2011). This form of UDP-arabinose is barely detectable in plants suggesting that UDP-arabinofuranose is strongly channeled, i.e. the mutase that makes the conversion of the pyranose to the furanose form is delivering the product directly to the arabinosyltransferase. This close association of the enzymatic steps in arabinosylation suggests that the enzymes are present in a complex.

Evidence that suggests complex formation in other aspects of cell wall biosynthesis has been presented. The cellulose synthase complex is well known (Taylor et al. 2000) and complexes involved in xylan biosynthesis have recently been reported (Zeng et al. 2010). Zeng et al, co-immunoprecipitated a non-covalently linked complex, consisting of at least three glycosyltransferases including the UDP-arabinose mutase and showed that the complex had xylan biosynthetic activity (Zeng et al. 2010). Very recently, a protein complex involved in homogalacturonan biosynthesis was reported (Atmodjo et al. 2011).

Complex formation by type-II Golgi-localized glycosyltransferases is known from the mammalian biosynthesis of *N*-linked glycoproteins where several of the glycosyltransferases have been shown by reducing and non-reducing SDS-PAGE analysis to form homo- and heterodimers by disulfide bridges (El-Battari et al. 2003; Hassinen et al. 2010). This complex formation apparently functions as part of a retention signal decreasing the secretion to the extracellular space, facilitates autoglycosylation or enhances activity (McCormick et al. 2000; El-Battari et al. 2003).

Here evidence for dimerisation through disulfide bridge formation between transiently expressed ARAD proteins is presented using bimolecular fluorescence complementation (BiFC), Förster resonance energy transfer (FRET) and non-reducing SDS-PAGE. Furthermore, mutant analysis by sugar composition analysis and immunolabelling show that ARAD2 is associated with arabinan biosynthesis and is clearly not redundant with ARAD1.

Materials and methods

35S DNA constructs used for complementation experiments, BiFC analysis and FRET

The coding region of *ARAD2* was amplified from the cDNA clone U13094 (TAIR accession Clone:1005797675) with primers 5′-GAGCTCATGAACCCCAAAATC AGA AAA-3′ and 5′-GAGCTCTTACTAGACACCATGGAT GA-3′ using Phusion polymerase (Finnzymes). The PCR product was cloned as a SacI/SacI fragment under the control of the 35S promoter and terminator in pPS48 (Kay et al. 1987) and checked for correct insert orientation by ClaI digestion, resulting in pPZP88.

When generating the ARAD1-Myc-6xHis and the ARAD1-GFP constructs the coding region of *ARAD1* was amplified from the cDNA clone OAO233 (TAIR accession 2337050) with the 5′ primer 5′-GTCCGGAGCTCATGGC GCGTAAATCTTC-3′ and with the 3′ primer 5′-GTCCGG AGCTCAATGGAAGTGATAAGACCG-3′ using Phusion polymerase. This PCR product was cloned as a SacI/SphI fragment under the control of the 35S promoter and terminator in two derivatives of pPS48, pPS-Myc-his and pPS-GFP, resulting in pJJ23 and pJJ26, respectively. pPS-GFP was generated by cloning GFP from pEGFP (Clontech) into pPS48 as a SacI/XhoI fragment using PCR and the primers 5′-GTCCGGAGCTCATGGTGAGCAAG GGCG-3′ and 5′-GTCCGCTCGAGTTACTTGTACAGCT CGTCCATGC-3′. pPS-Myc-his was generated by cloning Myc-his from pPICZα (Invitrogen) into pPS48 as a SacI/SphI fragment using PCR and the primers 5′-GTCCGGA GCTCGCGGAACAAAAACTCATCTCAGAAG-3′ and 5′-GACATGCATGCGCAAATGGCATTCTGACATCC-3′. All insert and vector-insert junctions were sequenced, and, subsequently, XbaI fragments of pPZP88, pJJ23, pJJ26 and pPS-GFP containing the CaMV 35S cassette with the respective inserts (*35S::ARAD2, 35S::ARAD1-Myc-6xHis, 35S::ARAD1-GFP* and *35S::GFP*) were transferred to pPZP221 (Hajdukiewicz et al. 1994).

Recombinant fusion proteins with fluorescent proteins (YFP, Yn, Yc, see below) were made following the USER cloning strategy as described previously (Nour-Eldin et al. 2006; Sakuragi et al. 2010). ARAD1 and ARAD2 C-terminal fluorescent fusion protein constructs were made in one-step cloning in pCAMBIA330035SuYFP (Jensen et al. 2008), pNB56, and pNB63, which harbor the unique USER cloning site followed by the full-length YFP, Yn and Yc coding sequences, respectively. UXS2, and MUR3 C-terminal fluorescent protein fusion constructs were made in two-step cloning (Sakuragi et al. 2010). pNB56 and pNB63 were derived from pCambia330035Su and pCambia230035Su (Nour-Eldin et al. 2006) and are kind gifts from Niels B Jensen. YFP used in this study are the followings: Venus YFP (1–238AA); Venus Yn (1–155AA), Venus Yc (156–238AA). The following primers used to amplify YFP, Yn, and Yc: nt59 and nt34; nt59 and nt35; nt61 and nt34. Recombinant fusion proteins with fluorescent proteins (CFP, YFP) for FRET studies were done using Gateway LR cloning reactions on *ARAD1* and *ARAD2* cDNA, provided by Dr. Masood Z. Hadi, Joint BioEnergy Institute, California, JBEI. Destination vectors used were the pEarleyGate 101 vector for full-length C-term YFP fusions and the pEarleyGate 102 vector for full-length C-term CFP fusions (Rual et al. 2004; Earley et al. 2006).

Oligonucleotide primers used are listed in Table 1. All inserts were verified by direct sequencing.

Subcellular localization, BiFC and FRET

Agrobacterial-mediated transient transformatioin of *N. benthamiana* leaves were carried out according to Sakuragi et al. (2010). Briefly, *Agrobacterium tumefaciens* pGV3850 C58C1 was transformed with the plasmid constructs (see above) and selected for their resistance to kanamycin 50 µg/mL, ampicillin 50 µg/mL, and rifampicin 100 µg/mL. The transformed agrobacteria cultured for 20 h at 28°C in LB liquid media were harvested and the pellets resupended in the infiltration medium (MES 10 mM, $MgCl_2$ 10 mM, acetosyringone 100 µM) to obtain the final cell density of $OD_{600} = 0.05$. Co-infiltration in *N. benthamiana* leaves of agrobacteria harboring the appropriate BiFC and FRET constructs were carried out using a syringe without needle. In BiFC studies the epidermal cell layers were observed 3, 4 and 5 days after infiltration using a Leica TCS SP2 AOBS confocal laser

Table 1 Primers used in generation of C-terminal fluorescent protein fusion constructs used in bioimaging analysis

Target	Primer name	Primer
ARAD1-forward	Nt122	*GGCTTAAU*ATGGCGCGTAAATCTTCCCT
ARAD1-reverse	JJ50	*GGTTTAAUCC*AATGGAAGTGATAAGACCGGT
ARAD2-forward	JJ61	*GGCTTAAU*ATGAACCCCAAAATCAGA
ARAD2-reverse	JJ62	*GGTTTAAUCC*GACACCATGGATGATCCC
MUR3-forward	Nt164	*GGCTTAAU*ATGTTTCCAAGGGTTTCTATG
MUR3-reverse	Nt165	*GGTTTAA*UTAAGGATCCTTAATTAAGCCTCAGCGGCTGTGTCTTATCTCTCTGCTC
UXS2-forward	Nt47	*GGCTTAAU*ATGGCGAGCGAGCTGATCAAT
UXS2-reverse	Nt48 (check)	*GGTTTAAU*TAAGGATCCTTAATTAAGCCTCAGCCTAGCTGAAGTTGTCTTGGTGGT
YFP-forward	Nt59	*GGCTTAAU*CTGGGTAGCGGTGGAATGGTGAGCAAGGGCGAGGAG
Yn- reverse	Nt35	*GGTTTAAU*TTAGGCGGTGATATAGACGTT
Yc-forward	Nt61	*GGCTTAAU*CTGGGTAGCGGTGGAATGGACAAGCAGAAGAACGGCATC
YFP-reverse	Nt34	*GGTTTAAU*TTACTTGTACAGCTCGTCCAT

Uracil-containing USER cloning linkers are shown in italics. Engineering USER cloning cassettes are underlined

scanning microscope. Excitation was with argon laser at 514 nm and the emission was detected between 520–550 nm. For FRET analysis, epidermal cell layers were observed 3 days after infiltration using Leica SP5 confocal laser scanning microscope. Quadric leaf pieces of 1 cm^2 were left in a 0.1 M PBS pH7, 4% paraformaldehyde fixation solution for 10 min and subsequently washed 2 × 10 min in water. Image acquisition was performed according to the method described by Sieben et al. (2008). The following argon laser lines were used for excitation of fluorescent proteins: 458 nm for CFP and 514 nm for YFP. The emission of CFP was detected at 465–505 nm and 525–600 nm for YFP. For spectral-FRET, CFP fluorescence was detected before and after bleaching between 460 and 595 nm with a 5-nm step size.

The acceptor (YFP) was bleached over 15 scan cycles with the 514 nm laser at maximum intensity and its emission was recorded between 525 and 600 nm. Spectral-fluorescence energy transfer was recorded by excitation of CFP at 458 nm, and detection between 475 and 595 nm. Spectrum was measured before (pre) and after (post) acceptor bleaching. The ratio between intensity of CFP (480 nm) and YFP (535 nm) was calculated pre- and postbleaching. Data were normalized towards the intensity at 595 nm.

The CFP emission was measured over five scan cycles pre- and postacceptor bleaching. Fluorescence energy transfer efficiency (FRET eff. %) was calculated as eff = (Dpost−Dpre)/Dpost, where D is short for donor. ARAD1/ARAD1: $n = 86$, 6 cells; ARAD2/ARAD2: $n = 42$, 4 cells; ARAD1/ARAD2: $n = 158$, 6 cells; ARAD2/ARAD1: $n = 56$, 5 cells; UXS2/ARAD1: $n = 65$, 5 cells; UXS2/ARAD2: $n = 65$, 5 cells (n number of Golgi vesicles analyzed in following number of cells).

Immunoblotting

ARAD1 and *ARAD2* fused to Myc-6xHis tags and full-length YFP respectively were constructed as per the cloning strategies described earlier. All tags were added to the C-terminal of ARAD1 and ARAD2. Constructs were co-expressed with p19 (Voinnet et al. 2003) in *N. benthamiana* leaves as in Jensen et al. (2008), but with $OD_{600} = 0.6$ for each of the *ARAD1* and *ARAD2* constructs and $OD_{600} = 0.1$ for the p19 construct. Two to four infiltrated leaves were harvested 2 days after infiltration. Microsomes were prepared as described (Orfila et al. 2005) with following modifications: Extraction buffer used consisted of 50 mM Tris–HCl pH 7.25, 100 mM sodium ascorbate, 400 mM sucrose, 2 mM 2-mercaptoethanol and 1 Complete Protease Inhibitor (Roche) tablet per 50 mL extraction buffer. The centrifugation conditions used were 3,000*g* in a F15 rotor (Piramoon Technologies Inc, CA, USA) for 15 min at 4°C, followed by ultracentrifugation at 113,000 g in a SW40 Ti rotor (Beckman Coulter Inc, CA, USA) for 1 h on a sucrose cushion (50 mM Tris–HCl pH 7.25, 1,400 mM sucrose, 2 mM 2-mercaptoethanol). Iodoacetamide was added to each sample to final concentration of 7 mM followed by 15 min incubation on ice to quench possible di-sulfide bridge formation. Protein content of each sample was measured by standard Bradford assay (Bradford 1976). Samples were mixed with 5 × sample buffer (0.125 M Tris–HCl pH 6.8, 20% glycerol, 4% SDS, 1% bromophenol blue) containing either no reductant or 200 mM DTT. Samples were heat treated for 10 min at either 50°C for samples containing DTT or 37°C for samples without DTT and electrophoresed on Criterion XT pre-cast 12% Bis–tris gels with MOPS buffer (Bio-Rad). Immunoblots were made using Protran nitrocellulose transfer membrane (Whatman) in a full wet Criterion blotting system (Bio-Rad). Primary antibody conditions were 1:5,000 dilution of rabbit anti-GFP antibody (A11122, Invitrogen) or 1:1,000 dilution of mouse anti-his antibody (His·Tag, Novagen). Secondary antibody conditions were 1:1,000 diluted anti-rabbit horseradish peroxidise-conjugated antibody (Dako PO217, DAKO Denmark, DK) or 1:1,000 diluted anti-mouse horseradish peroxidase-conjugated antibody (Dako PO161). Horseradish peroxidise signal were detected using a chemiluminescence detection system (Super-Signal; Pierce) according to the instructions of the manufacturer.

Plant growth conditions

Arabidopsis thaliana (L.) Heynh. plants were grown in soil with an 8 h photoperiod at 100–120 µmol photons m^{-2} s^{-1}, 20°C, 70% relative humidity and watered as necessary. To initiate bolting and synchronize stem growth plants were shifted to a 16 h photoperiod after 8 weeks growth in the 8 h photoperiod. Inflorescence stems were harvested when they were approximately 15 cm high. Secondary stems and flowers were removed before preparation of cell walls.

For the analysis of root surfaces, seeds were sterilized in 70% ethanol for 10 min, followed by 10% bleach for 20 min with shaking and then washed in sterile water. Seeds were incubated for 2 days in darkness at 4°C to promote uniform germination before growing for 7 days on solid sterile medium containing 2.2 g L^{-1} Murashige and Skoog basal medium (Duchefa Biochemie, Haarlem, The Netherlands), pH adjusted to 5.7, with 10 g L^{-1} sucrose and 9 g L^{-1} plant agar (Duchefa Biochemie, Haarlem, The Netherlands). Seedlings were grown in vertical 10 × 10 cm tissue culture dishes (Barloworld Scientific, Staffordshire, UK) with a 16 h photoperiod and at a constant temperature of 22°C.

N. benthamiana Domin. plants were grown on soil in greenhouse with supplemental light in a16 h photoperiod, 100–120 µmol photons m^{-2} s^{-1}, 25°C day/22°C night, 60% relative humidity. Seven to eight-weeks-old plants were used for the BiFC experiments.

Mutant screening

Genomic DNA from SAIL_881C10 was prepared as described in (Edwards et al. 1991). Homozygosity was verified by PCR as described by SALK (http://signal.salk.edu/tdnaprimers.2.html) using forward 5′-GTAGTTGTGT ATACCCTAGACT′-3 and reverse 5′-CGCCTCAGCCGG GTCAAAA′-3 primers with insert specific primer 5′-TA GCATCTGAATGTCATAACCAAT-3′.

Plant transformation for complementation experiments

Plants of WT and *arad1-2* were transformed with the empty pPZP221 vector or with vectors containing the *35S::ARAD2, 35S::ARAD1-Myc-6xHis, 35S::ARAD1-GFP* or the *35S::GFP* cassette by *A. tumefaciens*-mediated transformation using the *A. tumefaciens strain* PGV3850. Seeds were selected for 2 weeks on Murashige and Skoog medium containing 100 µg/mL gentamycin sulfate and subsequently transferred to soil. After 8 weeks on soil, the plants were transferred to 16 h light to induce bolting. Primary stems of five T1 primary transformants were harvested when 15–20 cm tall and used to prepare total alcohol insoluble residue (AIR) for determination of monosaccharide composition.

Cell wall preparation and sugar composition analysis

Cell walls were prepared as AIR as previously described (Fry 1988). The pectin-enriched fraction was extracted using endo-polygalacturonase and pectin methyl esterase as previously described (Harholt et al. 2006). For sugar composition analysis, AIR or pectin-enriched fraction was hydrolysed in 2 M triflouroacetic acid for 1 h at 120°C followed by quantitative analysis using HPAEC-PAD as previously described (Obro et al. 2004).

Immunofluorescence microscopy

Arabinan-directed monoclonal antibodies and the immunolabelling of Arabidopsis roots and stems have been described elsewhere (Willats et al. 1998; Verhertbruggen et al. 2009). For each antibody, at least 15 seven-day-old seedlings or 9 inflorescence stems were analyzed per genotype. The stems used for analysis (over 30 per genotypes) had an average height of 20 cm and the sections analyzed were ca. 10 cm distal from the rosette.

Results

Initial analysis of *ARAD2* included an in silico analysis of gene expression, co-expression and changes in expression level upon various treatments. As with *ARAD1*, *ARAD2* is ubiquitously expressed, but the transcript level is three- to fourfold lower than that of *ARAD1*. Neither the response viewer program in Genevestigator (Hruz et al. 2008), co-expression analysis using GeneCAT (Mutwil et al. 2008) or analysis using the AraNet probabilisitic network (Lee et al. 2010) gave any hints towards a particular function of ARAD2 or involvement in a known pathway.

ARAD proteins are involved in complex formation

ARAD1 is a putative arabinosyltransferase involved in pectin biosynthesis and was chosen as target candidate to test the hypothesis that pectic biosynthetic genes are involved in complex formation. In vivo complex formation would be difficult to identify due to low levels of expression. For example, complementation of the *arad1* phenotype could be accomplished by expression levels of ARAD1-GFP, which could not be detected using confocal laser scanning fluoresence microscopy or western blotting (data not shown). Therefore transient expression of ARAD1 in *N. benthamiana* was used as expression platform.

First, transient expression of ARAD1-YFP and ARAD2-YFP was observed at 3, 4 and 5 days following the infiltration of *N. benthamiana* leaves to evaluate the expression level and verify that the fusion proteins were efficiently targeted to Golgi stacks. A punctuate pattern of YFP fluorescence, typical of Golgi localization was observed with both fusion proteins expressed under the 35S promoter (Fig. 1a, b). The complementation experiments presented in Table 2 show that ARAD1 fusion proteins with C-terminal Myc-6xHis tag or GFP are functional. We therefore used C-terminally placed tags on ARAD1 and ARAD2.

After having ensured expression and functionality of fusion proteins, co-expression of ARAD1-Yn and ARAD1-Yc were carried out (the abbreviations Yn and Yc designate the N-terminal and C-terminal part of YFP, respectively). YFP fluorescence signals were visible until 5 days after infiltration in approximately 90% of the cells in the infiltrated area for ARAD1-Yn/ARAD1-Yc (Fig. 1e, f). The size (ca. 1 µm) and the mobility of the fluorescent signals observed are consistent with Golgi localisation.

As negative and positive control for the BiFC signals, we used UDP-Xylose synthase 2 (UXS2) and MUR3, which are known to be localized in Golgi. UXS2 operates at an early biosynthetic step common to synthesis of many different polymers; and MUR3 is a galactosyltransferase involved in xyloglucan synthesis (Madson et al. 2003;

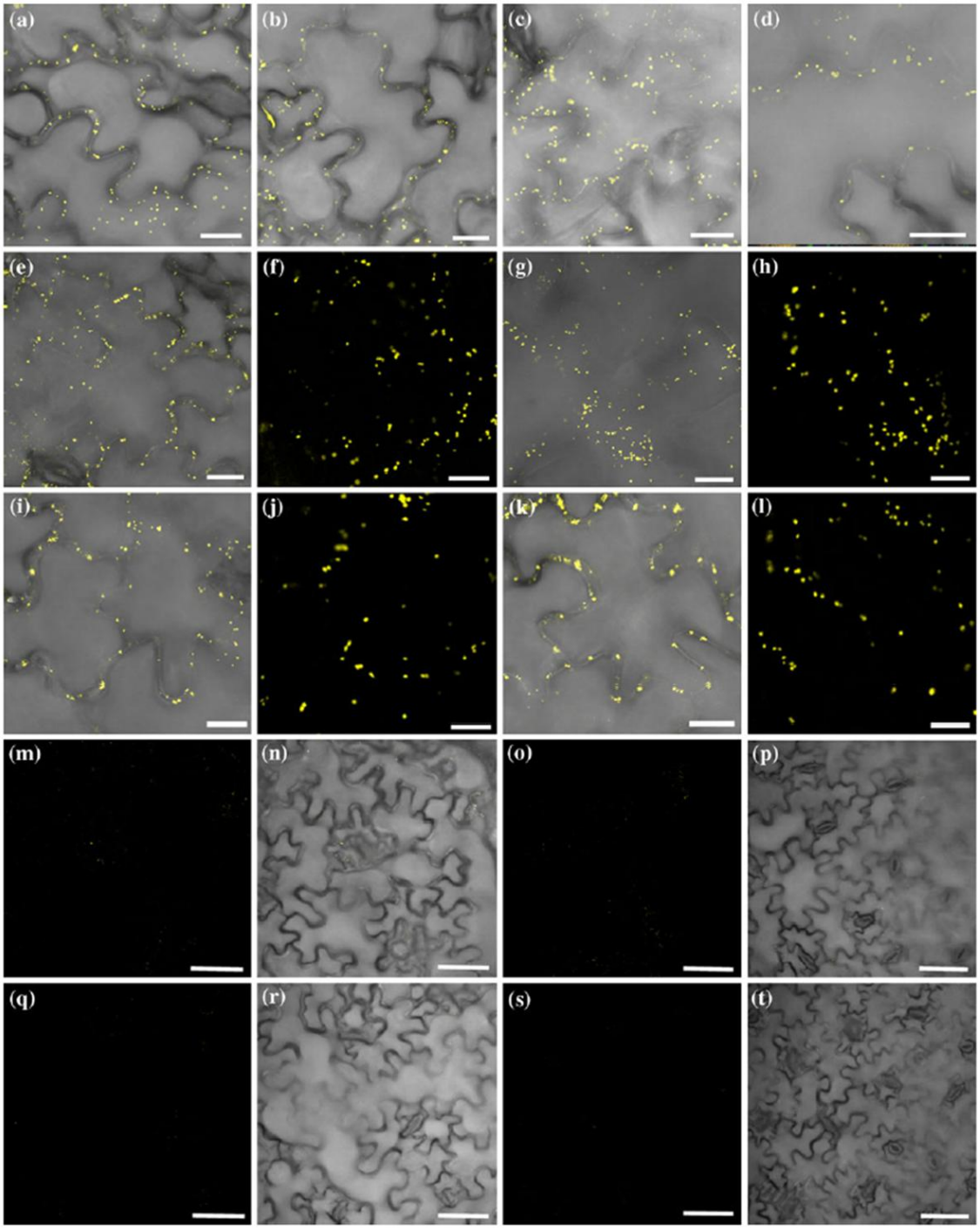
(a)
(b)
(c)
(d)
(e)
(f)
(g)
(h)
(i)
(j)
(k)
(l)
(m)
(n)
(o)
(p)
(q)
(r)
(s)
(t)

◀ **Fig. 1** Bimolecular fluorescence complementation (BiFC) with combinations of ARAD1 and ARAD2. First, Golgi localization of ARAD1-YFP (**a**) and ARAD2-YFP (**b**) was verified. Fluorescence signals typical of Golgi localization are seen following the co-expression of ARAD1-Yn/ARAD1-Yc (**e**, **f**); ARAD2-Yn/ARAD2-Yc (**g**, **h**); and ARAD1-Yn/ARAD2-Yc (**i**–**l**). The specificity of these interactions was tested using UXS2 and MUR3 as negative controls. UXS2-YFP and MUR3-YFP Golgi localization was verified (**c**, **d**). No fluorescence is observed for co-expression of ARAD1-Yn/UXS2-Yc (**m**, **n**) or ARAD2-Yn/UXS2-Yc (**q**, **r**); nor for co-expression of ARAD1-Yn/MUR3-Yc (**o**, **p**) or ARAD2-Yn/MUR3-Yc (**s**, **t**). As positive control, the interaction of UXS2-Yn/UXS2-Yc was observed (**x**) whereas UXS2-Yn (**u**) or UXS2-Yc (**v**) alone showed no fluorescence. *Scale bars* are 8 μm (**a**–**l**) or 20 μm (**m**–**t**)

Pattathil et al. 2005). Both UXS2-Yc and MUR3-Yn constructs are BiFC functional (Sakuragi et al. 2010; Søgaard et al. 2012). ARAD1-Yn (or Yc) did not complement fluorescence with UXS2-Yc (or Yn) (Fig. 1m) or MUR3-Yc (or Yn) (Fig. 1o) fusion proteins.

After establishing by BiFC that ARAD1 forms complexes with itself, ARAD2 was included in the study. It would be of interest to investigate if ARAD2 also made homocomplexes and if ARAD1/ARAD2 complexes could be observed.

Similarly to ARAD1, ARAD2 was transiently expressed in *N. benthamiana* and as with ARAD1 fluorescence typical for Golgi localisation was observed (Fig. 1b). Then combinations of ARAD1-Yn (or Yc) and ARAD2-Yn (or Yc) were expressed. Fifty percent of the cells for ARAD2-Yn/ARAD2-Yc (Fig. 1g, h), and 90% of cells for ARAD1-Yn/ARAD2-Yc (Fig. 1i, j) and ARAD2-Yn/ARAD1-Yc (Fig. 1k, l) resulted in a fluorescence signal, indicative of co-localization of ARAD1/ARAD2. As for ARAD1, ARAD2-Yn/UXS2-Yc (Fig. 1 q) and ARAD2-Yn/MUR3-Yc (Fig. 1s) co-expression did not result in detectable fluorescence. The BiFC signal between ARAD1 and ARAD2 may indicate that these proteins localized in a distinct sub-Golgi compartment that is free of MUR3 and UXS2. Alternatively, and more likely, the results may indicate that ARAD1 and ARAD2 form a complex that does not contain MUR3 nor UXS2.

In order to confirm the BiFC results, we conducted FRET analysis, where CFP as donor and YFP as acceptor were used and analyzed by acceptor photobleaching (Sieben et al. 2008).

FRET analysis for combinations of C-terminal fusion proteins with CFP and YFP as listed in Fig. 2 were conducted. Each combination was co-expressed transiently in *N. benthamiana* under 35S promoter. ARAD1-CFP and ARAD2-CFP showed a typical Golgi localization pattern, as shown for the YFP fusion proteins (Fig. 1 and data not shown). Results are summarized in Fig. 2. When the following combinations were tested: ARAD1-CFP/ARAD1-YFP; ARAD2-CFP/ARAD2-YFP; ARAD1-CFP/ARAD2-YFP; ARAD2-CFP/ARAD1-YFP (λ scan 458 nm, spectrum pre, in Fig. 2), the emission spectrum by excitation of CFP at 458 nm showed increase in peak around 535 nm which corresponds to the YFP emission. The increase of YFP emission suggested the occurrence of YFP excitation by FRET from CFP to YFP. Upon bleaching of YFP, the increase of YFP emission disappeared (λ scan 458 nm, spectrum post, in Fig. 2) and the ratio 480/535 nm (CFP/YFP) increased by 0.36, 0.31, 0.28 and 0.59, respectively. This change was most likely caused by an increase in CFP fluorescence due to reduced energy transfer from CFP to YFP as a result of YFP bleaching. Indeed, an increase of CFP emission was observed upon YFP bleaching (CFP intensity, Fig. 2) and FRET efficiency of 12–21% was observed. Overall, these results strongly indicated positive interaction in combinations of ARAD1-CFP/ARAD1-YFP; ARAD2-CFP/ARAD2-YFP; ARAD1-CFP/ARAD2-YFP; ARAD2-CFP/ARAD1-YFP.

In contrast, combinations of UXS2-CFP/ARAD1-YFP and UXS2-CFP/ARAD2-YFP did not show significant changes in YFP emission before and after bleaching of YFP (λ scan 458 nm, spectrum pre and post) and the ratio 480/535 nm (CFP/YFP) did not change significantly. The increase of CFP emission was not observed upon YFP bleaching (CFP intensity) and the FRET efficiency was calculated as −6 and −7%. These results indicated that

Table 2 Monosaccharide composition of stem or leaf AIR determined in wild-type, mutants and arad1 transformed with different construct

Genotype	Mean
Stem samples	
WT + *empty vector*	100 ± 8 a
arad1 + *35S::ARAD1-Myc-6xHis*	90 ± 6 a
arad1 + *35S::ARAD1-GFP*	72 ± 8 b
arad1 + *35S::ARAD2*	36 ± 3 c
arad1 + *35S::GFP*	33 ± 2 c
arad1 + empty vector	33 ± 3 c
Leaf samples	
WT	100 ± 5 a
arad1	57 ± 7 b
arad2	105 ± 3 a
arad1 arad2	61 ± 4 b
Pectin enriched fraction	
WT	100 ± 1 a
arad2	101 ± 1 a

The data (mean ± SD, $n = 4$) are expressed as mol% of arabinose relative to mol% of arabinose in WT. No difference in other sugars then arabinose was observed. Numbers followed by the same letter are not significantly different from same letter in same tissue or fraction analyzed (Tukey–Kramer test, $p > 0.05$)

Donor (CFP)	Acceptor (YFP)	480nm / 535nm pre bleach	480nm / 535nm post bleach	FRET eff. %	λ scan 458 nm Relative intensity / nm — Spectrum pre — Spectrum post	CFP intensity; bleach between scan cycle 5 and 6 (arrow) Relative intensity / Scan cycle
ARAD1	ARAD1	0,88	1,24	12	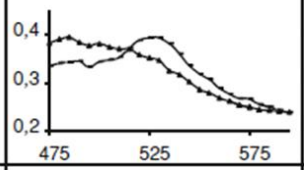	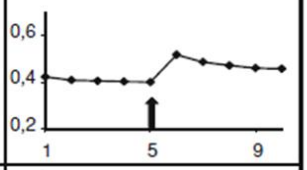
ARAD2	ARAD2	0,95	1,26	14	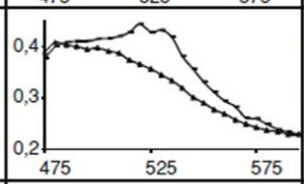	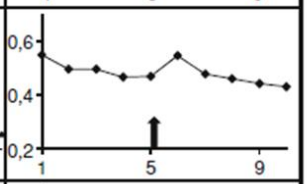
ARAD1	ARAD2	0,81	1,09	15	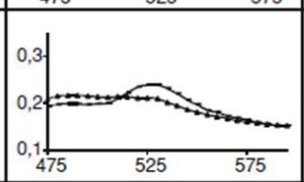	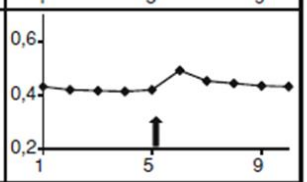
ARAD2	ARAD1	0,69	1,28	21	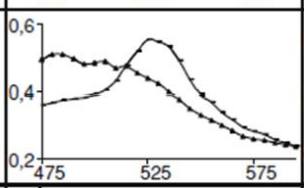	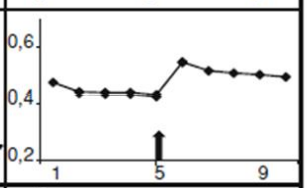
UXS2	ARAD1	1,11	1,25	-6	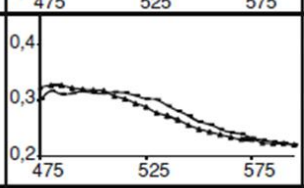	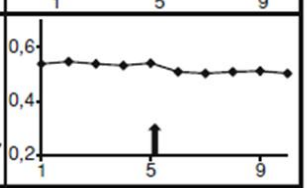
UXS2	ARAD2	1,21	1,28	-7	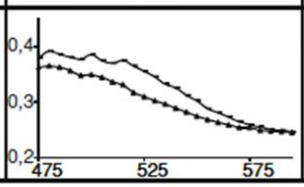	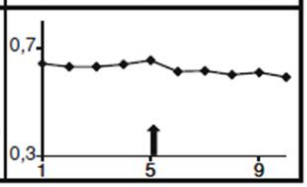

Fig. 2 FRET analysis of ARAD1, ARAD2 and ARAD1/ARAD2 interaction. Leaf epidermal cells of *N. benthamiana* co-expressing ARAD1-CFP, ARAD1-YFP, ARAD2-CFP, ARAD2-YFP, UXS2-CFP were analyzed with confocal laser scanning microscopy. Spectral-fluorescence energy transfer was recorded by excitation of CFP at 458 nm, and detection between 475 and 595 nm (λ scan 458 nm) pre- and postbleaching of acceptor (YFP). The ratio between intensity of CFP (480 nm) and YFP (535 nm) was calculated pre- and postbleaching. The CFP emission was also measured pre- and postacceptor bleaching (indicated by arrowhead) and fluorescence energy transfer efficiency (FRET eff. %) was calculated. FRET was observed for all combinations of ARAD1 and ARAD2, as opposed to the control UXS2 ARAD1 or ARAD2 combination. Number of Golgi vesicles analyzed >42 from more than four different cells

no interaction occurred between UXS2 and ARAD1 or ARAD2. In conclusion, these results provide a second set of evidence for the ability of ARAD1 and ARAD2 to form homodimers and heterodimers.

Alignments of the proteins in CAZy family GT47 showed two conserved cysteines in the C-terminus in four out of the eight Arabidopsis proteins in subgroup B, namely ARAD1, ARAD2, At5g16890 and At1g34270.

These proteins form their own subclade distinct from the remaining four proteins in the clade based on overall amino acid sequence similarity. This observation and the known involvement of disulfide bridges in establishing glycosyltransferase complexes in mammalian N-linked protein glycosylation led us to consider that the protein–protein interactions observed with BiFC could involve disulfide bridges. To investigate this possibility, microsomes were prepared from *N. benthamiana* transiently expressing ARAD1-Myc-6xHis and ARAD2-YFP and the microsomes were subjected to SDS-PAGE under reducing and non-reducing conditions. The tagged proteins were subsequently visualized by immunoblotting (Fig. 3). Under reducing conditions (+DTT) a single band of YFP or Myc-6xHis tagged protein was observed. The apparent molecular masses are ~ 5–10 kDa larger than the calculated molecular mass of ARAD2-YFP (75 kDa) and ARAD1-Myc-6xHis (53 kDa), most likely due to glycosylation of the proteins. Under non-reducing conditions (-DTT) and using anti-GFP antibody in the western blotting procedure two bands with apparent masses of approximately 150 and 170 kDa could be observed. These bands are consistent with heterodimerisation of ARAD2-YFP and ARAD1-Myc-6xHis (150 kDa band) and homodimerisation of ARAD2-YFP (170 kDa band). Development of the immunoblots with anti-His-tag antibody revealed the same 150 kDa band ascribed to the ARAD2-YFP and ARAD1-Myc-6xHis heterodimer and showed a 115 kDa band corresponding to the ARAD1-Myc-6xHis homodimer. While the presence of additional proteins in the complexes cannot be excluded, the observed molecular masses are consistent with dimers consisting only of ARAD1 and/or ARAD2.

ARAD2 is not functionally redundant with ARAD1

Redundant activities for ARAD1 and ARAD2 have previously been suggested (Harholt et al. 2006). To investigate this we identified a mutant line with a T-DNA insert located in the third and last exon of the *ARAD2* gene, designated *arad2*. The *arad2* mutant did not exhibit any noticeable morphological or developmental phenotype. Monosaccharide composition analysis of cell walls [alcohol insoluble residue (AIR)] isolated from leaves showed no difference between wild type (WT) and *arad2* (Table 2). In order to detect possible smaller and subtler changes in the pectin of *arad2*, a pectin-enriched fraction was isolated from leaf AIR and analyzed. However, as with the total cell walls, no difference was observed in monosaccharide composition of pectin from WT and *arad2* plants (Table 2). We subsequently generated the *arad1-1 arad2* double knockout mutant and analyzed the monosaccharide composition of leaf AIR. The *arad1 arad2* mutant also did not exhibit any noticeable morphological or developmental phenotype and no effect on sugar composition was observed beyond the reduction in arabinose content observed in *arad1* (Table 2). To further investigate the possibility of redundancy and confirm the in vivo activity of fusion proteins, *arad1* was used as background for a series of transformations (Table 2). We have previously shown that *ARAD1* driven by the 35S promoter will complement the *arad1* phenotype (Harholt et al. 2006). However, when *ARAD2* was expressed under control of the 35S promoter no complementation of the *arad1* phenotype could be observed. On the other hand, when *ARAD1* was introduced, this time either with a Myc-6xHis tag or GFP

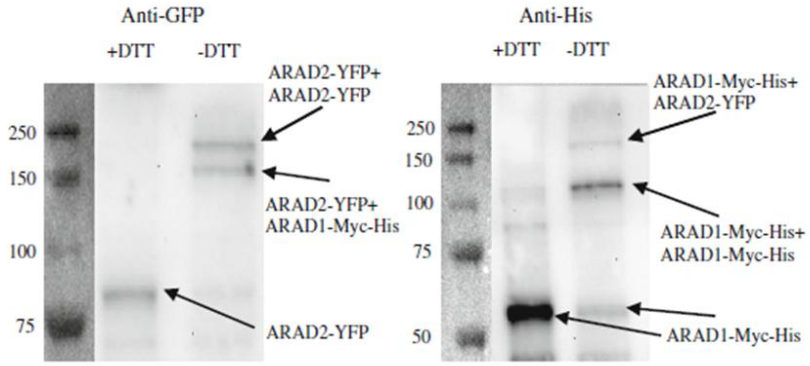

Fig. 3 Visualisation of ARAD1 and ARAD2 dimers by immunodetection. Microsomal preparations from *N. benthamiana* transiently expressing different combinations of ARAD1-Myc-6xHis tag and ARAD2-YFP was subjected to SDS-PAGE under reducing (+DTT) or non-reducing (−DTT) conditions before transfer onto nitrocellulose. Blots were incubated with anti-GFP primary antibody (*left hand panel*) or anti-His primary antibody (*right hand panel*) as indicated. Note that homo-dimerisation of ARAD1 (130 kDa) or ARAD2 (170 kDa) and hetero-dimerisation ARAD1 and ARAD2 (150 kDa) were only observed under non-reducing conditions. Under reducing conditions only monomeric forms of ARAD1 (60 kDa) and ARAD2 (85 kDa) was observed. Identified bands are marked by *arrows* and suggested composition of the proteins in the bands is indicated

fused to the C-terminus, the *arad1* phenotype was reverted to WT or near to WT as seen previously with the non-modified version of ARAD1 (Harholt et al. 2006).

ARAD2 is associated with arabinan biosynthesis

In order to investigate arabinan structure and abundance in *arad2* at a cellular level, we used immunolabelling with arabinan-specific monoclonal antibodies. The immunodetection of epitopes at intact root surfaces is a rapid and sensitive method, which has previously shown differences in epitope distribution between WT and genetically modified Arabidopsis seedlings (McCartney et al. 2003; Nguema-Ona et al. 2006). The intact root surfaces of 7-day-old seedlings of Arabidopsis WT, *arad1*, *arad1 arad2*, *arad2* and *arad2::35S::ARAD2* seedlings were studied with four monoclonal antibodies directed to epitopes associated with arabinan polysaccharides: LM6, LM13, LM16 and LM17 (Willats et al. 1998; Verhertbruggen et al. 2009). No differences in epitope detection were observed between WT and the mutants when immunolabeled with LM6, LM16 or LM17 (data not shown). LM6 and LM17 both recognize short chains of 1,5-linked arabinans and LM16 is proposed to bind to an epitope that relates to processed arabinan and that incorporates an attached galactosyl residue (Verhertbruggen et al. 2009). In contrast, immunolabelling with LM13, a monoclonal antibody that recognizes longer, unbranched regions of arabinans (Verhertbruggen et al. 2009), indicated changes in its epitope distribution in *arad2* when compared to WT, whereas *arad1* or *arad1 arad2* did not.

In WT, *arad1* and *arad1 arad2*, LM13 did not bind to the proximal meristematic zone/elongation zone of roots (Fig. 4). In contrast, a quite distinct occurrence of the LM13 epitope was observed at the proximal meristematic zone/elongation zone surface of the majority of *arad2* roots (Fig. 4). The proximal meristematic zone and the elongation zone corresponds to the region of cell division and maturation (Dolan et al. 1993). When the *arad2* mutation was complemented with *35S::ARAD2*, the LM13 epitope was not detected at the proximal meristematic zone/elongation zone of the roots, confirming that the alteration observed was due to the *arad2* mutation.

To extend the results obtained on intact root surfaces, immunolabelling with LM6, LM13, LM16 and LM17 was assessed on transverse sections of inflorescence stems (Fig. 5). No differences between WT and the *arad* mutants were observed when immunolabeled with LM6, LM16 and LM17. In contrast, the occurrence of the LM13 epitope was affected by the mutations. The LM13 antibody has been shown to be specific to epidermal cell walls in inflorescence stems (Verhertbruggen et al. 2009) and no difference of epitope detection was observed between WT and *arad2* (Fig. 5a, c). In contrast, the LM13 epitope was reduced in

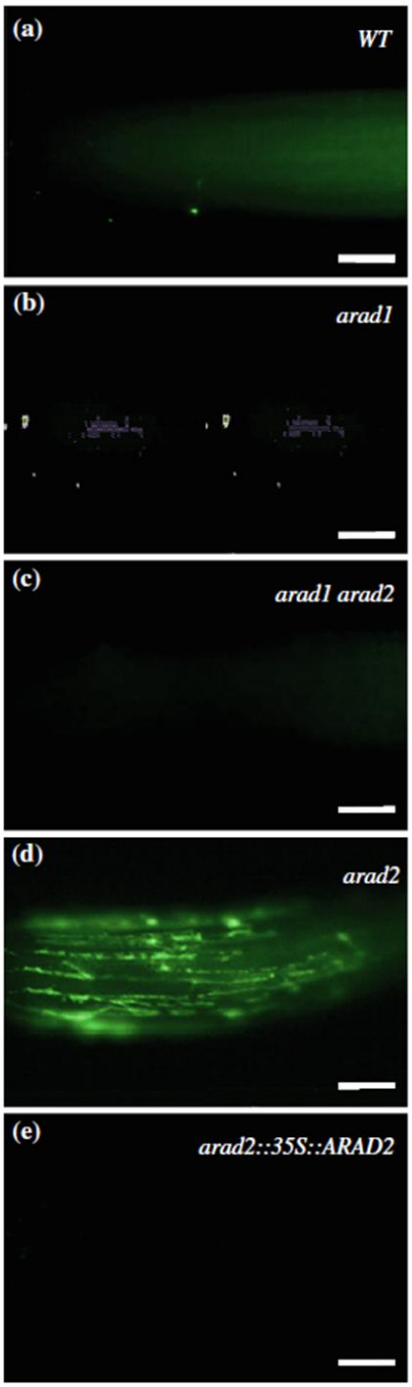

Fig. 4 Indirect immunofluorescence detection of the LM13 epitope at surface of proximal meristematic zone/elongation zone of roots. Indirect immunofluorescence detection of the LM13 arabinan epitope at surface of proximal meristematic zone/elongation zone of roots from seedlings of WT, *arad1*, *arad2*, *arad1 arad2*, and *arad2* complemented with *35S::ARAD2*. *Scale bars* = 50 µm

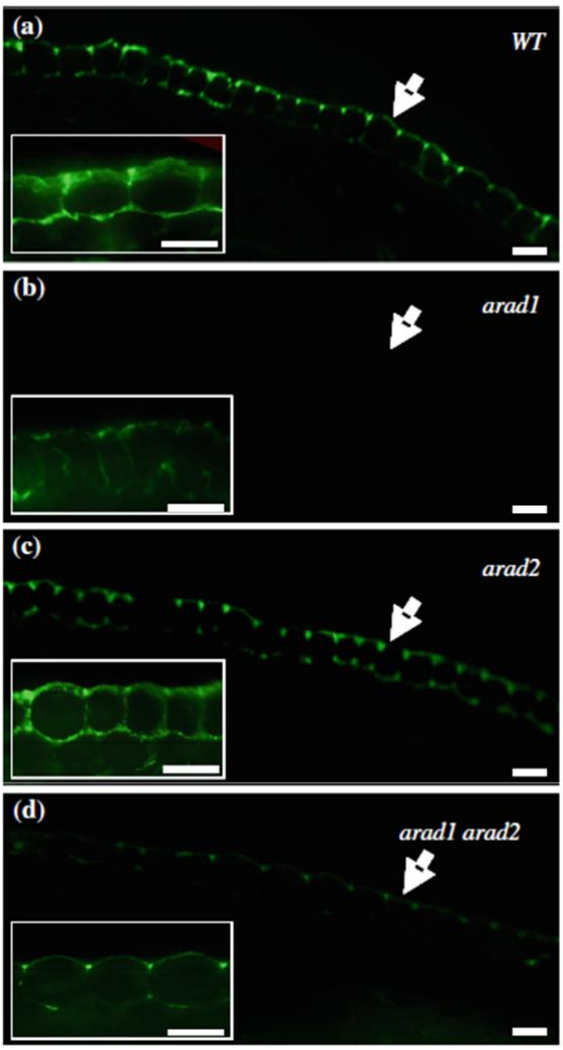

Fig. 5 Indirect immunofluorescence detection of the LM13 epitope in stem sections. Indirect immunofluorescence detection of the LM13 arabinan epitope in equivalent stem (middle of the stem) sections of WT, *arad1*, *arad2*, and *arad1 arad2*. *Arrows* indicate the outer edge of the stem. Higher magnification micrographs of epidermal cells (inserted) show details of the LM13 epitope occurrence in epidermal cell walls. *Scale bars* = 20 μm

the epidermal cell walls of *arad1* and *arad1 arad2* (Fig. 5b, d). An analysis of the *arad1* mutant stem sections under higher magnification showed that the LM13 epitope was still present in the epidermal cell walls of *arad1* but at a much lower level compared to WT (Fig. 5b insert). Notably, the LM13 epitope occurrence in *arad1 arad2* stem epidermal cell walls was not equivalent to that observed for *arad1*. The detection of the LM13 epitope was not as reduced as in *arad1* and in contrast to *arad1* in the double mutant the LM13 epitope was specifically detected in outer tangential epidermal cell walls and was relatively abundant in the intercellular regions between these cell walls (Fig. 5d).

Discussion

Three different methods, BiFC, FRET and non-reducing SDS-PAGE, consistently showed interaction between ARAD1 and ARAD2 both as homodimers and heterodimers. ARAD1/ARAD1, ARAD1/ARAD2 and ARAD2/ARAD2 split-YFP combinations resulted in the excitation of the fluorochrome (Fig. 1). The absence of fluorescence when the interaction of ARAD proteins was tested with UXS2 and MUR3 supported the possible dimerisation between the ARAD proteins as these controls did not show any false positive. BiFC can therefore be a useful technique to investigate protein–protein interaction between Golgi membrane proteins. Moreover, the results obtained by BiFC were confirmed by FRET. Both techniques demonstrated that proteins involved in the biosynthesis of pectins can form complexes.

Interaction between glycosyltransferases through intermolecular disulfide bridges is known from mammalian cells (El-Battari et al. 2003; Hassinen et al. 2010) and has been suggested for homogalacturonan synthase in plants (Atmodjo et al. 2011). Given the presence of conserved cysteine residues in the ARAD1 and ARAD2 proteins, we hypothesized that disulfide bridges could also be present in these proteins, and that was confirmed by non-denaturing SDS-PAGE and immunoblotting. Transient expression of the ARAD proteins in *N. Benthamiana* has its limitations since the proteins are overexpressed. Ideally, native promotors and stable transformants should be used to regulate the expression of tagged proteins, as done for instance for UDP-arabinose mutases (Rautengarten et al. 2011). Unfortunately, due to low levels of expression of ARAD1 and ARAD2, we were not able to investigate the protein–protein interaction under native conditions.

The physiological function of the ARAD complexes cannot be deduced from the interaction experiments. We have previously proposed that glycosyltransferases may work in a multifunctional way such that their acceptor specificities are affected by other proteins or compounds, for instance by protein–protein interactions (Scheller et al. 2007). Additionally, an increase in catalytic turnover could be suggested as reason for the complex formation, as observed in EXT1 and EXT2 complexes in animals (McCormick et al. 2000). Another role of complex formation could be to control retention in the Golgi, as reported for glycosyltransferases involved in mammalian *N*-glycosylation (El-Battari et al. 2003) and homogalacturonan biosynthesis (Atmodjo et al. 2011). In order to investigate these hypotheses an assay for arabinan

arabinosyltransferase activity using heterologously expressed proteins is required. We have so far been unsuccessful in developing such assays for ARAD1 and ARAD2. Expression of the proteins in *N. benthamiana* or in *Pichia pastoris* and using a well-established assay for arabinan synthesis (Konishi et al. 2006) did not enable us to detect significant activity (unpublished results).

From the in silico analysis of *ARAD2* it could be concluded that the expression of this gene is low and ubiquitous. No clear co-expression with other known or putative cell wall related genes could be observed. The monosaccharide composition analysis of *arad2* cell walls did not show any difference in cell wall composition. The double knock out *arad1 arad2* had a content of arabinose in the cell walls and in isolated pectin comparable to *arad1* and the overexpression of *ARAD2* in *arad1* using *35S::ARAD2* did not complement the arabinose deficiency (Table 2). Therefore, we conclude that ARAD2 is not functionally redundant with ARAD1.

Monosaccharide composition analysis has some limitations as all information relating to cell context is absent and arabinose is incorporated into several different cell wall polymers. Therefore further investigations were done using a series of monoclonal antibodies directed to pectic arabinans. The modulation of the LM13 epitope, which indicates a subset of arabinan polymers with longer, unsubstituted stretches of arabinan, revealed several subtle but clear differences in response to the *arad1* and *arad2* mutations.

The immunolabelling of intact root surfaces showed a novel pattern of LM13 labeling in *arad2*. In stem epidermal cell walls no difference could be observed between WT and *arad2*, but *arad1* and *arad1 arad2* showed differing LM13 labeling compared to WT. This may reflect the expression of redundant proteins in the stem or simply indicates that ARAD2 has a minor role in the synthesis of arabinans in that particular organ. The observations of the LM13 epitope at root surfaces suggest that ARAD2 requires ARAD1 for proper functionality. LM13 recognizes an unsubstituted arabinan epitope, thus it may be conceivable that ARAD1 synthesizes the arabinan backbone, which can subsequently be modified by ARAD2 directly or indirectly via another glycosyltransferase, e.g. by adding lateral chains. In the stem, the reduction of LM13 epitope occurrence in the double mutant was not as severe as observed for *arad1*. Here, the disruption of *ARAD2* in the *arad1* mutant background seemed to partially restore the loss of LM13 epitope occurrence produced by inactivation of ARAD1. Presumably, this reflects the presence of other glycosyltransferases involved in synthesis of arabinan. The *arad1* and the *arad1 arad2* mutants still contain about 50% of the wild type level of pectic arabinan in the leaves (Harholt et al. 2006; Table 2). Perhaps ARAD2 is also modulating the activity of other arabinan biosynthetic glycosyltransferases. Future investigation should isolate additional proteins associated with arabinan biosynthesis and study their interactions with ARAD proteins to increase our understanding of the dynamics of arabinan biosynthesis.

The immunolabelling observations support the developing understanding that the structures of arabinan polysaccharides are highly dynamic in plant cell walls. The functional implications of the extensive modulation of arabinan structures and substructures in relation to cell status and cell type are far from clear.

Conclusions

Transient overexpression of ARAD1 and ARAD2 in planta results in formation of homo- and heterodimers facilitated by interactions labile to reducing conditions, suggested to be disulfide bridges. Both ARAD1 and ARAD2 are associated with arabinan biosynthesis and are not redundant.

Acknowledgments We thank Dr. Niels B. Jensen for providing materials and technical advice. Dr. Maor Bar-Peled is thanked for providing UXS2 cDNA. Jesse Lee Walker is thanked for technical assistance. Imaging data were achieved at the Center for Advanced Bioimaging (CAB) Denmark, University of Copenhagen. This work was supported by The Villum Kann Rasmussen Foundation through the VKR Research Centre "Pro-Active Plants" [to JH, CS, CPP, NG, YS and HVS]; Danish Council for Independent Research [to CPP, YS, JKJ and HVS]; U. S. Department of Energy, Office of Science, Office of Biological and Environmental Research [DE-AC02-05CH11231 to YV and HVS]; 6th Framework Program of the European Commission, Marie Curie RTN 'WallNet' [MRTN-CT-2004-512265 to YV, JPK and HVS]; 7th Framework Program of the European Commission, large scale integrating project "Renewall" [project no. 211982 to NG]; DOE Great Lakes Bioenergy Research Center [DE-FC02-07ER64494 to JKJ]; University of Rouen, the French ministry for research and higher education [to SB and AD]; and by the regional council research network "VATA" of Haute Normandy [to SB and AD].

References

Atmodjo MA, Sakuragi Y, Zhu X, Burrell A, Mohanty SS, Atwood JA, Orlando R, Scheller HV, Mohnen D (2011) GAUT1:GAUT7 are the core of a pectin biosynthetic homogalacturonan: galacturonosyl-transferase complex. Proc Natl Acad Sci USA 108:20225–20230

Bouton S, Leboeuf E, Mouille G, Leydecker MT, Talbotec J, Granier F, Lahaye M, Hofte H, Truong HN (2002) Quasimodo1 encodes a putative membrane-bound glycosyltransferase required for normal pectin synthesis and cell adhesion in Arabidopsis. Plant Cell 14:2577–2590

Bradford MM (1976) Rapid and sensitive method for quantitation of microgram quantities of protein utilizing principle of protein-dye binding. Anal Biochem 72:248–254

Caffall KH, Mohnen D (2009) The structure, function, and biosynthesis of plant cell wall pectic polysaccharides. Carbohydr Res 344:1879–1900

Caffall KH, Pattathil S, Phillips SE, Hahn MG, Mohnen D (2009) *Arabidopsis thaliana* T-DNA mutants implicate GAUT genes in the biosynthesis of pectin and xylan in cell walls and seed testa. Mol Plant 2:1000–1014

Dolan L, Janmaat K, Willemsen V, Linstead P, Poethig S, Roberts K, Scheres B (1993) Cellular-organization of the *Arabidopsis-thaliana* root. Development 119:71–84

Earley, Keith, Jeremy R. Haag, Olga Pontes, Kristen Opper, Tom Juehne, Keming Song, and Craig S. Pikaard (2006). Gateway-compatible vectors for plant functional genomics and proteomics. Plant J 45:616–629

Edwards K, Johnstone C, Thompson C (1991) A simple and rapid method for the preparation of plant genomic DNA for PCR analysis. Nucleic Acids Res 19:1349

Egelund J, Petersen BL, Motawia MS, Damager I, Faik A, Olsen CE, Ishii T, Clausen H, Ulvskov P, Geshi N (2006) *Arabidopsis thaliana RGXT1* and *RGXT2* encode Golgi-localized (1,3)-alpha-D-xylosyltransferases involved in the synthesis of pectic rhamnogalacturonan-II. Plant Cell 18:2593–2607

Egelund J, Damager I, Faber K, Olsen CE, Ulvskov P, Petersen BL (2008) Functional characterisation of a putative rhamnogalacturonan II specific xylosyltransferase. FEBS Lett 582:3217–3222

El-Battari A, Prorok M, Angata K, Mathieu S, Zerfaoui M, Ong E, Suzuki M, Lombardo D, Fukuda M (2003) Different glycosyltransferases are differentially processed for secretion, dimerization, and autoglycosylation. Glycobiology 13:941–953

Fry SC (1988) The growing plant cell wall: Chemical and metabolic analysis. Longman Scientific and Technical, Harlow

Hajdukiewicz P, Svab Z, Maliga P (1994) The small, versatile PPZP family of agrobacterium binary vectors for plant transformation. Plant Mol Biol 25:989–994

Harholt J, Jensen JK, Sorensen SO, Orfila C, Pauly M, Scheller HV (2006) ARABINAN DEFICIENT 1 is a putative arabinosyltransferase involved in biosynthesis of pectic arabinan in Arabidopsis. Plant Physiol 140:49–58

Harholt J, Suttangkakul A, Scheller HV (2010) Biosynthesis of pectin. Plant Physiol 153:384–395

Hassinen A, Rivinoja A, Kauppila A, Kellokumpu S (2010) Golgi N-Glycosyltransferases form both homo- and heterodimeric enzyme complexes in live cells. J Biol Chem 285:17771–17777

Hruz T, Laule O, Szabo G, Wessendorp F, Bleuler S, Oertle L, Widmayer P, Gruissem W, Zimmermann P (2008) Genevestigator V3:a reference expression database for the meta-analysis of transcriptomes. Adv Bioinformatics 2008:20747

Jensen JK, Sorensen SO, Harholt J, Geshi N, Sakuragi Y, Moller I, Zandleven J, Bernal AJ, Jensen NB, Sorensen C, Pauly M, Beldman G, Willats WGT, Scheller HV (2008) Identification of a xylogalacturonan xylosyltransferase involved in pectin biosynthesis in Arabidopsis. Plant Cell 20:1289–1302

Kay R, Chan A, Daly M, Mcpherson J (1987) Duplication of camv-35S promoter sequences creates a strong enhancer for plant genes. Science 236:1299–1302

Konishi T, Ono H, Ohnishi-Kameyama M, Kaneko S, Ishii T (2006) Identification of a mung bean arabinofuranosyltransferase that transfers arabinofuranosyl residues onto (1, 5)-linked alpha-L-arabino-oligosaccharides. Plant Physiol 141:1098–1105

Konishi T, Takeda T, Miyazaki Y, Ohnishi-Kameyama M, Hayashi T, O'Neill MA, Ishii T (2007) A plant mutase that interconverts UDP-arabinofuranose and UDP-arabinopyranose. Glycobiology 17:345–354

Lee I, Ambaru B, Thakkar P, Marcotte EM, Rhee SY (2010) Rational association of genes with traits using a genome-scale gene network for *Arabidopsis thaliana*. Nat Biotechnol 28:149–U14

Liepman AH, Wightman R, Geshi N, Turner SR, Scheller HV (2010) Arabidopsis: a powerful model system for plant cell wall research. Plant J 61:1107–1121

Madson M, Dunand C, Li X, Verma R, Vanzin GF, Caplan J, Shoue DA, Carpita NC, Reiter WD (2003) The MUR3 gene of Arabidopsis encodes a xyloglucan galactosyltransferase that is evolutionarily related to animal exostosins. Plant Cell 15:1662–1670

McCartney L, Steele-King CG, Jordan E, Knox JP (2003) Cell wall pectic (1 - >4)-beta-D-galactan marks the acceleration of cell elongation in the Arabidopsis seedling root meristem. Plant J 33:447–454

McCormick C, Duncan G, Goutsos KT, Tufaro F (2000) The putative tumor suppressors EXT1 and EXT2 form a stable complex that accumulates in the Golgi apparatus and catalyzes the synthesis of heparan sulfate. Proc Natl Acad Sci USA 97:668–673

Mohnen D (2008) Pectin structure and biosynthesis. Curr Opin Plant Biol 11:266–277

Mutwil M, Obro J, Willats WGT, Persson S (2008) GeneCAT: novel webtools that combine BLAST and co-expression analyses. Nucleic Acids Res 36:W320–W326

Nguema-Ona E, Andème-Onzighi C, Aboughe-Angone S, Bardor M, Ishii T, Lerouge P, Driouich A (2006) The *reb1-1* mutation of Arabidopsis. Effect on the structure and localization of galactose-containing cell wall polysaccharides. Plant Physiol 140(4): 1406–1417

Nour-Eldin HH, Hansen BG, Norholm MHH, Jensen JK, Halkier BA (2006) Advancing uracil-excision based cloning towards an ideal technique for cloning PCR fragments. Nucleic Acids Res 34

Obro J, Harholt J, Scheller HV, Orfila C (2004) Rhamnogalacturonan I in *Solanum tuberosum* tubers contains complex arabinogalactan structures. Phytochemistry 65:1429–1438

Orfila C, Sorensen SO, Harholt J, Geshi N, Crombie H, Truong HN, Reid JSG, Knox JP, Scheller HV (2005) *QUASIMODO1* is expressed in vascular tissue of *Arabidopsis thaliana* inflorescence stems, and affects homogalacturonan and xylan biosynthesis. Planta 222:613–622

Pattathil S, Harper AD, Bar-Peled M (2005) Biosynthesis of UDP-xylose: characterization of membrane-bound At Uxs2. Planta 221:538–548

Ralet MC, Crepeau MJ, Lefebvre J, Mouille G, Hofte H, Thibault JF (2008) Reduced number of homogalacturonan domains in pectins of an Arabidopsis mutant enhances the flexibility of the polymer. Biomacromolecules 9:1454–1460

Rautengarten C, Ebert B, Herter T, Petzold CJ, Ishii T, Mukhopadhyay A, Usadel B, Scheller HV (2011) The Interconversion of UDP-Arabinopyranose and UDP-Arabinofuranose is Indispensable for Plant Development in *Arabidopsis thaliana*. Plant Cell 23:1373–1390

Rual JF, Hirozane-Kishikawa T, Hao T, Bertin N, Li S, Dricot A, Li N, Rosenberg J, Lamesch P, Vidalain PO, Clingingsmith TR, Hartley JL, Esposito D, Cheo D, Moore T, Simmons B, Sequerra R, Bosak S, Doucette-Stamm L, Le Peuch C, Vandenhaute J, Cusick ME, Albala JS, Hill DE (2004) Human ORFeome version 1.1: a platform for reverse proteomics. Genome Res 14:2128–2135

Sakuragi Y, Nørholm MHH, Scheller HV (2010) Visual mapping of cell wall biosynthesis. In: Popper ZA (ed) The plant cell wall: methods and protocols. Springer Science, Berlin

Scheller HV, Jensen JK, Sorensen SO, Harholt J, Geshi N (2007) Biosynthesis of pectin. Physiol Plant 129:283–295

Sieben C, Mikosch M, Brandizzi F, Homann U (2008) Interaction of the K(+)-channel KAT1 with the coat protein complex II coat component Sec24 depends on a di-acidic endoplasmic reticulum export motif. Plant J 56:997–1006

Søgaard C, Stenbæk A, Bernard S, Driouich A, Scheller HV, Sakuragi Y (2012) GO-PROMTO illuminates protein membrane topologies of glycan biosynthetic enzymes in the Golgi apparatus of living tissues. PLoS One (accepted)

Sterling JD, Atmodjo MA, Inwood SE, Kumar Kolli VS, Quigley HF, Hahn MG, Mohnen D (2006) Functional identification of an Arabidopsis pectin biosynthetic homogalacturonan galacturonosyltransferase. Proc Natl Acad Sci USA 103:5236–5241

Taylor NG, Laurie S, Turner SR (2000) Multiple cellulose synthase catalytic subunits are required for cellulose synthesis in Arabidopsis. Plant Cell 12:2529–2539

Verhertbruggen Y, Knox JP (2007) Pectic polysaccharides and expanding cell walls. In: Verbelen JP, Vissenberg K (eds) Plant cell monographs 5, the expanding cell. Springer-Verlag, Berlin, pp 139–158

Verhertbruggen Y, Knox JP (2009) Pectin, cell wall biology and elucidation of functions. In: Schols HA, Visser RGF, Voragen AGJ (eds) Pectin and pectinases. Wageningen Academic Publishers, Wageningen, pp 139–148

Verhertbruggen Y, Marcus SE, Haeger A, Verhoef R, Schols HA, McCleary BV, Mckee L, Gilbert HJ, Knox JP (2009) Developmental complexity of arabinan polysaccharides and their processing in plant cell walls. Plant J 59:413–425

Vincken JP, Schols HA, Oomen RJFJ, Mccann MC, Ulvskov P, Voragen AGJ, Visser RGF (2003) If homogalacturonan were a side chain of rhamnogalacturonan I. Implications for cell wall architecture. Plant Physiol 132:1781–1789

Voinnet O, Rivas S, Mestre P, Baulcombe D (2003) An enhanced transient expression system in plants based on suppression of gene silencing by the p19 protein of tomato bushy stunt virus. Plant J 33:949–956

Willats WGT, Marcus SE, Knox JP (1998) Generation of a monoclonal antibody specific to (1 - >5)-alpha-L-arabinan. Carbohydr Res 308:149–152

Zandleven J, Sorensen SO, Harholt J, Beldman G, Schols HA, Scheller HV, Voragen AJ (2007) Xylogalacturonan exists in cell walls from various tissues of *Arabidopsis thaliana*. Phytochemistry 68:1219–1226

Zeng W, Jiang N, Nadella R, Killen TL, Nadella V, Faik A (2010) A glucurono(arabino)xylan synthase complex from wheat contains members of the GT43, GT47, and GT75 families and functions cooperatively. Plant Physiol 154:78–97

Papier N°7: Article scientifique en collaboration avec Dr. Yumiko Sakuragi au sein du laboratoire de recherche « *Molecular plant biology: Cell wall* », dirigé par le Pr. Henrik Vibe Scheller, à l'université de Copenhague.

Résultats: Travaux effectués dans le cadre d'une collaboration

GO-PROMTO illuminates protein membrane topologies of glycan biosynthetic enzymes in the Golgi apparatus of living tissues.

Søgaard C, Stenbæk A, Bernard S, Hadi M, Driouich A, Scheller HV, Sakuragi Y.

PLoS One (2012) 7(2):e31324

OPEN ACCESS Freely available online

PLoS one

GO-PROMTO Illuminates Protein Membrane Topologies of Glycan Biosynthetic Enzymes in the Golgi Apparatus of Living Tissues

Casper Søgaard[1,2], Anne Stenbæk[1,2], Sophie Bernard[3], Masood Hadi[4], Azeddine Driouich[3], Henrik Vibe Scheller[5], Yumiko Sakuragi[1,2]*

1 Department of Plant Biology and Biotechnology, Faculty of Life Sciences, University of Copenhagen, Frederiksberg, Denmark, **2** Villum Kann Rasmussen Centre for ProActive Plants, Frederiksberg, Denmark, **3** Laboratoire de Glycobiologie et Matrice Extracellulaire-EA 4358, University of Rouen, Mont Saint Aignan, France, **4** Technologies Division, Joint BioEnergy Institute, Sandia National Laboratory, Emeryville, California, United States of America, **5** Feedstocks Division, Joint BioEnergy Institute, Lawrence Berkeley National Laboratory, Emeryville, California, United States of America

Abstract

The Golgi apparatus is the main site of glycan biosynthesis in eukaryotes. Better understanding of the membrane topology of the proteins and enzymes involved can impart new mechanistic insights into these processes. Publically available bioinformatic tools provide highly variable predictions of membrane topologies for given proteins. Therefore we devised a non-invasive experimental method by which the membrane topologies of Golgi-resident proteins can be determined in the Golgi apparatus in living tissues. A Golgi marker was used to construct a series of reporters based on the principle of bimolecular fluorescence complementation. The reporters and proteins of interest were recombinantly fused to split halves of yellow fluorescent protein (YFP) and transiently co-expressed with the reporters in the *Nicotiana benthamiana* leaf tissue. Output signals were binary, showing either the presence or absence of fluorescence with signal morphologies characteristic of the Golgi apparatus and endoplasmic reticulum (ER). The method allows prompt and robust determinations of membrane topologies of Golgi-resident proteins and is termed GO-PROMTO (for GOlgi PROtein Membrane TOpology). We applied GO-PROMTO to examine the topologies of proteins involved in the biosynthesis of plant cell wall polysaccharides including xyloglucan and arabinan. The results suggest the existence of novel biosynthetic mechanisms involving transports of intermediates across Golgi membranes.

Citation: Søgaard C, Stenbæk A, Bernard S, Hadi M, Driouich A, et al. (2012) GO-PROMTO Illuminates Protein Membrane Topologies of Glycan Biosynthetic Enzymes in the Golgi Apparatus of Living Tissues. PLoS ONE 7(2): e31324. doi:10.1371/journal.pone.0031324

Editor: Wanjin Hong, Institute of Molecular and Cell Biology, Singapore

Received October 3, 2011; **Accepted** January 5, 2012; **Published** February 21, 2012

This is an open-access article, free of all copyright, and may be freely reproduced, distributed, transmitted, modified, built upon, or otherwise used by anyone for any lawful purpose. The work is made available under the Creative Commons CC0 public domain dedication.

Funding: The Danish Council for Independent Research and Villum Kann Rasmussen foundation for YS. U.S. Department of Energy DE-AC02-05CH11231 for HVS. The funders had no role in study design, data collection and analysis, decision to publish, or preparation of the manuscript.

Competing Interests: The authors have declared that no competing interests exist.

* E-mail: ysa@life.ku.dk

Introduction

The Golgi apparatus is an organelle that plays a central role in the assembly of glycans associated with various macromolecules (*i.e.* matrix polysaccharides, proteins, lipids) in eukaryotic cells [1,2]. Biosynthesis of glycans requires concerted actions of enzymes and proteins including glycosyltransferases, modifying enzymes (*e.g.* methyltransferases, acetyltransferases, sulfatetransferases), nucleotide sugar transporters, and nucleotide sugar conversion enzymes, many of which are localized in the secretory pathway including endoplasmic reticulum (ER) and Golgi stacks. These enzymes and proteins must be oriented in the membrane so that the catalytic domains face the relevant sides of the membrane where the substrates are available and the products can be channeled to the enzymes and proteins in the proceeding steps during biosynthesis.

Because an experimental determination of protein membrane topology is often laborious, efforts have been directed towards bioinformatically predicting the topology of membrane proteins based on the structural and statistical evaluation of the amino acid sequences. The transmembrane domains of membrane proteins all have two common features: a hydrophobic middle section composed of mostly aliphatic amino acids [3,4] and a flanking sequence composed of aromatic amino acids, mostly tryptophan and tyrosine [5]. With the inclusion of the positive-inside rules and machine-learning techniques, a dozen of algorithms for predicting topology has been established and is widely used, including polyPhobius [6], HMMTOP [7], Prodiv-TMHMM [8], and TopPred [9].

These programs are said to correctly predict overall topologies of membrane proteins with an accuracy of ~70% [10–14]. This means approximately one out of three or four membrane topologies predicted by a program is incorrect. Furthermore, different algorithms often lead to different topological predictions for the same protein. This is partly attributed to marginally hydrophobic regions, which are not predicted as transmembrane domains by many of the predictors due to low degrees of hydrophobicity but are inserted into the membrane due to long range tertiary interactions during protein folding [15].

A range of experimental methods for examining the topology of membrane proteins in the endomembrane system of eukaryotes has been developed, each with advantages and drawbacks.

Biochemical approaches include recognition of glycosylation mapping [16], cysteine substitutions [17], and proteinase susceptibility assays [18]. These methods are invasive and require cell disruption, thus resulting in a loss of information about the subcellular localizations of the tested proteins.

Several non-invasive methods have been reported based on the use of green fluorescent protein (GFP) and its variants for detection of the topology of proteins localized in the endomembrane system in living cells. A classical biochemical protease susceptibility assay [19,20] coupled with fluorescent protein fusions was used to determine protein membrane topology in a variety of organelles including the Golgi apparatus, mitochondria, peroxisome, and autophagosomes [21]. The method has been shown to work robustly in human cell cultures; however, its applicability to intact, whole tissue samples of different biological systems has not been addressed. Bimolecular fluorescent complementation (BiFC) was used to determine the membrane orientation of N- and C-termini of a protein localized to the ER membranes in living plant tissues [22]. This method relies on cytosolic and ER lumenal reporters that detect the tagged amino acid termini if localized to the cytosol or ER lumen, respectively. pH-Dependent fluorescent intensity of yellow fluorescent protein (YFP) was used to determine the membrane topology of plasma membrane-associated proteins in plant tissues [23]. Due to the low pH values (ca. 5–6) in the apoplast, YFP fluorescence is decreased when exposed to the apoplast while a robust signal is detectable when exposed to the cytosol. The absence of signal is inferred, but not directly shown, as apoplastic localization. A redox-sensitive GFP (roGFP) has been utilized to probe the ER-localized membrane protein topology by exploiting the glutathione redox gradient across the ER membrane [24]. This method provides ratiometric outputs that distinguish the cytosolic and the ER luminal localizations of the fluorescent tags, but it requires an advanced filter setup and post-imaging processing. The application of any of these methods to Golgi lumen has not been demonstrated.

The lack of a reliable method allowing topology determinations of Golgi membrane proteins in complex living tissues prompted us to establish a method based on the BiFC system. GO-PROMTO (GOlgi PROtein Membrane TOpology analysis), produces binary signals illuminating the orientation of the N- and C-termini of the tested proteins in the Golgi apparatus. We have applied the method to determine the membrane topologies of eleven enzymes involved in the biosynthesis of cell wall polysaccharides in the higher plant Arabidopsis. The data reveal new insights into the mechanisms controlling the assembly of complex glycans within the Golgi membranes.

Results

Establishment of the GO-PROMTO method

There are four main criteria that need to be met for a topology reporter to prove robust: i) the signal-to-noise ratio must be high; ii) the topology reporter must recognize the luminal localization of protein termini of tested proteins; iii) the topology reporter must be promiscuous and recognize every tested protein; iv) the method must be simple, preferably inexpensive, and easily adapted to standard laboratories. In order to establish a method that produces excellent signal-to-noise ratio in the Golgi apparatus, we used BiFC. YFP (Venus) was split in two parts, "Yn" (amino acids 1–155 of YFP) and "Yc" (amino acids 156–238 of YFP) as previously reported [25]. The individual halves are not fluorescent, while the two parts can reconstitute if they are in the same microcompartment and emit fluorescence with a maximum peak at 535 nm upon excitation at 514 nm. Therefore the system gives either "on" or "off" output (Figure 1).

A series of topology reporters were generated by using a truncated rat sialyltransferase sequence. Sialyltransferase has the canonical type II membrane topology with N- and C-termini presented in the cytosol and the Golgi lumen, respectively. A truncated sialyltransferase consisting of the N-terminal 52 residues containing a transmembrane domain is widely used as a Golgi marker (hereafter "TMD") [26–28]. In-frame fusions of the TMD and the split YFP halves were made in order to create the GO-PROMTO topology reporters. Two with the sensor domain facing the cytosol ("cytosolic-TMD reporters"; Yn/Yc-TMD) and two lumen-oriented topology reporters with the sensor domains localized in the Golgi lumen ("lumenal-TMD reporters"; TMD-Yn/Yc).

When introduced individually into leaves of the tobacco plant *Nicotiana benthamiana* via transient transfection [29], none of these reporters alone produced detectable signals as shown in Figure 2. When expressed in combinations, the lumenal-TMD reporters

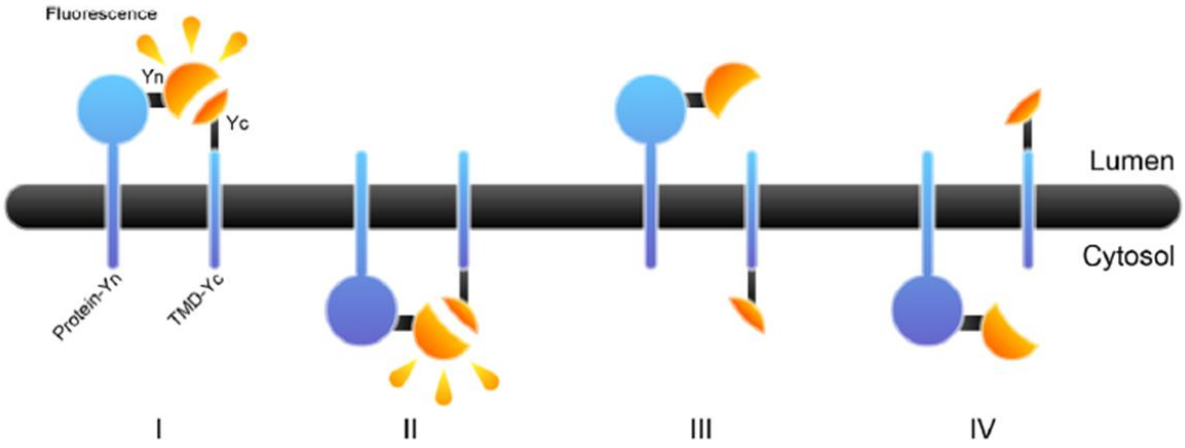

Figure 1. Illustrations of the principle of GO-PROMTO. Fluorescent complementation occurs when the two complementary domains of split YFP (Yn and Yc) fused to the test protein and TMD are present on the same side of the membrane (I and II), whereas no fluorescence occurs if they are on the opposite sides of the membrane (III and IV).
doi:10.1371/journal.pone.0031324.g001

complemented fluorescence signals characteristic of the Golgi apparatus as revealed by CLSM. Similarly, the cytosolic-TMD reporters complemented fluorescence and showed both the Golgi apparatus and ER-like signals. No complementation was observed when the lumenal- and cytosolic-TMD reporters were co-expressed. Yn and Yc without fusion proteins were included as reporters that localize in the cytosol without a membrane anchor ("cytosolic reporters"). The cytosolic reporters complemented fluorescence with the cytosolic-TMD reporters but not with the lumenal-TMD reporters under the current conditions (Figure 2). In rare occasions, we have noticed that negative interactions gave weak and sporadic positive signals if reporters were hyperexpressed and if the gain value of the microscope was set high. This could be due to a mistargeting, misinsertion, and/or flipping of these reporters across the membrane. It is noteworthy that ER signals were detectable even though the topology reporters were based on the well-defined Golgi marker, which is likely due to high-level expression of the reporters. These observations suggest that the topology reporters can be used to detect topologies of both Golgi- and ER-localized proteins.

Proteinase susceptibility assays were performed in order to validate the membrane orientation of the TMD fusion proteins.

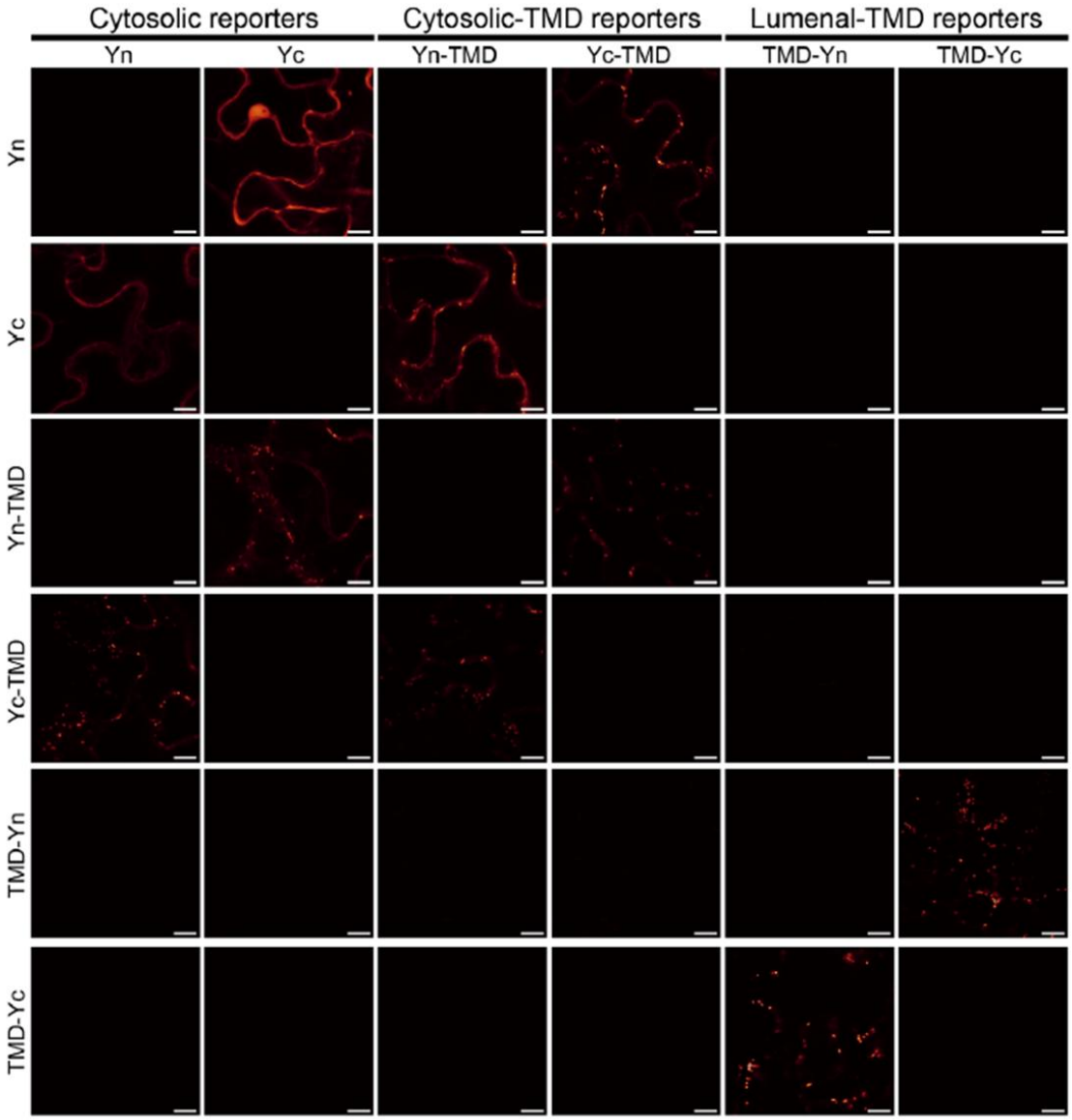

Figure 2. Fluorescence complementation among the GO-PROMTO reporters expressed in the whole leaf tissue of *Nicotiana benthamiana* at 3 days DPI. The GO-PROMTO reporters were co-expressed and fluorescence complementation was examined by CLSM upon excitation at 514 nm and detection between 529 nm and 599 nm. All scale bars indicate 10 µm. At least two individual experiments were performed for each combination with the similar results. Raw images are shown.
doi:10.1371/journal.pone.0031324.g002

TMD fused to the full-length YFP at N- and C-termini, YFP-TMD and TMD-YFP, respectively, were transiently and individually expressed in *N. benthamiana* leaves (Figure 3A). Microsomes isolated from these leaves were treated with proteinase K in the absence or presence of the detergent Triton X-100. Degradation of YFP was monitored by SDS-PAGE and immunoblotting with anti-GFP antibody which also recognizes YFP. The YFP tag in TMD-YFP was degraded by the protease only when the detergent was present, while the YFP tag in YFP-TMD was degraded regardless of the presence or absence of the detergent (Figure 3B). Untreated YFP-TMD migrated slightly faster than TMD-YFP in SDS-PAGE and an additional product with slightly lower apparent molecular mass that was resistant to proteinase K was observed. These results may indicate that the YFP tag, when localized to the cytosolic side of the membrane, is likely to be partially degraded. The combined results unequivocally demonstrate that the YFP tag localizes to the cytosol when fused to the N-terminus of TMD, whereas it localizes to the Golgi lumen when fused to the C-terminus of TMD. These results demonstrate that the reporters detect the cytosolic and lumenal orientations of the protein termini in the Golgi apparatus and ER with binary signal outputs.

Validating the robust performance of GO-PROMTO

In order to evaluate the performance of GO-PROMTO, the membrane topologies of Golgi-localized, predicted type II membrane proteins involved in cell wall polysaccharide biosynthesis in the model plant *Arabidopsis thaliana* were studied. RGXT2 is a 1,3-α-D-xylosyltransferase involved in rhamnogalacturonan II biosynthesis, whereas UXS2 is a UDP-glucuronic acid decarboxylase responsible for xylose biosynthesis. Both enzymes have been shown to localize to the Golgi apparatus by using C-terminal GFP fusions coupled to live-cell imaging [30–32]. IRX10-like (IRX10L) is a member of the GT47 glycosyltransferase family involved in xylan biosynthesis [33,34]. IRX10L has been suggested to localize to a Golgi fraction in a proteomics study [35].

The number of predicted transmembrane domains in these proteins varied considerably, between zero and three, depending on the prediction program (Figure 4). For example, TmHMM (ver. 2) predicts that RGXT2 and UXS2 contain single transmembrane domains while IRX10L contains no transmembrane domain. In contrast, TopPred (ver. 2) predicts that RGXT2 contains two transmembrane domains and IRX10L and UXS2 contain single transmembrane domains. Assuming that the N-terminus is placed in the cytosol, the presence of a single transmembrane domain would place the C-terminal catalytic domain in the Golgi lumen, whereas the absence (zero transmembrane domain) or the presence of two transmembrane domains would place it in the cytosol or at the cytosolic surface of the Golgi membrane, respectively. The cytosolic- and lumenal-TMD reporters were co-expressed with these proteins, fused with Yn and Yc at their C-termini, in order to address the membrane topology of these proteins. In all cases, fluorescence complementation was observed between the test proteins and the lumenal-TMD reporters but not between the test protein and the cytosolic-

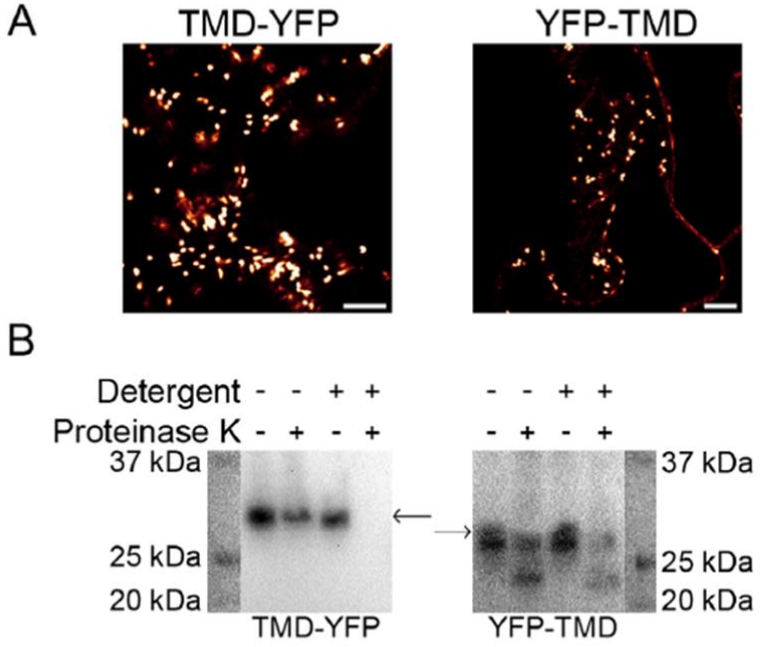

Figure 3. Proteinase protection assay of the TMD fused to YFP at the N- and C-terminus. A. TMD-YFP and YFP-TMD were transiently expressed in *Nicotiana benthamiana* whole leaves and CLSM was carried out at 3 DPI. Both fusion proteins show predominantly Golgi apparatus localization. Scale bars, 10 µm. **B.** Immunoblot analysis of the TMD-YFP and YFP-TMD after treatment with proteinase K in the presence or absence of TritonX-100. Molecular masses of TMD-YFP and YFP-TMD are estimated to be 33.8 kDa and 34.5 kDa, respectively (Compute pI/Mw server at Expasy.org). The full-length fusion proteins are indicated with the arrows. TMD-YFP is degraded only in the presence of detergent and protease indicating Golgi lumenal orientation of YFP tag. YFP-TMD was degraded regardless of detergent addition, indicating cytosolic orientation of YFP tag. Partial degradation of the YFP was observed for YFP-TMD (bands immediately below the full-length YFP). At least two individual experiments were performed for each combination with the similar results. Raw images are shown.
doi:10.1371/journal.pone.0031324.g003

GO-PROMTO

	RGXT2	IRX10L	UXS2	UGE4	XXT1	XXT2	XXT5	MUR3	ARAD1	MUR4
Alom_v2	1	1	1	0	1	1	1	1	3	1
DAS-TMfilter	2	2	1	0	1	1	1	2	3	1
Eiconda_v1	2	2	1	1	1	1	1	2	1	1
HmmTop_v2	1	1	1	0	1	1	1	1	1	3
MemSat_v3	1	0	1	0	1	1	1	1	2	1
Minnou	1	0	1	0	0	0	0	1	1	0
PHDhtm	2	1	0	0	0	0	1	2	2	0
Phobius	2	0	1	0	0	1	0	1	1	1
PredTmr_v1	2	1	1	0	1	1	1	1	1	1
S-Tmhmm_v0.9	2	1	1	0	1	1	0	2	1	0
Scampi	2	2	1	0	1	1	1	2	1	1
SosuiG_v1.1	2	2	1	0	0	0	1	1	1	0
SVMtm_v3	2	0	1	0	1	1	1	2	1	0
THUMBUP_v1	2	1	1	0	1	1	1	2	3	0
TmHMM_v2	1	0	1	0	1	1	1	1	1	0
TMMOD	2	0	1	0	1	1	0	1	1	0
TmPred	3	2	2	2	1	1	1	3	3	2
TopPred_v2	2	1	1	1	1	1	1	3	2	2

Figure 4. Prediction of the number of transmembrane domains for selected cell wall biosynthetic enzymes. The data compiled in Aramemnon (http://aramemnon.uni-koeln.de/) is summarized. Numbers indicate the number of transmembrane domains.
doi:10.1371/journal.pone.0031324.g004

TMD reporters (Figure 5). Furthermore, the fluorescence signals detected were typical of Golgi localization. These results clearly demonstrate that the C-termini of these proteins are localized to the Golgi lumen.

Next, a cytosolic protein and a multimembrane-spanning protein were tested against all six topology reporters. UGE4 is a UDP-glucose 4-epimerase and has previously been shown to be located in the cytosol [36]. As expected, UGE4-Yn did not complement fluorescence with the lumenal TMD reporters whereas it complemented fluorescence with the cytosolic TMD and soluble reporters (Figure 6). The similar results were obtained for the N-terminally tagged UGE4 (Yc-UGE4) (data not shown). Cellulose Synthase Like D2 (CSLD2) is a multimembrane-spanning protein that localizes to the Golgi apparatus and has

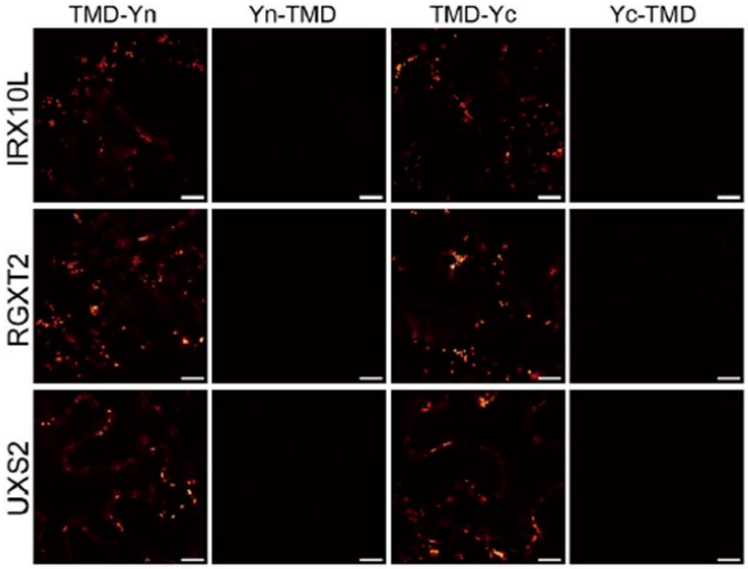

Figure 5. GO-PROMTO analysis of membrane proteins (IRX10L, RGXT2, and UXS2) known to be involved in cell wall polysaccharide biosynthesis in plant. The C-terminal Yc fusion of each of the proteins was co-expressed with TMD-Yn (1st column) or Yn-TMD (2nd column) and the C-terminal Yn fusion of each of the protein was co-expressed with TMD-Yc (3rd column) or Yc-TMD (4th column). The fluorescence complementation with the lumenal reporters and the lack of same with the cytosolic reporters indicate Golgi lumenal orientation of the IRX10L, RGXT2 and UXS2 catalytic domains. Scale bars, 10 µm. At least two individual experiments were performed for each combination with the similar results. Raw images are shown.
doi:10.1371/journal.pone.0031324.g005

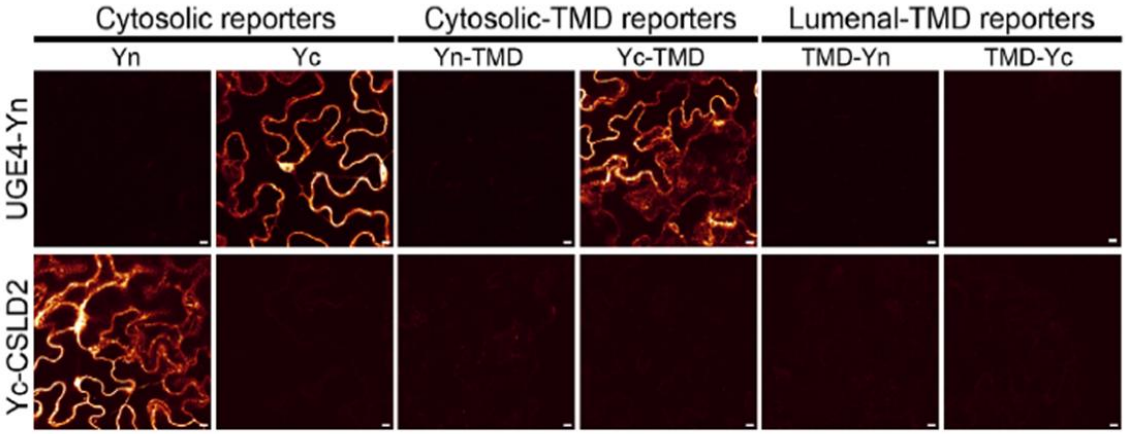

Figure 6. GO-PROMTO analysis of cytosolic (UGE4) and multimembrane spanning protein (CSLD2) known to be involved in cell wall polysaccharide biosynthesis in plant. UGE4 was fused to Yn at the C-terminus and CLSD2 was fused to Yc at the N-terminus and were transiently expressed in *Nicotiana benthamiana*. Observation was carried out by CLSM at 3 DPI. Scale bars, 10 µm. At least two individual experiments were performed for each combination with the similar results. Raw images are shown.
doi:10.1371/journal.pone.0031324.g006

been postulated to be involved in mannan synthesis [37]. The N-terminus of CSLD2 has been shown to be located in the cytosol [38]. Yc-CSLD2 complemented fluorescence with the cytosolic reporters whereas it did not complement fluorescence with the lumenal-TMD reporters (Figure 6). When Yn-TMD, a cytosolic-TMD reporter, was used, the detected signal was very weak, which is likely to be due to partial degradation of the N-terminus of Yn (Figure 3). It appears that the degree of degradation of the Yn-TMD reporter is highly variable. Taken together, the results presented in Figure 5 and 6 demonstrate that the five out of six topology reporters (Yn, Yc, Yc-TMD, TMD-Yn, TMD-Yc) specifically and robustly detect the topologies of the tested protein termini.

Membrane topologies of xyloglucan-biosynthesizing enzymes

GO-PROMTO was used to determine the membrane topology of enzymes involved in the biosynthesis of xyloglucan. Xyloglucan is a major hemicellulosic polysaccharide of primary cell wall, synthesis of which occurs in the Golgi apparatus [39–41]. In Arabidopsis, CSLC4 is thought to catalyze the synthesis of β-1,4-linked glucan backbone [42]. This glucan backbone is decorated with the side-chain α-1,6-xylosyl residues by XXT1, XXT2 and XXT5 [43,44], and can be further substituted with β-1,2-galactosyl and α-1,2-fucosyl residues by MUR3 and FUT1, respectively [43,45–47]. All these enzymes have been shown to localize to the Golgi cisternae [48,49]. A previous study has shown that the N- and C-termini and the catalytic domain of CSLC4 localize to the cytosolic side of the Golgi membrane [48]. This indicates that the backbone synthesis of xyloglucan occurs at the cytosolic face of the Golgi membrane and raises a question about the subcellular compartment in which the side-chain modifications occur.

The membrane topologies of the side chain biosynthetic enzymes have only partially been elucidated: it has been shown that the terminal fucosylation by FUT1 occurs in the Golgi lumen [50] and that XXT1 has its catalytic domain in the Golgi lumen [38]. Therefore we have investigated the membrane topology of four side-chain biosynthetic enzymes, XXT1, XXT2, XXT5 and MUR3. XXT1, XXT2 and XXT5 are predicted to contain zero or one transmembrane domain, while MUR3 is predicted to contain one, two and three transmembrane domains (Figure 4). Again, assuming cytosol-localized N-termini, odd-numbered transmembrane domains would place the C-terminal catalytic domains of these proteins in the Golgi lumen whereas zero and even-numbered transmembrane domains would place the catalytic domains in the cytosol. GO-PROMTO analysis was carried out in order to gain insight into the membrane topology of these side-chain synthesizing enzymes. N-terminal fusions of XXT1, XXT2, XXT5 and MUR3 complemented fluorescence with the cytosolic and cytosolic-TMD reporters, whereas they did not complement fluorescence with the lumenal-TMD reporters (Figure 7). This suggests that their N-termini are localized to the cytosol. The C-terminal fusions of XXT1, XXT5 and MUR3 did not complement fluorescence with the cytosolic and cytosolic-TMD reporters whereas they complemented fluorescence with the lumenal-TMD reporters and gave rise to signals characteristics of the Golgi apparatus (Figure 7). These results indicate that the catalytic domains of XXT1, XXT5 and MUR3 are localized to the Golgi lumen.

Membrane topologies of arabinan-biosynthesizing enzymes

Arabinan is mostly associated with the side chain of rhamnogalacturonan I. It consists of α-1,5-linked linear oligoarabinosaccharide with α-1,3- or α-1,2-linked branches also consisting of arabinose. Four gene products, MUR4, RGP1, RGP2 and ARAD1 have previously been shown to be involved in arabinan biosynthesis. MUR4 catalyzes the conversion of UDP-xylose to UDP-arabinopyranose [51]. RGP1 and RGP2 convert UDP-arabinopyranose to UDP-arabinofuranose [52,53]. ARAD1, a putative arabinosyltransferase, is involved in the incorporation of UDP-arabinofuranose into the growing arabinan structure [54].

It has been shown that RGP1 and RGP2 are located in the cytosolic face of the Golgi apparatus [52,53] whereas ARAD1 and MUR4 are thought to be membrane anchored and have been shown to localize to the Golgi membrane [29,51]. A previous study has indicated that MUR4 presents a predicted type II membrane topology [51]. However, a closer inspection of topology predictions revealed that the number of transmembrane domains

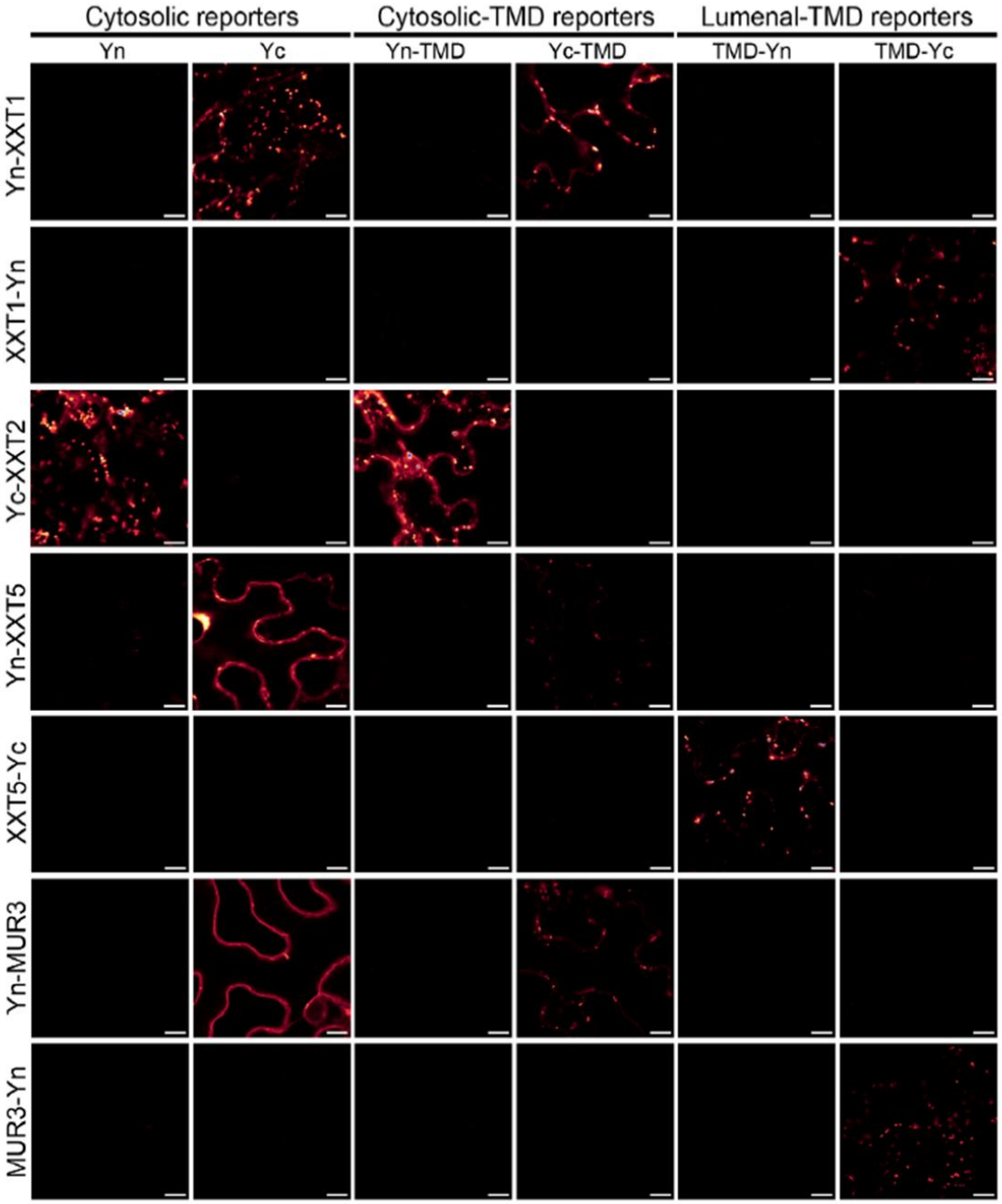

Figure 7. GO-PROMTO analysis of enzymes involved in the xyloglucan biosynthetic pathway. All proteins were fused to GO-PROMTO tags in the N-terminus. Additionally XXT1, XXT5 and MUR3 were fused to Yn or Yc at the C-termini. In all cases, the N-terminal of the proteins was found to localize to the cytosol by only reacting with the cytosolic GO-PROMTO reporters, concurrent with bioinformatic predictions. Furthermore, C-terminal fusions of MUR3, XXT5 and XXT1 showed Golgi lumenal localization. These fusion proteins were transiently expressed in *Nicotiana benthamiana*. Observation was carried out by CLSM at 3 DPI. Scale bars, 10 µm. At least two individual experiments were performed for each combination with the similar results. All of the images were processed identically by using Adobe Photoshop CS3.0 Extended v10.0.
doi:10.1371/journal.pone.0031324.g007

vary considerably from no transmembrane domain (Minnou, PHDhtm, S-Tmhmm_v0.9, TmHMM_v2, SosuiG_v1.1, SVMtm_v3, THUMBUP_v1, TMMOD) to one transmembrane domain (MemSat_v3, Phobius, PredTmr_v1, Scampi, Alom_v2, DAS-TMfilter, Eiconda_v1), two transmembrane domains (TmPred, TopPred_v2), and three transmembrane domains (HmmTop_v2) (Figure 4). Furthermore, the membrane topology predictions of ARAD1 also vary from one transmembrane domain (TmHMM_v2, TMMOD, SVMtm_v3, SosuiG_v1.1, Scampi, S_Tmhmm_v0.9, PredTmr_v1, Phobius, Minnou, HmmTop_v2, Eiconda_v1), two transmembrane domains (PHDhtm, TopPred_v2, MemSat_v3), and to three transmembrane domains (Alom_v2, DAS-TMfilter, TMUMBUP_v1, TmPred) (Figure 4).

GO-PROMTO analysis was carried out for ARAD1 and MUR4 (Figure 8). The cytosolic and cytosolic-TMD reporters did not complement fluorescence with the C-terminal fusions of ARAD1 and MUR4. In contrast, the lumenal-TMD reporters complemented fluorescence with both the C-terminal fusions of ARAD1 and MUR4. These results clearly demonstrate that the C-terminal catalytic domain of ARAD1 and MUR4 are located in the Golgi lumen.

Discussion

We have developed GO-PROMTO, a protein membrane topology method for fast and easy determination of the membrane topologies of proteins in the Golgi apparatus in living tissues. A series of topology reporters were generated and validated by live cell imaging and by the protease protection assay. The method is non-invasive, gives robust binary signal output, does not require further chemical treatments, and detects both the cytosolic and lumenal localization of the tagged termini for Golgi-resident proteins. GO-PROMTO was used to determine the membrane topologies of eleven proteins involved in plant cell wall biosynthesis as detailed below.

The membrane topology of the cell wall polysaccharide biosynthesis in plants is still not well understood. The previous topological studies of glucan synthases that catalyze the formation of the backbone of xyloglucan presented contradictory conclusions. In pea it was suggested that the catalytic site of a glucan synthase I, thought to synthesize the backbone glucan chain in the xyloglucan biosynthesis, is placed in the Golgi lumen [55]. In contrast a later study based on heterologous expression in *Pichia pastoris* provided compelling evidence that the catalytic site of the Arabidopsis glucan synthase CSLC4 is placed in the cytosol [48]. In this case, the synthesized glucan chain must be transported to the Golgi lumen where xyloglucan epitope is found [39]. The subcellular site(s) of side-chain synthesis have not yet been addressed except for that the terminal fucosylation has been shown to occur in the Golgi lumen [50] and that the putative catalytic domain of XXT1 has been shown to localize to the Golgi apparatus by protease protection assay [38]. By using GO-PROMTO we have validated the method by showing the C-terminus of XXT1 is located in the Golgi lumen, as previously shown [38] and have determined the membrane topology of enzymes responsible for two of the remaining steps of the side-chain synthesis (XXT5 and MUR3). Our results demonstrated that XXT5 and MUR3 have their C-terminal catalytic domains in the lumen (Figure 7). These results, together with the previous studies, indicate that the glucan backbone, if synthesized in the cytosol, is translocated across the membrane and that the side-chain modifications including the xylosylation by XXT1 and XXT5, galactosylation by MUR3 and the terminal fucosylation occur in the Golgi lumen.

The recent discovery that an enzymatic step in the pectic arabinan biosynthesis occurs in the cytosol has lead to an intriguing hypothesis about the mechanism of pectic arabinan biosynthesis. Scheller and colleagues have identified that the RGP1 and RGP2 encode UDP-arabinose mutases that are essential for the generation of UDP-arabinofuranose, an intermediate in arabinan biosynthesis [53]. Interestingly the authors also identified that RGP1 and RGP2 localize to the cytosolic surface of the Golgi apparatus as well as in the cytosol. On the other hand, it is generally regarded, though without experimental evidence, that the MUR4 and ARAD1 enzymes, involved in the arabinan biosynthesis at the preceding and proceeding steps of RGP1 and RGP2, respectively, posses the type II membrane topology with the catalytic C-termini located in the Golgi lumen. This apparent

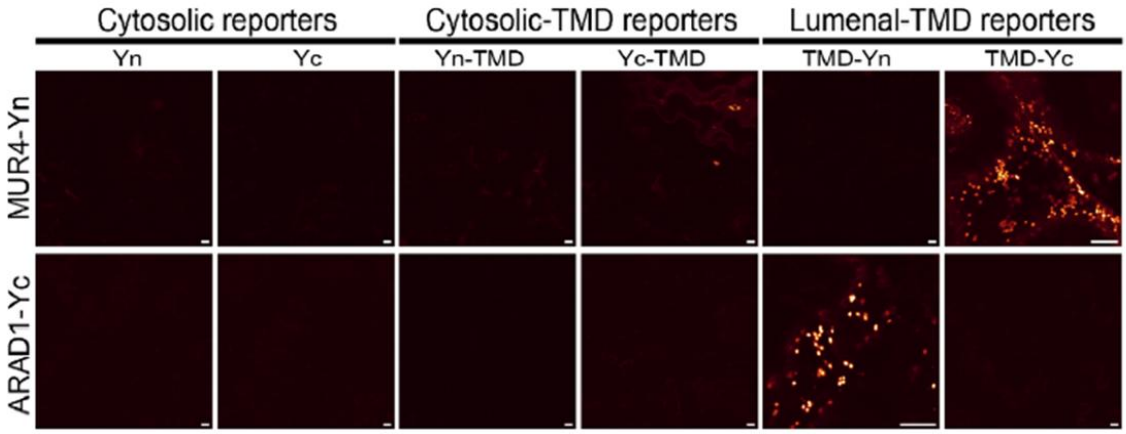

Figure 8. GO-PROMTO analysis of ARAD1 and MUR4, putative arabinosyltransferase and UDP-xylose/arabinose epimerase. ARAD1 and MUR4 fused with the Yc and Yn tags, respectively, at the C-termini were transiently expressed in *Nicotiana benthamiana*. Fluorescence complementation with lumenal reporters suggests Golgi-lumenal localization of ARAD1 and MUR4 C-termini. Observation was carried out by CLSM at 3 DPI. Scale bars, 10 µm. At least two individual experiments were performed for each combination with the similar results. Raw images are shown. doi:10.1371/journal.pone.0031324.g008

topology conundrum of arabinan biosynthesis prompted us to examine the subcellular localization of the C-termini of MUR4 and ARAD1.

Topology predictions of MUR4 and ARAD1 were found to be highly variable. Based on the topology prediction, three scenarios were considered: i) the catalytic domains of MUR4 and ARAD1 localize to the cytosol; ii) the catalytic domain of MUR4 localizes to the cytosol whereas that of ARAD1 localizes to the Golgi lumen; iii) the catalytic domains of both MUR4 and ARAD1 localize to the Golgi lumen. To test these hypotheses, we have carried out GO-PROMTO analysis of MUR4 and ARAD1. Our results clearly showed that the C-termini of both proteins are located in the Golgi lumen, therefore the third scenario is likely to be the case. This mode of biosynthesis, requiring a shuttling of intermediates across the membranes not only once but twice, is rather intriguing. Because the arabinose contents in the *mur4* knock-out mutants and the *rgp1/2* knock-down mutants were severely reduced [51,53], the possibility of the presence of other epimerases in the cytosol or mutases in the Golgi lumen is unlikely. Therefore, together with the previous reports [52,53], our results provide strong evidence of the existence of novel mechanisms of glycan biosynthesis involving intermediate shunts across the membrane (Figure 9).

The TMD topology reporters successfully detected the membrane topologies of all eleven proteins tested. This was initially unexpected because BiFC is also used to detect specific protein-protein interactions [51,53]. The apparent promiscuous fluorescence complementation by the TMD reporters could be attributed to the high level of expression under the experimental conditions tested. This is likely to result in ubiquitous distribution and high concentrations of the reporters across these subcellular compartments, thereby facilitating non-specific interaction between the reporters and the tested proteins. Additionally, the N- and C-terminal portions of TMD are predicted to be disordered by the three web-based programs, DisEMBL [56], DISOPRED [57], and GlobPlots [58]. Intrinsically disordered regions are thought to be structurally extended and flexible, which enhances the initial, relatively non-specific, associations that occur in protein-protein interactions [59]. It is plausible that the promiscuous fluorescence complementation between the TMD reporters and all the proteins tested is partly attributed to the disordered termini of TMD. Disordered regions may enhance the irreversible interaction between the split halves of YFP molecules [60], rendering the TMD-based reporters very robust.

It is noteworthy that the N-terminal fusions of tested proteins (XXT1, XXT2, XXT5 and MUR3) caused localization not only to the Golgi apparatus but also to ER, even though the C-terminal fusions of the same tested proteins localized predominantly in the Golgi apparatus (Figure 7). It is plausible that the partial ER localization is an artifact due to a combination of the presence of the tag in the N-termini and the effect of over-expression under the present conditions. In general, for protein topology analysis that relies on the tagging of protein termini, N-terminal tagging should be avoided. The N-termini of some proteins contain signal peptides that are cleaved after translation. In this case, the detected topology bears no information about the topology of the mature proteins. In addition, we have observed that YFP tagged to the N-termini of proteins and localized to the cytosol was partially degraded (Figure 3, Figure 6) or released from the fused protein (Figure 7, see Yn-MUR3 co-expressed with Yc). Lastly, the presence of a structured peptide (e.g. the Yn or Yc tag) preceding the first transmembrane domain may alter the overall topology of membrane proteins such as type I membrane proteins and multimembrane spanning proteins that insert N-terminal ends into the lumen of the secretory pathway. Most membrane proteins are co-translationally translocated across the membrane by the translocation channel, the Sec61 complex [61,62]. The first transmembrane domain, as it emerges from the ribosome, intercalates into the lateral gate of the channel complex. The N-terminus flips across the channel and subsequently exits the translocon laterally into the lumen if the hydrophobic region is long and the preceding segment does not contain positive charges or stable folding [62]. Otherwise the N-terminus is retained in the cytosol and the proceeding polypeptide is elongated and the C-terminus is translocated across the channel. To date, it is not clear to what extent the tagging of N-termini of membrane proteins with structured polypeptide tags impact the membrane topology. A systematic and thorough analysis addressing the impact of sizes and folding of tags on the N-terminal translocation across the membrane is needed.

This study developed and validated GO-PROMTO as a highly robust and easy method for determining topology of membrane proteins in the Golgi apparatus and ER in complex living tissues of higher plants. By using GO-PROMTO the membrane topology of xyloglucan and arabinan biosyntheses were examined. Even though GO-PROMTO was only tested in plant tissue, it can potentially be used in other organisms. Large-scale analysis of membrane protein topology has been performed previously in *Escherichia coli* and

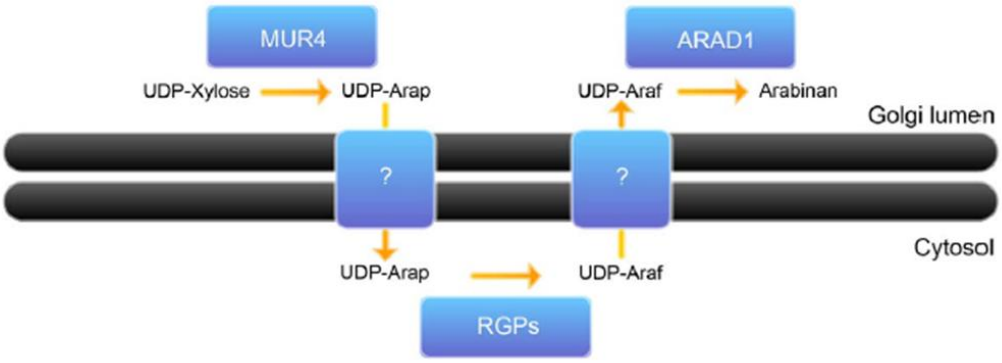

Figure 9. A topology model of Arabinan biosynthesis. UDP-arabinopyranose (UDP-Arap) generated by MUR4 in the Golgi lumen is transported to the cytosol possibly by a transporter; UDP-Arap is converted to UDP-Araf by RGP1 and RGP2 in the cytosol; UDP-Araf is transported from the cytosol to the Golgi lumen possibly by a transporter; UDP-Araf is incorporated into arabinan by glycosyltransferase(s) likely including ARAD1.
doi:10.1371/journal.pone.0031324.g009

Saccharomyces cerevisiae [13,14]. GO-PROMTO may be readily and universally adapted to global topology analyses in higher eukaryotes, either in cell cultures or in intact tissues. The binary signal output makes the detection and interpretation of the results straightforward and suitable for high-throughput applications.

Materials and Methods

Vector constructions and transformation of *Agrobacterium tumefaciens*

In-frame fusions of the *Arabidopsis thaliana* cDNA CSLD2 (At5g16910), ARAD1 (At2g35100), RGXT2 (At4g01750), UXS2 (At3g62830), UGE4 (At1g64440), MUR3 (At2g20370) and MUR4 (At1g30620) to Yn or Yc tags and that of XXT5 (At1g74380) to Yc were generated in pCAMBIA330035su using the USER cloning technique [63]. The design of the linker sequence was identical in all constructs as described previously [29]. In-frame fusions of the Arabidopsis cDNA XXT1 (At3g62720), XXT2 (At4g02500) and CSLC4 (At3g28180) to Yn, and Yc as well as that of XXT5 to Yn were carried out by Gateway cloning strategy according to the manufacturer's protocol (Invitrogen). The following destination vectors were used: the pEarlygate 104 vector for full length YFP fusions [64]; and Vyne or Vyce Gateway vectors for Yn and Yc, respectively [65]. *Agrobacterium tumefaciens* pGV3850 C58C01 [65] was transformed with plasmids bearing the in-frame fusions by electroporation and the transformants were selected in the presence of appropriate antibiotics. The transformants were stored at −80°C until used.

Transient expression in tobacco

Strains were grown in LB or YEP media with appropriate antibiotics overnight at 28°C with agitation at 220 rpm. After centrifugation, cell pellets were resuspended in 1 ml infiltration buffer containing 10 mM MES, pH 5.6, 100 µM acetosyringone and 10 mM $MgCl_2$ at the final optical density at 600 nm of 0.05. The viral suppressor of gene silencing, p19, [66] was co-infiltrated at an final optical density at 600 nm of 0.1 in combinations containing XXT1, XXT2, XXT5 or MUR3. Transient expression of the fusion proteins were carried out in 4-week-old *Nicotiana benthamiana* plants that have been grown in greenhouses at 24°C/17°C day/night temperatures, 16 hour photoperiod. Each strain combination was infiltrated into a separate leaf, in two independent plants. Infiltrations were done by injection on the bottom face of the leaf using a syringe without a needle, with a fingertip providing counter pressure. After infiltration, the plants were placed in the greenhouse for 3–4 days until observations by microscopy. At least two individual experiments were performed for each combination.

Confocal laser scanning microscopy

CLSM used in this study were Leica SP5 II and SP5-X AOBS CLSM with appropriate Leica Application Suite Advanced Fluorescence software as previously described [29]. Samples were excited with a 40% 514 nm Argon laser line. The emission of YFP was detected between 525 and 599 nm. Overall gain settings were in the range of 600 to 850 volts, and the gain setting was kept constant for each glycan biosynthetic fusion protein. The samples were observed with a Leica 40×/0.8 Numerical Aperture (NA) dipping lens with milliQ water as immersion media. Image processing, where it was necessary, was performed by using Adobe Photoshop CS3.0 Extended v10.0.

Protease protection assay and western blot of TMD constructs

Two to four infiltrated leaves at 2–4 days post infiltration (DPI) were harvested. Microsomes were prepared as follows. Leaves were frozen and ground in liquid nitrogen. The ground tissue was macerated in an extraction buffer, consisting of 100 mM HEPES-KOH pH 7.25, 300 mM sucrose, 5 mM EGTA, 5 mM $MgCl_2$ and 1 Complete Protease Inhibitor tablet (Roche) per 50 ml extraction buffer. The homogenates were subjected to centrifugation for 3000× g in a F15 rotor (Piramoon Technologies) for 15 min at 4°C, followed by ultracentrifugation of the supernatants at 113,000× g in a SW40 Ti rotor (Beckman Coulter) for 1 h at 4°C. The pellets were resuspended in the extraction buffer by light brushing with a small paint brush. The protein content of each sample was determined by the standard Bradford assay [67].

The protease protection assay was carried out as follows. Ten micrograms of protein from each sample was mixed with either Triton X-100, proteinase K (freshly made from a lyophilized stock, Sigma P6556) or both in the final volume of 15 µl. Final concentrations was 0.1% (v/v) and 0.1 µg μl^{-1}, respectively. The mix was incubated at 30°C for 30 min. The reaction was stopped by the addition of phenylmethanesulfonylfluoride at the final concentration of 6 mM. The samples were mixed with 5-fold strength sample buffer (0.125 M Tris-HCl, pH 6.8, 20% (v/v) glycerol, 4% (v/v) SDS, 1% (v/v) bromophenol blue) containing 200 mM dithiothreitol. The mixed samples were treated for 10 min at 55°C and proteins were separated in Criterion XT pre-cast 12% (v/v) bis-Tris gels with MOPS buffer (Bio-Rad). Immunoblots were carried out with Protran nitrocellulose transfer membrane (Whatman) in a full wet Criterion blotting system (Bio-Rad). The primary antibody, rabbit anti-GFP antibody (A11122, Invitrogen) was diluted by 5000 folds, and the secondary antibody, anti-rabbit horse radish peroxidase conjugated antibody (Dako PO217, DAKO Denmark, DK), was diluted by 1000 folds. The horse radish peroxidase signal was detected with a chemiluminescent detection system (Super-Signal; Pierce) according to the instructions of the manufacturer using an Autochemi UVP system (AH Diagnostics) with LabWorks version 4.5 software.

Acknowledgments

Imaging data were collected at the Center for Advanced Bioimaging (CAB) Denmark, University of Copenhagen. The authors would like to thank Jacob Lindborg for assistance with graphical design.

Author Contributions

Conceived and designed the experiments: CS YS. Performed the experiments: CS AS MH SB YS. Analyzed the data: CS AS YS. Contributed reagents/materials/analysis tools: CS AS SB AD MH HVS YS. Wrote the paper: CS AS SB AD HVS YS.

References

1. Wilson C, Venditti R, Rega LR, Colanzi A, D'Angelo G, et al. (2011) The Golgi apparatus: an organelle with multiple complex functions. Biochemical J 433: 1–9.
2. Emr S, Glick B, Linstedt A, Lippincott-Schwartz J, Luini A, et al. (2009) Journeys through the Golgi-taking stock in a new era. J Cell Biol 187: 449–453.
3. Wallin E, Tsukihara T, Yoshikawa S, VonHeijne G, Elofsson A (1997) Architecture of helix bundle membrane proteins: An analysis of cytochrome c oxidase from bovine mitochondria. Protein Sci 6: 808–815.
4. Seshadri K, Garemyr R, Wallin E, Von Heijne G, Elofsson A (1998) Architecture of beta-barrel membrane proteins: Analysis of trimeric porins. Protein Sci 7: 2026–2032.

5. Krogh A, Larsson B, von Heijne G, Sonnhammer E (2001) Predicting transmembrane protein topology with a hidden Markov model: Application to complete genomes. J Mol Biol 305: 567–580.
6. Kall L, Krogh A, Sonnhammer E (2005) An HMM posterior decoder for sequence feature prediction that includes homology information. Bioinformatics 21: I251–I257.
7. Tusnady G, Simon I (2001) The HMMTOP transmembrane topology prediction server. Bioinformatics 17: 849–850.
8. Viklund H, Elofsson A (2004) Best alpha-helical transmembrane protein topology predictions are achieved using hidden Markov models and evolutionary information. Protein Sci 13: 1908–1917.
9. Von Heijne G (1992) Membrane-protein structure prediction - hydrophobicity analysis and the positive-inside rule. J Mol Biol 225: 487–494.
10. Melen K, Krogh A, von Heijne G (2003) Reliability measures for membrane protein topology prediction algorithms. J Mol Biol 327: 735–744.
11. Bernsel A, Von Heijne G (2005) Improved membrane protein topology prediction by domain assignments. Protein Sci 14: 1723–1728.
12. von Heijne G (2006) Membrane-protein topology. Nat Rev Mol Cell Biol 7: 909–918.
13. Daley DO, Rapp M, Granseth E, Melén K, Drew D, et al. (2005) Global topology analysis of the *Escherichia coli* Inner membrane proteome. Science 308: 1321–1323.
14. Kim H, Melén K, Österberg M, von Heijne G (2006) A global topology map of the *Saccharomyces cerevisiae* membrane proteome. Proc Natl Acad Sci U S A 103: 11142–11147.
15. Kauko A, Hedin L, Thebaud E, Cristobal S, Elofsson A, et al. (2010) Repositioning of transmembrane alpha-helices during membrane protein folding. J Mol Biol 397: 190–201.
16. Chang X, Hou Y, Jensen T, Riordan J (1994) Mapping of cystic-fibrosis transmembrane conductance regulator membrane topology by glycosylation site insertion. J Biol Chem 269: 18572–18575.
17. Bogdanov M, Zhang W, Xie J, Dowhan W (2005) Transmembrane protein topology mapping by the substituted cysteine accessibility method (SCAM (TM)): Application to lipid-specific membrane protein topogenesis. Methods 36: 148–171.
18. Wilkinson B, Critchley A, Stirling C (1996) Determination of the transmembrane topology of yeast Sec61p, an essential component of the endoplasmic reticulum translocation complex. J Biol Chem 271: 25590–25597.
19. Akiyama Y, Ito K (1987) Topology analysis of the secY protein, an integral membrane-protein involved in protein expoert in *Escherichia coli*. EMBO J 6: 3465–3470.
20. Boyd D, Manoil C, Beckwith J (1987) Determinants of membrane-protein topology. Proc Natl Acad Sci U S A 84: 8525–8529.
21. Lorenz H, Hailey D, Lippincott-Schwartz J (2006) Fluorescence protease protection of GFP chimeras to reveal protein topology and subcellular localization. Nat Methods 3: 205–210.
22. Zamyatnin A, Solovyev A, Bozhkov P, Valkonen J, Morozov S, et al. (2006) Assessment of the integral membrane protein topology in living cells. Plant J 46: 145–154.
23. Swarup R, Kargul J, Marchant A, Zadik D, Rahman A, et al. (2004) Structure-function analysis of the presumptive Arabidopsis auxin permease AUX1. Plant Cell 16: 3069–3083.
24. Brach T, Soyk S, Muller C, Hinz G, Hell R, et al. (2009) Non-invasive topology analysis of membrane proteins in the secretory pathway. Plant J 57: 534–541.
25. Hu C, Chinenov Y, Kerppola T (2002) Visualization of interactions among bZip and Rel family proteins in living cells using bimolecular fluorescence complementation. Mol Cell 9: 789–798.
26. Munro S (1991) Sequences within an adjacent to the transmembrane segment of alpha-2,6-sialyltransferase specify Golgi retention. EMBO J 10: 3577–3588.
27. Wong S, Low S, Hong W (1992) The 17-residue transmembrane domain of beta-galactoside alpha-2,6-sialyltransferase is sufficient for Golgi retention. J Cell Biol 117: 245–258.
28. Colley K, Lee E, Paulson J (1992) The signal anchor and stem regions of the beta-galactoside alpha-2,6-sialyltransferase may each act to localize the enzyme to the Golgi-apparatus. J Biol Chem 267: 7784–7793.
29. Sakuragi Y, Nerholm M, Scheller H (2011) Visual mapping of cell wall biosynthesis. Methods MolBiol 715: 153–167.
30. Pattathil S, Harper AD, Bar-Peled M (2005) Biosynthesis of UDP-xylose: characterization of membrane-bound AtUXS2. Planta 221: 538–548.
31. Jensen JK, Sorensen SO, Harholt J, Geshi N, Sakuragi Y, et al. (2008) Identification of a xylogalacturonan xylosyltransferase involved in pectin biosynthesis in Arabidopsis. Plant Cell 20: 1289–1302.
32. Egelund J, Petersen B, Motawia M, Damager I, Faik A, et al. (2006) Arabidopsis thaliana RGXT1 and RGXT2 encode Golgi-localized (1,3)-alpha-D-xylosyltransferases involved in the synthesis of pectic rhamnogalacturonan-II. Plant Cell 18: 2593–2607.
33. Wu A-M, Rihouey C, Seveno M, Hörnblad E, Singh SK, et al. (2009) The Arabidopsis IRX10 and IRX10-LIKE glycosyltransferases are critical for glucuronoxylan biosynthesis during secondary cell wall formation. Plant J 57: 718–731.
34. David MB, Zhinong Z, Elaine S, Paul D, Simon RT (2009) Characterization of IRX10 and IRX10-like reveals an essential role in glucuronoxylan biosynthesis in Arabidopsis. The Plant Journal 57: 732–746.
35. Dunkley TP, Hester S, Shadforth IP, Runions J, Weimar T, et al. (2006) Mapping the Arabidopsis organelle proteome. Proc Natl Acad Sci U S A 103: 6518–6523.
36. Barber C, Rosti J, Rawat A, Findlay K, Roberts K, et al. (2006) Distinct properties of the five UDP-D-glucose/UDP-D-galactose 4-epimerase isoforms of Arabidopsis thaliana. J Biol Chem 281: 17276–17285.
37. Yin L, Verhertbruggen Y, Oikawa A, Manisseri C, Knierim B, et al. (2011) The cooperative activities of CSLD2, CSLD3, and CSLD5are required for normal Arabidopsis development. Molecular Plant.
38. Zeng W, Keegstra K (2008) AtCSLD2 is an integral Golgi membrane protein with its N-terminus facing the cytosol. Planta 228: 823–838.
39. Zhang G, Staehelin L (1992) Functional compartmentation of the Golgi-apparatus of plant cells - immunocytochemical analysis of high-pressure frozen-substituted and freeze-substituted sycamore maple suspension-culture cells. Plant Physiol 99: 1070–1083.
40. Norambuena L, Marchant L, Berninsone P, Hirschberg CB, Silva H, et al. (2002) Transport of UDP-galactose in plants. Identification and functional characterization of AtUTr1, an *Arabidopsis thaliana* UDP-galactos/UDP-glucose transporter. J Biol Chem 277: 32923–32929.
41. Driouich A, Faye L, Staehelin A (1993) The plant Golgi apparatus: a factory for complex polysaccharides and glycoproteins. Trends Biochem Sci 18: 210–214.
42. Cocuron J, Lerouxel O, Drakakaki G, Alonso A, Liepman A, et al. (2007) A gene from the cellulose synthase-like C family encodes a beta-1,4 glucan synthase. Proc Natl Acad Sci U S A 104: 8550–8555.
43. Zabotina O, van de Ven W, Freshour G, Drakakaki G, Cavalier D, et al. (2008) Arabidopsis XXT5 gene encodes a putative alpha-1,6-xylosyltransferase that is involved in xyloglucan biosynthesis. Plant J 56: 101–115.
44. Cavalier D, Lerouxel O, Neumetzler L, Yamauchi K, Reinecke A, et al. (2008) Disrupting two Arabidopsis thaliana xylosyltransferase genes results in plants deficient in xyloglucan, a major primary cell wall component. Plant Cell 20: 1519–1537.
45. Madson M, Dunand C, Li X, Verma R, Vanzin GF, et al. (2003) The MUR3 gene of Arabidopsis encodes a xyloglucan galactosyltransferase that is evolutionarily related to animal exostosins. Plant Cell 15: 1662–1670.
46. Faik A, Bar-Peled M, DeRocher A, Zeng W, Perrin R, et al. (2000) Biochemical characterization and molecular cloning of an alpha-1,2-fucosyltransferase that catalyzes the last step of cell wall xyloglucan biosynthesis in pea. J Biol Chem 275: 15082–15089.
47. Scheller HV, Ulvskov P (2010) Hemicelluloses. Annu Rev Plant Biol 61: 263–289.
48. Davis J, Brandizzi F, Liepman AH, Keegstra K (2010) Arabidopsis mannan synthase CSLA9 and glucan synthase CSLC4 have opposite orientations in the Golgi membrane. Plant J 64: 1028–1037.
49. Chevalier L, Bernard S, Ramdani Y, Lamour R, Bardor M, et al. (2010) Subcompartment localization of the side chain xyloglucan-synthesizing enzymes within Golgi stacks of tobacco suspension-cultured cells. Plant J 64: 977–989.
50. Wulff C, Norambuena L, Orellana A (2000) GDP-fucose uptake into the Golgi apparatus during xyloglucan biosynthesis requires the activity of a transporter-like protein other than the UDP-glucose transporter. Plant Physiol 122: 867–877.
51. Burget EG, Verma R, Molhoj M, Reiter WD (2003) The biosynthesis of L-arabinose in plants: molecular cloning and characterization of a Golgi-localized UDP-D-xylose 4-epimerase encoded by the MUR4 gene of Arabidopsis. Plant Cell 15: 523–531.
52. Konishi T, Takeda T, Miyazaki Y, Ohnishi-Kameyama M, Hayashi T, et al. (2007) A plant mutase that interconverts UDP-arabinofuranose and UDP-arabinopyranose. Glycobiology 17: 345–354.
53. Rautengarten C, Ebert B, Herter T, Petzold CJ, Ishii T, et al. (2011) The interconversion of UDP-arabinopyranose and UDP-arabinofuranose Is indispensable for plant development in Arabidopsis. Plant Cell 23: 1373–1390.
54. Harholt J, Jensen JK, Sorensen SO, Orfila C, Pauly M, et al. (2006) ARABINAN DEFICIENT 1 is a putative arabinosyltransferase involved in biosynthesis of pectic arabinan in Arabidopsis. Plant Physiol 140: 49–58.
55. Munoz P, Norambuena L, Orellana A (1996) Evidence for a UDP-Glucose transporter in Golgi apparatus-derived vesicles from pea and its possible role in polysaccharide biosynthesis. Plant Physiol 112: 1585–1594.
56. Linding R, Russell R, Neduva V, Gibson T (2003) GlobPlot: exploring protein sequences for globularity and disorder. Nucleic Acids Res 31: 3701–3708.
57. Ward J, McGuffin L, Bryson K, Buxton B, Jones D (2004) The DISOPRED server for the prediction of protein disorder. Bioinformatics 20: 2138–2139.
58. Linding R, Jensen LJ, Diella F, Bork P, Gibson TJ, et al. (2003) Protein disorder prediction: implications for structural proteomics. Structure 11: 1453–1459.
59. Tompa P, Szasz C, Buday L (2005) Structural disorder throws new light on moonlighting. Trends Biochem Sci 30: 484–489.
60. Magliery T, Wilson C, Pan W, Mishler D, Ghosh I, et al. (2005) Detecting protein-protein interactions with a green fluorescent protein fragment reassembly trap: Scope and mechanism. J Am Chem Soc 127: 146–157.
61. Rapoport T (2007) Protein translocation across the eukaryotic endoplasmic reticulum and bacterial plasma membranes. Nature 450: 663–669.
62. Rapoport T, Goder V, Heinrich S, Matlack K (2004) Membrane-protein integration and the role of the translocation channel. Trends Cell Biol 14: 568–575.

63. Geu-Flores F, Nour-Eldin HH, Nielsen MT, Halkier BA (2007) USER fusion: a rapid and efficient method for simultaneous fusion and cloning of multiple PCR products. Nucleic Acids Res 35.
64. Earley KW, Haag JR, Pontes O, Opper K, Juehne T, et al. (2006) Gateway-compatible vectors for plant functional genomics and proteomics. Plant J 45: 616–629.
65. Gehl C, Waadt R, Kudla J, Mendel R, Hansch R (2009) New GATEWAY vectors for high throughput analyses of protein-protein interactions by bimolecular fluorescence complementation. Mol Plant 2: 1051–1058.
66. Voinnet O, Rivas S, Mestre P, Baulcombe D (2003) An enhanced transient expression system in plants based on suppression of gene silencing by the p19 protein of tomato bushy stunt virus. Plant J 33: 949–956.
67. Bradford M (1976) Rapid and sensitive method for quantitation of microgram quantities of protein utilizing principle of protein-dye binding. Anal Biochem 72: 248–254.

CHAPITRE IV:

DISCUSSION/CONCLUSION

PARTIE A : LA SYNTHESE GOLGIENNE DU XYLOGLUCANE

I- Quels compartiments golgiens sont impliqués dans la synthèse du XyG ?

La cartographie golgienne des enzymes impliquées dans la synthèse des chaînes latérales du xyloglucane, fusionnées à la GFP, puis exprimées dans des cellules de tabac traitées par HPF/FS, nous a montré que la α(1,6)xylosyltransférase (AtXXT1) était localisée dans les compartiments *cis* et médian, la β(1,2)galactosyltransférase (AtMUR3) dans le compartiment médian et la α(1,2)fucosyltransférase (AtFUT1) dans le compartiment *trans*.

Zhang et Staehelin (1992) ont été les premiers à effectuer la cartographie golgienne d'épitopes polysaccharidiques spécifiques du xyloglucane sur des suspensions cellulaires de sycomore traitées par HPF/FS. Ils ont testé un anticorps nommé anti-XG, qui reconnaît la chaîne principale, et l'anticorps CCRC-M1, qui reconnaît spécifiquement le fucose terminal lié à un galactose d'une chaîne latérale. Ils ont constaté que ces deux épitopes étaient localisés dans le compartiment *trans* et le TGN.

Ainsi, nos résultats montrent que tous les compartiments golgiens seraient impliqués dans la synthèse du XyG, alors que ceux de Zhang et Staehelin (1992) montrent que seuls le compartiment *trans* et le TGN seraient inclus. Cette différence peut s'expliquer par le fait que nous avons effectué la cartographie sur des suspensions cellulaires de tabac, alors que Zhang et Staehelin (1992) ont testé des suspensions cellulaires de sycomore. La synthèse golgienne du xyloglucane pourrait impliquer compartiments qui diffèrent selon le type cellulaire, l'espèce ou le stade de croissance d'une plante.

Une autre différence réside dans la méthode de quantification et d'analyse des résultats. En effet, Zhang et Stahelin (1992) ont défini un pourcentage relatif par compartiment, par rapport au nombre total de particules d'un empilement golgien. Nous avons utilisé la méthode statistique de *Relative Labelling Index* (RLI), qui prend en compte la surface de chaque compartiment. Or, ce paramètre est important, puisque des citernes *cis* jusqu'au TGN, les saccules grandissent et le TGN peut être très diffus, augmentant ainsi le nombre de particules potentielles dans un compartiment. Il serait intéressant de traiter les données brutes de Zhang et Staehelin par la méthode statistique du RLI, et comparer les résultats avec ceux obtenus sur les cellules de tabac.

II- Les glycosyltransférases participant à la synthèse golgienne du XyG sont-elles organisées en complexes ?

A ce jour, un certain nombre de glycosyltransférases ont été identifiées et reconnues comme participant à la synthèse du XyG, et sont représentées **figure 58A**. Exceptée la glucane synthase qui possède 6 domaines transmembranaires, avec ses extrémités N- et C-terminales du côté cytosolique (**Figure 58B**, Davis et al., 2010), toutes les autres protéines sont des protéines transmembranaires de type II, avec un domaine transmembranaire et leur domaine catalytique (C-terminal) dans la lumière des saccules golgiennes (Søgaard et al., 2012).

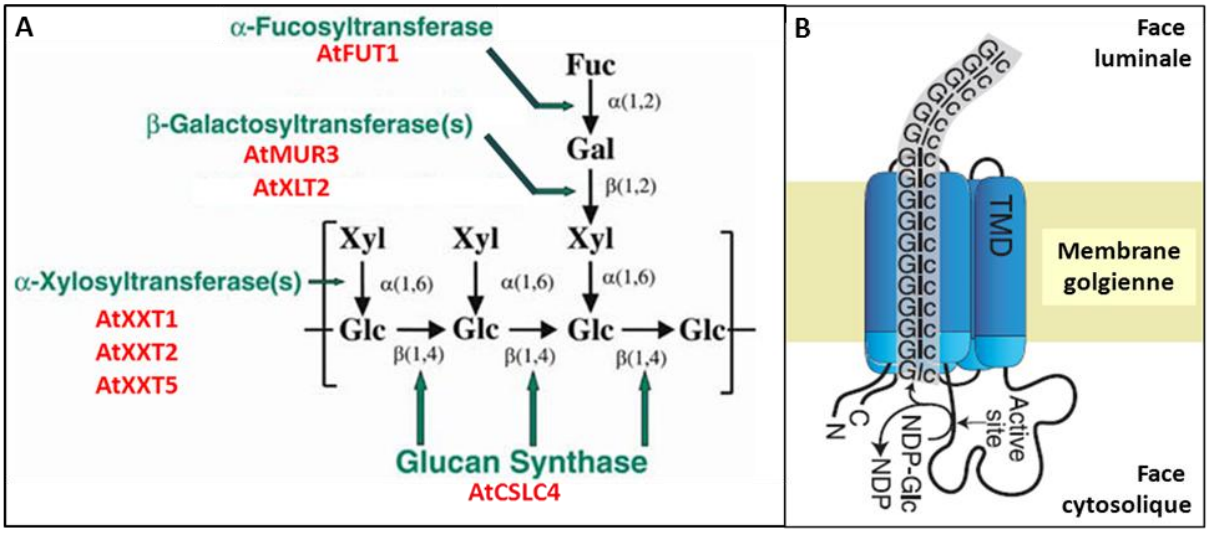

Figure 58 : Synthèse du xyloglucane (adapté de http://www.bmb.msu.edu/faculty/keegstra/cellwall.html et Davis, 2010)
A- Glycosyltransférases identifiées comme participant à la synthèse du XyG, B- Topologie de la glucane synthase AtCSLC4 au sein de la memebrane golgienne. Fuc : fucose, Gal : galactose, Glc : glucose, Xyl : xylose.

Dès les années 1980, des études portant sur la synthèse du XyG *in vitro* ont montré que l'incorporation du glucose pour la synthèse de la chaîne principale était étroitement liée à l'incorporation du xylose (Ray, 1980 ; Hayashi et Matsuda, 1981). Lorsque Cocuron et al. (2007) ont identifié la glucane synthase AtCSLC4 et l'ont exprimé dans *Pichia pastoris*, ils ont constaté un taux d'incorporation de glucose plus élevé quand la xylosyltransférase AtXXT1 était co-exprimée. Récemment, Chou et al. (2012) ont montré *in vivo* et *in vitro* l'existence d'un complexe multi-protéique impliquant la glucane synthase (AtCSLC4) et les xylosyltransférases (AtXXT1, AtXXT2 et AtXXT5) dans des protoplastes d'Arabidopsis, par des

techniques de BiFC et de co-immunoprécipitation. D'après leurs résultats, la glucane synthase forme un homodimère AtCSLC4-AtCSLC4, avec ses extrémités N- et C- terminales très proches, et la xylosyltransférase AtXXT2 forme un homodimère AtXXT2-AtXXT2 *via* des ponts disulfures. Trois hétérocomplexes ont été identifiés : AtXXT1-AtXXT2, AtXXT2-AtXXT5 et AtXXT5-AtCSLC4. L'interaction entre les 3 xylosyltransférases a lieu au niveau de leur domaine catalytique situé dans la lumière des saccules. La nature de l'interaction entre la glucane synthase et AtXXT5 n'a pas été identifiée, mais les auteurs postulent qu'elle peut avoir lieu au niveau de leur domaine transmembranaire.

Sachant que nous avons détecté la xylosyltransférase AtXXT1 dans les compartiments golgiens *cis* et médian, il semble probable que la glucane synthase AtCSLC4 ainsi que les xylosyltransférases AtXXT2 et AtXXT5 soient également présentes dans ces mêmes compartiments. De même, puisque nous détectons la galactosyltransférase AtMUR3 dans le compartiment médian, nous pouvons postuler qu'AtMUR3 rejoigne ce complexe dans le compartiment médian.

Ainsi, dans le compartiment *cis*, la synthèse du XyG commencerait par l'ajout de glucose par AtCSLC4 pour former la chaîne principale, suivi dans l'immédiat par l'ajout de xylose par les différentes xylosyltransférases AtXXT1, AtXXT2 et AtXXT5, formant un « complexe de xylosylation ». Dans le compartiment médian, la synthèse de la chaîne de glucose et l'ajout de xylose continuent, et l'ajout de galactose sur les résidus xylose commence. Sachant que la galactosyltransférase AtMUR3 se trouve dans le médian, on peut également postuler que l'autre galactosyltransférase AtXLT2 se situe dans le médian et forme avec AtMUR3 un « complexe de galactosylation » du XyG. Enfin, dans le compartiment *trans*, l'unique fucosyltransférase AtFUT1 effectuerait l'étape de fucosylation.

PARTIE B : LA SYNTHESE GOLGIENNE DU RG-I

I- Quels compartiments golgiens sont impliqués dans la synthèse du RG-I ?

Grâce au développement de nouveaux anticorps spécifiques du RG-I dont la nature des épitopes est connue, nous avons pu effectuer une cartographie golgienne de ces épitopes sur des suspensions cellulaires de tabac préparées par HPF/FS, et mettre en évidence l'implication des compartiments median, *trans* ainsi que du TGN.

Une précédente étude de cartographie golgienne sur des épitopes du RG-I a été effectuée sur des suspensions cellulaires de sycomore (Zhang et Staehelin, 1992). Les auteurs ont testé un anticorps, nommé PGA/RG-I, reconnaissant la zone de transition entre un homogalacturonane non estérifié et un résidu rhamnose provenant de la chaîne principale du RG-I (Moore et al., 1991), dans les compartiments golgiens *cis* et médian. Après un traitement de dé-estérification au Na_2CO_3, ils ont également détecté cet épitope dans le compartiment *trans* et le TGN, suggérant que la méthylestérification des acides galacturoniques avait lieu dans ces mêmes compartiments. Ces résultats ayant été confirmés par la localisation d'une pectine méthyl transférase putative, nommée AtQUA2, fusionnée à la GFP et localisée dans le compartiment *trans* et le TGN dans des empilements golgiens de cellules de pointe de racine d'Arabidopsis (Driouich et al., 2012; Follet-Gueye et al., 2012).

A partir de toutes ces données, nous avons proposé un modèle qui représente les grandes étapes de la synthèse du RG-I dans les différents compartiments golgiens, et résumé **figure 59**. Dans le compartiment *cis*, l'initiation de la chaîne principale du RG-I débuterait à partir d'une chaîne d'homogalacturonane, sachant qu'il a été montré que ces deux polysaccharides étaient liés de façon covalente (Coenen et al., 2007), puis la chaîne principale du RG-I serait rallongée dans le compartiment median. Dans le compartiment *trans*, les chaînes arabinanes linéaires seraient rallongées, puis branchées au sein du TGN. Les chaînes galactanes seraient rallongées dans le TGN et les chaînes arabinogalactanes constituées d'un ou plusieurs galactoses associés à des arabinanes branchés y seraient synthétisées.

Golgi compartment labeled	Antibody used	Corresponding epitope detected	Possible reaction occuring in this compartment
cis	PGA/RG-I	Transition region between deesterified HG and the first Rha linked residue of RG-I	• Association of HG and RG-I backbone • Initiation of RG-I backbone synthesis
medial	PGA/RG-I	Transition region between deesterified HG and the first Rha linked residue of RG-I	• Elongation of RG-I backbone
	INRA-RU1	6 to 7 [GalUA /Rha] units which are unbranched, non-methylated and non-acetylated	
trans	PGA/RG-I after deesterification treatment	Transition region between deesterified HG and the first Rha linked residue of RG-I	• Methylesterification of GalA
	LM13	Long (5 to 11 Ara), unbranched and linear arabinan chain	• Elongation of (1→5)-α-L-arabinan chain
TGN	PGA/RG-I after deesterification treatment	Transition region between deesterified HG and the first Rha linked residue of RG-I	• (Methylesterification of GalA ?)
	LM5	Short (4 Gal) galactan chain	• Elongation of galactan chain
	LM6	Short (2 to 6 Ara), possibly branched and non linear arabinan chain	• Branching of linear arabinan chain with 2- or 3-linked arabinose
	LM16	Galactosyl residue/galactan stub between arabinan chain and RG-I backbone	• Branching of branched arabinan on galactose residue or galactan stub to form arabinogalactan chain

Figure 59 : Modèle représentant les grandes étapes de la synthèse du RG-I dans les différents compartiments golgiens.

Une fois localisés des épitopes spécifiques du RG-I, nous avons cartographié l'arabinosyltransférase potentielle AtARAD1, ainsi que la xylose-épimérase AtUXE1/MUR4 et son homologue AtUXE3 ; ces enzymes étant de bons candidats pour synthétiser des chaînes arabinanes du RG-I. Nous avons localisé AtARAD1 et AtUXE3 dans le compartiment median et AtMUR4 dans le TGN. L'arabinosyltransférase AtARAD1 est certainement une enzyme processive responsable de l'élongation des chaînes arabinanes (Harholt et al. 2006). Elle possède un homologue, nommé AtARAD2, qui semble être une arabinosyltransférase participant à la synthèse des chaînes arabinanes branchées. Il a été montré que ces deux enzymes existent sous forment d'homo- et d'hétéro-dimère (Harholt et al. 2012). Ainsi on peut postuler qu'AtARAD2 colocalise avec AtARAD1 dans le compartiment median.

D'après la cartographie golgienne des épitopes, nous avons postulé que les chaînes arabinanes linéaires étaient rallongées dans le compartiment *trans* et qu'elles étaient certainement branchées dans le TGN. Comment expliquer cette différence ? Si AtARAD1 effectue l'élongation des chaînes dans le median, il n'est pas surprenant que le produit final ne puisse être détecté par l'anticorps LM13 que dans le compartiment suivant, puisqu'il

reconnaît 5 à 11 résidus linéaires d'arabinoses. Cependant, la présence des chaînes arabinanes branchées dans le TGN et celle d'AtARAD2 dans le compartiment median ne coïncident pas. L'activité de la protéine AtARAD2 n'a pas été clairement démontrée, et son rôle en tant qu'arabinosyltransférase responsable du branchement des chaînes arabinanes reste donc hypothétique.

II- Les glycosyltransférases participant à la synthèse golgienne des chaînes arabinanes du RG-I sont-elles organisées en complexes ?

La synthèse des chaînes arabinanes nécessite l'action de plusieurs partenaires potentiellement organisés en complexe : une épimérase qui va transformer de l'UDP-D-xylose en UDP-L-arabinopyranose, puis une mutase qui va le transformer en UDP-L-arabinofuranose. Si ces deux réactions ont lieu au sein du cytosol dans l'environnement très proche d'une saccule golgienne, l'UDP-L-arabinofuranose traversera la membrane golgienne *via* un transporteur, avant d'être pris en charge par une arabinosyltransférase dans la lumière golgienne, comme schématisé **figure 60**.

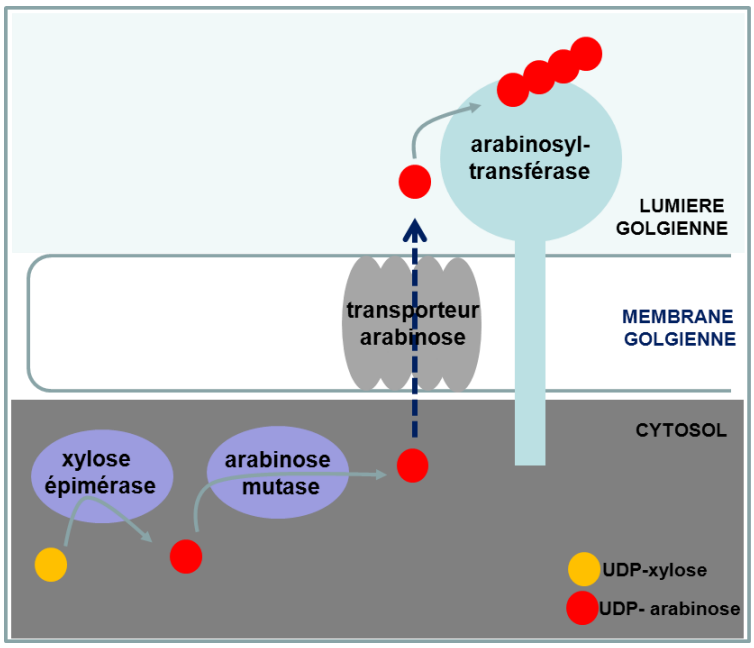

Figure 60 : Représentation schématique des enzymes potentiellement impliquées dans la synthèse golgienne des chaînes arabinanes du RG-I.

Grâce à la technique de split-ubiquitin, nous avons testé l'interaction directe entre plusieurs candidats pouvant participer à la synthèse des chaînes arabinanes pour former un

complexe multiprotéique. AtUXE3 est l'homologue de la xylose épimérase AtMUR4, elle ne possède pas de domaine transmembranaire d'après les analyses *in silico*, et elle est localisée au niveau du compartiment median. AtRGP1 et AtRGP2 sont des mutases, elles n'ont pas de domaine transmembranaire, elles sont cytosoliques et également associées aux empilements golgiens (e.g. protéines périphériques). AtARAD1 est une arabinosyltransférase potentielle, c'est une protéine transmembranaire de type II, et elle est localisée au niveau du compartiment median.

Aucune interaction directe n'a été détectée entre l'épimérase potentielle, les mutases et l'arabinosyltransférase potentielle. Seule l'homo- et l'hétéro-dimérisation des deux mutases a été observée, confirmant les observations de Rautengarten et al. (2011). Bien que ce premier test s'avère négatif, cela ne signifie pas que ces candidats ne soient pas impliqués dans un complexe multiprotéique. En effet, d'autres partenaires potentiels font peut-être le lien entre ces différents candidats. De Pino et al. (2013) ont observé que les mutases RGP n'existaient pas toujours en complexe. C'est la glycosylation des RGPs qui engendre la formation d'un complexe dans le cytsosol et qu'une autre RGP, qui elle n'a pas d'activité mutase, se lie aux saccules golgiennes. D'après l'étude des différentes RGPs, il semble qu'AtRGP5 soit un très bon candidat pour lier AtRGP1 et AtRGP2 à la membrane golgienne. De même, l'homologue de l'arabinosyltransférase, nommé AtARAD2, participe cretainement à ce complexe multiprotéique, puisqu'elle est liée à AtARAD1. Enfin, le dernier partenaire manquant est le transporteur d'arabinose, mais actuellement aucun transporteur spécifique de l'UDP-arabinose n'a été identifié.

PARTIE C : CONCLUSION

Les connaissances sur la synthèse golgienne des polysaccharides pariétaux sont encore très peu développées. L'identification des enzymes d'interconversion, des transporteurs et des glycosyltransférases est la première étape clef pour comprendre le processus de synthèse. L'identification de ces différents acteurs pour la synthèse du XyG est plus avancée que pour le RG-I, en particulier pour les glycosyltransférases. Le RG-I possède une structure très variable comparée au XyG, et la présence d'enzymes homologues ne facilite pas la tâche pour étudier un mutant et caractériser clairement l'activité d'une protéine candidate.

Bien que l'ensemble des acteurs de la synthèse golgienne du XyG et du RG-I ne soit pas identifié, les résultats de ces travaux de recherche tendent à montrer que leur synthèse au sein de l'appareil de Golgi est séquentielle, où les différents sous-compartiments golgiens et le TGN sont chacun dédiés à une étape (représentant une ou plusieurs réactions) de synthèse du XyG et du RG-I.

De plus, les techniques de biochimie et d'imagerie ont mis en évidence *in vitro* et *in vivo* que différents partenaires identifiés s'associent en complexe au sein des empilements golgiens. L'organisation de ces complexes protéiques est encore très peu connue, et ce pour plusieurs raisons. En premier lieu, la topologie des partenaires au sein des membranes est très différente, puisque certaines enzymes d'interconversion se situent dans le cytosol, quand d'autres sont des protéines golgiennes transmembranaires de type II, tout comme les glycosyltransférases. Enfin, les transporteurs d'UDP-sucre et certaines synthases sont des protéines ayant plusieurs domaines transmembranaires, avec leurs extrêmités N- et C-terminales orientées ou non du même côté. Ainsi, la nature des liens qui associent les différents partenaires semble complexe, sachant qu'en plus, nombre de ces partenaires existent en homo-dimères.

Pour compliquer encore la tâche d'étudier ces complexes, il faut également prendre en compte que l'appareil de Golgi n'est pas une structure figée, puisque ses saccules évoluent continuellement du compartiment *cis* vers le *trans*, puis le TGN. Si la synthèse des polysaccharides est séquentielle, cela implique l'association et la dissociation des partenaires pour rester dans un type de compartiment donné, et ce en fonction du micro-environnement golgien (composition de la membrane golgienne, pH).

Enfin, l'existence de complexes multi-protéiques de synthèse du XyG et du RG-I au sein même de l'appareil de Golgi n'est peut-être pas continue dans le temps. L'appareil de Golgi étant le lieu de synthèse de tous les polysaccharides complexes pariétaux, il est fort possible que la cellule végétale régule la synthèse d'un ou plusieurs types de polysaccharides complexes pariétaux, en fonction de ses besoins le long de sa vie au sein d'un tissu donné et/ou en réponse à des stimuli biotique ou abiotique.

BIBLIOGRAPHIE

A

Abiodun MOlabiyi and Matsuoka K (2013). Evidence that Proliferation of Golgi Apparatus Depends on Both De Novo Generation from the Endoplasmic Reticulum and Formation from Pre-Existing Stacks During the Growth of Tobacco BY-2 Cells. *Plant Cell Physiology* 54(4): 541-554

Albersheim P, Darvill AG, O'Neill MA, Schols HA, Voragen AGJ (1996) An hypothesis: the same six polysaccharides are components of the primary cell walls of all higher plants. In Pectins and Pectinases. Edited by Visser J, Voragen AGJ. Amsterdam: Elsevier Sciences B.V.; p 47-53

Anders N, Wilkinson MD, Lovegrove A, Freeman J, Tryfona T, Pellny TK, Weimar T, Mortimer JC, Stott K, Baker JM, Defoin-Platel M, Shewry PR, Dupree P, Mitchell RA. (2012) Glycosyl transferases in family 61 mediate arabinofuranosyl transfer onto xylan in grasses. Proc Natl Acad Sci U S A. 109(3):989-93

Atmodjo MA, Sakuragi Y, Zhu X, Burrell AJ, Mohanty SS, Atwood JA 3rd, Orlando R, Scheller HV, Mohnen D. (2011) Galacturonosyltransferase (GAUT)1 and GAUT7 are the core of a plant cell wall pectin biosynthetic homogalacturonan:galacturonosyltransferase complex. *Proc Natl Acad Sci U S A.* 108(50):20225-30

Atmodjo MA, Hao Z, Mohnen D (2013) Evolving views of pectin biosynthesis. *Annu Rev Plant Biol.* 64:747-79

B

Bakker H, Routier F, Oelmann S, Jordi W, Lommen A, Gerardy-Schahn R, Bosch D (2005) Molecular cloning of two Arabidopsis UDP-galactose transporters by complementation of a deficient Chinese hamster ovary cell line. *Glycobiology* 15:193-201

Banfield DK. (2011) Mechanisms of protein retention in the Golgi. *Cold Spring Harb Perspect Biol.* 3(8):a005264

Barber C., Rösti J., Rawat A., Findlay K., Roberts K., and Seifert G J. (2006) Distinct Properties of the Five UDP-D-glucose/UDP-D-galactose 4-Epimerase Isoforms of *Arabidopsis thaliana The journal of biological chemistry* 281(25):17276–17285

Barratt, D.H., Derbyshire, P., Findlay, K., Pike, M., Wellner, N., Lunn, J., Feil, R., Simpson, C., Maule, A.J., and Smith, A.M. (2009). Normal growth of Arabidopsis requires cytosolic invertase but not sucrose synthase. *Proc. Natl Acad. Sci. U S A.* 106:13124–13129

Becker B, Bölinger B, Melkonian M (1995). Anterograde transport of algal scales through the Golgi complex is not mediated by vesicles. *Trends Cell Biology* 5 : 305–307

Boevink, P., Oparka, K., Santa Cruz, S.,Martin, B., Betteridge, A., and Hawes, C. (1998). Stacks on tracks: the plant Golgi apparatus traffics on an actin/ER network. *Plant J.* 15:441-447

Bonfanti L, Mironov AA Jr, Martínez-Menárguez JA, Martella O, Fusella A, Baldassarre M, Buccione R, Geuze HJ, Mironov AA, Luini A (1998). Procollagen traverses the Golgi stack without leaving the lumen of cisternae: evidence for cisternal maturation. *Cell* 95 : 993–1003

Bonin C P. , Potter I. , Vanzin Gary F., And Wolf-Dieter Reiter (1997) The mur1 gene of arabidopsis thaliana encodes an isoform of gdp-d-mannose-4,6-dehydratase,catalyzing the first step in the de novo synthesis of gdp-l-fucose. *proc Natl Acad Sci U S A.* 94(5):2085-90

Bonin CP, Reiter WD (2000) A bifunctional epimerase-reductase acts downstream of the MUR1 gene product and completes the de novo synthesis of GDP-L-fucose in Arabidopsis. Plant J. Mar;21(5):445-54

Bonin CP., Freshour G., Hahn MG., Vanzin G F., and Reiter WD (2003) The GMD1 and GMD2 genes of Arabidopsis encode isoforms of GDP-D-mannose 4,6-dehydratase with cell type-specific expression patterns. *Plant Physiol.* 132(2):883-92

Brandizzi F, Snapp EL, Roberts AG, Lippincott-Schwartz J, Hawes C. (2002a) Membrane protein transport between the endoplasmic reticulum and the Golgi in tobacco leaves is energy dependent but cytoskeleton independent: evidence from selective photobleaching. *Plant Cell.* 14(6):1293-309

Brandizzi F., Frangne N. ,Marc-Martin S., Hawes C., Neuhaus J.M.,and Paris N.(2002b).The destination for single-pass membrane proteins is influenced markedly by the length of the hydrophobic domain. *Plant Cell* 14: 1077–1092

Bretscher MS, Munro S. (1993) Cholesterol and the Golgi apparatus. *Science*. 261(5126):1280-1

Brown, R.M. (1996). The biosynthesis of cellulose. *J. Macromol. Sci.* 33: 1345–1373

Brummell DA, Camirand A, Maclachlan GA. (1990) Differential distribution of xyloglucan glycosyltransferase in pea golgi dictyosomes and secretory vesicles. *J Cell Sci*. 96: 705-710

Burget EG, Reiter WD. (1999) The mur4 mutant of arabidopsis is partially defective in the de novo synthesis of uridine diphospho L-arabinose.*Plant Physiol*. 121(2):383-9

Burget EG, Verma R, Mølhøj M, Reiter WD. (2003) The biosynthesis of L-arabinose in plants: molecular cloning and characterization of a Golgi-localized UDP-D-xylose 4-epimerase encoded by the MUR4 gene of Arabidopsis. *Plant Cell*. 15(2):523-31

C

Caffall K.H., Mohnen D. (2009) The structure, function, and biosynthesis of plant cell wall pectic polysaccharides Carbohydrate Research 344: 1879–1900

Camirand A, Brummell D, Maclachlan G. (1987) Fucosylation of xyloglucan: localization of the transferase in dictyosomes of pea stem cells. *Plant Physiol*. 84: 753-756

Cavalier DM, Keegstra K. (2006) Two xyloglucan xylosyltransferase catalyze the addition of multiple xylosyl residues to a cellohexaose. *J Biol Chem*. 281: 34197-34207

Chevalier L, Bernard S, Ramdani Y, Lamour R, Bardor M, Lerouge P, Follet-Gueye ML, Driouich A. (2010) Subcompartment localization of the side chain xyloglucan-synthesizing enzymes within Golgi stacks of tobacco suspension-cultured cells. Plant J 64: 977–989.

Chou YH, Pogorelko G, Zabotina OA (2012) Xyloglucan xylosyltransferases XXT1, XXT2, and XXT5 and the glucan synthase CSLC4 form Golgi-localized multiprotein complexes. *Plant Physiol.* 159(4):1355-66

Cocuron JC, Lerouxel O, Drakakaki G, Alonso AP, Liepman AH, Keegstra K, Raikhel N, Wilkerson CG. (2007) A gene from the cellulose synthase-like C family encodes a beta-1,4 glucan synthase. *Proc Natl Acad Sci USA*. 104: 8550-8555

Coenen GJ, Bakx EJ, Verhoef RP, Schols HA, Voragen AGJ (2007) Identification of the connecting linkage between homo- or xylogalacturonan and rhamnogalacturonan type I *Carbohydrate Polymers* 70 :224–235

Cosgrove DJ. (2005) Growth of the plant cell wall. *Nature Reviews Molecular Cell Biology* 6, 850–861

D

Darvill JE., Mcneil M., Darvill AG., and Albersheim P. (1980) Structure of plant cell walls xi. glucuronoarabinoxylan, a second hemicellulose in the primary cell walls of suspension-cultured sycamore cells *Plant Physiol.* 66 : 1135-1139

daSilva LLP, Snapp EL, Denecke J, Lippincott-Schwartz J, Hawes C, Brandizzi F. (2004) Endoplasmic reticulum export sites and Golgi bodies behave as single mobile secretory units in plant cells. *Plant Cell* 16:1753–1771

Dauwalder, M. and Whaley, W.G. (1974). Patterns of incorporation of (3H)galactose by cells of Zea mays root tips. *J. Cell Sci.* 14 (1): 11-27

Davis, J., Brandizzi, F., Liepman, A., and Keegstra, K. (2010). Arabidopsis mannan synthase CSLA9 and glucan synthase CSLC4 have opposite orientations in the Golgi membrane. *Plant J.* 64: 1028-1037

Davis JK (2012) Combining polysaccharide biosynthesis and transport in a single enzyme: dual-function cell wall glycan synthases. *Frontiers in plant science* Volume 3 | Article 138

Delgado IJ, Wang Z, de Rocher A, Keegstra K and Raikhel NV (1998) Cloning and Characterization of AtRGP11 - A Reversibly Autoglycosylated Arabidopsis Protein Implicated in Cell Wall Biosynthesis *Plant Physiol*. 116: 1339–1349

De Pino V, Borán M, Norambuena L, González M, Reyes F, Orellana A, Moreno S. (2007) Complex formation regulates the glycosylation of the reversibly glycosylated polypeptide. *Planta.* 226(2):335-45

De Pino V, Marino Busjle C, Moreno S. (2013) Oligomerization of the reversibly glycosylated polypeptide: its role during rice plant development and in the regulation of self-glycosylation. *Protoplasma.* 250(1):111-9

Dettmer J, Hong-Hermesdorf A, Stierhof YD, Schumacher K. (2006) Vacuolar H+-ATPase activity is required for endocytic and secretory trafficking in Arabidopsis. *Plant Cell.* 18(3):715-30

Diet A., Link B., Seifert G.J., Schellenberg B., Wagner U., Pauly M., Reiter W.D., Ringli C. (2006) The Arabidopsis root hair cell wall formation mutant lrx1 is suppressed by mutations in the RHM1 gene encoding a UDP-L-rhamnose synthase. *Plant Cell* 18: 1630–1641

Dirnberger D., Bencúr P., Mach L., Steinkellner H. (2002) The Golgi localization of Arabidopsis thaliana β1,2-xylosyltransferase in plant cells is dependent on its cytoplasmic and transmembrane sequences *Plant Molecular Biology* 50(2):273-281

Donohoe BS, Kang BH, Gerl MJ, Gergely ZR, McMichael CM, Bednarek SY, Staehelin LA. (2013) Cis-Golgi cisternal assembly and biosynthetic activation occur sequentially in plants and algae. *Traffic.* 14(5):551-67

Dörmann P. and Benning C. (1996) Functional Expression of Uridine 5'-Diphospho-Glucose 4-Epimerase (EC 5.1.3.2) from *Arabidopsis thaliana* in *Saccharomyces cerevisiae* and *Escherichia coli Archives of biochemistry and biophysics* 327(1): 27–34

Drakakaki G, Zabotina O, Delgado I, Robert S, Keegstra K and Raikhel N (2006) Arabidopsis Reversibly Glycosylated Polypeptides 1 and 2 Are Essential for Pollen Development *Plant Physiology*, 142: 1480–1492

Driouich A, Zhang GF, Staehelin LA. (1993) Effect of Brefeldin A on the structure of the golgi apparatus and on the synthesis and secretion of proteins and polysaccharides in sycamore maple suspension-cultured cells. *Plant Physiol*. 101: 1363-1373

E

Eda S, Akiyama Y, Kato K (1983) Methylation Analysis of Cell Wall Polysaccharides from Suspension-cultured Cells of Nicotiana tabacum *Agric. Biol Chem.,* 47 (8): 1783-1789

Eda S., Akiyama Y., Kato K. (1985) A galactoglucomannan from cell walls of suspension cultured tobacco (nicotiana tabacum) cells *Carbohydrate Research,* 137: 173-181

Edwards ME, Dickson CA, Chengappa S, Sidebottom C, Gidley MJ, Reid GJS. (1999) Molecular characterization of a membrane-bound galactosyltransferase of plant cell wall matrix polysaccharide biosynthesis. *Plant J.* 19: 691-697

Endler A, Persson S (2011) Cellulose synthases and synthesis in Arabidopsis. *Mol Plant.* 4(2):199-211

F

Faik A, Price NJ, Raikhel NV, Keegstra K. (2002) An Arabidopsis gene encoding an α-xylosyltransferase involved in xyloglucan biosynthesis. *Proc Natl Acad Sci USA*. 99: 7797-7802

Fry, S.C., York, W.S., Albersheim, P., Darvill, A., Hayashi, T., Joseleau, J.-P., Kato, Y., Lorences, E.P.,Maclachlan, G.A., McNeil, M., Mort, A.J., Reid, J.S.G., Seitz, H.U., Selvendran, R.R., Voragen,A.G.J. and White, A.R. (1993) An unambiguous nomenclature for xyloglucan-derived oligosaccharides. *Physiol. Plant*. 89: 1-3

Fujii, S., Hayashi, T., and Mizuno, K. (2010). Sucrose synthase is an integral component of the cellulose synthesis machinery. *Plant Cell Physiol.* 51: 294–301

Fujimoto M and Ueda T (2012) Conserved and plant-unique mechanisms regulating plant post-Golgi traffic *Frontiers in plant sciences* Volume 3, article 197

G

Gardiner,M.,and Chrispeels,M.J. (1975). Involvement of the Golgi apparatus in the synthesis and secretion of hydroxyproline-rich cell wall glycoproteins. *Plant Physiol.* 55: 536–541

Geshi N, Pauly M and Ulvskov P (2002) Solubilization of galactosyltransferase that synthesizes 1,4-*b*-galactan side chains in pectic rhamnogalacturonan *Physiologia Plantarum* 114: 540–548

Geshi N, Jørgensen B, Ulvskov P (2004) Subcellular localization and topology of b(1,4) galactosyltransferase that elongates b(1 ,4)galactan side chains in rhamnogalacturonan I in potato *Planta* 218: 862–868

Gibeaut D.M. and Carpita N.C. (1994). Biosynthesis of plant cell wall polysaccharides. *FASEB J.* 8 (12), 904-915

Green,J.R.,andNorthcote,D.H.(1978) The structure and function of glycoproteins synthesized during slime-polysaccharide production by membranes of the root-cap cells of maize(*Zea mays*). *Biochem.J.* 170: 599–608

Gu X. and Bar-Peled M. (2004) The Biosynthesis of UDP-Galacturonic Acid in Plants.
Functional Cloning and Characterization of Arabidopsis UDP-D-Glucuronic Acid 4-Epimerase1 *Plant Physiology,* 136: 4256–4264

H

Handford M, Rodríguez-Furlán C, Marchant L, Segura M, Gómez D, Alvarez-Buylla E, Xiong GY, Pauly M, Orellana A. (2012) Arabidopsis thaliana AtUTr7 encodes a golgi-localized UDP-glucose/UDP-galactose transporter that affects lateral root emergence. *Mol Plant*. 5(6):1263-80

Harholt J, Jensen JK, Sorensen SO, Orfila C, Pauly M, Scheller HV (2006) ARABINAN DEFICIENT 1 is a putative arabinosyltransferase involved in biosynthesis of pectic arabinan in Arabidopsis. *Plant Physiol* 140: 49–58

Harholt,J., Suttangkakul,A., and Vibe Scheller,H.(2010) Biosynthesis of pectin. *Plant Physiol.* 153: 384–395

Harholt J, Jensen JK, Verhertbruggen Y, Søgaard C, Bernard S, Nafisi M, Poulsen CP, Geshi N, Sakuragi Y, Driouich A, Knox JP, Scheller HV (2012) ARAD proteins associated with pectic Arabinan biosynthesis form complexes when transiently overexpressed in planta. *Planta.* 236(1):115-28

Harper AD, Bar-Peled M. Biosynthesis of UDP-xylose (2002) Cloning and characterization of a novel Arabidopsis gene family, UXS, encoding soluble and putative membrane-bound UDP-glucuronic acid decarboxylase isoforms. *Plant Physiol.* 130(4):2188-98

Harris, P.J. and Northcote, D.H. (1971). Polysaccharide formation in plant Golgi bodies. *Biochem. Biophys. Acta*. 237(1): 56-64

Hawes C, Satiat-Jeunemaitre B (2005) The plant Golgi apparatus--going with the flow. *Biochim Biophys Acta.* 1744(3):466-80

Hawes C, Schoberer J, Hummel E, Osterrieder A. (2010) Biogenesis of the plant Golgi apparatus. *Biochem Soc Trans.* 38(3):761-7

Hayashi T, Kato Y, Matsuda K. (1981) Biosynthesis of xyloglucan in suspensions-cultured soybean cells. An assay method for xyloglucan xylosyltransferase and attempted synthesis of xyloglucan from UDP-D-xylose. *J Biochem*. 89: 325-328

Hayashi T, Koyama T, Matsuda K. (1988) Formation of UDP-Xylose and xyloglucan in soybean golgi membranes. *Plant Physiol*. 87:341-345

Hayashi T. and Kaida R. (2011) Functions of Xyloglucan in Plant Cells *Molecular Plant* 4 (1): 17–24

Hisamatsu M, York WS, Darvill AG, Albersheim P. (1992) Characterization of seven xyloglucan oligosaccharides containing from seventeen to twenty glycosyl residues. *Carbohydr Res*. 227:45-71

Hoffman M, Jia Z, Pena MJ, Cash M, Harper A, Blackburn AR II, Darvill A, York WS. (2005) Structural analysis of xyloglucans in primary cell walls of plants in the subclass Asteridae. *Carbohydrate Res.* 340:1826-1840

Hood EE, Gelvin SB, Melchers LS and Hoekema A (1993) New *Agrobacterium* helper plasmids for gene transfer to plants *Transgenic Research.* 2:208-218

Hu CD, Chinenov Y, Kerppola TK. (2002) Visualization of interactions among bZIP and Rel family proteins in living cells using bimolecular fluorescence complementation *Mol Cell.* 9(4):789-98

Huisman MMH, Brüll LP, Thomas-Oates JE, Haverkamp J, Schols HA, Voragen AGJ (2001) The occurrence of internal (1-5)-linked arabinofuranose and arabinopyranose residues in arabinogalactan side chains from soybean pectic substances. *Carbohydrate Research* 330: 103–114

Hwang,J.W.,and Kokini,J.L.(1991). Structure and rheological function of side branches of carbohydrate polymers. *J. TextureStud.* 22: 123–167

I

Ishii, T. and Matsunaga, T. (1996). Isolation and characterization of a boron-rhamnogalacturonan II complex from cell walls of sugar beet pulp. *Carbohydrate Res.* 284: 1-9

Ishii T., Matsunaga T., Hayashi N. (2001) Formation of Rhamnogalacturonan II-Borate Dimer in Pectin Determines Cell Wall Thickness of Pumpkin Tissue. *Plant Physiology* 126: 1698–1705

Ishii T, Konishi T, Ito Y, Ono H, Ohnishi-Kameyama M, Maeda I (2005) A β-(1→3)-arabinopyranosyltransferase that transfers a single arabinopyranose onto arabino-oligosaccharides in mung bean (*Vigna radiate*) hypocotyls. *Phytochemistry* 66(20):2418-2425

Ito Y, Uemura T, Shoda K, Fujimoto M, Ueda T, Nakano A. (2012) cis-Golgi proteins accumulate near the ER exit sites and act as the scaffold for Golgi regeneration after brefeldin A treatment in tobacco BY-2 cells. *Mol Biol Cell.* Aug;23(16):3203-14

J

Jarvis MC (1984) Structure and properties of pectin gels in plant cell wall. *Plant Cell Environ.* 7:153–164

Jia Z, Qin Q, Darvill AG, and York WS (2003) Structure of the xyloglucan produced by suspension-cultured tomato cells. *Carbohydrate Research*, 338:1197-1208

Jensen JK, Schultink A, Keegstra K, Wilkerson CG, Pauly M. (2012) RNA-Seq Analysis of Developing Nasturtium Seeds (Tropaeolum majus): Identification and Characterization of an additional Galactosyltransferase Involved in Xyloglucan Biosynthesis. *Mol Plant.* Apr 2. [Epub ahead of print]

Jones, L.; Milne, J. L.; Ashford, D.; McQueen-Mason, S. (2003) Cell wall arabinan is essential for guard cell function. *Proc. Natl. Acad. Sci. U.S.A.*, 100:11783–11788

Jordan D B., Bowman M J., Braker J D., Dien B S., Hector R E. , Lee C C. , Mertens J A. and Wagschal K. (2012) Plant cell walls to ethanol *Biochem. J.*, 442 : 241–252

K

Kang BH (2011) Shrinkage and fragmentation of the trans-Golgi network in non-meristematic plant cells. *Plant Signaling & Behavior* 6(6): 884-886

Kang BH, Nielsen E, Preuss ML, Mastronarde D, Staehelin LA. (2011) Electron tomography of RabA4b- and PI-4Kbeta1-labeled trans golgi network compartments in arabidopsis. *Traffic* 12:313-29

Keegstra K., Talmadge K W., Bauer W. D. and Albersheim P.(1973) The structure of plant cell walls iii. A model of the walls of suspension-cultured sycamore cells based on the interconnections of the macromolecular components *Plant physiol.* 51: 188-196

Kerppola KT (2008) Bimolecular Fluorescence Complementation (BiFC) Analysis as a Probe of Protein Interactions in Living Cells *Annu. Rev. Biophys.* 37:465–87

Kimura, S., Laosinchai, W., Itoh, T., Cui, X., Linder, C.R., and Brown, R.M. (1999). Immunogold labeling of rosette terminal cellulose-synthesizing complexes in the vascular plant Vigna angularis. *Plant Cell.* 11: 2075–2086

Klemm, R.W., Ejsing, C.S., Surma, M.A. et al. (2009) Segregation of sphingolipids and sterols during formation of secretory vesicles at the trans-Golgi network. *J. Cell Biol.* 185: 601–612

Kobayashi, M., Matoh, T., Azuma, J. (1996). Two chains of rhamnogalacturonan-II are cross-linked by borate-diol ester bonds in higher plant cell walls. *Plant Physiol*. 110: 1017-1020

Koncz C. and Jeff Schell J. (1986) The promoter of TL-DNA gene 5 controls the tissue-specific expression of chimaeric genes carried by a novel type of *Agrobacterium* binary vector *Mol. Gen. Genet.* 204:383-396

Kondylis, V. and Rabouille, C. (2009) The Golgi apparatus: lessons from *Drosophila*. *FEBS Lett.* 583:3827–3838

Konishi T, Mitome T, Hatsushika H, Md. Haque A, Kotake T, Tsumuraya Y (2004) Biosynthesis of pectic galactan by membrane-bound galactosyltransferase from soybean (Glycine max Merr.) seedlings *Planta* 218: 833–842

Konishi T, Kotake T, Tsumuraya Y (2007a) Chain elongation of pectic β(1,4)-galactan by a partially purified galactosyltransferase from soybean (*Glycine max* Merr.) hypocotyls *Planta* 226:571–579

Konishi T, Takeda T, Miyazaki Y, Ohnishi-Kameyama M, Hayashi T, O'Neill MA and Ishii T (2007b) A plant mutase that interconverts UDP-arabinofuranose and UDP-arabinopyranose *Glycobiology* 17:345-354

Kristen U (1978) Ultrastructure and a Possible Function of the Intercisternai Elements in Dictyosomes *Planta* 138: 29-33

L

Latijnhouwers M, Gillespie T, Boevink P, Kriechbaumer V, Hawes C, Carvalho CM (2007) Localization and domain characterization of Arabidopsis golgin candidates. *J Exp Bot.* 58(15-16):4373-86

LeGoff, A., Renard, C.M.G.C., Bonnin, E., Thibault, J.-F., (2001). Extraction, purification and chemical characterisation of xylogalacturonans from pea hulls. *Carbohydr. Polym.* 45: 325–334

Lerouxel O, Cavalier DM, Liepman AH, Keegstra K. (2006) Biosynthesis of plant cell wall polysaccharides: a complex process. *Curr. Opin. Plant Biol.* 9: 621-630

Li X, Cordero I, Caplan J, Mølhøj M, Reiter WD. (2004) Molecular analysis of 10 coding regions from Arabidopsis that are homologous to the MUR3 xyloglucan galactosyltransferase. *Plant Physiol.* 134(3):940-50.

Li Y, Smith C, Corke F, Zheng L, Merali Z, Ryden P, Derbyshire P, Waldron K, and Bevana MW, (2007) Signaling from an Altered Cell Wall to the Nucleus Mediates Sugar-Responsive Growth and Development in Arabidopsis thaliana *The Plant Cell* 19: 2500–2515

Liepman AH. and Cavalier DM. (2012) The Cellulose Synthase-Like A And Cellulose Synthase-Like C families: recent advances and future perspectives *Frontiers in plant science* Volume3 | Article 109

Lippincott-Schwartz J, Phair RD. (2010) Lipids and cholesterol as regulators of traffic in the endomembrane system. *Annu Rev Biophys* 39: 559–578

Liwanag AJ, Ebert B, Verhertbruggen Y, Rennie EA, Rautengarten C, Oikawa A, Andersen MC, Clausen MH, Scheller HV. (2012) Pectin biosynthesis: GALS1 in Arabidopsis thaliana is a β-1,4-galactan β-1,4-galactosyltransferase. *Plant Cell.* 24(12):5024-36

Losev E, Reinke CA, Jellen J, Strongin DE, Bevis BJ, Glick BS (2006). Golgi maturation visualized in living yeast. *Nature* 441: 1002–1006

M

Madson M, Dunand C, Li X, Verma R, Vanzin GF, Caplan J, Shoue DA, Carpita NC, Reiter WD. (2003) The MUR3 gene of Arabidopsis encode a xyloglucan galactosyltransferase that is evolutionarily related to animal exostosins. *Plant Cell*. 15: 1662-1670

Matoh, T., Ishigaki, K., Ohno, K., Azuma, J. (1993). Isolation and characterization of a boron-polysaccharide complex from radish roots. *Plant Cell Physiol*. 34: 639-642

Matsuura-Tokita K, Takeuchi M, Ichihara A, Mikuriya K, Nakano A (2006). Live imaging of yeast Golgi cisternal maturation. *Nature* 441 : 1007–1010

Mayhew, T.M., Lucocq, J.M. and Griffiths, G. (2002) Relative labelling index: a novel stereological approach to test for non-random immunogold labeling of organelles and membranes on transmission electron microscopy thin sections. *J. Microsc*. 205: 153–164

Mayhew T. M. (2011) Quantifying immunogold localization on electron microscopic thin sections: a compendium of new approaches for plant cell biologists *J. Exp. Bot*. 62(12): 4101-4113.

McCann MC, Roberts K. (1991) Architecture of the primary cell wall. In *The Cytoskeletal Basis of Plant Growth and Form*, ed. CW Lloyd, pp. 109–29. New York: Academic

McDougall GJ, Fry SC. (1989) Structure-activity relationships for xyloglucan oligosaccharides with antiauxin activity. *Plant Physiol.* 89:883–87

McNeil,M.,Darvill,A.G.,andAlber- sheim, P.(1982).Structure of plant cell walls. Identification of seven glycosyl residues attached to O-4 of the 2-4 linked L-rhamnosyl residues of rhamnogalacturonan I. *PlantPhysiol.* 70: 1586–1591

Meier H, Reid JSG. 1982. Reserve polysaccharides other than starch in higher plants. In *Encyclopedia of Plant Physiology.* NS 13A: *Plant Carbohydrates I*, ed. FA Loewus,WTanner, pp. 418–71. Berlin: Springer

Melser S, Molino D, Batailler B, Peypelut M, Laloi M, Wattelet-Boyer V, Bellec Y, Faure JD, Moreau P (2011) Links between lipid homeostasis, organelle morphodynamics and protein trafficking in eukaryotic and plant secretory pathways. *Plant Cell Rep* 30:177–193

Mohnen,D.(2008).Pectin structure and biosynthesis. *Curr.Opin.Plant Biol.* 11: 266–277

Mølhøj M., Verma R., and Reiter WD.(2004) The Biosynthesis of D-Galacturonate in Plants. Functional Cloning and Characterization of a Membrane-Anchored UDP-D-Glucuronate 4-Epimerase from Arabidopsis *Plant Physiology* 135: 1221–1230

Moore JP, Nguema-Ona E, Chevalier L, Lindsey GG, Brandt WF, Lerouge P, Farrant JM, Driouich A. (2006) Response of the leaf cell wall to desiccation in the resurrection plant Myrothamnus flabellifolius. *Plant Physiol.* 141(2):651-62

Moreau P, Brandizzi F, Hanton S, Chatre L, Melser S, Hawes C, Satiat-Jeunemaitre B. (2007) The plant ER-Golgi interface: a highly structured and dynamic membrane complex. *Journal Experimental Botany* 58(1):49-64

Mori M et Kato K (1981) An arabinoglucuronomannan from suspension-cultured cells of *Nicotiana tabacum. Carbohydrate research* 91: 49-58

Munro S (2011) The Golgin Coiled-Coil Proteins of the Golgi Apparatus *Cold Spring Harb Perspect Biol* 3:a005256

N

Nakamura, A., Furuta, H., Maeda, H., Takao, T., Nagamatsu, Y., (2002). Analysis of the molecular construction of xylogalacturonan isolated from soluble soybean polysaccharides. *Biosci. Biotechnol. Biochem.* 66: 1155–1158

Nakayama K, Maeda Y, Jigami Y (2003) Interaction of GDP-4-keto-6-deoxymannose-3,5-epimerase-4-reductase with GDP-mannose-4,6-dehydratase stabilizes the enzyme activity for formation of GDP-fucose from GDP-mannose. *Glycobiology.* 13(10):673-80

Nebenführ A., Gallagher L., Dunahay T.G., Frohlick J.A., Mazurkiewicz A.M., Meehl J.B., Staehelin L.A. (1999) Stop-and-go movements of plant Golgi stacks are mediated by the acto-myosin system. *Plant Physiol*. 121:1127-1141

Nemati N, Karapetyan G, Nolting B, Endress HU, Vogel C (2008) Synthesis of rhamnogalacturonan I fragments by a modular design principle. *Carbohydr. Res.* 343: 1730-1742

Nguema-Ona E, Andeme-Onzighi C, Aboughe-Angone S, Bardor M, Ishii T, Lerouge P, Driouich A. (2006) The *reb1-1* mutation of Arabidopsis: Effect on the structure and the localization of galactose containing cell wall polysaccharides. *Plant Physiol*. 140, 1406-1417.

Nikolovski N, Rubtsov D, Segura MP, Miles GP, Stevens TJ, Dunkley TP, Munro S, Lilley KS, Dupree P (2012) Putative glycosyltransferases and other plant Golgi apparatus proteins are revealed by LOPIT proteomics. *Plant Physiol.* 160(2):1037-51

Nilsson T, Slusarewicz P, HoeMH,Warren G. (1993) Kin recognition. A model for the retention of golgi enzymes. *FEBS Lett* 330: 1–4

Norambuena L, Marchant L, Berninsone P, Hirschberg C, Silva H, Orellana A (2002) Transport of UDP-Galactose in plants. *J Biol Chem* 277:32923-32929

Norambuena L, Nilo R, Handford M, Reyes F, Marchant L, Meisel L, Orellana A (2005) AtUTr2 is an Arabidopsis thaliana nucleotide sugar transporter located in the Golgi apparatus capable of transporting UDP galactose. Planta, 222:521-529

Nour-Eldin HH, Hansen BG, Nørholm MH, Jensen JK, Halkier BA. (2006) Advancing uracil-excision based cloning towards an ideal technique for cloning PCR fragments. *Nucleic Acids Res.* 34(18):e122

Nour-Eldin HH, Geu-Flores F, Halkier BA. (2010) USER cloning and USER fusion: the ideal cloning techniques for small and big laboratories. *Methods Mol Biol.* 643:185-200.

O

Øbro J, Harholt J, Scheller HV, Orfila C (2004) Rhamnogalacturonan I in Solanum tuberosum tubers contains complex arabinogalactan structures. *Phytochemistry* 65:1429–1438

Oechslin, R., Lutz, M. V., & Amado, R. (2003). Pectic substances isolated from apple cellulosic residue: Structural characterisation of a new type of rhamnogalacturonan I. *Carbohydrate Polymers*, 51: 301–310

Oka T., Nemoto T., Jigami Y. (2007) Functional analysis of Arabidopsis thaliana RHM2/MUM4, a multidomain protein involved in UDP-D-glucose to UDP-L-rhamnose conversion. *J. Biol. Chem.* 282: 5389–5403

Oikawa A, Lund CH, Sakuragi Y, Scheller HV. (2013) Golgi-localized enzyme complexes for plant cell wall biosynthesis. *Trends Plant Sci.* 18(1):49-58

O'Neill, M.A., Warrenfeltz, D., Kates, K., Pellerin, P., Doco, T., Darvill, A.G., Albersheim, P. (1996). Rhamnogalacturonan-II, a pectic polysaccharide in the walls of growing plant cell, forms a dimer that is covalently crosslinked by a borate ester. *J. Biol. Chem.* 271: 22923-22930

O'Neill, M.A, Eberhard, S., Albersheim, P., Darvill, A.G. (2001). Requirement of borate cross-linking of cell wall rhamnogalacturonan II for Arabidopsis growth. *Science* 294(5543): 846-849

O'Neill, M.A., Ishii, T., Albersheim, P., Darvill, A.G. (2004). Rhamnogalacturonan II: structure and function of a borate cross-linked cell wall pectic polysaccharide. *Annu. Rev. Plant Biol*. 55: 109-139

Orfila, C.; Seymour, G. B.; Willats, W. G. T.; Huxham, I. M.; Jarvis, M. C.; Dover, C. J.; Thompson, A. J.; Knox, J. P. (2001) Altered Middle Lamella Homogalacturonan and Disrupted Deposition of (1,5)-a-L-Arabinan in the Pericarp of *Cnr*, a Ripening Mutant of Tomato. *Plant Physiol.*, 126: 210–221

P

Pagnussat G.C., Yu HJ,, Ngo Q.A., Rajani S., Mayalagu S.,. Johnson C. S, Capron A., Xie L.F, Ye D., and Sundaresan V. (2004) Genetic and molecular identification of genes required for female gametophyte development and function in Arabidopsis *Development* 132: 603-614

Pagny S, Bouissonie F, Sarkar M, Follet-Gueye ML, Driouich A, Schachter H, Faye L, Gomord V. (2003) Structural requirements for Arabidopsis β 1-2 xylosyltransferase activity and targeting to the golgi. *Plant J*. 33: 189-203

Park YB. and Cosgrove DJ. (2012) A Revised Architecture of Primary Cell Walls Based on Biomechanical Changes Induced by Substrate-Specific Endoglucanases *Plant Physiology*, 158: 1933–1943

Parsons HT, Drakakaki G, Heazlewood JL. (2013) Proteomic dissection of the Arabidopsis Golgi and trans-Golgi network. *Front Plant Sci.* Volume 3| Article 298.

Pattathil S., Harper AD., Bar-Peled M. (2005) Biosynthesis of UDP-xylose: characterization of membrane-bound AtUxs2. *Planta.* 221(4):538-48

Pattathil S., Avci U., Baldwin D., Swennes AG., McGill JA., Popper Z., Booten T., Albert A., Davis RH., Chennareddy C., Dong R., O'Shea B., Rossi R., Leoff C., Freshour G., Narra R., O'Neil M., York WS., Hahn M. (2010) A comprehensive toolkit of plant cell wall glycan-directed monoclonal antibodies. *Plant Physiol.*. 153(2): 514-525

Patterson GH, Hirschberg K, Polishchuk RS, Gerlich D, Phair RD, Lippincott-Schwartz J. (2008) Transport through the golgi apparatus by rapid partitioning within a two-phase membrane system. *Cell* 133: 1055-1067

Pauly M, Eberhard S, Albersheim P, Darvill A, York WS. (2001) Effects of the mur1 mutation on xyloglucans produced by suspension-cultured Arabidopsis thaliana cells. *Planta* 214(1):67-74

Pédelacq JD, Cabantous S, Tran T, Terwilliger TC, Waldo GS. (2006) Engineering and characterization of a superfolder green fluorescent protein. *Nat Biotechnol.* 24(1):79-88

Peng, L.C., Kawagoe, Y., Hogan, P., and Delmer, D. (2002). Sitosterol-b-glucoside as primer for cellulose synthesis in plants. *Science.* 295:147–150

Perrin RM, DeRocher AE, Bar-Peled M, Zeng W, Norambuena L, Orellana A, Raikhel NV, Keegstra K. (1999) Xyloglucan fucosyltransferase, an enzyme involved in plant cell wall biosynthesis. *Science*. 284: 1976-1979

Pickett-Heaps, J.D. (1966). Incorporation of radiactivity into wheat xylem walls. *Planta* 71:1-14

Pickett-Heaps, J.D. (1968) Further ultrastructural observations on polysaccharide localization in plant cells. *J. Cell Sci.* 3(1): 55-64

Popper ZA, Michel G, Hervé C, Domozych DS, Willats WG, Tuohy MG, Kloareg B, Stengel DB. (2011) Evolution and diversity of plant cell walls: from algae to flowering plants. *Annu Rev Plant Biol.* 62:567-90

Q

Qu Y, Egelund J, Gilson PR, Houghton F, Gleeson PA, Schultz CJ, Bacic A (2008) Identification of a novel group of putative Arabidopsis thaliana *b*-(1,3)-galactosyltransferases *Plant Mol Biol* 68:43–59

R

Ralet MC, André-Leroux G, Quéméner B, Thibault JF. (2005). Sugar beet (*Beta vulgaris*) pectins are covalently cross-linked through diferulic bridges in the cell wall. *Phytochemistry* 66:2800–14

Rautengarten C, Ebert B, Herter T, Petzold CJ, Ishii T, Mukhopadhyay A, Usadel B and Scheller HV (2011) The Interconversion of UDP-Arabinopyranose and UDP-Arabinofuranose Is Indispensable for Plant Development in Arabidopsis *The Plant Cell* 23: 1373–1390

Ray PM. (1980) Cooperative action of beta-glucan synthetase and UDP-xylose xylosyl transferase of Golgi membranes in the synthesis of xyloglucan-like polysaccharide. *Biochim Biophys Acta.* 629, 431-444

Reboul R, Geserick C, Pabst M, Frey B, Wittmann D, Lütz-Meindl U, Léonard R, Tenhaken R. (2011) Down-regulation of UDP-glucuronic acid biosynthesis leads to swollen plant cell walls and severe developmental defects associated with changes in pectic polysaccharides. *J Biol Chem*. 286(46):39982-92

Reichardt I, Stierhof YD, Mayer U, Richter S, Schwarz H, Schumacher K, Jürgens G. (2007). Plant cytokinesis requires de novo secretory trafficking but not endocytosis. *Curr. Biol.* 17: 2047-2053

Reid JSG. (1985) Cell wall storage carbohydrates in seeds—biochemistry of the seed “gums” and “hemicelluloses.”*Adv. Bot. Res.* 11:125–55

Reiffarth D, Reimer KB (2008) Synthesis of two repeat units corresponding to the backbone of the pectic polysaccharide rhamnogalacturonan I. *Carbohydr. Res.* 343: 179-188

Reiter, W.-D., Chapple, C. C. S. & Somerville, C. R. (1993) Altered Growth and Cell Walls in a Fucose-Deficient Mutant of Arabidopsis *Science* 261:1032–1035

Renna L, Stefano G, Majeran W, Micalella C, Meinnel T, Giglione C, Brandizzi F (2013) Golgi traffic and integrity depend on N-myristoyl transferase-1 in Arabidopsis. *Plant Cell.* 25(5):1756-73

Reuhs, B.L, Glenn, J., Stephens, S.B., Kim, J.S., Christie, D.B., Glushka, J.G., Zablackis, E., Albersheim, P., Darvill, A.G., O'Neill, M.A. (2004). L-Galactose replaces L-fucose in the pectic polysaccharide rhamnogalacturonan II synthesized by the L-fucose-deficient *mur1* Arabidopsis mutant. *Planta* 219(1):147-157

Reyes F, Orellana A. (2008) Golgi transporters: opening the gate to cell wall polysaccharide biosynthesis. Curr Opin Plant Biol. 11(3):244-51

Richmond,T.,and Somerville,C.R. (2001). Integrative approaches to determining Csl function. *PlantMol. Biol.* 47: 131–143

Ridley, B.L., O'Neill, M.A., Mohnen, D. (2001). Pectins: structure, biosynthesis, and oligogalacturonide-related signaling. *Phytochemistry* 57(6): 929-967

Rollwitz I, Santaella M, Hille D, Flugge UI, Fischer K (2006) Characterization of AtNST-KT1, a novel UDP-galactose transporter from Arabidopsis thaliana. *FEBS Lett* 580:4246–4251

Rösti J, Barton CJ, Albrecht S, Dupree P, Pauly M, Findlay K, Roberts K, Seifert GJ. (2007) UDP-glucose 4-epimerase isoforms UGE2 and UGE4 cooperate in providing UDP-galactose for cell wall biosynthesis and growth of Arabidopsis thaliana. *Plant Cell*. 19(5):1565-79

S

Sagi G, Katz A, Guenoune-Gelbart D, and Epel BL (2005) Class 1 Reversibly Glycosylated Polypeptides Are Plasmodesmal-Associated Proteins Delivered to Plasmodesmata via the Golgi Apparatus *The Plant Cell* 17:1788–1800

Saint-Jore-Dupas C, Nebenführ A, Boulaflous A, Follet-Gueye ML, Plasson C, Hawes C, Driouich A, Faye L, Gomord V. (2006) Plant N-glycan processing enzymes employ different targeting mechanisms for their spatial arrangement along the secretory pathway. *Plant Cell*. 18: 3182-3200

Sarria R, Wagner TA, O'Neill MA, Faik A, Wilkerson CG, Keegstra K, Raikhel NV. (2001) Characterization of a family of Arabidopsis genes related to xyloglucan fucosyltransferase. *Plant Physiol*. 127: 1595-1606

Scheible WR and Pauly M (2004) Glycosyltransferases and cell wall biosynthesis: novel players and insights. *Current Opinion in Plant Biology* 7:285–295

Scheller, H.V, Jensen J.K, Sørensen S.O, Harholt J, Geshi N (2007) Biosynthesis of pectins. *Physiol. Plant.* 129: 283–295

Scheller H V. and Ulvskov P. (2010) Hemicelluloses *Annu. Rev. Plant Biol.* 61:263–89

Scheuring D, Viotti C, Krüger F, Künzl F, Sturm S, Bubeck J, Hillmer S, Frigerio L, Robinson DG, Pimpl P, Schumacher K (2011) Multivesicular bodies mature from the trans-Golgi network/early endosome in Arabidopsis. *Plant Cell*. 23(9):3463-81

Schoberer J, Vavra U, Stadlmann J, Hawes C, Mach L, Steinkellner Herta, Strasser R (2009) Arginine/Lysine Residues in the Cytoplasmic Tail Promote ER Export of Plant Glycosylation Enzymes.*Traffic* 10(1): 101–115

Schoberer J. and Strasser R. (2011) Sub-Compartmental Organization of Golgi-Resident N-Glycan Processing Enzymes in Plants *Molecular Plant* 4(2): 220-228

Schols HA, Posthumus MA and Voragent AGJ (1990) Structural features of hairy regions of pectins isolated from apple juice produced by the liquefaction process. *Carbohydrate Research,* 206: 17- 129

Schrick, K., Fujioka, S., Takatsuto, S., Stierhof, Y.D., Stransky, H., Yoshida, S., and Jurgens, G. (2004). A link between sterol biosynthesis, the cell wall, and cellulose in Arabidopsis. *Plant J.* 38: 227–243

Schröder, R., Nicolas, P., Vincent, S.J.F., Fischer, M., Reymond, S. and Redgwell, R. (2001) Purification and characterisation of a galactoglucomannan from kiwi fruit. *Carbohydr. Res.* 331:291–306

Segui-Simarro, J.M. and Staehelin, L.A. (2006) Cell cycle-dependent changes in Golgi stacks, vacuoles, clathrin-coated vesicles and multivesicular bodies in meristematic cells of *Arabidopsis thaliana*: a quantitative and spatial analysis. *Planta* 223: 223–236

Seifert GJ, Barber C, Wells B, Roberts K. (2004) Growth regulators and the control of nucleotide sugar flux. *Plant Cell*. 16:723-730

Sharpe HJ, Stevens TJ, Munro S. (2010) A comprehensive comparison of transmembrane domains reveals organelle-specific properties. *Cell.* 142(1):158-69

Shyu YJ, Liu H, Deng X, and Hu CD (2006) Identification of new fluorescent protein fragments for bimolecular fluorescence complementation analysis under physiological conditions. *BioTechniques* 40:61-66

Sims IM., Munro SLA., Currie G., Craik D., Bacic A. (1996) Structural characterization of xyloglucan secreted by suspension-cultured cells of *Nicotiana plumbaginifolia*. *Carbohydrate Research* 293: 147-172

Sims IM, Craik DJ, Bacic A (1997) Structural characterisation of galactoglucomannan secreted by suspension-cultured cells of *Nicotiana plumbaginifolia. Carbohydrate Research* 303:79-92

Sjostrand FS, Hanzon V (1954) Ultrastructure of Golgi apparatus of exocrine cells of mouse pancreas. *Experimental Cell Research* 7: 415–429

Sparkes, I.A., Ketelaar, T., de Ruijter, N.C.A. and Hawes, C. (2009) Grab a Golgi: laser trapping of Golgi bodies reveals in vivo interaction with the endoplasmic reticulum. *Traffic* 10: 567–571

Staehelin LA, Giddings TH Jr, Kiss JZ, Sack FD. (1990) Macromolecular differentiation of Golgi stacks in root tip of Arabidopsis and Nicotiana seedlings as vizualized in high pressure frozen and freeze-substituted samples. *Protoplasma*. 157:75-91

Staehelin LA, Driouich A. (1997) Brefeldin A Effects in Plants (Are Different Golgi Responses Caused by Different Sites of Action?). *Plant Physiol.* 114 (2), 401-403

Staehelin, L.A. and Kang, B.H. (2008). Nanoscale architecture of endoplasmic reticulum export sites and of Golgi membranes as determined by electron tomography. *Plant Physiol.* 147: 1454-1468

Strasser R, Schoberer J, Jin C, Glo¨ ssl J, Mach L, Steinkellner H. (2006) Molecular cloning and characterization of Arabidopsis thaliana Golgi alpha-mannosidase II, a key enzyme in the formation of complex N-glycans in plants. *Plant J*. 45:789–803

Strasser R, Bondili JS, Vavra U, Schoberer J, Svoboda B, Glossl J, Leonard R, Stadlmann J, Altmann F, Steinkellner H, Mach L (2007) A unique 1,3-Galactosyltransferase is indispensable for the biosynthesis of N-glycans containing Lewis a structures in *Arabidopsis thaliana*. *Plant Cell* 19:2278–2292

Studer D., Graber W., Al-Amoudi A. and Eggli P. (2001) A new approach for cryofixation by high-pressure freezing. *Journal of microscopy* 203 (3): 285-294

Surma MA, Klose C, Simons K. (2012) Lipid-dependent protein sorting at the trans-Golgi network. *Biochim Biophys Acta*. 1821(8):1059-67

T

Talbott L D. and Ray PM. (1992) Molecular Size and Separability Features of Pea Cell Wall Polysaccharides- Implications for Models of Primary Wall Structure *Plant Physiol.* 98: 357-368

Tamura K., Shimada T., Kondo M., Nishimura M. and Hara-Nishimura I. (2005) KATAMARI1/MURUS3 Is a Novel Golgi Membrane Protein That Is Required for Endomembrane Organization in Arabidopsis. *The Plant Cell*. 17: 1764–1776

Tuskan GA et al. (2006) The genome of black cottonwood, Populus trichocarpa (Torr. & Gray). *Science* 313(5793):1596-604

U

Usadel B, Schlüter U, Mølhøj M, Gipmans M, Verma R, Kossmann J, Reiter WD, Pauly M. (2004) Identification and characterization of a UDP-D-glucuronate 4-epimerase in Arabidopsis. *FEBS Lett.* 569(1-3):327-31

Usadel B., Kuschinsky A.M., Rosso M.G., Eckermann N., Pauly M. (2004b) RHM2 is involved in mucilage pectin synthesis and is required for the development of the seed coat in Arabidopsis. *Plant Physiol.* 134: 286–295

V

Vanzin GF, Madson M, Carpita NC, Keegstra K, Reiter WD. (2002) The *mur*2 mutant of *Arabidopsis thaliana* lacks fucosylated xyloglucan because of a lesion in fucosyltransferase AtFUT1. *Proc Natl Acad Sci USA*. 99:3340-3345

Verhoef, R., Lu, Y., Knox, J.P., Voragen, A.G.J. and Schols, H.A. (2009) Fingerprinting complex pectins by chromatographic separation combined with ELISA detection. *Carbohydr. Res*. 344: 1808-1817

Vicré M, Santaella C, Blanchet S, Gateau A, Driouich A. (2005) Root border-like cells of Arabidopsis. Microscopical characterization and role in the interaction with rhizobacteria. *Plant Physiol.* 138(2):998-1008

Vicré M, Jauneau A, Knox JP, Driouich A (1998) Immunolocalization of beta-(1 -> 4) and beta-(1 -> 6)-D-galactan epitopes in the cell wall and Golgi stacks of developing flax root tissues. *Protoplasma* 203: 26-34.

Vincken JP, York WS, Beldman G, Voragen AG. (1997) Two general branching patterns of xyloglucan, XXXG and XXGG. *Plant Physiol.* 114(1):9-13

Vincken,J.P.,Schols,H.A.,Oomen,R.J.,F.J.,Beldman,G.,Visser,R.G.F.,andVoragen,A.G.J.(2003).“ Pectin–the hairy thing,” in *Advances in Pectin and Pectinase Research*, edsA.G. J. Voragen,H.ScholsandR.Visser (Dordrecht: Kluwer Academic Publishers), 47–59

Viotti C, Bubeck J, Stierhof YD, Krebs M, Langhans M, van den Berg W, van Dongen W, Richter S, Geldner N, Takano J, Jürgens G, de Vries SC, Robinson DG, Schumacher K. (2010) Endocytic and secretory traffic in Arabidopsis merge in the trans-Golgi network/early endosome, an independent and highly dynamic organelle. *Plant Cell.* 22(4):1344-57

Voxeur A, Gilbert L, Rihouey C, Driouich A, Rothan C, Baldet P, Lerouge P. (2011) Silencing of the GDP-D-mannose 3,5-epimerase affects the structure and cross-linking of the pectic polysaccharide rhamnogalacturonan II and plant growth in tomato. *J Biol Chem.* 286(10):8014-20

W

Wang J, Ji Q, Jiang L, Shen S, Fan Y, Zhang C (2009) Overexpression of a cytosol-localized rhamnose biosynthesis protein encoded by Arabidopsis RHM1 gene increases rhamnose content in cell wall *Plant Physiology and Biochemistry* 47: 86–93

Watt G., Leoff C., Harper A.D., Bar-Peled M. (2004) A bifunctional 3,5-epimerase/4-keto reductase for nucleotide-rhamnose synthesis in Arabidopsis. *Plant Physiol.* 134: 1337–1346

Wee, E.G., Sherrier, D.J., Prime, T.A., and Dupree, P. (1998). Targeting of active sialyltransferase to the plant Golgi apparatus. *Plant Cell.* 10:1759-1768

Western T.L., Young D.S., Dean G.H., Tan W.L., Samuels A.L., Haughn G.W. (2004) MUCILAGE-MODIFIED4 encodes a putative pectin biosynthetic enzyme developmentally regulated by APETALA2, TRANSPARENT TESTA GLABRA1, and GLABRA2 in the Arabidopsis seed coat. *Plant Physiol.* 134: 296–306

Willats,W.G.T.,McCartney,L.,Mackie, W.,andKnox,J.P.(2001) Pectin: cell biology and prospects for functional analysis. *PlantMol.Biol.* 47: 9–27

Winicur ZM, Zhang GF, Staehelin A. (1998) Auxin deprivation induces Golgi differentiation in suspension-cultured tobacco BY-2 cells. *Plant Physiol*. 117: 501-513

Wolf S, Mouille G and Pelloux J (2009) Homogalacturonan Methyl-Esterification and Plant Development *Molecular Plant* 2(5): 851–860

X

Xu R, Li QQ. (2008) Protocol: Streamline cloning of genes into binary vectors in Agrobacterium via the Gateway(R) TOPO vector system. *Plant Methods.* 4:4

Y

Yang YD, Elamawi R, Bubeck J, Pepperkok R, Ritzenthaler C, Robinson DG (2005) Dynamics of COPII vesicles and the Golgi apparatus in cultured Nicotiana tabacum BY-2 cells provides evidence for transient association of Golgi stacks with endoplasmic reticulum exit sites. *Plant Cell.* 17(5):1513-31

Yang H, Richter GL, Wang X, Młodzińska E, Carraro N, Ma G, Jenness M, Chao DY, Peer WA, Murphy AS. (2013) Sterols and sphingolipids differentially function in trafficking of the Arabidopsis ABCB19 auxin transporter. *Plant J.* 74(1):37-47

Yin Y, Huang J, Gu X, Bar-Peled M, Xu Y (2011) Evolution of Plant Nucleotide-Sugar Interconversion Enzymes. *PLoS ONE* 6(11): e27995

York WS, van Halbeek H, Darvill AG, Albersheim P (1990) Structure of plant cell walls. 29. Structural analysis of xyloglucan oligosaccharides by ^{1}H NMR spectroscopy and fast atom bombardment mass spectrometry. *Carbohydrate Research* 200: 9-31

York WS, Kolli VS, Orlando R, Albersheim P, Darvill AG (1996) The structures of arabinoxyloglucans produced by solanaceous plants *Carbohydrate Research* 285: 99- 128

Z

Zablackis E, Huang J, Müllerz B, Darvill AC, and Albersheim P (1995) Characterization of the Cell-Wall Polysaccharides of *Arabidopsis thaliana* Leaves *Plant Physiol.* 107: 1129-1138

Zabotina OA, van de Ven WT, Freshour G, Drakakaki G, Cavalier D, Mouille G, Hahn MG, Keegstra K, Raikhel NV (2008) Arabidopsis XXT5 gene encodes a putative alpha-1,6-xylosyltransferase that is involved in xyloglucan biosynthesis. *Plant J.* 56(1):101-15.Erratum in *Plant J.* (2009) 57(2):386

Zakharova AN, Madsen R and Clausen MH (2013) Synthesis of a Backbone Hexasaccharide Fragment of the Pectic Polysaccharide Rhamnogalacturonan I *Organic Letters* 15(8): 1826–1829

Zandleven, J., Beldman, G., Bosveld,M., Schols, H.A., Voragen, A. (2006). Enzymatic degradation studies of xylogalacturonans from apple and potato, using XGH. *Carbohydr. Polym.* 65: 495–503

Zhang GF, Staehelin LA. (1992); Functional compartmentation of the golgi apparatus of plant cells: immunocytochemical analysis of high-pressure frozen- and freeze-substituted sycamore maple suspension culture cells. *Plant Physiol.* 99:1070-1083

CURICULUM VITAE

Sophie BERNARD
Née le 26-09-1980
Célibataire
Nationalité : Française

Ingénieur d'études en Microscopie Electronique à Transmission

EXPERIENCE PROFESSIONNELLE

Depuis 09/2009 : **Ingénieur d'étude en microscopie électronique à transmission**
Laboratoire de recherche universitaire « Glycobiologie et Matrice Extracellulaire Végétale », EA4358 et plateforme d'imagerie cellulaire PRMACEN (Université de Rouen, France). Mission : gestion technique et administrative du service de microscopie électronique à transmission.

10/2008 à 08/2009 : **Attaché temporaire d'enseignement et de recherche**
Université de Rouen, Faculté des Sciences et techniques. Mission : Travaux pratiques : niveau L1 « Introduction à la biochimie » et « Projet professionnel » ; niveau L2 « Biochimie générale » et « Physiologie végétale ».

09/2005 à 09/2008 : **Doctorante en biologie cellulaire**
Laboratoire de recherche universitaire « Glycobiologie et Matrice Extracellulaire Végétale », EA4358 (Université de Rouen, France). Mission : Cartographie golgienne d'enzymes impliquées dans la synthèse de la paroi végétale et recherche de complexes enzymatiques par microscopie électronique à transmission.
Séjours scientifiques au cours du doctorat :
Laboratoire de recherche universitaire « Plant cell wall biotechnology: cell wall elaboration » (Université d'Athens, Ohio,USA, 6 mois) et Laboratoire de recherche universitaire « Molecular Biology of Plant Cell Walls » (Université de Copenhague, Danemark, 2 mois).

09/2004 à 08/2005 : **Stage de formation master 2 recherche**
Laboratoire de recherche universitaire « Glycobiologie et Parois chez les Végétaux », CNRS-FRE3090 (Université de Rouen, France). Mission : Développement d'une nouvelle technique de préparation d'échantillon (la *High Pressure Freezing)* pour l'observation en microscopie électronique à transmission, sur 2 modèles végétaux *Nicotiana tabacum* et *Arabidopsis thaliana.*

Eté 2000 et 2001 : **Technicienne de laboratoire**
Entreprise pharmaceutique PHARMACIA (Louviers, France). Mission : Validation d'appareillage (Coulomètre, Lyophilisateur, Turbidimètre, Spectrocolorimètre) au sein du service contrôle qualité physico-chimique de l'entreprise.

COMPETENCES TECHNIQUES

- Préparation d'échantillons biologiques animal ou végétal, biopolymères.
- Préparation d'échantillons par fixation chimique classique, cryofixation sous haute pression (EMPACT1, LEICA), cryosubstitution (AFS1, LEICA), enrésinement en résines acrylique ou époxy.
- Ultramicrotomie sur coupes semi-fines et ultrafines (UCT et UC6, LEICA).
- Immunocytochimie appliquée à la microscopie électronique à transmission.
- Utilisation du microscope TECNAI 12 BIOTWIN, FEI.
- Analyses d'images et statistiques (Gatan Digital Micrograph, Image J).

DIPLOMES

2005 : Master 2 Recherche Biologie Cellulaire - Ecophysiologie et Biotechnologies végétales
2004 : Maîtrise Biochimie - Biochimie moléculaire et cellulaire, Microscopie
2003 : Licence Biochimie - Biochimie analytique
2002 : DEUG 2 Sciences de la vie - Biochimie
2001 : Brevet de Technicien Supérieur Biochimiste
1998 : Baccalauréat Sciences et Techniques de laboratoires - Biochimie et génie biologique

PUBLICATIONS

2012

• Harholt J, Jensen JK, Verhertbruggen Y, Søgaard C, Bernard S, Nafisi M, Poulsen CP, Geshi N, Sakuragi Y, Driouich A, Knox JP, Scheller HV. ARAD proteins associated with pectic Arabinan biosynthesis form complexes when transiently overexpressed in planta. Planta, 236(1):115-28

• C.Søgaard, A.Stenbaek, S. Bernard, M. Hadi, A. Driouich, HV. Scheller,Y. Sakuragi. GO-PROMTO Illuminates Protein Membrane Topologies of Glycan Biosynthetic Enzymes in the Golgi Apparatus of Living Tissues. PloS One, 7(2): e31324

• Driouich A, Follet-Gueye ML, Bernard S, Kousar S, Chevalier L, Vicré-Gibouin M, Lerouxel O. Golgi-mediated synthesis and secretion of matrix polysaccharides of the primary cell wall of higher plants. Frontiers in Plant Science, 3:79

• Follet-Gueye ML., Mollet JC., Vicré-Gibouin M., Bernard S., Chevalier L., Plancot B.,Dardelle F., Ramdani Y, Coimbra S. and Driouich A. Immuno-Glyco-Imaging in Plant Cells:Localization of Cell Wall Carbohydrate Epitopes and Their Biosynthesizing Enzymes. In Applications of Immunocytochemistry. Ed. Hesam Dehghani ISBN 978-953-51-0229-8. pp 297-320.

• Elias S, Delestre C, Ory S, Marais S, Courel M, Vazquez-Martinez R, Bernard S, Coquet L, Malagon MM, Driouich A, Chan P, Gasman S, Anouar Y and Montero-Hadjadje M (2012) Chromogranin A induces the biogenesis of granules with calcium- and actin-dependent dynamics and exocytosis in constitutively secreting cells. Endocrinology 153: 4444-56.

2011

• Chevalier L., Bernard S., Vicré-Gibouin M., Driouich A., and Follet-Gueye ML. Cryopreparation of tobacco Bright Yellow-2 (BY-2) suspension-cultured cells and application to immunogold localization of Green Fluorescent Protein-tagged-membrane- proteins. Journal of Biological Research - Thessaloniki, 16:212-216

• Driouich A., Cannesan MC., Dardelle F., Durand C., Plancot B., Bernard S., Follet-Gueye ML., and Vivré-Gibouin M. Unity is strenght : the power of border cells and border-like cells in relation with plant defense. In Secretions and Exudates in Biological Systems, Signalling and Communication in Plants. Springer-Verlag Berlin Heidelberg.

2010

• Chevalier L.*, Bernard S.*, Ramdani Y., Lamour R., Bardor M., Lerouge P., Follet-Gueye ML. and Driouich A. Subcompartment localization of the side chain xyloglucan-synthesizing enzymes within Golgi stacks of tobacco suspension-cultured cells. The Plant Journal, 64: 977-989

• Wu Y, Williams M, Bernard S, Driouich A, Showalter AM, Faik A. Functional identification of two nonredundant Arabidopsis alpha(1,2)fucosyltransferases specific to arabinogalactan proteins. Journal of biological chemistry 285(18): 13638-45